

# Hanford Double-Shell Tank Thermal and Seismic Project - Dytran Analysis of Seismically Induced Fluid-Structure Interaction in a Hanford Double Shell Primary Tank

**TC Mackey**  
Washington River Protection Solutions  
Richland, WA 99352  
U.S. Department of Energy Contract DE-AC27-08RV14800

EDT/ECN: ECN-726549 R0 UC:  
Cost Center: Charge Code:  
B&R Code: Total Pages: 343

Key Words: Double-Shell Tank, Tanks, DST, Seismic, Thermal, Buckling, J Bolt.

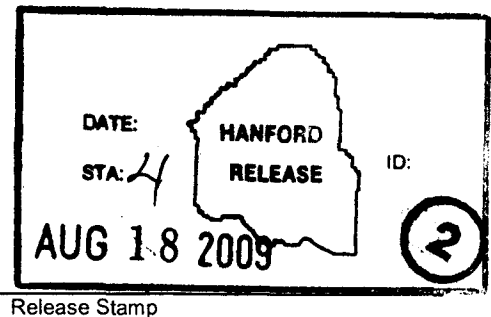
Abstract: This report (Revision 1) incorporates corrections and clarifications regarding the interpretation of solutions in BNL (1995) per reviewer comments from a June 7-8, 2007, review meeting. The review comments affect Appendixes C and D of this report – the body of the report is unchanged.

---

TRADEMARK DISCLAIMER. Reference herein to any specific commercial product, process, or service by trade name, trademark, manufacturer, or otherwise, does not necessarily constitute or imply its endorsement, recommendation, or favoring by the United States Government or any agency thereof or its contractors or subcontractors.

*TEF*  
Release Approval

*8-18-2009*  
Date



**Approved For Public Release**

<b>Tank Operations Contractor (TOC) RECORD OF REVISION</b>		(1) Document Number: <b>RPP-RPT-28963</b>	Page 1
(2) Title: <b>Dytran Analysis of Seismically Induced Fluid-Structure Interaction in a Hanford Double Shell Primary Tank</b>			
<b>Change Control Record</b>			
(3) Revision	(4) Description of Change – Replace, Add, and Delete Pages	Authorized for Release	
		(5) Resp. Engr. (print/sign/date)	(6) Resp. Mgr. (print/sign/date)
Rev. 1 <b>RS</b>	This document incorporates changes per ECN 726549 Rev. 0.	TC Mackey <i>TC Mackey</i> 8/18/09	EA Nelson <i>EA Nelson</i> 9/10/09

# Hanford Double-Shell Tank Thermal and Seismic Project – Dytran<sup>®</sup> Benchmark Analysis of Seismically Induced Fluid-Structure Interaction in a Hanford Double- Shell Primary Tank

F. G. Abatt  
M. W. Rinker

January 2008

Prepared for  
CH2M HILL Hanford Group, Inc.  
in Support of the  
Double-Shell Tank Integrity Program



Sponsored by the U.S. Department of Energy  
under Contract DE-AC05-76RL01830

---

## DISCLAIMER

This report was prepared as an account of work sponsored by an agency of the United States Government. Neither the United States Government nor any agency thereof, nor Battelle Memorial Institute, nor any of their employees, makes **any warranty, express or implied, or assumes any legal liability or responsibility for the accuracy, completeness, or usefulness of any information, apparatus, product, or process disclosed, or represents that its use would not infringe privately owned rights.** Reference herein to any specific commercial product, process, or service by trade name, trademark, manufacturer, or otherwise does not necessarily constitute or imply its endorsement, recommendation, or favoring by the United States Government or any agency thereof, or Battelle Memorial Institute. The views and opinions of authors expressed herein do not necessarily state or reflect those of the United States Government or any agency thereof.

PACIFIC NORTHWEST NATIONAL LABORATORY  
*operated by*  
BATTELLE  
*for the*  
UNITED STATES DEPARTMENT OF ENERGY  
*under Contract DE-AC05-76RL01830*



This document was printed on recycled paper.

**Hanford Double-Shell Tank Thermal and Seismic  
Project – Dytran<sup>®</sup> Benchmark Analysis of  
Seismically Induced Fluid-Structure Interaction  
in a Hanford Double-Shell Primary Tank**

F. G. Abatt<sup>(a)</sup>  
M. W. Rinker

January 2008

Prepared for  
CH2M HILL Hanford Group, Inc.  
in Support of the Double-Shell Tank Integrity Program

Pacific Northwest National Laboratory  
Richland, Washington 99352

---

(a) M&D Professional Services, Richland, Washington.

RPP-RPT-28963, Rev. 1  
M&D-2008-005-RPT-01, Rev. 1

Intentionally left blank.

# Dytran Benchmark Analysis of Seismically Induced Fluid-Structure Interaction in a Hanford Double Shell Primary Tank

F.G. Abatt

January 2008

Prepared by  
M&D Professional Services, Inc.  
for  
Pacific Northwest National Laboratory



Prepared by F. G. Abatt 1/28/08  
F.G. Abatt

Appendices C and D checked by M. Meyer 1/28/08  
Milon Meyer

RPP-RPT-28963, Rev. 1  
M&D-2008-005-RPT-01, Rev. 1

Intentionally left blank.

## Executive Summary

M&D Professional Services, Inc. (M&D) is under subcontract to Pacific Northwest National Laboratory (PNNL) to perform seismic analysis of the Hanford Site double-shell tanks (DSTs) in support of a project entitled *Double-Shell Tank (DST) Integrity Project – DST Thermal and Seismic Analyses*. The overall scope of the project is to complete an up-to-date comprehensive analysis of record of the DST system at Hanford in support of Tri-Party Agreement Milestone M-48-14. The work described in this report was performed in support of the seismic analysis of the Hanford double-shell tanks. The thermal and operating loads analysis of the DSTs is documented in Rinker et al. (2004).

The overall seismic analysis of the DSTs is being performed with the general-purpose finite element code ANSYS<sup>®</sup>.<sup>1</sup> The global model used for the seismic analysis of the Hanford DSTs includes the DST structure, the contained waste, and the surrounding soil. The seismic analysis of the DSTs must address the fluid-structure interaction behavior and sloshing response of the primary tank and contained liquid. ANSYS<sup>®</sup> has demonstrated capabilities for structural analysis, but has more limited capabilities for fluid-structure interaction analysis.

The purpose of this study is to demonstrate the capabilities and investigate the limitations of the finite element code MSC.Dytran<sup>®</sup><sup>2</sup> for performing a dynamic fluid-structure interaction analysis of the primary tank and contained waste. To this end, the Dytran<sup>®</sup> solutions are benchmarked against theoretical solutions appearing in BNL (1995), when such theoretical solutions exist. When theoretical solutions were not available, comparisons were made to theoretical solutions to similar problems and to the results from ANSYS<sup>®</sup> simulations.

Both rigid tank and flexible tank configurations were analyzed with Dytran<sup>®</sup>. The response parameters of interest that are evaluated in this study are the total hydrodynamic reaction forces, the impulsive and convective mode frequencies, the waste pressures, and the slosh heights. To a limited extent, primary tank stresses are also reported.

The capabilities and limitations of ANSYS<sup>®</sup> for performing a fluid-structure interaction analysis of the primary tank and contained waste were explored in a parallel investigation and documented in a companion report (Carpenter and Abatt 2006). The results of this study were used in conjunction with the results of the global ANSYS<sup>®</sup> analysis reported in Carpenter et al. (2006) and the parallel ANSYS<sup>®</sup> fluid-structure interaction analysis to help determine if a more refined sub-model of the primary tank is necessary to capture the important fluid-structure interaction effects in the tank and if so, how to best utilize a refined sub-model of the primary tank.

The results of this study demonstrate that Dytran<sup>®</sup> has the capability to perform fluid-structure interaction analysis of a primary tank subjected to seismic loading. With the exception of some isolated peak pressures, and to a lesser extent peak stresses, the results agreed very well with theoretical solutions.

The benchmarking study documented in Carpenter and Abatt (2006) showed that the ANSYS<sup>®</sup> model used in that study captured much of the fluid-structure interaction (FSI) behavior, but did have limitations

---

<sup>1</sup> ANSYS<sup>®</sup> is a registered trademark of ANSYS, Inc., Canonsburg, Pennsylvania.

<sup>2</sup> MSC.Dytran<sup>®</sup> is a registered trademark of MSC.Software, Inc., Santa Ana, California.

for predicting the convective response of the waste. While Dytran<sup>®</sup> appears to have stronger capabilities for the analysis of the FSI behavior in the primary tank, it is more practical to use ANSYS<sup>®</sup> for the global evaluation of the tank. Thus, Dytran<sup>®</sup> served the purpose of helping to identify limitations in the ANSYS<sup>®</sup> FSI analysis, so that those limitations can be addressed in the structural evaluation of the primary tank.

Revision 0A of this report (Rinker and Abbot 2006) introduced new Appendixes C and D. Appendix C contains a reanalysis of the rigid and flexible tanks at the 460-inch liquid level and was motivated by recommendations from a project review meeting held on March 20–21, 2006 (Deibler et al. 2007, Appendix E). Appendix D contains the benchmark solutions in support of the analyses in Appendix C.

This report (Revision 1) incorporates corrections and clarifications regarding the interpretation of solutions in BNL (1995) per reviewer comments from a June 7–8, 2007, review meeting. The review comments affect Appendixes C and D of this report – the body of the report is unchanged. The complete set of review comments appear as Appendix A of Deibler et al. (2008), as referenced in Appendix C of this report.

## Contents

1.0	Introduction .....	1.1
1.1	Discussion .....	1.2
1.2	Summary .....	1.6
1.3	Conclusions .....	1.8
2.0	Model Description .....	2.1
2.1	Model Geometry .....	2.2
2.2	Material Properties and Element Types .....	2.8
2.3	Boundary Conditions.....	2.9
2.4	Initial Conditions.....	2.9
2.5	Seismic Input.....	2.10
3.0	Rigid Dytran® Model at 422-Inch Waste Level.....	3.1
3.1	Hydrodynamic Forces .....	3.1
3.1.1	Horizontal Excitation .....	3.2
3.1.2	Vertical Excitation.....	3.4
3.2	Waste Pressures.....	3.6
3.2.1	Horizontal Excitation Run at Absolute Pressure .....	3.6
3.2.2	Vertical Excitation.....	3.11
3.3	Slosh Height Results .....	3.16
4.0	Rigid Tank Model at 460-Inch Waste Level .....	4.1
4.1	Hydrodynamic Forces .....	4.1
4.1.1	Horizontal Excitation at Absolute Pressure.....	4.1
4.1.2	Vertical Excitation at Absolute Pressure .....	4.3
4.2	Waste Pressures.....	4.4
4.2.1	Horizontal Excitation Run at Absolute Pressure .....	4.4
4.2.2	Vertical Excitation Run at Absolute Pressure .....	4.10
4.3	Slosh Height Results .....	4.16
5.0	Flexible Tank Dytran® Model at 422-Inch Waste Level .....	5.1
5.1	Damping Implementation and Calibration .....	5.1
5.2	Hydrodynamic Forces .....	5.3
5.2.1	Horizontal Excitation .....	5.3
5.2.2	Vertical Excitation.....	5.15
5.3	Waste Pressures.....	5.18
5.3.1	Horizontal Excitation Run at Absolute Pressure .....	5.18
5.3.2	Wall and Base Pressures Due to Vertical Excitation Run at Absolute Pressure .....	5.26
5.4	Maximum Slosh Height Results.....	5.32

RPP-RPT-28963, Rev. 1  
M&D-2008-005-RPT-01, Rev. 1

5.5	Element Stresses.....	5.33
5.5.1	Horizontal Excitation Run at Absolute Pressure .....	5.33
6.0	Flexible Tank Dytran® Model at 460-Inch Waste Level .....	6.1
6.1	Hydrodynamic Forces .....	6.1
6.1.1	Horizontal Excitation Run at Absolute Pressure .....	6.1
6.1.2	Vertical Excitation Run at Absolute Pressure .....	6.4
6.2	Waste Pressures.....	6.4
6.2.1	Horizontal Excitation Run at Absolute Pressure .....	6.5
6.2.2	Wall and Base Pressures Due to Vertical Excitation Run at Absolute Pressure .....	6.10
6.3	Maximum Slosh Height Results.....	6.17
6.4	Element Stresses.....	6.17
6.4.1	Horizontal Excitation Run at Absolute Pressure .....	6.17
6.4.2	Vertical Excitation Run at Absolute Pressure .....	6.21
7.0	ANSYS® to Dytran® Comparisons .....	7.1
7.1	Frequencies and Slosh Heights .....	7.1
7.2	Hydrodynamic Forces .....	7.2
7.3	Waste Pressures.....	7.5
7.4	Element Stresses.....	7.8
8.0	References .....	8.1
	Appendix A – Description of Input and Results Files .....	A.1
	Appendix B – Theoretical Solutions.....	B.1
	Appendix C – Reanalysis of the Rigid and Flexible Wall Tanks at the 460-Inch Initial Liquid Level with Increased Mesh Refinement.....	C.1
	Appendix D – Benchmark Solutions in Support of Reanalysis Contained in Appendix C .....	D.1

## Figures

2-1	AY Primary Tank Dimensions.....	2.2
2-2	Plot of Primary Tank and Base .....	2.3
2-3	Plot of Tank and Waste at 422-Inch Waste Level.....	2.4
2-4	Plot of Tank and Waste at 460-Inch Waste Level.....	2.4
2-5	Top View of Model Showing the Angular Locations of Fluid Elements at Which Pressures Were Monitored .....	2.5
2-6	Waste Element Numbering for Element Sets “Plusx_els,” Minusx_els”, and Cent_press” .....	2.6
2-7	Waste Element Numbering for Element Sets “Press_45” and Plusz_els” .....	2.6
2-8	Shell Element Numbering for Tank Wall Stress Results at $\theta=0$ and $\theta=90^\circ$ .....	2.7
2-9	Shell Element Numbering for Tank Wall Stress Results at $\theta=45^\circ$ and $\theta=180^\circ$ .....	2.7
2-10	Section Plot of Flexible Primary Tank.....	2.8
2-11	ANSYS® Composite Tank Model Detail .....	2.10
2-12	Excavated Soil Model Detail for Global ANSYS® Model.....	2.11
2-13	Far-Field Soil Model Detail for Global ANSYS® Model .....	2.11
2-14	Tank with Hinged-Top Boundary Condition per BNL (1995).....	2.12
2-15	Horizontal Acceleration Time History Output from ANSYS® Model.....	2.13
2-16	Vertical Acceleration Time History Output from ANSYS® Model.....	2.13
2-17	Velocity Time Histories Output from ANSYS® Model.....	2.14
2-18	Displacement Time Histories Output from ANSYS® Model.....	2.14
2-19	4% Damped Response Spectra for Acceleration Time Histories Extracted from ANSYS® Model .....	2.15
2-20	Comparison of Horizontal Dome Apex Response Spectra at Different Damping Values .....	2.15
2-21	Comparison of Horizontal Dome Apex Response Spectra at Different Damping Values for Low Frequencies .....	2.16
3-1	Coupling Surface Reaction Forces for the Rigid Tank at 422-Inch Waste Level Under Horizontal Seismic Input.....	3.2
3-2	Horizontal Coupling Surface Reaction Force for the Rigid Tank at 422-Inch Waste Level Under Horizontal Seismic Input.....	3.3
3-3	Horizontal Coupling Surface Reaction Force for Rigid Tank at 422-Inch Waste Level Under Horizontal Seismic Excitation – Convective Response .....	3.4
3-4	Coupling Surface Reaction Forces for Rigid Tank at 422-Inch Waste Level Under Vertical Seismic Input.....	3.5
3-5	Vertical Coupling Surface Reaction Force for Rigid Tank at 422-Inch Waste Level Under Vertical Seismic Input.....	3.5
3-6	Waste Pressure Time Histories for the Rigid Tank with 422 Inches of Waste Under Horizontal Excitation at $\theta=0$ Run at Absolute Pressure.....	3.7
3-7	Waste Pressure Time Histories for the Rigid Tank with 422 Inches of Waste Under Horizontal Excitation at $\theta=45^\circ$ Run at Absolute Pressure .....	3.8

RPP-RPT-28963, Rev. 1  
M&D-2008-005-RPT-01, Rev. 1

3-8	Waste Pressure Time Histories for the Rigid Tank with 422 Inches of Waste Under Horizontal Excitation at $\theta=90^\circ$ Run at Absolute Pressure .....	3.8
3-9	Maximum and Minimum Waste Pressures vs. Normalized Height from Tank Bottom for Horizontal Excitation at $\theta=0$ Run at Absolute Pressure .....	3.9
3-10	Maximum and Minimum Waste Pressures vs. Normalized Height from Tank Bottom for Horizontal Excitation at $\theta=45^\circ$ Run at Absolute Pressure.....	3.10
3-11	Maximum and Minimum Waste Pressures vs. Normalized Height from Tank Bottom for Horizontal Excitation at $\theta=90^\circ$ Run at Absolute Pressure.....	3.10
3-12	Selected Waste Pressure Time Histories for the Rigid Tank with 422 Inches of Waste Under Horizontal Excitation at $\theta=0$ Run at Absolute Pressure.....	3.11
3-13	Waste Pressure Time Histories for the Rigid Tank with 422 Inches of Waste Under Vertical Excitation at $\theta=0$ Run at Absolute Pressure.....	3.12
3-14	Waste Pressure Time Histories for the Rigid Tank with 422 Inches of Waste Under Vertical Excitation at $\theta=45^\circ$ Run at Absolute Pressure .....	3.13
3-15	Waste Pressure Time Histories for the Rigid Tank with 422 Inches of Waste Under Vertical Excitation at $\theta=90^\circ$ Run at Absolute Pressure .....	3.13
3-16	Pressure Time History for Bottom Center Waste Element for the Rigid Tank at the 422-Inch Waste Level and Vertical Excitation Run at Absolute Pressure .....	3.14
3-17	Maximum and Minimum Waste Pressures vs. Normalized Height from Tank Bottom for Vertical Excitation of Rigid Tank at 422-Inch Waste Level and $\theta=0$ Run at Absolute Pressure .....	3.15
3-18	Maximum and Minimum Waste Pressures vs. Normalized Height from Tank Bottom for Vertical Excitation of Rigid Tank at 422-Inch Waste Level and $\theta=45^\circ$ Run at Absolute Pressure .....	3.15
3-19	Maximum and Minimum Waste Pressures vs. Normalized Height from Tank Bottom for Vertical Excitation of Rigid Tank at 422-Inch Waste Level and $\theta=90^\circ$ Run at Absolute Pressure .....	3.16
3-20	Maximum Slosh Height Time History Over All Waste Elements for Horizontal Excitation .....	3.17
4-1	Coupling Surface Reaction Forces at the 460-Inch Waste Level for the Rigid Tank Under Horizontal Seismic Excitation.....	4.1
4-2	Horizontal Coupling Surface Reaction Force for Rigid Tank at 460-Inch Waste Level Under Horizontal Seismic Excitation.....	4.2
4-3	Horizontal Coupling Surface Reaction Force for Rigid Tank at 460-Inch Waste Level Under Horizontal Seismic Excitation – Convective Response .....	4.3
4-4	Vertical Coupling Surface Reaction Force for Rigid Tank at 460-Inch Waste Level Under Vertical Seismic Excitation.....	4.4
4-5	Waste Pressure Time Histories for the Rigid Tank with 460 Inches of Waste Under Horizontal Excitation at $\theta=0$ Run at Absolute Pressure.....	4.6
4-6	Selected Waste Pressure Time Histories for the Rigid Tank with 460 Inches of Waste Under Horizontal Excitation at $\theta=0$ Run at Absolute Pressure.....	4.6
4-7	Waste Pressure Time Histories for the Rigid Tank with 460 Inches of Waste Under Horizontal Excitation at $\theta=45^\circ$ Run at Absolute Pressure .....	4.7

RPP-RPT-28963, Rev. 1  
M&D-2008-005-RPT-01, Rev. 1

4-8	Selected Waste Pressure Time Histories for the Rigid Tank with 460 Inches of Waste Under Horizontal Excitation at $\theta=45^\circ$ Run at Absolute Pressure .....	4.7
4-9	Waste Pressure Time Histories for the Rigid Tank with 460 Inches of Waste Under Horizontal Excitation at $\theta=90^\circ$ Run at Absolute Pressure .....	4.8
4-10	Maximum and Minimum Waste Pressures vs. Normalized Height from Tank Bottom for Horizontal Excitation of Rigid Tank at 460-Inch Waste Level and $\theta=0$ Run at Absolute Pressure .....	4.9
4-11	Maximum and Minimum Waste Pressures vs. Normalized Height from Tank Bottom for Horizontal Excitation of Rigid Tank at 460-Inch Waste Level and $\theta=45^\circ$ Run at Absolute Pressure .....	4.9
4-12	Maximum and Minimum Waste Pressures vs. Normalized Height from Tank Bottom for Horizontal Excitation of Rigid Tank at 460-Inch Waste Level and $\theta=90^\circ$ Run at Absolute Pressure .....	4.10
4-13	Waste Pressure Time Histories for the Rigid Tank with 460 Inches of Waste Under Vertical Excitation at $\theta=0$ Run at Absolute Pressure .....	4.11
4-14	Selected Waste Pressure Time Histories for the Rigid Tank with 460 Inches of Waste Under Vertical Excitation at $\theta=0$ Run at Absolute Pressure .....	4.11
4-15	Waste Pressure Time Histories for the Rigid Tank with 460 Inches of Waste Under Vertical Excitation at $\theta=45^\circ$ Run at Absolute Pressure .....	4.12
4-16	Selected Waste Pressure Time Histories for the Rigid Tank with 460 Inches of Waste Under Vertical Excitation at $\theta=45^\circ$ Run at Absolute Pressure .....	4.12
4-17	Waste Pressure Time Histories for the Rigid Tank with 460 Inches of Waste Under Vertical Excitation at $\theta=90^\circ$ Run at Absolute Pressure .....	4.13
4-18	Selected Waste Pressure Time Histories for the Rigid Tank with 460 Inches of Waste Under Vertical Excitation at $\theta=90^\circ$ Run at Absolute Pressure .....	4.13
4-19	Pressure Time History for Bottom Center Waste Element for the Rigid Tank at the 460-Inch Waste Level and Vertical Excitation Run at Absolute Pressure .....	4.14
4-20	Maximum and Minimum Waste Pressures vs. Normalized Height from Tank Bottom for Vertical Excitation of Rigid Tank at 460-Inch Waste Level and $\theta=0$ Run at Absolute Pressure .....	4.14
4-21	Maximum and Minimum Waste Pressures vs. Normalized Height from Tank Bottom for Vertical Excitation of Rigid Tank at 460-Inch Waste Level and $\theta=45^\circ$ Run at Absolute Pressure .....	4.15
4-22	Maximum and Minimum Waste Pressures vs. Normalized Height from Tank Bottom for Vertical Excitation of Rigid Tank at 460-Inch Waste Level and $\theta=90^\circ$ Run at Absolute Pressure .....	4.15
4-23	Maximum Slosh Height Time History Over All Waste Elements for Horizontal Excitation of the Rigid Tank at the 460-Inch Waste Level .....	4.16
4-24	Plot of Waste-Free Surface Under Gravity Loading Only for the Rigid Tank at the 460-Inch Waste Level .....	4.17
5-1	Coupling Surface Reaction Forces for the Flexible Tank Under Horizontal Seismic Input at Gage Pressure– Case 1 .....	5.4
5-2	Coupling Surface Reaction Forces for the Flexible Tank Under Horizontal Seismic Input at Gage Pressure During the Initial Free-Vibration Phase – Case 1 .....	5.4

RPP-RPT-28963, Rev. 1  
M&D-2008-005-RPT-01, Rev. 1

5-3	Mid-Wall Hoop Stress for Flexible Tank at Gage Pressure and $\theta=0$ – Case 1 .....	5.5
5-4	Coupling Surface Reaction Forces at the 422-Inch Waste Level for the Flexible Tank at Gage Pressure Under Horizontal Seismic Input During the Initial Free-Vibration Phase – Case 2a ( $\alpha=0.08$ ) .....	5.6
5-5	Coupling Surface Reaction Forces at the 422-Inch Waste Level for the Flexible Tank at Gage Pressure Under Horizontal Seismic Input – Case 2a ( $\alpha=0.08$ ).....	5.6
5-6	Coupling Surface Reaction Forces at the 422-Inch Waste Level for the Flexible Tank at Gage Pressure Under Horizontal Seismic Input During the Initial Free-Vibration Phase – Case 2b ( $\alpha=0.04$ ) .....	5.7
5-7	Coupling Surface Reaction Forces at the 422-Inch Waste Level for the Flexible Tank at Gage Pressure Under Horizontal Seismic Input – Case 2b ( $\alpha=0.04$ ).....	5.8
5-8	Coupling Surface Reaction Forces at the 422-Inch Waste Level for the Flexible Tank at Gage Pressure Under Horizontal Seismic Input During the Initial Free-Vibration Phase – Case 2c ( $\alpha=0.02$ ) .....	5.9
5-9	Coupling Surface Reaction Forces at the 422-Inch Waste Level for the Flexible Tank at Gage Pressure Under Horizontal Seismic Input – Case 2c ( $\alpha=0.02$ ).....	5.9
5-10	Coupling Surface Reaction Forces at the 422-Inch Waste Level for the Flexible Tank at Gage Pressure Under Horizontal Seismic Input During the Final Free-Vibration Phase – Case 2c ( $\alpha=0.02$ ) .....	5.10
5-11	Coupling Surface Reaction Forces at the 422-Inch Waste Level for the Flexible Tank at Absolute Pressure Under Horizontal Seismic Input During the Initial Free-Vibration Phase – Case 2c ( $\alpha=0.02$ ) .....	5.10
5-12	Horizontal Coupling Surface Reaction Force at the 422-Inch Waste Level for the Flexible Tank at Absolute Pressure Under Horizontal Seismic Input – Case 2c ( $\alpha=0.02$ ).....	5.11
5-13	Coupling Surface Reaction Forces at the 422-Inch Waste Level for the Flexible Tank at Absolute Pressure Under Horizontal Seismic Input During the Final Free-Vibration Phase – Case 2c ( $\alpha=0.02$ ) .....	5.11
5-14	Coupling Surface Reaction Forces at the 422-Inch Waste Level for the Flexible Tank at Gage Pressure Under Horizontal Seismic Input During the Initial Free-Vibration Phase – Case 2d ( $\alpha=0.01$ ) .....	5.12
5-15	Coupling Surface Reaction Forces at the 422-Inch Waste Level for the Flexible Tank at Gage Pressure Under Horizontal Seismic Input – Case 2d ( $\alpha=0.01$ ).....	5.13
5-16	Coupling Surface Reaction Forces at the 422-Inch Waste Level for the Flexible Tank at Gage Pressure Under Horizontal Seismic Input During the Final Free-Vibration Phase – Case 2d ( $\alpha=0.01$ ) .....	5.13
5-17	Coupling Surface Reaction Forces for the Flexible Tank at Gage Pressure Under Horizontal Seismic Input – Case 3.....	5.14
5-18	Coupling Surface Reaction Forces for the Flexible Tank at Gage Pressure Under Horizontal Seismic Input from 23.0 to 25.0 seconds – Case 3.....	5.14
5-19	Coupling Surface Reaction Forces for the Flexible Tank at Gage Pressure Under Vertical Seismic Input – Case 2c .....	5.16
5-20	Coupling Surface Reaction Forces for the Flexible Tank at Gage Pressure Under Vertical Seismic Input – Case 3 .....	5.17

RPP-RPT-28963, Rev. 1  
M&D-2008-005-RPT-01, Rev. 1

5-21	Coupling Surface Reaction Forces for the Flexible Tank at Absolute Pressure Under Vertical Seismic Input – Case 2c .....	5.18
5-22	Waste Pressures Time Histories for the Flexible Tank at the 422-Inch Waste Level for Horizontal Excitation at $\theta=0$ , Case 2c ( $\alpha=0.02$ ) Run at Absolute Pressure.....	5.20
5-23	Selected Element Pressure Time Histories for the Flexible Tank at the 422-Inch Waste Level for Horizontal Excitation at $\theta=0$ , Case 2c ( $\alpha=0.02$ ) Run at Absolute Pressure .....	5.20
5-24	Waste Pressures Time Histories for the Flexible Tank at the 422-Inch Waste Level for Horizontal Excitation at $\theta=45$ , Case 2c ( $\alpha=0.02$ ) Run at Absolute Pressure.....	5.21
5-25	Selected Element Pressure Time Histories for the Flexible Tank at the 422-Inch Waste Level for Horizontal Excitation at $\theta=45$ , Case 2c ( $\alpha=0.02$ ) Run at Absolute Pressure .....	5.21
5-26	Waste Pressures Time Histories for the Flexible Tank at the 422-Inch Waste Level for Horizontal Excitation at $\theta=90$ , Case 2c ( $\alpha=0.02$ ) Run at Absolute Pressure.....	5.22
5-27	Selected Element Pressure Time Histories for the Flexible Tank at the 422-Inch Waste Level for Horizontal Excitation at $\theta=90$ , Case 2c ( $\alpha=0.02$ ) Run at Absolute Pressure .....	5.22
5-28	Comparison of Waste Pressures in the Flexible Tank at the 422-Inch Waste Level at Absolute and Gage Pressure for Selected Elements at $\theta=0$ .....	5.23
5-29	Comparison of Waste Pressures in the Flexible Tank at the 422-Inch Waste Level at Absolute and Gage Pressure for Selected Elements at $\theta=45^\circ$ .....	5.24
5-30	Comparison of Waste Pressures in the Flexible Tank at the 422-Inch Waste Level at Absolute and Gage Pressure for Selected Elements at $\theta=90^\circ$ .....	5.24
5-31	Maximum and Minimum Waste Pressures vs. Normalized Height from Tank Bottom for the Flexible Tank at the 422-Inch Waste Level Under Horizontal Excitation for $\alpha=0.02$ and $\theta=0$ .....	5.25
5-32	Maximum and Minimum Waste Pressures vs. Normalized Height from Tank Bottom for the Flexible Tank at the 422-Inch Waste Level Under Horizontal Excitation for $\alpha=0.02$ and $\theta=45^\circ$ .....	5.25
5-33	Maximum and Minimum Waste Pressures vs. Normalized Height from Tank Bottom for the Flexible Tank at the 422-Inch Waste Level Under Horizontal Excitation for $\alpha=0.02$ and $\theta=90^\circ$ .....	5.26
5-34	Waste Pressure Time Histories for the Flexible Tank at the 422-Inch Waste Level for Vertical Excitation Run at Absolute Pressure for $\theta=0$ and $\alpha=0.02$ .....	5.27
5-35	Selected Waste Pressure Time Histories for the Flexible Tank at the 422-Inch Waste Level for Vertical Excitation Case 2c ( $\alpha=0.02$ ) Run at Absolute Pressure .....	5.28
5-36	Selected Waste Pressure Time Histories for the Flexible Tank at the 422-Inch Waste Level for Vertical Excitation Case 2c ( $\alpha=0.02$ ) Run at Absolute Pressure – Time 0 to 3 Seconds.....	5.28
5-37	Maximum and Minimum Waste Pressures vs. Normalized Height from Tank Bottom for the Flexible Tank at the 422-Inch Waste Level Under Vertical Excitation at $\theta=0$ and $\alpha=0.02$ .....	5.29
5-38	Comparison of Waste Pressure to Tank Wall Hoop Stress for the Flexible Tank at the 422-Inch Waste Level and Vertical Excitation at Absolute Pressure Near the Tank Bottom at $\theta=0$ .....	5.29

RPP-RPT-28963, Rev. 1  
M&D-2008-005-RPT-01, Rev. 1

5-39	Maximum and Minimum Waste Pressures vs. Normalized Height from Tank Bottom for the Flexible Tank at the 422-Inch Waste Level Under Vertical Excitation at $\theta=45^\circ$ and $\alpha=0.02$ .....	5.30
5-40	Maximum and Minimum Waste Pressures vs. Normalized Height from Tank Bottom for the Flexible Tank at the 422-Inch Waste Level at Absolute Pressure with $\theta=90^\circ$ and $\alpha=0.02$ .....	5.31
5-41	Pressure Time History for Bottom Center Waste Element for 422 Inches Waste Level and Vertical Excitation at Absolute Pressure and $\alpha=0.02$ .....	5.31
5-42	Comparison of Maximum Slosh Height Time Histories for the Flexible Tank at the 422-Inch Waste Level and $\alpha=0.02$ .....	5.32
5-43	Dependence of the Maximum Slosh Height on the Damping Parameter $\alpha$ .....	5.33
5-44	Mid-Plane Hoop Stress for the Flexible Tank at the 422-Inch Waste Level at $\theta=0$ and $\alpha=0.02$ Run at Absolute Pressure .....	5.34
5-45	Mid-Plane Hoop Stress for the Flexible Tank at the 422-Inch Waste Level at $\theta=45^\circ$ and $\alpha=0.02$ Run at Absolute Pressure .....	5.34
5-46	Mid-Plane Hoop Stress for the Flexible Tank at the 422-Inch Waste Level at $\theta=90^\circ$ and $\alpha=0.02$ Run at Absolute Pressure .....	5.35
5-47	Comparison of Mid-Plane Hoop Stress in Tank Wall Element 433 to pr/t for Waste Element 6108 at Wall Mid-Height and $\theta=0$ .....	5.35
5-48	Comparison of Mid-Plane Hoop Stress at Absolute and Gage Pressure for Selected Elements at $\theta=90^\circ$ .....	5.36
6-1	Coupling Surface Reaction Forces at the 460-Inch Waste Level for the Flexible Tank Under Horizontal Seismic Input During the Initial Free-Vibration Phase – $\alpha=0.02$ .....	6.1
6-2	Coupling Surface Reaction Forces at the 460-Inch Waste Level for the Flexible Tank Under Horizontal Seismic Input – $\alpha=0.02$ .....	6.2
6-3	Coupling Surface Reaction Forces at the 460-Inch Waste Level for the Flexible Tank Under Horizontal Seismic Input During the Final Free-Vibration Phase – $\alpha=0.02$ .....	6.3
6-4	Comparison of the Horizontal Coupling Surface Reaction Force for the 460- and 422-Inch Waste Levels During the Final Free-Vibration Period – $\alpha=0.02$ .....	6.3
6-5	Vertical Coupling Surface Reaction Force at the 460-Inch Waste Level for the Flexible Tank Under Vertical Seismic Input .....	6.4
6-6	Waste Pressures Time Histories for the Flexible Tank at the 460-Inch Waste Level for Horizontal Excitation at $\theta=0$ and $\alpha=0.02$ Run at Absolute Pressure .....	6.6
6-7	Selected Element Pressure Time Histories for the Flexible Tank at the 460-Inch Waste Level for Horizontal Excitation at $\theta=0$ and $\alpha=0.02$ Run at Absolute Pressure .....	6.6
6-8	Waste Pressures Time Histories for the Flexible Tank at the 460-Inch Waste Level for Horizontal Excitation at $\theta=45$ and $\alpha=0.02$ Run at Absolute Pressure .....	6.7
6-9	Selected Element Pressure Time Histories for the Flexible Tank at the 460-Inch Waste Level for Horizontal Excitation at $\theta=45$ and $\alpha=0.02$ Run at Absolute Pressure .....	6.7
6-10	Waste Pressures Time Histories for the Flexible Tank at the 460-Inch Waste Level for Horizontal Excitation at $\theta=90$ and $\alpha=0.02$ Run at Absolute Pressure .....	6.8

RPP-RPT-28963, Rev. 1  
M&D-2008-005-RPT-01, Rev. 1

6-11	Maximum and Minimum Waste Pressures vs. Normalized Height from Tank Bottom for the Flexible Tank Under Horizontal Excitation at the 460-Inch Waste Level at $\theta=0$ and $\alpha=0.02$ .....	6.9
6-12	Maximum and Minimum Waste Pressures vs. Normalized Height from Tank Bottom for the Flexible Tank Under Horizontal Excitation at the 460-Inch Waste Level at $\theta=45^\circ$ and $\alpha=0.02$ .....	6.9
6-13	Maximum and Minimum Waste Pressures vs. Normalized Height from Tank Bottom for the Flexible Tank Under Horizontal Excitation at the 460-Inch Waste Level at $\theta=90^\circ$ and $\alpha=0.02$ .....	6.10
6-14	Waste Pressure Time Histories for the Flexible Tank at the 460-Inch Waste Level for Vertical Excitation at $\theta=0$ and $\alpha=0.02$ .....	6.11
6-15	Selected Element Waste Pressure for the Flexible Tank at the 460-Inch Waste Level for Vertical Excitation at $\theta=0$ and $\alpha=0.02$ .....	6.11
6-16	Selected Element Waste Pressures for the Flexible Tank at the 460-Inch Waste Level for Vertical Excitation at $\theta=0$ and $\alpha=0.02$ – Time 0 to 3 Seconds .....	6.12
6-17	Waste Pressure Time Histories for the Flexible Tank at the 460-Inch Waste Level for Vertical Excitation at $\theta=45^\circ$ and $\alpha=0.02$ .....	6.12
6-18	Selected Element Waste Pressure for the Flexible Tank at the 460-Inch Waste Level for Vertical Excitation at $\theta=45^\circ$ and $\alpha=0.02$ .....	6.13
6-19	Waste Pressure Time Histories for the Flexible Tank at the 460-Inch Waste Level for Vertical Excitation at $\theta=90^\circ$ and $\alpha=0.02$ .....	6.13
6-20	Selected Element Waste Pressure for the Flexible Tank at the 460-Inch Waste Level for Vertical Excitation at $\theta=90^\circ$ and $\alpha=0.02$ .....	6.14
6-21	Maximum and Minimum Waste Pressures vs. Normalized Waste Height from Tank Bottom for 460-Inch Waste Level for Vertical Excitation at $\theta=0$ and $\alpha=0.02$ .....	6.14
6-22	Maximum and Minimum Waste Pressures vs. Normalized Waste Height from Tank Bottom for 460-Inch Waste Level for Vertical Excitation at $\theta=45^\circ$ and $\alpha=0.02$ .....	6.15
6-23	Maximum and Minimum Waste Pressures vs. Normalized Waste Height from Tank Bottom for 460-Inch Waste Level for Vertical Excitation at $\theta=90^\circ$ and $\alpha=0.02$ .....	6.15
6-24	Pressure Time History for Bottom Center Waste Element for 460-Inch Waste Level and Vertical Excitation for $\alpha=0.02$ .....	6.16
6-25	Maximum Slosh Height Time History for the Flexible Tank at the 460-Inch Waste Level for $\alpha=0.02$ .....	6.17
6-26	Mid-Plane Hoop Stress for the Flexible Tank at the 460-Inch Waste Level at $\theta=0$ and $\alpha=0.02$ Run at Absolute Pressure .....	6.18
6-27	Mid-Plane Hoop Stress for the Flexible Tank at the 460-Inch Waste Level at $\theta=45^\circ$ and $\alpha=0.02$ Run at Absolute Pressure .....	6.19
6-28	Mid-Plane Hoop Stress for the Flexible Tank at the 460-Inch Waste Level at $\theta=90^\circ$ and $\alpha=0.02$ Run at Absolute Pressure .....	6.19
6-29	Comparison of Waste Pressure to Tank Wall Hoop Stress for the Flexible Tank at the 460-Inch Waste Level at Absolute Pressure for Waste Element 9753 and Tank Wall Element 406 Near the Free Surface at $\theta=0$ .....	6.20

RPP-RPT-28963, Rev. 1  
M&D-2008-005-RPT-01, Rev. 1

6-30	Comparison of Waste Pressure to Tank Wall Hoop Stress for the Flexible Tank at the 422-Inch Waste Level at Absolute Pressure for Waste Element 9024 and Tank Wall Element 431 Near the Free Surface at $\theta=0$ .....	6.20
6-31	Mid-Plane Hoop Stress for the Flexible Tank at the 460-Inch Waste Level for Vertical Excitation at $\theta=0$ and $\alpha=0.02$ Run at Absolute Pressure .....	6.21
6-32	Mid-Plane Hoop Stress for the Flexible Tank at the 460-Inch Waste Level for Vertical Excitation at $\theta=45^\circ$ and $\alpha=0.02$ Run at Absolute Pressure.....	6.22
6-33	Mid-Plane Hoop Stress for the Flexible Tank at the 460-Inch Waste Level for Vertical Excitation at $\theta=90^\circ$ and $\alpha=0.02$ Run at Absolute Pressure.....	6.22
6-34	Comparison of Waste Pressure to Tank Wall Hoop Stress for the Flexible Tank at the 460-Inch Waste Level Under Vertical Excitation at Absolute Pressure Near the Free Surface at $\theta=45^\circ$ .....	6.23
6-35	Comparison of Waste Pressure to Tank Wall Hoop Stress for the Flexible Tank at the 460-Inch Waste Level Under Vertical Excitation at Absolute Pressure Near the Free Surface at $\theta=90^\circ$ .....	6.23
7-1	Comparison of ANSYS <sup>®</sup> and Dytran <sup>®</sup> Total Horizontal Reaction Forces for the Flexible Tank at the 422-Inch Waste Level Under Horizontal Seismic Excitation .....	7.3
7-2	Comparison of ANSYS <sup>®</sup> and Dytran <sup>®</sup> Total Vertical Reaction Forces for the Flexible Tank at the 422-Inch Waste Level Under Vertical Seismic Excitation.....	7.3
7-3	Comparison of ANSYS <sup>®</sup> and Dytran <sup>®</sup> Total Horizontal Reaction Forces for the Flexible Tank at the 460-Inch Waste Level Under Horizontal Seismic Excitation .....	7.4
7-4	Comparison of ANSYS <sup>®</sup> and Dytran <sup>®</sup> Total Vertical Reaction Forces for the Flexible Tank at the 460-Inch Waste Level Under Vertical Seismic Excitation.....	7.4
7-5	Comparison of ANSYS <sup>®</sup> and Dytran <sup>®</sup> Waste Pressures for the Flexible Tank at the 422-Inch Waste Level Under Horizontal Excitation – Waste Elements Near Tank Top and Bottom at $\theta=0$ .....	7.6
7-6	Comparison of ANSYS <sup>®</sup> and Dytran <sup>®</sup> Waste Pressures for the Flexible Tank at the 422-Inch Waste Level Under Horizontal Excitation – Waste Elements at Elevation 292 Inches Above Tank Bottom at $\theta=0$ .....	7.6
7-7	Comparison of ANSYS <sup>®</sup> and Dytran <sup>®</sup> Waste Pressures for the Flexible Tank at the 460-Inch Waste Level Under Horizontal Excitation – Waste Elements Near Tank Top and Bottom at $\theta=0$ .....	7.7
7-8	Comparison of ANSYS <sup>®</sup> and Dytran <sup>®</sup> Waste Pressures for the Flexible Tank at the 460-Inch Waste Level Under Horizontal Excitation – Waste Elements at Elevation 292 Inches Above Tank Bottom at $\theta=0$ .....	7.7
7-9	Comparison of ANSYS <sup>®</sup> and Dytran <sup>®</sup> Mid-Plane Hoop Stress at Primary Tank Wall Element Near the Waste-Free Surface for the Flexible Tank at the 422-Inch Waste Level for Horizontal Excitation and $\theta=0$ .....	7.9
7-10	Comparison of ANSYS <sup>®</sup> and Dytran <sup>®</sup> Mid-Plane Hoop Stress at an Elevation of 292 Inches from the Tank Bottom for the Flexible Tank at the 422-Inch Waste Level for Horizontal Excitation and $\theta=0$ .....	7.10
7-11	Comparison of ANSYS <sup>®</sup> and Dytran <sup>®</sup> Mid-Plane Hoop Stress at Primary Tank Wall Element Near the Tank Bottom for the Flexible Tank at the 422-Inch Waste Level for Horizontal Excitation and $\theta=0$ .....	7.10

7-12	Comparison of ANSYS® and Dytran® Mid-Plane Hoop Stress at Primary Tank Wall Element Near the Waste-Free Surface for the Flexible Tank at the 460-Inch Waste Level for Horizontal Excitation and $\theta=0$ .....	7.11
7-13	Comparison of ANSYS® and Dytran® Mid-Plane Hoop Stress at an Elevation of 292 Inches from the Tank Bottom for the Flexible Tank at the 460-Inch Waste Level for Horizontal Excitation and $\theta=0$ .....	7.11
7-14	Comparison of ANSYS® and Dytran® Mid-Plane Hoop Stress at Primary Tank Wall Element Near the Tank Bottom for the Flexible Tank at the 460-Inch Waste Level for Horizontal Excitation and $\theta=0$ .....	7.12

## Tables

1-1	Summary of Frequencies and Maximum Slosh Heights .....	1.7
1-2	Summary of Global Reaction Forces .....	1.7
3-1	Expected Hydrostatic Pressure of Waste Elements.....	3.1
3-2	Theoretical Maximum Waste Pressures for Horizontal Excitation in the Rigid Tank at 422-Inch Waste Level for Elements at $\theta=0$ Run at Absolute Pressure .....	3.6
3-3	Theoretical Maximum Waste Pressures for Horizontal Excitation in the Rigid Tank at 422-Inch Waste Level for Elements at $\theta=45^\circ$ Run at Absolute Pressure.....	3.7
3-4	Theoretical Maximum Wall Pressures for Vertical Excitation in the Rigid Tank at 422-Inch Waste Level .....	3.12
4-1	Theoretical Maximum Absolute Waste Pressures for Horizontal Excitation in the Rigid Open-Top Tank at 460-Inch Waste Level for Elements at $\theta=0$ .....	4.5
4-2	Theoretical Maximum Absolute Waste Pressures for Horizontal Excitation in the Rigid Open-Top Tank at 460-Inch Waste Level for Elements at $\theta=45^\circ$ .....	4.5
5-1	Theoretical Maximum Absolute Waste Pressures for Horizontal Excitation in the Flexible Tank at 422-Inch Waste Level for Elements at $\theta=0$ .....	5.19
5-2	Theoretical Maximum Absolute Waste Pressures for Horizontal Excitation in the Flexible Tank at 422-Inch Waste Level for Elements at $\theta=45^\circ$ .....	5.19
5-3	Theoretical Maximum Absolute Wall Pressures for Vertical Excitation at the 422-Inch Waste Level.....	5.27
6-1	Theoretical Maximum Absolute Waste Pressures for Horizontal Excitation in the Flexible Open-Top Tank at 460-Inch Waste Level for Elements at $\theta=0$ .....	6.5
6-2	Theoretical Maximum Absolute Waste Pressures for Horizontal Excitation in the Flexible Open-Top Tank at 460-Inch Waste Level for Elements at $\theta=45$ .....	6.5
6-3	Theoretical Maximum Absolute Wall Pressures for Vertical Excitation of an Open-Top Tank at the 460-Inch Waste Level .....	6.16
7-1	Comparison of ANSYS® and Dytran® Frequencies and Maximum Slosh Heights .....	7.1
7-2	Summary of Centroidal Elevations for ANSYS® and Dytran® Selected Waste Elements at $\theta=0$ .....	7.5
7-3	Summary of Centroidal Elevations for Tank Wall Elements at $\theta=0$ .....	7.8

## 1.0 Introduction

M&D Professional Services, Inc. (M&D) is under subcontract to Pacific Northwest National Laboratory (PNNL) to perform seismic analysis of the Hanford Site double-shell tanks (DSTs) in support of a project entitled *Double-Shell Tank (DST) Integrity Project – DST Thermal and Seismic Analyses*. The overall scope of the project is to complete an updated analysis of record of the DST system at Hanford. The work described herein was performed in support of the seismic analysis of the double-shell tanks. The seismic analysis of the DSTs is part of an overall project to provide an up-to-date comprehensive analysis of record for the tanks.

The overall seismic analysis of the double-shell tanks is being performed with the general-purpose finite element code ANSYS®.<sup>1</sup> The overall model used for the seismic analysis of the DSTs includes the tank structure, the contained waste, and the surrounding soil. The seismic analysis of the DSTs must address the fluid-structure interaction behavior and sloshing response of the primary tank and contained liquid. ANSYS® has demonstrated capabilities for structural analysis, but has more limited capabilities for fluid-structure interaction analysis.

The purpose of this study is to demonstrate the capabilities and investigate the limitations of Dytran® for performing a dynamic fluid-structure interaction analysis of the primary tank and contained waste. The explicit code MSC.Dytran®<sup>2</sup> was developed to analyze fluid-structure interaction problems. MSC.Dytran® resulted from a unification of Dyna-3D and the Pisces code, in which the latter was developed specifically for the analysis of fluid-structure interaction problems. The Dytran® solutions are benchmarked against theoretical solutions appearing in BNL (1995), when such theoretical solutions exist. When theoretical solutions were not available, comparisons were made to theoretical solutions to similar problems, and to the results from ANSYS® simulations.

The capabilities and limitations of ANSYS® for performing a fluid-structure interaction analysis of the primary tank and contained waste were explored in a parallel investigation and documented in a companion report (Carpenter and Abatt 2006). The results of this study will be used in conjunction with the results of the global ANSYS® analysis documented in Carpenter et al. (2006) and the parallel ANSYS® fluid-structure interaction analysis to help determine if a more refined sub-model of the primary tank is necessary to capture the important fluid-structure interaction (FSI) effects in the tank – and if so, how to best analyze a refined sub-model of the primary tank.

Both rigid tank and flexible tank configurations were analyzed with Dytran®. Numerous cases of damping or dynamic relaxation were studied to determine the best way to implement damping in Dytran® for the flexible tank problems. The options available are to introduce dynamic relaxation solely as a means to obtain a stable solution to the initial gravity loading, and then remove it from the problem and run seismic loading without damping, or to keep the dynamic relaxation parameter constant throughout the problem. The first method is probably the more typical use of dynamic relaxation in Dytran®. The second method requires calibrating the dynamic relaxation coefficient by iteration and comparison to known solutions.

---

<sup>1</sup> ANSYS® is a registered trademark of ANSYS, Inc., Canonsburg, Pennsylvania.

<sup>2</sup> MSC.Dytran® is a registered trademark of MSC.Software Corporation, Santa Ana, California.

The response parameters of interest that are evaluated in this study are the total hydrodynamic reaction forces, the impulsive and convective mode frequencies, the waste pressures, and the slosh heights. To a limited extent, primary tank stresses are also reported.

## 1.1 Discussion

The earlier Dytran<sup>®</sup> runs performed were run at gage rather than absolute pressure for the simple reason that stable solutions were easier to obtain using gage pressure. However, it was recognized from the beginning of the study that it would be preferable to perform the analyses at absolute pressure. Running at absolute pressure eliminates any potential problems that can arise when dynamic pressures exceed static pressures, and total pressures become negative, at least in theory.

Eventually, stable solutions were achieved in most instances running at absolute pressure, and the focus of the discussion and results in the body of the report will be on the absolute pressure results. In a few places, results of gage pressure runs are shown alongside results from absolute pressure runs to illustrate some differences in the solutions.

Hand in hand with the discussion of running the problem at absolute or gage pressure is the subject of how to best implement damping into the solution to achieve the desired effective damping. It turned out that solution stability depended both on whether the problem was run at absolute or gage pressure, and, in the case of flexible wall tanks, how damping was introduced into the problem. Typically, damping is introduced into a Dytran<sup>®</sup> analysis through the use of dynamic relaxation parameters that are intended to aid in finding the steady-state part of a dynamic solution to a transient loading. The dynamic relaxation factors available in Dytran<sup>®</sup> are introduced directly into the central difference integration scheme of the equations of motion. The tie to overall system damping is loose, especially for complex systems. Thus, using dynamic relaxation to produce a target effective damping in a complex system becomes a matter of trial and error. For these reasons, dynamic relaxation is normally introduced to achieve a steady-state response to a transient loading (e.g., gravity), and then is removed for the remainder of the problem. It is not typically used to achieve a desired effective damping in a complex system such as a double-shell tank.

Several implementations of damping or dynamic relaxation were investigated. The first attempt at utilizing dynamic relaxation was made by introducing a constant dynamic relaxation value throughout the complete analysis based on a guideline given in the Dytran Theory Manual (MSC 2005a). This resulted in the system being significantly under-damped to the point that it was difficult to achieve a steady-state solution to gravity loading.

The second attempt (referred to as Case 3 later in this report) was the more traditional approach of introducing a much larger dynamic relaxation factor during the initial gravity loading, and then removing the damping for the remainder of the problem that consisted of the seismic transient and an ensuing free-vibration phase. This approach resulted in good agreement with the theoretical value of the total horizontal hydrodynamic reaction force when the problem was run at gage pressure, but had the deficiency that a stable solution was not achieved when the problem was run at absolute pressure.

The final approach was to use a constant dynamic relaxation factor throughout the whole problem and to calibrate the value based on trial and error. The value that was finally selected was much larger than that suggested in the Dytran Theory Manual (MSC 2005a), but somewhat less than was used in the more

traditional approach. This approach had the desired outcome that it produced stable solutions at absolute pressure and gave good agreement with theoretical solutions.

The four tank configurations investigated were a rigid tank with a waste level of 422 inches, a rigid tank with a waste level of 460 inches, a flexible wall tank with a waste level of 422 inches, and a flexible wall tank with a waste level of 460 inches. The 422-inch waste level is intended to represent a baseline waste level for the Hanford DSTs, while the 460-inch waste level represents a higher level being proposed to increase the capacity of the Hanford AP DSTs. Each of the four configurations was subjected to horizontal and vertical seismic excitation as separate cases.

For the rigid tank configurations, dynamic relaxation was not necessary, but the bulk viscosities were assigned non-default values to help achieve stable solutions. The response parameters investigated for the rigid tanks were the total hydrodynamic force components, the convective frequency, the waste pressures, and the slosh height. The analyses of the flexible wall tanks used the dynamic relaxation schemes described above, and the response parameters were those for the rigid tanks, plus impulsive frequencies and element stresses.

The solution for the rigid tank at the 422-inch level was compared to the theoretical solution for an open-top rigid tank with a hinged-top boundary condition (although the boundary condition is irrelevant for a rigid tank). The peak hydrodynamic forces and the convective frequency closely matched theoretical predictions, although the convective component of the horizontal hydrodynamic force was somewhat lower than expected. The waste pressures and pressure distributions also matched well to theoretical values, except for a few isolated peaks in the pressure time histories. Such isolated peaks were present to some degree in all of the simulations and will be discussed further below. The maximum slosh height was 7% greater than predicted by theory.

Theoretical solutions are not available at the 460-inch waste level because of the interaction between the waste and the dome curvature. However, comparisons were made to the corresponding solution for a tank at the 460-inch waste level with vertical walls, open top, and a hinged-top boundary condition.

The simulation for the rigid tank at the 460-inch waste level showed that the total peak horizontal reaction force agreed with that predicted by the theoretical solution for an open-top tank with a 460-inch waste level, and the total peak vertical reaction force was slightly higher than predicted by the open-top theoretical solution. The convective component of the horizontal reaction force was low, indicating that the presence of the dome acts to inhibit the convective response. The fundamental convective frequency matches that for the open-top tank, but the reaction time history for the convective response shows some high-frequency content that was not present at the 422-inch waste level.

The waste pressures are generally as predicted for the open-top tank, but isolated peaks exist in the pressure time histories, especially for elements near the elevation of the waste-free surface. More such isolated pressure peaks were evident in the simulation at the 460-inch waste level than at the 422-inch waste level. The maximum slosh height was 86% of that predicted for the open-top tank.

The total horizontal reaction force for the flexible wall tank at the 422-inch waste level was 96% of the theoretical value, while the total vertical reaction force was 20% greater than predicted by theory. The

response showed a breathing mode<sup>1</sup> frequency of 6 Hz and an impulsive mode frequency of slightly less than 7 Hz – both in good agreement with theoretical predictions. The fundamental convective frequency was 0.19 Hz, also in agreement with theory. Based on the decay of the total horizontal reaction force during the final free-vibration phase, the effective damping associated with the convective response is approximately 1% of critical damping.

The waste pressures due to horizontal excitation show generally good agreement with theory, but as with the other solutions, isolated peaks that are not predicted by theory exist in the pressure time histories. The peaks are more prevalent in elements closer to the waste surface. The pressures associated with vertical excitation of the tank also show general agreement with theory and contain a few isolated peak pressures. Both the pressure and hoop stress time histories show a gradual drift down over time toward the end of solution. The maximum slosh height of 24.5 inches calculated by Dytran<sup>®</sup> is 3% greater than the theoretical value.

The Dytran<sup>®</sup> analysis of the flexible wall tank at the 460-inch waste level showed that the total horizontal reaction force was as predicted by the open-top theory, and the total vertical reaction force was 6% greater than the theoretical value. *That is, according to the Dytran<sup>®</sup> model, the peak horizontal hydrodynamic force is essentially the same as predicted for the open-top tank, and any interaction of the fluid with the dome has not significantly changed the peak force from that predicted for an open-top tank.* The breathing mode frequency was 5.5 Hz, and the impulsive frequency was 6.5 Hz, both in agreement with open-top theory, and both approximately ½ Hz less than for the 422-inch waste level. The fundamental convective frequency is 0.2 Hz, as expected from the theory.

As was the case for the rigid tank at the 460-inch waste level, the convective component of the total horizontal reaction force is less than predicted for an open-top tank, and less than was observed for the flexible tank at the 422-inch waste level. Once again, it appears that the dome curvature inhibits the convective response.

The waste pressure responses for horizontal and vertical seismic input both showed isolated peaks that were similar to those seen for the rigid tank at the 460-inch waste level. In the case of vertical input, both pressures and hoop stresses showed a slight downward drift over time. The tank wall hoop stresses from horizontal seismic input are as expected and generally do not reflect the isolated spikes in waste pressures. Hoop stresses in tank wall elements near the free surface that are caused by vertical excitation appear to be only loosely correlated to the waste pressures of adjacent waste elements. The hoop stresses show a few isolated spikes, but the spikes do not appear well correlated with the more frequent spikes in the waste pressures. The maximum slosh height was 20 inches or 82% of the value predicted for an open-top tank.

The interpretation of isolated peaks in the waste pressure time histories that occurred in all four analysis configurations warrants discussion. The fundamental issue is whether the peaks are physically real or whether they are numerical noise in the Dytran<sup>®</sup> solution. To some degree, the question is irrelevant, or at least ill-posed, since ultimately the interest is in performing a stress analysis on the primary tank, and the behavior of the stress time histories is not the same as the pressure time histories. It appears that the primary tank structure acts to filter out at least some of the localized high (and low) waste pressures.

---

<sup>1</sup> The breathing mode is the axisymmetric vibratory mode associated with volumetric expansion and contraction of the cylinder. It is the fundamental mode for the transient response of the model to gravity loading.

However, although the waste pressure time histories are of less importance than the stress time histories for the structural assessment of the primary tank, it is still informative to look closely at the waste pressure behavior. The positive and negative spikes in the waste pressure time histories occurred in all four analyses and for both horizontal and vertical excitation. The spikes occurred at both the top and bottom of the waste, and occurred during the seismic excitation, and afterwards during the unforced vibration phase when the seismic excitation was not present. The spikes were more prevalent at the higher waste level, but still occurred at the lower waste level.

The frequency of output for the pressure time histories was 10 ms – the same as the frequency of the seismic input. The isolated peaks typically occurred at one output point at a time meaning that the duration of a peak on the pressure time history output files was 20 ms. There is some evidence to suggest that the pressure spikes are real and are due to impact pressures generated by waves impacting the boundary of the structure. Such phenomena were observed in experiments reported by Kurihara et al. (1994) for liquid sloshing in flat-top tanks. The fact that the pressure spikes occur more frequently at the higher liquid level where interaction with the dome curvature is important is consistent with the observations for the flat-top tanks.

On the other hand, the manifestation of the spikes in the pressure time histories also showed behavior that suggests that the spikes may be numerical in origin. For instance, some spikes occur in waste elements near the bottom of the tank and some spikes occurred during the second free-vibration phase of the analysis after the seismic input was terminated. These observations make it seem less plausible that the pressure spikes are real. Moreover, if the highest isolated peak pressures are disregarded, the agreement between the computer simulations and the theoretical solutions (for exact solutions at the 422-inch waste level) improves markedly. Indeed, it is likely that excellent agreement between the simulations and theory would result either by filtering the pressure time histories via post-processing, or rerunning the simulations using the technique of bulk scaling in which the bulk modulus of the liquid is reduced, thereby providing a natural filtering mechanism for the high-frequency pressure response.

Although it is not clear whether the pressure spikes are physical or numerical in origin, the most important aspect of the response is the stress in the primary tank. As noted above, most of the high-frequency peaks in the pressures do not show up in the stress response. In a few instances, similar peaks do show up in the stress time histories, but the stress magnitudes are low enough to not cause concern.

Further investigation of the phenomenon could include rerunning the simulations and requesting the pressure time histories at a higher frequency to better characterize the nature of the response, and to run a simulation of a tank with vertical walls and no fluid-structure interaction with the dome. The analyses at the 422-inch liquid level nearly satisfy this condition, but not exactly, since the free surface of the waste will have very mild interaction with the dome. If high-frequency pressure spikes still showed up in this situation, it is more likely that the peaks are numerical in origin.

Some unexpected behavior was noted in the slosh height time histories at the 460-inch waste level. Specifically, maximum waste-free surface heights of nearly 10 inches were recorded during the initial gravity loading of the structure before seismic excitation commenced. Investigation of the deformed shape of the waste showed that the initial change in the waste-free surface height under gravity loading was due to an axisymmetric increase in the waste-free surface near the tank boundary that had the appearance of a meniscus. This effect was attributed to either a limitation of the post-processing routine

used to calculate the maximum waste-free surface height, or else a limitation caused by lack of sufficient resolution in the model discretization. Nonetheless, the maximum slosh heights recorded for these analyses did appear reasonable relative to theoretical predictions.

Section 7.0 of this report contains direct comparisons between the results from the flexible tank ANSYS® models reported in Carpenter and Abatt (2006) and the flexible tank Dytran® models described in this report. Both codes predict frequencies that agree well with theoretical values, although the Dytran® predictions are generally closer to expected values than the ANSYS® predictions. Comparison of the reaction forces from the ANSYS® and Dytran® models showed that the responses from the models are similar with ANSYS® generally being conservative relative to Dytran®, and both codes generally showing good agreement with theoretical predictions. At the 422-inch waste level, the ANSYS® reaction forces were slightly greater than the reaction force predicted by Dytran® for both horizontal and vertical seismic input. At the 460-inch waste level, the horizontal reaction force predicted by ANSYS® is the same as predicted by theory and essentially the same as predicted by Dytran®. In the case of the vertical reaction forces, somewhat higher peaks are predicted by Dytran® than ANSYS®. In particular, since the loads into the j-bolts connecting the primary tank to the concrete dome are driven by the overall forces on the primary tank, it appears that a global ANSYS® model is sufficient for analysis of the j-bolts, and that any sub-model of the primary tank need not contain the j-bolts.

Comparison of a limited set of waste pressures due to horizontal excitation from ANSYS® and Dytran® showed that at the 422-inch waste level, the waste pressures were very similar near the bottom of the tank. In the middle and upper portions of the waste, the ANSYS® solution showed more of a convective response than the Dytran® solution. At the 460-inch waste level, the peak pressures near the bottom of the waste are higher in Dytran® than in ANSYS®. Near the top of the waste, the responses are similar, with ANSYS® predicting somewhat higher pressures. The appearance of a convective response in ANSYS® is less evident at the higher waste level. At an elevation of 292 inches up from the tank bottom, the pressure predictions are very similar, with the ANSYS® response being slightly higher.

Finally, comparisons were made between membrane hoop stress predictions for the models. It is difficult to draw conclusions from these comparisons because of differences in modeling techniques, mesh resolution in the tank wall, mesh resolution near the tank knuckle, and differences in the elevation of the tank wall element centroids. The two models do give very similar results for membrane hoop stress at the middle elevation of 292 inches up from the tank bottom, with the ANSYS® results being slightly higher than the Dytran® results. A couple of interesting observations on the hoop stresses are that whereas the convective response was more apparent in the waste pressures predicted by ANSYS® near the free surface at the 422-inch waste level, this response is more apparent in the Dytran® hoop stress predictions at that elevation. Also, the convective response that was observed from ANSYS® in the waste pressure time history at 292 inches above the tank bottom at the 422-inch waste level is not readily apparent in the hoop stress time history.

## 1.2 Summary

The purpose of this study was to demonstrate the capabilities and to investigate the limitations of Dytran® for performing an FSI analysis of the primary tank and contained waste. The results of this study were used in conjunction with the results of the global ANSYS® analysis (Carpenter et al. 2006) and the

parallel ANSYS® FSI analysis (Carpenter and Abatt 2006) to help determine if a more refined sub-model of the primary tank is necessary to capture the important FSI effects in the tank – and if so, how to best utilize a refined sub-model of the primary tank.

The results of this study demonstrate that Dytran® has the capability to perform FSI analysis of a primary tank subjected to seismic loading. With the exception of some isolated peak pressures, and to a lesser extent peak stresses, the results agreed very well with theoretical solutions as shown in Table 1-1 and Table 1-2.

**Table 1-1. Summary of Frequencies and Maximum Slosh Heights**

Configuration	First Convective Mode Frequency (Hz)		Impulsive Mode Frequency (Hz)		Breathing Mode Frequency (Hz)		Maximum Slosh Height (in.)	
	Theory	Dytran®	Theory	Dytran®	Theory	Dytran®	Theory	Dytran®
Rigid 422	0.19	0.19	Rigid	Rigid	Rigid	Rigid	23.7	25.4
Rigid 460 <sup>(a)</sup>	0.2	0.2	Rigid	Rigid	Rigid	Rigid	24.5	21.1
Flexible 422	0.19	0.19	7.0	6.85	6.1	6.0	23.7	24.5
Flexible 460 <sup>(a)</sup>	0.2	0.2	6.5	6.4	5.5	5.5	24.5	20.1

(a) Theoretical solutions for the 460-in. waste level are based on an open tank with vertical walls and a hinged-top boundary condition.

**Table 1-2. Summary of Global Reaction Forces**

Configuration	Peak Horizontal Reaction Force (lbf)		Peak Vertical Reaction Force (lbf)	
	Theory	Dytran®	Theory <sup>(a)</sup>	Dytran® <sup>(a)</sup>
Rigid 422	2.42x10 <sup>6</sup>	2.45x10 <sup>6</sup>	1.96x10 <sup>6</sup>	2.15x10 <sup>6</sup>
Rigid 460 <sup>(b)</sup>	3.0x10 <sup>6</sup>	3.02x10 <sup>6</sup>	2.3x10 <sup>6</sup>	3.1x10 <sup>6</sup>
Flexible 422	7.56x10 <sup>6</sup>	7.25x10 <sup>6</sup>	5.24x10 <sup>6</sup>	6.3x10 <sup>6</sup>
Flexible 460 <sup>(b)</sup>	1.03x10 <sup>7</sup>	1.02x10 <sup>7</sup>	4.54x10 <sup>6</sup>	5.98x10 <sup>6</sup>

(a) Values shown are the dynamic components of the vertical reaction forces exclusive of the waste weight.  
(b) Theoretical solutions for the 460-in. waste level are based on an open tank with vertical walls and a hinged-top boundary condition.

The results of the ANSYS® FSI benchmark analysis documented in Carpenter and Abatt (2006) showed that the ANSYS® model was suitable for predicting the global response of the tank and contained waste and was capable of adequately predicting waste pressures in a large portion of the waste. However, the ANSYS® model did not accurately capture the waste pressures near the free surface due to the convective response, nor did the model give accurate predictions of maximum slosh heights.

While Dytran® appears to have stronger capabilities for the analysis of the FSI behavior in the primary tank, it is more practical to use ANSYS® for the global evaluation of the tank. Thus, Dytran® served the

purpose of helping to identify limitations in the ANSYS® FSI analysis so that those limitations can be addressed in the structural evaluation of the primary tank.

Due to the limitations identified in the ANSYS® model for predicting the convective response of the waste, the evaluation of primary tank stresses near the waste-free surface should be supplemented by results from an ANSYS® sub-model of the primary tank that incorporates pressures from theoretical solutions or from Dytran® solutions. However, the primary tank is expected to have low demand-to-capacity ratios in the upper wall.

### 1.3 Conclusions

1. The results of the Dytran® analyses of the rigid and flexible wall tanks at the 422-inch waste level generally agree well with known theoretical solutions.
2. Although theoretical solutions for a domed tank with the static liquid level near the dome as in the 460-inch waste level simulation do not exist, the results of Dytran® analyses of the rigid and flexible wall tanks at the 460-inch waste level appear reasonable and show many similarities to solutions for an open-top tank with a hinged-top boundary condition.
3. The peak horizontal reaction force for the both the rigid and flexible tanks at the 460-inch waste level under horizontal seismic excitation agree with the theoretical predictions for the corresponding open-top tanks. *That is, any interaction of the fluid with the dome during the simulations at the 460-inch waste level has not significantly changed the peak force from that theoretically predicted for the corresponding open-top tanks.*
4. Dytran® appears capable of providing a realistic FSI analysis of a primary tank and contained waste. However, the features and configurations of a Dytran® model should be compatible with the strengths of the program.
5. All solutions showed instances of isolated high-frequency spikes in the pressure time histories that deviate from theoretical solutions.
6. Such high-frequency pressure spikes typically did not show up as stress spikes in the primary tank since the tank structure evidently acts as a natural mechanical filter. In the few instances where higher spikes appeared in stress time histories, the magnitudes of the stresses were low enough to not cause concern.
7. It is preferable to analyze the problem at absolute rather than gage pressure, but it was more difficult to get stable solutions using absolute pressure.
8. The implementation of dynamic relaxation or damping can have a significant affect on solution stability and solution accuracy.
9. Once the dynamic relaxation parameter was properly calibrated, a single value worked well for all cases. That is, a single value appeared to work well for both waste heights, for horizontal and vertical excitation, and for predicting total hydrodynamic reaction forces, pressures, and slosh heights.

10. Although the damping was calibrated based on response decay during an initial free oscillation phase and peak responses during forced motion, critical damping values for the convective response in a final free oscillation phase were in the range of 1% or less.
11. The convective component of the total reaction force is small relative to the total reaction force. That is, the total reaction force is dominated by the impulsive response.
12. The Dytran<sup>®</sup> model has better capabilities than the ANSYS<sup>®</sup> model for predicting slosh heights and for predicting waste pressures and tank stresses near the free surface of the waste.
13. Based on good agreement between ANSYS<sup>®</sup>, Dytran<sup>®</sup>, and theoretical solutions for reaction forces, a global ANSYS<sup>®</sup> model is sufficient for analysis of the j-bolts and any sub-model of the primary tank need not contain the j-bolts.

Intentionally left blank.

## 2.0 Model Description

A simplified model of a Hanford double-shell tank (DST) was created using the 2005 version of MSC.Patran<sup>®</sup>,<sup>1</sup> and was analyzed using the Dytran<sup>®</sup> 2006 Development Version. The verification and validation of the software on the local computer platform is documented in M&D (2005). The purpose of the analysis was to investigate the fluid-structure interaction behavior for several tank structural configurations, liquid levels, loadings, and damping implementations. Results from theoretical solutions are presented and summarized for each of the cases in the body of the report. The details of the theoretical solutions are included in Appendix B.

The two structural configurations studied include a completely rigid primary tank, and a primary tank with a rigid dome and base, but with flexible walls. All Dytran<sup>®</sup> models are full three-dimensional (3-D) representations of the tanks. Simulations were performed for both the 422- and 460-inch waste levels. Applied loads include gravity loading and seismic loading, with seismic loading applied in the horizontal and vertical directions as separate load cases.

The first configuration studied was a completely rigid tank with a waste depth of 422 inches. This case is intended to simulate the response of a rigid tank with vertical walls without significant fluid interaction with the dome. The second case was a completely rigid tank with a waste depth of 460 inches. At the 460-inch waste level, significant fluid-structure interaction occurs in the dome under seismic excitation. This configuration does not have a theoretical solution, but it is useful as a comparison to the solution for the flexible tank at the 460-inch waste level.

In the third case, the walls of the tank were flexible, and the waste depth was 422 inches. This case is intended to simulate the response of a tank with flexible vertical walls without significant fluid interaction with the dome. The fourth configuration studied was a flexible wall tank with a waste depth of 460 inches. In the case of the flexible wall models, the material properties and wall thickness were based on the AY tank configuration, though the model was simplified to have a uniform wall thickness to allow more direct comparisons with theoretical solutions. All four configurations were run for horizontal and vertical seismic excitation independently. The solutions to the first and third configurations at the 422-inch waste level were compared to theoretical solutions from BNL (1995). The results from the second and fourth configurations at the 460-inch waste depth were compared to the first and third cases as well as to theoretical solution to similar configurations, but no closed form solutions exist for the actual configurations.

The rigid tank configuration was run without damping other than the artificial viscosities inherent in the Dytran<sup>®</sup> program. The artificial viscosities implemented in Dytran<sup>®</sup> are referred to as the linear (BULKL) and quadratic (BULKQ) bulk viscosities. The bulk viscosities act to control the formation of shock waves by introducing viscosity to the bulk straining of the fluid. Trial and error showed that increased bulk viscosity coefficients relative to the default values were necessary to achieve stable solutions, at least in some cases. As a result of the trial-and-error investigation, all results reported were run with the linear and quadratic bulk viscosity parameters set to 0.2 and 1.1, respectively. The default values for the bulk viscosity coefficients are 0 for the linear coefficient and 1.0 for the quadratic coefficient.

---

<sup>1</sup> MSC.Patran<sup>®</sup> is a registered trademark of MSC.Software Corporation, Santa Ana, California.



**RPP-RPT-28963, Rev. 1**  
**M&D-2008-005-RPT-01, Rev. 1**

A notable difference between the Dytran<sup>®</sup> model and the actual tank as shown in Figure 2-2 is that the junction between the vertical wall and the tank bottom is modeled as a right angle. Consequently, the details of the tank lower knuckle region and its support by the insulating concrete have not been captured by this simplified model.

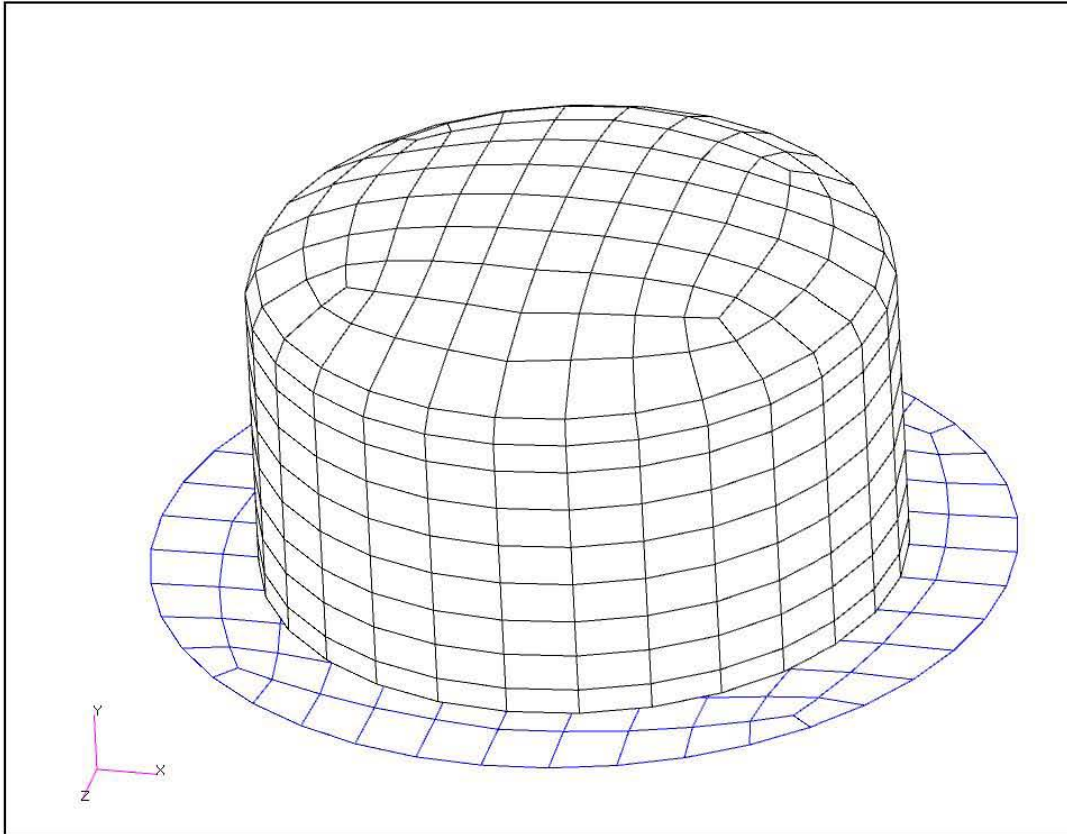


**Figure 2-2.** Plot of Primary Tank and Base

The relative height of the waste to the tank for the 422- and 460-inch waste levels is shown in Figure 2-3 and Figure 2-4, respectively. The tank floor and walls form what is known as a Dytran<sup>®</sup> coupling surface with the water. The coupling surface allows the Eulerian waste mesh to interact with the Lagrangian structural mesh, and although the Eulerian mesh extends beyond the tank boundary, all the fluid dynamics occurs inside the tank.

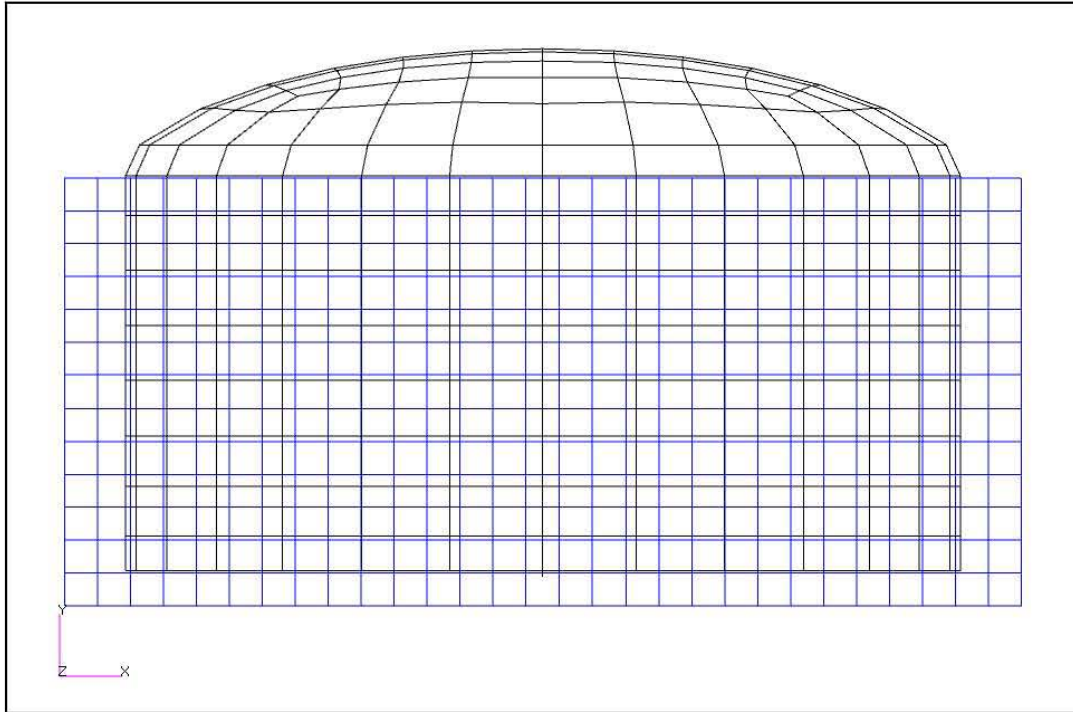


**Figure 2-3.** Plot of Tank and Waste at 422-Inch Waste Level

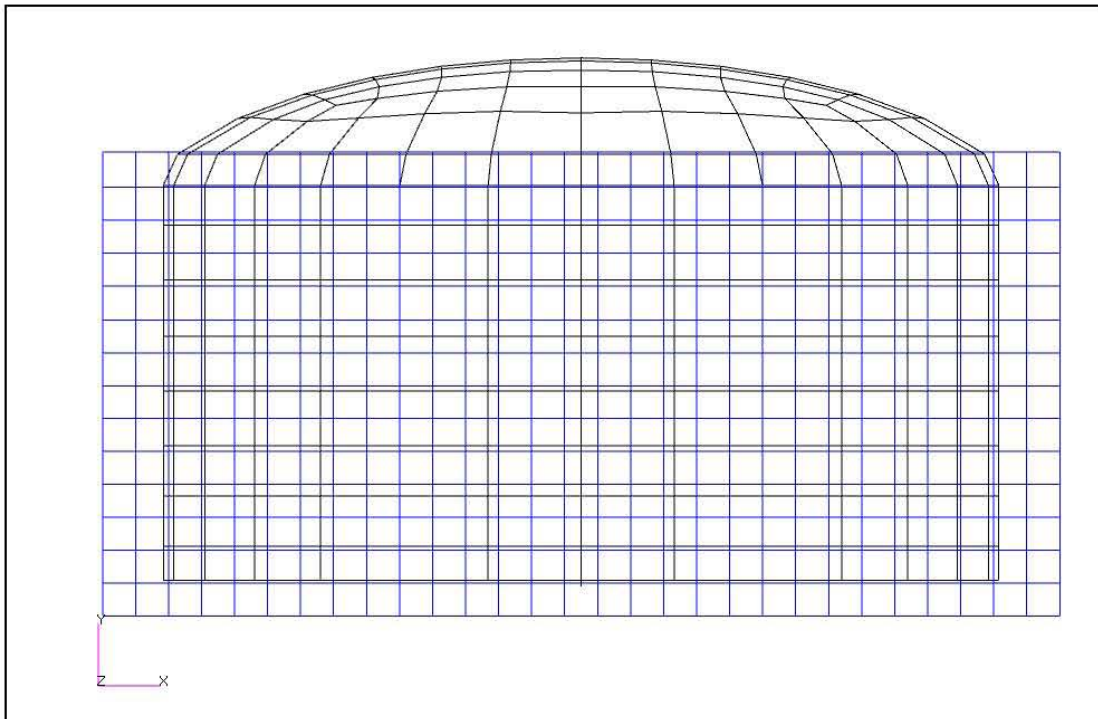


**Figure 2-4.** Plot of Tank and Waste at 460-Inch Waste Level

**RPP-RPT-28963, Rev. 1**  
**M&D-2008-005-RPT-01, Rev. 1**

Dynamic waste pressures are a function of depth, angular location, and radial location of the fluid element. Waste pressures were extracted from five sets of fluid elements throughout the tank as shown in Figure 2-5. The element set “plusx\_els” is located near the tank wall in the positive x-direction ( $\theta=0$ ) in the plane of the seismic excitation. Note that the angle  $\theta$  is measured from the positive x-axis to the positive z-axis to describe the angular position of elements in the model. Element sets “press\_45” and “plusz\_els” are located near the tank wall at 45° (approximately) and 90° from the excitation direction. Element set “minusx\_els” is near the tank wall in the negative x-direction, and the set “cent\_press” is near the center of the tank at a radial location of approximately zero. Figure 2-5 and Figure 2-7 show the waste element numbering for four element sets described above. In Figure 2-5, the center pressure elements are in the middle, the plusx\_els” are on the right, and the “minusx\_els” are on the left. In Figure 2-7, the set “press\_45” is on the right, and the “set plusz\_els” is on the left.

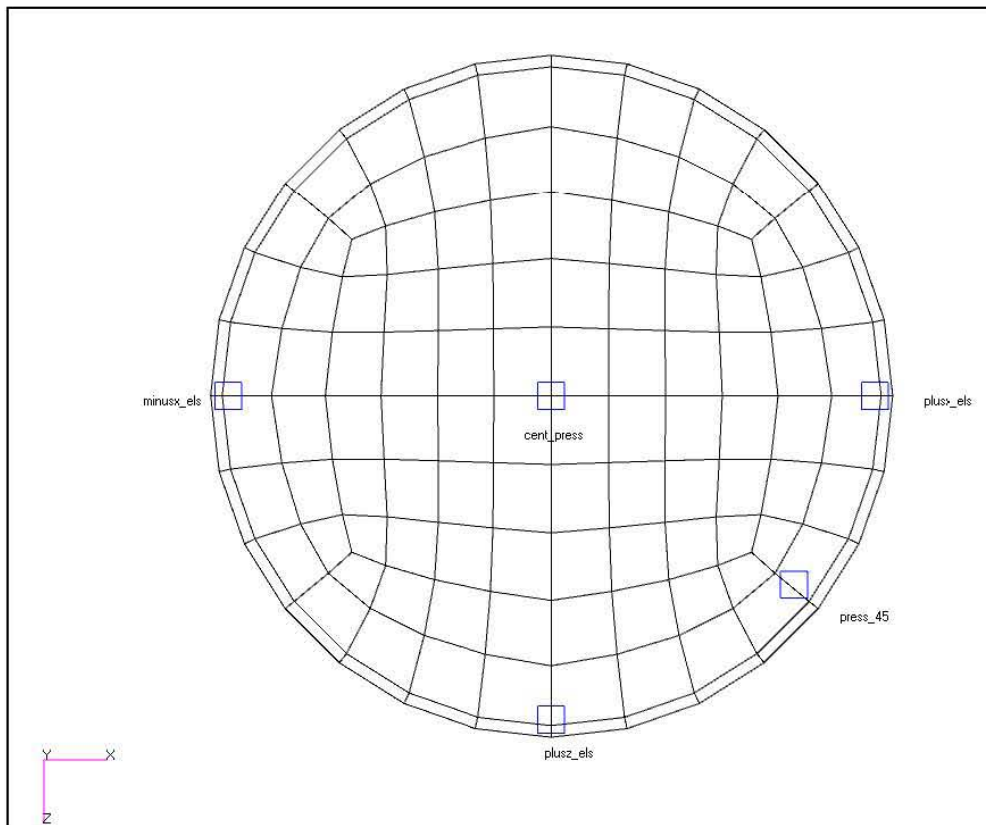


**Figure 2-5.** Top View of Model Showing the Angular Locations of Fluid Elements at Which Pressures Were Monitored

RPP-RPT-28963, Rev. 1  
M&D-2008-005-RPT-01, Rev. 1

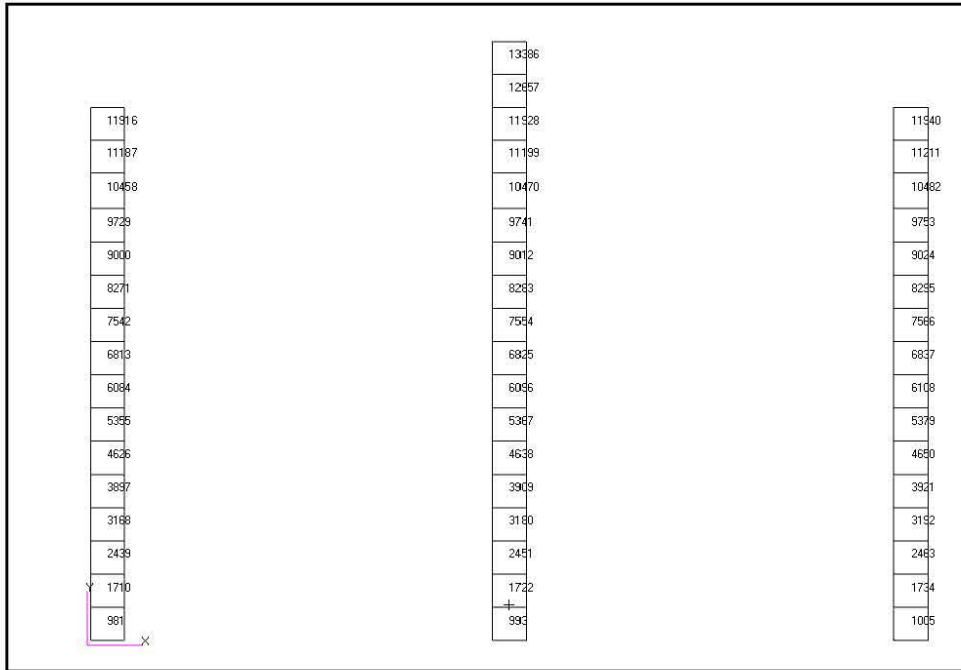


Figure 2-6. Waste Element Numbering for Element Sets “Plusx\_els”, “Minux\_els”, and “Cent\_press”

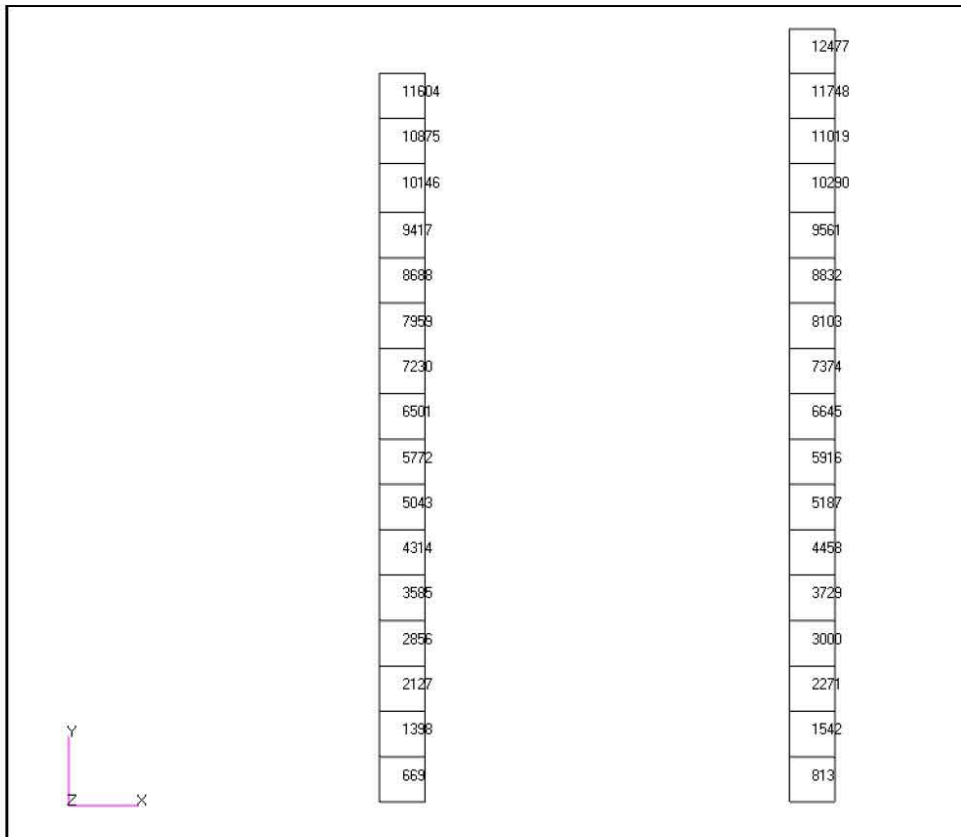
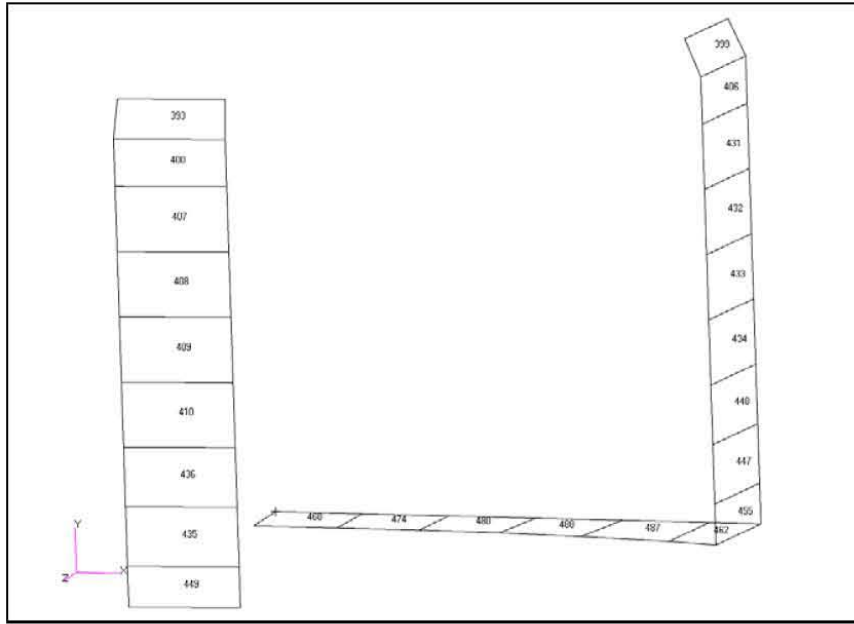


Figure 2-7. Waste Element Numbering for Element Sets “Press\_45” and “Plusz\_els”

**RPP-RPT-28963, Rev. 1**  
**M&D-2008-005-RPT-01, Rev. 1**

In the case of the flexible wall model, tank wall stresses were extracted at angular locations of  $\theta=0$ , 45, 90, and 180°. The shell element numbering for the  $\theta=0$  and  $\theta=90^\circ$  sets is shown in Figure 2-8, with the elements at  $\theta=0$  and on the right, and the elements at  $\theta=90^\circ$  on the left. The numbering for the  $\theta=45^\circ$  and  $\theta=180^\circ$  sets is shown in Figure 2-9, with the elements at  $\theta=45^\circ$  on the right and the elements at  $\theta=180^\circ$  on the left.



**Figure 2-8.** Shell Element Numbering for Tank Wall Stress Results at  $\theta=0$  and  $\theta=90^\circ$

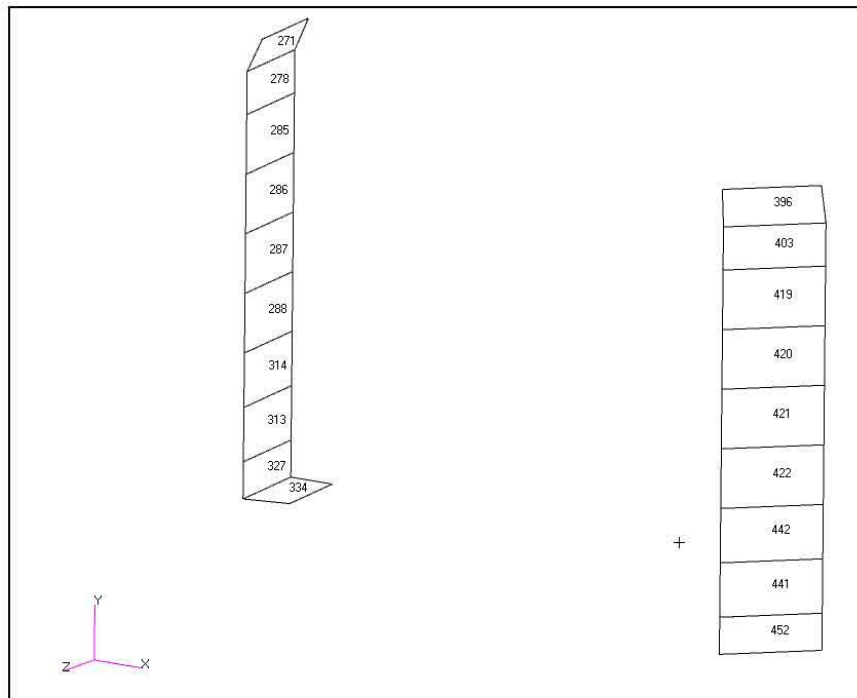


**Figure 2-9.** Shell Element Numbering for Tank Wall Stress Results at  $\theta=45^\circ$  and  $\theta=180^\circ$

## 2.2 Material Properties and Element Types

The tank was modeled in Dytran<sup>®</sup> using CQUAD4 shell elements. In the case of the rigid tank, the complete tank was modeled as a rigid body using the “MATRIG” command. The mass of the tank was much larger than the mass of the waste to faithfully reflect the applied seismic motion.

In the case of the flexible wall tank, the elastic modulus, Poisson’s ratio, and the specific weight of the steel walls were set to  $29 \times 10^6$  lbf/in<sup>2</sup>, 0.3, and 0.284 lbf/in<sup>3</sup>, respectively. The tank wall was assigned a thickness of 0.65 inch, which is the approximate average thickness of the lower two-thirds of the AY tank wall. The uniform wall thickness was introduced to simplify the benchmarking model – it is not used for any analysis of record of the primary tank.

For the flexible wall tank, the dome was kept rigid above the primary tank tangent line, and the central portion of the primary tank bottom was also kept rigid. The outer ring of elements in the primary tank bottom was flexible and was assigned normal steel properties. Both of the rigid regions were assigned artificially high mass density as in the completely rigid case. A section plot of the flexible tank configuration is presented in Figure 2-10 with the rigid elements shown in black and the deformable elements shown in blue.

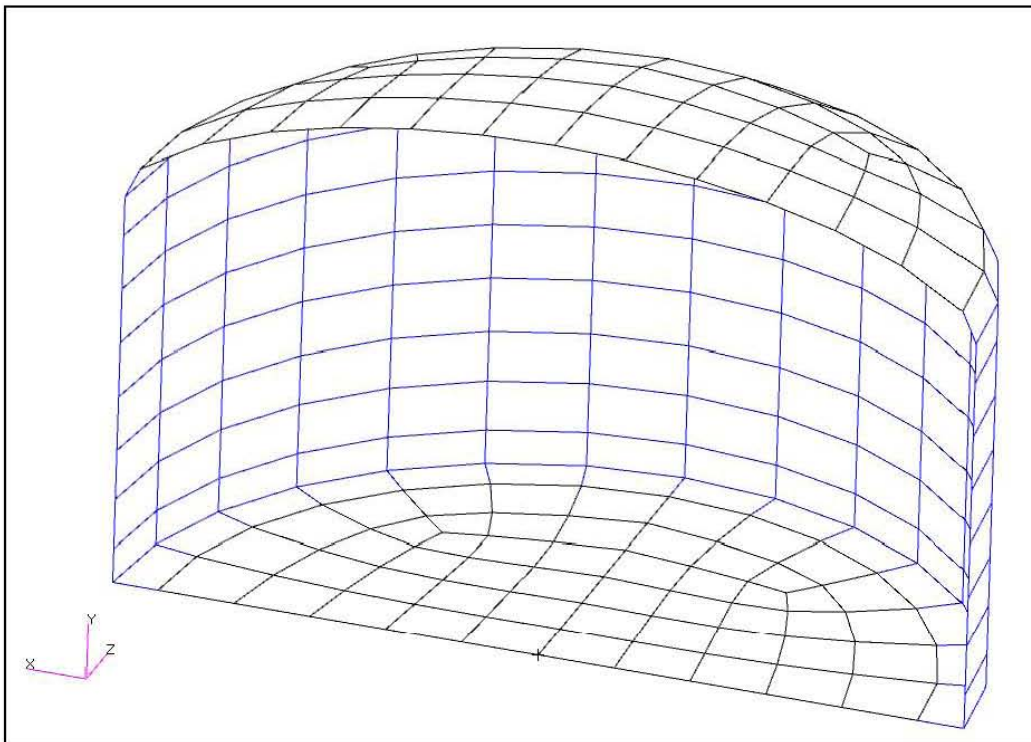


**Figure 2-10.** Section Plot of Flexible Primary Tank

The waste and air in the dome space were modeled using 8-node CHEXA Eulerian solid elements. Because two fluids are present, the Eulerian elements were assigned multi-material hydrodynamic material properties (MMHYDRO). Both the air and the waste were modeled as homogeneous, inviscid fluids.

The waste was modeled using a polynomial equation of state (EOSPOL) that requires the initial mass density and the bulk modulus of the fluid as input. The initial density of the waste was set to  $1.59 \times 10^{-4} \text{ lbf-s}^2/\text{in}^4$  (specific gravity=1.7) for the 422-inch waste level models and it was set to  $1.71 \times 10^{-4} \text{ lbf-s}^2/\text{in}^4$  (specific gravity=1.83) for the 460-inch waste level models. The bulk modulus of the waste was set to  $305,000 \text{ lbf/in}^2$ , which is a typical bulk modulus for water. The results are expected to be insensitive to the value of the bulk modulus since fluid compressibility is not critical to the response in this problem. Although the bulk modulus of water is realistic for this problem, scaling the bulk modulus down over several orders of magnitude can be an effective solution technique to reduce computer run time without unduly affecting the solution of problems where compressibility is not critical.

The air was modeled using the gamma law equation of state (EOSGAM), where the pressure is a function of the density  $\rho$ , the specific internal energy per unit mass  $e$ , and the ideal gas ratio of specific heats  $\gamma$  via  $p = (\gamma - 1)\rho e$ . The mass density of air is  $1.167 \times 10^{-7} \text{ lbf-s}^2/\text{in}^4$ , and the ratio of constant-pressure specific heat to constant-volume specific heat is 1.4. The specific internal energy per unit mass of the air was set to  $3.15 \times 10^8 \text{ in}^2/\text{s}^2$  for the absolute pressure simulations and zero for gage pressure simulations. The internal energy for the absolute pressure simulations corresponds to an air pressure of  $14.7 \text{ lbf/in}^2$ .

### 2.3 Boundary Conditions

In the case of horizontal seismic excitation, the rigid regions were free in the x-direction and fixed in the other five degrees-of-freedom. For vertical excitation, the rigid regions were free in the vertical direction and fixed in the other five degrees-of-freedom.

The Dytran<sup>®</sup> general coupling algorithm was used to allow the Eulerian waste mesh to interact with the Lagrangian structural mesh. The problem was set up to take advantage of the “fast coupling” option in Dytran<sup>®</sup>.

### 2.4 Initial Conditions

In general, it is preferable to run at absolute pressure to avoid any difficulties associated with dynamic pressures exceeding static pressures and total pressures becoming negative.

Earlier in the project, runs were performed at gage pressure simply because it was more difficult to achieve stable solutions when running at absolute pressure. For the most part, those issues were resolved, and stable solutions are now achieved using either method in most cases. For the remainder of the report, the emphasis will be on absolute pressure results.

The results from the absolute pressure runs are presented in the body of the report. Selected results are included in the body of the report that show the comparison between absolute and gage pressure results. The results from other gage pressure runs are included as background information in electronic format on the accompanying DVD; however, those results do not have a direct bearing on the analysis.

The changes required to run at absolute pressure are to set the atmospheric pressure to 14.7 lbf/in<sup>2</sup> in the parameters section of the input file, and set the specific internal energy per unit mass of the air to  $3.15 \times 10^8$  in<sup>2</sup>/s<sup>2</sup>, according to the gamma law equation of state

$$e = \frac{P}{(\gamma-1)\rho} \quad (2-1)$$

As a convenience, a balancing pressure of 14.7 lbf/in<sup>2</sup> was applied to the outside of the tank using the Dytran<sup>®</sup> COUOPT command (MSC 2005b) to keep the tank stresses in terms of gage pressures.

## 2.5 Seismic Input

The seismic time histories used to excite the tank model were output from a more complete linear ANSYS<sup>®</sup> model of the DST and surrounding soil shown in Figure 2-11, Figure 2-12, and Figure 2-13. The horizontal time history was taken from the dome apex of the ANSYS<sup>®</sup> model, and the vertical time history was taken from the haunch region 90° from the direction of horizontal excitation to minimize rocking effects. The ANSYS<sup>®</sup> model was subjected to simultaneous horizontal and vertical seismic excitation in the absence of gravity. The seismic input for the ANSYS<sup>®</sup> model was applied at the base of the far-field soil shown in Figure 2-13. The extracted time histories consisted of 2,048 points defined at 0.01-second intervals giving seismic records with durations of 20.48 seconds.

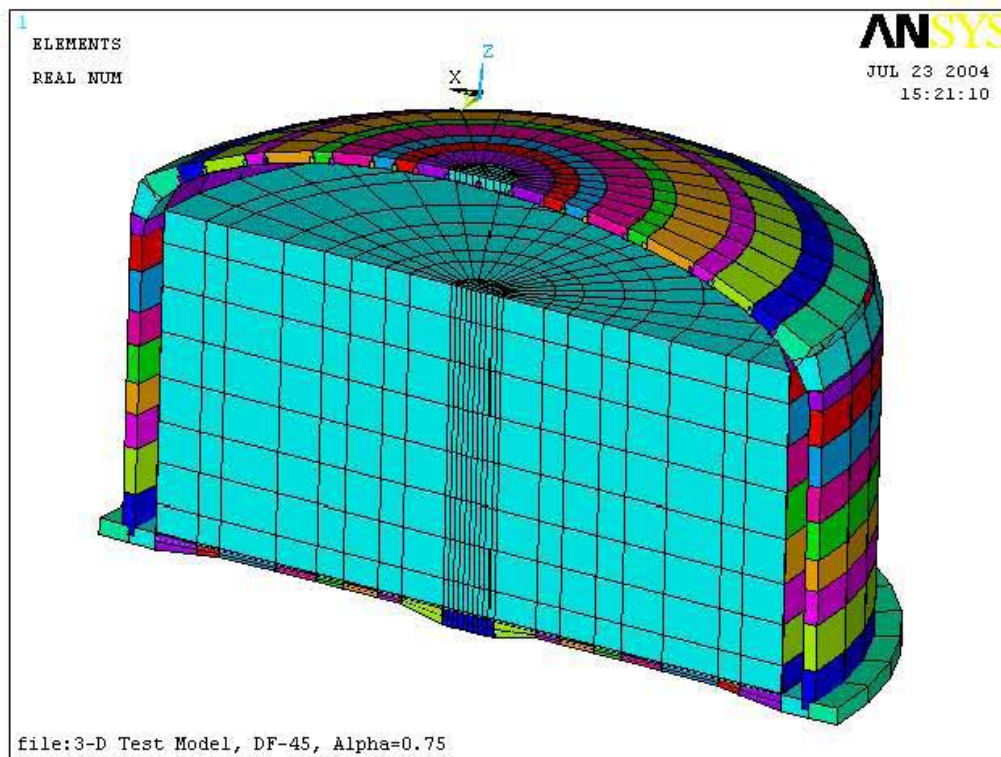


Figure 2-11. ANSYS<sup>®</sup> Composite Tank Model Detail

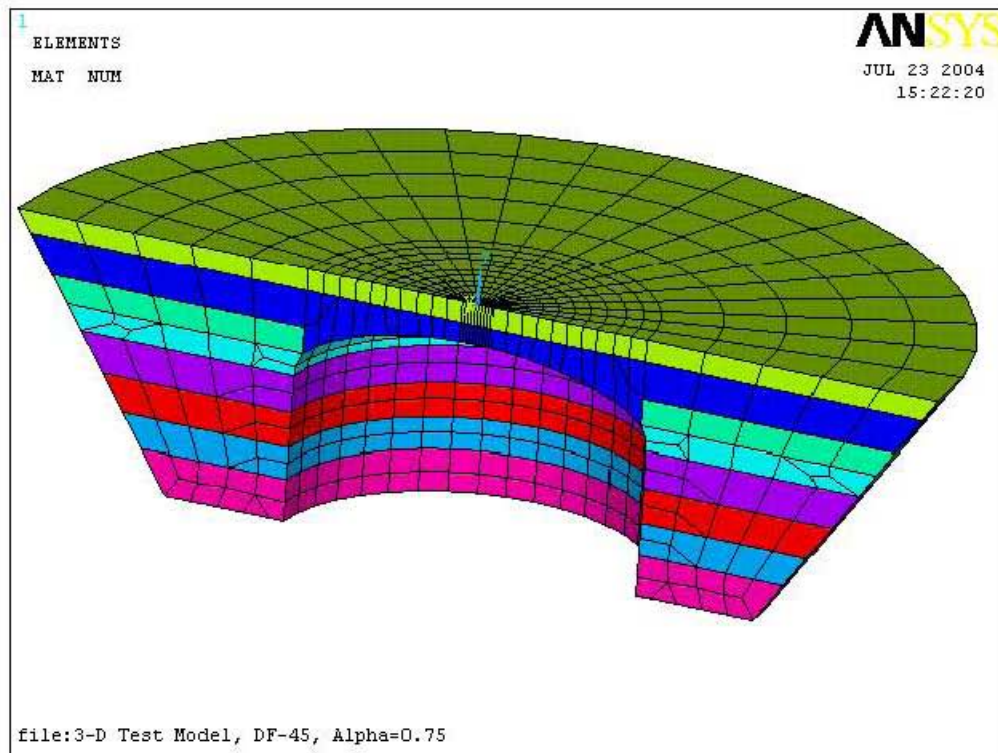


Figure 2-12. Excavated Soil Model Detail for Global ANSYS® Model

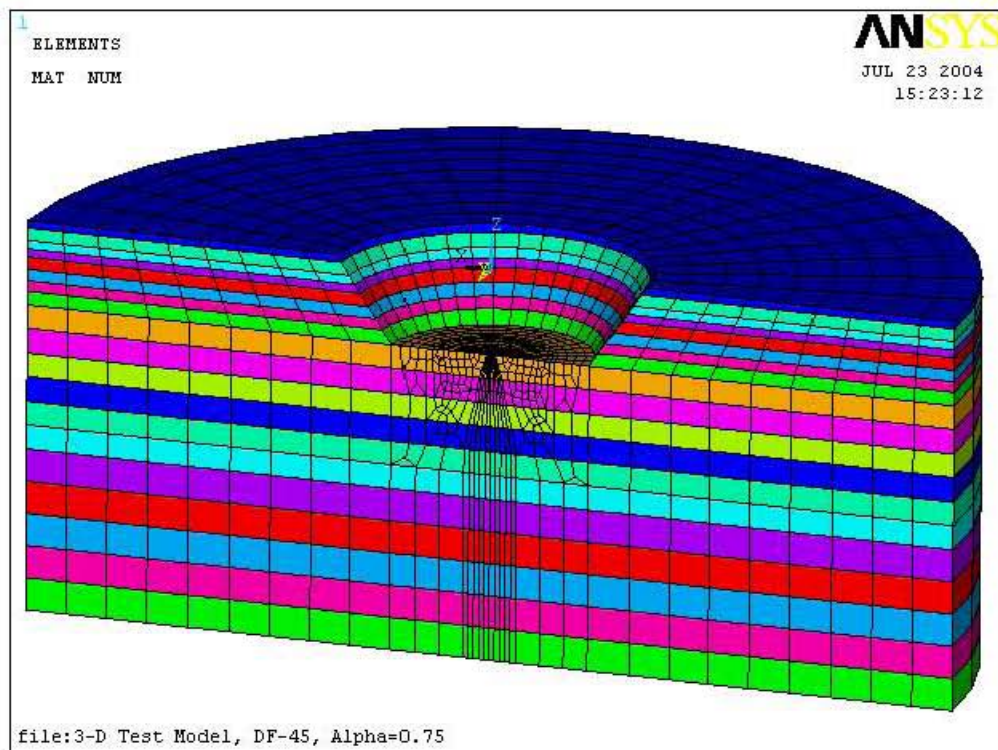


Figure 2-13. Far-Field Soil Model Detail for Global ANSYS® Model

For the completely rigid tank, the whole tank was subjected to the seismic motion. In the flexible tank configuration, the rigid dome and rigid central portion of the tank bottom were subjected to the same input simultaneously. This represents the hinged-top boundary condition discussed in BNL (1995) and shown in Figure 2-14.

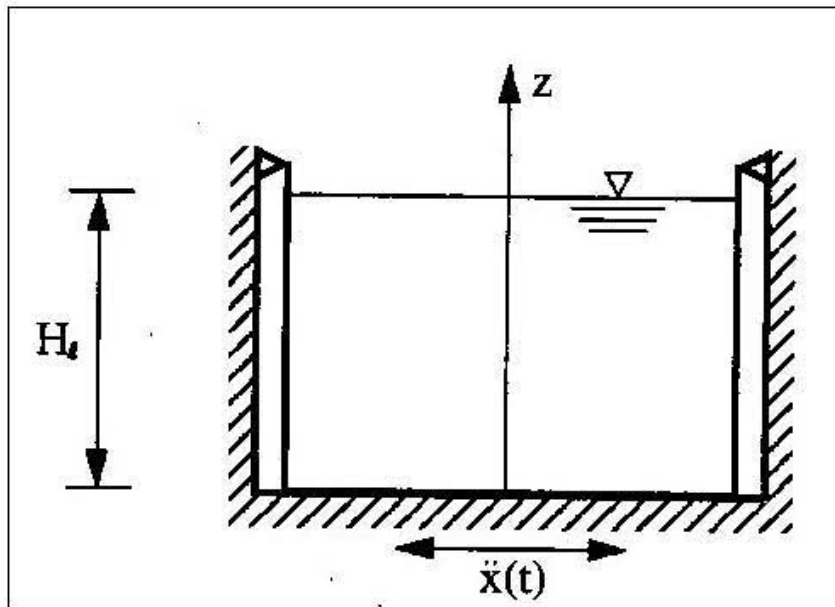


Figure 2-14. Tank with Hinged-Top Boundary Condition per BNL (1995)

In the case of horizontal ( $x$ -direction) excitation, the seismic time histories were applied to both the rigid and flexible tank Dytran<sup>®</sup> models as body force accelerations per unit mass on the nodes of the rigid portions of the tank that have artificially high mass. The vertical seismic time history was applied as a velocity time history to the rigid portions of the tank. The reason that the vertical input was applied as a velocity rather than an acceleration time history is that this approach prevents having to exactly balance the vertical gravity load with the vertical acceleration time history, thus preventing any vertical drift.

The horizontal acceleration, vertical acceleration, and the velocity and displacement time histories for horizontal and vertical input are shown in Figure 2-15, Figure 2-16, Figure 2-17, and Figure 2-18, respectively. The 4% damped response spectra for the horizontal and vertical time histories are shown in Figure 2-19. A comparison of horizontal response spectra at damping values of 0.5% and 4% is shown in Figure 2-20 and Figure 2-21, respectively. The plots in Figure 2-21 show that the spectral acceleration near the first convective frequency of approximately 0.2 Hz is 20% greater at 0.5% damping than at 4% damping. That is, in this range of damping values, the convective response is not highly sensitive to damping. The spectra for 0.5% and 4% critical damping are of particular interest because these are the target effective damping for the convective and impulsive response of the tank and waste according to DOE-STD-1020-2002.

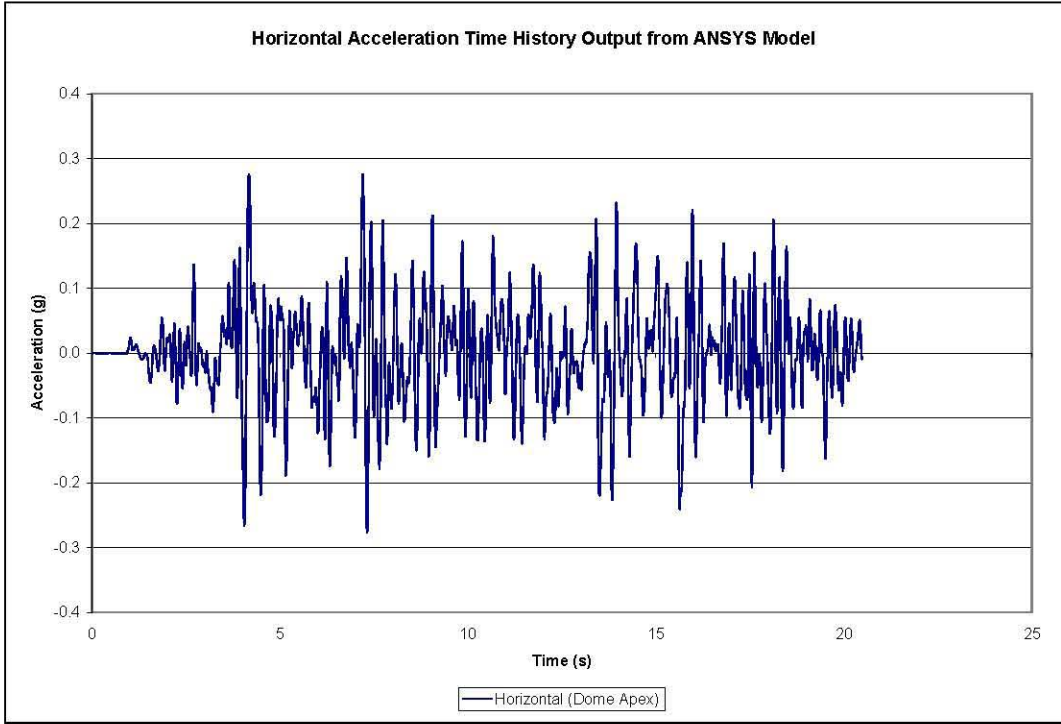


Figure 2-15. Horizontal Acceleration Time History Output from ANSYS® Model

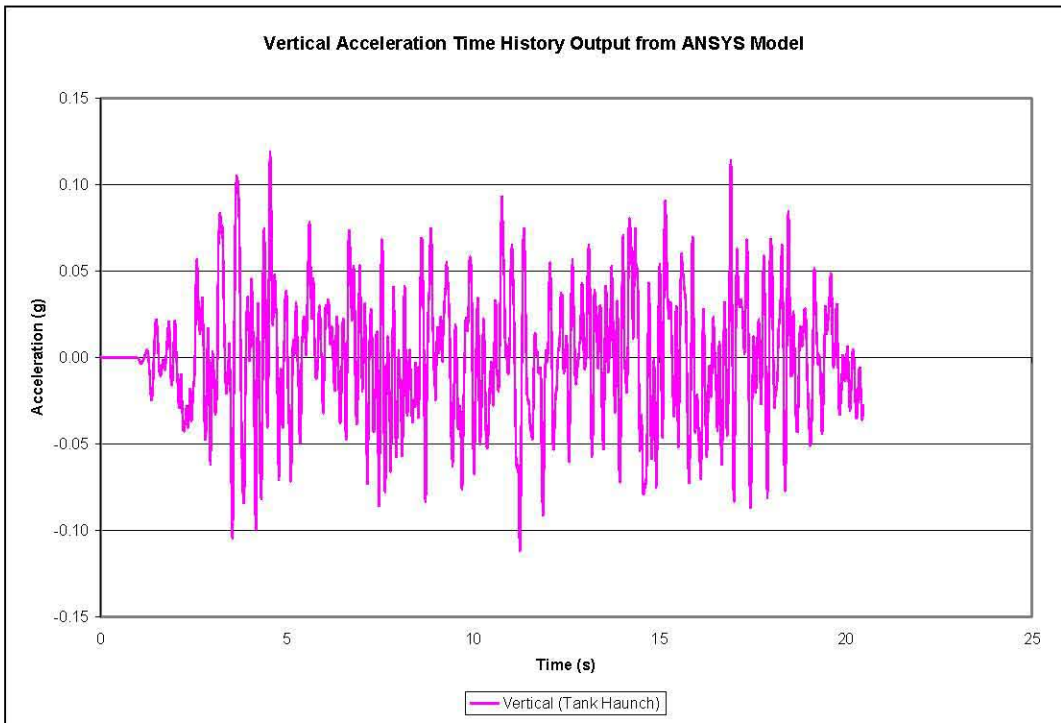


Figure 2-16. Vertical Acceleration Time History Output from ANSYS® Model

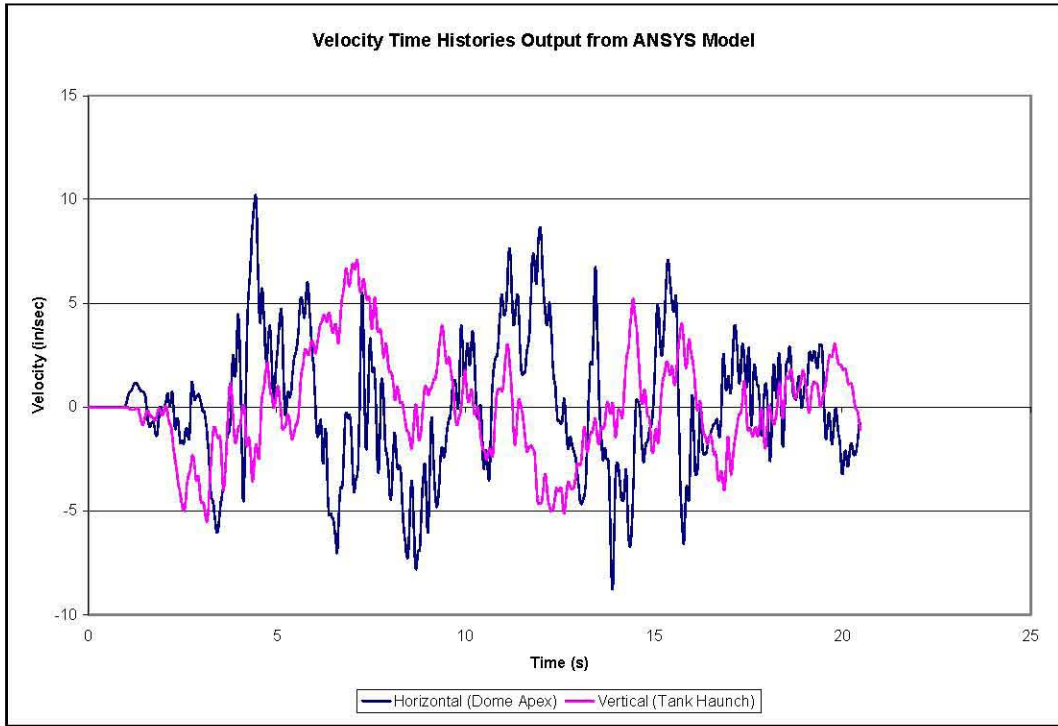


Figure 2-17. Velocity Time Histories Output from ANSYS® Model

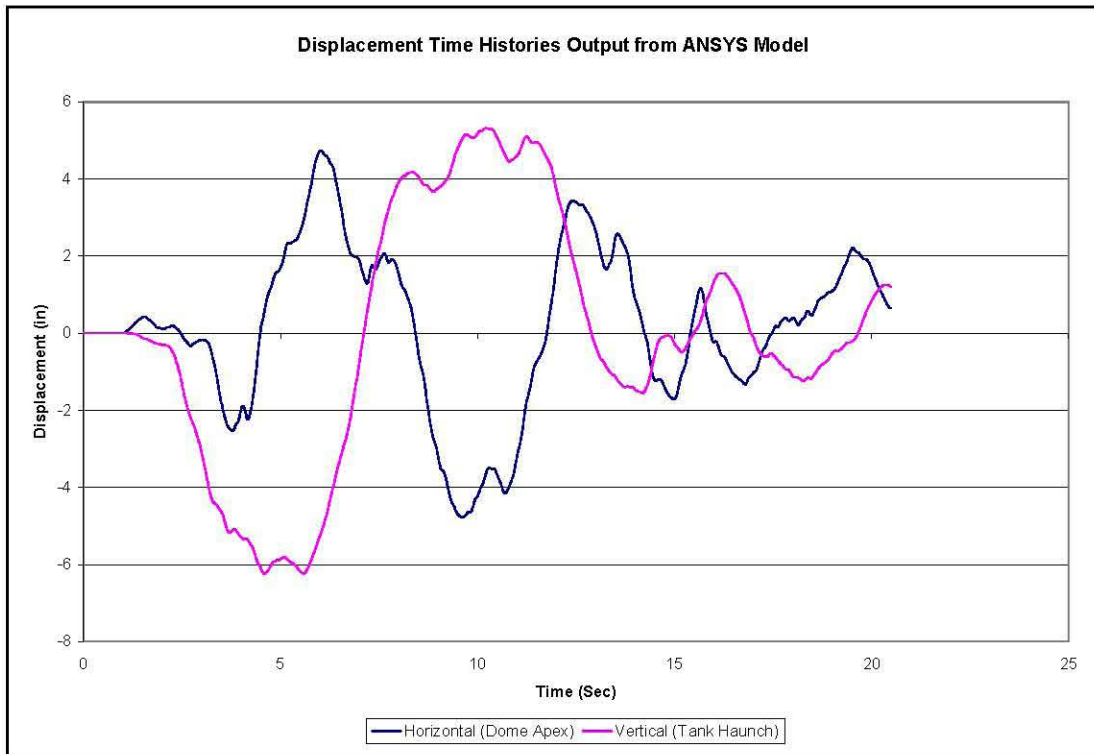


Figure 2-18. Displacement Time Histories Output from ANSYS® Model

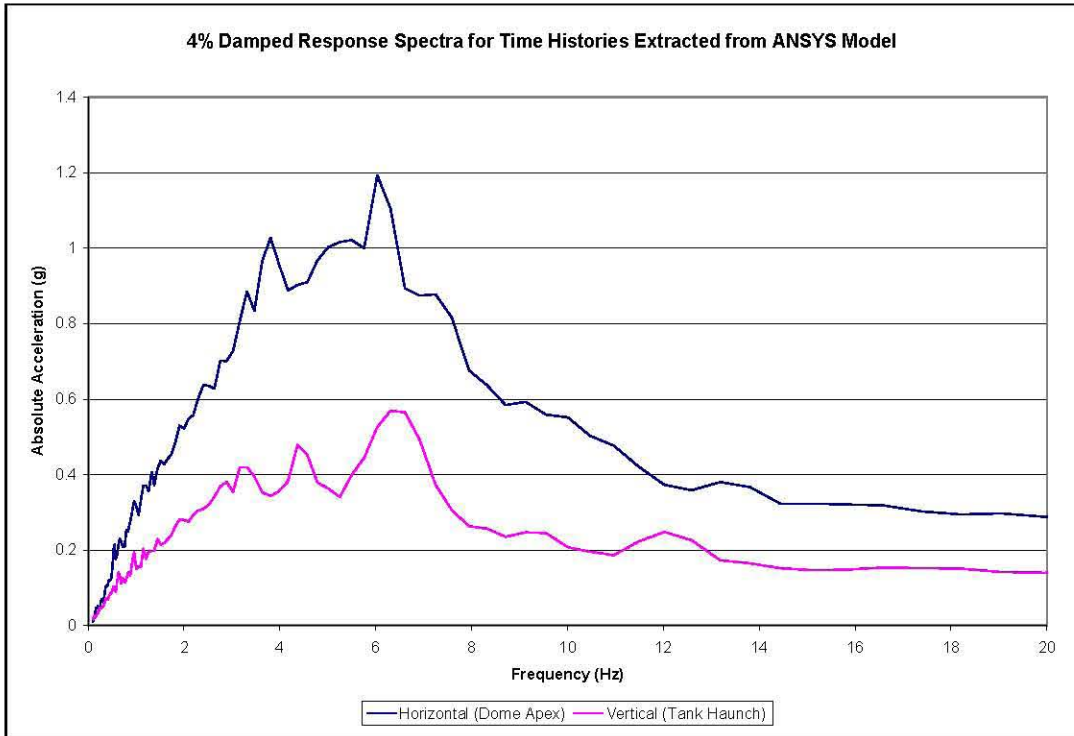


Figure 2-19. 4% Damped Response Spectra for Acceleration Time Histories Extracted from ANSYS® Model

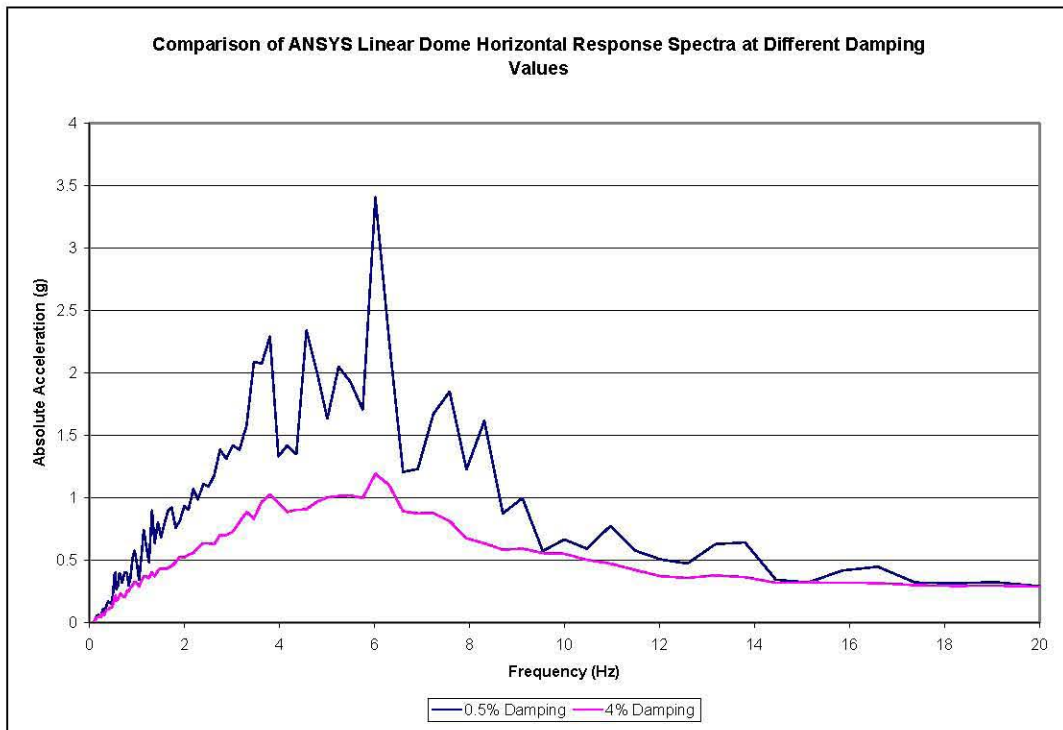


Figure 2-20. Comparison of Horizontal Dome Apex Response Spectra at Different Damping Values

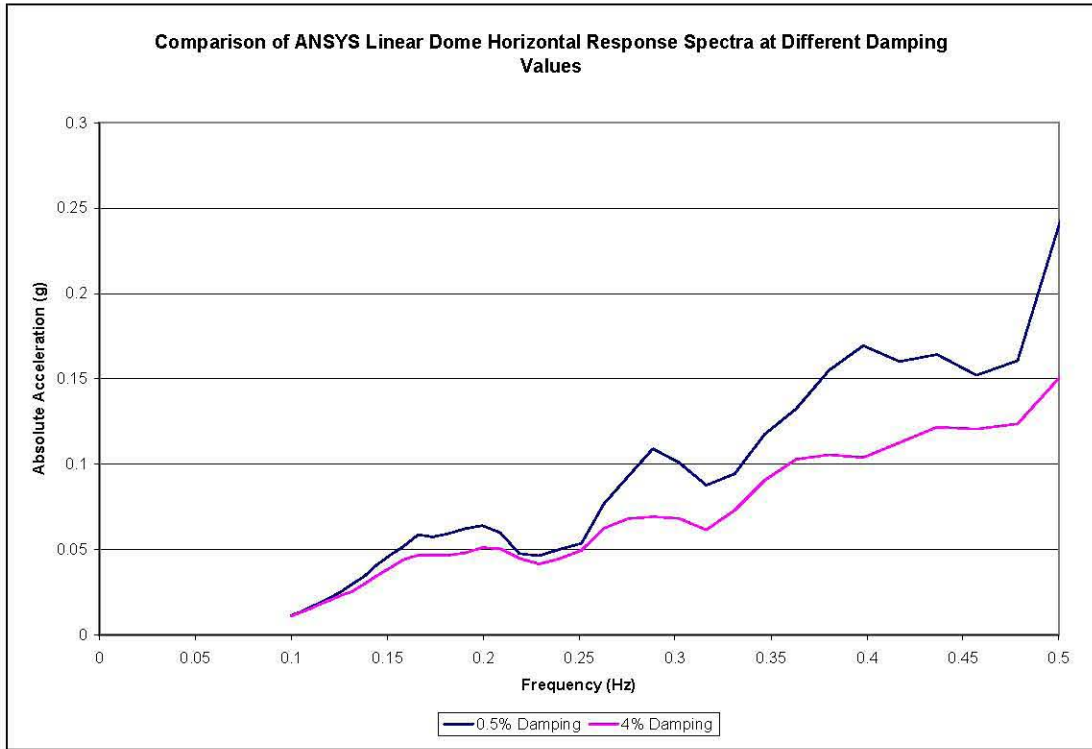


Figure 2-21. Comparison of Horizontal Dome Apex Response Spectra at Different Damping Values for Low Frequencies

### 3.0 Rigid Dytran<sup>®</sup> Model at 422-Inch Waste Level

The expected hydrostatic pressure at the centroid of the waste elements is easily calculated knowing the vertical location of the waste elements and the initial pressure using the equation  $p = p_0 + \rho g \Delta h$ , where  $p_0$  is the ambient pressure at the free surface. The expected hydrostatic pressures for the element sets “plusx\_els”, “press\_45”, and “plusz\_els” are shown in Table 3-1.

Table 3-1. Expected Hydrostatic Pressure of Waste Elements

“Plusx_els” Element No.	“Press_45” Element No.	“Plusz_els” Element No.	Hydrostatic Pressure (psi absolute)
10482	10290	10146	14.7
9753	9561	9417	15.8
9024	8832	8688	18.0
8295	8103	7959	20.1
7566	7374	7230	22.3
6837	6645	6501	24.5
6108	5916	5772	26.7
5379	5187	5043	28.8
4650	4458	4314	31.0
3921	3729	3585	33.2
3192	3000	2856	35.4
2463	2271	2127	37.5
1734	1542	1398	39.7

In the case of horizontal excitation, the gravity load was run for 5 seconds before beginning the seismic input. The 20.48-second seismic record was followed by 20 seconds of unforced motion with gravity loading. For vertical excitation, the gravity load was run for 2 seconds before beginning the seismic input. The 20.48-second seismic record was followed by 20 seconds of unforced motion with gravity loading.

The problem was originally run at gage pressure, but all results reported are from subsequent runs made at absolute pressure.

### 3.1 Hydrodynamic Forces

Dytran<sup>®</sup> provides output of the overall reaction forces between the Euler elements (fluid elements) and the coupling surface that is the interface between the fluid elements and the structural elements. The coupling surface reaction forces are compared to the total hydrodynamic forces calculated using the methodology described in BNL (1995) and shown in Appendix B.

### 3.1.1 Horizontal Excitation

The peak hydrodynamic force induced against the tank wall due to horizontal excitation can be calculated using Equation 4.31 in BNL (1995) with the instantaneous accelerations replaced by the appropriate spectral accelerations. If the contributions of the impulsive mode and first three convective modes are combined in a square-root-sum-of-squares (SRSS) fashion, the theoretical maximum horizontal hydrodynamic force is  $2.42 \times 10^6$  lbf, based on a zero-period acceleration for the impulsive response, and convective accelerations from the 0.5% damped spectrum. The coupling surface reaction force time histories reported by Dytran® for horizontal excitation are shown in Figure 3-1. The peak reaction force is  $2.45 \times 10^6$  lbf, which is approximately 1% greater than the predicted value. A plot of the horizontal reaction force is shown in Figure 3-2.

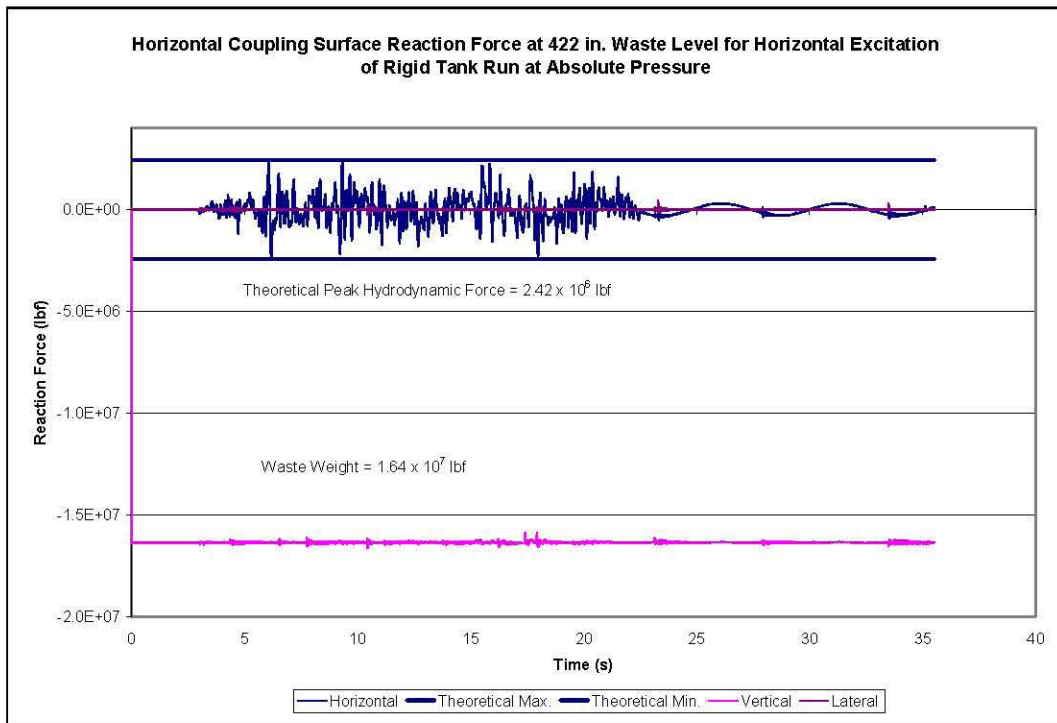


**Figure 3-1.** Coupling Surface Reaction Forces for the Rigid Tank at 422-Inch Waste Level Under Horizontal Seismic Input

Although the total horizontal hydrodynamic force is slightly greater than predicted by theory, the convective contribution is less than predicted by theory. The theoretical peak reaction force due to the first three convective modes only is  $4.62 \times 10^5$  lbf. The Dytran® calculated convective component of the horizontal reaction force during the free-vibration phase following the seismic excitation appears as Figure 3-3. The peak reaction force due to the convective response is approximately  $3 \times 10^5$  lbf or 65% of the theoretical value, if only the long-period first mode response is considered. Also apparent in the free-vibration response is the period of the first convective mode. The period shown in Figure 3-1 during the free-vibration phase is approximately 5.25 seconds, which matches the theoretical fundamental convective frequency of 0.19 Hz.

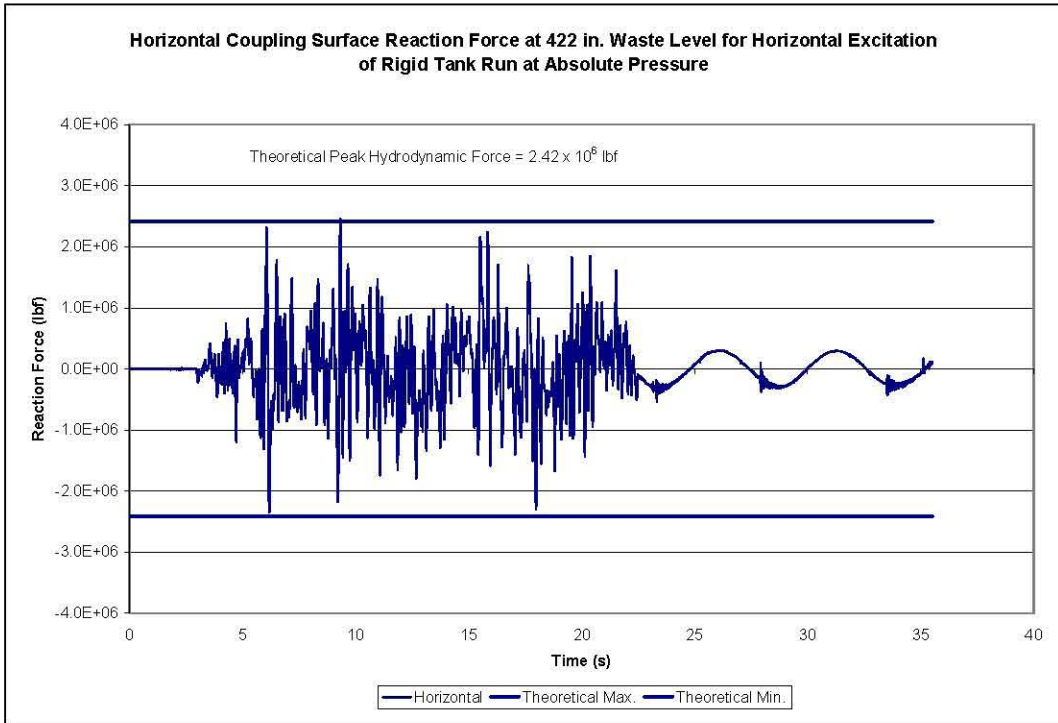


Figure 3-2. Horizontal Coupling Surface Reaction Force for the Rigid Tank at 422-Inch Waste Level Under Horizontal Seismic Input

The theoretical solution for the rigid tank is for an open tank with vertical walls. The rigid tank modeled in Dytran<sup>®</sup> nearly reflects that configuration, but not exactly. It can be seen from Figure 2-3 that the initial waste level corresponds to the top of the vertical wall. The next structural element up the tank begins to reflect the dome curvature to a mild degree, and the expected slosh height is less than the height of this next row of elements. However, this is a slightly different configuration than represented by the theoretical solution. It may be that the beginning of the dome curvature has the effect of inhibiting the convective response and increasing the impulsive response, and may account for the difference in the two solutions. This behavior will be seen clearly when results from the simulations at the 460-inch waste level are presented.

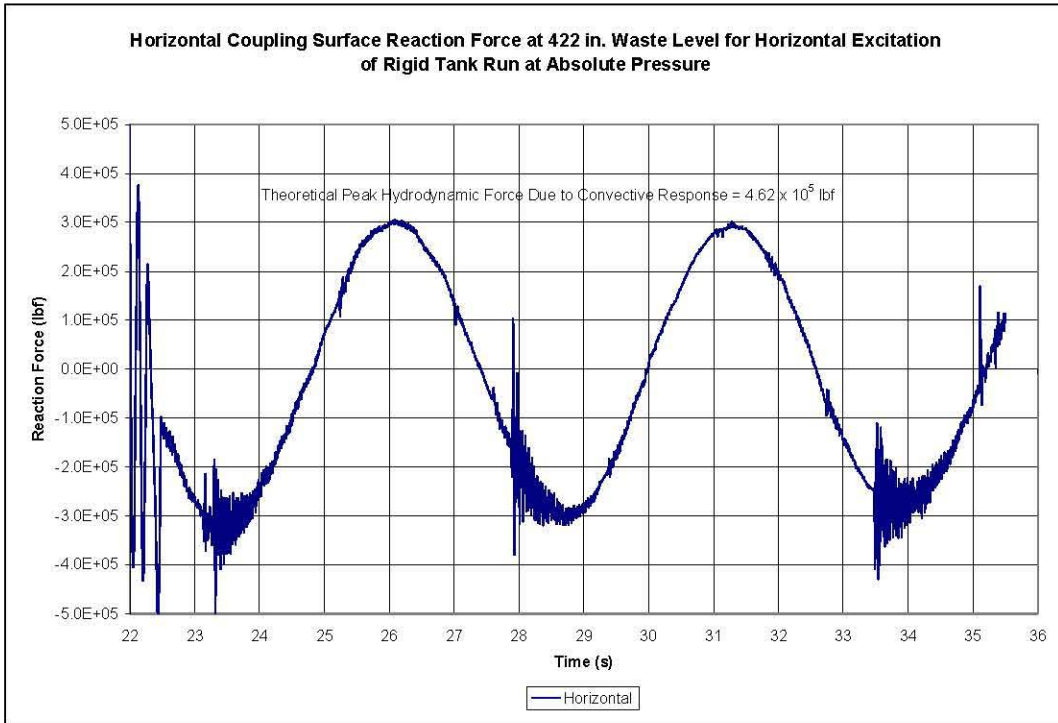


Figure 3-3. Horizontal Coupling Surface Reaction Force for Rigid Tank at 422-Inch Waste Level Under Horizontal Seismic Excitation – Convective Response

### 3.1.2 Vertical Excitation

Under vertical seismic excitation, the peak vertical hydrodynamic force for a rigid tank is simply the product of the waste mass and the peak acceleration. Given the waste mass of  $4.23 \times 10^4$  lbf-s<sup>2</sup>/in. and the vertical zero period acceleration of 0.12g (shown in the vertical acceleration time history in Figure 2-15), the peak vertical hydrodynamic base force is  $1.96 \times 10^6$  lbf. The coupling surface reaction force shown in Figure 3-4 is slightly greater than predicted by theory, with the peak hydrodynamic force of  $2.15 \times 10^6$  lbf. The spike in the vertical reaction force at 22.5 seconds is due to the final point in the vertical velocity time history being zero, bringing the tank to a sudden stop.

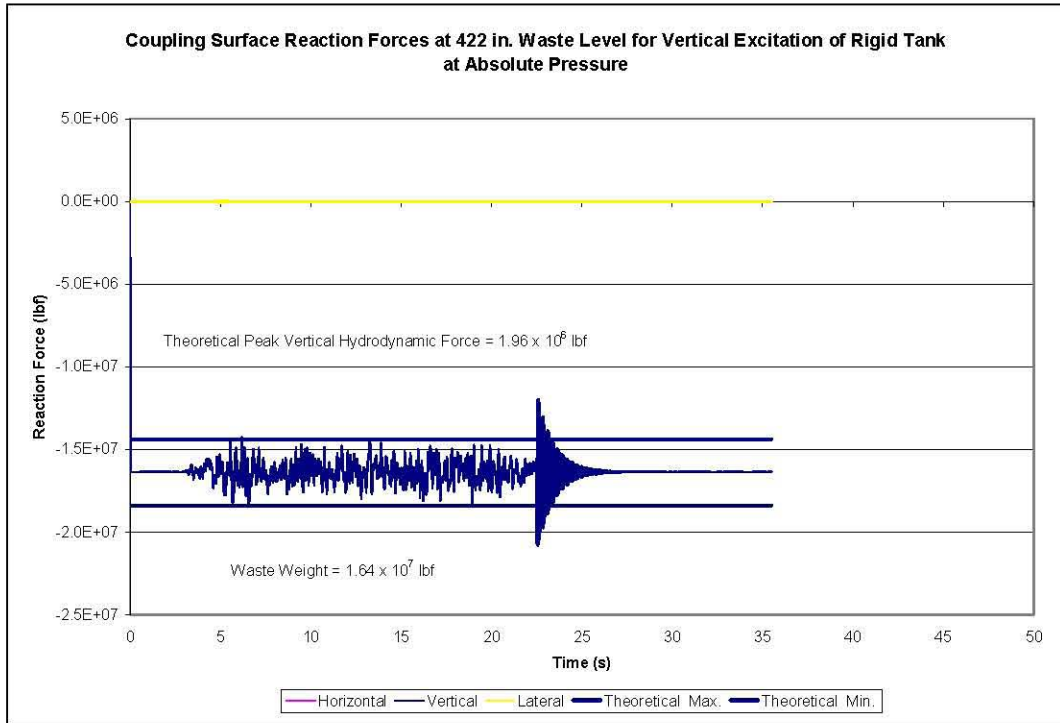


Figure 3-4. Coupling Surface Reaction Forces for Rigid Tank at 422-Inch Waste Level Under Vertical Seismic Input

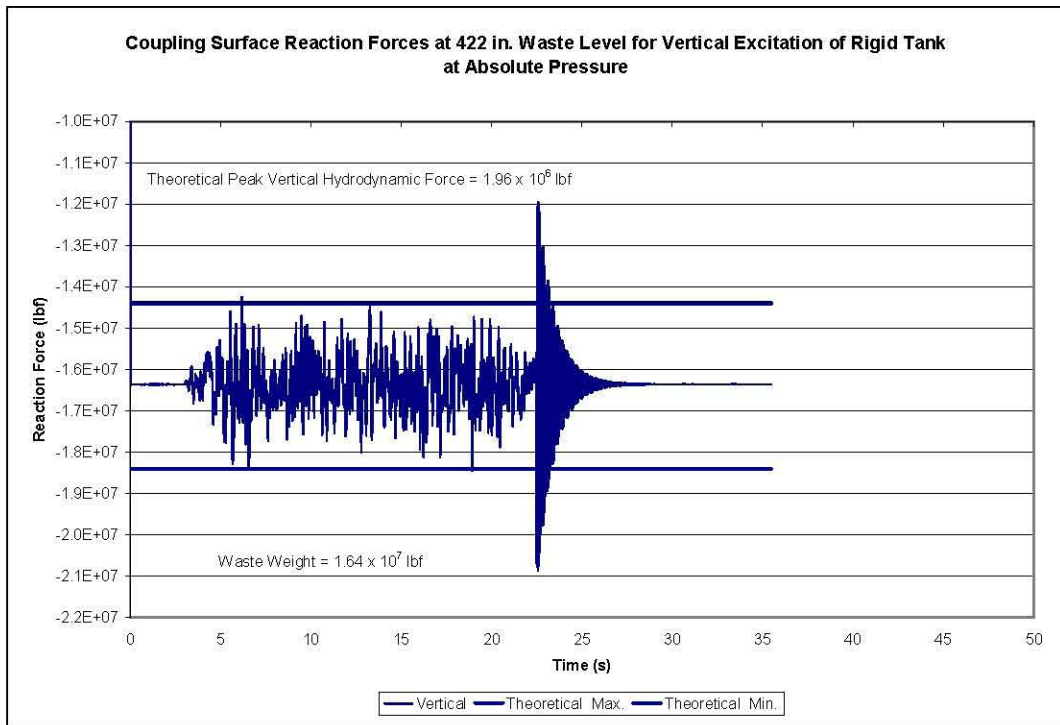


Figure 3-5. Vertical Coupling Surface Reaction Force for Rigid Tank at 422-Inch Waste Level Under Vertical Seismic Input

## 3.2 Waste Pressures

### 3.2.1 Horizontal Excitation Run at Absolute Pressure

The hydrodynamic pressures in the tank are caused by impulsive and convective components and depend on the location of the fluid element within the tank. In the case of horizontal excitation, both the impulsive and convective components vary in the circumferential direction as  $\cos\theta$ , with the maximum theoretical values occurring along the plane of excitation, and decreasing to zero hydrodynamic pressure at  $\theta=90^\circ$  to the plane of excitation. The impulsive hydrodynamic pressure increases with depth, while the convective dynamic pressure is a maximum at the top of the waste. The theoretical peak hydrodynamic pressures are given by Equation 4.24 in BNL (1995), and the total pressures are the sum of the hydrostatic pressures and the hydrodynamic pressures. The hydrostatic, peak hydrodynamic, and peak total pressures for the elements in the sets “plusx\_els” and “press\_45” are shown in Table 3-2 and Table 3-3. The maximum theoretical pressures for the elements set “plusz\_els” are simply the hydrostatic pressures shown in Table 3-1, because the theoretical hydrodynamic pressures are zero at  $\theta=90^\circ$ . The pressure time histories for the waste element sets at  $\theta=0$ , 45, and  $90^\circ$  are shown in Figure 3-6, Figure 3-7, and Figure 3-8.

**Table 3-2.** Theoretical Maximum Waste Pressures for Horizontal Excitation in the Rigid Tank at 422-Inch Waste Level for Elements at  $\theta=0$  Run at Absolute Pressure

“Plusx_els” Element No.	Hydrostatic Pressure (psi absolute)	Peak Hydrodynamic Pressure (psi absolute)	Peak Total Pressure (psi absolute)
10482	14.7	0	14.7
9753	15.8	1.7	17.5
9024	18.0	2.4	20.3
8295	20.1	3.0	23.1
7566	22.3	3.6	25.9
6837	24.5	4.0	28.5
6108	26.7	4.4	31.1
5379	28.8	4.7	33.6
4650	31.0	5.0	36.0
3921	33.2	5.2	38.3
3192	35.4	5.3	40.7
2463	37.5	5.4	42.9
1734	39.7	5.4	45.1

Table 3-3. Theoretical Maximum Waste Pressures for Horizontal Excitation in the Rigid Tank at 422-Inch Waste Level for Elements at  $\theta=45^\circ$  Run at Absolute Pressure

“Press_45” Element No.	Hydrostatic Pressure (psi absolute)	Peak Hydrodynamic Pressure (psi absolute)	Peak Total Pressure (psi absolute)
10290	14.7	0	14.7
9561	15.8	1.2	17.0
8832	18.0	1.7	19.6
8103	20.1	2.1	22.2
7374	22.3	2.5	24.8
6645	24.5	2.8	27.3
5916	26.7	3.1	29.8
5187	28.8	3.3	32.2
4458	31.0	3.5	34.5
3729	33.2	3.7	36.8
3000	35.4	3.8	39.1
2271	37.5	3.8	41.3
1542	39.7	3.9	43.5

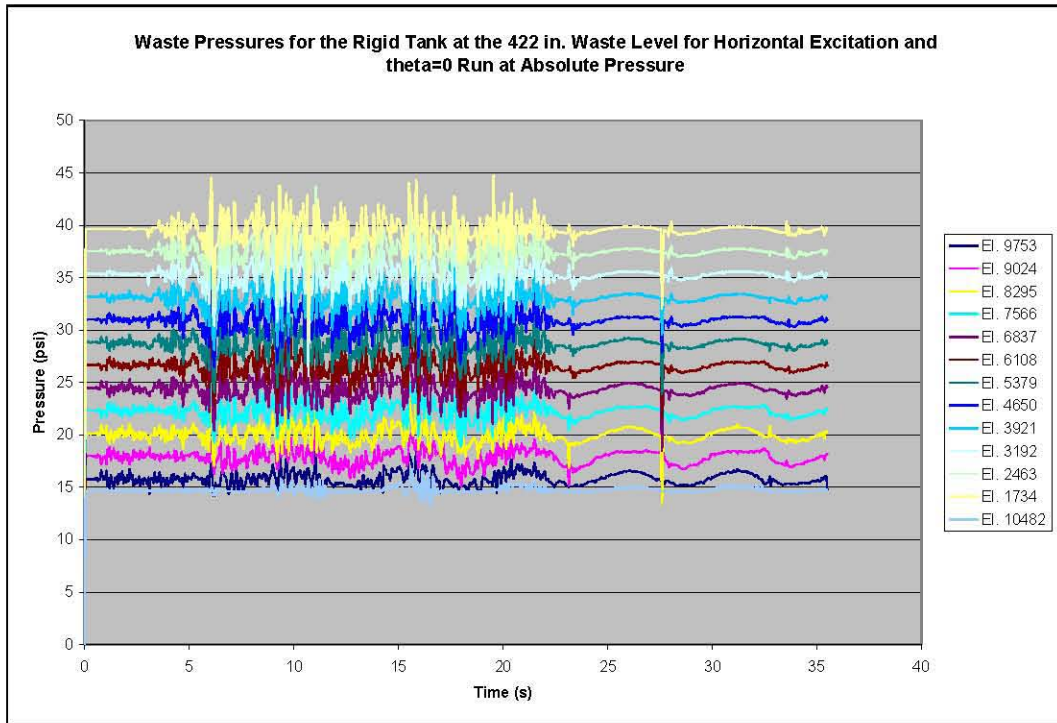


Figure 3-6. Waste Pressure Time Histories for the Rigid Tank with 422 Inches of Waste Under Horizontal Excitation at  $\theta=0$  Run at Absolute Pressure

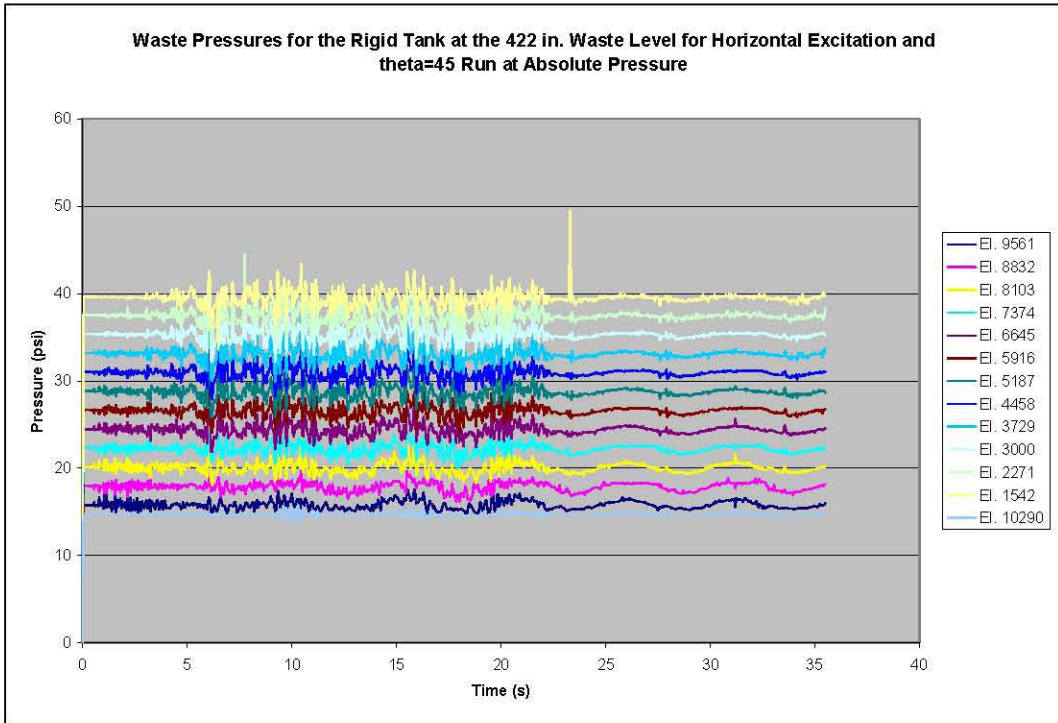


Figure 3-7. Waste Pressure Time Histories for the Rigid Tank with 422 Inches of Waste Under Horizontal Excitation at  $\theta=45^\circ$  Run at Absolute Pressure

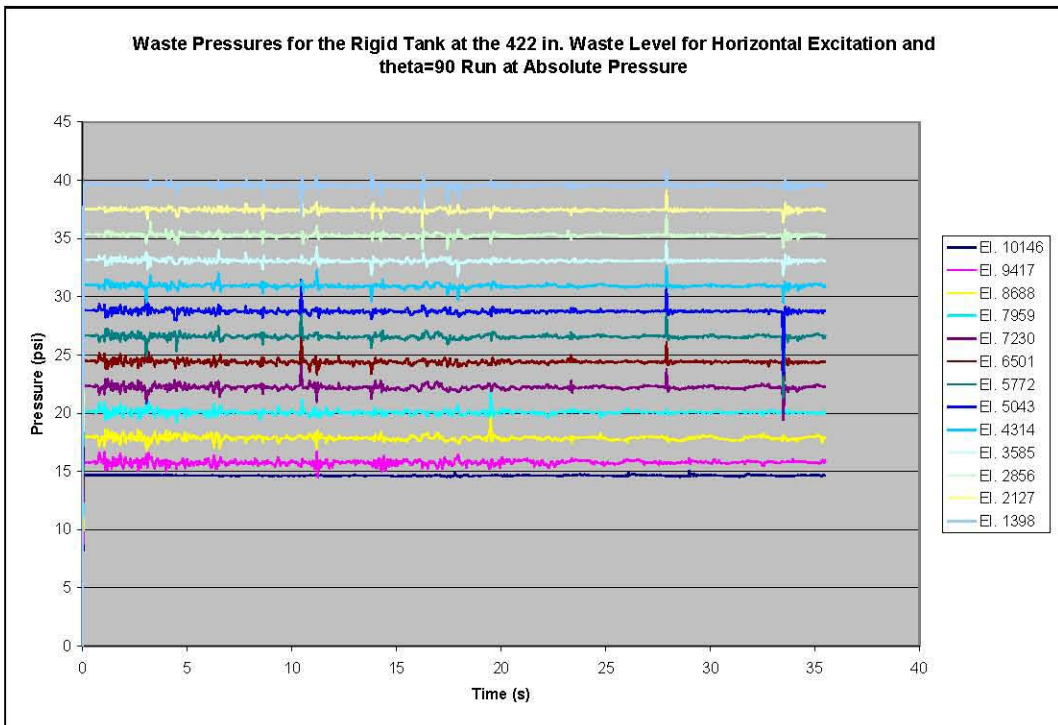


Figure 3-8. Waste Pressure Time Histories for the Rigid Tank with 422 Inches of Waste Under Horizontal Excitation at  $\theta=90^\circ$  Run at Absolute Pressure

Another way of presenting some of the information in the previous plots is to look at maximum and minimum pressures as a function of angular position and waste depth. Plots of the actual (as calculated by Dytran® – hereafter referred to as “actual”) and theoretical maximum and minimum waste pressures at  $\theta=0, 45,$  and  $90^\circ$  are shown in Figure 3-9, Figure 3-10, and Figure 3-11. As shown in Figure 3-12, the lower than predicted minimum pressures for the waste elements near the bottom of the tank as shown in Figure 3-9 are due to the isolated low peak pressures in waste elements 1734, 2463, and 3192. This behavior of isolated maxima and minima that stray from theoretical predictions will be observed in other simulations presented in this report.

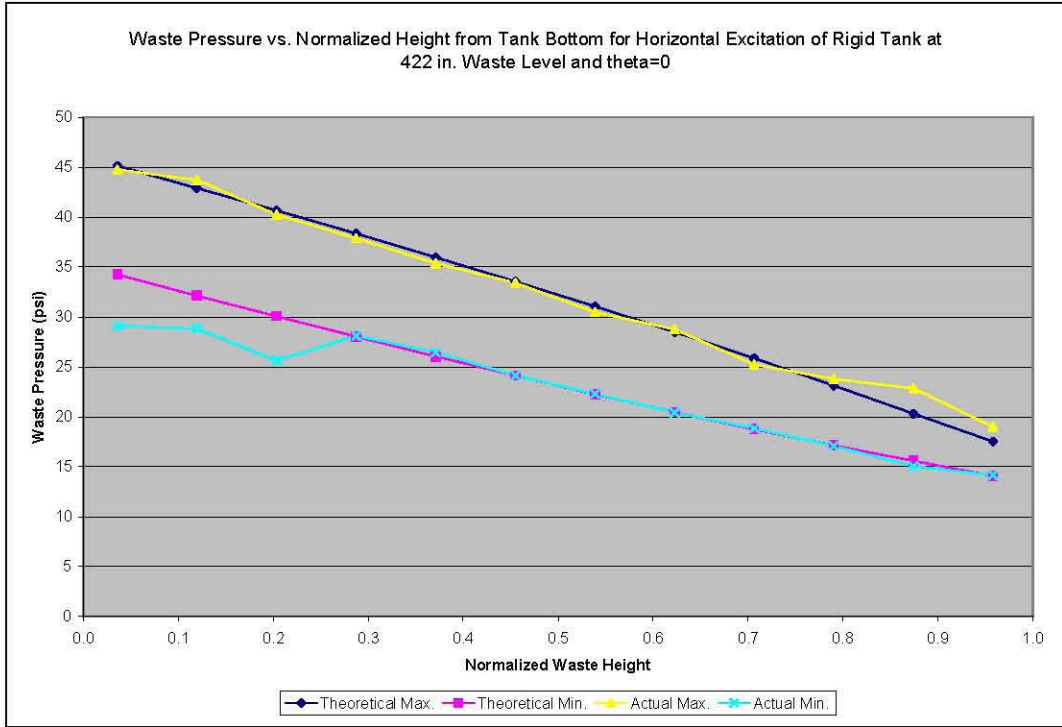


Figure 3-9. Maximum and Minimum Waste Pressures vs. Normalized Height from Tank Bottom for Horizontal Excitation at  $\theta=0$  Run at Absolute Pressure

RPP-RPT-28963, Rev. 1  
M&D-2008-005-RPT-01, Rev. 1

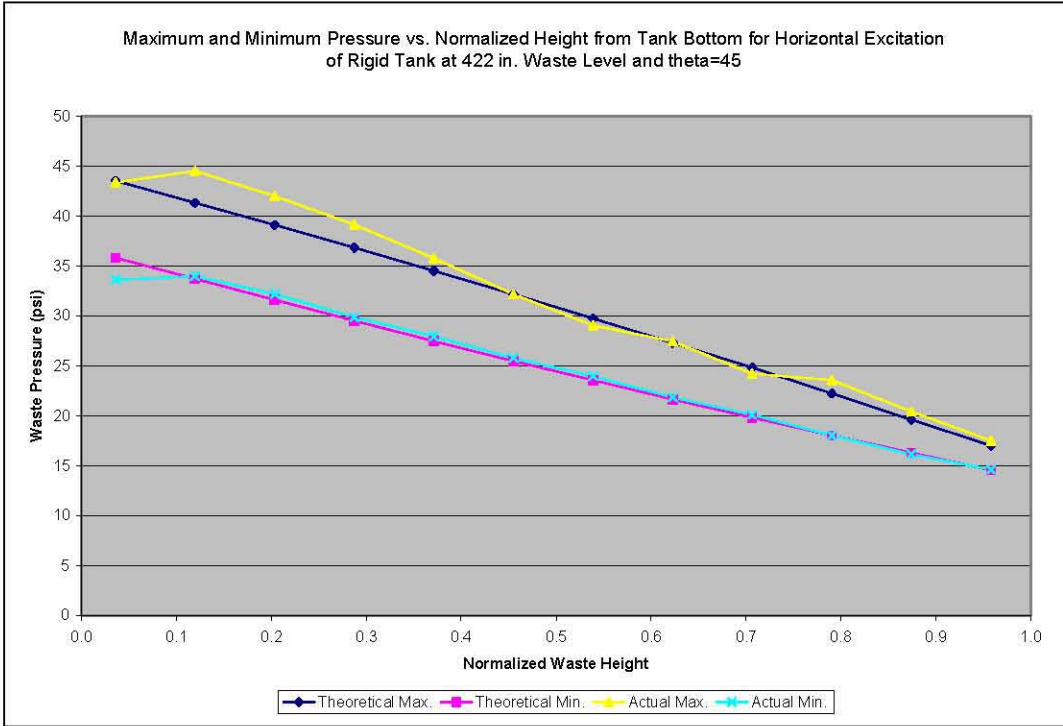


Figure 3-10. Maximum and Minimum Waste Pressures vs. Normalized Height from Tank Bottom for Horizontal Excitation at  $\theta=45^\circ$  Run at Absolute Pressure

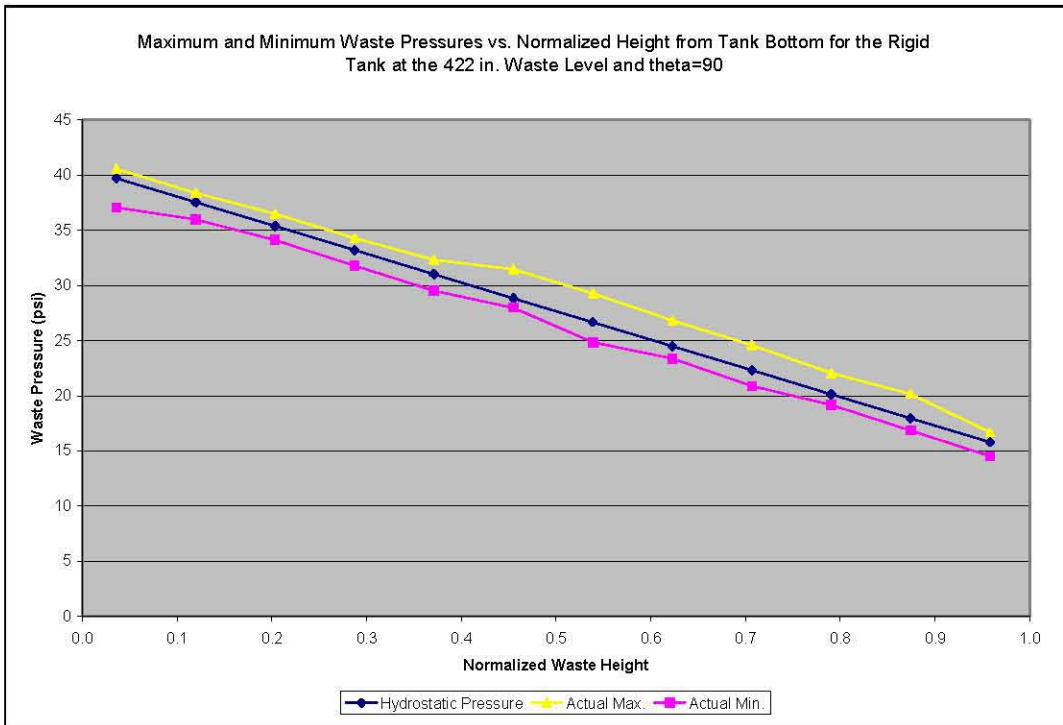


Figure 3-11. Maximum and Minimum Waste Pressures vs. Normalized Height from Tank Bottom for Horizontal Excitation at  $\theta=90^\circ$  Run at Absolute Pressure

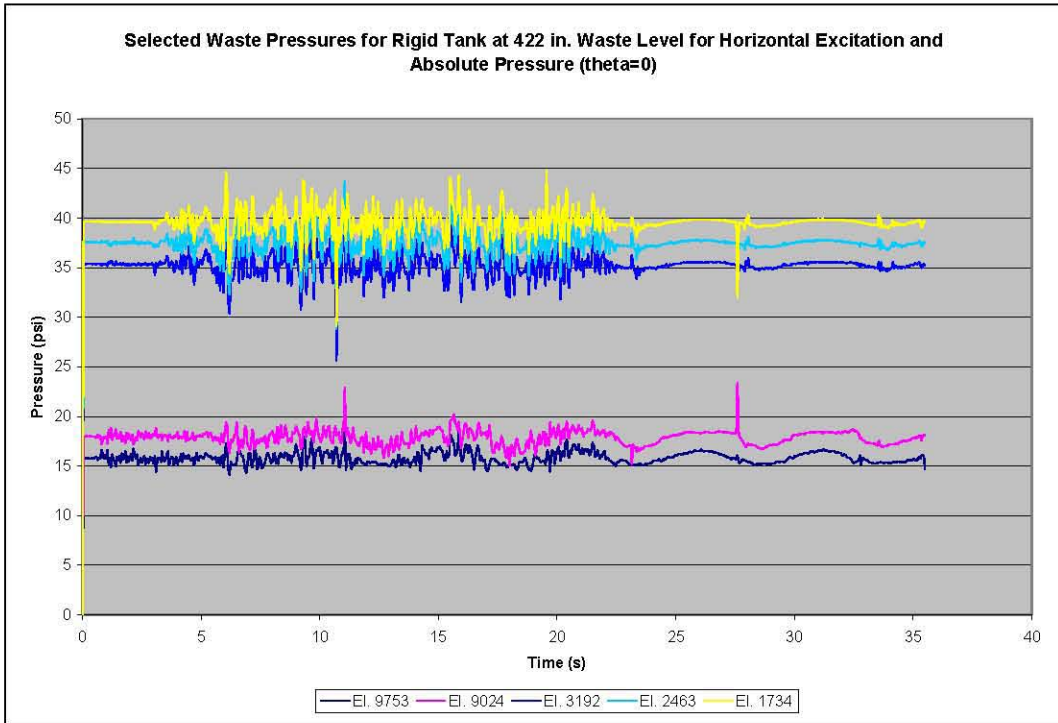


Figure 3-12. Selected Waste Pressure Time Histories for the Rigid Tank with 422 Inches of Waste Under Horizontal Excitation at  $\theta=0$  Run at Absolute Pressure

### 3.2.2 Vertical Excitation

The maximum hydrodynamic pressures induced by the waste on the tank wall due to vertical excitation depend on the vertical location in the waste and are given by Equation 4.55 in BNL (1995). The maximum hydrodynamic and total pressures for the elements in sets “plusx\_els”, “press\_45”, and “plusz\_els” are given in Table 3-4.

Waste pressure time histories for the waste elements at  $\theta=0$ ,  $45^\circ$ , and  $90^\circ$  are shown in Figure 3-13, Figure 3-14, and Figure 3-15.

Table 3-4. Theoretical Maximum Wall Pressures for Vertical Excitation in the Rigid Tank at 422-Inch Waste Level

“Plusx_els”	“Press_45”	“Plusz_els”	Hydrostatic Pressure (psi absolute)	Peak Hydrodynamic Wall Pressure (psi absolute)	Peak Total Pressure (psi absolute)
Element No.	Element No.	Element No.			
10482	10290	10146	14.7	0	14.7
9753	9561	9417	15.8	0.2	16.0
9024	8832	8688	18.0	0.5	18.5
8295	8103	7959	20.1	0.8	20.9
7566	7374	7230	22.3	1.1	23.4
6837	6645	6501	24.5	1.4	25.9
6108	5916	5772	26.7	1.7	28.4
5379	5187	5043	28.8	1.9	30.7
4650	4458	4314	31.0	2.1	33.1
3921	3729	3585	33.2	2.2	35.4
3192	3000	2856	35.4	2.4	37.8
2463	2271	2127	37.5	2.5	40.0
1734	1542	1398	39.7	2.5	42.2

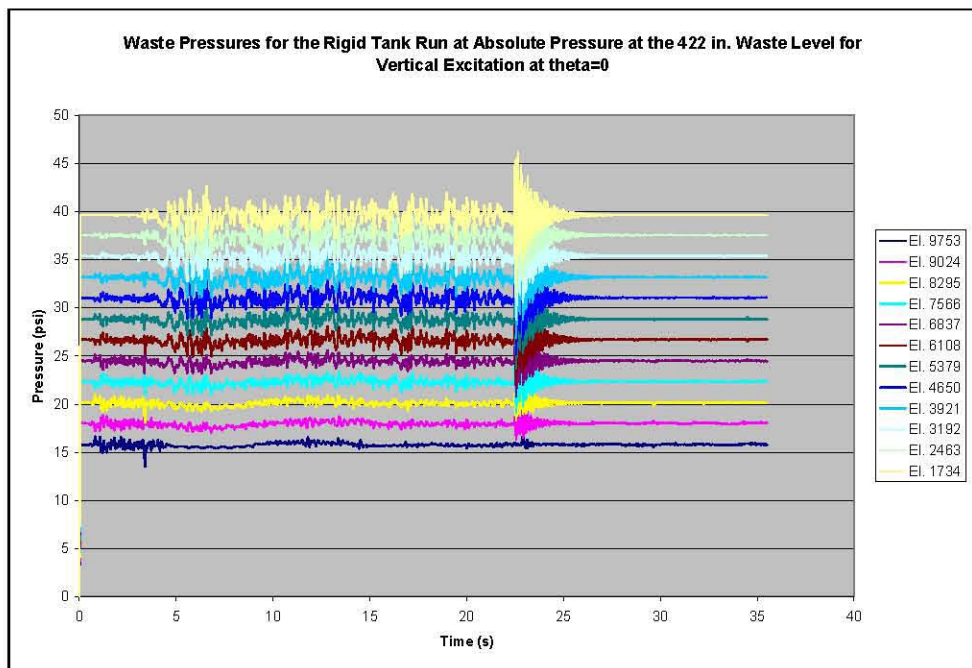


Figure 3-13. Waste Pressure Time Histories for the Rigid Tank with 422 Inches of Waste Under Vertical Excitation at  $\theta=0$  Run at Absolute Pressure

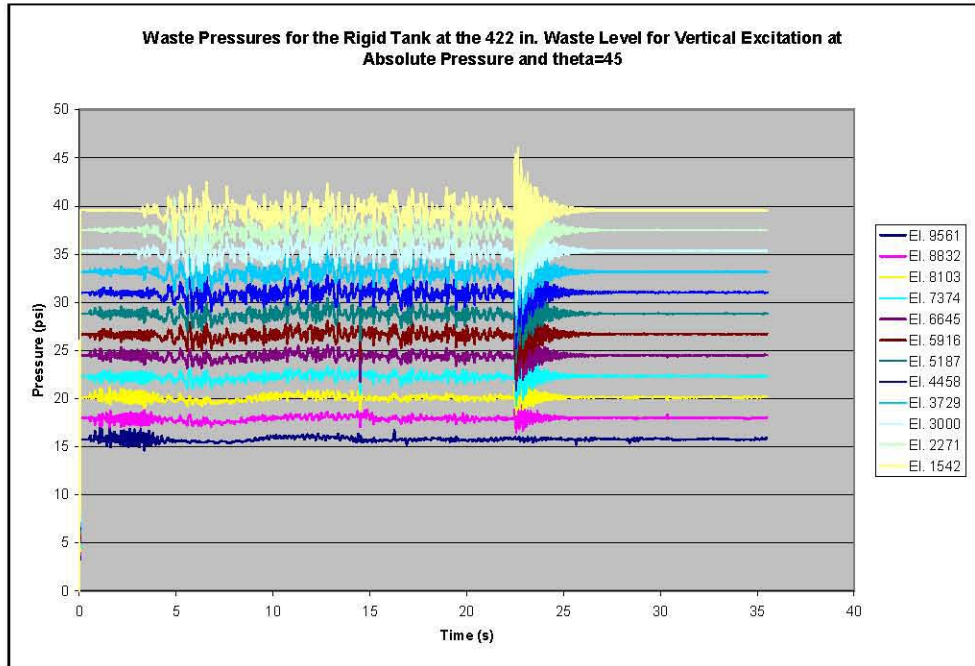


Figure 3-14. Waste Pressure Time Histories for the Rigid Tank with 422 Inches of Waste Under Vertical Excitation at  $\theta=45^\circ$  Run at Absolute Pressure

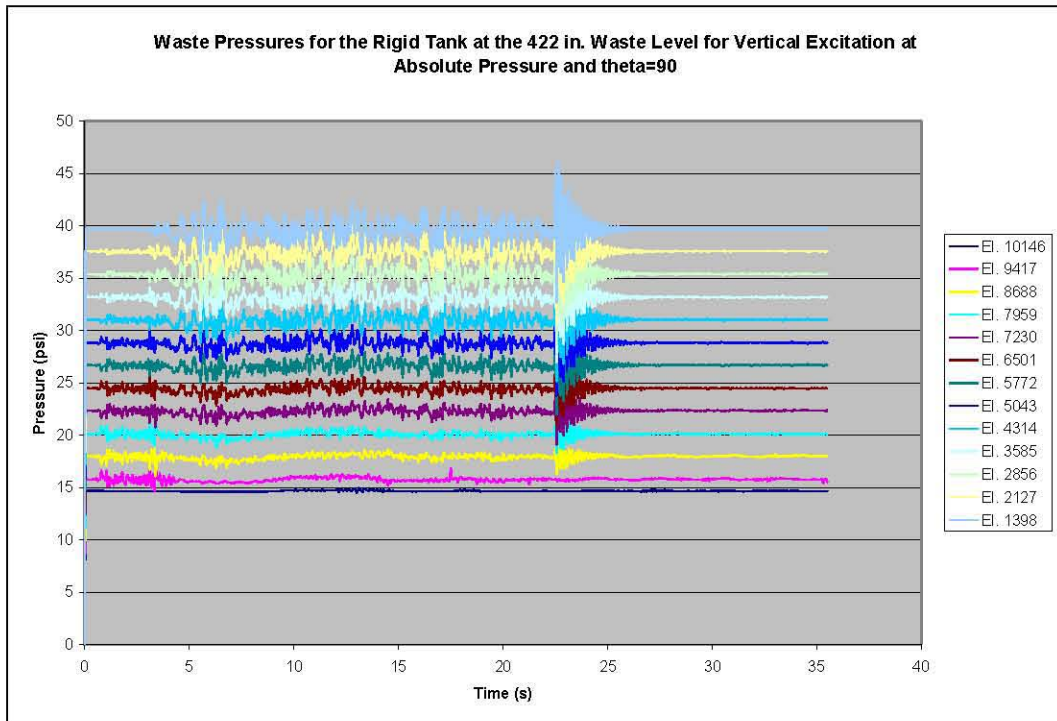
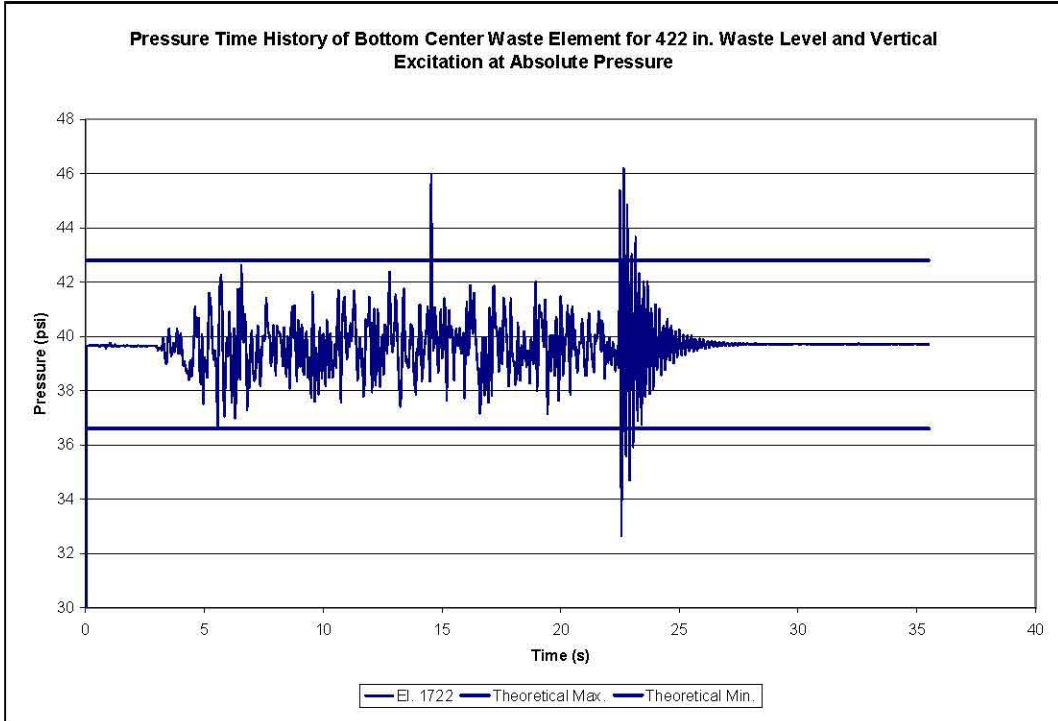


Figure 3-15. Waste Pressure Time Histories for the Rigid Tank with 422 Inches of Waste Under Vertical Excitation at  $\theta=90^\circ$  Run at Absolute Pressure

The pressure time history of waste element 1722 located at the center of the tank near the bottom is shown as Figure 3-16. The maximum total pressure is 7% greater than predicted by theory, and the peak dynamic pressure is approximately twice that predicted by theory, although this appears to occur at a single isolated point at approximately 15 seconds. The minimum pressure is as predicted by theory.



**Figure 3-16.** Pressure Time History for Bottom Center Waste Element for the Rigid Tank at the 422-Inch Waste Level and Vertical Excitation Run at Absolute Pressure

The actual (that is, as predicted by Dytran<sup>®</sup>) maximum and minimum pressure for the elements at  $\theta=0$ ,  $45^\circ$ , and  $90^\circ$  is shown in Figure 3-17, Figure 3-18, and Figure 3-19, along with the theoretical maximum and minimum pressures for the elements. The results show very good agreement with theoretical predictions.

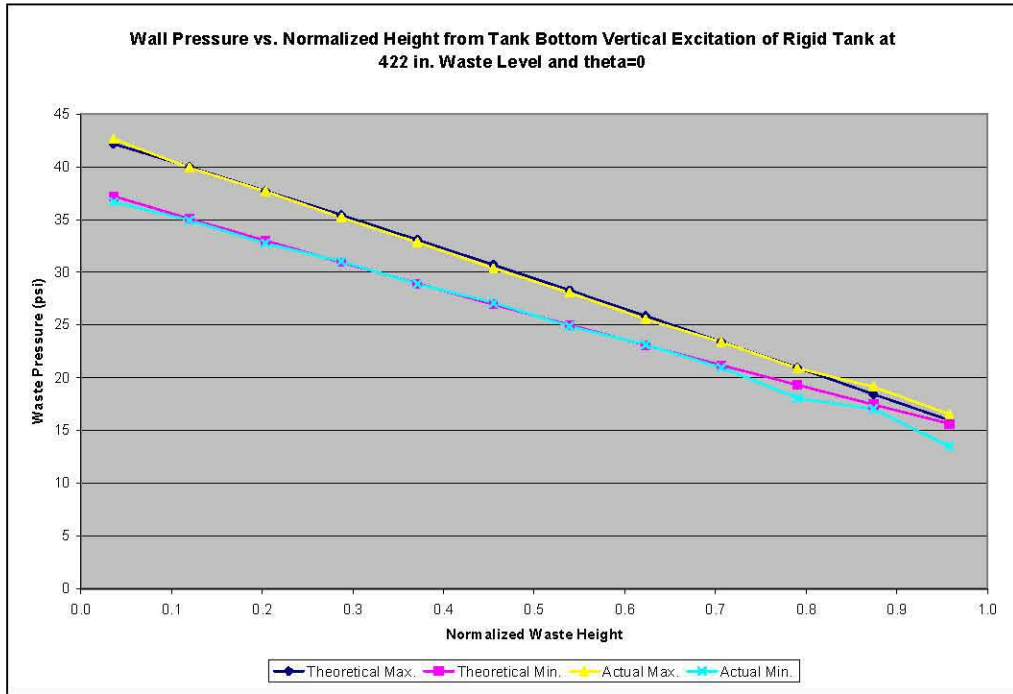


Figure 3-17. Maximum and Minimum Waste Pressures vs. Normalized Height from Tank Bottom for Vertical Excitation of Rigid Tank at 422-Inch Waste Level and  $\theta=0$  Run at Absolute Pressure

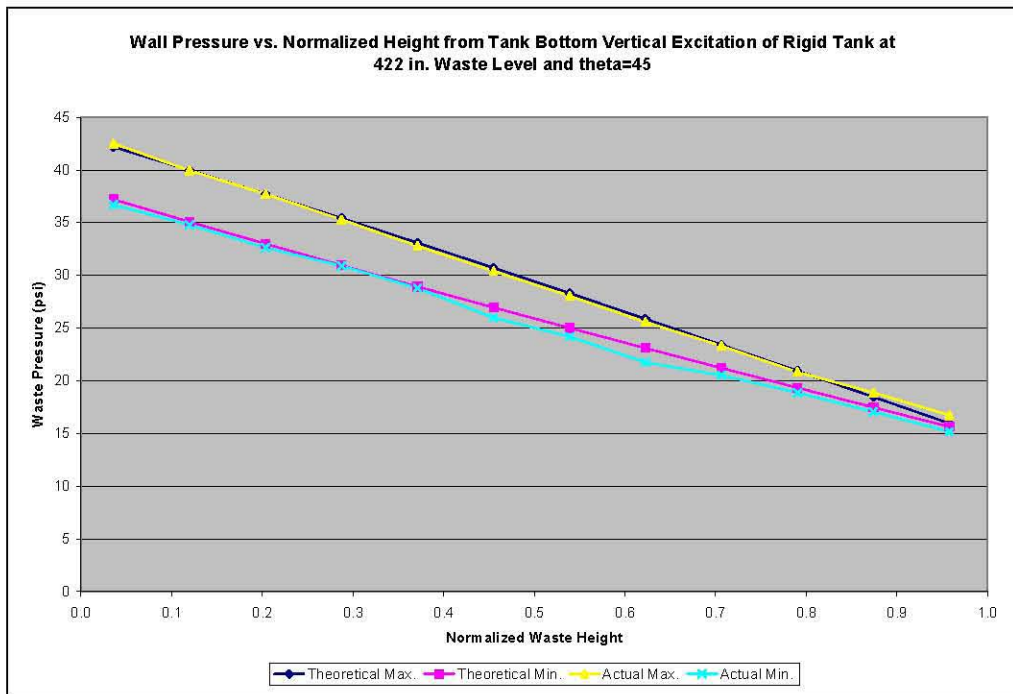


Figure 3-18. Maximum and Minimum Waste Pressures vs. Normalized Height from Tank Bottom for Vertical Excitation of Rigid Tank at 422-Inch Waste Level and  $\theta=45^\circ$  Run at Absolute Pressure

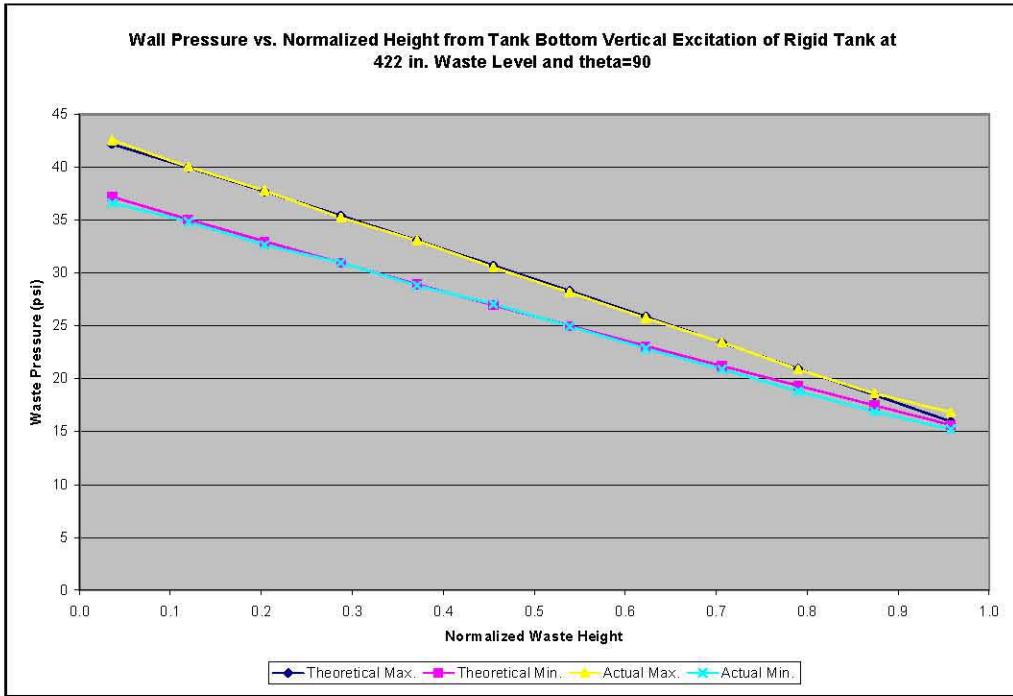


Figure 3-19. Maximum and Minimum Waste Pressures vs. Normalized Height from Tank Bottom for Vertical Excitation of Rigid Tank at 422-Inch Waste Level and  $\theta=90^\circ$  Run at Absolute Pressure

### 3.3 Slosh Height Results

According to Equation 4.60 in BNL (1995), the maximum predicted slosh height due to horizontal excitation is 23.7 inches. The time history of the maximum slosh height across all elements is shown in Figure 3-20, where the maximum height of the free surface is shown as 25.4 inches above the initial level.

The slosh height subroutine works by representing the waste-free surface as discrete triangular facets in space. At each output time step, the position of each corner node of each facet is known. At each time, the maximum slosh height is reported as the maximum height over all corner nodes representing the free surface position. A physical interpretation of slosh height time history is to think of a massless rigid plate that remains horizontal at all times and floats on top of the waste-free surface. The vertical position of the plate corresponds to the peak height of any point on the free surface. The slosh height time history may then be thought of as the vertical displacement time history of the floating plate, starting from the initial position.

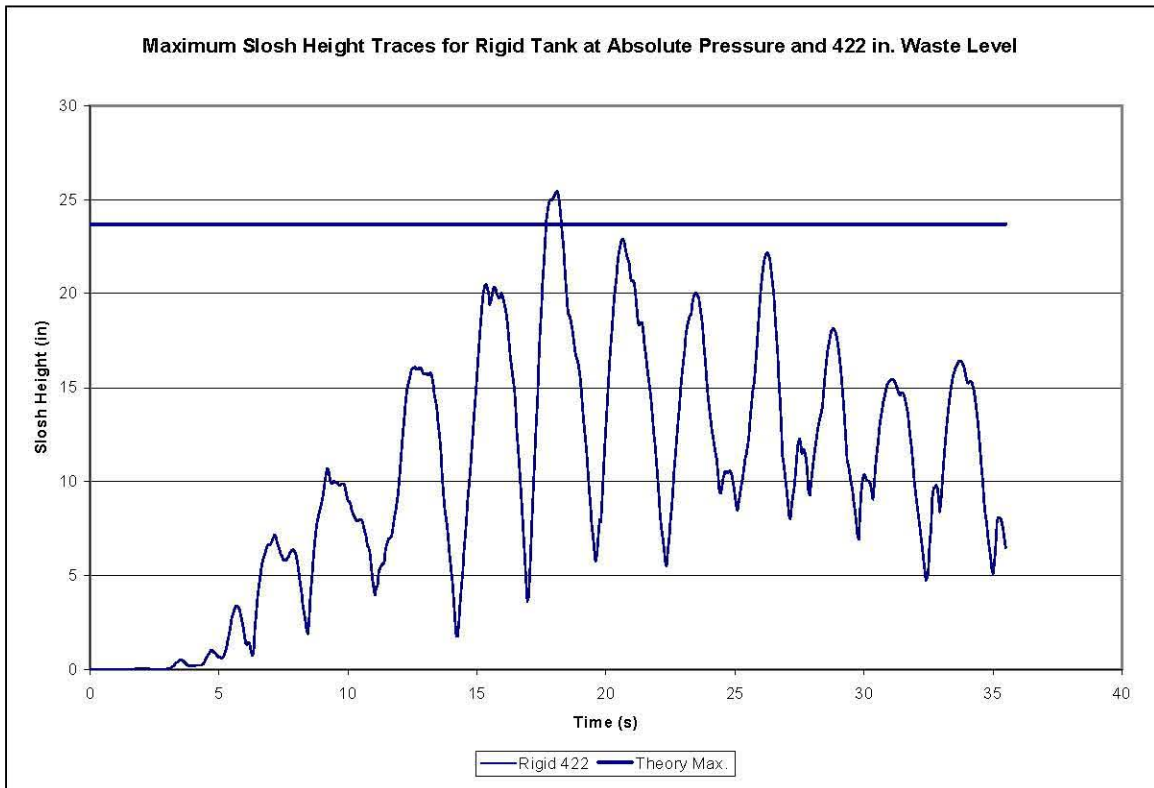


Figure 3-20. Maximum Slosh Height Time History Over All Waste Elements for Horizontal Excitation

Intentionally left blank.

## 4.0 Rigid Tank Model at 460-Inch Waste Level

The response of the tank and contained liquid to seismic excitation with the liquid initially at the 460-inch level *does not have a closed form analytical solution* because of the interaction of the liquid-free surface with the curved surface of the tank dome. However, the *solutions obtained with Dytran® will be compared to the theoretical solution for the rigid open tank with the hinged-top condition and 460-inch waste level* as well as with the Dytran® solution for the rigid tank at the 422-inch level.

The problem was originally run at gage pressure, but all results reported are from subsequent runs made at absolute pressure.

### 4.1 Hydrodynamic Forces

#### 4.1.1 Horizontal Excitation at Absolute Pressure

If the contributions of the impulsive mode and first three convective modes are combined in a square-root-sum-of-squares (SRSS) fashion, the theoretical maximum horizontal hydrodynamic force is  $3.0 \times 10^6$  lbf, based on a zero-period acceleration for the impulsive response, and convective accelerations from the 0.5% damped spectrum. The coupling surface reaction force time histories reported by Dytran® for horizontal excitation are shown in Figure 4-1. The horizontal coupling surface reaction force appears as Figure 4-2. The peak reaction force is  $3.02 \times 10^6$  lbf, which is essentially the same as the theoretical maximum.

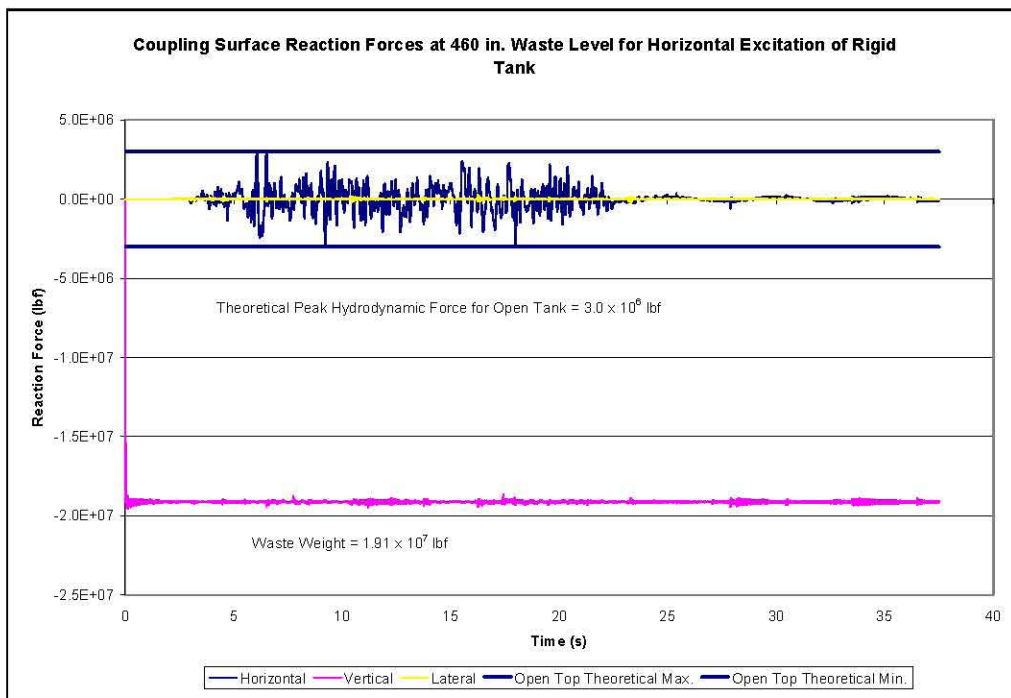


Figure 4-1. Coupling Surface Reaction Forces at the 460-Inch Waste Level for the Rigid Tank Under Horizontal Seismic Excitation

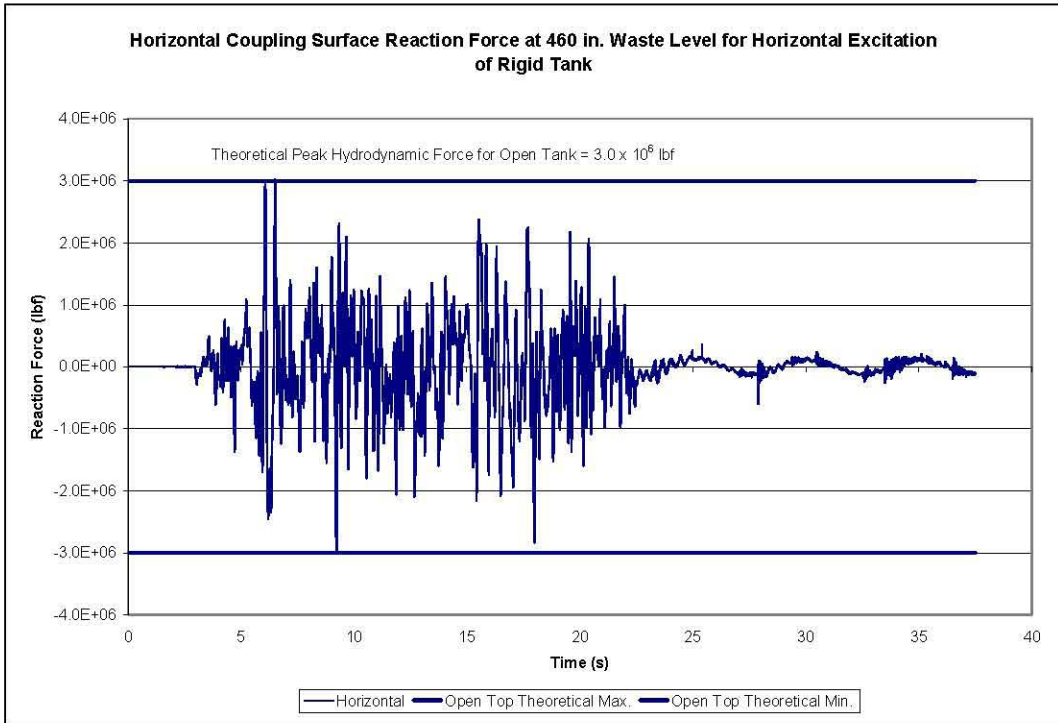


Figure 4-2. Horizontal Coupling Surface Reaction Force for Rigid Tank at 460-Inch Waste Level Under Horizontal Seismic Excitation

The theoretical peak reaction force due to the first three convective modes only is  $5.21 \times 10^5$  lbf. The convective component of the horizontal reaction force during the free-vibration phase following the seismic excitation appears as Figure 4-3. The peak reaction force due to the convective response is approximately  $2 \times 10^5$  lbf – much less than the predicted value. Also apparent in the free-vibration response is the period of the first convective mode. The period shown in Figure 4-3 during the free-vibration phase is approximately 5 seconds, which matches the theoretical fundamental convective frequency of 0.2 Hz, and is slightly lower than the 5.25-second period for the rigid tank at the 422-inch level.

As noted in Section 3.1.1, it appears that the presence of the tank dome acts to inhibit the convective waste response.

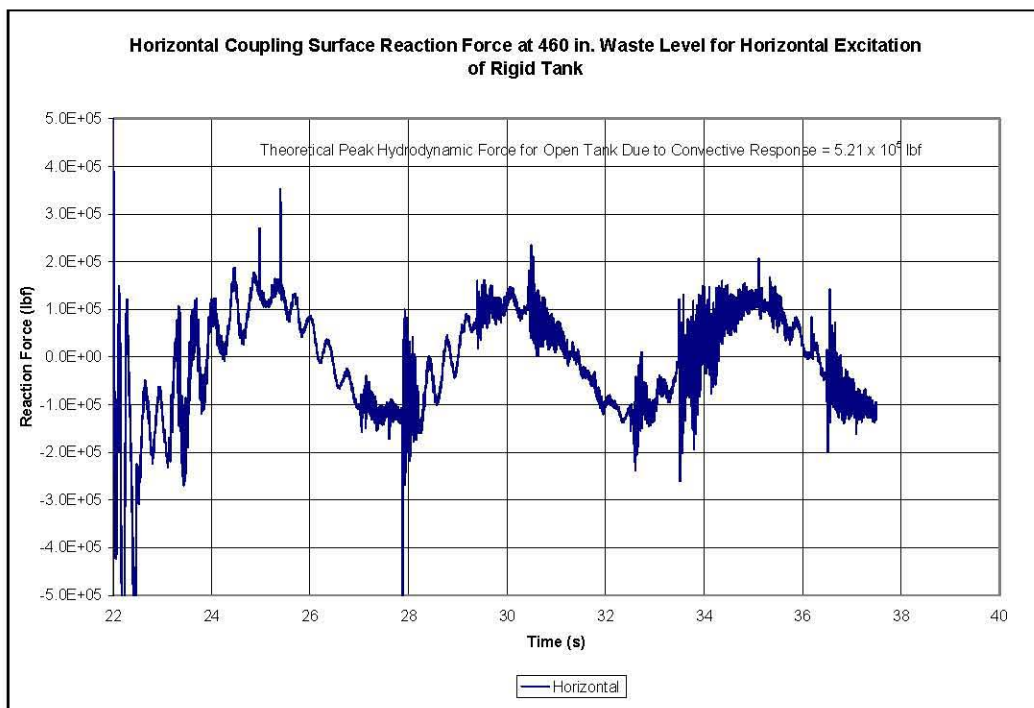


Figure 4-3. Horizontal Coupling Surface Reaction Force for Rigid Tank at 460-Inch Waste Level Under Horizontal Seismic Excitation – Convective Response

#### 4.1.2 Vertical Excitation at Absolute Pressure

Given the waste mass of  $4.95 \times 10^4$  lbf-s<sup>2</sup>/in. and the vertical zero period acceleration of 0.12g (shown in the vertical acceleration time history in Figure 2-15), the peak theoretical vertical hydrodynamic base force is  $2.30 \times 10^6$  lbf. The coupling surface reaction force shown in Figure 4-4 is greater than predicted by theory with the peak hydrodynamic force of  $3.1 \times 10^6$  lbf. The spike in the vertical reaction force at 22.5 seconds is due to the final point in the vertical velocity time history being zero, bringing the tank to a sudden stop.

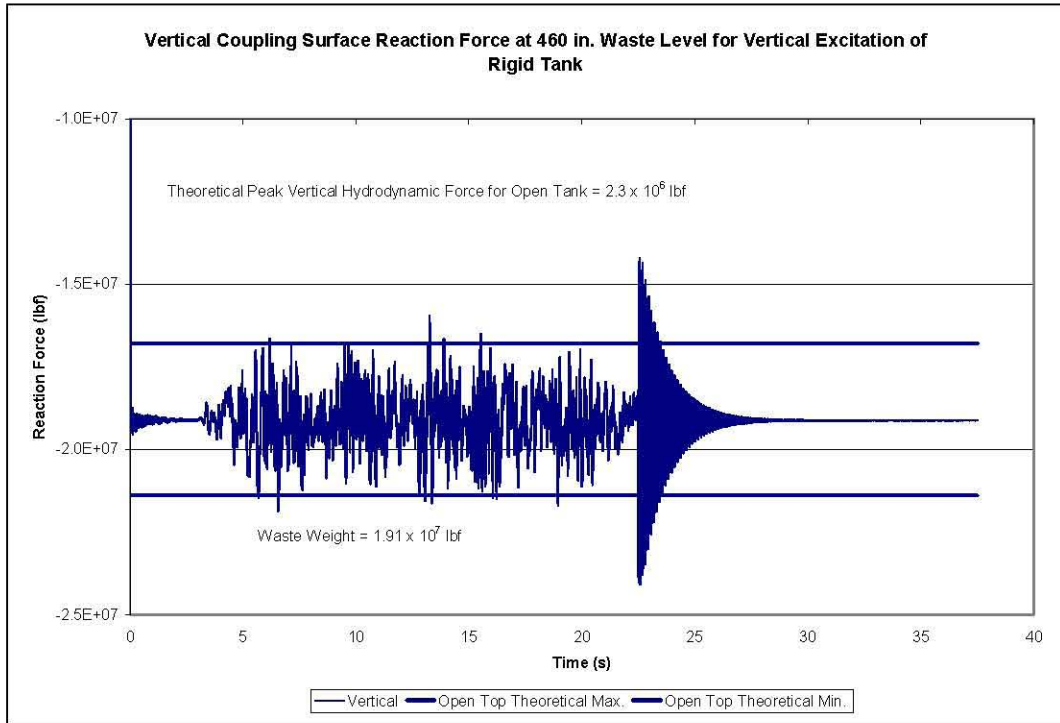


Figure 4-4. Vertical Coupling Surface Reaction Force for Rigid Tank at 460-Inch Waste Level Under Vertical Seismic Excitation

## 4.2 Waste Pressures

### 4.2.1 Horizontal Excitation Run at Absolute Pressure

Although no closed form solution exists for the 460-inch waste level, theoretical dynamic pressures were calculated using Equation 4.24 in BNL (1995) based on an open tank with 460 inches of waste and a hinged-top condition. This solution is presented along with the actual results for comparison purposes.

The hydrostatic, peak hydrodynamic, and peak total pressures for the elements in the sets “plusx\_els” and “press\_45” are shown in Table 4-1 and Table 4-2. The maximum theoretical pressures for the elements set “plusz\_els” are simply the hydrostatic pressures shown in the two tables because the theoretical hydrodynamic pressures are zero at  $\theta=90^\circ$ . The pressure time histories for waste element sets at  $\theta=0$ , 45, and  $90^\circ$  are shown in Figure 4-5 through Figure 4-9.

RPP-RPT-28963, Rev. 1  
M&D-2008-005-RPT-01, Rev. 1

**Table 4-1.** Theoretical Maximum Absolute Waste Pressures for Horizontal Excitation in the Rigid Open-Top Tank at 460-Inch Waste Level for Elements at  $\theta=0$

<b>“Plusx_els”</b>	<b>Hydrostatic Pressure (psi)</b>	<b>Peak Hydrodynamic Pressure (psi)</b>	<b>Peak Total Pressure (psi)</b>
<b>Element No.</b>			
11211	14.7	0	14.7
10482	16.0	1.9	17.9
9753	18.4	2.6	21.0
9024	20.7	3.3	24.0
8295	23.1	3.9	27.0
7566	25.4	4.4	29.8
6837	27.7	4.9	32.6
6108	30.1	5.2	35.3
5379	32.4	5.5	37.9
4650	34.7	5.7	40.4
3921	37.1	5.9	43.0
3192	39.4	6.1	45.5
2463	41.8	6.1	47.9
1734	44.1	6.2	50.3

**Table 4-2.** Theoretical Maximum Absolute Waste Pressures for Horizontal Excitation in the Rigid Open-Top Tank at 460-Inch Waste Level for Elements at  $\theta=45^\circ$

<b>“Press_45”</b>	<b>Hydrostatic Pressure (psi)</b>	<b>Peak Hydrodynamic Pressure (psi)</b>	<b>Peak Total Pressure (psi)</b>
<b>Element No.</b>			
11019	14.7	0	14.7
10290	16.0	1.4	17.4
9561	18.4	1.9	20.3
8832	20.7	2.3	23.0
8103	23.1	2.8	25.9
7374	25.4	3.1	28.5
6645	27.7	3.4	31.1
5916	30.1	3.7	33.8
5187	32.4	3.9	36.3
4458	34.7	4.1	38.8
3729	37.1	4.2	41.3
3000	39.4	4.3	43.7
2271	41.8	4.3	46.1
1542	44.1	4.4	48.5

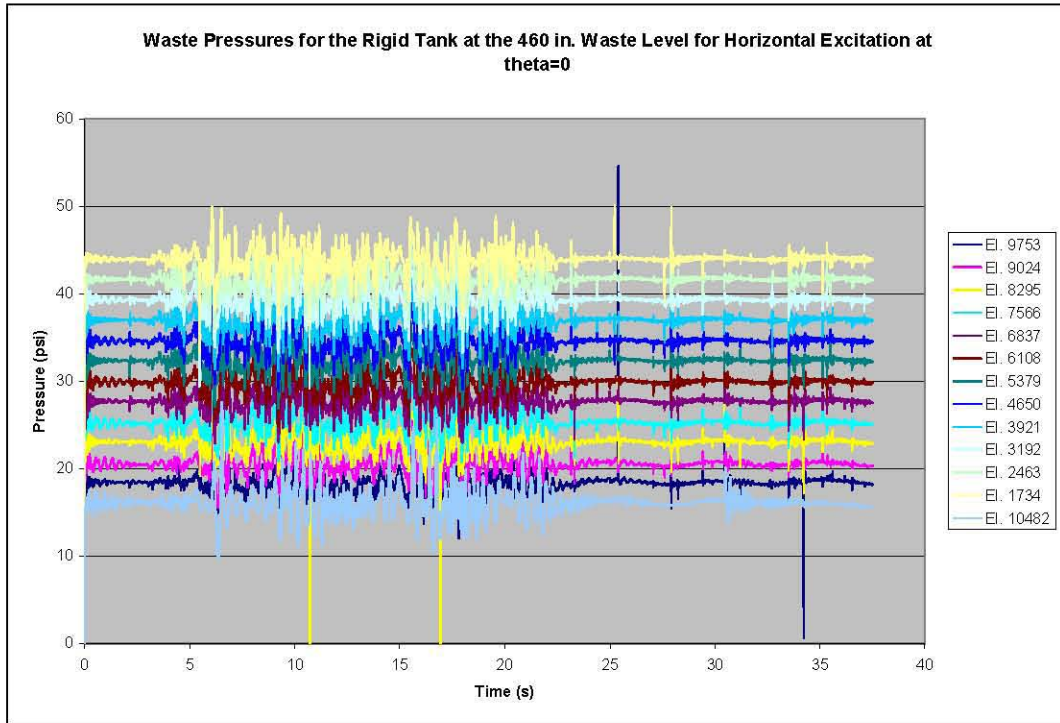


Figure 4-5. Waste Pressure Time Histories for the Rigid Tank with 460 Inches of Waste Under Horizontal Excitation at  $\theta=0$  Run at Absolute Pressure

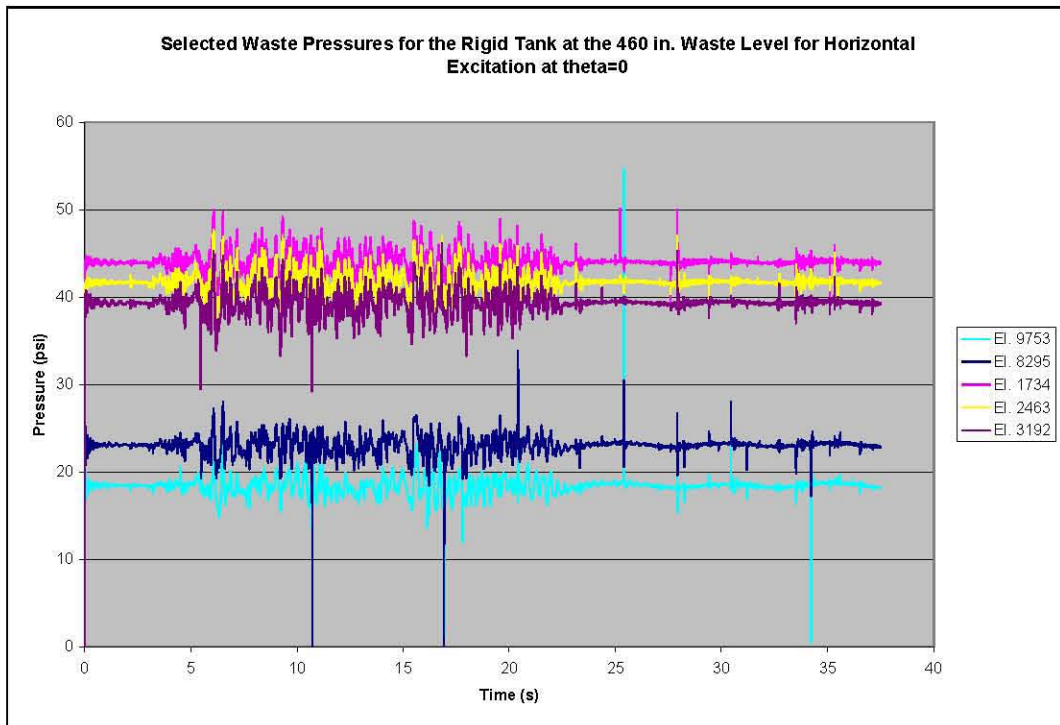


Figure 4-6. Selected Waste Pressure Time Histories for the Rigid Tank with 460 Inches of Waste Under Horizontal Excitation at  $\theta=0$  Run at Absolute Pressure

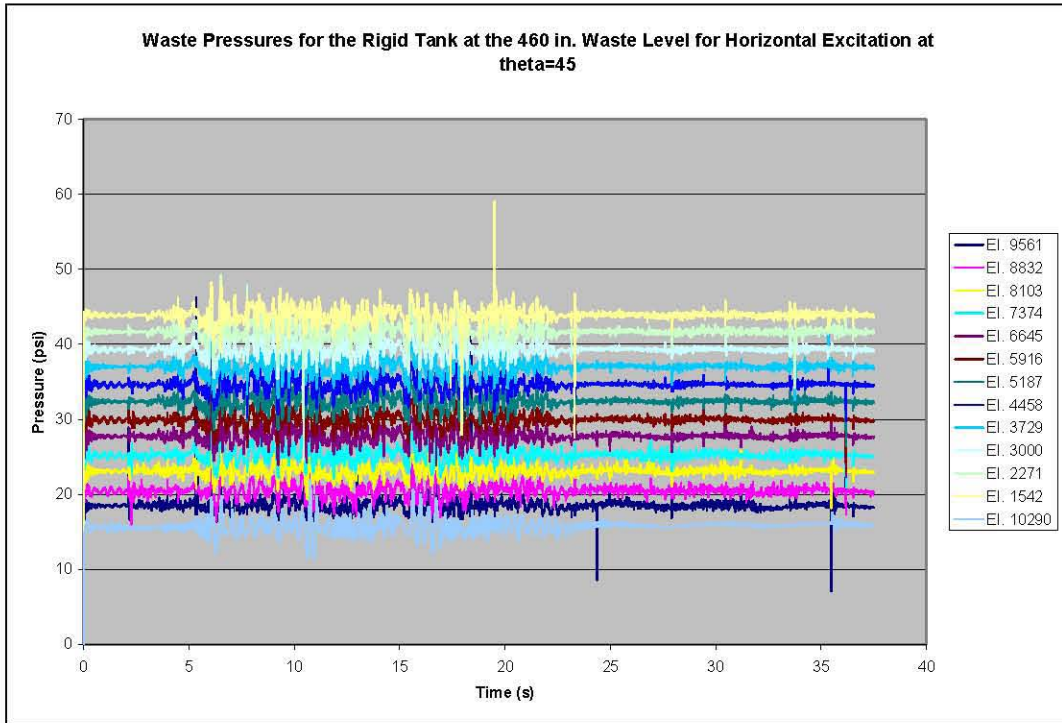


Figure 4-7. Waste Pressure Time Histories for the Rigid Tank with 460 Inches of Waste Under Horizontal Excitation at  $\theta=45^\circ$  Run at Absolute Pressure

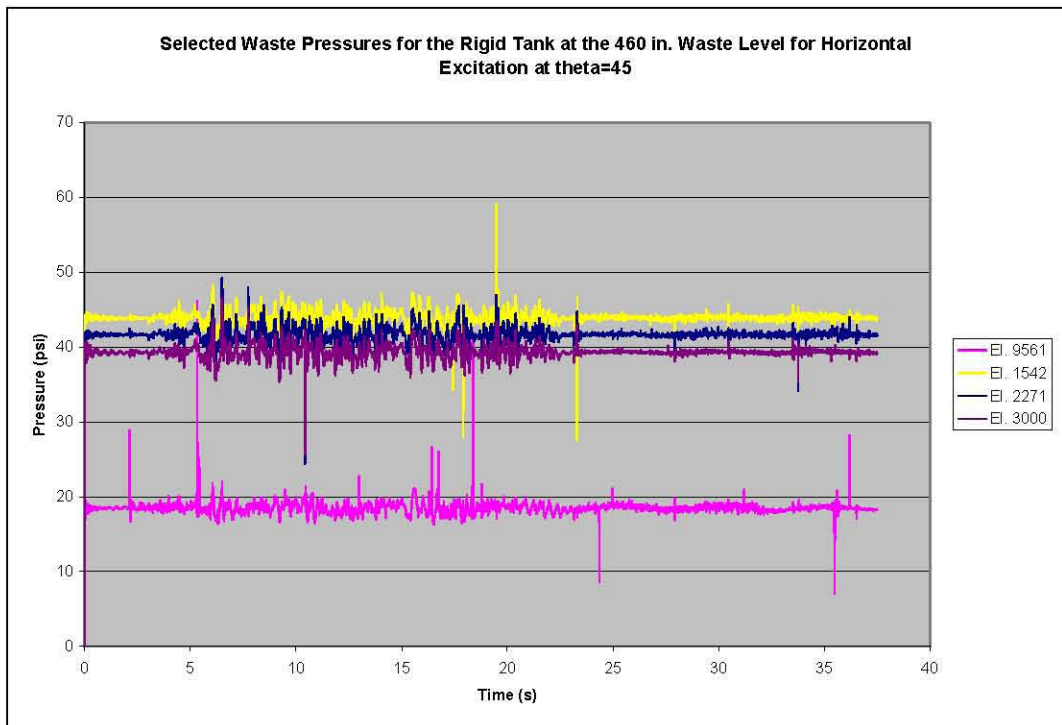


Figure 4-8. Selected Waste Pressure Time Histories for the Rigid Tank with 460 Inches of Waste Under Horizontal Excitation at  $\theta=45^\circ$  Run at Absolute Pressure

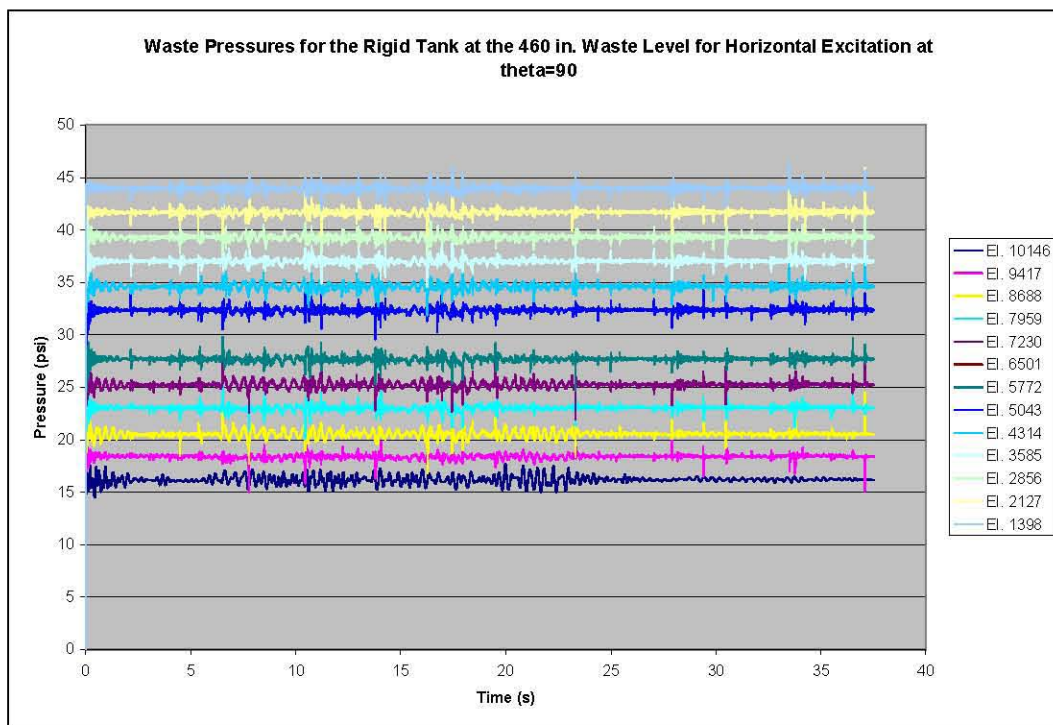


Figure 4-9. Waste Pressure Time Histories for the Rigid Tank with 460 Inches of Waste Under Horizontal Excitation at  $\theta=90^\circ$  Run at Absolute Pressure

Comparisons of the maximum and minimum pressures expected for an open-top tank to the maximum and minimum pressures obtained from the computer simulations (labeled as “actual max.” and “actual min.”) are shown in Figure 4-10, Figure 4-11, and Figure 4-12. Excursions from the open-top solution are evident in Figure 4-10 and Figure 4-11. In Figure 4-10 the biggest differences occur in waste elements 8295 and 9753 near the free surface. The pressure time histories for these elements are shown in Figure 4-6 where it can be seen that the large differences from the theoretical solution for the open-top tank come at isolated points. Similar remarks apply to Figure 4-11 and the time history plots shown in Figure 4-8.

The time history data were saved every 0.01 second, which is the same resolution as the seismic input. It is difficult to know which peaks in a time history record are physically meaningful and which peaks are due to numerical noise. However, two observations are readily apparent. First, if the high isolated peaks are neglected, the time history records show good agreement with the theory. Second, some of the high isolated peaks occur after 22.48 seconds, which is the end of the seismic input and after which the tank experiences unforced motion. These two observations suggest that peaks of this nature are caused by numerical noise in the solution and may not be physically meaningful.

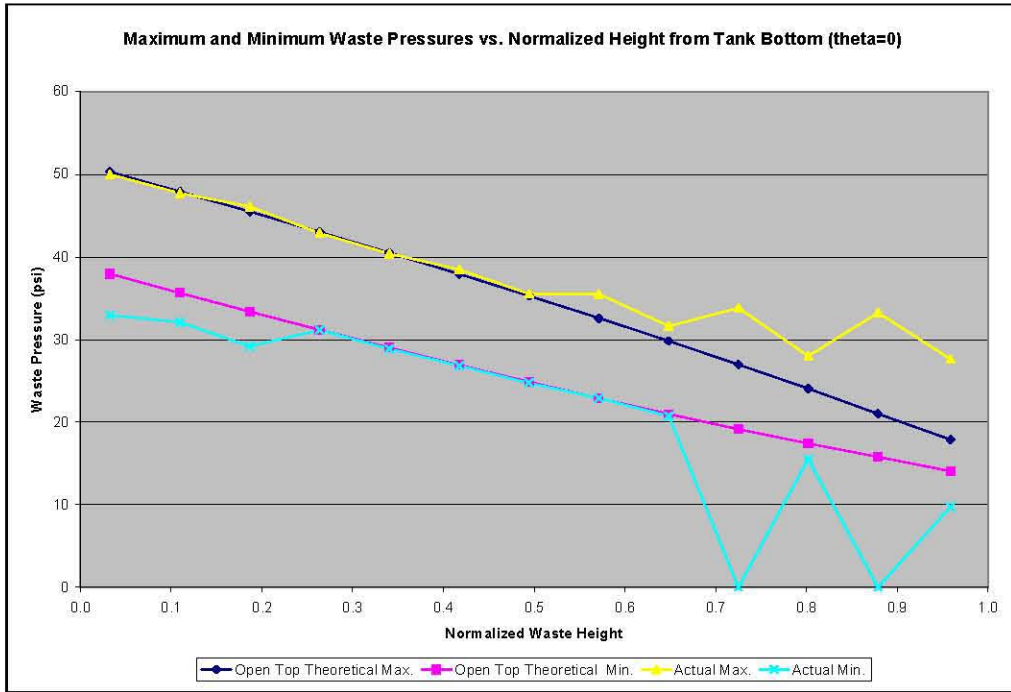


Figure 4-10. Maximum and Minimum Waste Pressures vs. Normalized Height from Tank Bottom for Horizontal Excitation of Rigid Tank at 460-Inch Waste Level and  $\theta=0$  Run at Absolute Pressure

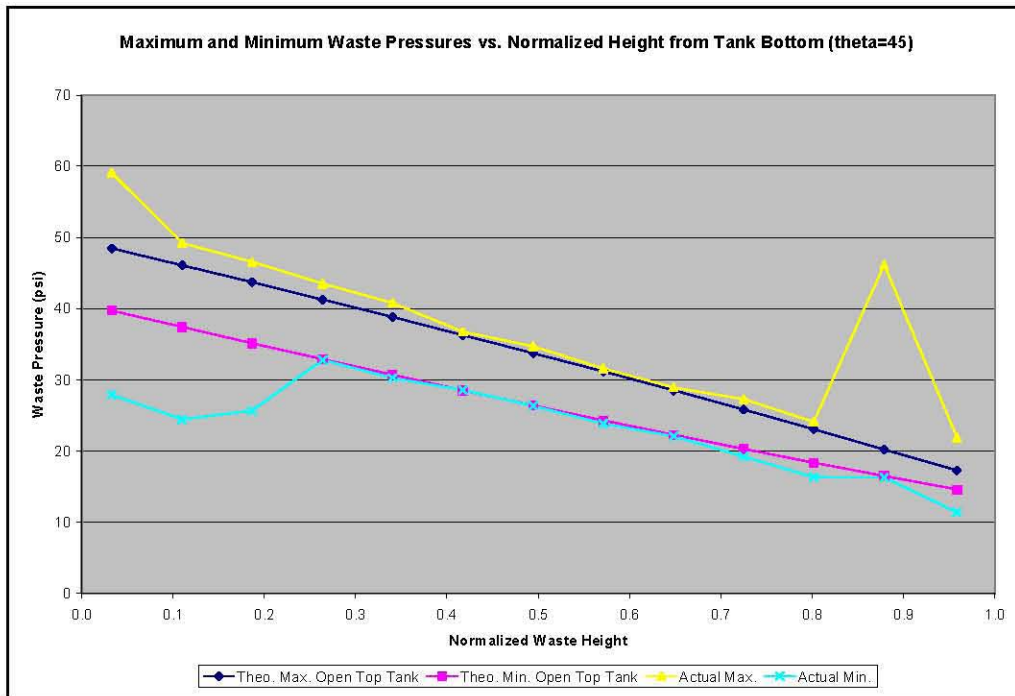
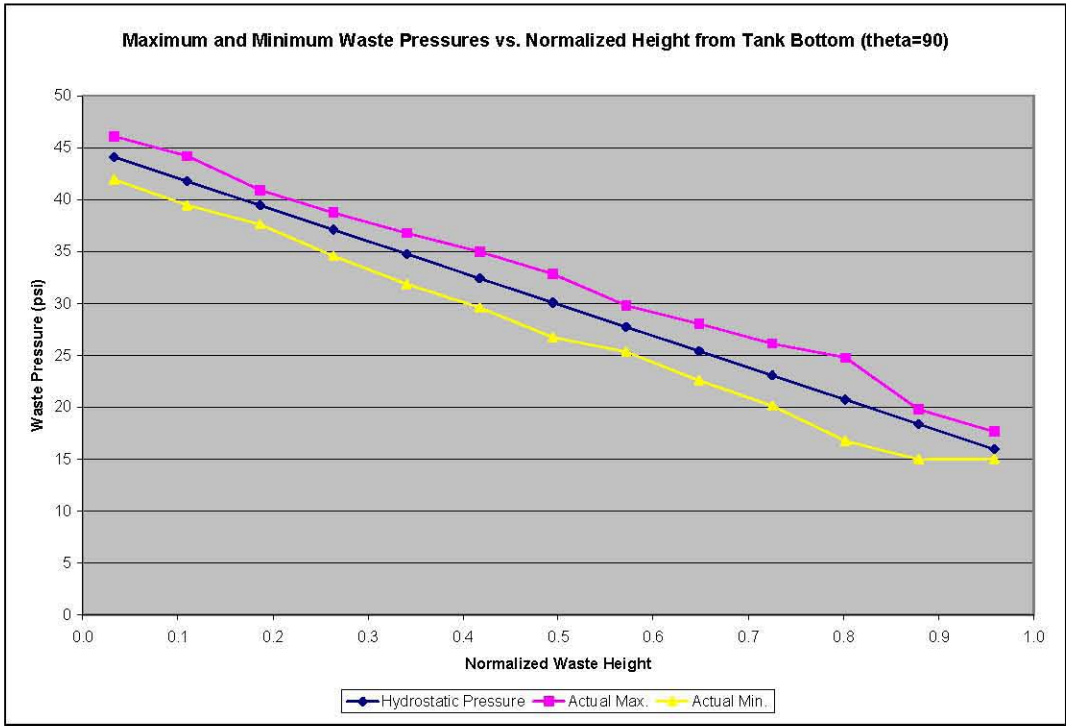


Figure 4-11. Maximum and Minimum Waste Pressures vs. Normalized Height from Tank Bottom for Horizontal Excitation of Rigid Tank at 460-Inch Waste Level and  $\theta=45^\circ$  Run at Absolute Pressure



**Figure 4-12.** Maximum and Minimum Waste Pressures vs. Normalized Height from Tank Bottom for Horizontal Excitation of Rigid Tank at 460-Inch Waste Level and  $\theta=90^\circ$  Run at Absolute Pressure

**4.2.2 Vertical Excitation Run at Absolute Pressure**

Waste element time histories for vertical excitation are shown in Figure 4-13 through Figure 4-19. Comparisons of maximum and minimum pressures from the simulation (labeled as “actual max.” and “actual min”) and the open-top solution are presented as Figure 4-20, Figure 4-21, and Figure 4-22. The agreement between the simulation and the open-top theory is good, but shows some deviations at elements near the free surface. The details for the  $\theta=0$ ,  $45$ , and  $90^\circ$  locations are shown in Figure 4-14, Figure 4-15, and Figure 4-16. Once again, at least some of the differences appear to be due to isolated peaks in the time history records.

According to the theory for an open-top tank, the maximum and minimum waste pressures for the bottom center waste element are  $47.7$  and  $40.4$  lbf/in<sup>2</sup>, respectively. The actual maximum and minimum pressures (that is, as calculated by Dytran®) shown in Figure 4-19 are  $48.4$  and  $38.3$  lbf/in<sup>2</sup>, respectively.

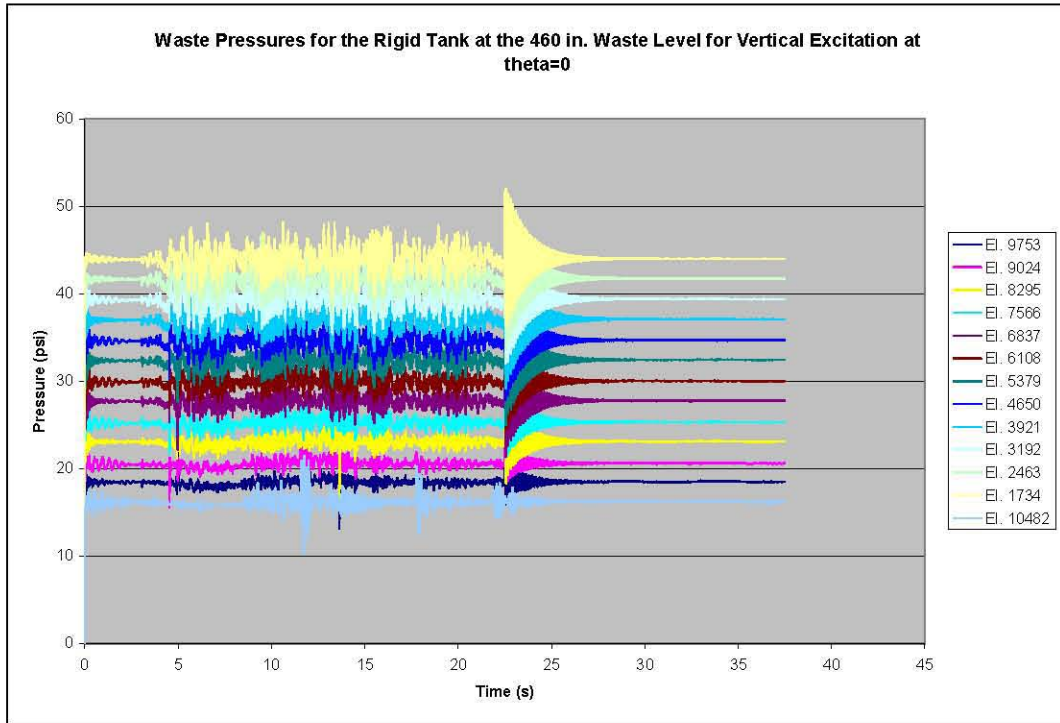


Figure 4-13. Waste Pressure Time Histories for the Rigid Tank with 460 Inches of Waste Under Vertical Excitation at  $\theta=0$  Run at Absolute Pressure

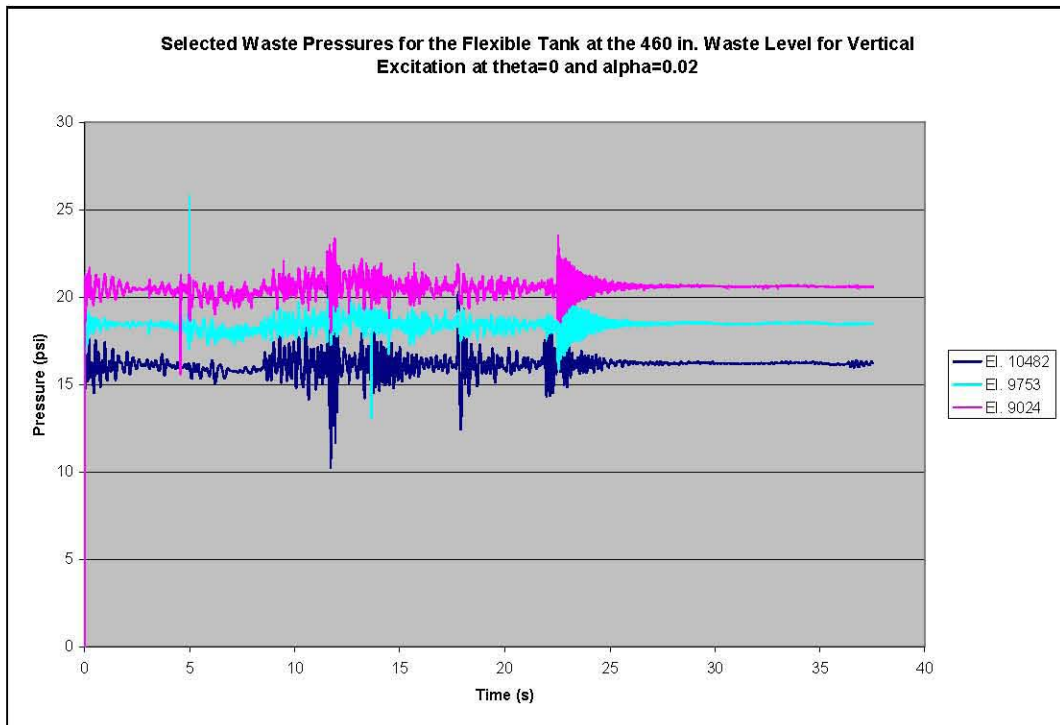


Figure 4-14. Selected Waste Pressure Time Histories for the Rigid Tank with 460 Inches of Waste Under Vertical Excitation at  $\theta=0$  Run at Absolute Pressure

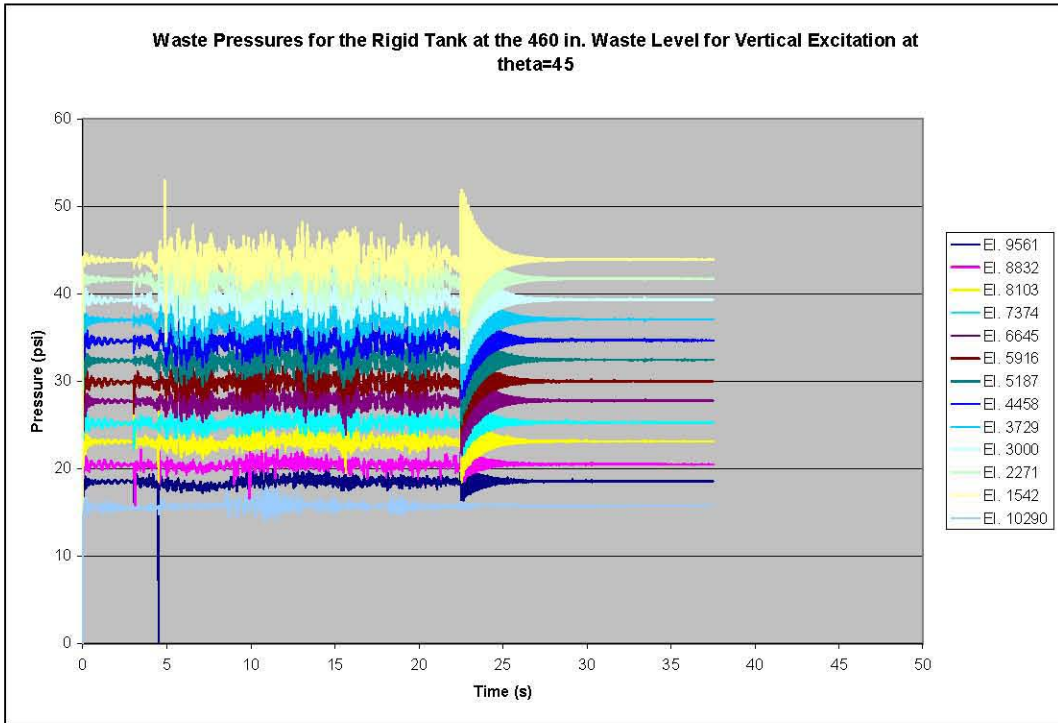


Figure 4-15. Waste Pressure Time Histories for the Rigid Tank with 460 Inches of Waste Under Vertical Excitation at  $\theta=45^\circ$  Run at Absolute Pressure

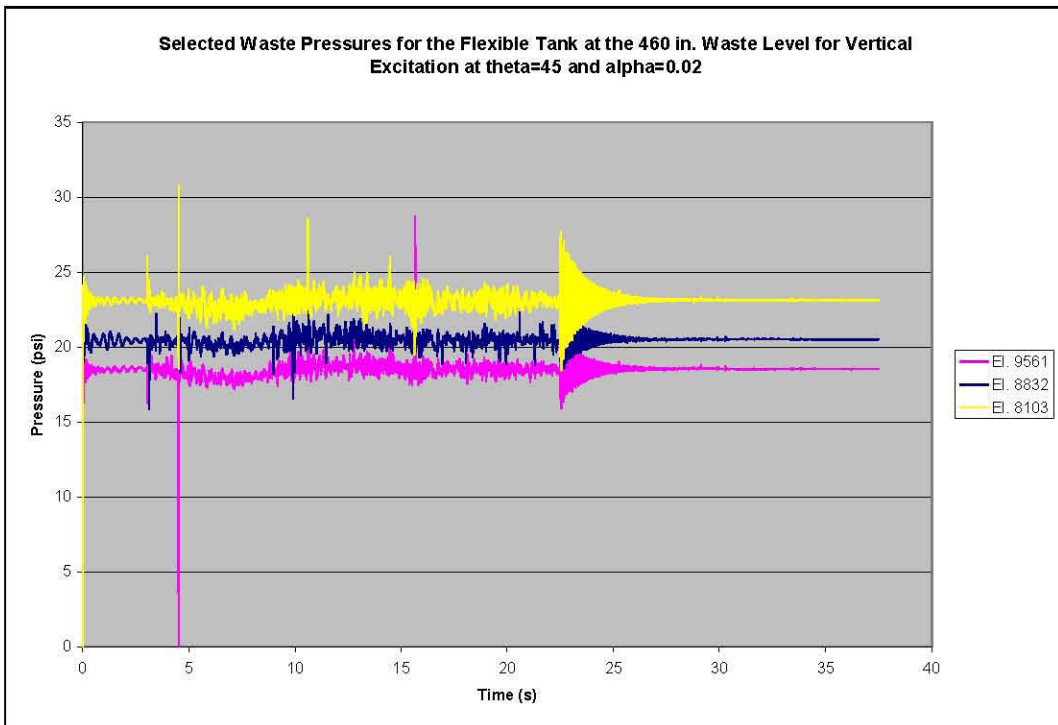


Figure 4-16. Selected Waste Pressure Time Histories for the Rigid Tank with 460 Inches of Waste Under Vertical Excitation at  $\theta=45^\circ$  Run at Absolute Pressure

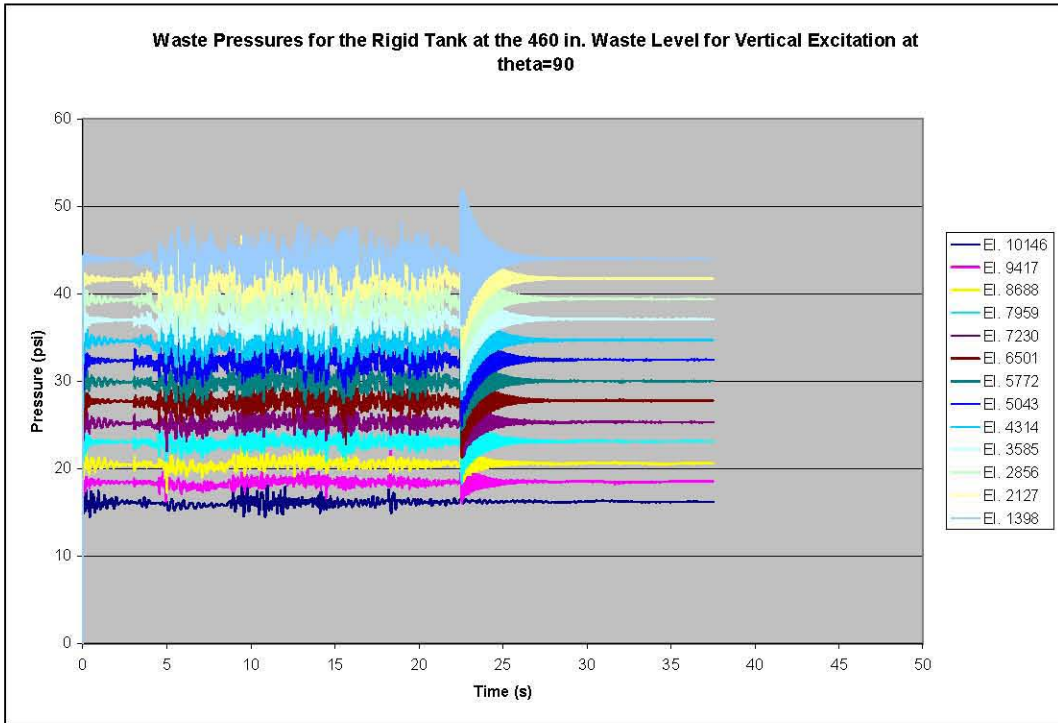


Figure 4-17. Waste Pressure Time Histories for the Rigid Tank with 460 Inches of Waste Under Vertical Excitation at  $\theta=90^\circ$  Run at Absolute Pressure

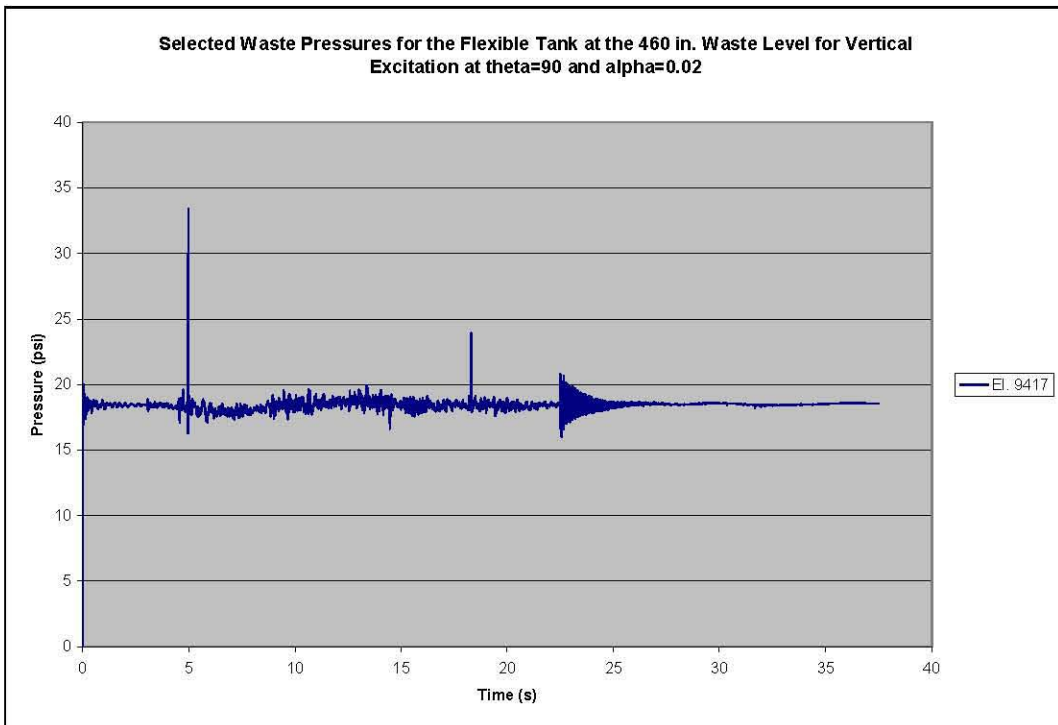


Figure 4-18. Selected Waste Pressure Time Histories for the Rigid Tank with 460 Inches of Waste Under Vertical Excitation at  $\theta=90^\circ$  Run at Absolute Pressure

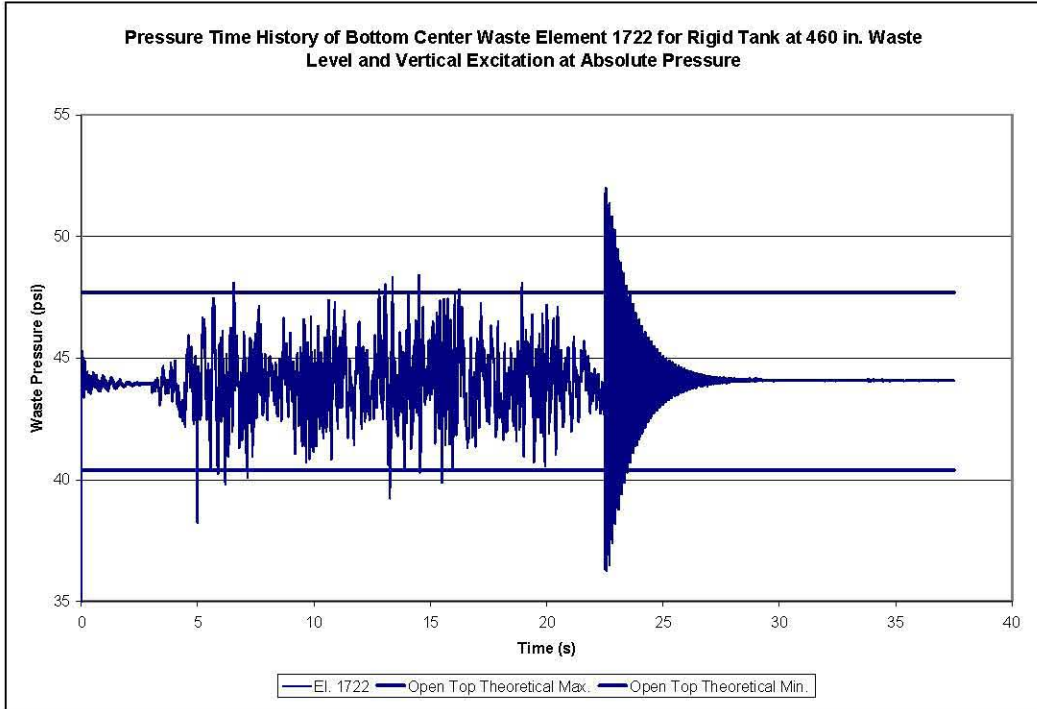


Figure 4-19. Pressure Time History for Bottom Center Waste Element for the Rigid Tank at the 460-Inch Waste Level and Vertical Excitation Run at Absolute Pressure

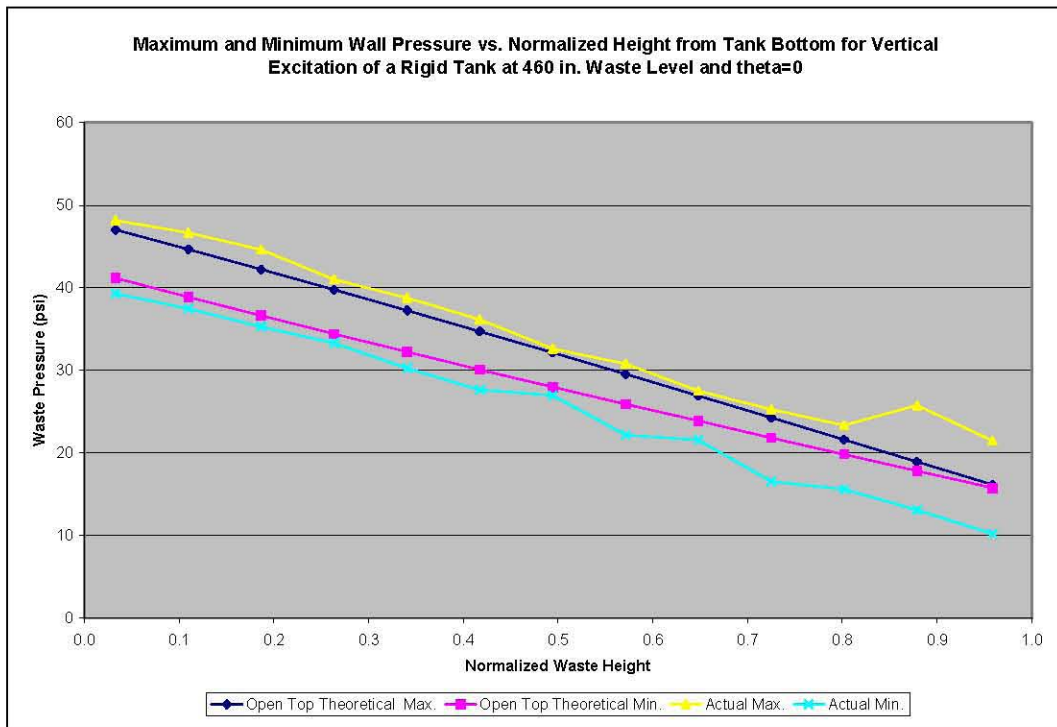


Figure 4-20. Maximum and Minimum Waste Pressures vs. Normalized Height from Tank Bottom for Vertical Excitation of Rigid Tank at 460-Inch Waste Level and  $\theta=0$  Run at Absolute Pressure

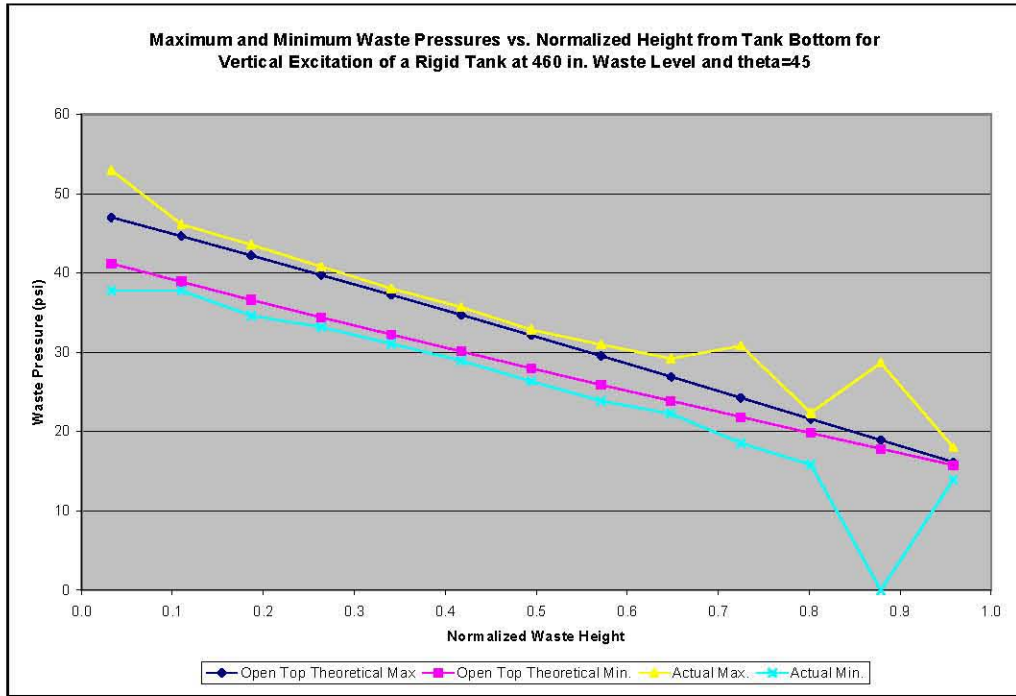


Figure 4-21. Maximum and Minimum Waste Pressures vs. Normalized Height from Tank Bottom for Vertical Excitation of Rigid Tank at 460-Inch Waste Level and  $\theta=45^\circ$  Run at Absolute Pressure

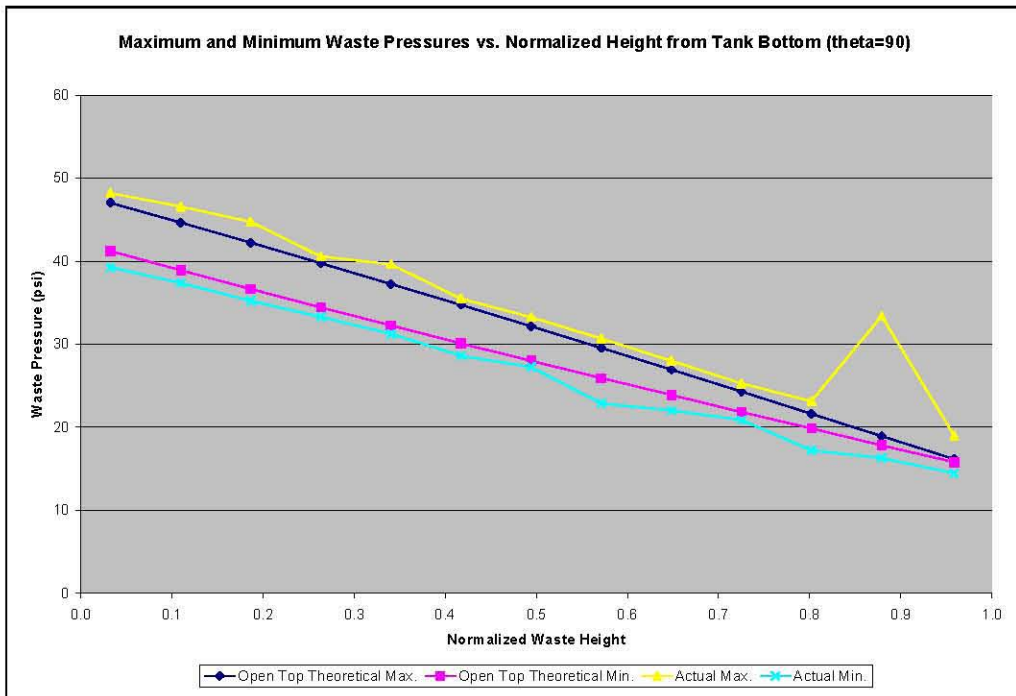


Figure 4-22. Maximum and Minimum Waste Pressures vs. Normalized Height from Tank Bottom for Vertical Excitation of Rigid Tank at 460-Inch Waste Level and  $\theta=90^\circ$  Run at Absolute Pressure

### 4.3 Slosh Height Results

The time history of the maximum slosh height over all waste elements is shown as Figure 4-23. The maximum slosh height according to the theory for the open-top tank is 24.5 inches while the maximum slosh height from the simulation is 21.1 inches or 86% of the open-top theoretical value. Again, it appears that the presence of the dome acts to inhibit the convective response. Recall also that the only damping present for the rigid tank simulations are the artificial bulk viscosities that are not expected to affect the convective response or maximum slosh height. In other words, the lower maximum slosh height does appear to be due to the presence of the dome rather than by over-damping of the convective response.

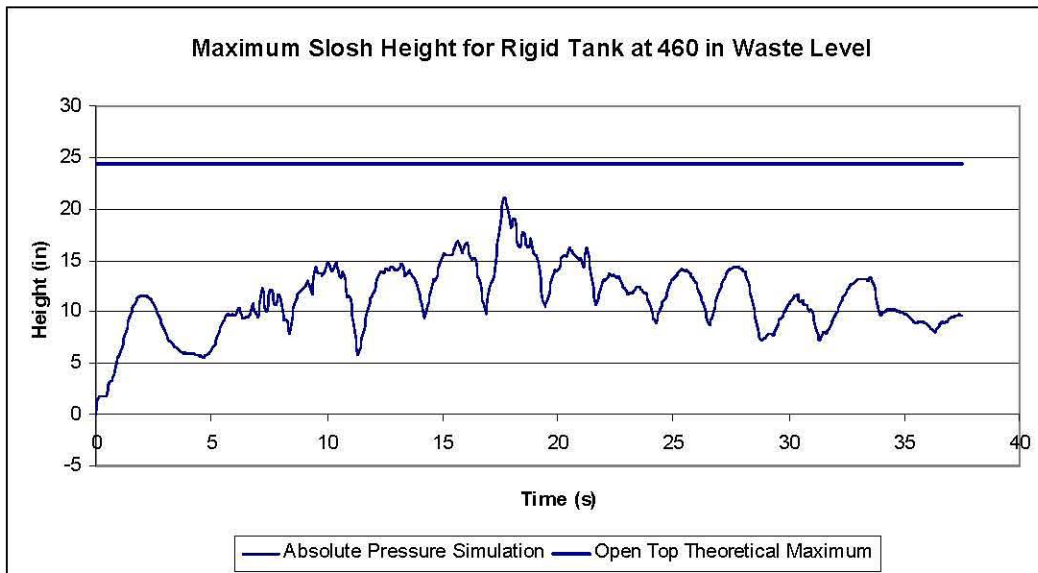
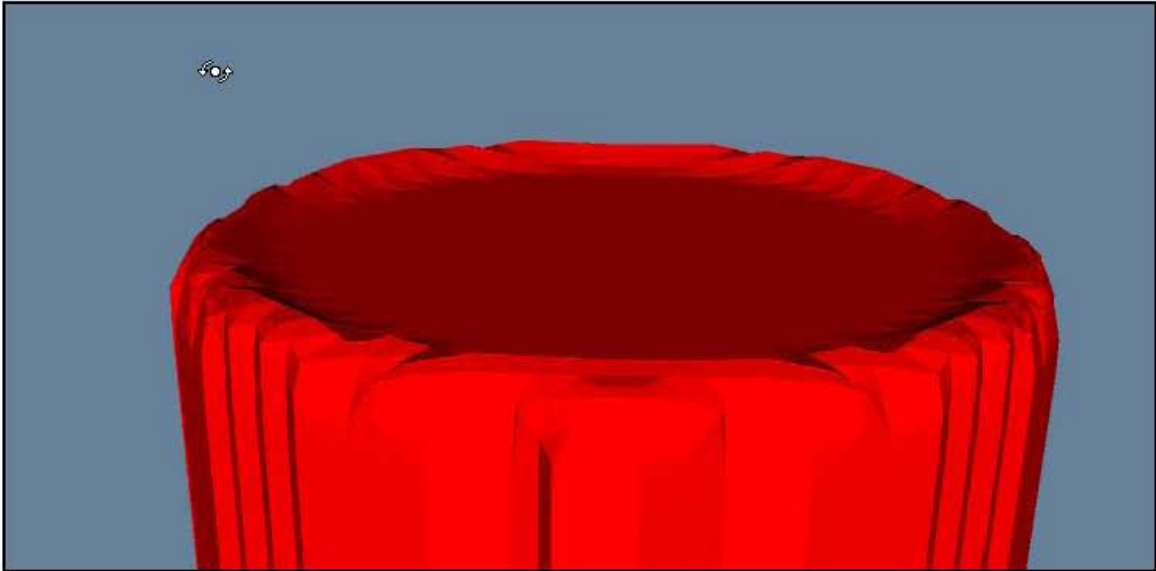


Figure 4-23. Maximum Slosh Height Time History Over All Waste Elements for Horizontal Excitation of the Rigid Tank at the 460-Inch Waste Level

The unusual behavior noted in Figure 4-23 is that the maximum height of the free surface is greater than 10 inches during the first 5 seconds under gravity load alone. This was not seen in the maximum slosh height time histories shown in Figure 3-20 for the 422-inch waste level, and it appears to be either a limitation in the post-processing routine used to calculate the free surface height at the higher waste level or else a result of the mesh density. It may very well be that this effect could be minimized by including more resolution in the waste element mesh where the waste elements contact the dome, but this was not tested.

Investigation of the waste-free surface shape under gravity loading showed that the initial “slosh height” under gravity loading was actually the result of increased waste height near the tank boundary that appears similar to a meniscus, as shown in Figure 4-24.



**Figure 4-24.** Plot of Waste-Free Surface Under Gravity Loading Only for the Rigid Tank at the 460-Inch Waste Level

Intentionally left blank.

## 5.0 Flexible Tank Dytran® Model at 422-Inch Waste Level

### 5.1 Damping Implementation and Calibration

The section presents the results of several runs that were performed to determine the best way to implement damping and the best value of the dynamic relaxation factor to be used in Dytran® in order to achieve the desired effective damping. The target effective damping was based on the guidelines given in DOE-STD-1020-2002. Target damping for the fluid convective response is 0.5% critical damping, and the target effective damping for the fluid impulsive response is in the range of 2-4% critical damping.

The initial screening as to the appropriate value of the dynamic relaxation factor was made based on the decay behavior and peak values of the horizontal hydrodynamic force time history. However, very similar behavior occurs in other response parameters such as pressure time histories and nodal displacement time histories.

The initial calibration study was performed by running the simulations at gage rather than absolute pressure, because initially it was more difficult to get stable solutions running at absolute pressure. Once stable solutions were achieved using absolute pressure, and the best damping implementation had been identified tentatively, this configuration was rerun at absolute pressure to ensure that the gage and absolute pressure simulations behaved similarly. Not all cases described below were rerun at absolute pressure – in fact, a stable solution was not achieved running Case 3 (described below) at absolute pressure.

The damping implemented in the Dytran® tank models consists of a single damping or dynamic relaxation parameter that is introduced in the central difference integration scheme of the equations of motion using the VISCDMP command. The damping takes the form

$$v^{n+\frac{1}{2}} = v^{n-\frac{1}{2}}(1 - \alpha) + a^n \cdot \Delta t, \quad (5-1)$$

where  $v$  denotes the grid point velocity,  $a$  is the acceleration,  $\Delta t$  is the time step, and  $\alpha$  is the dynamic relaxation parameter or damping coefficient (not the same as the mass proportional damping parameter  $\alpha$  in ANSYS®). The dynamic relaxation parameter can be defined individually for each available structural element type. In the tank models, the damping was applied to the grid points of the tank shell elements, including the shell elements that form the rigid portion of the tank model.

The choice of the dynamic relaxation parameter depends on the frequency, and the critical damping value at a given frequency, and according to the guideline given in MSC (2005a), should be taken to be approximately 5/3 times the product of the frequency and the time step. That is,

$$\alpha_{crit} = \frac{5}{3} \omega \cdot \Delta t. \quad (5-2)$$

It is clear from the Dytran® damping formulation that frequencies below the selected frequency will be over-damped and frequencies above the selected frequency will be under-damped.

The impulsive frequency for the tank calculated via Equation 4.16 in BNL (1995) is approximately 7 Hz. The nominal damping value to enforce 4% critical damping at the impulsive frequency of 7 Hz is  $3.4 \times 10^{-4}$ .

$$\alpha_{impulsive} = (0.04)\left(\frac{5}{3}\right)(2\pi f_i)\Delta t = (0.04)\left(\frac{5}{3}\right)(2\pi \cdot 7\text{Hz})(1.158 \times 10^{-4} \text{ s}) = 3.4 \times 10^{-4} \quad (5-3)$$

Several different combinations of damping were run to determine the effect of damping on the solution. The cases presented are as follows:

**Case 1:** The damping parameter ( $\alpha$ ) was fixed throughout the simulation at the nominal value of  $3.4 \times 10^{-4}$  per MSC (2005a) with the intent of enforcing 4% critical damping at the impulsive frequency.

**Case 2 (a, b, c, and d):** The damping parameter was fixed throughout the simulation at much higher values of 0.08, 0.04, 0.02, and 0.01. These values were selected by trial and error by attempting to achieve a balance between an appropriate effective damping during the initial free-vibration period and the response during the seismic transient. These damping values were intended to provide approximately 4% critical damping during the initial free-vibration phase of the breathing mode under the gravity load. According to Equation 4.53 in BNL (1995), the breathing mode frequency of the tank is 6.1 Hz for the 422-inch waste level.

**Case 3:** The damping parameter was set to 0.08 during the initial application of the gravity load, then was set to zero at the beginning of the seismic loading and left at zero for the remainder of the simulation.

The damping in Cases 2 a, b, c, and d was increased significantly above the damping in Case 1 because it was apparent from the results in Case 1 that the initial free-vibration period was highly under-damped, in spite of the guideline given in MSC (2005a).

The effects of damping in each of the cases will be determined from the results of the initial free-vibration period and the horizontally applied seismic load. The results reviewed consist of the peak horizontal hydrodynamic force, waste pressures, stresses, and displacement time history of a node near the middle of the tank wall.

Due to the extensive amount of data, the results presented during the initial evaluation of damping will focus mostly on the coupling surface reaction forces for the different cases. However, the same conclusions would be reached by studying the behavior of the other system responses such as the waste pressures, tank stresses, or nodal displacements.

The effective damping during the initial free-vibration phase was quantified by determining the rate of decay of the various responses. The effective damping during the seismic excitation was qualitatively determined by comparing the actual peak responses to the theoretical peak responses.

Application of the logarithmic decrement  $\delta$  to the decay of a selected response implies that for a constant critical damping ratio  $\xi$ , the ratio of successive peak responses is constant. For small critical damping ratios, the logarithmic decrement can be approximated as

$$\delta \equiv \ln\left(\frac{x_1}{x_2}\right) \approx 2\pi\xi. \quad (5-4)$$

More generally, the number of cycles  $n$  required to achieve a  $R\%$  reduction in amplitude for a given critical damping ratio  $\xi$  is

$$n \approx \frac{1}{2\pi\xi} \ln\left(\frac{100}{100-R}\right). \quad (5-5)$$

The investigation showed that the effective damping appeared to be slightly higher during the seismic excitation than during the initial free-vibration phase. Because damping is applied to grid point motion in Dytran<sup>®</sup>, this is likely due to the fact that many more grid points are moving during the seismic excitation (the dome and primary tank bottom), and much more mass is in motion.

The simulation time of the initial free-vibration phase varied depending on the case. The goals of the initial phase were to achieve a steady-state solution to the gravity loading before introducing the seismic load, to quantify the effective system damping by response decay, and to isolate the breathing mode frequency of the tank. The simulation time needed to achieve a steady-state solution to the gravity load depends on the damping. A lower value of the damping parameter requires a longer initial period, whereas a shorter initial phase will suffice with a higher value of the damping parameter. All cases could have been run with a long initial phase, but this would have resulted in significant run time penalties.

## 5.2 Hydrodynamic Forces

### 5.2.1 Horizontal Excitation

The peak horizontal hydrodynamic forces for the flexible tank are again calculated via Equation 4.31 in BNL (1995) with the instantaneous accelerations replaced by the appropriate spectral accelerations. If the contributions of the impulsive mode and first three convective modes are combined in a square-root-sum-of-squares (SRSS) fashion, the theoretical maximum horizontal hydrodynamic force is  $7.56 \times 10^6$  lbf. The above value is based on spectral accelerations from the 4% damped spectrum.

For horizontal excitation in Case 1, gravity was run for 15 seconds before the application of the seismic input. At the end of the seismic input, the simulation was run for approximately 16 seconds of unforced motion.

The peak horizontal reaction force shown in Figure 5-1 for Case 1 is  $7.52 \times 10^6$  lbf, or 99% of the theoretical value. The sloshing period of approximately 5 seconds is reflected at the end of the horizontal force time history. The effective damping can be evaluated by reviewing the decay of the vertical coupling surface reaction force shown in Figure 5-1. The vertical reaction force trace reflects the breathing mode frequency of approximately 6 Hz as shown in Figure 5-2.

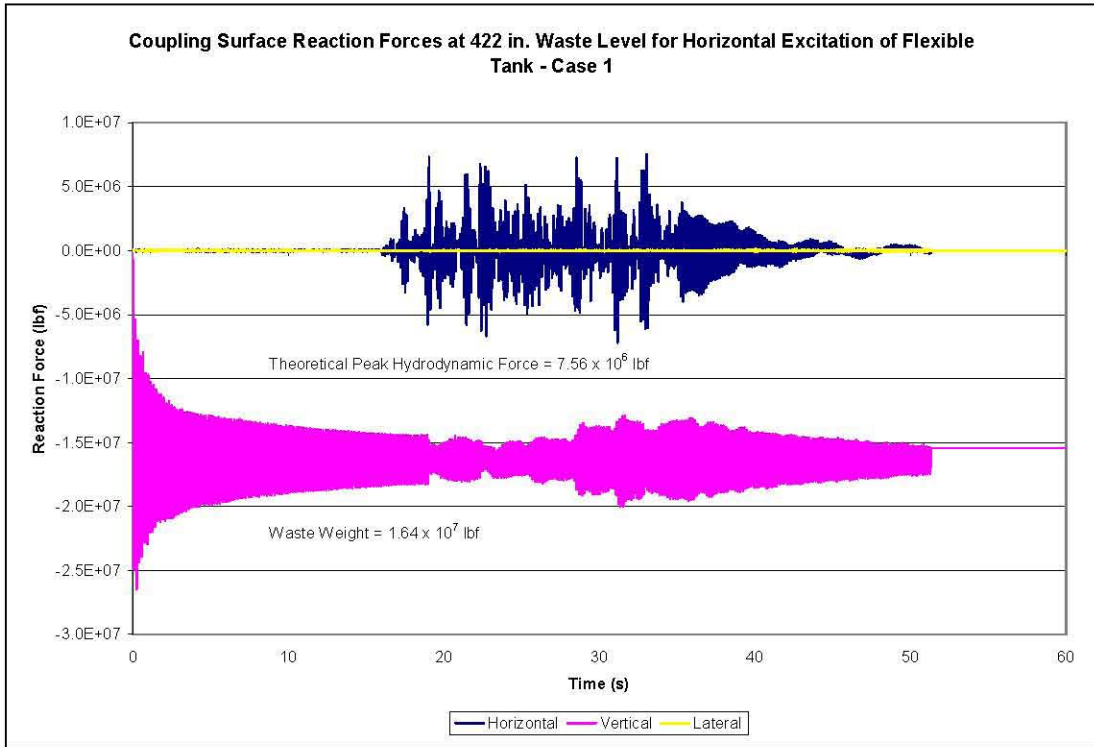


Figure 5-1. Coupling Surface Reaction Forces for the Flexible Tank Under Horizontal Seismic Input at Gage Pressure– Case 1

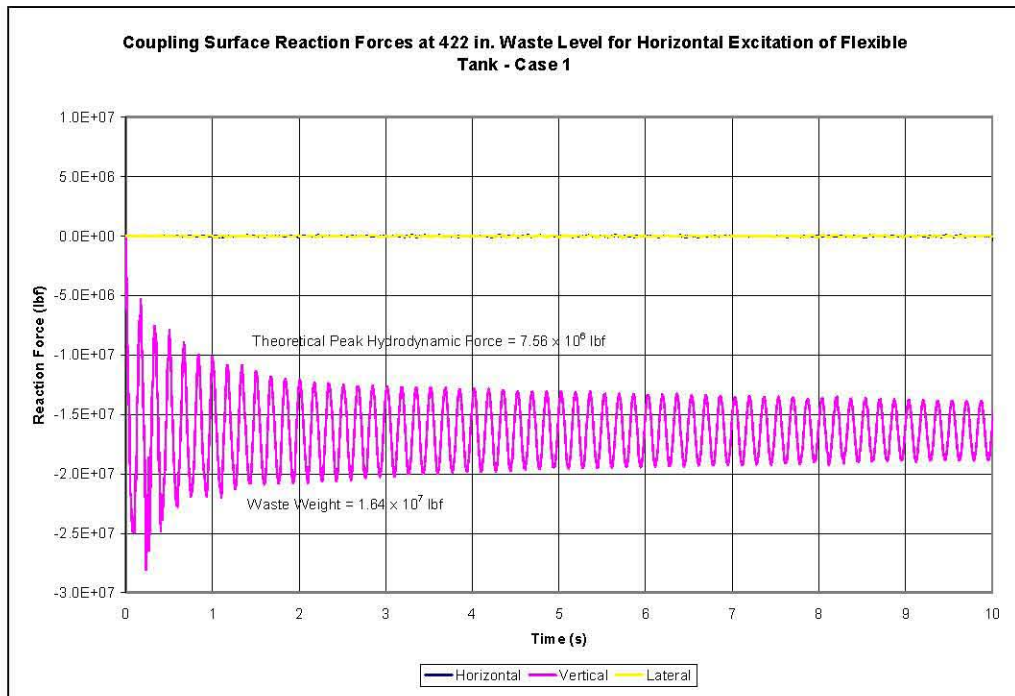


Figure 5-2. Coupling Surface Reaction Forces for the Flexible Tank Under Horizontal Seismic Input at Gage Pressure During the Initial Free-Vibration Phase – Case 1

It is evident in Figure 5-1 and Figure 5-2 that with the relatively low damping parameter in Case 1, the effective damping decreases during the initial free-vibration phase. The logarithmic decrement equation also shows that for 4% critical damping, the ratio of successive peaks should be 1.29. That is, each subsequent peak should be approximately 78% of the preceding peak. With this rate of decay, the vertical reaction force should be within 10% of the steady-state value within nine cycles (~1.5 seconds) and within 1% of the steady-state value within 18 cycles (~3 seconds). Clearly, the decay rate shown in Figure 5-1 and Figure 5-2 is much slower, showing that the solution is under-damped during the initial free-vibration phase. Similarly, the solution is under-damped during the final free-vibration phase following the seismic excitation. On the other hand, because the peak horizontal reaction force achieves 99% of the theoretical value during the seismic transient, the solution is apparently not under-damped during the seismic excitation.

Similar behavior is displayed in the decay of waste pressures and tank stresses. As an example, the hoop stress time history for element 433 near the mid-height of the tank wall at  $\theta=0$  is shown in Figure 5-3.

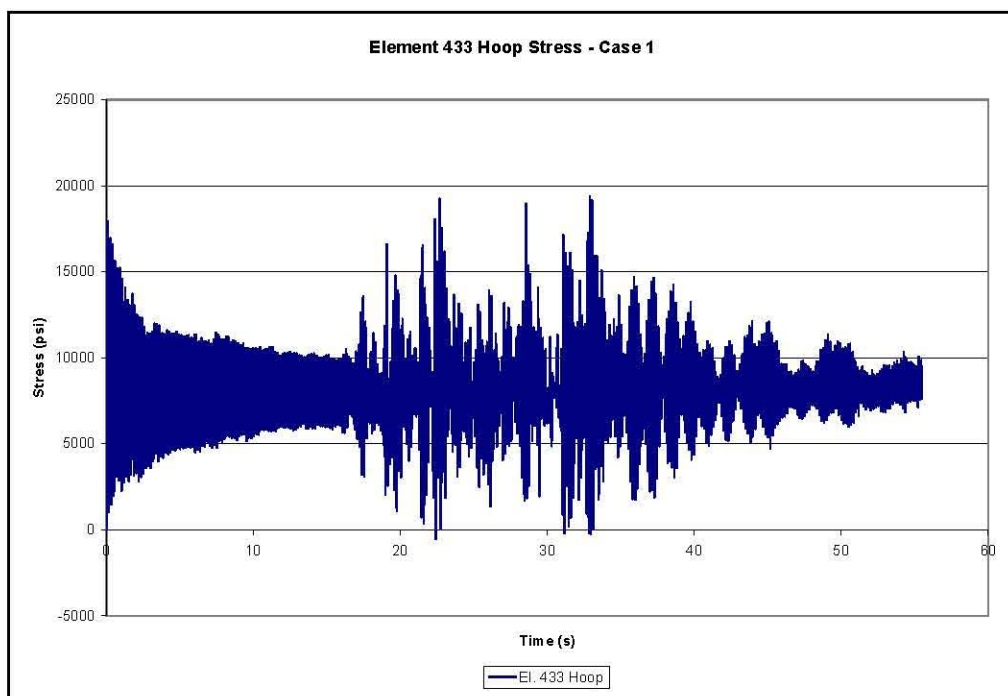


Figure 5-3. Mid-Wall Hoop Stress for Flexible Tank at Gage Pressure and  $\theta=0$  – Case 1

Since the initial free-vibration phase was under-damped in Case 1, the damping parameter was increased in Cases 2a, 2b, 2c, and 2d in an attempt to achieve approximately 4% damping during the initial free-vibration phase. The values of 0.08, 0.04, 0.02, and 0.01 were selected based on trial and error and gave initial damping in the range of a few percent based on the decay during the initial gravity phase.

For horizontal excitation in Case 2a, gravity was run for 2 seconds before the application of the seismic input. At the end of the seismic input, the simulation was run for an additional 20 seconds of unforced motion. The coupling surface reaction forces for Case 2a are shown in Figure 5-4 and Figure 5-5. The results show that the vertical reaction force has essentially reached the steady-state value in 1.5 seconds (9 cycles), giving an effective damping during the initial phase of approximately 7-8% critical damping.

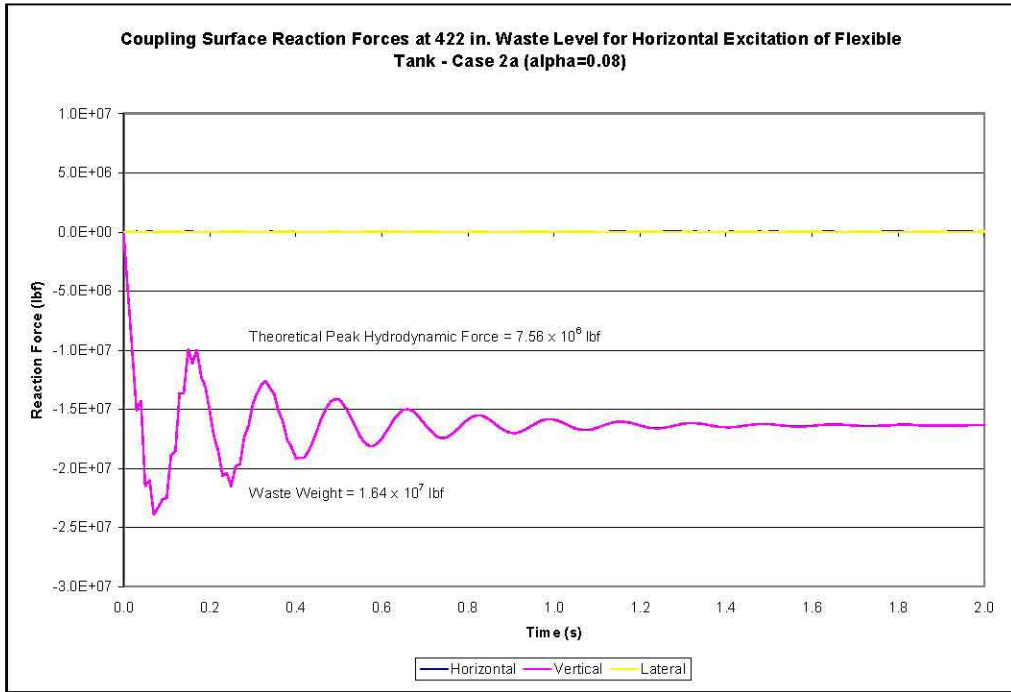


Figure 5-4. Coupling Surface Reaction Forces at the 422-Inch Waste Level for the Flexible Tank at Gage Pressure Under Horizontal Seismic Input During the Initial Free-Vibration Phase – Case 2a (alpha=0.08)

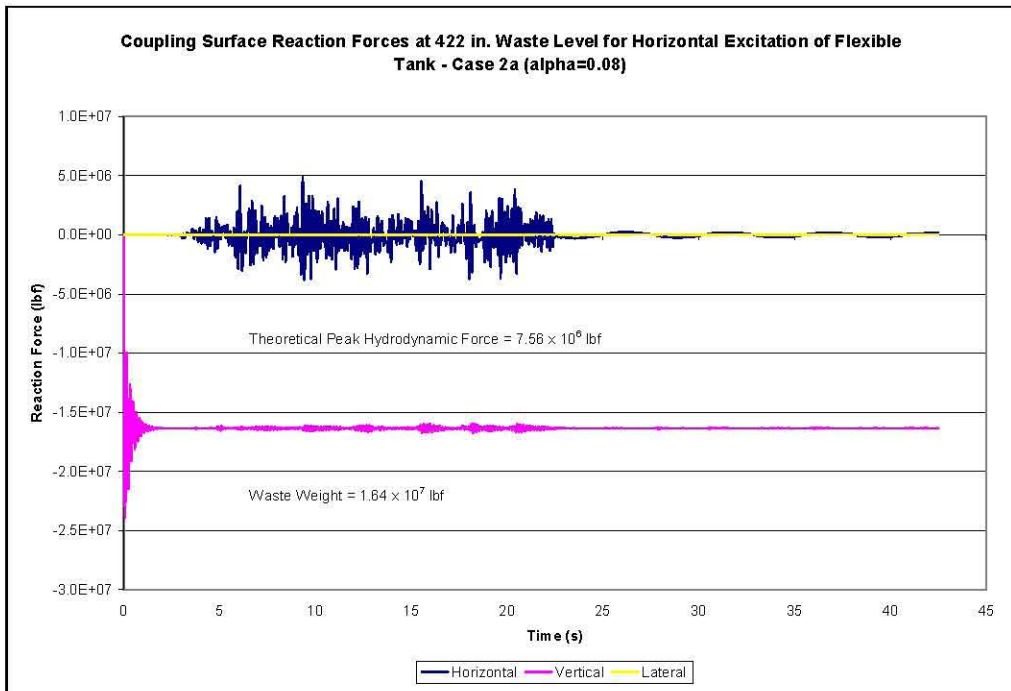
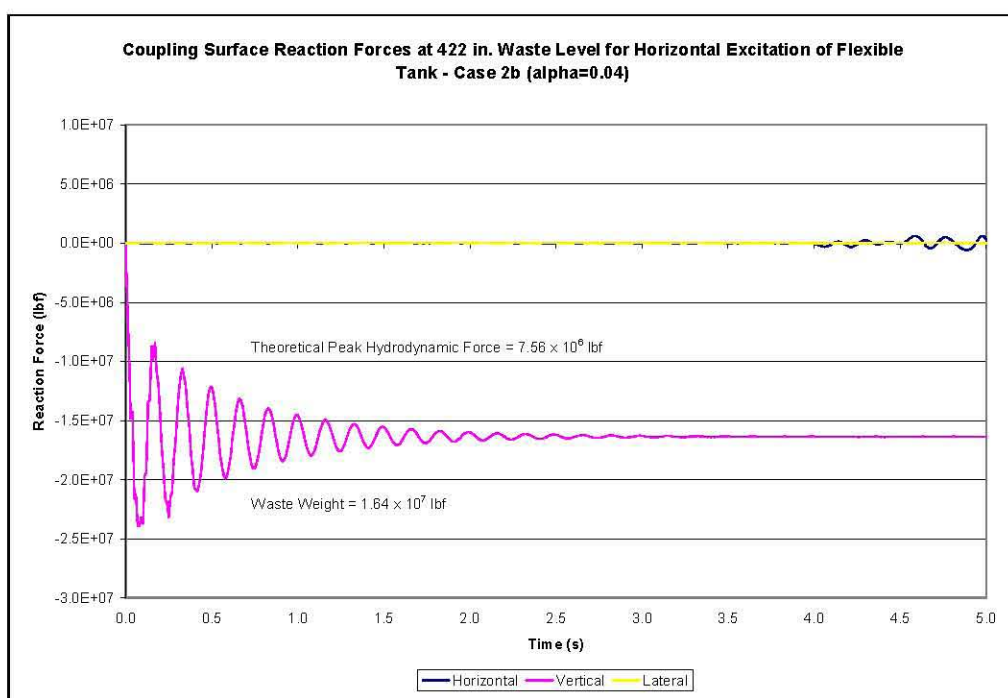


Figure 5-5. Coupling Surface Reaction Forces at the 422-Inch Waste Level for the Flexible Tank at Gage Pressure Under Horizontal Seismic Input – Case 2a (alpha=0.08)

The peak horizontal hydrodynamic reaction force shown in Figure 5-5 is approximately  $5 \times 10^6$  lbf, or 63% of the theoretical value, showing that the solution is still over-damped during the seismic excitation.

Essentially, the same conclusions regarding effective damping during free-vibration can be drawn from other response parameters such as pressure time-history plots or from time-history plots of nodal displacements along the tank wall.

For horizontal excitation in Case 2b, gravity was run for 3 seconds before the application of the seismic input. At the end of the seismic input, the simulation was run for an additional 19 seconds of unforced motion. The coupling surface reaction forces for Case 2b are shown in Figure 5-6 and Figure 5-7. The results show that the vertical reaction force has essentially reached the steady-state value in 3.0 seconds (18 cycles) giving an effective damping during the initial phase of approximately 4% critical damping.



**Figure 5-6.** Coupling Surface Reaction Forces at the 422-Inch Waste Level for the Flexible Tank at Gage Pressure Under Horizontal Seismic Input During the Initial Free-Vibration Phase – Case 2b (alpha=0.04)

The peak horizontal hydrodynamic reaction force shown in Figure 5-7 is approximately  $6.4 \times 10^6$  lbf, or 85% of the theoretical value, showing that the solution is still over-damped during the seismic excitation.

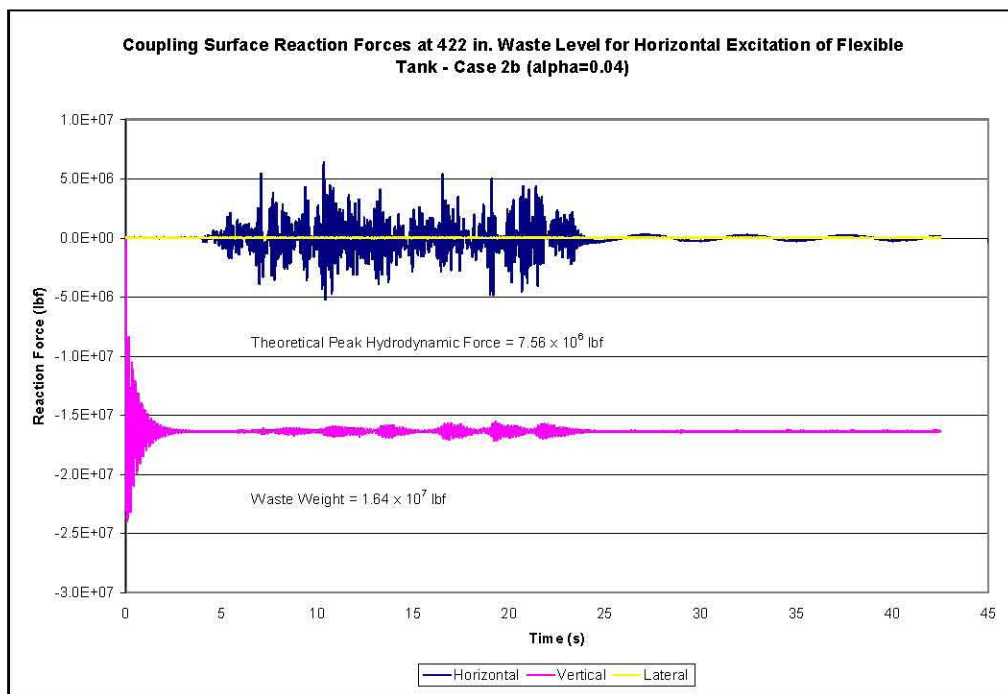


Figure 5-7. Coupling Surface Reaction Forces at the 422-Inch Waste Level for the Flexible Tank at Gauge Pressure Under Horizontal Seismic Input – Case 2b (alpha=0.04)

In Case 2c, gravity was run for 5 seconds before the application of the seismic input, and the simulation was run for an additional 20 seconds of unforced motion after the end of the seismic excitation. The coupling surface reaction forces for Case 2c are shown in Figure 5-8 and Figure 5-9. The vertical reaction force has essentially reached the steady-state value in 5-6 seconds (30-36 cycles), giving an effective damping during the initial phase of approximately 2% critical damping. The breathing mode frequency of approximately 6 Hz is apparent in the vertical reaction force.

The peak horizontal hydrodynamic reaction force shown in Figure 5-9 is  $7.09 \times 10^6$  lbf, or 94% of the theoretical value, when the problem is run at gauge pressure. The first convective period of slightly greater than 5 seconds is displayed in the horizontal reaction force during the period of unforced motion during the last 20 seconds of the simulation. The coupling surface reaction force during the first 3 seconds of the second period of unforced motion is shown as Figure 5-10. Evident in that plot are the impulsive frequency of slightly less than 7 Hz in the horizontal reaction force and the breathing mode frequency of approximately 6 Hz in the vertical reaction force.

When this case was rerun at absolute pressure as discussed in Section 5.3, the peak horizontal reaction force increased slightly to  $7.25 \times 10^6$  lbf, or 96% of the theoretical value as shown in Figure 5-12. The frequency behavior remained the same as shown in Figure 5-11 and Figure 5-13. The peak reaction force during the final free-vibration phase shown in Figure 5-12 decays approximately 20% over three cycles from the peak at 29 seconds to the peak at 45 seconds. This results in slightly greater than 1% damping for the convective response during free oscillation.

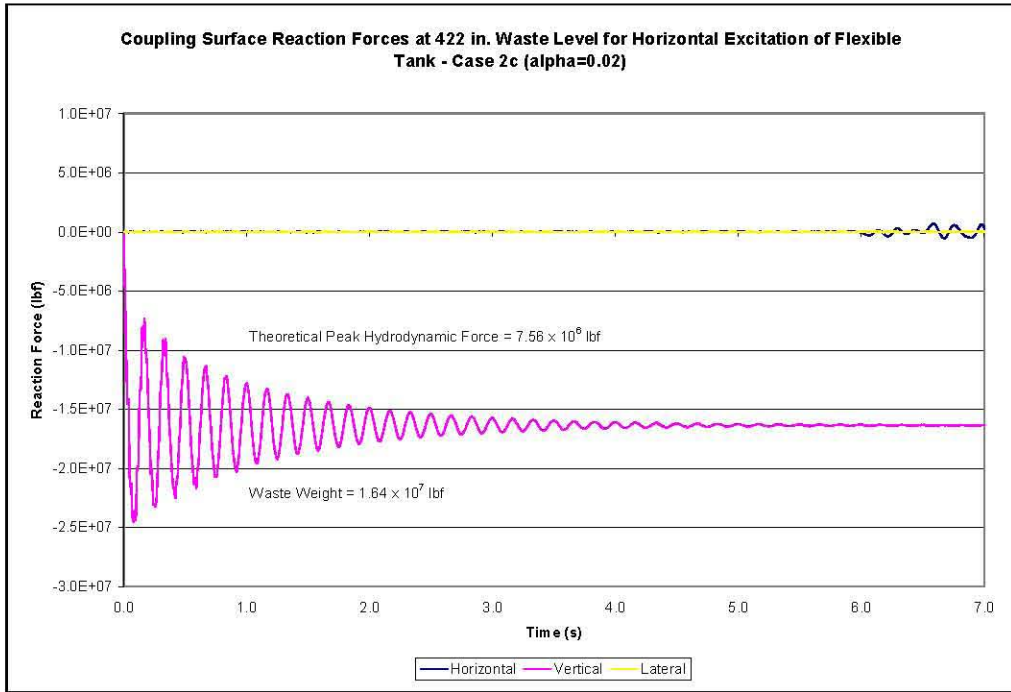


Figure 5-8. Coupling Surface Reaction Forces at the 422-Inch Waste Level for the Flexible Tank at Gage Pressure Under Horizontal Seismic Input During the Initial Free-Vibration Phase – Case 2c (alpha=0.02)

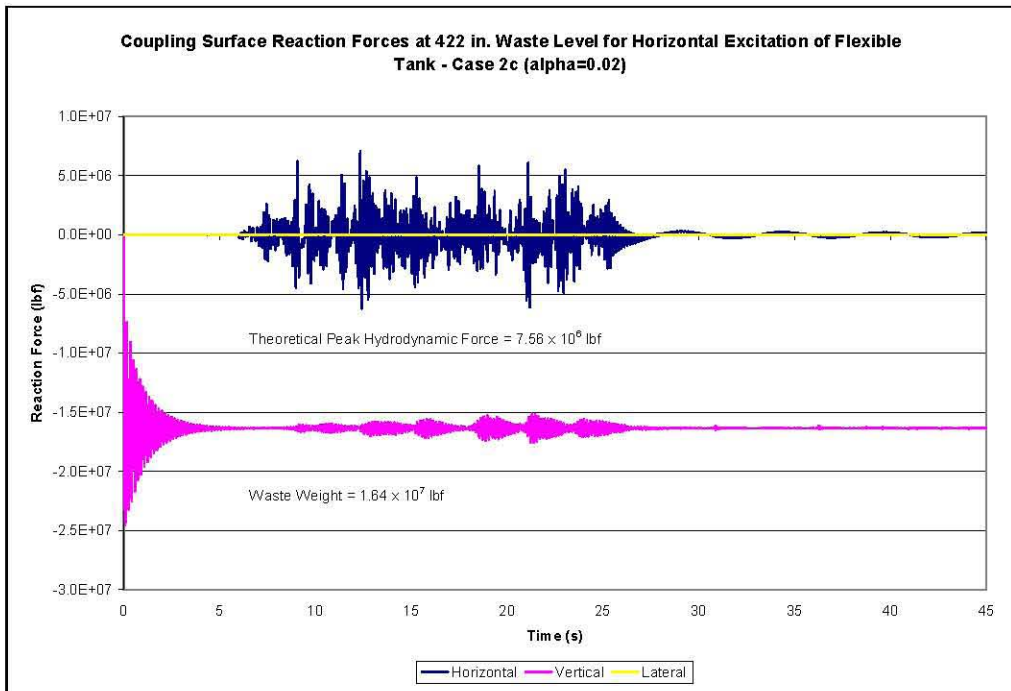


Figure 5-9. Coupling Surface Reaction Forces at the 422-Inch Waste Level for the Flexible Tank at Gage Pressure Under Horizontal Seismic Input – Case 2c (alpha=0.02)

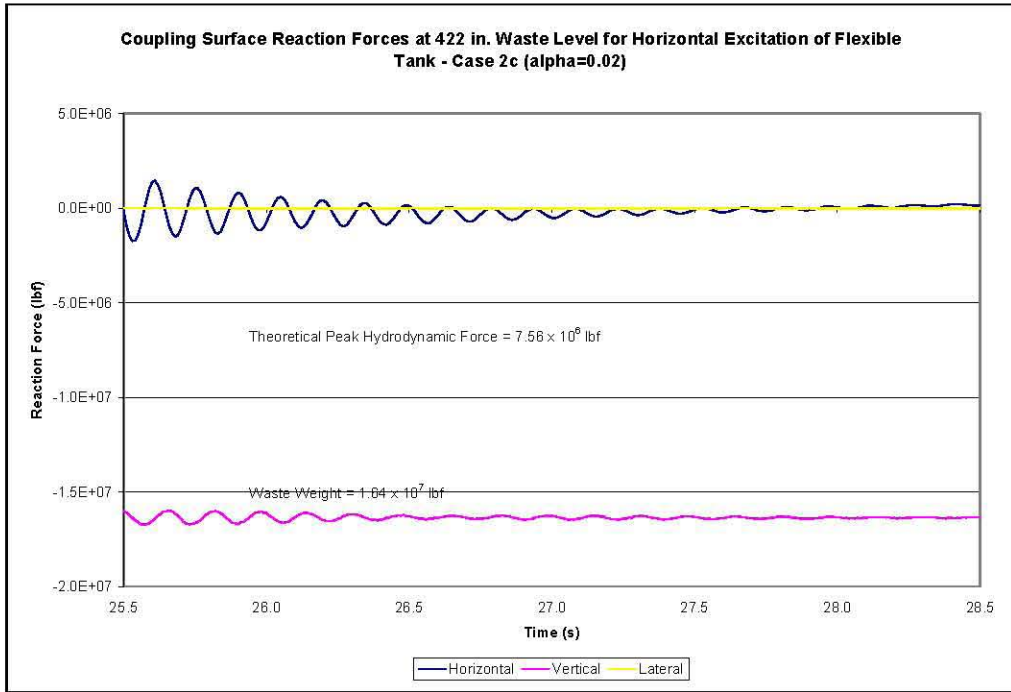


Figure 5-10. Coupling Surface Reaction Forces at the 422-Inch Waste Level for the Flexible Tank at Gage Pressure Under Horizontal Seismic Input During the Final Free-Vibration Phase – Case 2c (alpha=0.02)

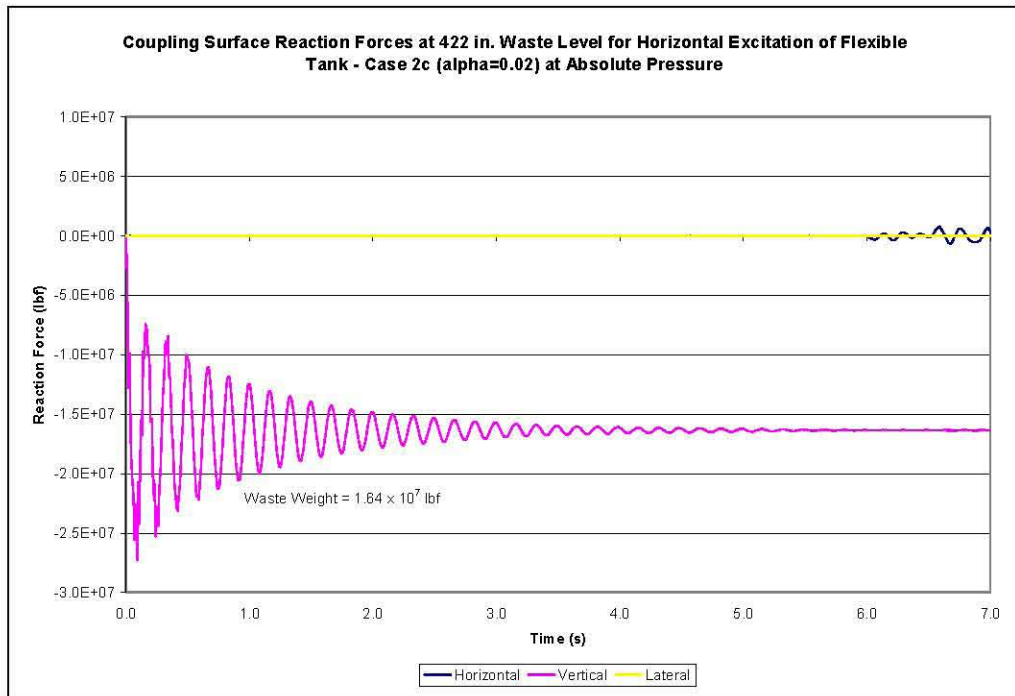


Figure 5-11. Coupling Surface Reaction Forces at the 422-Inch Waste Level for the Flexible Tank at Absolute Pressure Under Horizontal Seismic Input During the Initial Free-Vibration Phase – Case 2c (alpha=0.02)

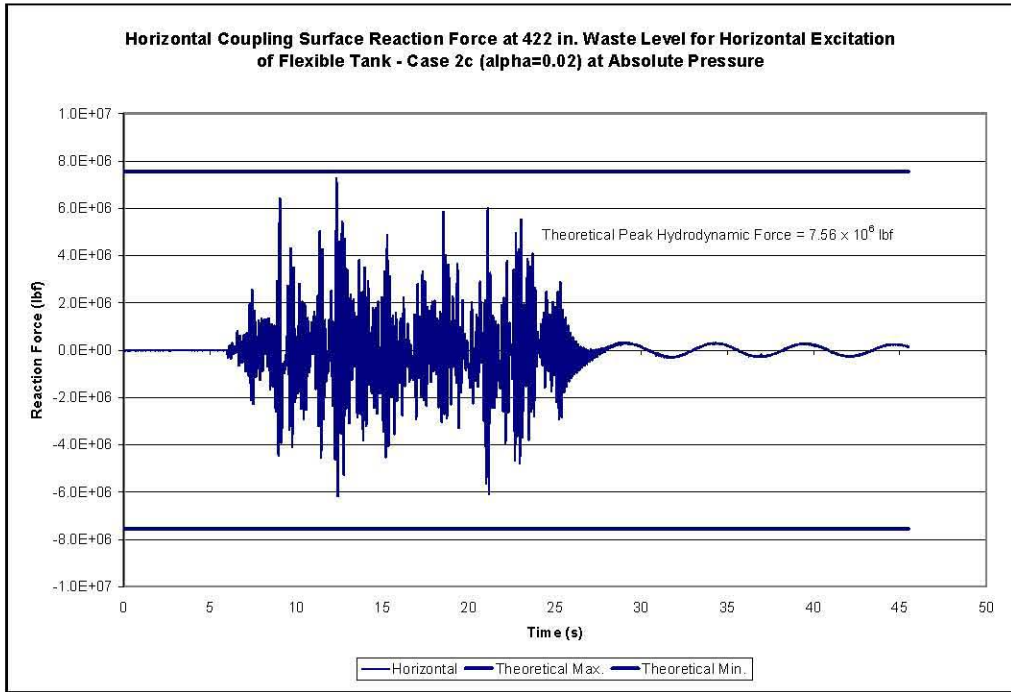


Figure 5-12. Horizontal Coupling Surface Reaction Force at the 422-Inch Waste Level for the Flexible Tank at Absolute Pressure Under Horizontal Seismic Input – Case 2c (alpha=0.02)

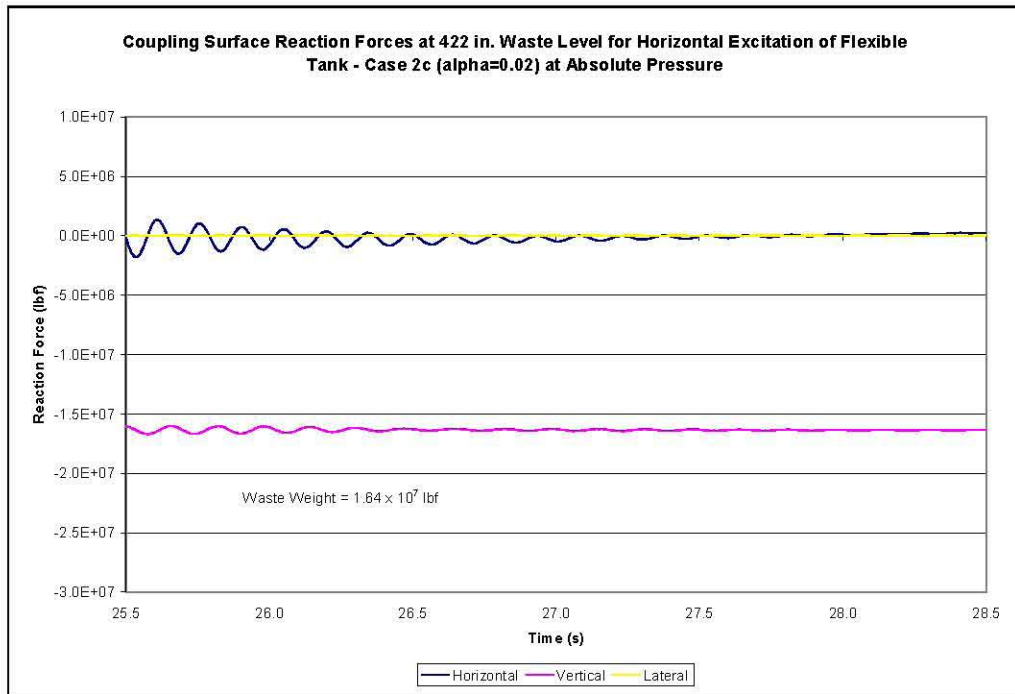
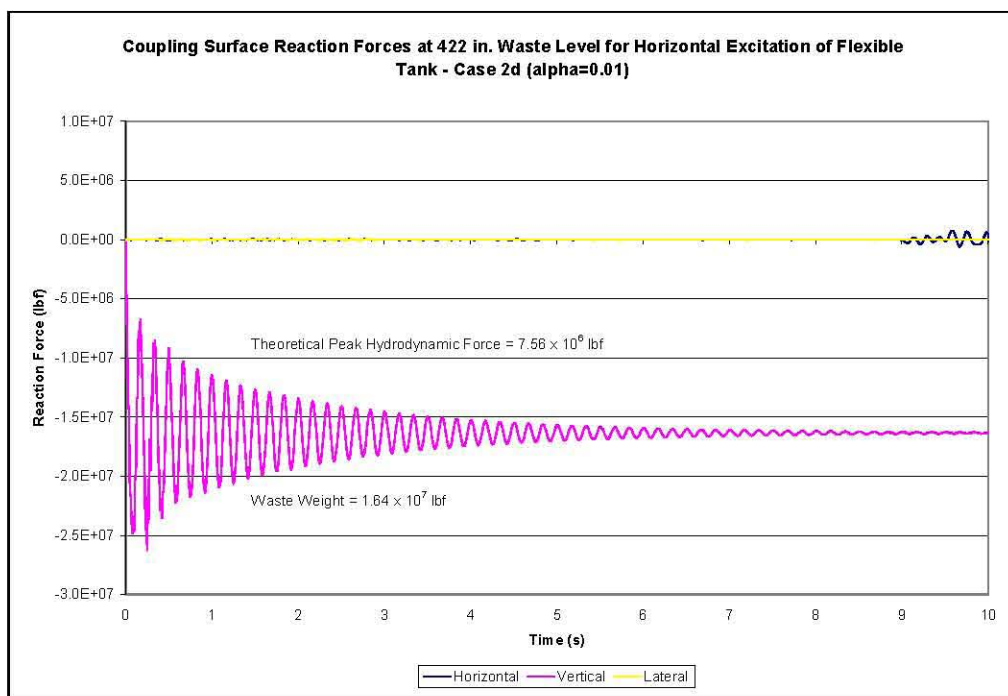


Figure 5-13. Coupling Surface Reaction Forces at the 422-Inch Waste Level for the Flexible Tank at Absolute Pressure Under Horizontal Seismic Input During the Final Free-Vibration Phase – Case 2c (alpha=0.02)

In Case 2d, gravity was run for 8 seconds before the application of the seismic input, and the simulation was run for an additional 20 seconds of unforced motion after the end of the seismic excitation. The coupling surface reaction forces for Case 2d are shown in Figure 5-14, Figure 5-15, and Figure 5-16. The vertical reaction force has essentially reached the steady-state value in 10 seconds (60 cycles), giving an effective damping during the initial phase of approximately 1% critical damping. The breathing mode frequency of approximately 6 Hz is apparent in the vertical reaction force.



**Figure 5-14.** Coupling Surface Reaction Forces at the 422-Inch Waste Level for the Flexible Tank at Gage Pressure Under Horizontal Seismic Input During the Initial Free-Vibration Phase – Case 2d (alpha=0.01)

The peak horizontal hydrodynamic reaction force shown in Figure 5-15 is approximately  $7.08 \times 10^6$  lbf, also 94% of the theoretical value. The first convective period of slightly greater than 5 seconds is displayed in the horizontal reaction force during the period of unforced motion during the last 20 seconds of the simulation. The coupling surface reaction force during the first 3 seconds of the second period of unforced motion is shown as Figure 5-16. As before, the impulsive frequency of approximately 7 Hz is reflected in the horizontal reaction force, and the breathing mode frequency of approximately 6 Hz is reflected in the vertical reaction force.

In Case 3, gravity was run for 2 seconds before the application of seismic input, and the simulation was run for an additional 20 seconds of unforced motion after the end of the seismic excitation. The peak horizontal reaction force shown in Figure 5-17 for Case 3 is  $7.57 \times 10^6$  lbf, or 101% of the theoretical value. The sloshing period of approximately 5 seconds is reflected at the end of the horizontal force time history. Figure 5-18 shows the coupling surface reaction forces for Case 3 during the period of unforced motion from 23.0 to 25.0 seconds. The impulsive frequency of 7 Hz is evident in the horizontal reaction force, while the breathing mode frequency of approximately 6 Hz is displayed in the vertical reaction force.

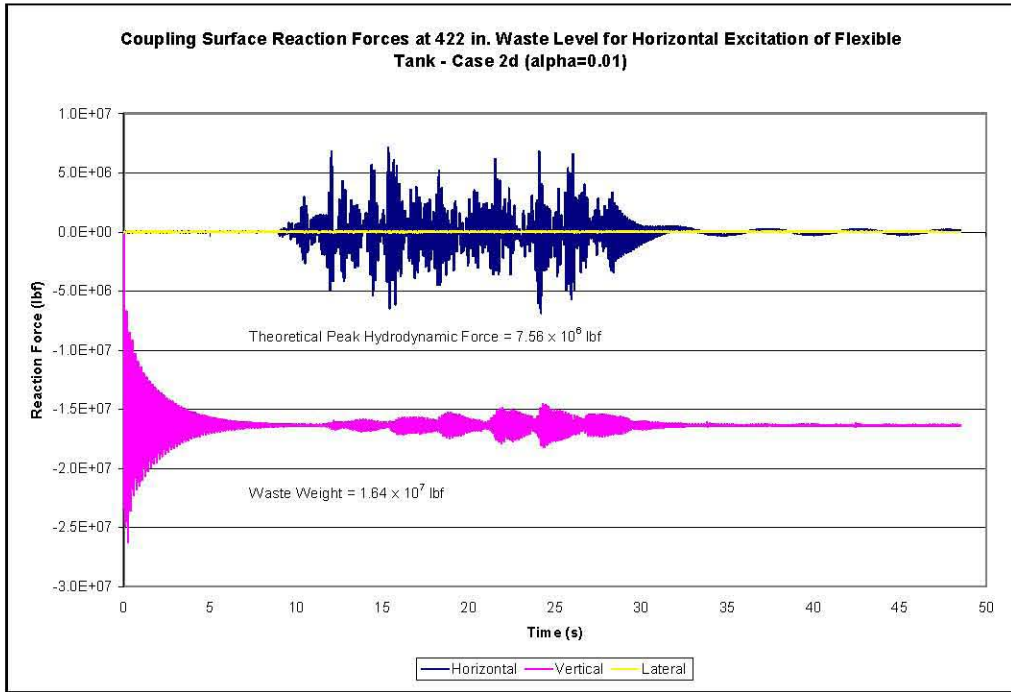


Figure 5-15. Coupling Surface Reaction Forces at the 422-Inch Waste Level for the Flexible Tank at Gage Pressure Under Horizontal Seismic Input – Case 2d (alpha=0.01)

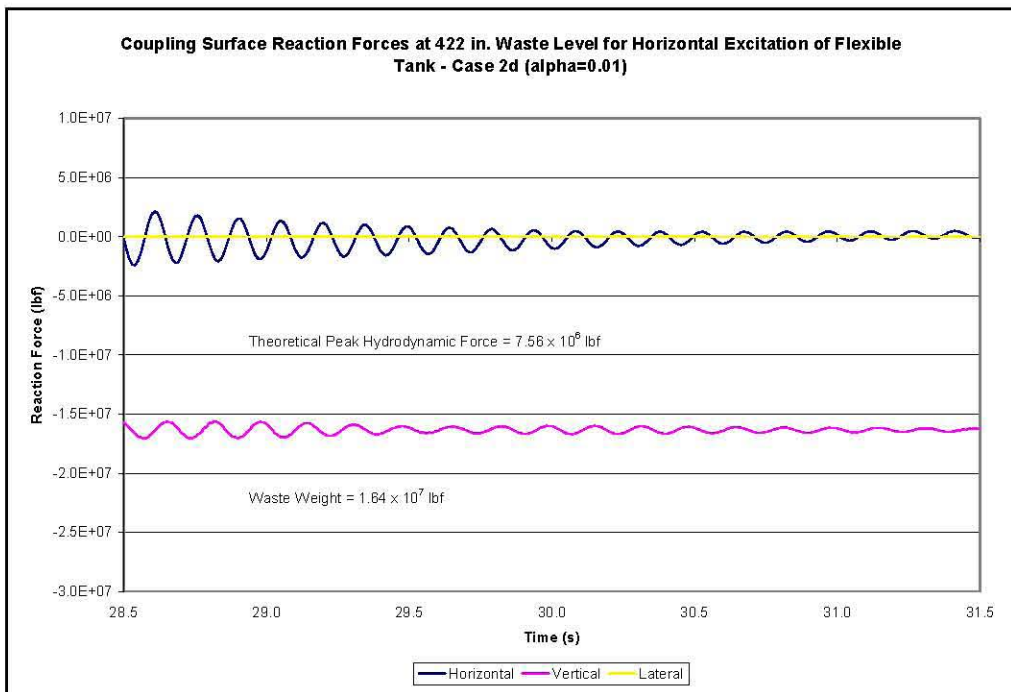


Figure 5-16. Coupling Surface Reaction Forces at the 422-Inch Waste Level for the Flexible Tank at Gage Pressure Under Horizontal Seismic Input During the Final Free-Vibration Phase – Case 2d (alpha=0.01)

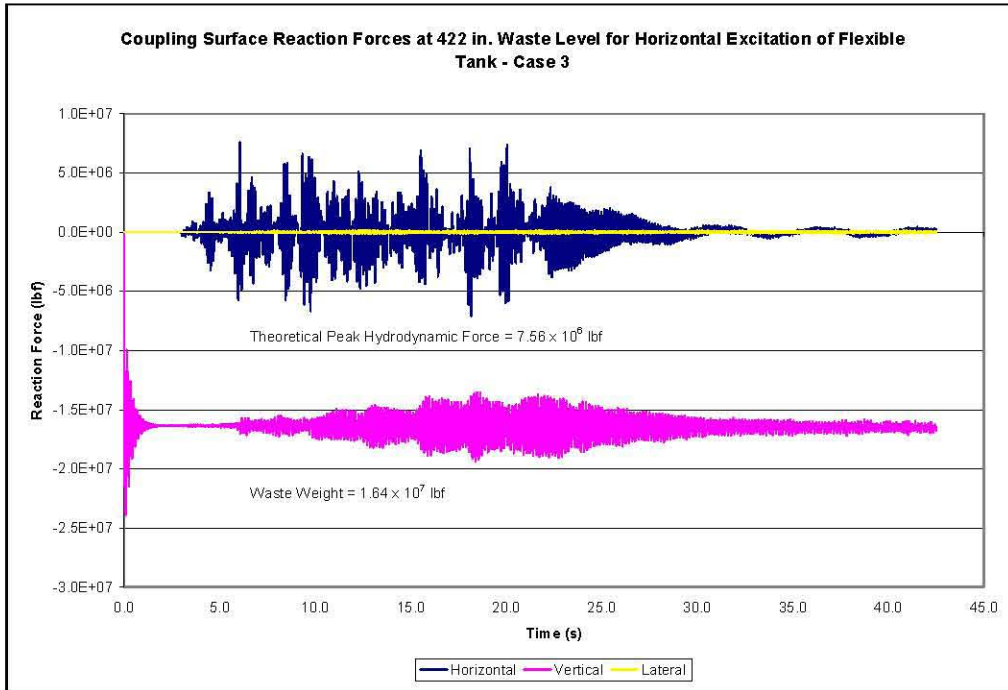


Figure 5-17. Coupling Surface Reaction Forces for the Flexible Tank at Gage Pressure Under Horizontal Seismic Input – Case 3

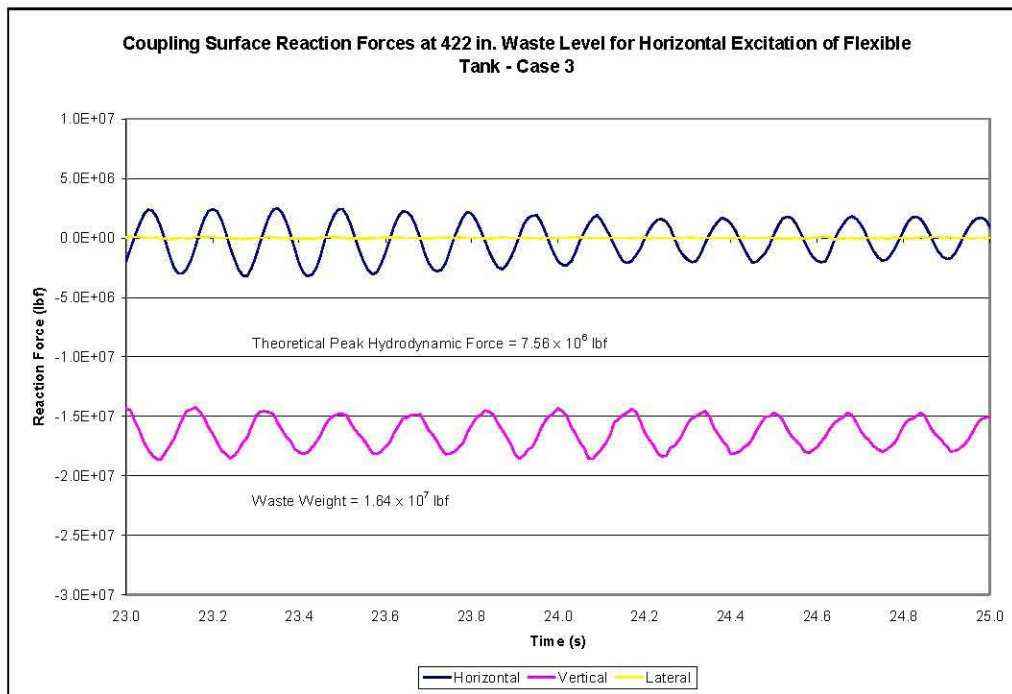


Figure 5-18. Coupling Surface Reaction Forces for the Flexible Tank at Gage Pressure Under Horizontal Seismic Input from 23.0 to 25.0 seconds – Case 3

The coupling surface reaction forces show that Case 1 is significantly under-damped, and Cases 2a and 2b are somewhat over-damped. Cases 2c and 2d are nearly the same, very slightly over-damped, and both agree well with theory. Case 3 also shows good agreement with theory, but as noted above, a stable solution was not achieved for Case 3 when run at absolute pressure – a decided disadvantage for this damping implementation. Thus, on the basis of the results of horizontal excitation, only the results for Cases 2c and 3 will be presented for vertical excitation.

It will be shown in Section 5.2.2 that the response to Case 2c under vertical excitation is slightly under-damped, and the response to vertical excitation for Case 3 is significantly under-damped. This behavior coupled with the noted deficiencies of the damping implementation in Case 3 will lead to Case 2c being the best overall choice for the implementation of damping.

### 5.2.2 Vertical Excitation

The peak vertical hydrodynamic forces for the flexible tank are calculated using Equation 4.57 in BNL (1995), with the instantaneous accelerations replaced by the appropriate spectral accelerations and the impulsive and convective components combined via the SRSS rule. The theoretical maximum vertical hydrodynamic force based on spectral accelerations from the 4% damped spectrum is  $5.24 \times 10^6$  lbf. Accordingly, the vertical coupling surface reaction force should vary between

$$(-1.64 \times 10^7 - 5.24 \times 10^6) \text{ lbf} = -2.16 \times 10^7 \text{ lbf} \quad (5-6)$$

and

$$(-1.64 \times 10^7 + 5.24 \times 10^6) \text{ lbf} = -1.12 \times 10^7 \text{ lbf.} \quad (5-7)$$

The results in Section 5.2 show that damping implemented in Case 2c and Case 3 provided the best match to theoretical results. Accordingly, additional results from the other cases will not be presented in the body of the report.

The coupling surface reaction force due to vertical excitation for Case 2c at gage pressure is shown as Figure 5-19. The maximum and minimum values for the vertical force are  $-1.07 \times 10^7$  and  $-2.27 \times 10^7$  lbf, respectively. That is, the peak vertical hydrodynamic force is 109% of the theoretical value in the positive direction

$$((1.64 \times 10^7 - 1.07 \times 10^7) / (5.24 \times 10^6)) \times 100 = 109, \quad (5-8)$$

and 120% of the theoretical value in the negative direction

$$((2.27 \times 10^7 - 1.64 \times 10^7) / (5.24 \times 10^6)) \times 100 = 120. \quad (5-9)$$

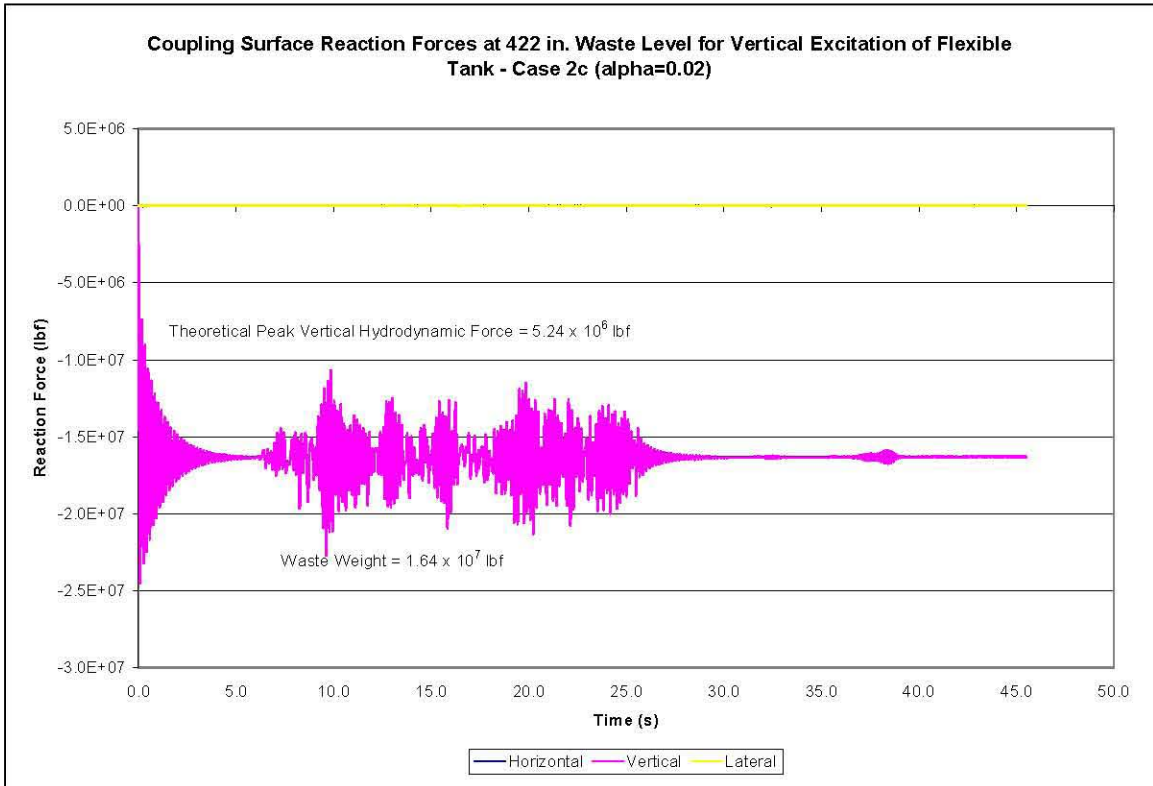


**Figure 5-19.** Coupling Surface Reaction Forces for the Flexible Tank at Gage Pressure Under Vertical Seismic Input – Case 2c

The coupling surface reaction force due to vertical excitation for Case 3 is shown as Figure 5-20. The maximum and minimum values for the vertical force are  $-97.7 \times 10^7$  and  $-2.35 \times 10^7$  lbf, respectively. That is, the peak vertical hydrodynamic force is 127% of the theoretical value in the positive direction

$$((1.64 \times 10^7 - 97.7 \times 10^7)/(5.24 \times 10^6)) \times 100=127, \tag{5-9}$$

and 135% of the theoretical value in the negative direction

$$((2.35 \times 10^7 - 1.64 \times 10^7)/(5.24 \times 10^6)) \times 100=135. \tag{5-10}$$

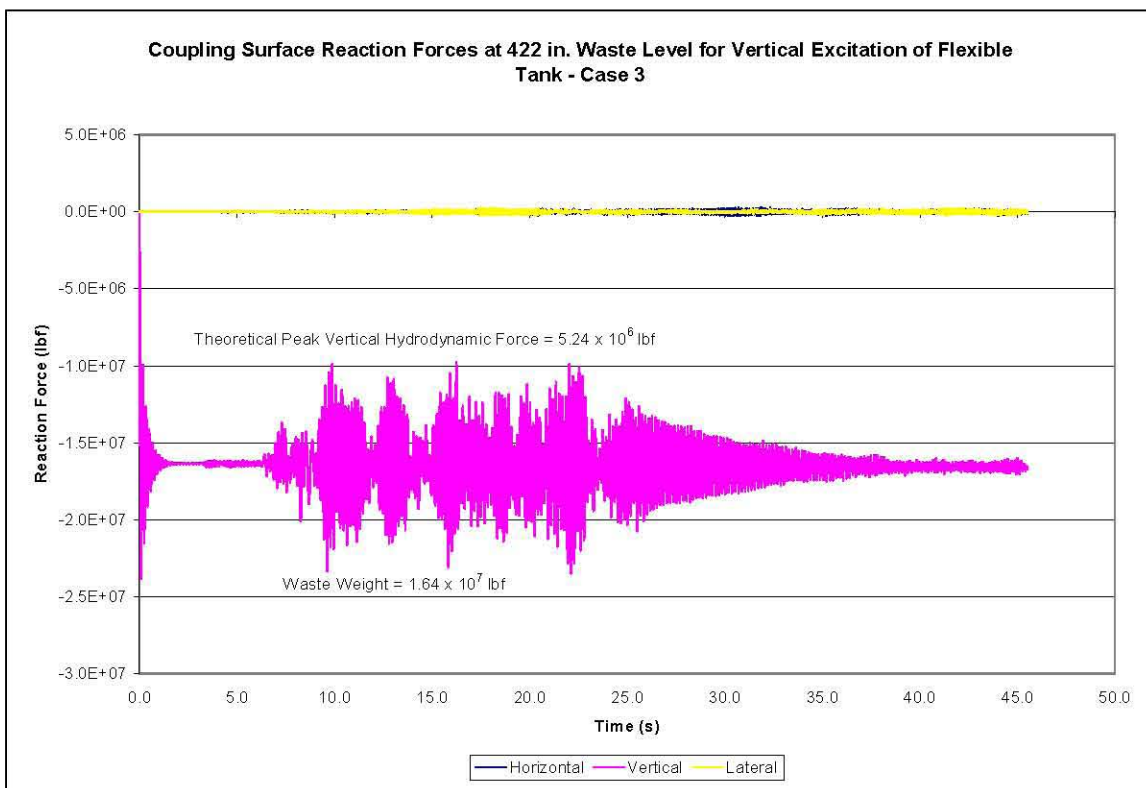


Figure 5-20. Coupling Surface Reaction Forces for the Flexible Tank at Gage Pressure Under Vertical Seismic Input – Case 3

Based on the peak hydrodynamic forces caused by vertical excitation, Case 3 is significantly under-damped, and Case 2c is slightly under-damped. Since Case 3 is somewhat under-damped for horizontal excitation (evidenced by pressure and hydrodynamic force results), and Case 2c is slightly over-damped for horizontal excitation, the damping value used in Case 2c is judged to provide the best overall match to the theoretical predictions.

Consequently, the focus of the remainder of the analysis will be on results from Case 2c. Results from other cases are included in the appendixes.

For reference, the coupling surface reaction forces for vertical excitation at absolute pressure are shown in Figure 5-21. The maximum and minimum vertical reaction forces are  $-1.07 \times 10^7$  lbf and  $-2.27 \times 10^7$  lbf, exactly the same as in the gage pressure simulation.

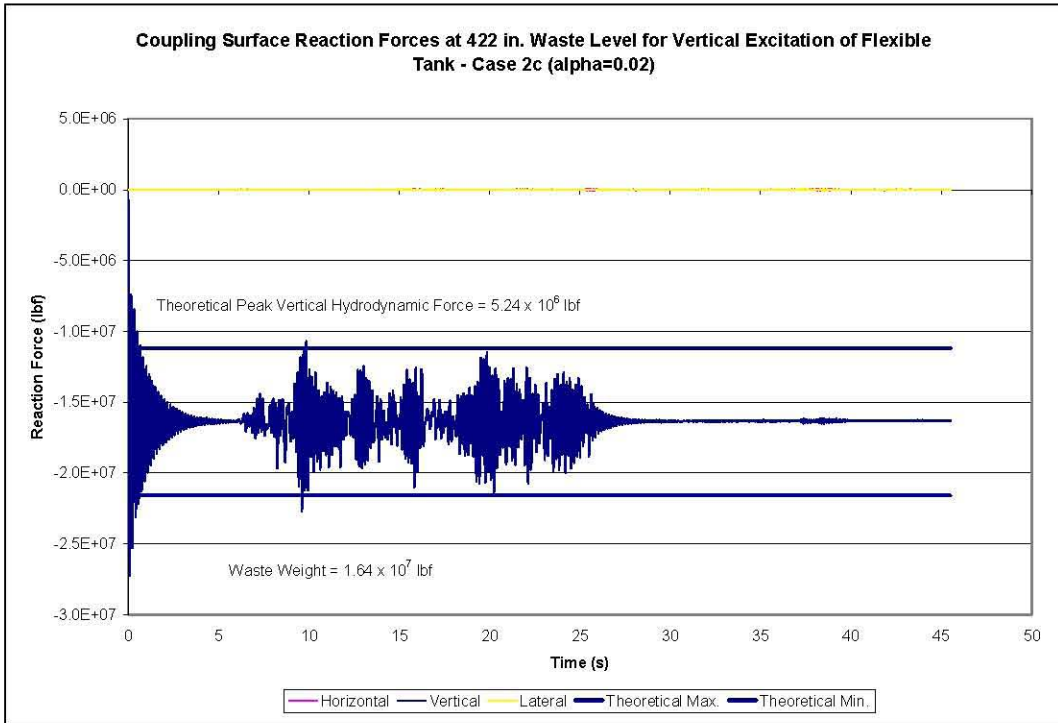


Figure 5-21. Coupling Surface Reaction Forces for the Flexible Tank at Absolute Pressure Under Vertical Seismic Input – Case 2c

### 5.3 Waste Pressures

#### 5.3.1 Horizontal Excitation Run at Absolute Pressure

The theoretical peak hydrodynamic pressures due to horizontal excitation are given by Equation 4.24 in BNL (1995). The total pressures are the sum of the hydrostatic pressures and the hydrodynamic pressures. The hydrostatic, peak hydrodynamic, and peak total pressures for the elements in the sets “plusx\_els” and “press\_45” are shown in Table 5-1 and Table 5-2. The maximum theoretical pressures for the elements set “plusz\_els” are simply the hydrostatic pressures shown in Table 3-1, because the theoretical hydrodynamic pressures are zero at  $\theta=90^\circ$ .

RPP-RPT-28963, Rev. 1  
M&D-2008-005-RPT-01, Rev. 1

**Table 5-1.** Theoretical Maximum Absolute Waste Pressures for Horizontal Excitation in the Flexible Tank at 422-Inch Waste Level for Elements at  $\theta=0$

<b>“Plusx_els”</b>	<b>Hydrostatic Pressure (psi)</b>	<b>Peak Hydrodynamic Pressure (psi)</b>	<b>Peak Total Pressure (psi)</b>
<b>Element No.</b>			
10482	14.7	0	14.7
9753	15.8	3.6	19.4
9024	18.0	6.6	24.6
8295	20.1	9.0	29.1
7566	22.3	10.9	33.2
6837	24.5	12.5	37.0
6108	26.7	13.8	40.5
5379	28.8	14.8	43.6
4650	31.0	15.7	46.7
3921	33.2	16.3	49.5
3192	35.4	16.8	52.2
2463	37.5	17.1	54.6
1734	39.7	17.2	56.9

**Table 5-2.** Theoretical Maximum Absolute Waste Pressures for Horizontal Excitation in the Flexible Tank at 422-Inch Waste Level for Elements at  $\theta=45^\circ$

<b>“Press_45”</b>	<b>Hydrostatic Pressure (psi)</b>	<b>Peak Hydrodynamic Pressure (psi)</b>	<b>Peak Total Pressure (psi)</b>
<b>Element No.</b>			
10290	14.7	0	14.7
9561	15.8	2.6	18.4
8832	18.0	4.6	22.6
8103	20.1	6.3	26.4
7374	22.3	7.7	30.0
6645	24.5	8.8	33.3
5916	26.7	9.8	36.5
5187	28.8	10.5	39.3
4458	31.0	11.1	42.1
3729	33.2	11.5	44.7
3000	35.4	11.9	47.3
2271	37.5	12.1	49.6
1542	39.7	12.2	51.9

The pressure time histories for the waste elements along the tank wall at  $\theta=0$  are shown in Figure 5-22. The pressure time histories for elements 1734, 6108, and 9753 are shown again in Figure 5-23. These three elements were selected since they are near the bottom, mid-height, and top of the waste, respectively. Figure 5-24, Figure 5-25, Figure 5-26, and Figure 5-27, show similar plots for the waste elements located at  $\theta=45$  and  $90^\circ$ .

The data in Figure 5-22 through Figure 5-27 indicate that the hydrostatic pressures match the theoretical values, and that the decay in waste pressures is very similar to the decay in the hydrodynamic forces. The typical peak pressures are approximately 95% of the theoretical peak values, but at waste elements higher in the tank, pressures exceed theoretical values at a few isolated peaks.

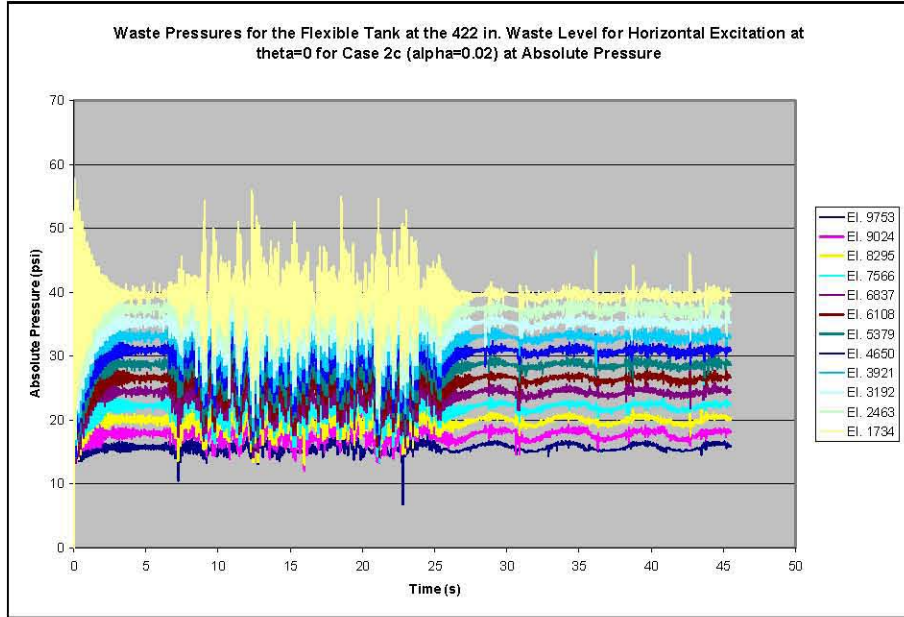


Figure 5-22. Waste Pressures Time Histories for the Flexible Tank at the 422-Inch Waste Level for Horizontal Excitation at  $\theta=0$ , Case 2c ( $\alpha=0.02$ ) Run at Absolute Pressure

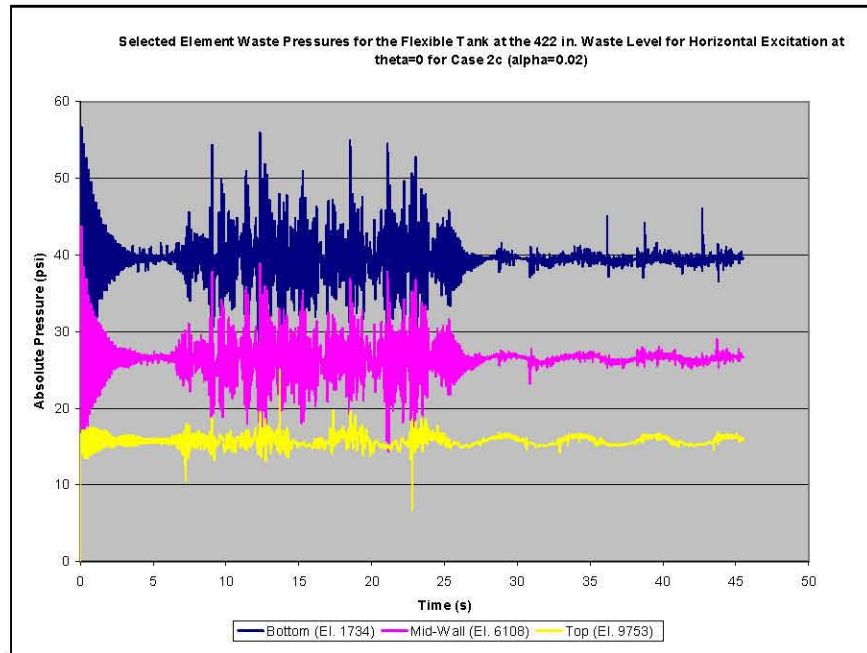


Figure 5-23. Selected Element Pressure Time Histories for the Flexible Tank at the 422-Inch Waste Level for Horizontal Excitation at  $\theta=0$ , Case 2c ( $\alpha=0.02$ ) Run at Absolute Pressure

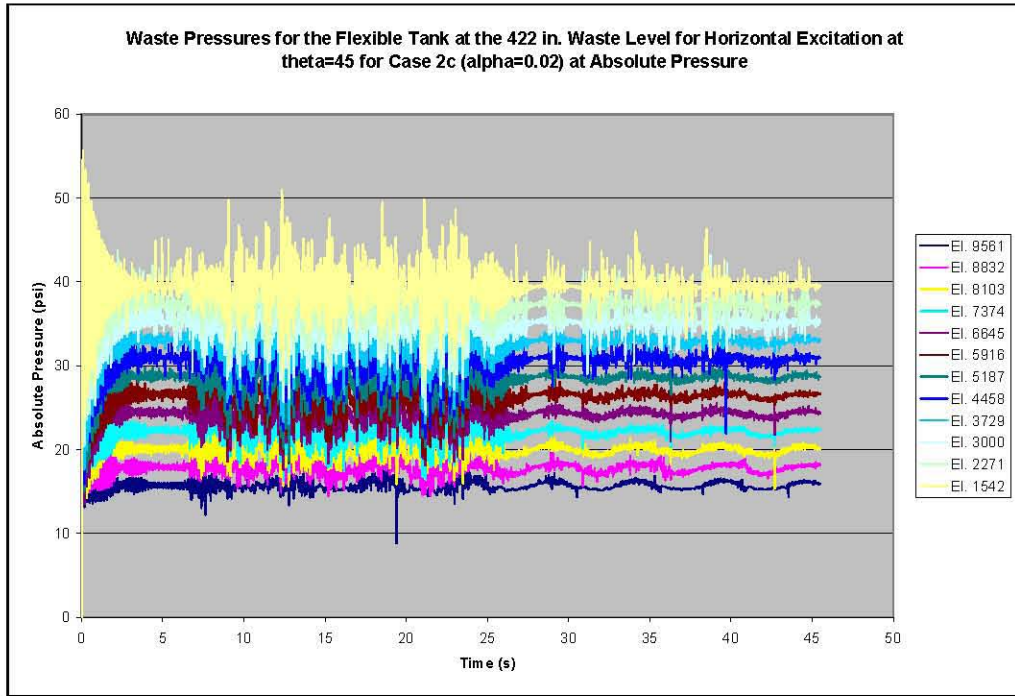


Figure 5-24. Waste Pressures Time Histories for the Flexible Tank at the 422-Inch Waste Level for Horizontal Excitation at  $\theta=45$ , Case 2c ( $\alpha=0.02$ ) Run at Absolute Pressure

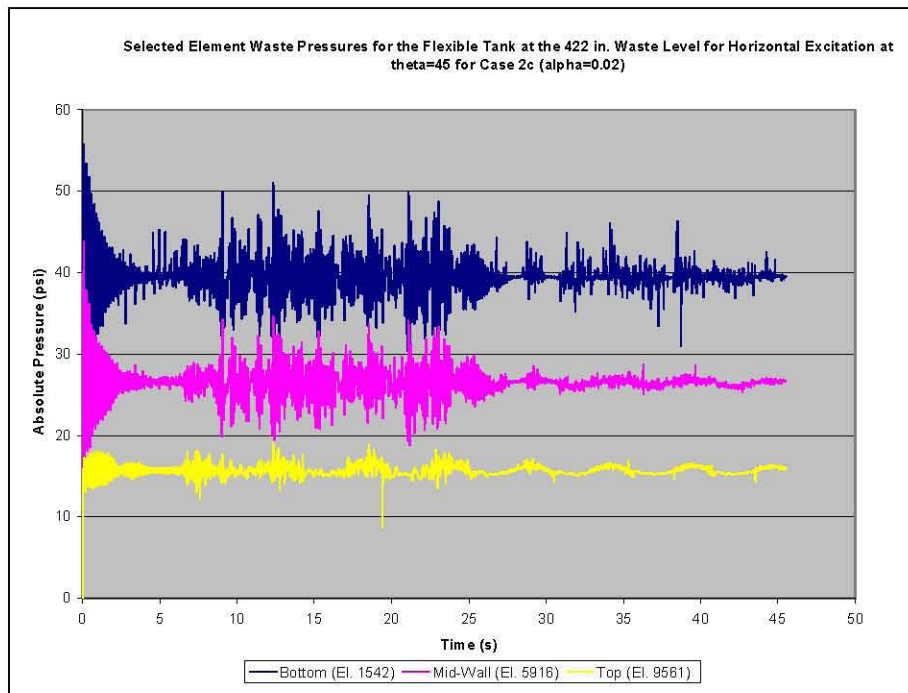


Figure 5-25. Selected Element Pressure Time Histories for the Flexible Tank at the 422-Inch Waste Level for Horizontal Excitation at  $\theta=45$ , Case 2c ( $\alpha=0.02$ ) Run at Absolute Pressure

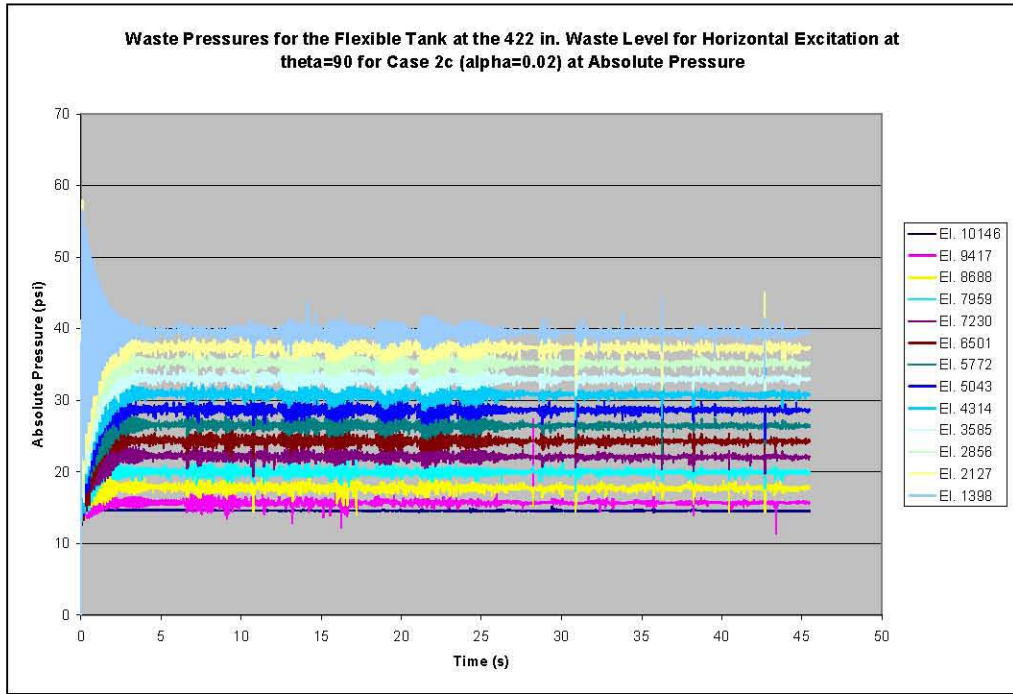


Figure 5-26. Waste Pressures Time Histories for the Flexible Tank at the 422-Inch Waste Level for Horizontal Excitation at  $\theta=90$ , Case 2c ( $\alpha=0.02$ ) Run at Absolute Pressure

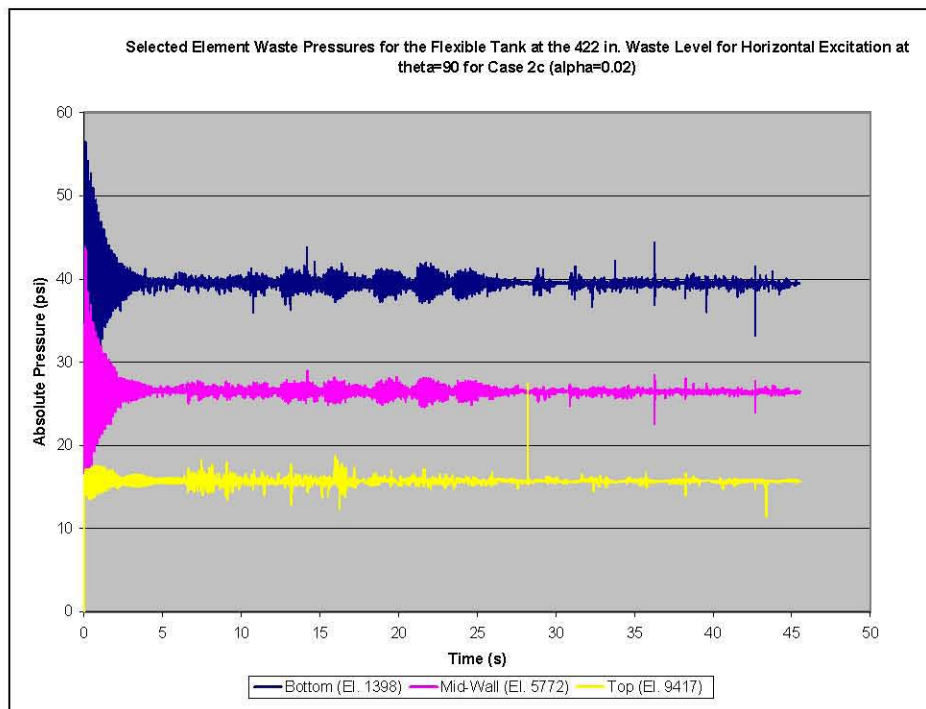


Figure 5-27. Selected Element Pressure Time Histories for the Flexible Tank at the 422-Inch Waste Level for Horizontal Excitation at  $\theta=90$ , Case 2c ( $\alpha=0.02$ ) Run at Absolute Pressure

Figure 5-28, Figure 5-29, and Figure 5-30 show comparisons between the solutions at absolute and gage pressure for selected waste elements at  $\theta=0$ , 45, and 90°. Comparison of the two solutions shows several trends. When the problem is run at absolute pressure, the pressure time histories in the upper portion of the waste are much more regular since the pressures are not near zero. This also has the effect of eliminating some of the high isolated spikes, or spurious peaks that occurred in the uppermost waste elements when the problem was run at gage pressure. This can be seen most easily in Figure 5-29 and Figure 5-30. It is also apparent from the plots that during the final free-vibration phase, the gage pressure solution shows some slight upward drift in the pressures that is not present in the absolute pressure solution.

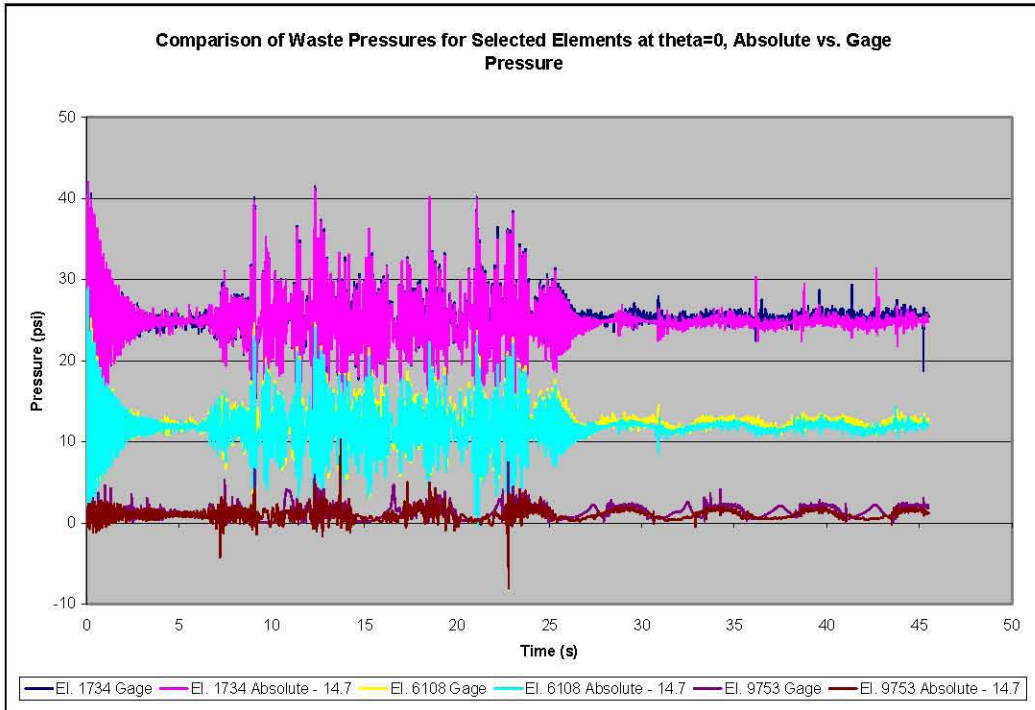


Figure 5-28. Comparison of Waste Pressures in the Flexible Tank at the 422-Inch Waste Level at Absolute and Gage Pressure for Selected Elements at  $\theta=0$

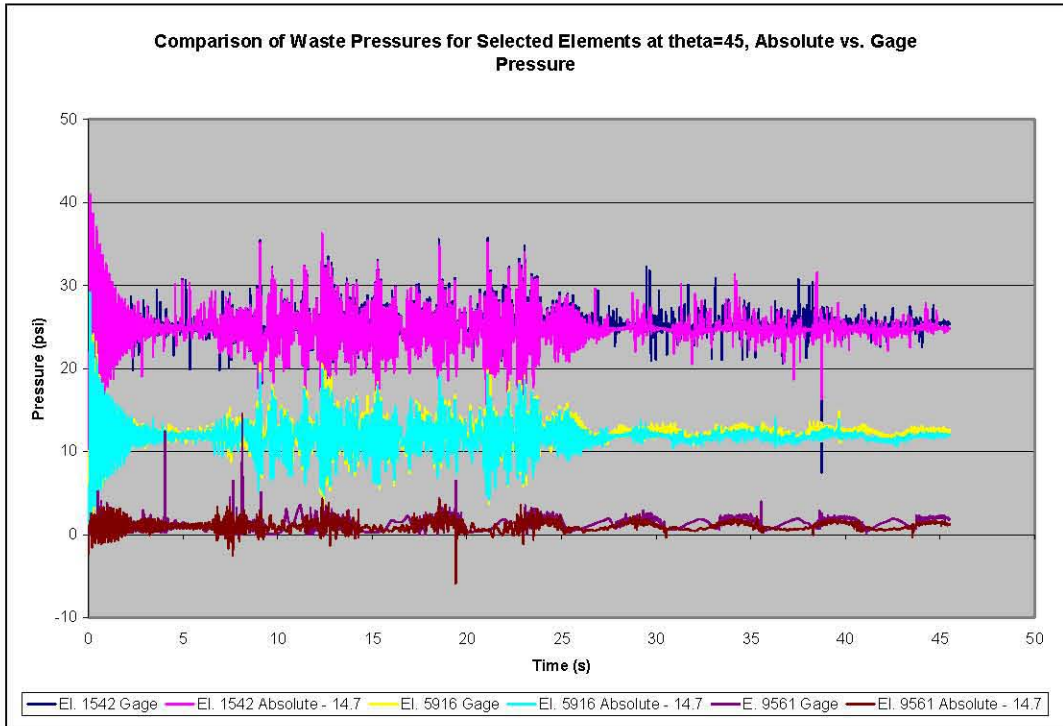


Figure 5-29. Comparison of Waste Pressures in the Flexible Tank at the 422-Inch Waste Level at Absolute and Gage Pressure for Selected Elements at  $\theta=45^\circ$

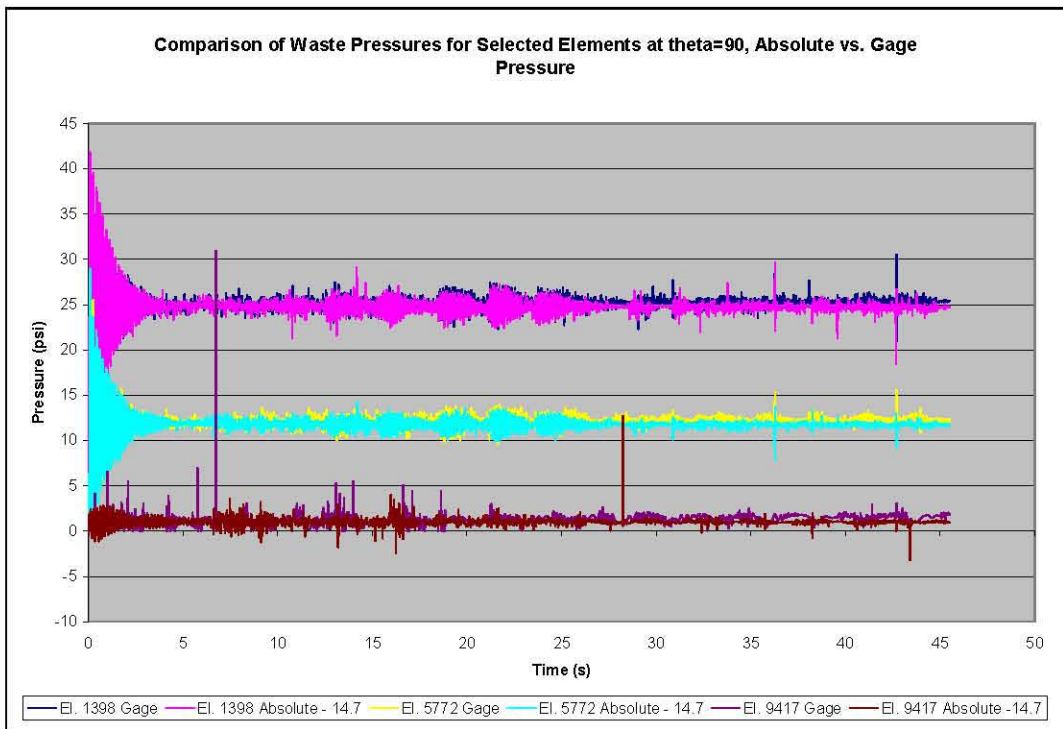


Figure 5-30. Comparison of Waste Pressures in the Flexible Tank at the 422-Inch Waste Level at Absolute and Gage Pressure for Selected Elements at  $\theta=90^\circ$

Plots of the actual (that is, as calculated by Dytran<sup>®</sup>) and theoretical maximum and minimum waste pressures at  $\theta=0$ , 45, and 90° are shown in Figure 5-31 through Figure 5-33.

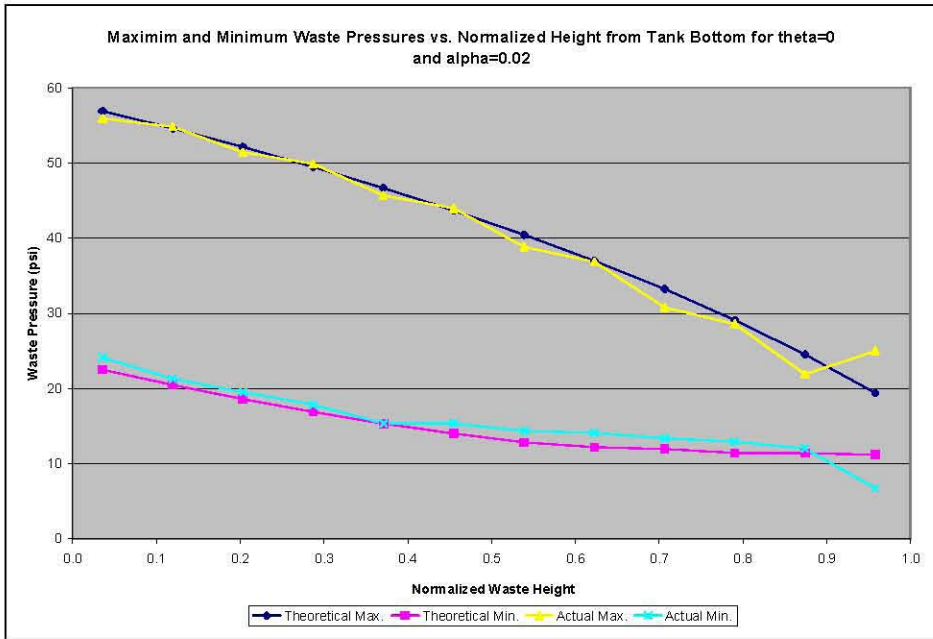


Figure 5-31. Maximum and Minimum Waste Pressures vs. Normalized Height from Tank Bottom for the Flexible Tank at the 422-Inch Waste Level Under Horizontal Excitation for  $\alpha=0.02$  and  $\theta=0$

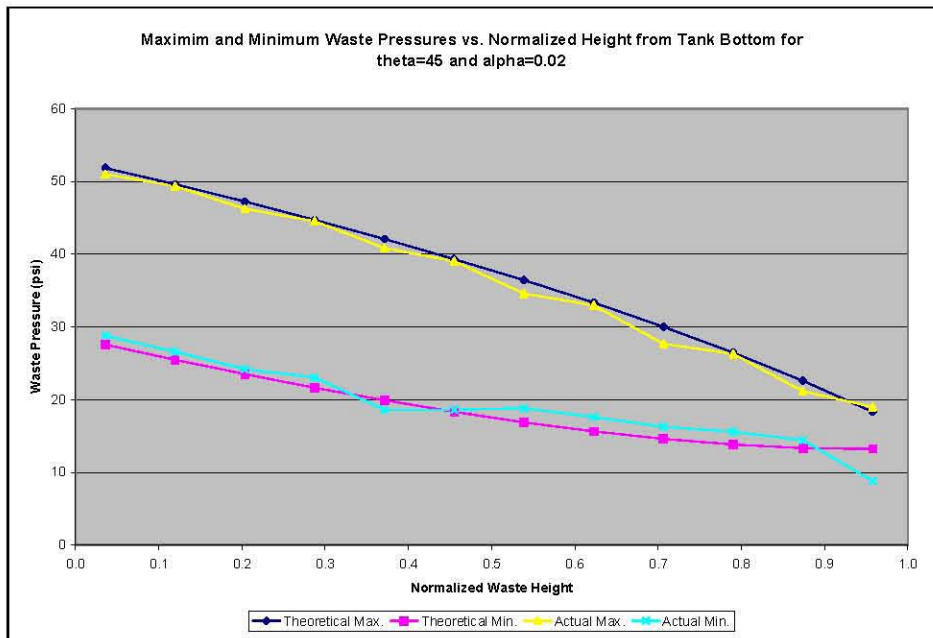
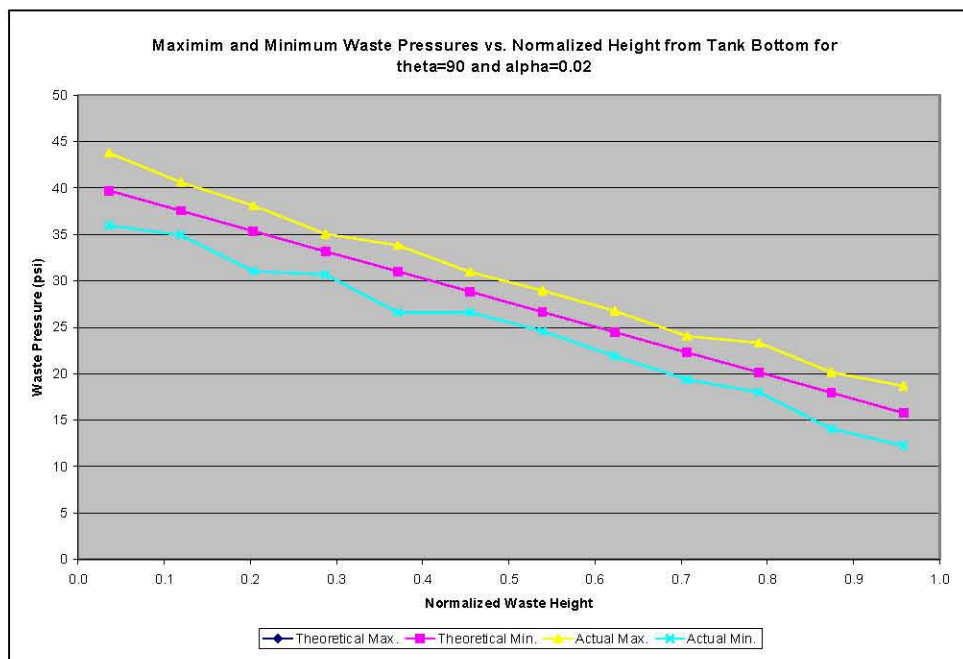


Figure 5-32. Maximum and Minimum Waste Pressures vs. Normalized Height from Tank Bottom for the Flexible Tank at the 422-Inch Waste Level Under Horizontal Excitation for  $\alpha=0.02$  and  $\theta=45^\circ$



**Figure 5-33.** Maximum and Minimum Waste Pressures vs. Normalized Height from Tank Bottom for the Flexible Tank at the 422-Inch Waste Level Under Horizontal Excitation for  $\alpha=0.02$  and  $\theta=90^\circ$

### 5.3.2 Wall and Base Pressures Due to Vertical Excitation Run at Absolute Pressure

The maximum hydrodynamic pressures induced by the waste on the tank wall and base due to vertical excitation depend on the vertical and radial location in the waste, respectively. The peak wall pressures are given by Equation 4.52 in BNL (1995), and the peak base pressures are given by Equation 4.55 in BNL (1995). The theoretical wall pressures are shown in Table 5-3.

The pressure time histories for the waste elements adjacent to the tank wall at  $\theta=0$  are shown in Figure 5-34, and pressure time histories for three selected elements near the top, middle, and bottom of the waste are shown in Figure 5-35. A plot of the pressure decay for the same three elements during the initial gravity loading is shown in Figure 5-36. Evident in the plot is the breathing mode frequency of 6 Hz.

A plot of the maximum and minimum waste pressures as a function of waste depth is shown in Figure 5-37, where the results labeled as “actual” refer to the values predicted by Dytran<sup>®</sup>. The results of the computer simulation are conservative relative to the theoretical results, and are generally in quite good agreement. The maximum pressure of 58 lbf/in<sup>2</sup> near the bottom of the tank wall in element 2463 is significantly higher than the 48 lbf/in<sup>2</sup> value predicted by theory. However, that maximum value occurs at a single isolated point as seen in Figure 5-34 and Figure 5-35.

A comparison of the pressure in element 2463 and the hoop stress in the adjacent tank wall element 447 is shown in Figure 5-38. It can be seen from this plot that the isolated spike in the pressure time history does not appear in the stress time history. The absence of high isolated peaks in the hoop stresses is typical. Apparently brief pressure spikes at single waste elements are transparent to the tank wall stresses, at least in some cases.

Table 5-3. Theoretical Maximum Absolute Wall Pressures for Vertical Excitation at the 422-Inch Waste Level

“Plusx_els”	“Press_45”	“Plusz_els”	Hydrostatic Pressure (psi)	Peak Hydrodynamic Wall Pressure (psi)	Peak Total Pressure (psi)
Element No.	Element No.	Element No.			
10482	10290	10146	14.7	0	14.7
9753	9561	9417	15.8	0.7	16.5
9024	8832	8688	18.0	2.2	20.2
8295	8103	7959	20.1	3.6	23.7
7566	7374	7230	22.3	4.9	27.2
6837	6645	6501	24.5	6.1	30.6
6108	5916	5772	26.7	7.3	34.0
5379	5187	5043	28.8	8.3	37.1
4650	4458	4314	31.0	9.2	40.2
3921	3729	3585	33.2	9.9	43.1
3192	3000	2856	35.4	10.4	45.8
2463	2271	2127	37.5	10.8	48.3
1734	1542	1398	39.7	11.0	50.7

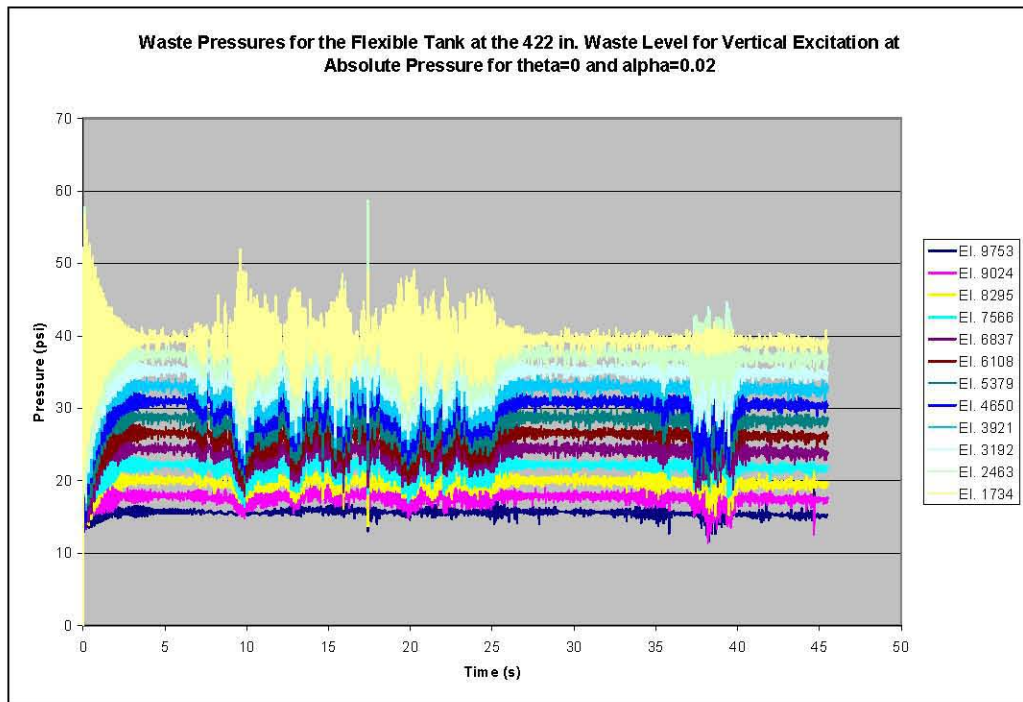


Figure 5-34. Waste Pressure Time Histories for the Flexible Tank at the 422-Inch Waste Level for Vertical Excitation Run at Absolute Pressure for  $\theta=0$  and  $\alpha=0.02$

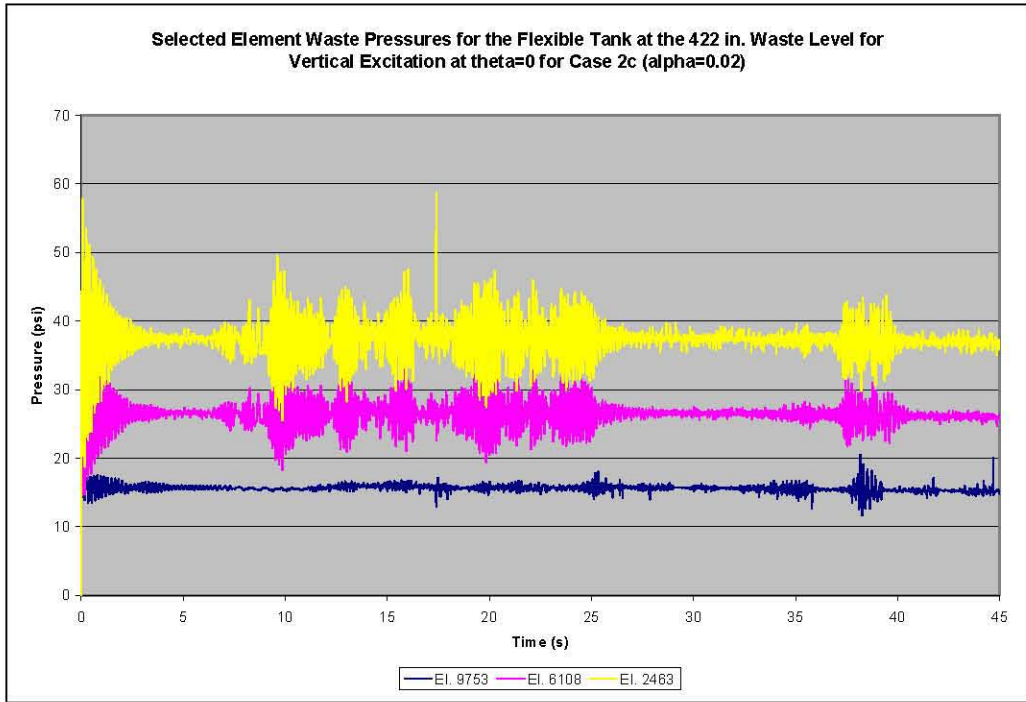


Figure 5-35. Selected Waste Pressure Time Histories for the Flexible Tank at the 422-Inch Waste Level for Vertical Excitation Case 2c ( $\alpha=0.02$ ) Run at Absolute Pressure

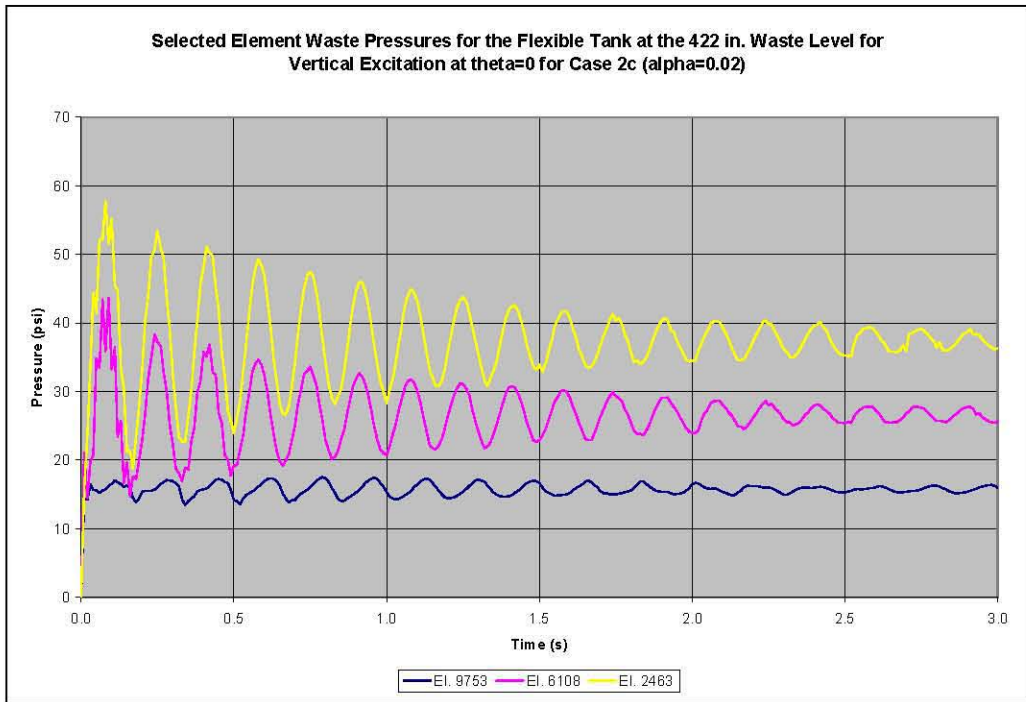


Figure 5-36. Selected Waste Pressure Time Histories for the Flexible Tank at the 422-Inch Waste Level for Vertical Excitation Case 2c ( $\alpha=0.02$ ) Run at Absolute Pressure – Time 0 to 3 Seconds

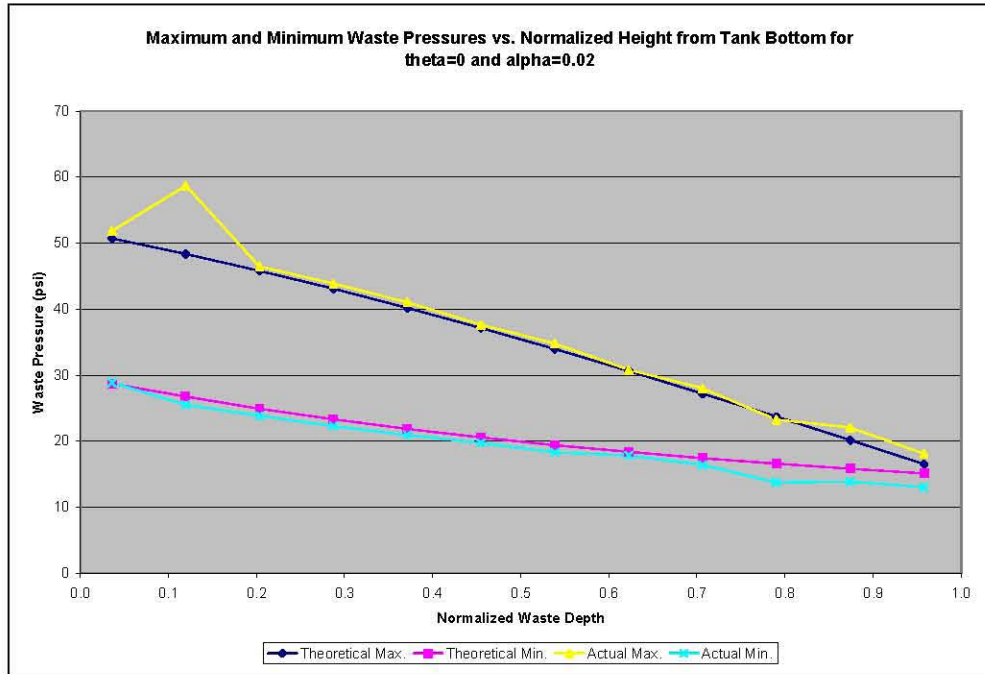


Figure 5-37. Maximum and Minimum Waste Pressures vs. Normalized Height from Tank Bottom for the Flexible Tank at the 422-Inch Waste Level Under Vertical Excitation at  $\theta=0$  and  $\alpha=0.02$

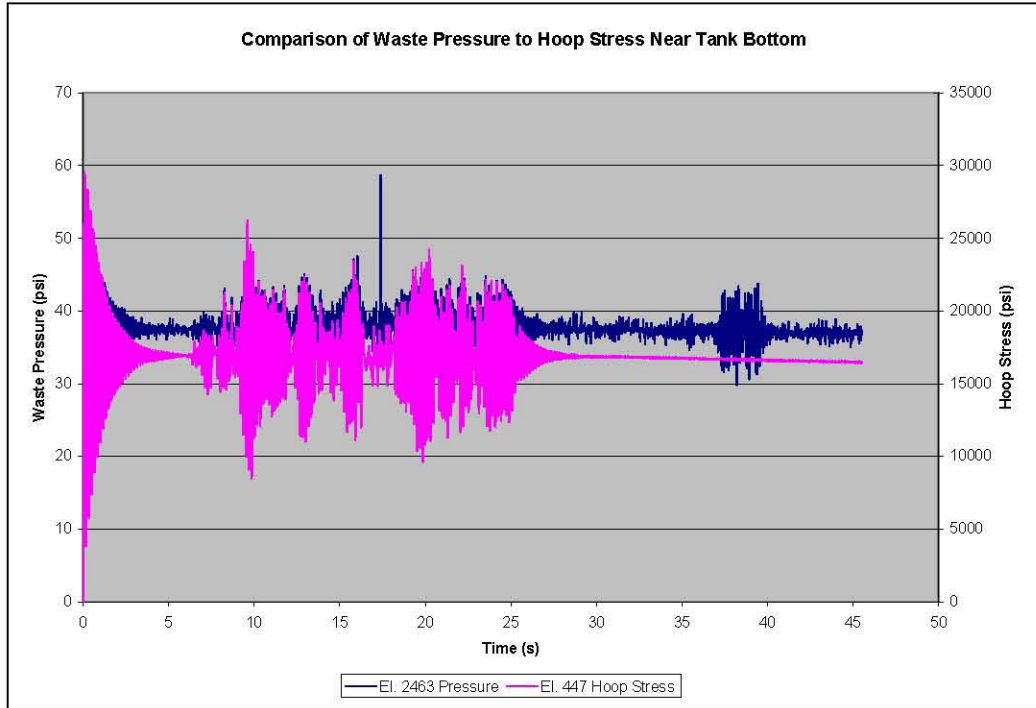


Figure 5-38. Comparison of Waste Pressure to Tank Wall Hoop Stress for the Flexible Tank at the 422-Inch Waste Level and Vertical Excitation at Absolute Pressure Near the Tank Bottom at  $\theta=0$

The pressure spikes generally occur at a single isolated point and the frequency of output is 0.01 second. This results in a triangular pulse with duration of 0.02 second. Given that the fundamental breathing mode frequency of the tank is 6 Hz, this nominally leads to a ratio of 0.12 for pulse duration to the natural period of the structure. Depending on the assumed actual pulse shape, the resulting dynamic magnification factor is in the range of 0.4 to 0.8 (Clough and Penzien 1975). However, the pulse duration should be viewed as an upper bound, since it depends on the output frequency. In fact, the true pulse duration, and hence the dynamic magnification factor, may be less. This could be investigated by rerunning the problem with a higher output frequency, although this was not done.

It is also obvious from Figure 5-38 and evident in Figure 5-34 and Figure 5-35 that there is a slight downward drift in the pressure time histories that did not occur during the horizontal excitation.

Comparisons of the actual (that is, as predicted by Dytran<sup>®</sup>) maximum and minimum waste pressures to the theoretical maximum pressures at the 45 and 90° locations are shown in Figure 5-39 and Figure 5-40.

The pressure time history for the bottom center waste element (element 1722) is shown as Figure 5-41. The theoretical hydrostatic pressure at the centroid of element 1722 is 39.7 lbf/in<sup>2</sup>, and the theoretical peak hydrodynamic pressure is 8.0 lbf/in<sup>2</sup>. That is, the predicted maximum and minimum pressures at this location are 47.7 and 31.7 lbf/in<sup>2</sup>, respectively. The maximum and minimum values shown in Figure 5-41 are 47.2 and 32.6 lbf/in<sup>2</sup>, respectively.

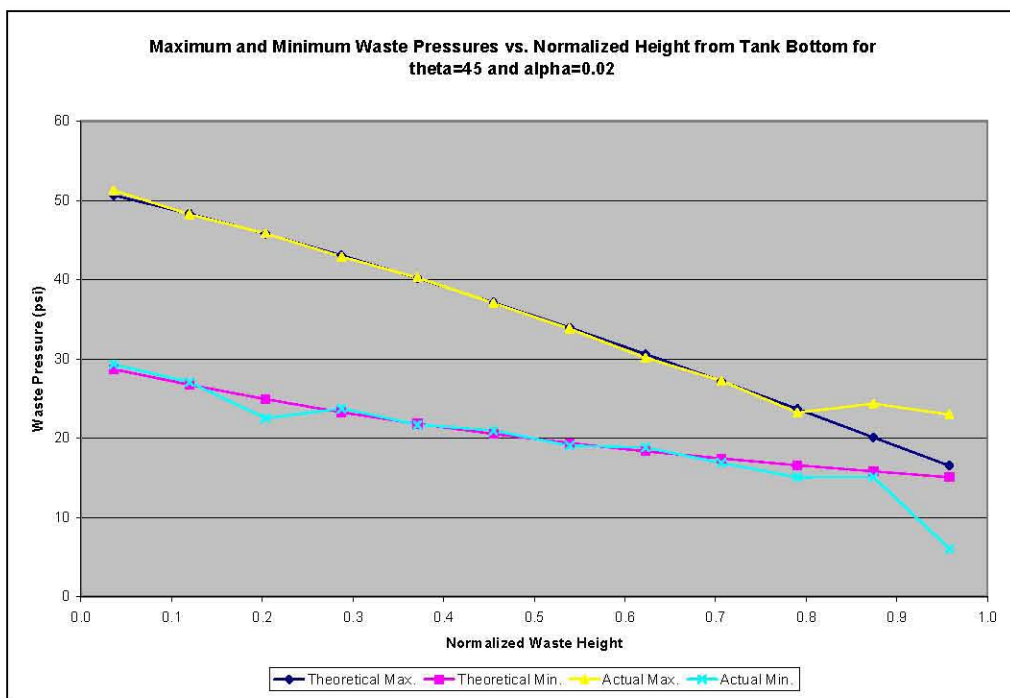


Figure 5-39. Maximum and Minimum Waste Pressures vs. Normalized Height from Tank Bottom for the Flexible Tank at the 422-Inch Waste Level Under Vertical Excitation at  $\theta=45^\circ$  and  $\alpha=0.02$

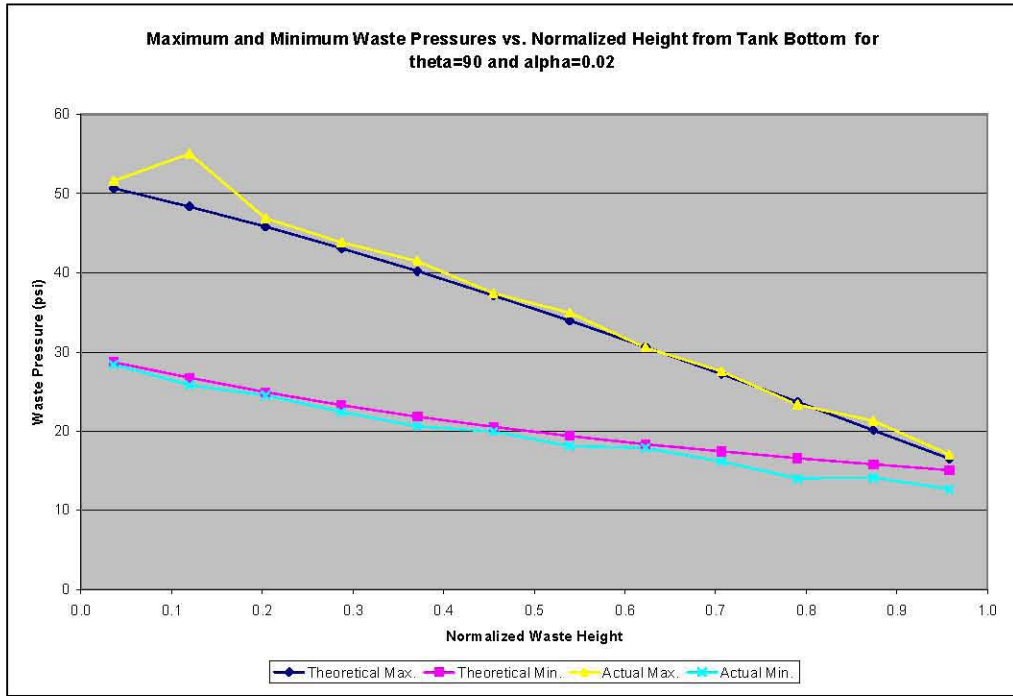


Figure 5-40. Maximum and Minimum Waste Pressures vs. Normalized Height from Tank Bottom for the Flexible Tank at the 422-Inch Waste Level at Absolute Pressure with  $\theta=90^\circ$  and  $\alpha=0.02$

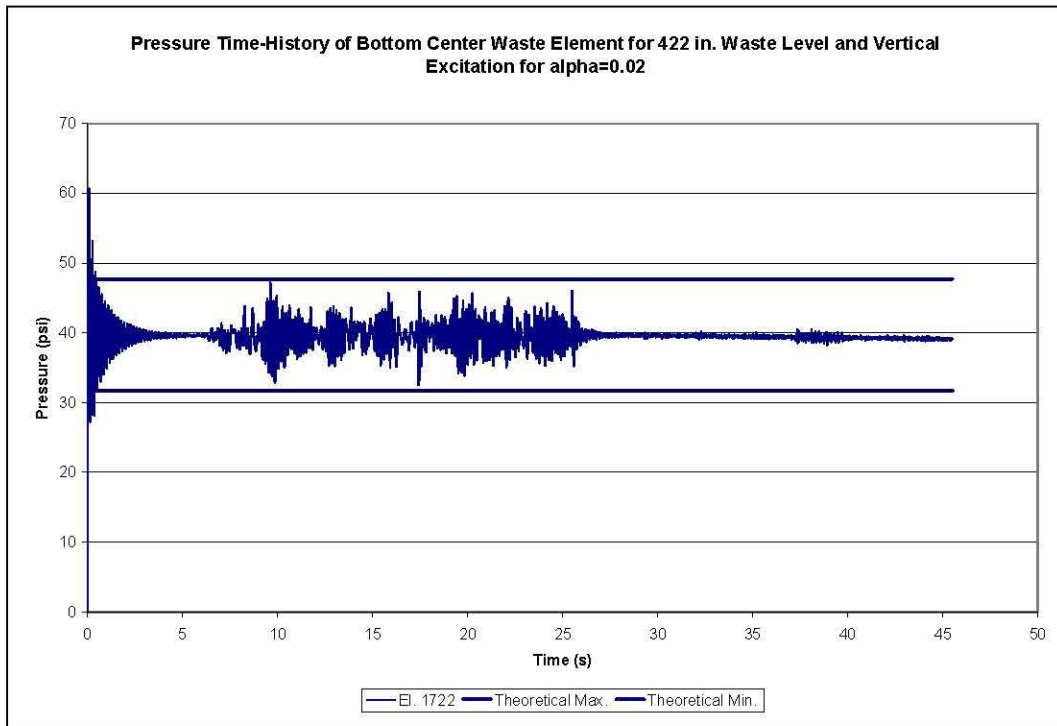


Figure 5-41. Pressure Time History for Bottom Center Waste Element for 422 Inches Waste Level and Vertical Excitation at Absolute Pressure and  $\alpha=0.02$

## 5.4 Maximum Slosh Height Results

The maximum slosh height traces for the runs at gage and absolute pressure are shown in Figure 5-42. The results show minor differences, but the peak slosh heights both compare well with the theoretical value of 23.7 inches.

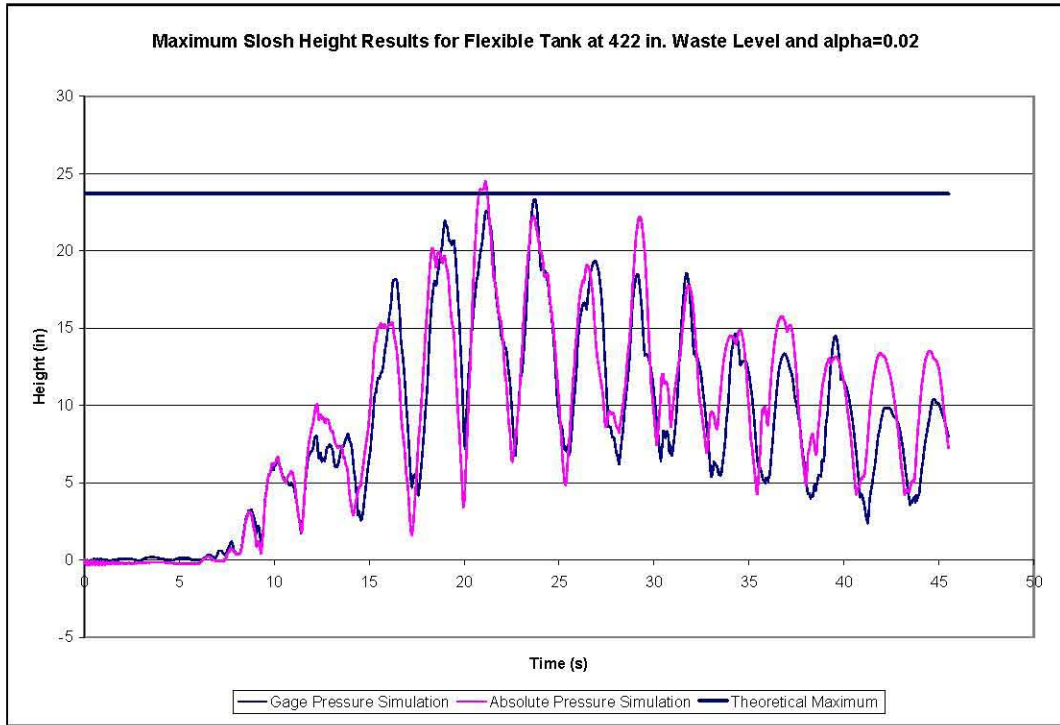


Figure 5-42. Comparison of Maximum Slosh Height Time Histories for the Flexible Tank at the 422-Inch Waste Level and  $\alpha=0.02$

Figure 5-43 shows the effect of the damping parameter alpha on the maximum slosh height time histories. The data show that there is very little difference in the maximum slosh height for values of alpha of 0.01 and 0.02, and that both agree well with theory. The maximum slosh height corresponding to alpha=0.04 is approximately 4% less than the maximum slosh height for alpha=0.01, or 0.02.

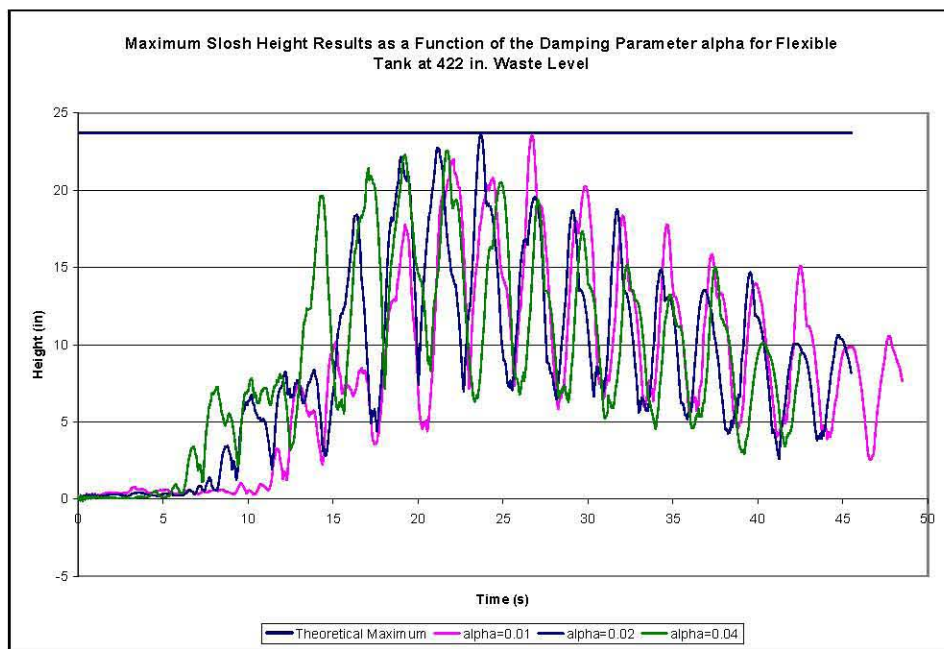


Figure 5-43. Dependence of the Maximum Slosh Height on the Damping Parameter  $\alpha$

## 5.5 Element Stresses

Selected stress results will be presented for the absolute pressure run. The pressure plots are presented to illustrate trends and as a general check on the behavior of the solution. Although some checks exist for the expected stress values, because of the complexity of the structure, the stress fields will be more complicated than the fluid pressure fields. The primary reason for assuming a uniform wall thickness for the benchmark primary tank model was to simplify the distribution of stress in the tank wall and, in particular, to simplify the hoop stress distribution that can be approximated as

$$\sigma_{hoop} = \frac{pr}{t}, \quad (5-12)$$

where  $p$  is the fluid pressure,  $r$  is the tank radius, and  $t$  is the tank wall thickness. This relationship is, of course, expected to breakdown near the upper and lower portions of the tank wall due to local end-effects, but should give a good approximation in the central portion of the tank wall.

### 5.5.1 Horizontal Excitation Run at Absolute Pressure

Mid-plane or membrane hoop stress is shown in Figure 5-44, Figure 5-45, and Figure 5-46 for tank wall elements at  $\theta=0$ ,  $45$ , and  $90^\circ$ , respectively. A comparison between membrane hoop stress and the expected value of that stress for a tank wall element at mid-height in the wall is shown as Figure 5-47. The hoop stresses are generally as expected and show the proper dependence on the angle  $\theta$ . A comparison of the hoop stresses at the  $90^\circ$  for the absolute and gage pressure solutions is shown as Figure 5-48. Examination of Figure 5-48 shows that the stresses in the gage pressure solution drift slightly upward over time while the stresses from the absolute pressure solutions are steady. The same behavior was observed in Figure 5-28, Figure 5-29, and Figure 5-30 for the waste pressures.

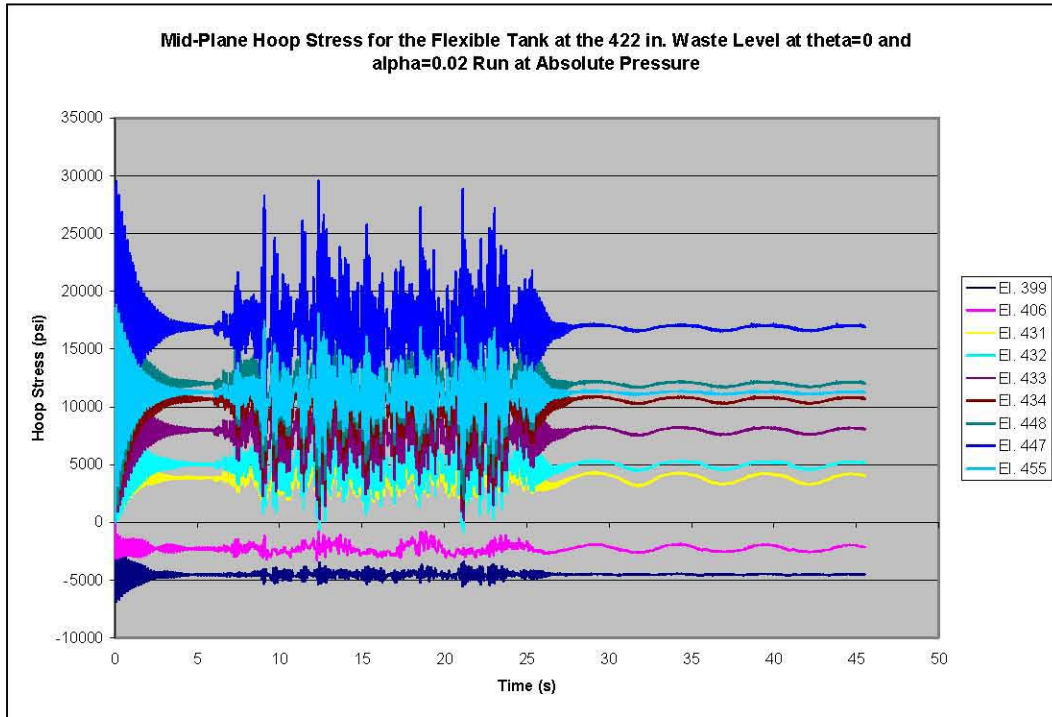


Figure 5-44. Mid-Plane Hoop Stress for the Flexible Tank at the 422-Inch Waste Level at  $\theta=0$  and  $\alpha=0.02$  Run at Absolute Pressure

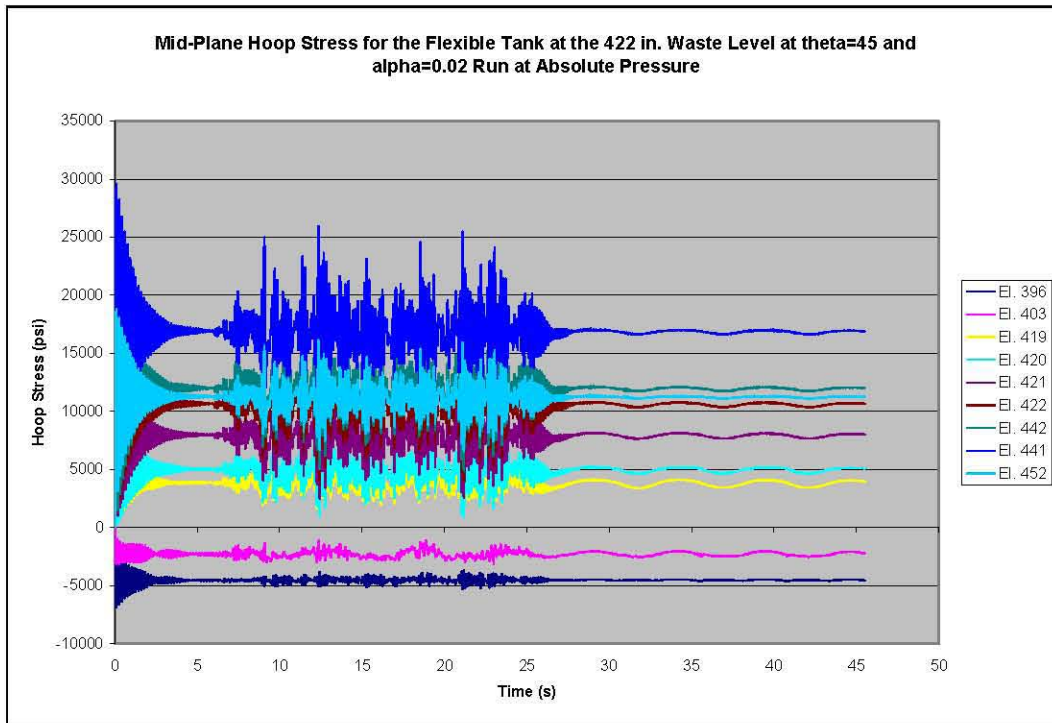


Figure 5-45. Mid-Plane Hoop Stress for the Flexible Tank at the 422-Inch Waste Level at  $\theta=45^\circ$  and  $\alpha=0.02$  Run at Absolute Pressure

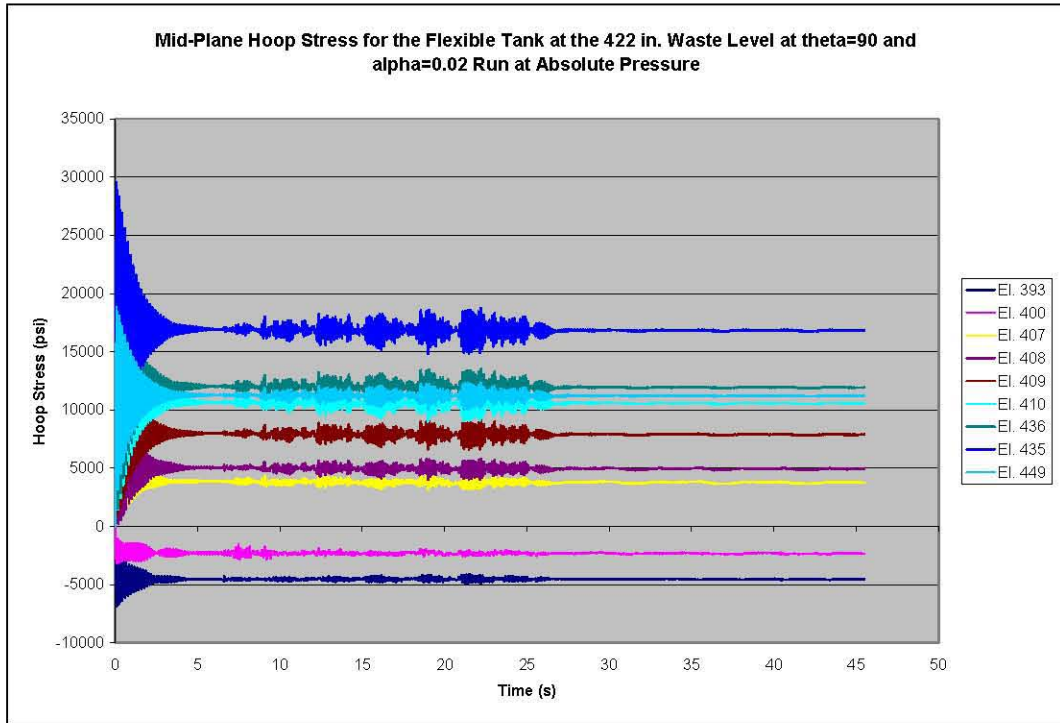


Figure 5-46. Mid-Plane Hoop Stress for the Flexible Tank at the 422-Inch Waste Level at  $\theta=90^\circ$  and  $\alpha=0.02$  Run at Absolute Pressure

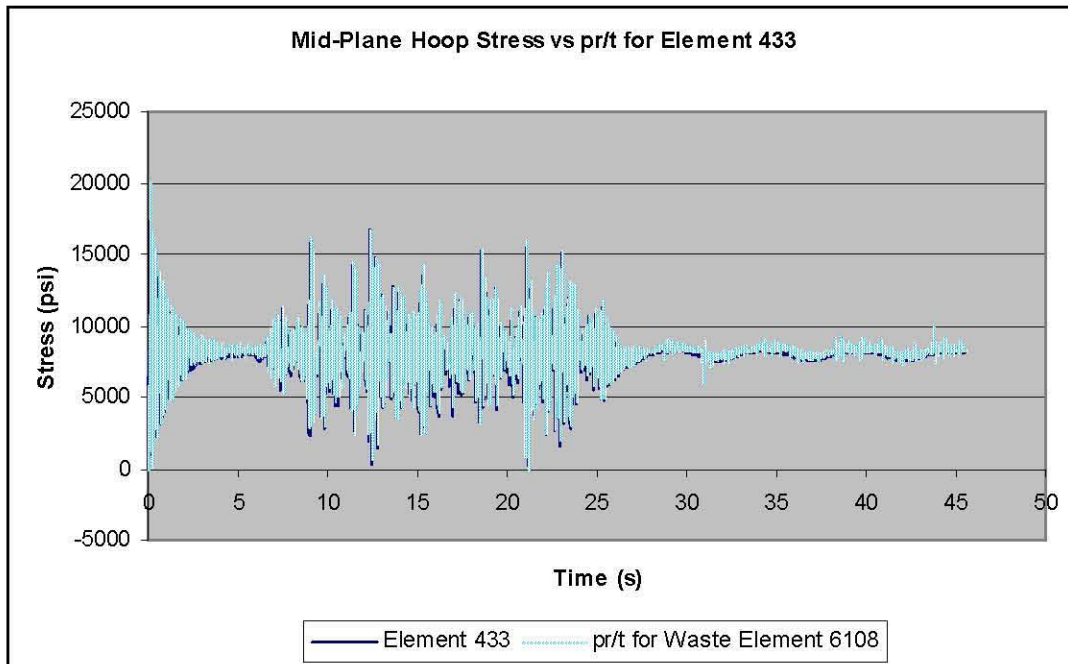


Figure 5-47. Comparison of Mid-Plane Hoop Stress in Tank Wall Element 433 to  $pr/t$  for Waste Element 6108 at Wall Mid-Height and  $\theta=0$

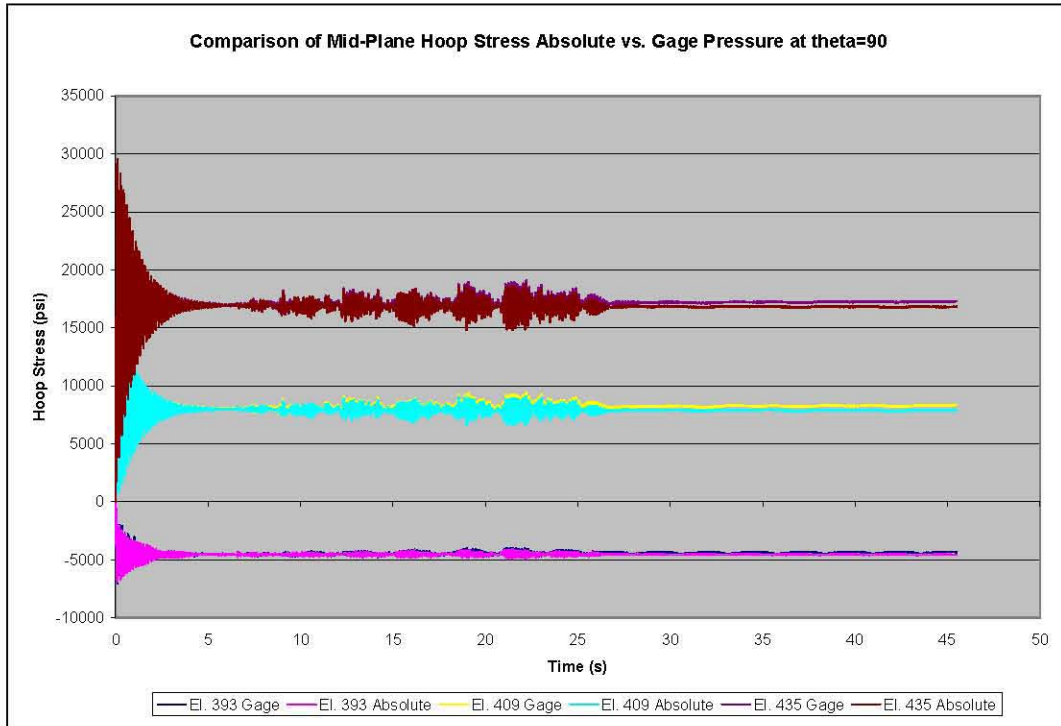


Figure 5-48. Comparison of Mid-Plane Hoop Stress at Absolute and Gage Pressure for Selected Elements at  $\theta=90^\circ$

## 6.0 Flexible Tank Dytran® Model at 460-Inch Waste Level

The response of the tank and contained liquid to seismic excitation with the liquid initially at the 460-inch level does not have a closed form analytical solution because of the interaction of the liquid-free surface with the curved surface of the tank dome. However, the solutions obtained with Dytran® will be compared to *the theoretical solution for the open tank with the hinged-top condition and 460-inch waste level* as well as with the Dytran® solution at the 422-inch level.

The problem was run initially at gage pressure. Pressure time histories for the waste elements showed that several waste elements experienced zero pressure, indicating that the dynamic pressure exceeded the static pressure. Consequently, the problem was rerun at absolute pressure, and the results presented below are from the absolute pressure case.

### 6.1 Hydrodynamic Forces

#### 6.1.1 Horizontal Excitation Run at Absolute Pressure

The vertical reaction force shown in Figure 6-1 during the initial free-vibration phase exhibits a breathing mode frequency of 5.5 Hz in agreement with theory, and it has essentially reached steady-state in 5-6 seconds (28-33 cycles), indicating an effective damping of approximately 2.5% during this phase.

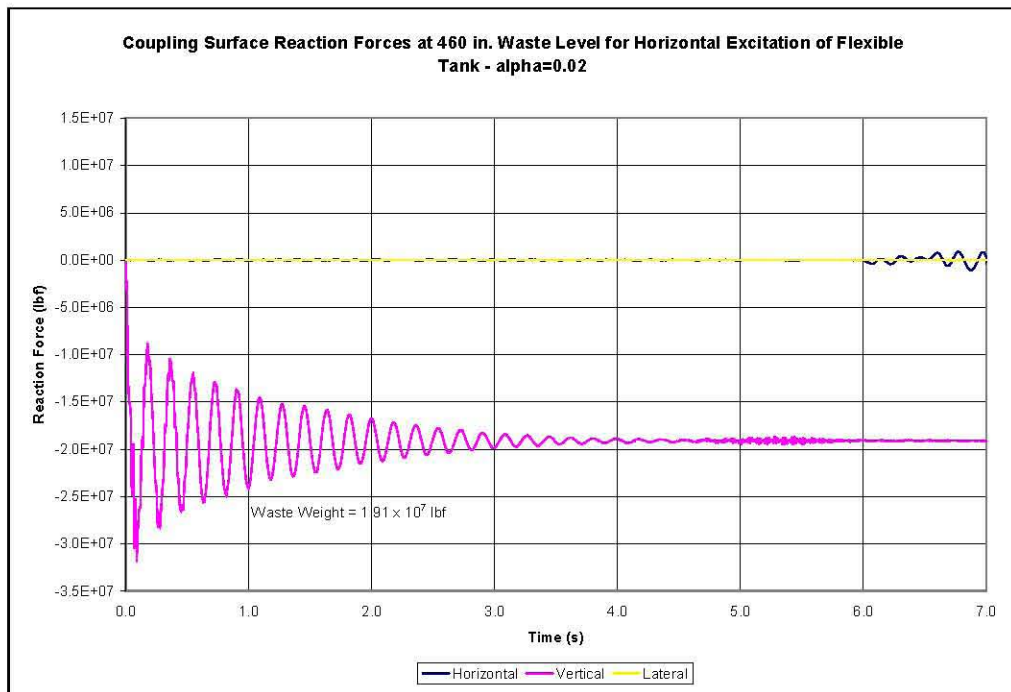


Figure 6-1. Coupling Surface Reaction Forces at the 460-Inch Waste Level for the Flexible Tank Under Horizontal Seismic Input During the Initial Free-Vibration Phase – alpha=0.02

The peak hydrodynamic force is  $1.02 \times 10^7$  lbf as shown in Figure 6-2, or 99% of the value of  $1.03 \times 10^7$  lbf predicted for the open tank with the hinge-top condition at the 460-inch waste level. That is, according to the Dytran® model, the peak horizontal hydrodynamic force is essentially the same as predicted for the open-top tank, and any interaction of the fluid with the dome has not significantly changed the peak force from that predicted for the open-top tank.

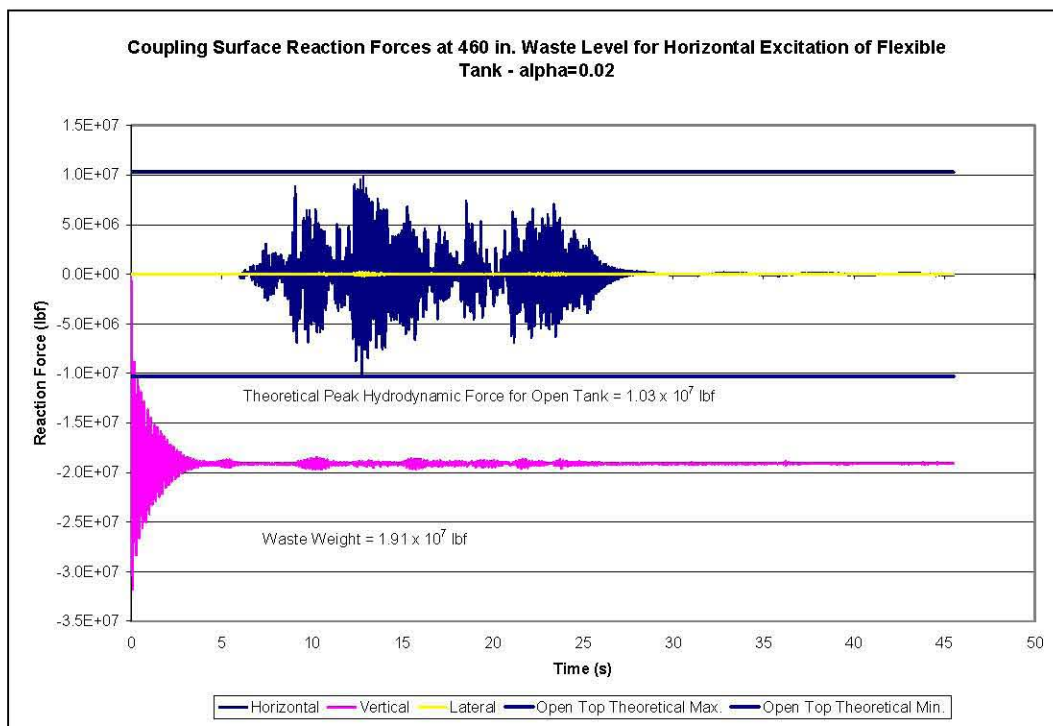


Figure 6-2. Coupling Surface Reaction Forces at the 460-Inch Waste Level for the Flexible Tank Under Horizontal Seismic Input – alpha=0.02

As shown in Figure 6-3, the horizontal reaction force time history during the second free-vibration period beginning at 25.5 seconds indicates that the impulsive frequency is approximately 6.5 Hz. Thus, both the impulsive and breathing mode frequencies have decreased approximately 0.5 Hz relative to the 422-inch case as predicted by theory. The 36% increase in peak horizontal hydrodynamic force relative to the 422-inch waste level is due not only to the increased waste mass, but also because the lower impulsive frequency associated with the 460-inch waste level has a higher associated spectral acceleration.

Figure 6-4 presents a comparison of the horizontal hydrodynamic force time histories for the 460- and 422-inch waste levels during the second free-vibration period beginning at 25.5 seconds. During this period, the response is dominated by convective effects. The data show that the peak hydrodynamic force during this period is  $3.31 \times 10^5$  lbf for the 422-inch waste level (72% of theoretical value of  $4.62 \times 10^5$  lbf), and  $2.85 \times 10^5$  lbf for the 460-inch waste level (55% of open-top theoretical value of  $5.21 \times 10^5$  lbf). Because of system damping, the values above should not be interpreted as the peak of the convective response, but the relative magnitude shows that the presence of the dome reduces the convective response of the waste. The fundamental convective period is approximately 5 seconds. Comparison of the two responses shows less-effective damping at the 460-inch waste level during the convective response in final free-oscillation phase than the 1% critical damping at the 422-inch level.

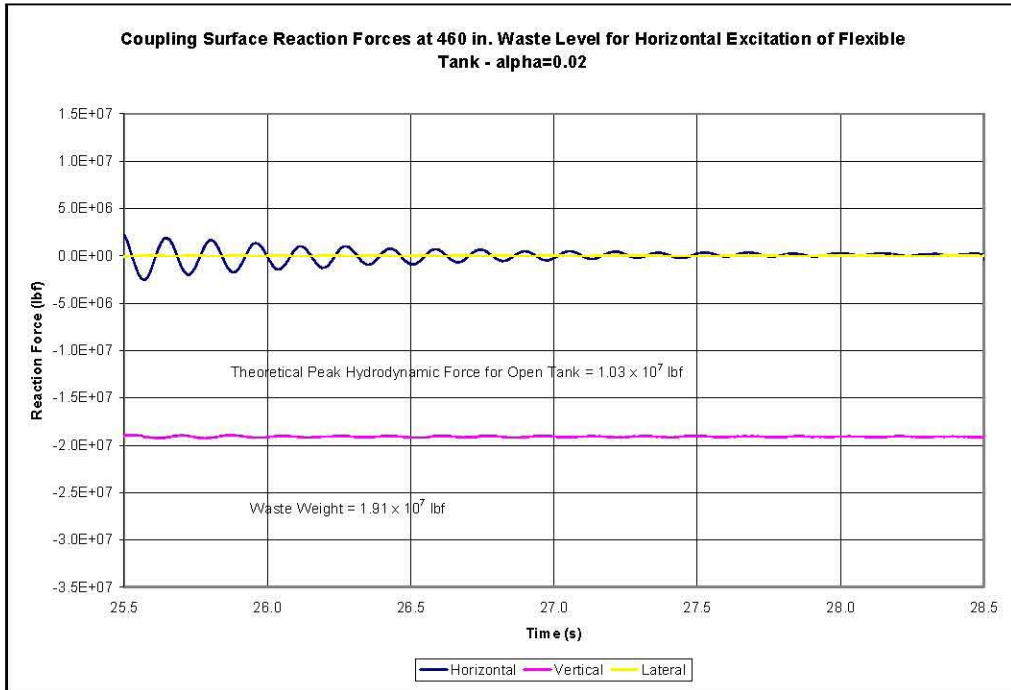


Figure 6-3. Coupling Surface Reaction Forces at the 460-Inch Waste Level for the Flexible Tank Under Horizontal Seismic Input During the Final Free-Vibration Phase –  $\alpha=0.02$

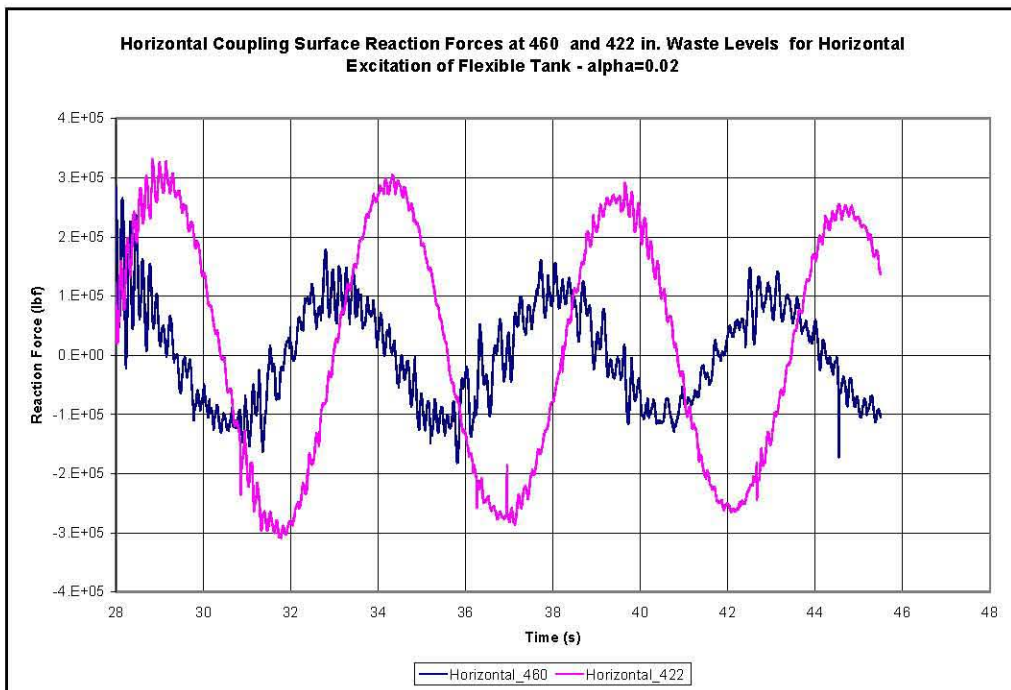


Figure 6-4. Comparison of the Horizontal Coupling Surface Reaction Force for the 460- and 422-Inch Waste Levels During the Final Free-Vibration Period –  $\alpha=0.02$

### 6.1.2 Vertical Excitation Run at Absolute Pressure

The peak vertical hydrodynamic force from the computer simulation was  $5.98 \times 10^6$  lbf, or 32% greater than the value of  $4.54 \times 10^6$  lbf predicted by theory for the open tank at the 460-inch waste level. The majority of the vertical coupling surface reaction force is due to the weight of the waste rather than the hydrodynamic force, so viewed this way, the total peak reaction force of  $2.51 \times 10^7$  lbf is 6% greater than the theoretical value of  $2.36 \times 10^7$  lbf (Figure 6-5).

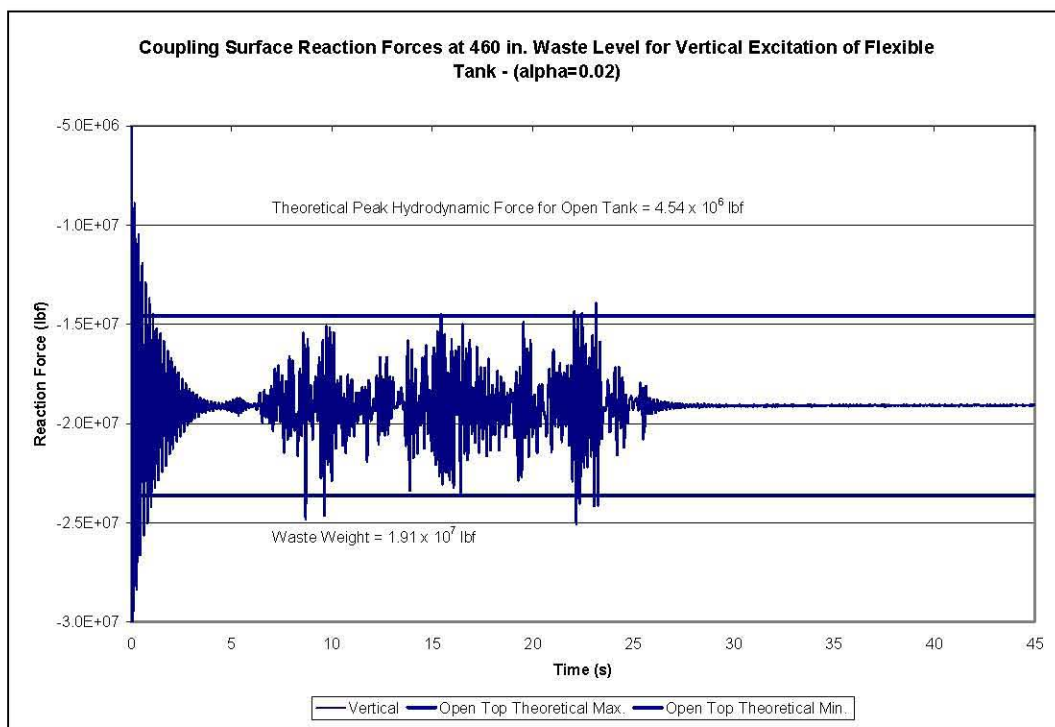


Figure 6-5. Vertical Coupling Surface Reaction Force at the 460-Inch Waste Level for the Flexible Tank Under Vertical Seismic Input

## 6.2 Waste Pressures

Although no closed form solution exists for the 460-inch waste level, theoretical dynamic pressures were calculated from Equation 4.24 in BNL (1995) based on an open tank with 460 inches of waste and a hinged-top condition. This solution is presented along with the actual results for comparison purposes.

As in Section 5.3, the total pressures are the sum of the hydrostatic pressures and the hydrodynamic pressures. The hydrostatic, peak hydrodynamic, and peak total pressures for the elements in the sets “plusx\_els” and “press\_45” are shown in Table 6-1 and Table 6-2. The maximum theoretical pressures for the elements set “plusx\_els” are simply the hydrostatic pressures shown in Table 6-1, because the theoretical hydrodynamic pressures are zero at  $\theta=90^\circ$ .

**Table 6-1.** Theoretical Maximum Absolute Waste Pressures for Horizontal Excitation in the Flexible Open-Top Tank at 460-Inch Waste Level for Elements at  $\theta=0$

“Plusx_els” Element No.	Hydrostatic Pressure (psi)	Peak Hydrodynamic Pressure (psi)	Peak Total Pressure (psi)
11211	14.7	0	14.7
10482	16.0	4.4	20.4
9753	18.4	8.1	26.5
9024	20.7	11.0	31.7
8295	23.1	13.3	36.4
7566	25.4	15.2	40.6
6837	27.7	16.8	44.5
6108	30.1	18.1	48.2
5379	32.4	19.2	51.6
4650	34.7	20.0	54.7
3921	37.1	20.7	57.8
3192	39.4	21.1	60.5
2463	41.8	21.4	63.2
1734	44.1	21.6	65.7

**Table 6-2.** Theoretical Maximum Absolute Waste Pressures for Horizontal Excitation in the Flexible Open-Top Tank at 460-Inch Waste Level for Elements at  $\theta=45$

“Press_45” Element No.	Hydrostatic Pressure (psi)	Peak Hydrodynamic Pressure (psi)	Peak Total Pressure (psi)
11019	14.7	0	14.7
10290	16.0	3.1	19.1
9561	18.4	5.7	24.1
8832	20.7	7.8	28.5
8103	23.1	9.4	32.5
7374	25.4	10.8	36.2
6645	27.7	11.9	39.6
5916	30.1	12.8	42.9
5187	32.4	13.6	46.0
4458	34.7	14.2	48.9
3729	37.1	14.6	51.7
3000	39.4	14.9	54.4
2271	41.8	15.1	56.9
1542	44.1	15.3	59.3

### 6.2.1 Horizontal Excitation Run at Absolute Pressure

The pressure time histories for the elements adjacent to the tank wall at  $\theta=0$  are shown in Figure 6-6. The hydrostatic pressures are evenly spaced between 16 and 44 lbf/in<sup>2</sup> in agreement with the values in

Table 6-1. The pressure time histories for elements 9753 and 9024 in the upper portion of the waste are shown separately in Figure 6-7. Evident are several isolated peaks in the waste pressures. Similar behavior is seen in the upper waste elements 9561 and 8103 at the 45° location as shown in Figure 6-8 and Figure 6-9. The pressure time histories for the waste elements at  $\theta=90^\circ$  do not show the isolated peaks present at the other two locations (Figure 6-10).

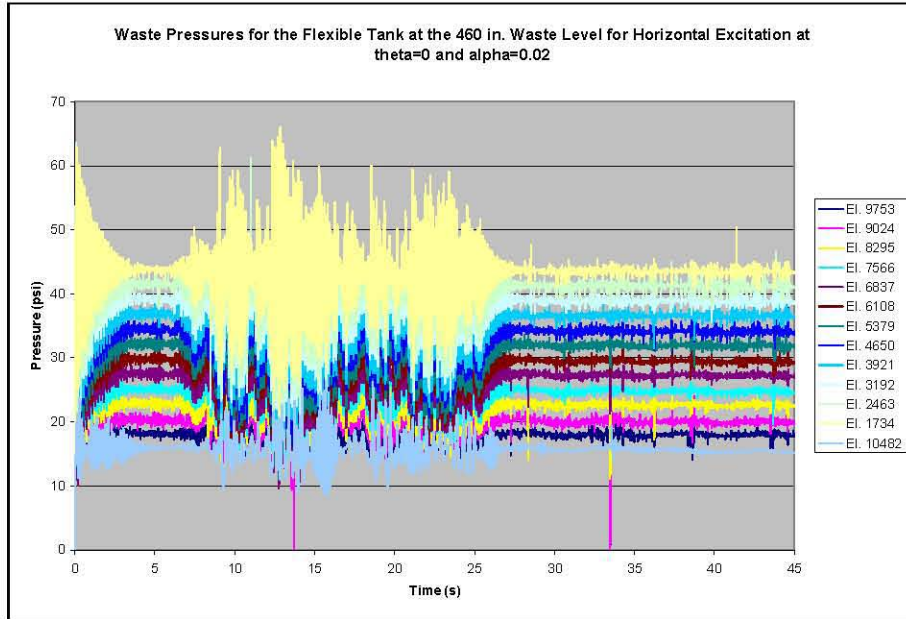


Figure 6-6. Waste Pressures Time Histories for the Flexible Tank at the 460-Inch Waste Level for Horizontal Excitation at  $\theta=0$  and  $\alpha=0.02$  Run at Absolute Pressure

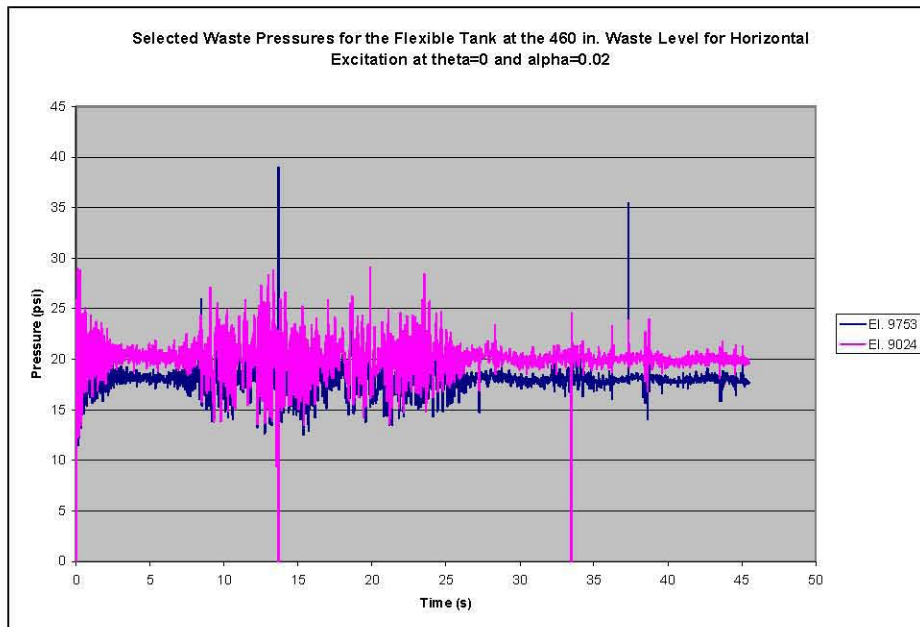


Figure 6-7. Selected Element Pressure Time Histories for the Flexible Tank at the 460-Inch Waste Level for Horizontal Excitation at  $\theta=0$  and  $\alpha=0.02$  Run at Absolute Pressure

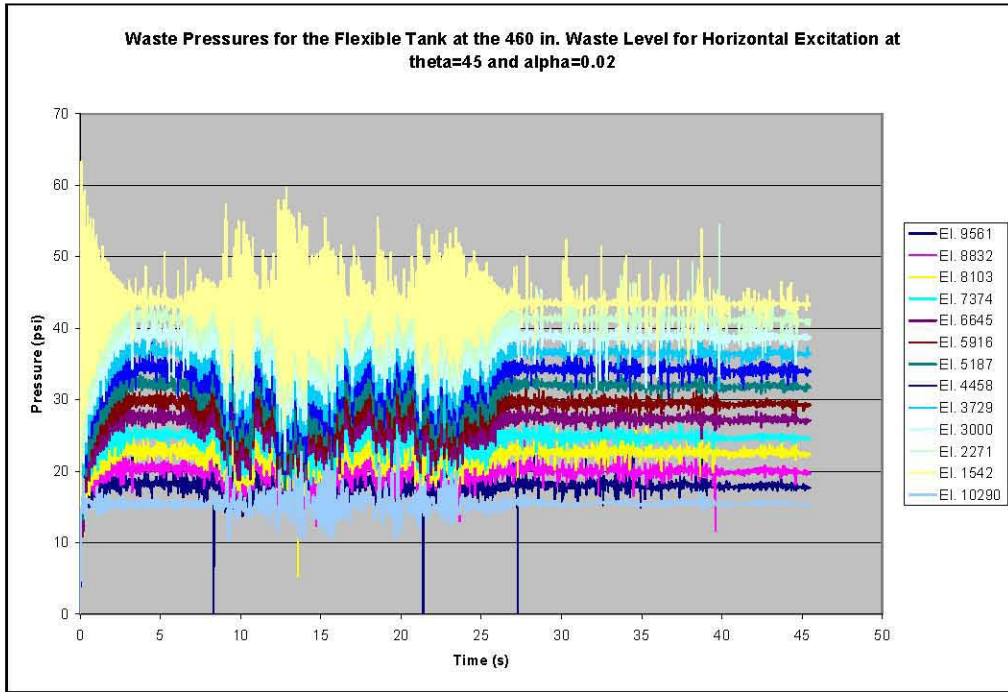


Figure 6-8. Waste Pressures Time Histories for the Flexible Tank at the 460-Inch Waste Level for Horizontal Excitation at  $\theta=45$  and  $\alpha=0.02$  Run at Absolute Pressure

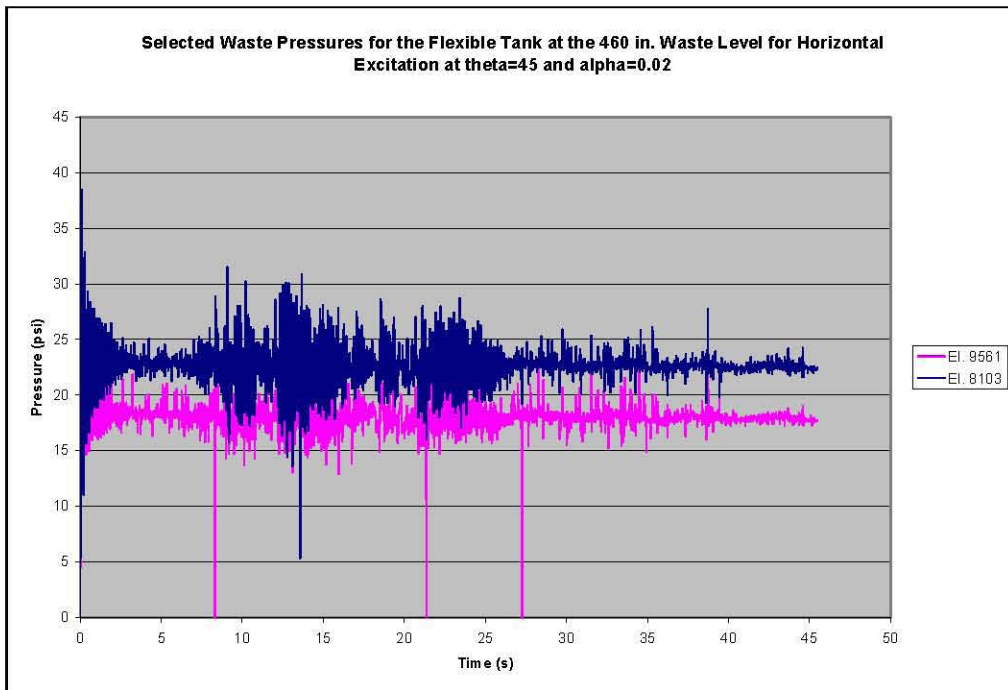
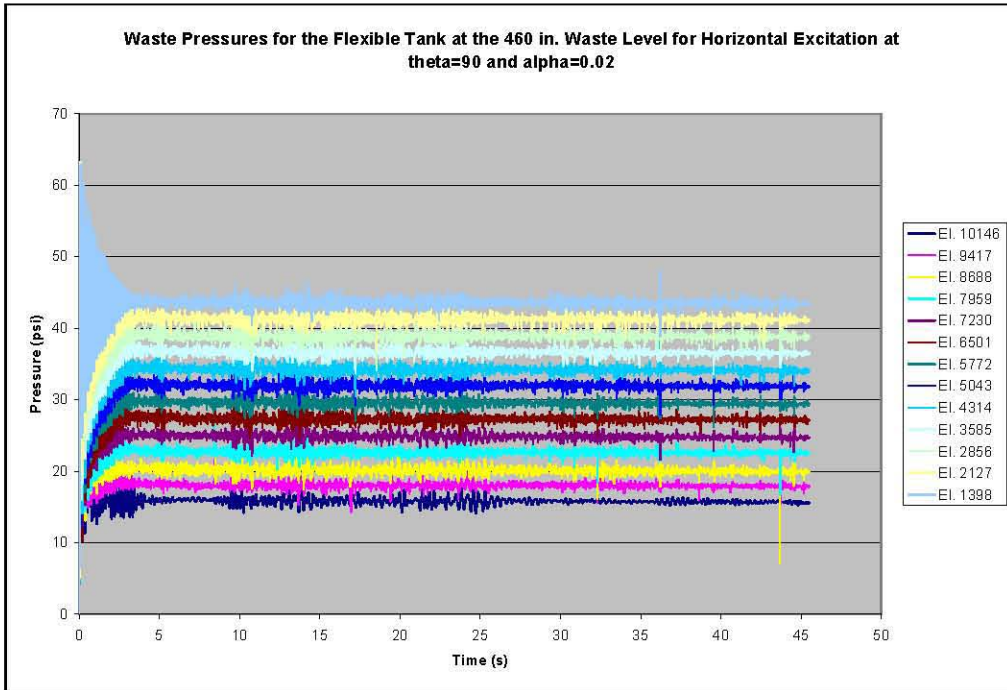


Figure 6-9. Selected Element Pressure Time Histories for the Flexible Tank at the 460-Inch Waste Level for Horizontal Excitation at  $\theta=45$  and  $\alpha=0.02$  Run at Absolute Pressure



**Figure 6-10.** Waste Pressures Time Histories for the Flexible Tank at the 460-Inch Waste Level for Horizontal Excitation at  $\theta=90$  and  $\alpha=0.02$  Run at Absolute Pressure

Comparisons of the maximum and minimum waste pressures from the computer simulation (labeled at “actual max.” and “actual min.”) to the maximum and minimum pressures from the theoretical solution for the open tank at the 460-inch waste level are shown in Figure 6-11, Figure 6-12, and Figure 6-13. In the lower portions of the waste, the results agree well with the theoretical solution for the open tank at the 460-inch waste level. In the upper waste elements, the results for  $\theta=0$  and  $45^\circ$  deviate from the theoretical value. The differences, of course, correspond to the isolated peaks shown in Figure 6-7 and Figure 6-9. If the single point isolated peaks shown in Figure 6-7 are neglected, the remaining maximum and minimum waste pressures are approximately 29 and 9 lbf/in<sup>2</sup>, respectively, and the correlation in Figure 6-11 would be much better at the upper waste elements. Likewise, if the isolated high peaks in Figure 6-9 are neglected, the correlation at the upper waste elements in Figure 6-12 would improve. Because no significant isolated peaks exist in the traces shown in Figure 6-10, the correlation of computer results to theoretical results shown in Figure 6-13 is good.

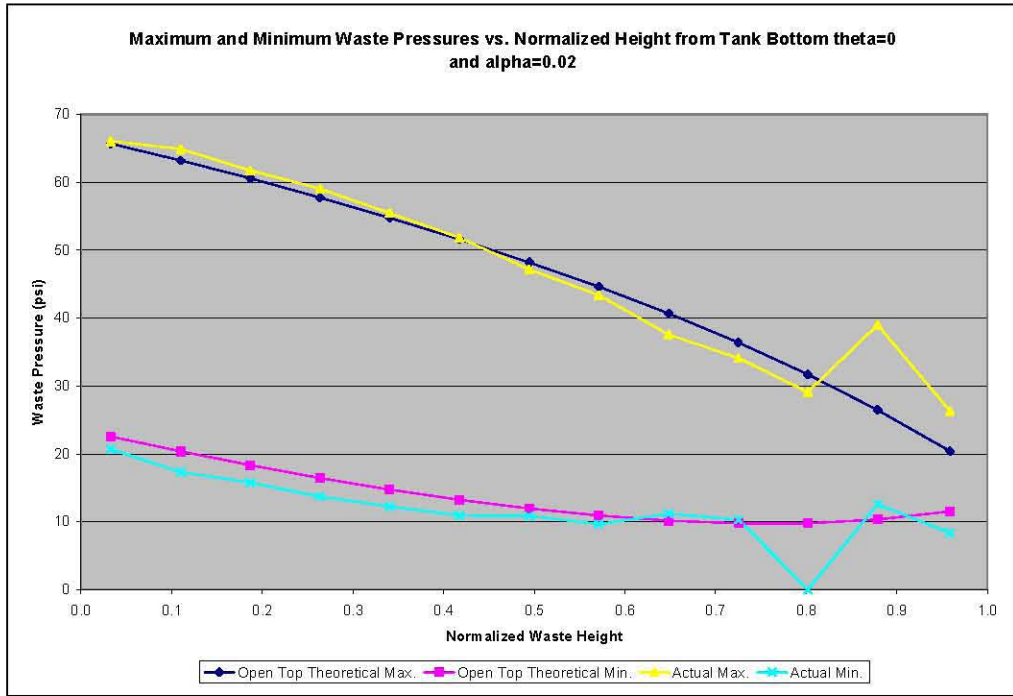


Figure 6-11. Maximum and Minimum Waste Pressures vs. Normalized Height from Tank Bottom for the Flexible Tank Under Horizontal Excitation at the 460-Inch Waste Level at  $\theta=0$  and  $\alpha=0.02$

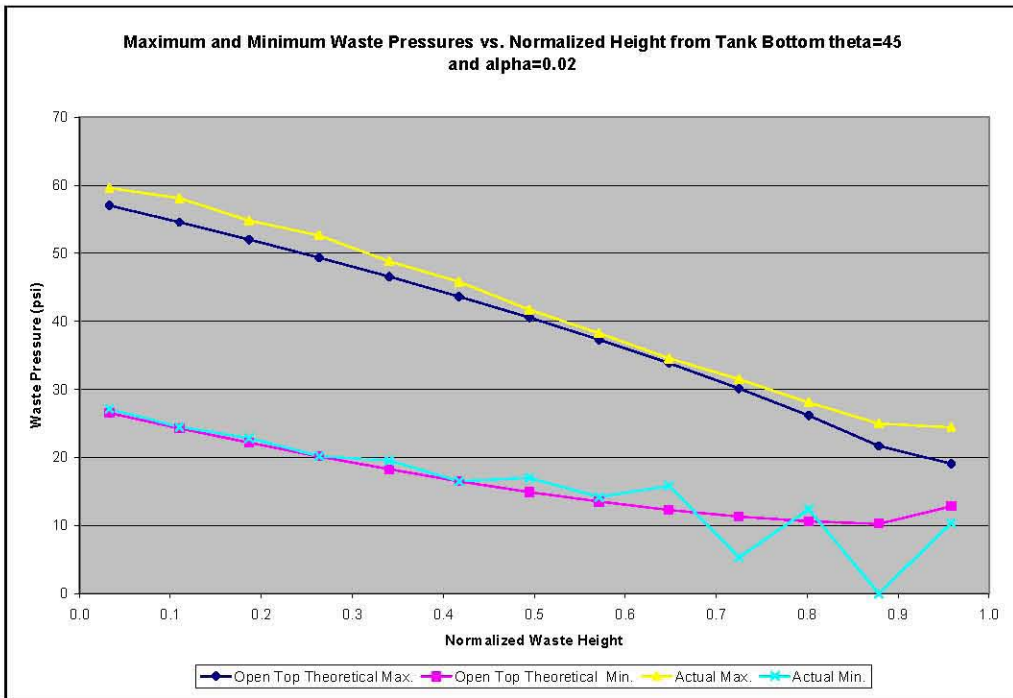
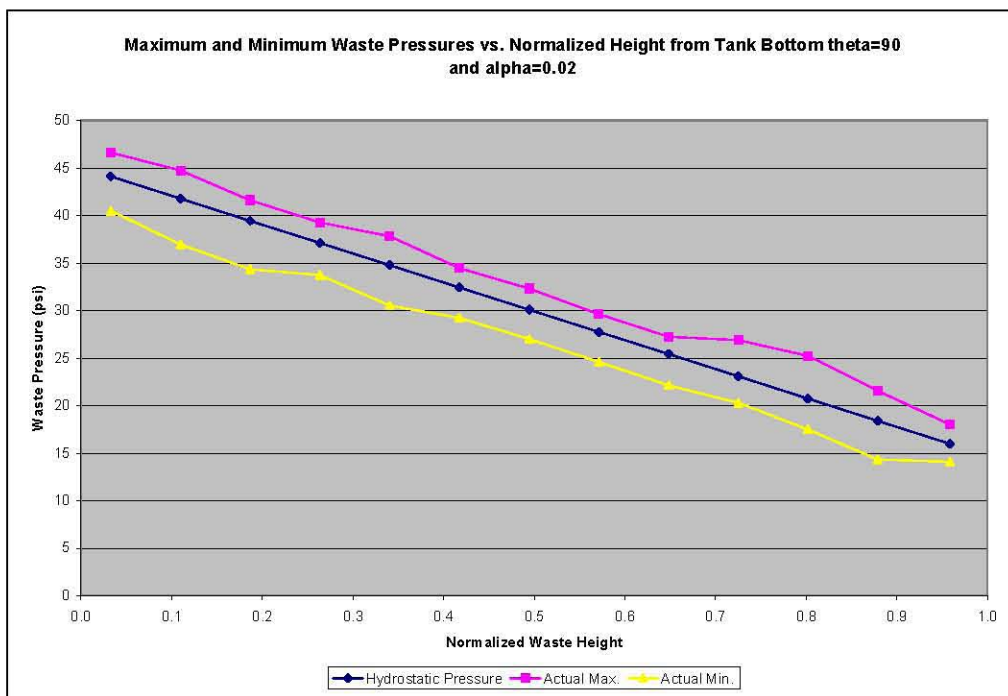


Figure 6-12. Maximum and Minimum Waste Pressures vs. Normalized Height from Tank Bottom for the Flexible Tank Under Horizontal Excitation at the 460-Inch Waste Level at  $\theta=45^\circ$  and  $\alpha=0.02$



**Figure 6-13.** Maximum and Minimum Waste Pressures vs. Normalized Height from Tank Bottom for the Flexible Tank Under Horizontal Excitation at the 460-Inch Waste Level at  $\theta=90^\circ$  and  $\alpha=0.02$

### 6.2.2 Wall and Base Pressures Due to Vertical Excitation Run at Absolute Pressure

The pressure time histories for the waste elements adjacent to the tank wall at  $\theta=0$  are shown in Figure 6-14, and pressure time histories for elements 2463 and 8295 are shown in Figure 6-15. A plot of the pressure decay for the same two elements during the initial gravity loading is shown in Figure 6-16. Evident in the plot is the breathing mode frequency of 5.5 Hz. Similar plots for waste elements at  $\theta=45$  and  $90^\circ$  are shown in Figure 6-17 through Figure 6-20.

Plots of the maximum and minimum waste pressures as a function of waste depth are shown in Figure 6-21, Figure 6-22, and Figure 6-23, where the values predicted by Dytran<sup>®</sup> are labeled as “actual max.” and “actual min.” The general agreement with open-top theory (Table 6-3) is good, but in each case, isolated peaks in the time histories result in deviations from the theoretical values. The very low value of minimum pressure that occurs at a normalized waste height of 0.11 is in element 2463. This minimum value occurs as an isolated peak at approximately 17 seconds as shown in Figure 6-15. Similar isolated peaks occur at the  $45$  and  $90^\circ$  locations, and the pressure time histories for the associated waste elements are shown in Figure 6-18 and Figure 6-20.

The pressure time history for the bottom center waste element (element 1722) is shown as Figure 6-24. The theoretical hydrostatic pressure at the centroid of element 1722 is  $44.1 \text{ lbf/in}^2$ , and the theoretical peak hydrodynamic pressure is  $7.3 \text{ lbf/in}^2$ . That is, the predicted maximum and minimum pressures at this location are  $51.4$  and  $36.8 \text{ lbf/in}^2$ , respectively. The maximum and minimum values shown in Figure 6-24 are  $54.3$  and  $36.3 \text{ lbf/in}^2$ , respectively.

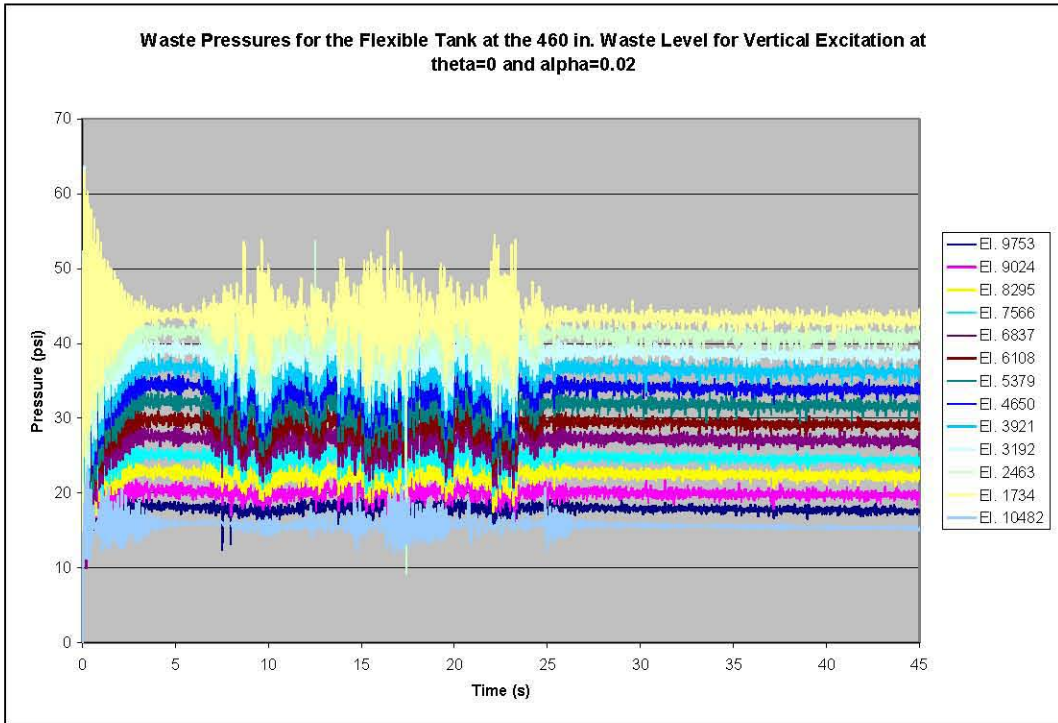


Figure 6-14. Waste Pressure Time Histories for the Flexible Tank at the 460-Inch Waste Level for Vertical Excitation at  $\theta=0$  and  $\alpha=0.02$

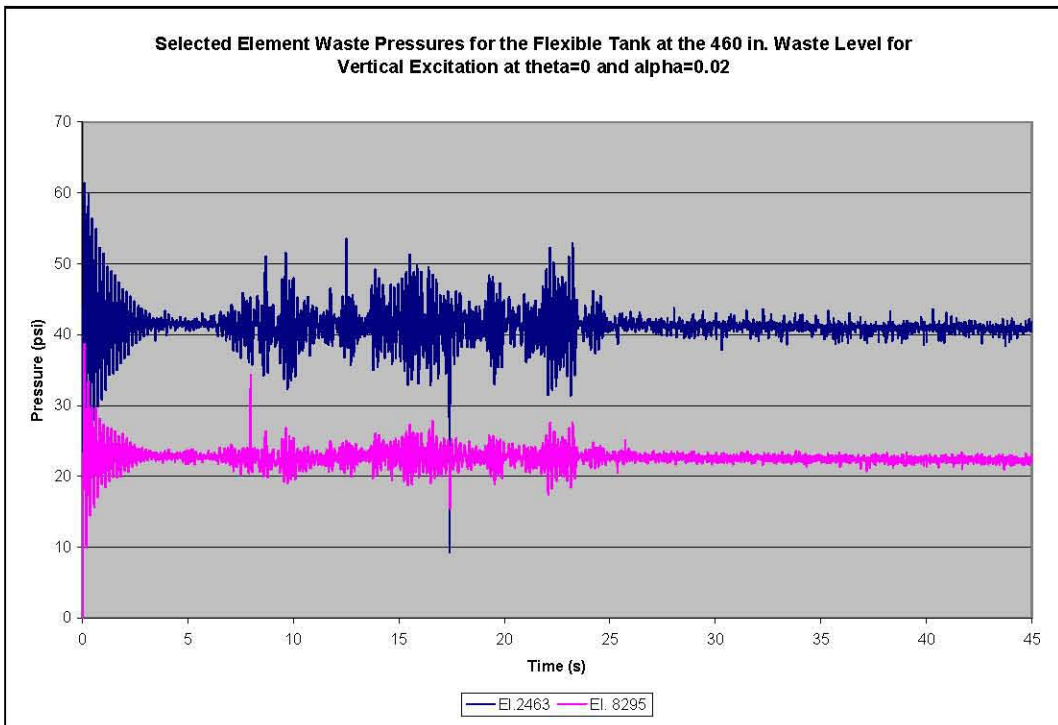


Figure 6-15. Selected Element Waste Pressure for the Flexible Tank at the 460-Inch Waste Level for Vertical Excitation at  $\theta=0$  and  $\alpha=0.02$

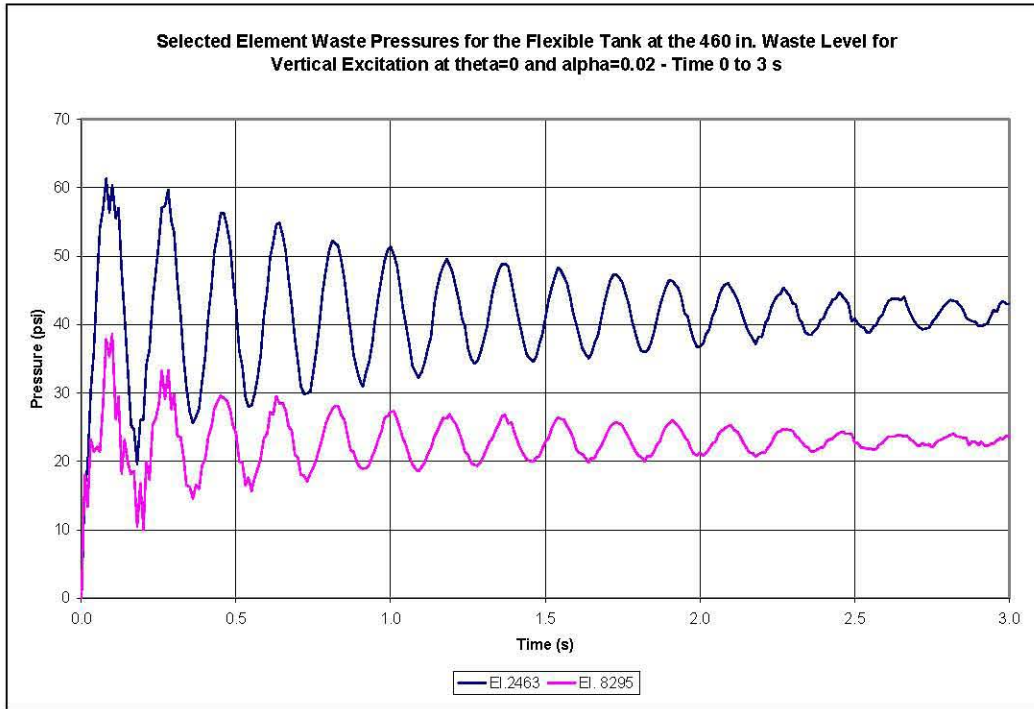


Figure 6-16. Selected Element Waste Pressures for the Flexible Tank at the 460-Inch Waste Level for Vertical Excitation at  $\theta=0$  and  $\alpha=0.02$  – Time 0 to 3 Seconds

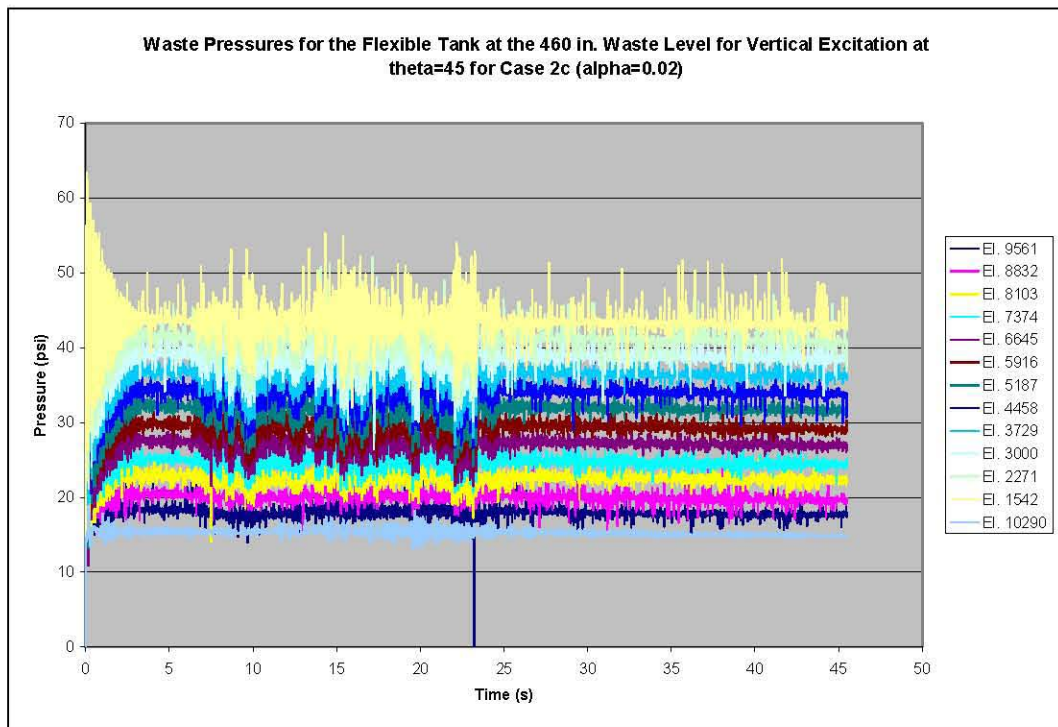


Figure 6-17. Waste Pressure Time Histories for the Flexible Tank at the 460-Inch Waste Level for Vertical Excitation at  $\theta=45^\circ$  and  $\alpha=0.02$

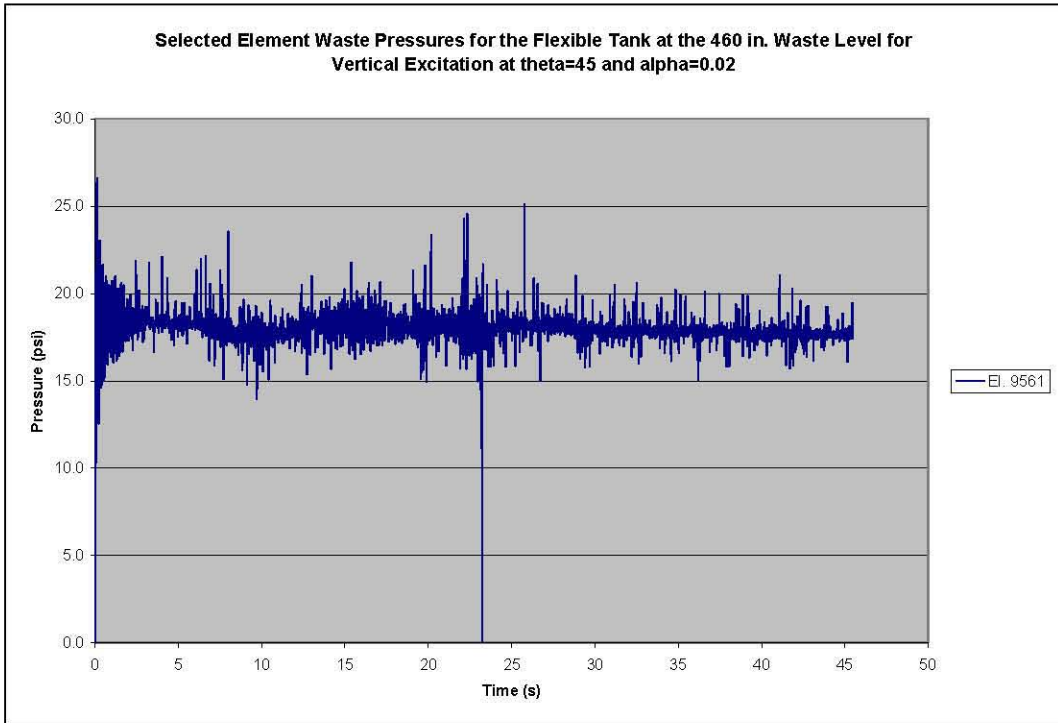


Figure 6-18. Selected Element Waste Pressure for the Flexible Tank at the 460-Inch Waste Level for Vertical Excitation at  $\theta=45^\circ$  and  $\alpha=0.02$

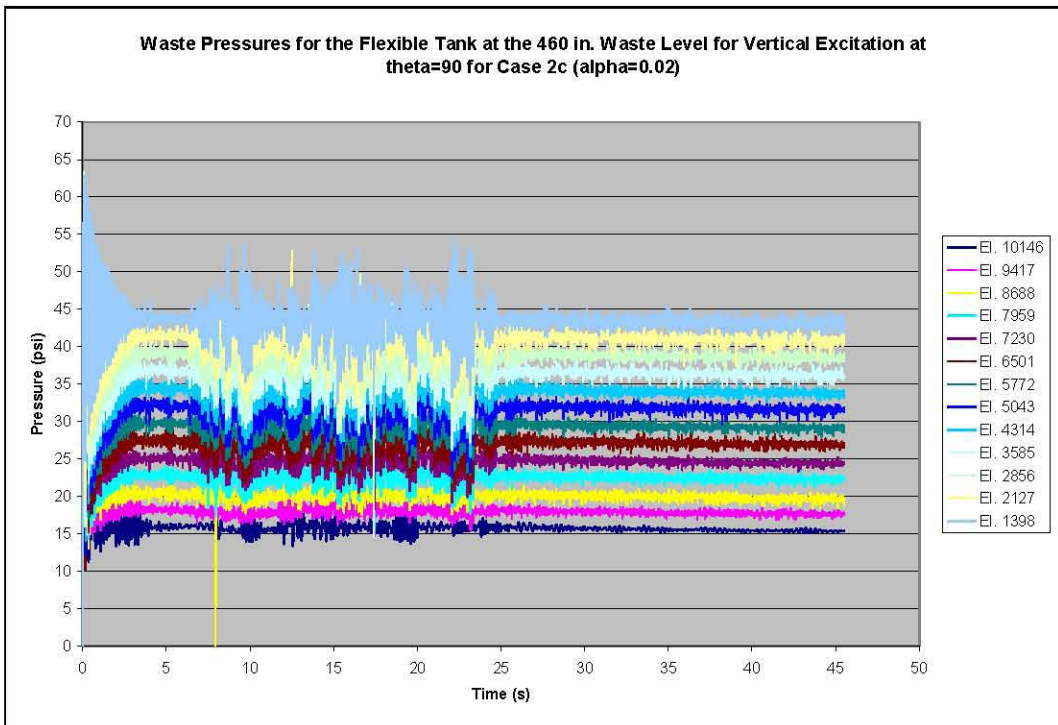


Figure 6-19. Waste Pressure Time Histories for the Flexible Tank at the 460-Inch Waste Level for Vertical Excitation at  $\theta=90^\circ$  and  $\alpha=0.02$

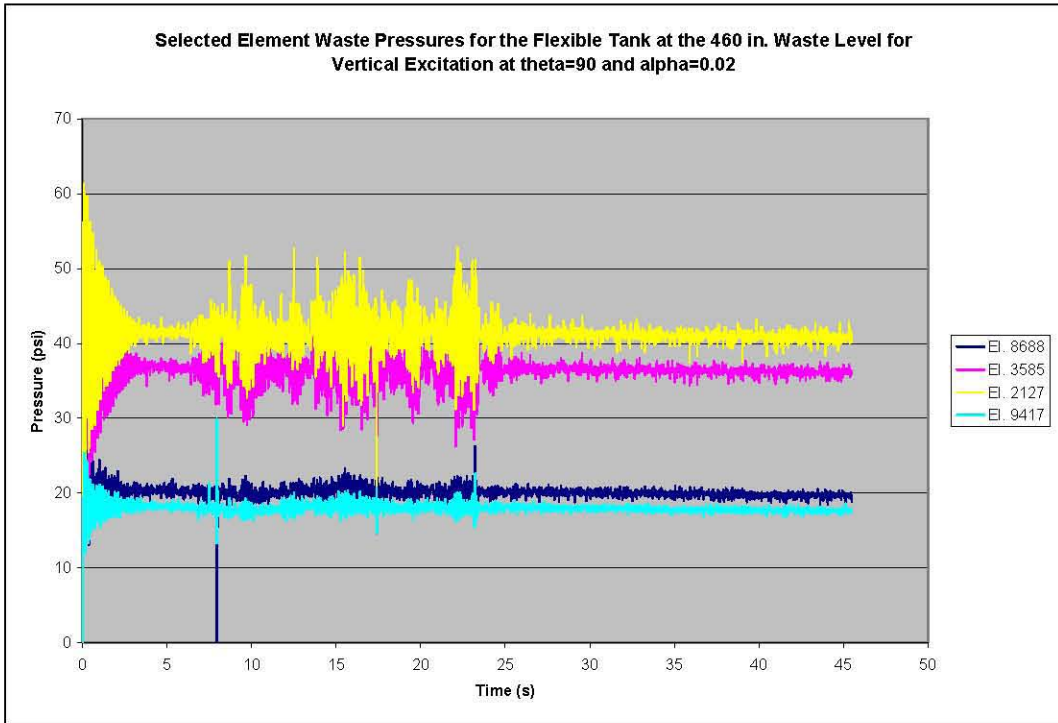


Figure 6-20. Selected Element Waste Pressure for the Flexible Tank at the 460-Inch Waste Level for Vertical Excitation at  $\theta=90^\circ$  and  $\alpha=0.02$

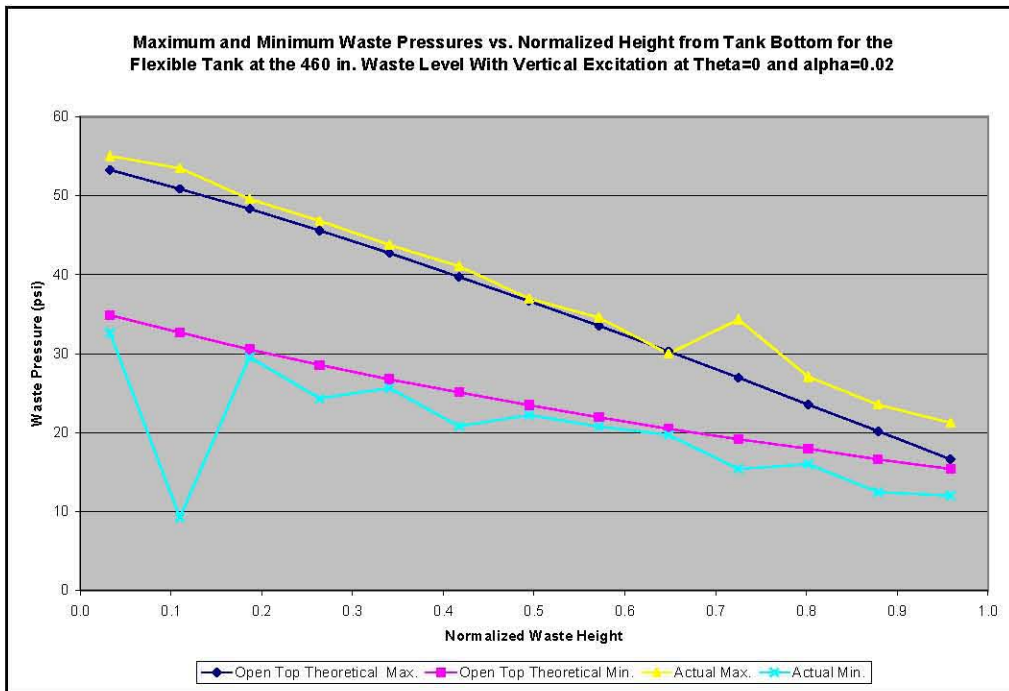


Figure 6-21. Maximum and Minimum Waste Pressures vs. Normalized Waste Height from Tank Bottom for 460-Inch Waste Level for Vertical Excitation at  $\theta=0$  and  $\alpha=0.02$

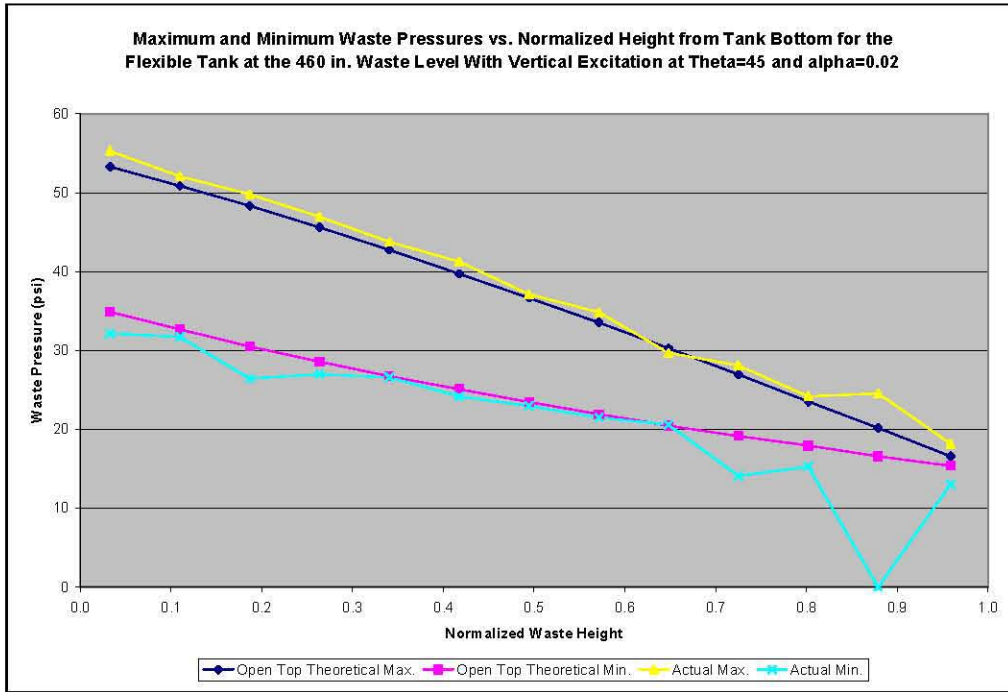


Figure 6-22. Maximum and Minimum Waste Pressures vs. Normalized Waste Height from Tank Bottom for 460-Inch Waste Level for Vertical Excitation at  $\theta=45^\circ$  and  $\alpha=0.02$

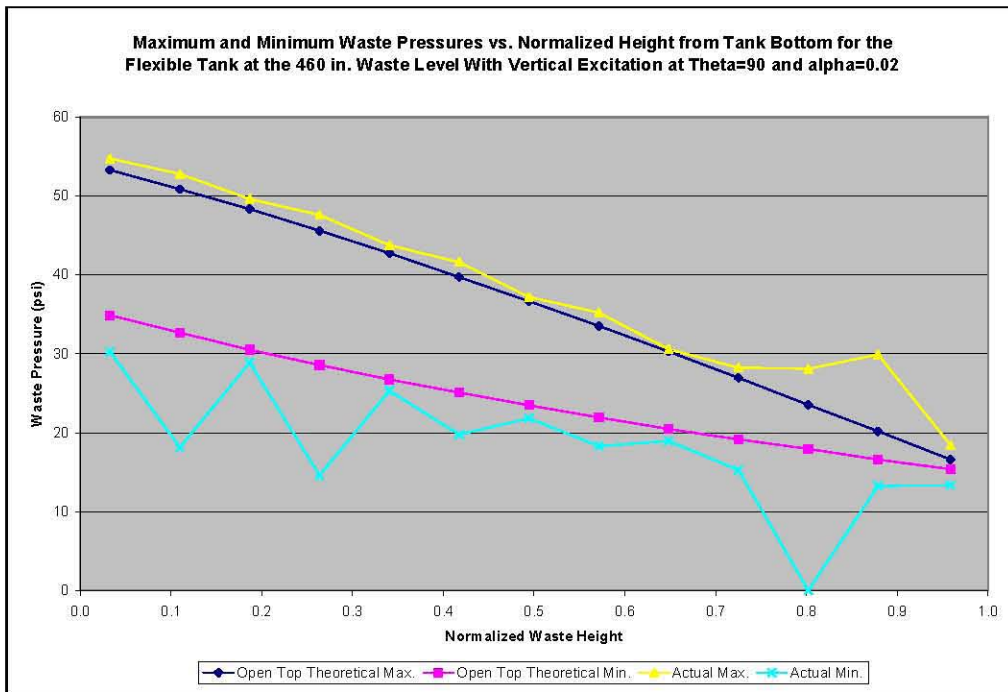
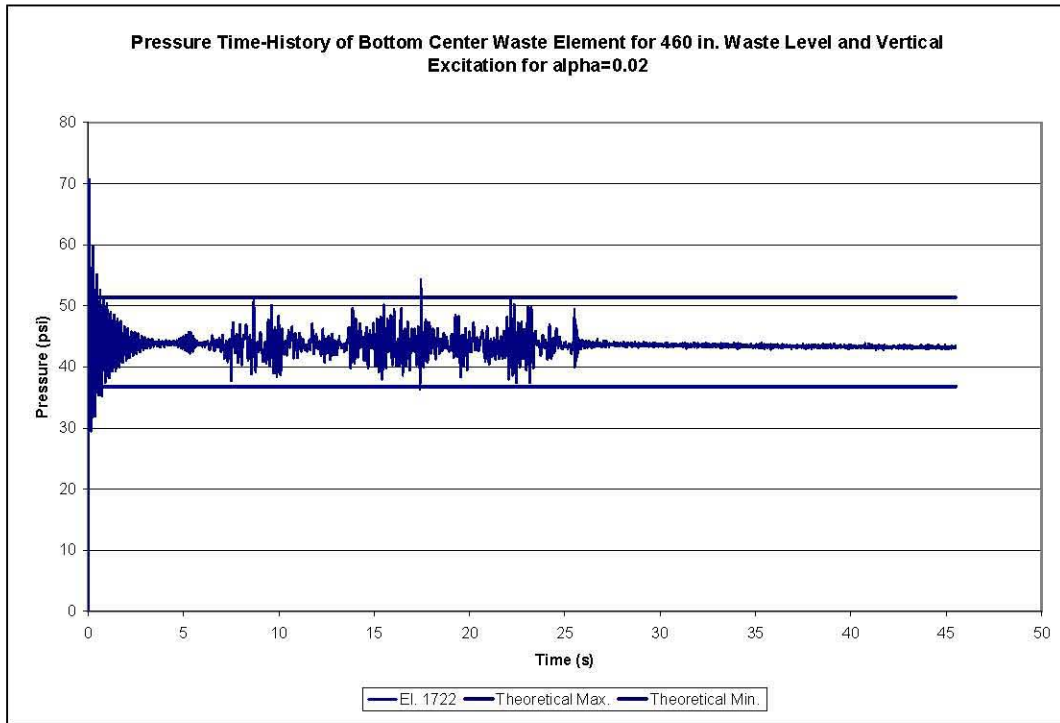


Figure 6-23. Maximum and Minimum Waste Pressures vs. Normalized Waste Height from Tank Bottom for 460-Inch Waste Level for Vertical Excitation at  $\theta=90^\circ$  and  $\alpha=0.02$

RPP-RPT-28963, Rev. 1  
M&D-2008-005-RPT-01, Rev. 1

**Table 6-3.** Theoretical Maximum Absolute Wall Pressures for Vertical Excitation of an Open-Top Tank at the 460-Inch Waste Level

“Plusx_els”	“Press_45”	“Plusz_els”	Hydrostatic Pressure (psi absolute)	Peak Hydrodynamic Wall Pressure (psi absolute)	Peak Total Pressure (psi absolute)
Element No.	Element No.	Element No.			
10482	10290	10146	16.0	0.9	16.9
9753	9561	9417	18.4	2.7	21.1
9024	8832	8688	20.7	4.4	25.1
8295	8103	7959	23.1	6.0	29.1
7566	7374	7230	25.4	7.5	32.9
6837	6645	6501	27.7	9.0	36.7
6108	5916	5772	30.1	10.2	40.3
5379	5187	5043	32.4	11.4	43.8
4650	4458	4314	34.7	12.3	47.0
3921	3729	3585	37.1	13.1	50.2
3192	3000	2856	39.4	13.7	53.1
2463	2271	2127	41.8	14.1	55.9
1734	1542	1398	44.1	14.3	58.4



**Figure 6-24.** Pressure Time History for Bottom Center Waste Element for 460-Inch Waste Level and Vertical Excitation for  $\alpha=0.02$

### 6.3 Maximum Slosh Height Results

The time histories of the maximum height of the waste-free surface for the simulations at absolute and gage pressure are presented in Figure 6-25. The maximum slosh height predicted for an open tank at the 460-inch waste level is 24.5 inches as shown by the horizontal line in the plot. The maximum value predicted by the Dytran<sup>®</sup> simulation run at absolute pressure is slightly greater than 20 inches, and the maximum value predicted for the run at gage pressure is approximately 18 inches. Also plotted is the slosh height trace for a rigid tank at the 460-inch waste level run at absolute pressure. The maximum free surface height from that run is just over 21 inches. It should not be surprising that the maximum slosh height for the closed tank is less than for the open tank since the presence of the dome should be expected to inhibit the convective response.

The same nonzero slosh heights during gravity loading that were observed in Figure 4-23 show up in Figure 6-25. As remarked in Section 4.3, this may be a limitation with either the slosh height subroutine, or the model discretization.

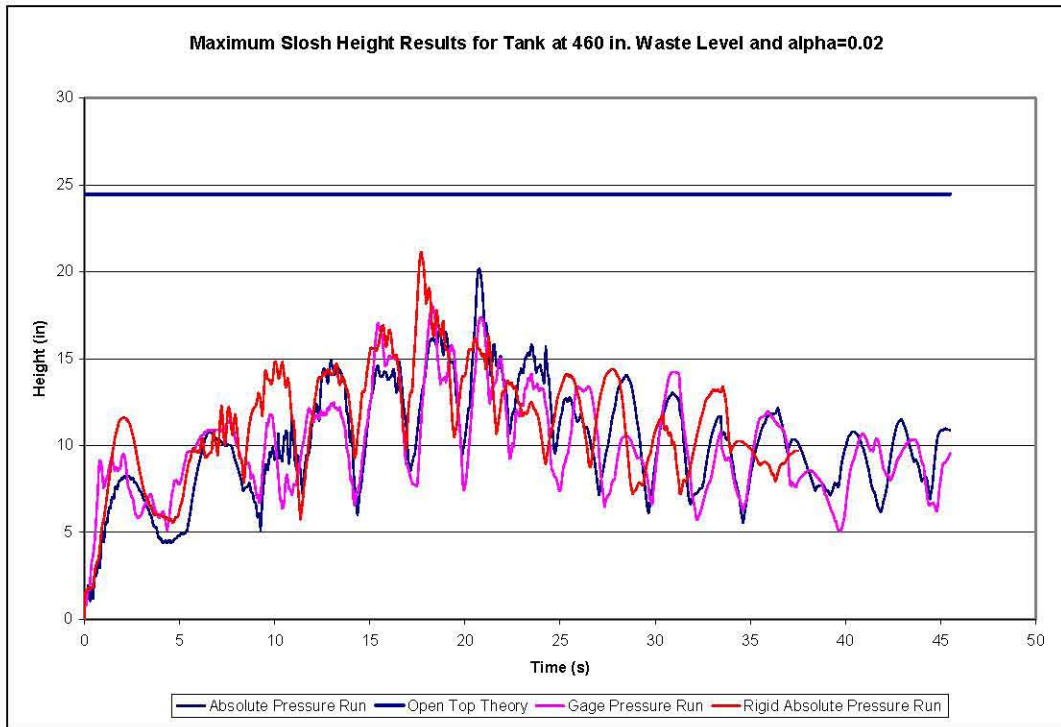


Figure 6-25. Maximum Slosh Height Time History for the Flexible Tank at the 460-Inch Waste Level for  $\alpha=0.02$

### 6.4 Element Stresses

#### 6.4.1 Horizontal Excitation Run at Absolute Pressure

Mid-plane hoop stresses for the tank shell elements at  $\theta=0, 45,$  and  $90^\circ$  are presented as Figure 6-26, Figure 6-27, and Figure 6-28, respectively. The general behavior of the hoop stresses is reasonable, with

the peak stresses generally increasing with waste depth, and decreasing with the angular distance from the plane of excitation in accordance with the waste pressures.

A comparison of the hoop stress to the waste pressures for tank wall element 406 and waste element 9753 is shown as Figure 6-29. Both elements are near the waste-free surface at  $\theta=0$ . Notable in the plot is that the hoop stress does not reflect the spikes in the waste pressure that occur at approximately 14 and 36 seconds. Similar behavior is displayed in Figure 6-30 for the 422-inch waste level.

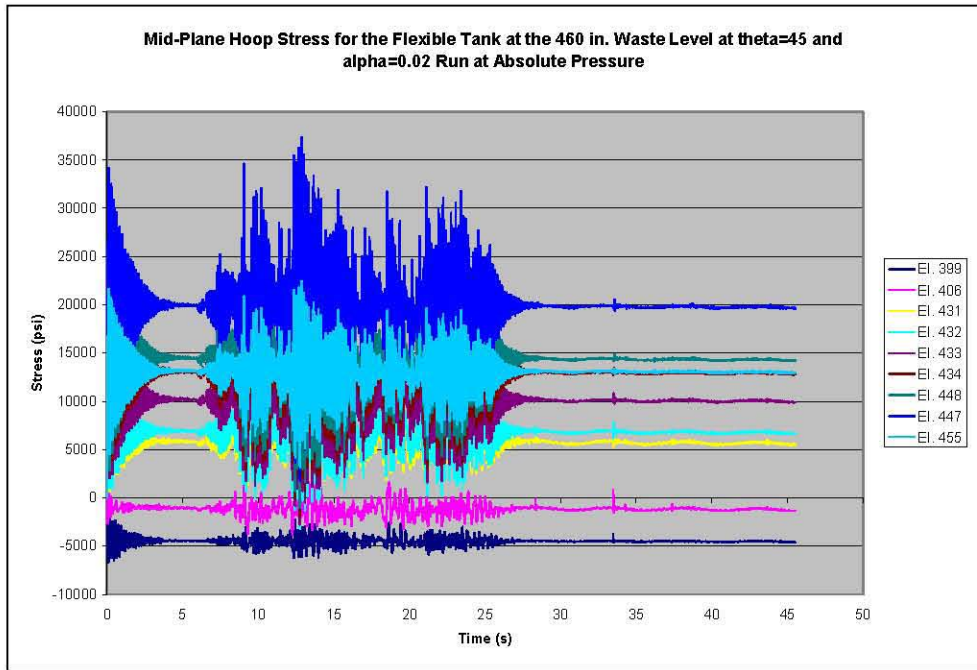


Figure 6-26. Mid-Plane Hoop Stress for the Flexible Tank at the 460-Inch Waste Level at  $\theta=0$  and  $\alpha=0.02$  Run at Absolute Pressure

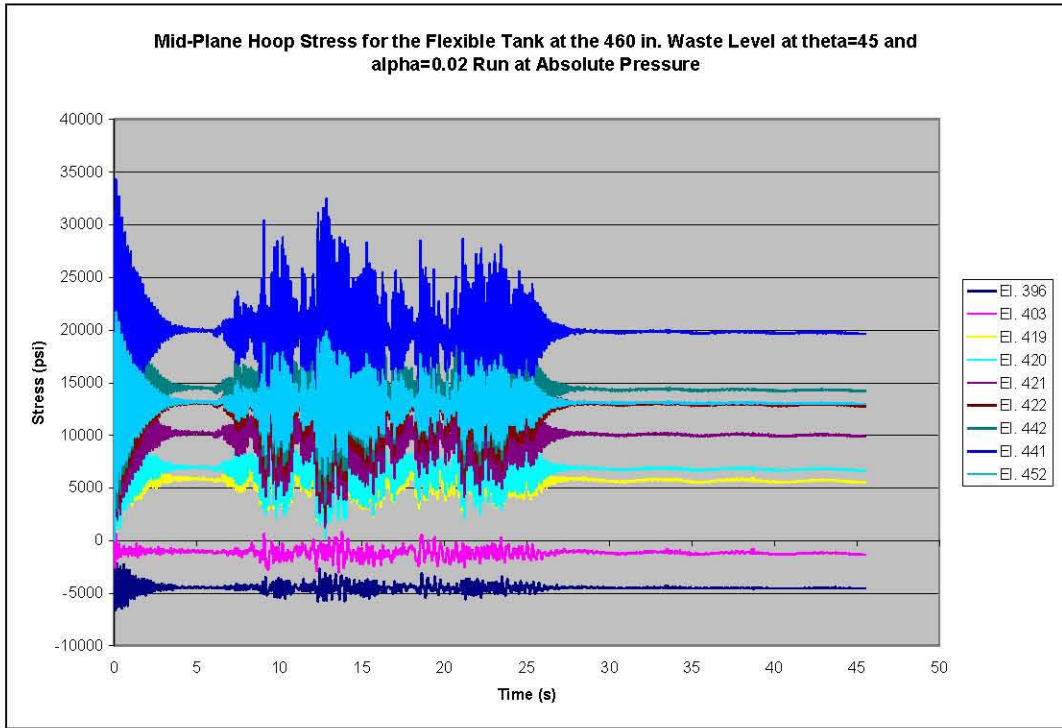


Figure 6-27. Mid-Plane Hoop Stress for the Flexible Tank at the 460-Inch Waste Level at  $\theta=45^\circ$  and  $\alpha=0.02$  Run at Absolute Pressure

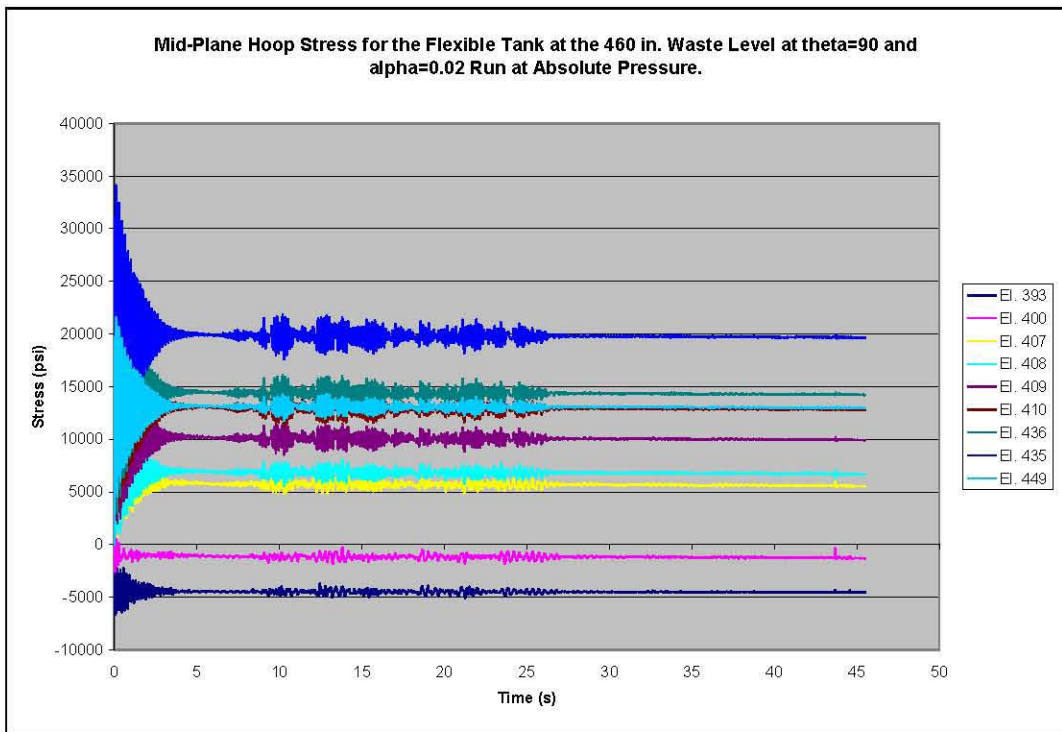


Figure 6-28. Mid-Plane Hoop Stress for the Flexible Tank at the 460-Inch Waste Level at  $\theta=90^\circ$  and  $\alpha=0.02$  Run at Absolute Pressure

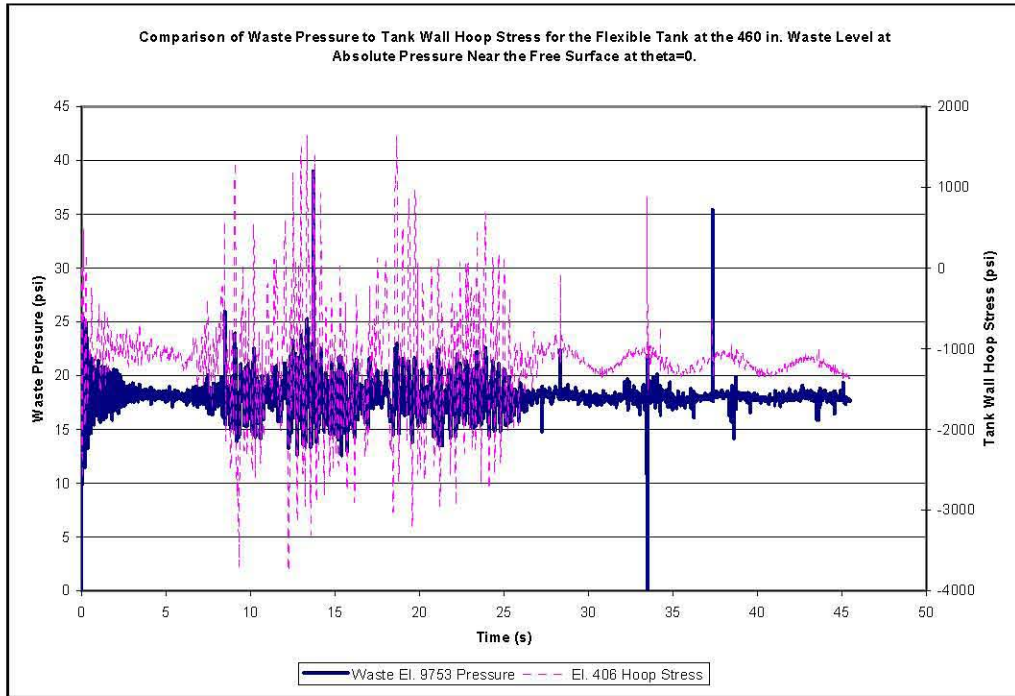


Figure 6-29. Comparison of Waste Pressure to Tank Wall Hoop Stress for the Flexible Tank at the 460-Inch Waste Level at Absolute Pressure for Waste Element 9753 and Tank Wall Element 406 Near the Free Surface at  $\theta=0$

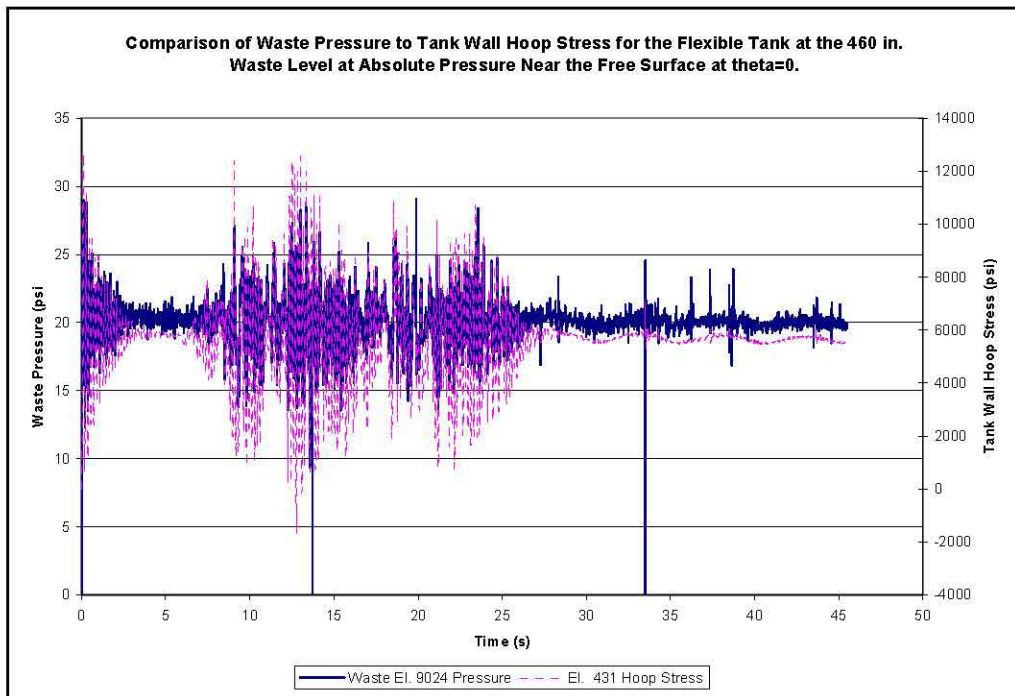


Figure 6-30. Comparison of Waste Pressure to Tank Wall Hoop Stress for the Flexible Tank at the 422-Inch Waste Level at Absolute Pressure for Waste Element 9024 and Tank Wall Element 431 Near the Free Surface at  $\theta=0$

### 6.4.2 Vertical Excitation Run at Absolute Pressure

Mid-plane hoop stresses for tank shell elements located at  $\theta=0$ , 45, and  $90^\circ$  are shown in Figure 6-31, Figure 6-32, and Figure 6-33. The general behavior of the hoop stresses is reasonable with similar values and distributions at  $\theta=0$ , 45, and  $90^\circ$  as expected. A slight downward drift is apparent in the stress that had been observed earlier for the vertical runs. Because of the isolated pressure spikes at waste elements near the free surface shown in Figure 6-18 and Figure 6-20 at the  $\theta=45$ , and  $90^\circ$  locations, comparisons between the waste pressure and the hoop stress in the adjacent tank wall element are shown in Figure 6-34 and Figure 6-35. In the vertical run, the hoop stress does not follow the pattern of the waste pressure as well as in the horizontal run.

In Figure 6-34, the downward spike in the waste pressure is not reflected in the hoop stress of the adjacent element, but the upward spike in waste pressure shown in Figure 6-35 at approximately 8 seconds for element 9417 is reflected as a concomitant increase in hoop stress in tank wall element 400. However, magnitude of hoop stress in element 400 is low even with the isolated spike.

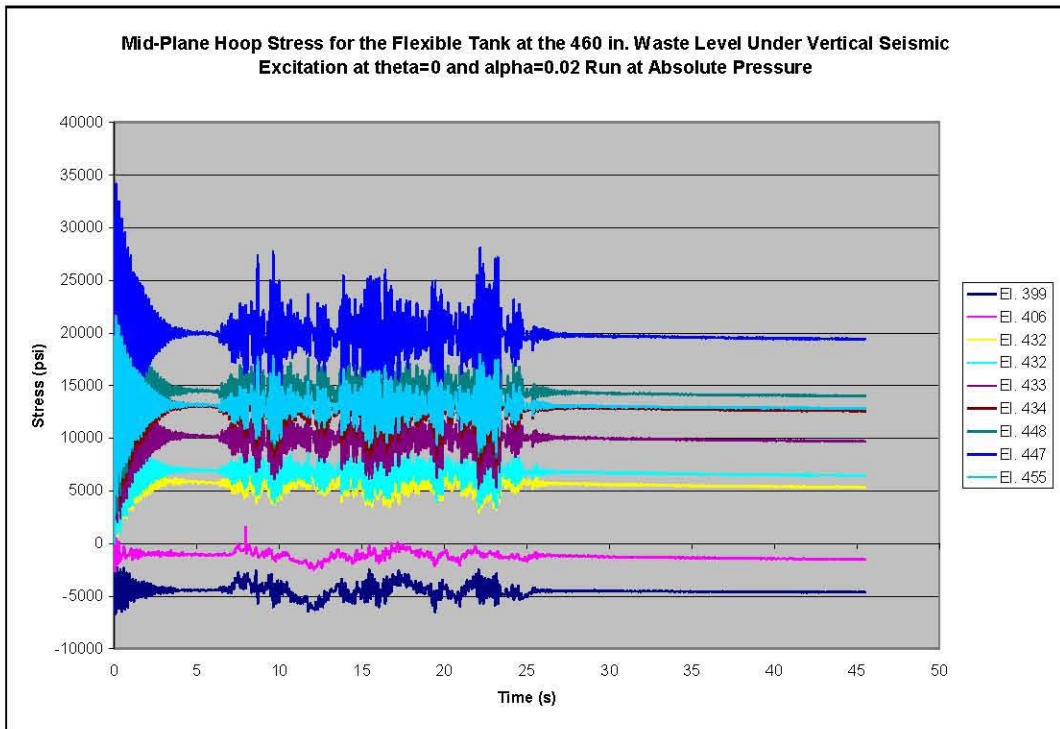


Figure 6-31. Mid-Plane Hoop Stress for the Flexible Tank at the 460-Inch Waste Level for Vertical Excitation at  $\theta=0$  and  $\alpha=0.02$  Run at Absolute Pressure

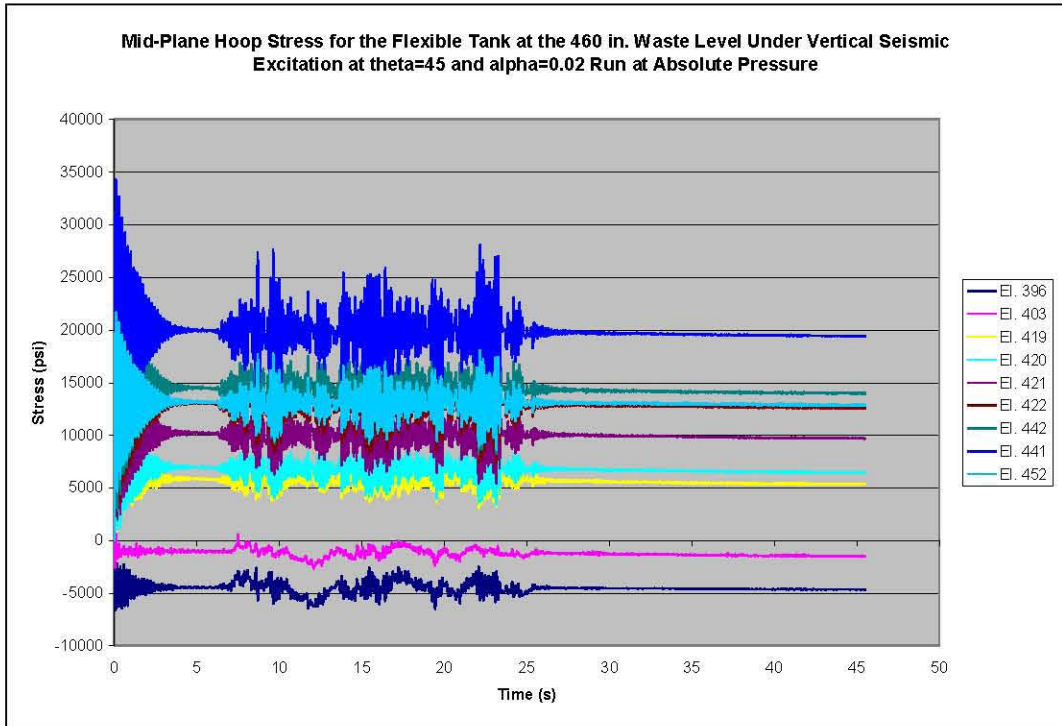


Figure 6-32. Mid-Plane Hoop Stress for the Flexible Tank at the 460-Inch Waste Level for Vertical Excitation at  $\theta=45^\circ$  and  $\alpha=0.02$  Run at Absolute Pressure

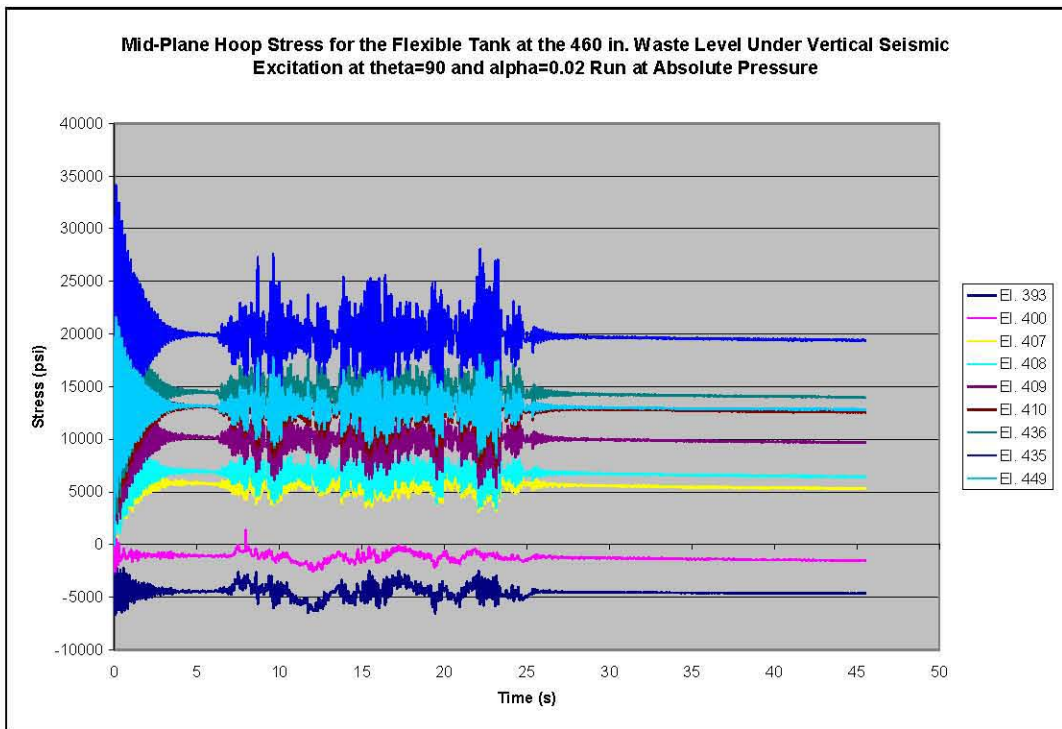


Figure 6-33. Mid-Plane Hoop Stress for the Flexible Tank at the 460-Inch Waste Level for Vertical Excitation at  $\theta=90^\circ$  and  $\alpha=0.02$  Run at Absolute Pressure

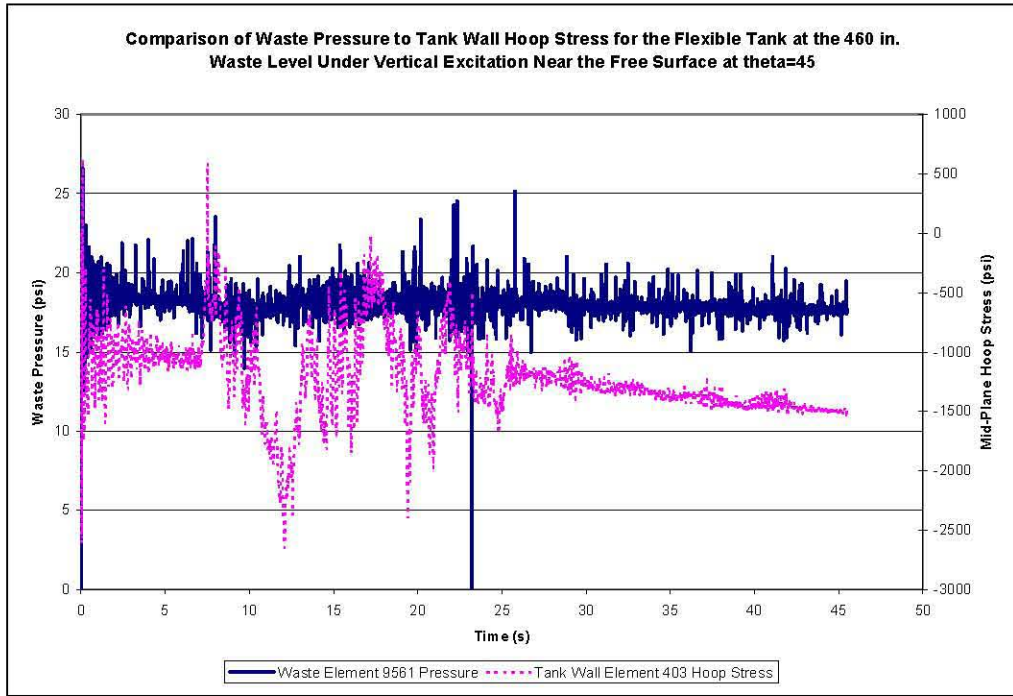


Figure 6-34. Comparison of Waste Pressure to Tank Wall Hoop Stress for the Flexible Tank at the 460-Inch Waste Level Under Vertical Excitation at Absolute Pressure Near the Free Surface at  $\theta=45^\circ$

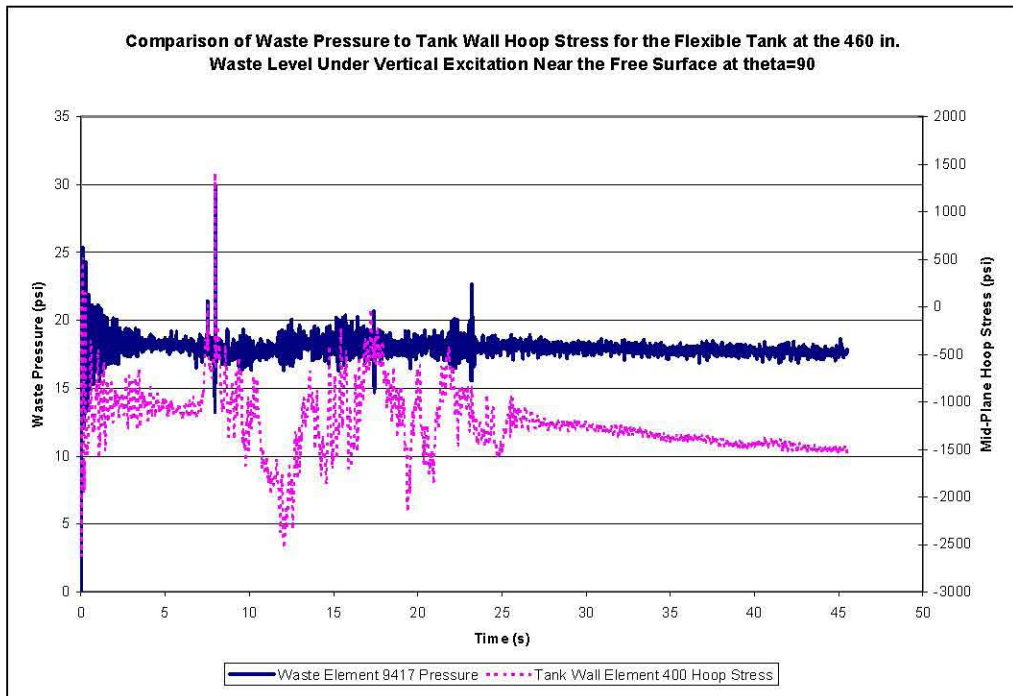


Figure 6-35. Comparison of Waste Pressure to Tank Wall Hoop Stress for the Flexible Tank at the 460-Inch Waste Level Under Vertical Excitation at Absolute Pressure Near the Free Surface at  $\theta=90^\circ$

Intentionally left blank.

## 7.0 ANSYS® to Dytran® Comparisons

This report has presented the results of a series of Dytran® analyses of simplified primary tank models. A parallel study was conducted using the finite element code ANSYS®, and the results of that study are documented in a companion report (Carpenter and Abatt 2006). The goal of the two studies was to evaluate the capabilities and limitations of each code for performing fluid-structure interaction analysis of a double-shell primary tank. Although the investigations are documented in separate reports, selected results are compared directly in the following sections.

As described in the companion report documenting the ANSYS® analyses, the two waste levels of interest are 422 inches and 460 inches. The Dytran® analyses were performed at these two waste levels. Due to modeling limitations, the lower waste level was modeled in ANSYS® at 424 inches. At the higher waste level, the ANSYS® models were performed at 460 inches for horizontal runs and at 452 inches for vertical runs. In the comparison plots to follow, the configurations are generically referred to as the 422- and 460-inch levels, but the actual waste levels used for the ANSYS® analyses are as described above. Thus, slight inherent differences exist in some of the solutions due to the difference in waste levels. The theoretical values shown in the plots are for the intended waste levels of 422 and 460 inches.

### 7.1 Frequencies and Slosh Heights

A summary of fundamental frequencies and maximum slosh heights predicted by both ANSYS® and Dytran® is given in Table 7-1. Both ANSYS® and Dytran® predict fundamental frequencies that agree well with theory, although Dytran® agrees better with theoretical values, particularly for predicting the breathing mode frequencies. It is clear that the ANSYS® model is deficient in its ability to predict meaningful slosh heights.

Table 7-1. Comparison of ANSYS® and Dytran® Frequencies and Maximum Slosh Heights

Configuration	First Convective Mode Frequency (Hz)			Impulsive Mode Frequency (Hz)		
	Theory	Dytran®	ANSYS®	Theory	Dytran®	ANSYS®
Rigid 422	0.19	0.19	0.184 <sup>(b)</sup>	Rigid	Rigid	Rigid
Rigid 460 <sup>(a)</sup>	0.2	0.2	0.192	Rigid	Rigid	Rigid
Flexible 422	0.19	0.19	0.184 <sup>(c)</sup>	7.0	6.85	7.5 <sup>(b)</sup>
Flexible 460 <sup>(a)</sup>	0.2	0.2	0.192 <sup>(c)</sup>	6.5	6.4	6.6 <sup>(d)</sup>
Configuration	Breathing Mode Frequency (Hz)			Maximum Slosh Height (in.)		
	Theory	Dytran®	ANSYS®	Theory	Dytran®	ANSYS®
Rigid 422	Rigid	Rigid	Rigid	23.7	25.4	8
Rigid 460 <sup>(a)</sup>	Rigid	Rigid	Rigid	24.5	21.1	8
Flexible 422	6.1	6.0	6.6 <sup>(b)</sup>	23.7	24.5	8
Flexible 460 <sup>(a)</sup>	5.5	5.5	5.7	24.5	20.1	8

(a) Theoretical solutions for the 460-in. waste level are based on an open tank with vertical walls and a hinged-top boundary condition.  
(b) Based on 424-in. waste level.  
(c) Convective frequency response based on rigid tank.  
(d) Based on 452-in. waste level.

## 7.2 Hydrodynamic Forces

Comparisons between the overall reaction forces predicted by ANSYS® and Dytran® for the flexible tank models are presented in this section. In order to match the Dytran® data to the ANSYS® data, time scales were shifted as appropriate and the Dytran® data were reversed in sign. The correct signs for the reactions are those predicted by Dytran® since the ANSYS® data were a result of nodal force post-processing. The results are presented for comparison, but if a physical interpretation of the reaction force is desired, the signs should be reversed from those shown in the plots. For example, in Figure 7-4, the static portion of the vertical reaction force is a downward force due to gravity, and the peak dynamic component of the reaction force occurs in the same direction as the waste weight.

A comparison of the overall horizontal reaction force due to horizontal seismic excitation for the flexible tank at the 422-inch waste level is shown in Figure 7-1. The general agreement between the two responses is good, with the peak reaction force predicted by ANSYS® slightly higher (that is, conservative) relative to that predicted by Dytran®. The comparison of vertical responses to vertical input shown in Figure 7-2 also shows similar signals, and again, the peak response from ANSYS® is slightly conservative relative to the Dytran® prediction.

A comparison of the total horizontal reaction force for horizontal seismic excitation of the flexible tank at the 460-inch waste level is shown as Figure 7-3. Once again, the responses are very similar and the peak reaction force predicted by ANSYS® is slightly greater than the peak reaction force predicted by Dytran®. Figure 7-4 shows the comparison of the total vertical reaction forces for vertical seismic input for the flexible tank at the 460-inch waste level. This time, although the responses are similar, the higher peak response is predicted by Dytran® rather than ANSYS®. A review of Figure 6-5 also shows that both models predict a higher peak vertical force than would be expected from the corresponding open-top theoretical solution.

Comparison of the reaction forces from the ANSYS® and Dytran® models shows that the responses from the models are similar, with ANSYS® generally being conservative relative to Dytran®. Both models predict responses that are in good agreement with theoretical solutions. In terms of global reactions on the primary tank, both ANSYS® and Dytran® appear capable of providing good results. In particular, since the loads into the j-bolts connecting the primary tank to the concrete dome are driven by the overall forces on the primary tank, it appears that a global ANSYS® model is sufficient for analysis of the j-bolts and that any sub-model of the primary tank need not contain the j-bolts.

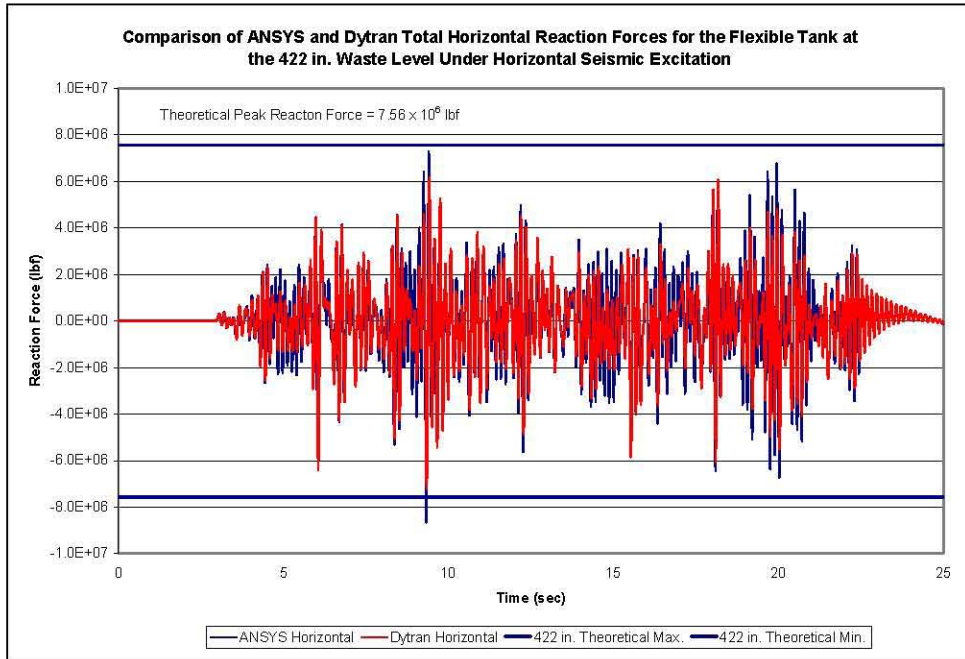


Figure 7-1. Comparison of ANSYS® and Dytran® Total Horizontal Reaction Forces for the Flexible Tank at the 422-Inch Waste Level Under Horizontal Seismic Excitation

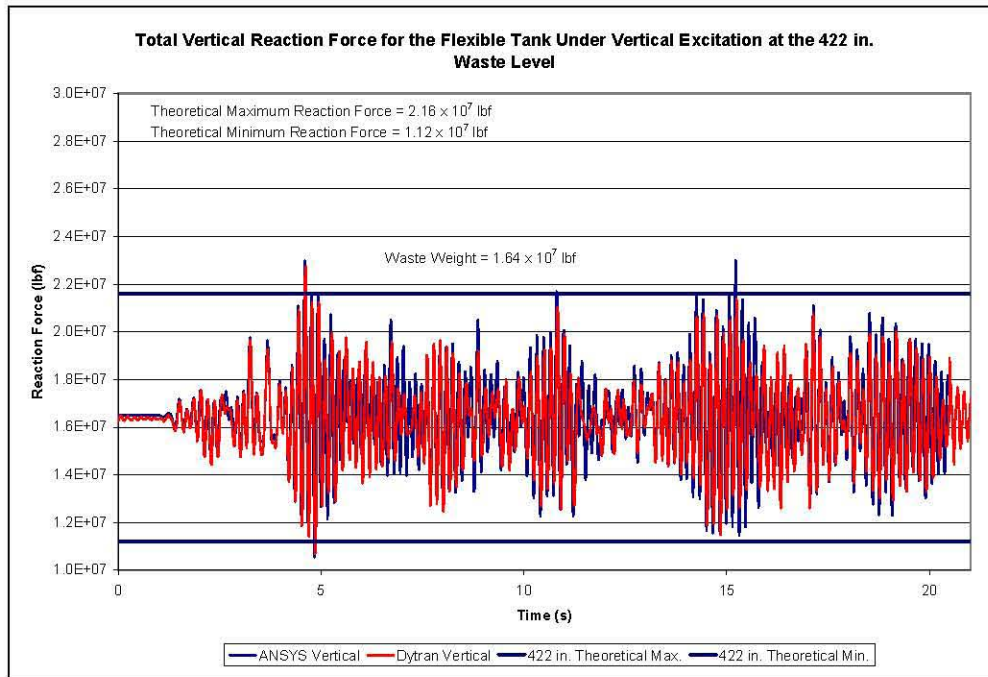


Figure 7-2. Comparison of ANSYS® and Dytran® Total Vertical Reaction Forces for the Flexible Tank at the 422-Inch Waste Level Under Vertical Seismic Excitation

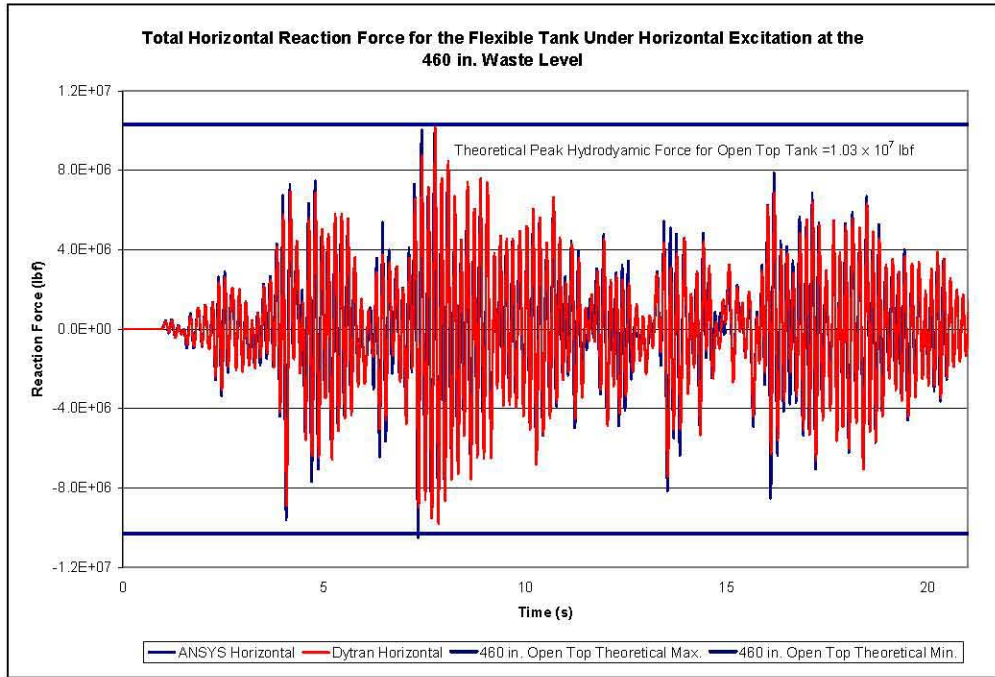


Figure 7-3. Comparison of ANSYS® and Dytran® Total Horizontal Reaction Forces for the Flexible Tank at the 460-Inch Waste Level Under Horizontal Seismic Excitation

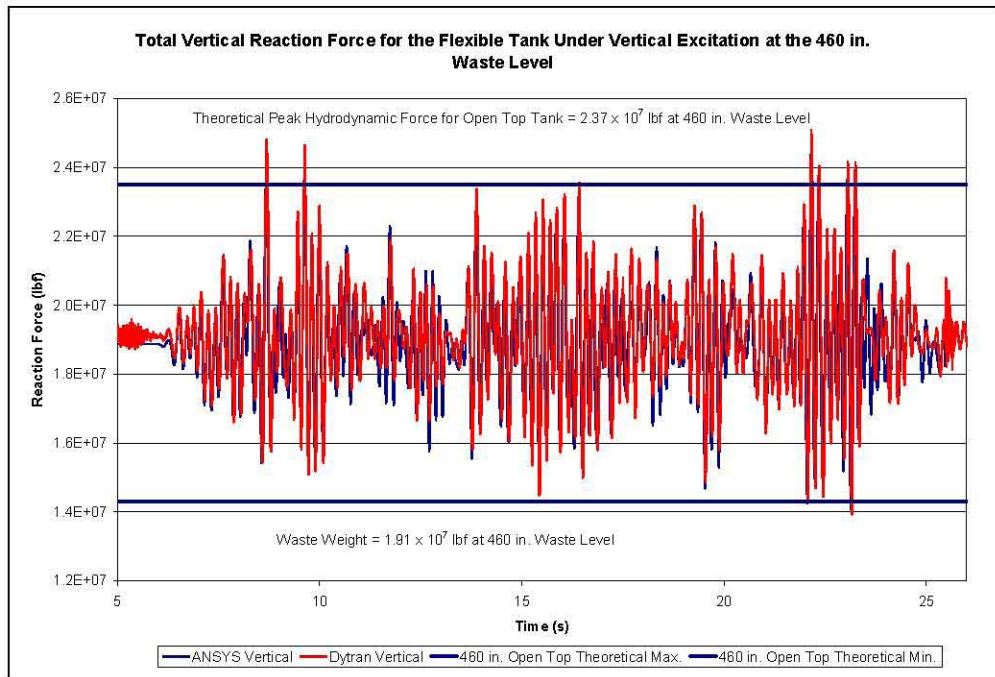


Figure 7-4. Comparison of ANSYS® and Dytran® Total Vertical Reaction Forces for the Flexible Tank at the 460-Inch Waste Level Under Vertical Seismic Excitation

### 7.3 Waste Pressures

Direct comparisons of waste pressures predicted by ANSYS® and Dytran® are presented in this section. To be consistent with the pressures reported by ANSYS®, the Dytran® pressures have been shifted down by 14.7 lbf/in<sup>2</sup>, since the ANSYS® simulations were run at gage pressure and the Dytran® simulations were performed at absolute pressure. The ANSYS® and Dytran® model meshes were not identical, so comparisons are made for waste elements at similar elevations. All comparisons were made for elements along the plane of excitation ( $\theta=0$ ). The waste element numbers, centroidal elevations, and theoretical hydrostatic pressures are summarized in Table 7-2. The element numbers for ANSYS® are actually contact element numbers between the waste and the primary tank, since these are the elements used to report the waste pressures from ANSYS®.

Waste element pressures at the 422-inch waste level are presented as Figure 7-5 and Figure 7-6. A comparison of waste pressures near the top and bottom of the tank is shown in Figure 7-5, and a comparison of waste pressures approximately two-thirds the way up the waste is shown in Figure 7-6. Both plots show reasonably good agreement with the dynamic pressures reported by ANSYS® tending to run slightly higher than those from Dytran® except at a few isolated peaks near the waste surface in Figure 7-5. The plots also show that in the upper portion of the waste, the low-frequency convective response is more pronounced in ANSYS® than in Dytran®.

Wastes pressures from the simulations at the 460-inch waste level are shown in Figure 7-7 and Figure 7-8. The responses are again similar, but at the bottom of the waste, the peak pressures reported by Dytran® exceed those reported by ANSYS®. In the upper portion of the waste, the peak pressures from ANSYS® are greater than the peak pressures from Dytran®. The convective response is also less apparent in the ANSYS® simulation at the 460-inch waste level than at the 422-inch waste level.

**Table 7-2.** Summary of Centroidal Elevations for ANSYS® and Dytran® Selected Waste Elements at  $\theta=0$ .

ANSYS® Element No.	Centroidal Elevation from Tank Bottom (in.)	Theoretical Hydrostatic Pressure (psi)	Dytran® Element No.	Centroidal Elevation from Tank Bottom (in.)	Theoretical Hydrostatic Pressure (psi) <sup>(a)</sup>
<b>422-in. Waste Level</b>					
5521	401.9	1.4	9753	404.3	1.1
5581	291.8	8.1	7566	298.2	7.6
5721	54.5	22.7	2463	50.5	22.8
<b>460-in. Waste Level</b>					
5511	438.3	1.4	10482	441.0	1.3
5831	291.8	11.1	7566	298.2	10.7
5971	54.5	26.8	2463	50.5	27.1
(a) Dytran® waste pressures have been shifted down by 14.7 lbf/in <sup>2</sup> to be consistent with ANSYS®.					

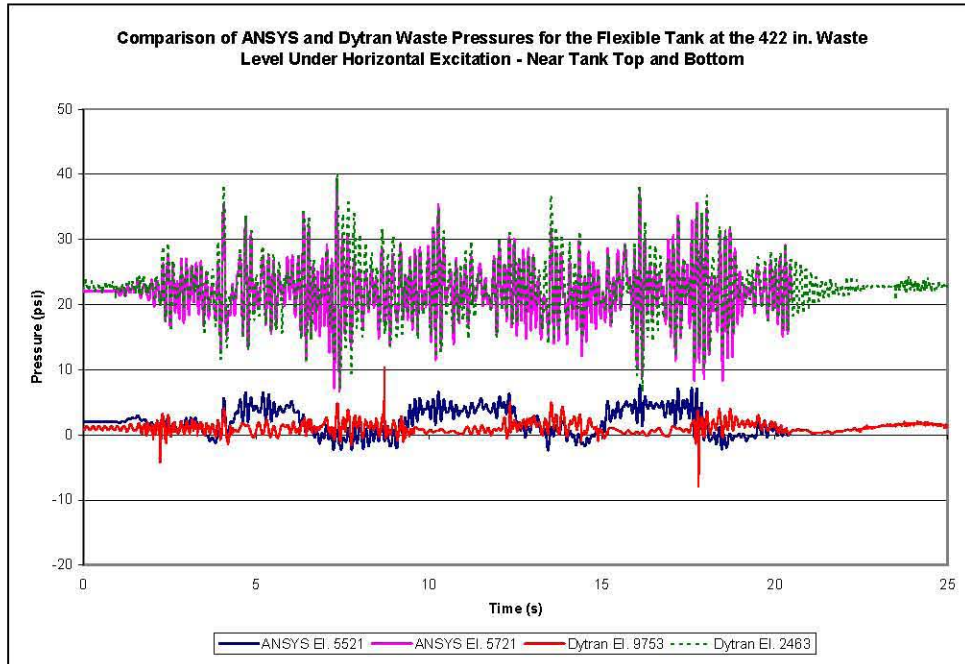


Figure 7-5. Comparison of ANSYS® and Dytran® Waste Pressures for the Flexible Tank at the 422-Inch Waste Level Under Horizontal Excitation – Waste Elements Near Tank Top and Bottom at  $\theta=0$

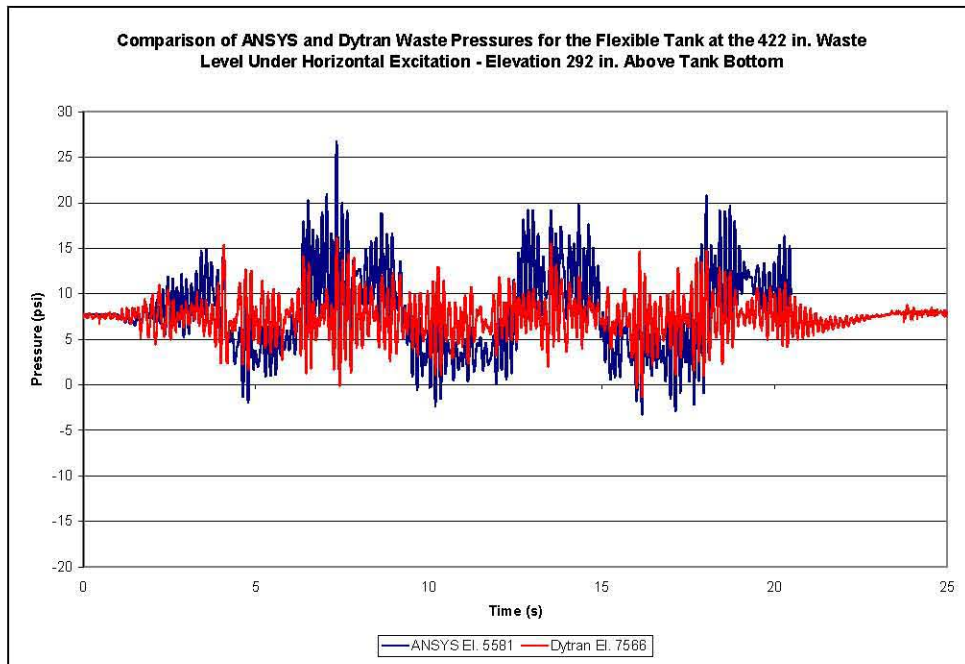


Figure 7-6. Comparison of ANSYS® and Dytran® Waste Pressures for the Flexible Tank at the 422-Inch Waste Level Under Horizontal Excitation – Waste Elements at Elevation 292 Inches Above Tank Bottom at  $\theta=0$

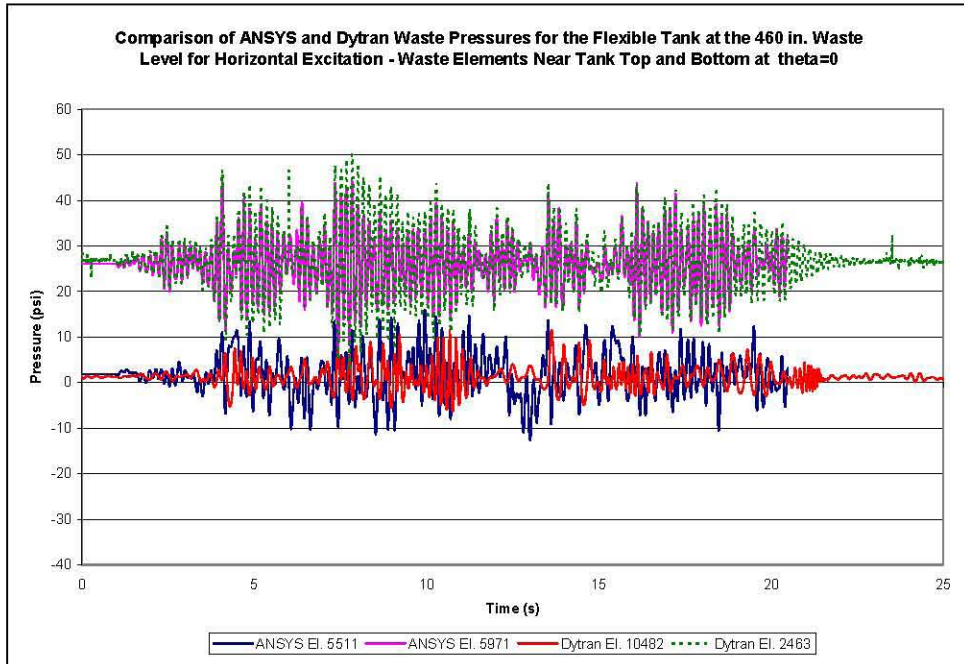


Figure 7-7. Comparison of ANSYS® and Dytran® Waste Pressures for the Flexible Tank at the 460-Inch Waste Level Under Horizontal Excitation – Waste Elements Near Tank Top and Bottom at  $\theta=0$

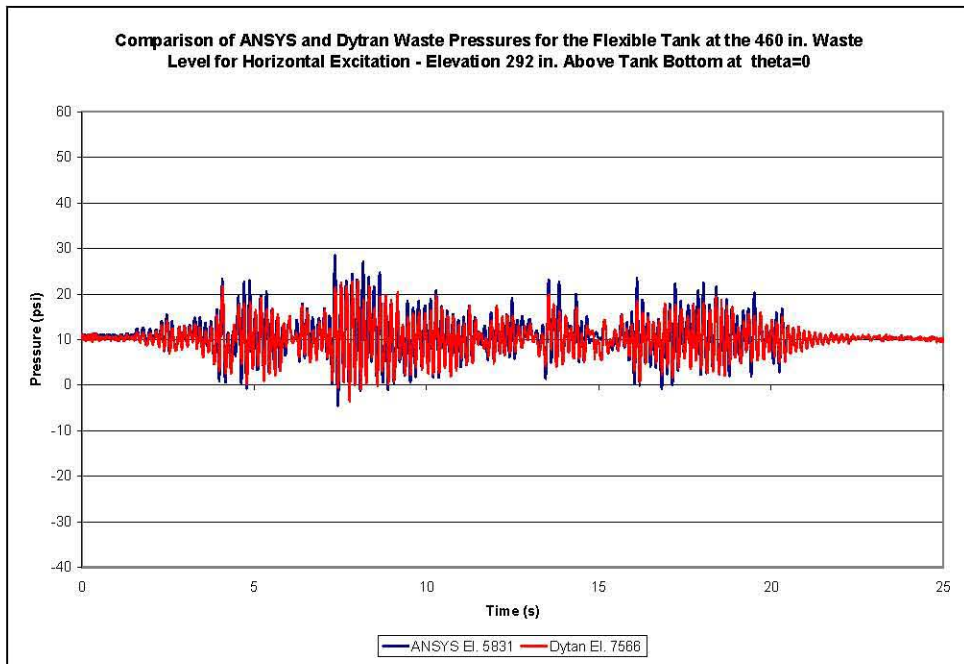


Figure 7-8. Comparison of ANSYS® and Dytran® Waste Pressures for the Flexible Tank at the 460-Inch Waste Level Under Horizontal Excitation – Waste Elements at Elevation 292 Inches Above Tank Bottom at  $\theta=0$

## 7.4 Element Stresses

Direct comparisons of element mid-wall hoop stresses predicted by ANSYS® and Dytran® are presented in this section. The ANSYS® and Dytran® model meshes were not identical, so comparisons are made for tank wall elements at elevations as close as possible. However, the difference in mesh resolutions and the local modeling of the tank knuckle region are expected to cause differences in the reported stresses even at similar elevations. All comparisons were made for elements along the plane of excitation ( $\theta=0$ ). The tank wall element numbers and centroidal elevations are summarized in Table 7-3.

Table 7-3. Summary of Centroidal Elevations for Tank Wall Elements at  $\theta=0$

ANSYS® Element No.	Centroidal Elevation from Tank Bottom (in.)	Dytran® Element No.	Centroidal Elevation from Tank Bottom (in.)
961	438.3	399	441.8
981	401.9	406	402.9
1041	291.8	432	292.77
1181	54.5	447	63.9

Mid-wall hoop stresses at the 422-inch waste level are presented for tank elements near the waste-free surface, approximately two-thirds of the way up from the tank bottom, and near the tank bottom in Figure 7-9, Figure 7-10, and Figure 7-11, respectively. The static portion of the hoop stresses shown in Figure 7-9 differ by approximately 1,000 lbf/in<sup>2</sup>, even though the element elevations are nearly the same as shown in Table 7-3. According to Figure 7-5, the waste pressures adjacent to these elements are nearly the same, so apparently the difference in stresses is due to a combination of the difference in mesh resolution and the difference in how the two codes transmit the waste pressures into the structure. Interestingly, whereas the convective response was more pronounced in the waste pressures predicted by ANSYS® at this elevation, the convective response is more apparent in the stresses predicted by Dytran®. This may be due to the difference in the Lagrangian vs. Eulerian formulation of the waste elements.

At the 292-inch elevation and at the bottom, the responses are similar, with ANSYS® predicting a slightly higher stresses at the 292-inch level and Dytran® predicting a slightly higher stresses near the tank bottom. The differences near the tank bottom may be due partly to the difference in the details of the mesh in the tank knuckle region and partly due to the more than 9-inch difference in the elevation of the wall element centroids.

Mid-wall hoop stresses at the 460-inch waste level are shown in Figure 7-12, Figure 7-13, and Figure 7-14. The hoop stresses shown in Figure 7-12 are for tank wall elements located approximately 20 inches below the nominal level of the waste surface. The corresponding pressure plots in Figure 7-7 show that the static pressures are nearly the same for the ANSYS® and Dytran® models, but the dynamic pressures are somewhat higher in the ANSYS® model. In Figure 7-12, the static portion of hoop stresses differ by approximately 3,500 lbf/in<sup>2</sup> and the dynamic stresses are higher in Dytran® than in ANSYS®. The differences in static and dynamic pressure shown in Figure 7-12 do not correspond to the pressure traces shown in Figure 7-7, so the differences must be because of differences in mesh resolution and the difference in how the two codes transmit the waste pressures into the structure.

Figure 7-13 shows a comparison of mid-wall hoop stresses at an elevation of 292 inches above the tank bottom (64% of the way up the tank wall). Figure 7-8 shows that the static pressures are nearly the same at that location, and that the dynamic pressures are slightly higher in ANSYS®. In Figure 7-13, the ANSYS® static stress is higher than the Dytran® static stress by approximately 1,000 lbf/in<sup>2</sup>. The dynamic components of the stresses are in good agreement in Figure 7-13, with the ANSYS® dynamic stress tending to be slightly higher, which agrees with the slightly higher dynamic pressures in Figure 7-8.

Figure 7-14 shows a comparison of mid-wall hoop stresses at an elevation of approximately 60 inches above the tank bottom. The corresponding pressure time-histories in Figure 7-7 show that the static pressures are nearly the same in both models, and that the dynamic component of the pressure tends to be larger for the Dytran® model. The stress plot in Figure 7-14 shows that the static hoop stress is approximately 2,000 lbf/in<sup>2</sup> (~10%) higher for the Dytran® model than for the ANSYS® model. The difference in static stress is not due to a difference in static pressure, so it must be due to mesh resolution and the difference in how the two codes transmit the waste pressures into the structure. The higher dynamic stress shown in Figure 7-14 for the Dytran® model corresponds to the higher dynamic pressure in Figure 7-7. It appears that the difference in total pressures between the Dytran® and ANSYS® models as shown in Figure 7-14 is due to a combination of the offset static stress and the higher dynamic pressures from the Dytran® model.

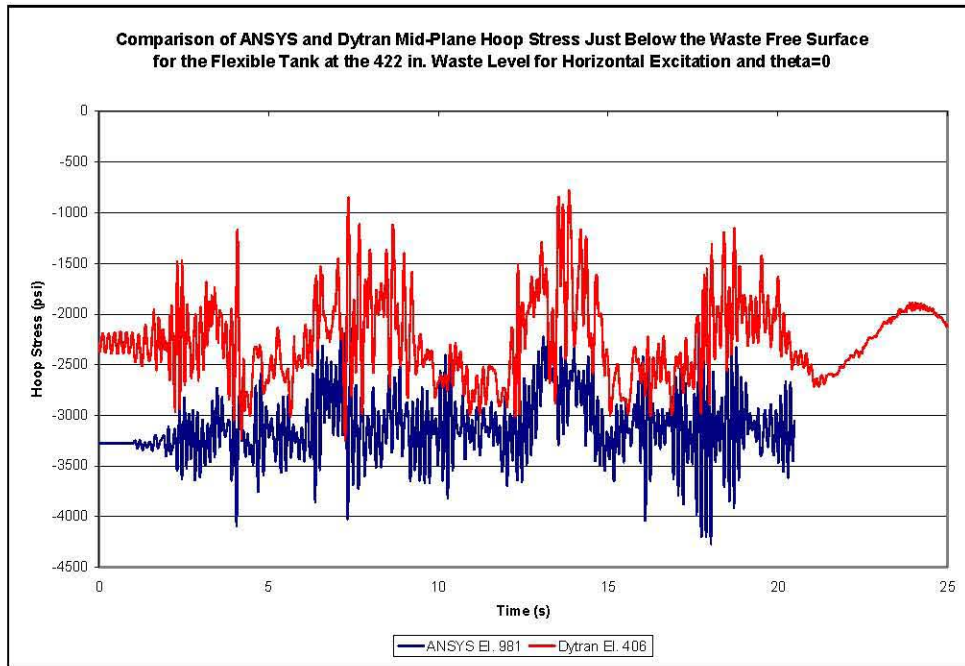


Figure 7-9. Comparison of ANSYS® and Dytran® Mid-Plane Hoop Stress at Primary Tank Wall Element Near the Waste-Free Surface for the Flexible Tank at the 422-Inch Waste Level for Horizontal Excitation and  $\theta=0$

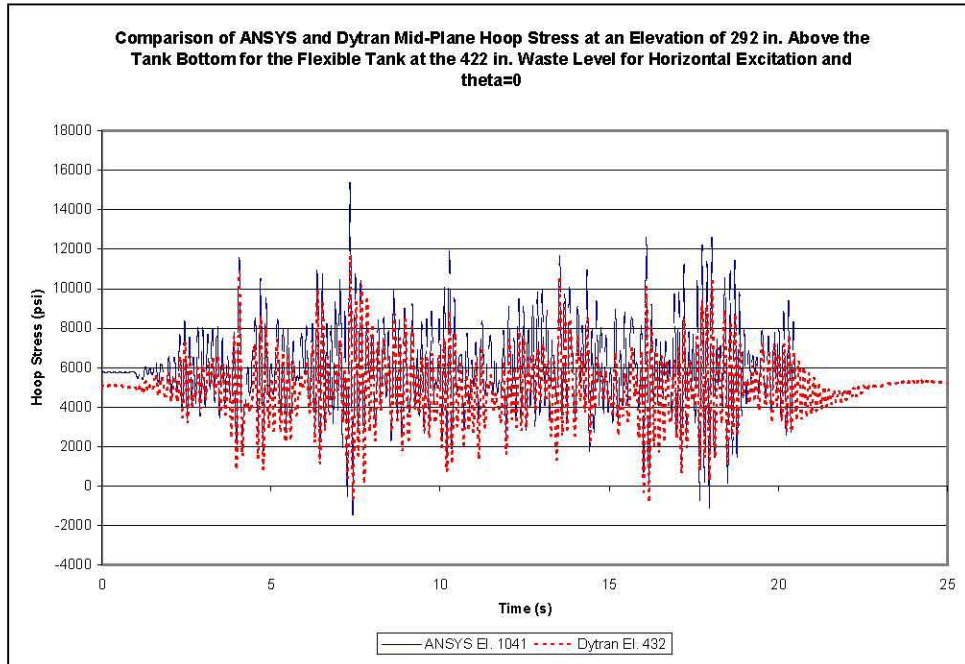


Figure 7-10. Comparison of ANSYS® and Dytran® Mid-Plane Hoop Stress at an Elevation of 292 Inches from the Tank Bottom for the Flexible Tank at the 422-Inch Waste Level for Horizontal Excitation and  $\theta=0$

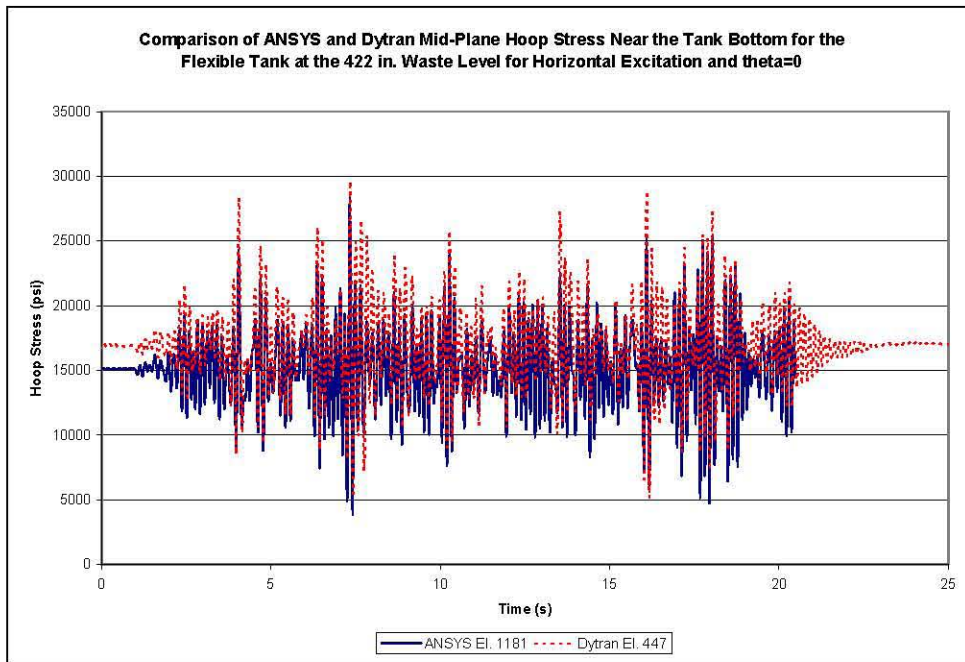


Figure 7-11. Comparison of ANSYS® and Dytran® Mid-Plane Hoop Stress at Primary Tank Wall Element Near the Tank Bottom for the Flexible Tank at the 422-Inch Waste Level for Horizontal Excitation and  $\theta=0$

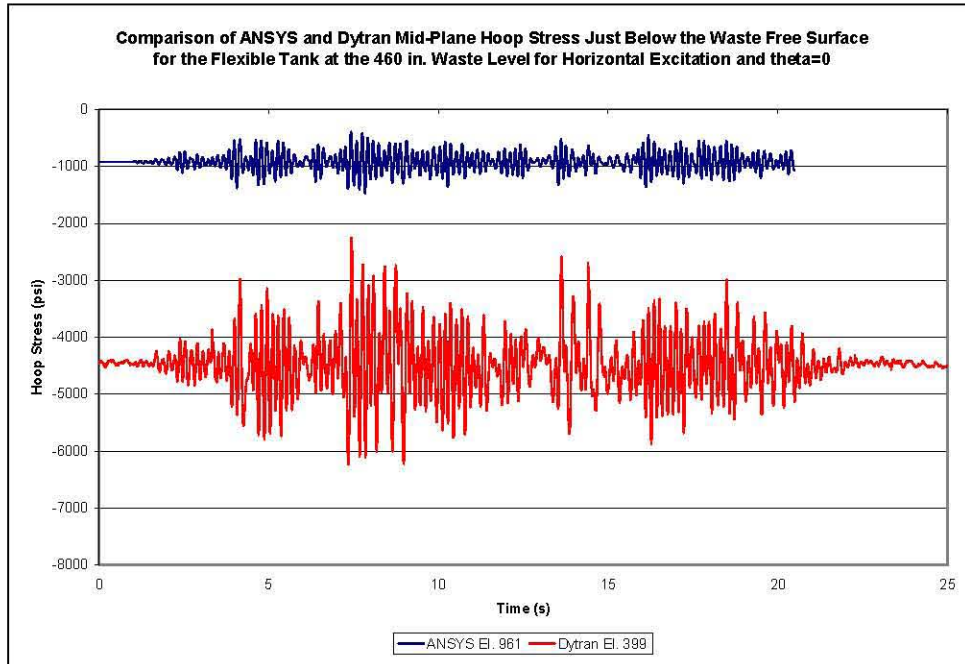


Figure 7-12. Comparison of ANSYS® and Dytran® Mid-Plane Hoop Stress at Primary Tank Wall Element Near the Waste-Free Surface for the Flexible Tank at the 460-Inch Waste Level for Horizontal Excitation and  $\theta=0$

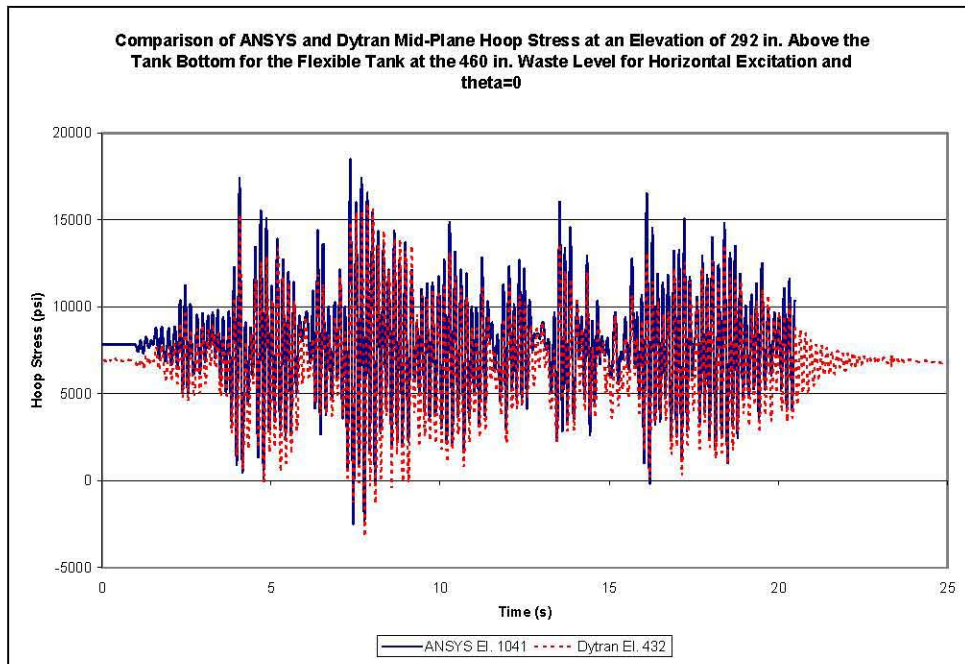


Figure 7-13. Comparison of ANSYS® and Dytran® Mid-Plane Hoop Stress at an Elevation of 292 Inches from the Tank Bottom for the Flexible Tank at the 460-Inch Waste Level for Horizontal Excitation and  $\theta=0$

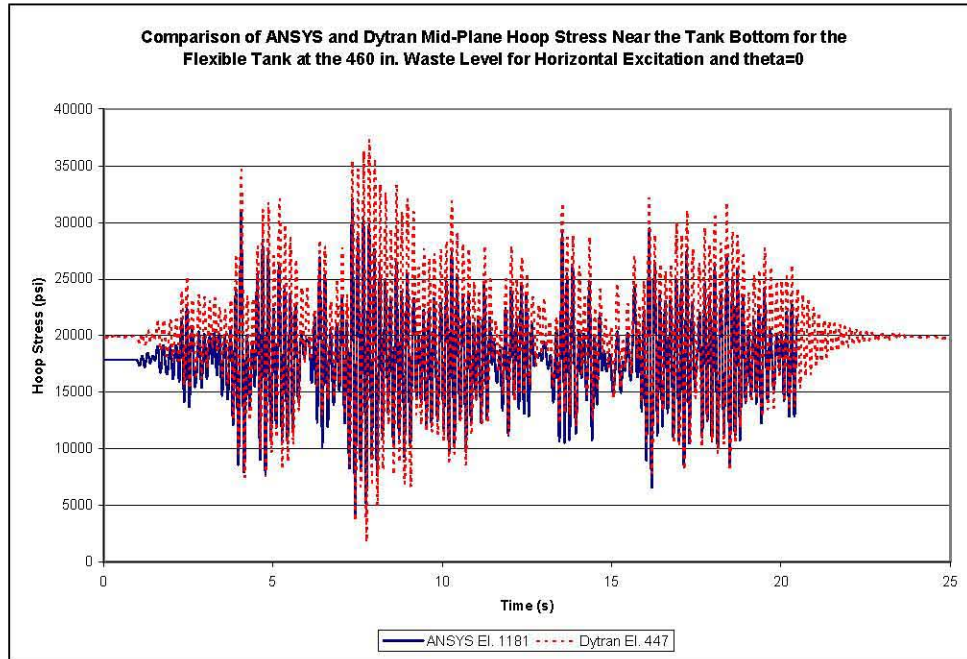


Figure 7-14. Comparison of ANSYS® and Dytran® Mid-Plane Hoop Stress at Primary Tank Wall Element Near the Tank Bottom for the Flexible Tank at the 460-Inch Waste Level for Horizontal Excitation and  $\theta=0$

## 8.0 References

BNL. 1995. *Seismic Design and Evaluation Guidelines for the Department of Energy High-Level Waste Storage Tanks and Appurtenances*. Report No. 52361, October 1995, Engineering Research and Applications Division, Department of Advanced Technology, Brookhaven National Laboratory, Associated Universities, Inc., Upton, New York.

Carpenter BG and FG Abatt. 2006. *ANSYS Benchmark Analysis of Seismically Induced Fluid-Structure Interaction in a Hanford Double Shell Primary Tank*. M&D-2008-004-RPT-02, Rev. 0, prepared by M&D Professional Services, Inc. for Pacific Northwest National Laboratory, Richland, Washington.

Carpenter BG, CA Hendrix, and FG Abatt. 2006. *ANSYS Soil-Structure Interaction Analysis of a Hanford Double Shell Tank*. M&D-2008-004-CALC-01, Rev. 0, prepared by M&D Professional Services, Inc. for Pacific Northwest National Laboratory, Richland, Washington.

Clough RW and J Penzien. 1975. *Dynamics of Structures*. McGraw-Hill Book Company, New York, New York.

Deibler JE, KI Johnson, SP Pilli, MW Rinker, FG Abatt, and NK Karri. 2008. *Hanford Double-Shell Tank Thermal and Seismic Project – Increased Liquid Level Analysis for 241-AP Tank Farm*. RPP-RPT-32237, Rev. 1, Pacific Northwest National Laboratory, Richland, Washington.

Deibler JE, KI Johnson, NK Karri, SP Pilli, MW Rinker, FG Abatt, BF Carpenter, and C Hendrix. 2007. *Hanford Double-Shell Tank Thermal and Seismic Project - Summary of Combined Thermal and Operating Loads with Seismic Analysis*. RPP-RPT-28969, Rev. 0A, Pacific Northwest National Laboratory, Richland, Washington.

DOE-STD-1020-2002. January 2002. *Natural Phenomenon Hazards Design and Evaluation Criteria for Department of Energy Facilities*. U.S. Department of Energy, Washington, D.C.

Hanford Drawing H-2-64449, Rev. 6, dated 5/12/1970, *Tank Elevation and Details, 241-AY*, Vitro Hanford Engineering Services, Richland, Washington.

Kurihara C, Y Masuko, and A Sakurai. 1994. “Sloshing Impact Pressure in Roofed Liquid Tanks.” *Journal of Pressure Vessel Technology* 116(2):193-200.

M&D. 2005. *DYTRAN 2006 Development Version Verification of M&D Workstation Kingair*. M&D-V&V-DYT-2006DV-001 R0, M&D Professional Services, Inc., Richland, Washington.

MSC. 2005a. *MSC.Dytran 2005 Theory Manual, Version 2005*. MSC.Software Corporation, Santa Ana, California.

MSC. 2005b. *MSC.Dytran Reference Manual, Version 2005*. MSC.Software Corporation, Santa Ana, California.

**RPP-RPT-28963, Rev. 1**  
**M&D-2008-005-RPT-01, Rev. 1**

Rinker MW and FG Abatt. 2006. *Dytran Benchmark Analysis of Seismically Induced Fluid-Structure Interaction in a Hanford Double Shell Primary Tank*. RPP-RPT-28963, Rev. 0 and Rev. 0A, prepared by M&D Professional Services, Inc. for Pacific Northwest National Laboratory, Richland, Washington.

Rinker MW, JE Deibler, KI Johnson, SP Pili, CE Guzman-Leong, and OD. Mullen. 2004. *Hanford Double-Shell Tank Thermal and Seismic Project – Thermal and Operating Loads Analysis*. RPP-RPT-23308, Rev. 0, Pacific Northwest National Laboratory, Richland, Washington.

**Appendix A**  
**Description of Input and Results Files**

RPP-RPT-28963, Rev. 1  
M&D-2008-005-RPT-01, Rev. 1

Intentionally left blank

## Appendix A

### Description of Input and Results Files

**Table A-1.** Description of Input and Results Files

<b>File Extension</b>	<b>Typical File Name</b>	<b>Description</b>
.db	Rigid_422.db	Patran database file used for model creation. The Dytran input files are created by translating this file to Dytran input file format within Patran.
.dat	alpha_02_abs.dat	Main Dytran input file. Required bulk data files are called from this file
.bdf	Flex_422_horiz.bdf	Dytran bulk data file containing node and element information. This file is called by the main input file and is common to a given tank configuration (rigid or flexible) and waste level. Total of four files.
.bdf	DomeTH.bdf	Dytran bulk data file containing the seismic time history. Two files – one for horizontal excitation and one for vertical excitation (Vert_TH.bdf).
.xls	Results_422_Flex_Horizontal_alpha02_ABS.xls	Excel spreadsheet containing results from a given run. In the example at left, the results are for the flexible tank at the 422 in. waste level with horizontal excitation run at absolute pressure with a damping parameter of 0.02.

Intentionally left blank.

## **Appendix B**

### **Theoretical Solutions**

RPP-RPT-28963, Rev. 1  
M&D-2008-005-RPT-01, Rev. 1

Intentionally left blank

**RPP-RPT-28963, Rev. 1**  
**M&D-2008-005-RPT-01, Rev. 1**

Prepared by: F. G. Abatt  
M&D Professional Services  
8/10/05  
Rev. 1 *GA*

Theoretical Fluid Response  
Calculations for Rigid Primary Tank  
at 422 in. Waste Level

Checked by: B.G. Carpenter  
M&D Professional Services  
*BAC* 2/1/06

$H_1 := 422\text{-in}$       Baseline waste level

$H_t := 460\text{-in}$       Height to primary tank tangent line

$\frac{H_1}{H_t} = 0.92$       Ratio of waste height to tank height

$$g_w = 386.4 \frac{\text{in}}{\text{sec}^2}$$

$R := 450\text{-in}$       Tank radius

$\frac{H_1}{R} = 0.94$       Ratio of waste height to tank radius

$i := 0..2$

$\lambda := \begin{pmatrix} 1.841 \\ 5.331 \\ 8.536 \end{pmatrix}$       Bessel function roots

$\theta := \begin{pmatrix} 0\text{-deg} \\ 45\text{-deg} \\ 90\text{-deg} \end{pmatrix}$       Circumferential location of waste elements for which pressures are reported

**Convective Frequencies**

$$f_{con_i} := \frac{1}{2 \cdot \pi} \cdot \sqrt{\left[ \lambda_i \cdot \frac{g}{R} \cdot \tanh \left[ \lambda_i \cdot \left( \frac{H_1}{R} \right) \right] \right]} \quad \text{Eqn. 4.14 BNL 1995}$$

$f_{con} = \begin{pmatrix} 0.19 \\ 0.34 \\ 0.43 \end{pmatrix} \text{ Hz}$       First three convective frequencies

$\rho_1 := 1.59 \cdot 10^{-4} \frac{\text{lb} \cdot \text{sec}^2}{\text{in}^4}$       waste density - specific gravity = 1.7

RPP-RPT-28963, Rev. 1  
M&D-2008-005-RPT-01, Rev. 1

Prepared by: F. G. Abatt  
M&D Professional Services  
8/10/05  
Rev. 1

Theoretical Fluid Response  
Calculations for Rigid Primary Tank  
at 422 in. Waste Level

Checked by: B.G. Carpenter  
M&D Professional Services  
2/1/06

Determine Convective Pressures on the Tank Wall:

$z :=$

15-in
50.5-in
85.8-in
121.2-in
156.6-in
192.0-in
227.4-in
262.8-in
298.2-in
333.5-in
368.9-in
404.3-in

Vertical location of Euler element centroids at which pressures are reported.

$$\eta_1 := \frac{z}{H_1}$$

Ratio of tank wall vertical location to waste height for waste element centroids.

$\eta_1 =$

	0
0	0.04
1	0.12
2	0.2
3	0.29
4	0.37
5	0.45
6	0.54
7	0.62
8	0.71
9	0.79
10	0.87
11	0.96

RPP-RPT-28963, Rev. 1  
M&D-2008-005-RPT-01, Rev. 1

Prepared by: F. G. Abatt  
M&D Professional Services  
8/10/05  
Rev. 1

Theoretical Fluid Response  
Calculations for Rigid Primary Tank  
at 422 in. Waste Level

Checked by: B.G. Carpenter  
M&D Professional Services  
2/1/06

Determine convective coefficients as a function of dimensionless height per Eqn. 4.4 BNL 1995

$$\text{con}_0(\eta_1) := \frac{2 \cdot \cosh\left[\lambda_0 \cdot \left(\frac{H_1}{R}\right) \cdot \eta_1\right]}{\left(\lambda_0\right)^2 - 1 \cdot \cosh\left[\lambda_0 \cdot \left(\frac{H_1}{R}\right)\right]}$$

$$\text{con}_1(\eta_1) := \frac{2 \cdot \cosh\left[\lambda_1 \cdot \left(\frac{H_1}{R}\right) \cdot \eta_1\right]}{\left(\lambda_1\right)^2 - 1 \cdot \cosh\left[\lambda_1 \cdot \left(\frac{H_1}{R}\right)\right]}$$

$$\text{con}_2(\eta_1) := \frac{2 \cdot \cosh\left[\lambda_2 \cdot \left(\frac{H_1}{R}\right) \cdot \eta_1\right]}{\left(\lambda_2\right)^2 - 1 \cdot \cosh\left[\lambda_2 \cdot \left(\frac{H_1}{R}\right)\right]}$$

$$\text{con}_0(\eta_1) =$$

	0
0	0.29
1	0.29
2	0.31
3	0.32
4	0.35
5	0.38
6	0.42
7	0.47
8	0.53
9	0.6
10	0.68
11	0.78

$$\text{con}_1(\eta_1) =$$

	0
0	9.99·10 <sup>-4</sup>
1	1.16·10 <sup>-3</sup>
2	1.54·10 <sup>-3</sup>
3	2.18·10 <sup>-3</sup>
4	3.22·10 <sup>-3</sup>
5	4.83·10 <sup>-3</sup>
6	7.31·10 <sup>-3</sup>
7	0.01
8	0.02
9	0.03
10	0.04
11	0.06

$$\text{con}_2(\eta_1) =$$

	0
0	1.93·10 <sup>-5</sup>
1	2.78·10 <sup>-5</sup>
2	4.91·10 <sup>-5</sup>
3	9.35·10 <sup>-5</sup>
4	1.82·10 <sup>-4</sup>
5	3.55·10 <sup>-4</sup>
6	6.94·10 <sup>-4</sup>
7	1.36·10 <sup>-3</sup>
8	2.66·10 <sup>-3</sup>
9	5.19·10 <sup>-3</sup>
10	0.01
11	0.02

RPP-RPT-28963, Rev. 1  
M&D-2008-005-RPT-01, Rev. 1

Prepared by: F. G. Abatt  
M&D Professional Services  
8/10/05  
Rev. 1

Theoretical Fluid Response  
Calculations for Rigid Primary Tank  
at 422 in. Waste Level

Checked by: B.G. Carpenter  
M&D Professional Services  
2/1/06

Impulsive pressure coefficient as a function of dimensionless wall height

$$c_i(\eta_1) := 1 - \text{con}_0(\eta_1) - \text{con}_1(\eta_1) - \text{con}_2(\eta_1) \quad \text{Eqn. 4.7 BNL 1995}$$

	0
0	0.71
1	0.7
2	0.69
3	0.67
4	0.65
5	0.61
6	0.57
7	0.52
8	0.45
9	0.37
10	0.27
11	0.14

Calculate maximum values of dynamic wall pressures from spectral acceleration of dome input TH.

Consider the first three convective mode spectral accelerations for the 0.5% damped spectrum

$$SA_{c0} := 0.062 \cdot g \quad SA_{c0} = 23.96 \frac{\text{in}}{\text{sec}^2} \quad \text{Figure 2-21 of main report}$$

$$SA_{c1} := 0.108 \cdot g \quad SA_{c1} = 41.73 \frac{\text{in}}{\text{sec}^2}$$

$$SA_{c2} := 0.163 \cdot g \quad SA_{c2} = 62.98 \frac{\text{in}}{\text{sec}^2}$$

Associate the impulsive mode with the ZPA, since the tank is rigid.

$$PGA := 0.276 \cdot g \quad PGA = 106.65 \frac{\text{in}}{\text{sec}^2} \quad \text{ANSYS dome RS from Spectr - Figure 2-19 of main report.}$$

**RPP-RPT-28963, Rev. 1**  
**M&D-2008-005-RPT-01, Rev. 1**

Prepared by: F. G. Abatt  
M&D Professional Services  
8/10/05  
Rev. 1

Theoretical Fluid Response  
Calculations for Rigid Primary Tank  
at 422 in. Waste Level

Checked by: B.G. Carpenter  
M&D Professional Services  
2/1/06

$$P_{\max\text{conv}}(\eta_1, \theta) := \left[ \sqrt{(\text{con}_0(\eta_1) \cdot SA_{c0})^2 + (\text{con}_1(\eta_1) \cdot SA_{c1})^2 + (\text{con}_2(\eta_1) \cdot SA_{c2})^2} \right] \cdot (\rho_1 \cdot R \cdot \cos(\theta \cdot \text{deg}))$$

$$P_{\max\text{impulsive}}(\eta_1, \theta) := \left[ \sqrt{[c_i(\eta_1) \cdot (PGA)]^2} \right] \cdot (\rho_1 \cdot R \cdot \cos(\theta \cdot \text{deg}))$$

$$P_{\max}(\eta_1, \theta) := \left[ \sqrt{[c_i(\eta_1) \cdot (PGA)]^2 + (\text{con}_0(\eta_1) \cdot SA_{c0})^2 + (\text{con}_1(\eta_1) \cdot SA_{c1})^2 + (\text{con}_2(\eta_1) \cdot SA_{c2})^2} \right] \cdot (\rho_1 \cdot R \cdot \cos(\theta \cdot \text{deg}))$$

Eqn. 4.24 BNL 1995

$P_{\max\text{impulsive}}(\eta_1, 0) =$

	0
0	5.42
1	5.37
2	5.28
3	5.13
4	4.93
5	4.67
6	4.34
7	3.93
8	3.43
9	2.8
10	2.03
11	1.06

$\frac{\text{lb}}{\text{in}^2}$

Maximum impulsive dynamic pressures at theta = 0.

$P_{\max\text{conv}}(\eta_1, 0) =$

	0
0	0.5
1	0.51
2	0.53
3	0.56
4	0.6
5	0.66
6	0.73
7	0.81
8	0.91
9	1.03
10	1.18
11	1.36

$\frac{\text{lb}}{\text{in}^2}$

Maximum convective dynamic pressures at theta = 0.

RPP-RPT-28963, Rev. 1  
M&D-2008-005-RPT-01, Rev. 1

Prepared by: F. G. Abatt  
M&D Professional Services  
8/10/05  
Rev. 1

Theoretical Fluid Response  
Calculations for Rigid Primary Tank  
at 422 in. Waste Level

Checked by: B.G. Carpenter  
M&D Professional Services  
2/1/06

$$p_{\max}(\eta_1, 0) =$$

	0
0	5.44
1	5.39
2	5.3
3	5.16
4	4.97
5	4.72
6	4.4
7	4.01
8	3.55
9	2.99
10	2.35
11	1.72

$$\frac{\text{lbf}}{\text{in}^2}$$

Maximum total dynamic pressure at  
theta = 0.

$$p_{\max}(\eta_1, 45) =$$

	0
0	3.85
1	3.81
2	3.75
3	3.65
4	3.51
5	3.34
6	3.11
7	2.84
8	2.51
9	2.11
10	1.66
11	1.22

$$\frac{\text{lbf}}{\text{in}^2}$$

Maximum total dynamic pressure at  
theta = 45 degrees.

$$p_{\max}(\eta_1, 90) =$$

	0
0	0
1	0
2	0
3	0
4	0
5	0
6	0
7	0
8	0
9	0
10	0
11	0

$$\frac{\text{lbf}}{\text{in}^2}$$

Maximum total dynamic pressure at  
theta = 90 degrees.

RPP-RPT-28963, Rev. 1  
M&D-2008-005-RPT-01, Rev. 1

Prepared by: F. G. Abatt  
M&D Professional Services  
8/10/05  
Rev. 1

Theoretical Fluid Response  
Calculations for Rigid Primary Tank  
at 422 in. Waste Level

Checked by: B.G. Carpenter  
M&D Professional Services  
2/1/06

Calculate Maximum Slosh Height:

$$\text{conmax} := \begin{pmatrix} 0.837 \\ 0.073 \\ 0.028 \end{pmatrix} \quad \text{Maximum value of convective coefficients at } \eta_1=1$$

$$h_{\text{maxslosh}} := R \cdot \sqrt{\left(\text{conmax}_0 \cdot \frac{SA_{c0}}{g}\right)^2 + \left(\text{conmax}_1 \cdot \frac{SA_{c1}}{g}\right)^2 + \left(\text{conmax}_2 \cdot \frac{SA_{c2}}{g}\right)^2} \quad \text{Eqn. 4.60 BNL 1995}$$

$$h_{\text{maxslosh}} = 23.71 \text{ in} \quad \text{Maximum theoretical slosh height}$$

Calculate Maximum Total Hydrodynamic Force:

The maximum hydrodynamic force induced on the tank wall is given by Eqn. 4.31 of BNL 1995 with the instantaneous accelerations replaced by the maximum spectral accelerations. First determine the effective impulsive and convective masses.

$$m_{l\text{approx}} := \pi \cdot R^2 \cdot H_1 \cdot \rho_1 \quad m_{l\text{approx}} = 4.27 \times 10^4 \frac{\text{lb} \cdot \text{sec}^2}{\text{in}} \quad \text{Total waste mass based on circular cylinder approximation.}$$

$$m_1 := 4.23 \cdot 10^4 \frac{\text{lb} \cdot \text{sec}^2}{\text{in}} \quad \text{Actual waste mass reported by Dytran model.}$$

$$m_{c0} := \left[ \frac{2}{\lambda_0 \cdot \left[ (\lambda_0)^2 - 1 \right] \cdot \left( \frac{H_1}{R} \right)} \right] \cdot \tanh \left[ \lambda_0 \cdot \left( \frac{H_1}{R} \right) \right] \cdot m_1$$

$$m_{c0} = 1.93 \times 10^4 \frac{\text{lb} \cdot \text{sec}^2}{\text{in}} \quad \text{First mode convective mass}$$

$$m_{c1} := \left[ \frac{2}{\lambda_1 \cdot \left[ (\lambda_1)^2 - 1 \right] \cdot \left( \frac{H_1}{R} \right)} \right] \cdot \tanh \left[ \lambda_1 \cdot \left( \frac{H_1}{R} \right) \right] \cdot m_1 \quad \text{Second mode convective mass}$$

**RPP-RPT-28963, Rev. 1**  
**M&D-2008-005-RPT-01, Rev. 1**

Prepared by: F. G. Abatt  
M&D Professional Services  
8/10/05  
Rev. 1

Theoretical Fluid Response  
Calculations for Rigid Primary Tank  
at 422 in. Waste Level

Checked by: B.G. Carpenter  
M&D Professional Services  
2/1/06

$$m_{c1} = 617.11 \frac{\text{lb} \cdot \text{sec}^2}{\text{in}}$$

$$m_{c2} := \left[ \frac{2}{\lambda_2 \left[ (\lambda_2)^2 - 1 \right] \left( \frac{H_1}{R} \right)} \right] \cdot \tanh \left[ \lambda_2 \cdot \left( \frac{H_1}{R} \right) \right] \cdot m_1 \quad \text{Third mode convective mass}$$

$$m_{c2} = 147.06 \frac{\text{lb} \cdot \text{sec}^2}{\text{in}}$$

$$m_i := m_1 - (m_{c0} + m_{c1} + m_{c2}) \quad \text{Impulsive mass}$$

$$m_i = 2.23 \times 10^4 \frac{\text{lb} \cdot \text{sec}^2}{\text{in}}$$

$$F_{\text{max}} := m_i \cdot \text{PGA} + m_{c0} \cdot \text{SA}_{c0} + m_{c1} \cdot \text{SA}_{c1} + m_{c2} \cdot \text{SA}_{c2} \quad \text{Eqn. 4.31 BNL 1995}$$

$$F_{\text{max}} = 2.87 \times 10^6 \text{ lbf} \quad \text{Conservative estimate of maximum hydrodynamic force}$$

The above expression is a conservative estimate because it assumes that the peak impulsive and convective forces occur simultaneously. A less conservative estimate can be made via a square-root-sum-of-the-squares (SRSS) combination.

$$F_{\text{srss}} := \sqrt{(m_i \cdot \text{PGA})^2 + (m_{c0} \cdot \text{SA}_{c0})^2 + (m_{c1} \cdot \text{SA}_{c1})^2 + (m_{c2} \cdot \text{SA}_{c2})^2} \quad \text{Eqn. 4.31 BNL 1995}$$

$$F_{\text{srss}} = 2.42 \times 10^6 \text{ lbf} \quad \text{SRSS estimate of peak hydrodynamic force}$$

$$F_{\text{conmax}} := \sqrt{(m_{c0} \cdot \text{SA}_{c0})^2 + (m_{c1} \cdot \text{SA}_{c1})^2 + (m_{c2} \cdot \text{SA}_{c2})^2}$$

$$F_{\text{conmax}} = 4.62 \times 10^5 \text{ lbf} \quad \text{Peak hydrodynamic force due to convective response - shows up in free oscillations.}$$

RPP-RPT-28963, Rev. 1  
M&D-2008-005-RPT-01, Rev. 1

Prepared by: F. G. Abatt  
M&D Professional Services  
8/10/05  
Rev. 1

Theoretical Fluid Response  
Calculations for Rigid Primary Tank  
at 422 in. Waste Level

Checked by: B.G. Carpenter  
M&D Professional Services  
2/1/06

Consider Vertical Excitation:

For a rigid tank, the period of the breathing mode is zero and the associated spectral acceleration is the vertical ZPA.

$ZPA_{\text{vert}} := 0.12 \cdot g$       ANSYS Haunch RS from Spectr - see also Figure 2-16 of main report.

The maximum wall pressure as a function of the dimensionless vertical distance is given by

$$P_{\text{maxv}}(\eta_1) := (0.8) \cdot \left( \cos\left(\frac{\pi}{2} \cdot \eta_1\right) \right) \cdot (\rho_1 \cdot H_1 \cdot ZPA_{\text{vert}}) \quad \text{Eqn. 4.52 BNL 1995}$$

	0	
0	2.49	
1	2.45	
2	2.36	
3	2.24	
4	2.08	
5	1.88	
6	1.65	
7	1.39	
8	1.11	
9	0.81	
10	0.49	
11	0.16	

$P_{\text{maxv}}(\eta_1) =$        $\frac{\text{lbf}}{\text{in}^2}$



The maximum base pressure and force are given by

$$P_{\text{maxbasevert}} := \rho_1 \cdot H_1 \cdot ZPA_{\text{vert}} \quad P_{\text{maxbasevert}} = 3.11 \frac{\text{lbf}}{\text{in}^2} \quad \text{Eqn. 4.55 BNL 1995}$$

$$F_{\text{maxbasevert}} := m_1 \cdot ZPA_{\text{vert}} \quad F_{\text{maxbasevert}} = 1.96 \times 10^6 \text{ lbf} \quad \text{Eqn. 4.57 BNL 1995}$$

**RPP-RPT-28963, Rev. 1**  
**M&D-2008-005-RPT-01, Rev. 1**

Prepared by: F. G. Abatt  
M&D Professional Services  
8/17/05  
Rev. 1 *FA*

Theoretical Fluid Response  
Calculations for Rigid Primary Tank  
at 460 in. Waste Level - Dytran  
Configuration

Checked by: B.G. Carpenter  
M&D Professional Services  
2/1/06  
*BGC*

$H_1 := 460.0 \text{ in}$  Baseline waste level

$H_t := 460.0 \text{ in}$  Height to primary tank tangent line

$\frac{H_1}{H_t} = 1$  Ratio of waste height to tank height

$$g_w := 386.4 \frac{\text{in}}{\text{sec}^2}$$

$R := 450 \text{ in}$  Tank radius

$\frac{H_1}{R} = 1.02$  Ratio of waste height to tank radius

$i := 0..2$

$\lambda := \begin{pmatrix} 1.841 \\ 5.331 \\ 8.536 \end{pmatrix}$  Bessel function roots

$\theta := \begin{pmatrix} 0 \text{ deg} \\ 45 \text{ deg} \\ 90 \text{ deg} \end{pmatrix}$  Circumferential location of waste elements for which pressures are reported

**Convective Frequencies**

$$f_{con_i} := \frac{1}{2 \cdot \pi} \cdot \left[ \sqrt{\lambda_i \left[ \frac{g}{R} \cdot \tanh \left[ \lambda_i \left( \frac{H_1}{R} \right) \right] \right]} \right] \quad \text{Eqn. 4.14 BNL 1995}$$

$f_{con} = \begin{pmatrix} 0.2 \\ 0.34 \\ 0.43 \end{pmatrix} \text{ Hz}$  First three convective frequencies

$\rho_1 := 1.71 \cdot 10^{-4} \frac{\text{lb} \cdot \text{sec}^2}{\text{in}^4}$  waste density - specific gravity = 1.83

**RPP-RPT-28963, Rev. 1**  
**M&D-2008-005-RPT-01, Rev. 1**

Prepared by: F. G. Abatt  
M&D Professional Services  
8/17/05  
Rev. 1

Theoretical Fluid Response  
Calculations for Rigid Primary Tank  
at 460 in. Waste Level - Dytran  
Configuration

Checked by: B.G. Carpenter  
M&D Professional Services  
2/1/06

Determine Convective Pressures on the Tank Wall:

$$z := \begin{pmatrix} 15\text{-in} \\ 50.5\text{-in} \\ 85.8\text{-in} \\ 121.2\text{-in} \\ 156.6\text{-in} \\ 192.0\text{-in} \\ 227.4\text{-in} \\ 262.8\text{-in} \\ 298.2\text{-in} \\ 333.5\text{-in} \\ 368.9\text{-in} \\ 404.3\text{-in} \\ 441\text{-in} \end{pmatrix}$$

Vertical location of Euler element centroids at which pressures are reported.

$$\eta_1 := \frac{z}{H_1}$$

Ratio of tank wall vertical location to waste height for waste element centroids.

$$\eta_1 = \begin{array}{|c|c|} \hline & 0 \\ \hline 0 & 0.03 \\ \hline 1 & 0.11 \\ \hline 2 & 0.19 \\ \hline 3 & 0.26 \\ \hline 4 & 0.34 \\ \hline 5 & 0.42 \\ \hline 6 & 0.49 \\ \hline 7 & 0.57 \\ \hline 8 & 0.65 \\ \hline 9 & 0.73 \\ \hline 10 & 0.8 \\ \hline 11 & 0.88 \\ \hline 12 & 0.96 \\ \hline \end{array}$$

RPP-RPT-28963, Rev. 1  
M&D-2008-005-RPT-01, Rev. 1

Prepared by: F. G. Abatt  
M&D Professional Services  
8/17/05  
Rev. 1

Theoretical Fluid Response  
Calculations for Rigid Primary Tank  
at 460 in. Waste Level - Dytran  
Configuration

Checked by: B.G. Carpenter  
M&D Professional Services  
2/1/06

Determine convective coefficients as a function of dimensionless height per BNL 1995 Eqn. 4.4

$$\text{con}_0(\eta_1) := \frac{2}{\left(\lambda_0\right)^2 - 1} \cdot \frac{\cosh\left[\lambda_0 \cdot \left(\frac{H_1}{R}\right) \cdot \eta_1\right]}{\cosh\left[\lambda_0 \cdot \left(\frac{H_1}{R}\right)\right]}$$

$$\text{con}_1(\eta_1) := \frac{2}{\left(\lambda_1\right)^2 - 1} \cdot \frac{\cosh\left[\lambda_1 \cdot \left(\frac{H_1}{R}\right) \cdot \eta_1\right]}{\cosh\left[\lambda_1 \cdot \left(\frac{H_1}{R}\right)\right]}$$

$$\text{con}_2(\eta_1) := \frac{2}{\left(\lambda_2\right)^2 - 1} \cdot \frac{\cosh\left[\lambda_2 \cdot \left(\frac{H_1}{R}\right) \cdot \eta_1\right]}{\cosh\left[\lambda_2 \cdot \left(\frac{H_1}{R}\right)\right]}$$

$$\text{con}_0(\eta_1) =$$

	0
0	0.25
1	0.25
2	0.26
3	0.28
4	0.3
5	0.33
6	0.37
7	0.41
8	0.46
9	0.52
10	0.59
11	0.68
12	0.78

$$\text{con}_1(\eta_1) =$$

	0
0	6.37·10 <sup>-4</sup>
1	7.43·10 <sup>-4</sup>
2	9.8·10 <sup>-4</sup>
3	1.39·10 <sup>-3</sup>
4	2.05·10 <sup>-3</sup>
5	3.08·10 <sup>-3</sup>
6	4.66·10 <sup>-3</sup>
7	7.07·10 <sup>-3</sup>
8	0.01
9	0.02
10	0.02
11	0.04
12	0.06

$$\text{con}_2(\eta_1) =$$

	0
0	9.41·10 <sup>-6</sup>
1	1.35·10 <sup>-5</sup>
2	2.39·10 <sup>-5</sup>
3	4.55·10 <sup>-5</sup>
4	8.84·10 <sup>-5</sup>
5	1.73·10 <sup>-4</sup>
6	3.38·10 <sup>-4</sup>
7	6.61·10 <sup>-4</sup>
8	1.29·10 <sup>-3</sup>
9	2.53·10 <sup>-3</sup>
10	4.94·10 <sup>-3</sup>
11	9.68·10 <sup>-3</sup>
12	0.02

RPP-RPT-28963, Rev. 1  
M&D-2008-005-RPT-01, Rev. 1

Prepared by: F. G. Abatt  
M&D Professional Services  
8/17/05  
Rev. 1

Theoretical Fluid Response  
Calculations for Rigid Primary Tank  
at 460 in. Waste Level - Dytran  
Configuration

Checked by: B.G. Carpenter  
M&D Professional Services  
2/1/06

Impulsive pressure coefficient as a function of dimensionless wall height

$$c_i(\eta_1) := 1 - \cos_0(\eta_1) - \cos_1(\eta_1) - \cos_2(\eta_1) \quad \text{Eqn. 4.7 BNL 1995}$$

	0
0	0.75
1	0.74
2	0.73
3	0.72
4	0.7
5	0.67
6	0.63
7	0.58
8	0.53
9	0.46
10	0.38
11	0.28
12	0.14

Calculate maximum values of dynamic wall pressures from spectral acceleration of dome input TH.

Consider the first three convective mode spectral accelerations for the 0.5% damped spectrum

$$SA_{c0} := 0.064\text{-g} \quad SA_{c0} = 24.73 \frac{\text{in}}{\text{sec}^2} \quad \text{Figure 2-21 of main report}$$

$$SA_{c1} := 0.108\text{-g} \quad SA_{c1} = 41.73 \frac{\text{in}}{\text{sec}^2}$$

$$SA_{c2} := 0.163\text{-g} \quad SA_{c2} = 62.98 \frac{\text{in}}{\text{sec}^2}$$

Associate the impulsive mode with the ZPA, since the tank is rigid.

$$PGA := 0.276\text{-g} \quad PGA = 106.65 \frac{\text{in}}{\text{sec}^2} \quad \text{ANSYS dome RS from Spectr - Figures 2-15 and 2-19 of main report.}$$

RPP-RPT-28963, Rev. 1  
M&D-2008-005-RPT-01, Rev. 1

Prepared by: F. G. Abatt  
M&D Professional Services  
8/17/05  
Rev. 1

Theoretical Fluid Response  
Calculations for Rigid Primary Tank  
at 460 in. Waste Level - Dytran  
Configuration

Checked by: B.G. Carpenter  
M&D Professional Services  
2/1/06

$$P_{\max\text{conv}}(\eta_1, \theta) := \left[ \sqrt{(\text{con}_0(\eta_1) \cdot SA_{c0})^2 + (\text{con}_1(\eta_1) \cdot SA_{c1})^2 + (\text{con}_2(\eta_1) \cdot SA_{c2})^2} \right] \cdot (\rho_1 \cdot R \cdot \cos(\theta \cdot \text{deg}))$$

$$P_{\max\text{impulsive}}(\eta_1, \theta) := \left[ \sqrt{[c_1(\eta_1) \cdot (PGA)]^2} \right] \cdot (\rho_1 \cdot R \cdot \cos(\theta \cdot \text{deg}))$$

$$P_{\max}(\eta_1, \theta) := \left[ \sqrt{[c_1(\eta_1) \cdot (PGA)]^2 + (\text{con}_0(\eta_1) \cdot SA_{c0})^2 + (\text{con}_1(\eta_1) \cdot SA_{c1})^2 + (\text{con}_2(\eta_1) \cdot SA_{c2})^2} \right] \cdot (\rho_1 \cdot R \cdot \cos(\theta \cdot \text{deg}))$$

Eqn. 4.24 BNL 1995

	0
0	6.15
1	6.11
2	6.03
3	5.89
4	5.71
5	5.47
6	5.17
7	4.8
8	4.34
9	3.79
10	3.11
11	2.28
12	1.19

$P_{\max\text{impulsive}}(\eta_1, 0) =$

$\frac{\text{lbf}}{\text{in}^2}$

Maximum impulsive dynamic pressures at  
theta = 0.

	0
0	0.48
1	0.48
2	0.5
3	0.53
4	0.57
5	0.63
6	0.69
7	0.78
8	0.87
9	0.99
10	1.13
11	1.29
12	1.49

$P_{\max\text{conv}}(\eta_1, 0) =$

$\frac{\text{lbf}}{\text{in}^2}$

Maximum convective dynamic pressures at  
theta = 0.

**RPP-RPT-28963, Rev. 1**  
**M&D-2008-005-RPT-01, Rev. 1**

Prepared by: F. G. Abatt  
M&D Professional Services  
8/17/05  
Rev. 1

Theoretical Fluid Response  
Calculations for Rigid Primary Tank  
at 460 in. Waste Level - Dytran  
Configuration

Checked by: B.G. Carpenter  
M&D Professional Services  
2/1/06

$$P_{\max}(\eta_1, 0) =$$

	0
0	6.17
1	6.13
2	6.05
3	5.92
4	5.74
5	5.51
6	5.22
7	4.86
8	4.43
9	3.92
10	3.31
11	2.62
12	1.91

$\frac{\text{lb}}{\text{in}^2}$

Maximum total dynamic pressure at  
theta = 0.

$$P_{\max}(\eta_1, 45) =$$

	0
0	4.36
1	4.34
2	4.28
3	4.18
4	4.06
5	3.89
6	3.69
7	3.44
8	3.13
9	2.77
10	2.34
11	1.85
12	1.35

$\frac{\text{lb}}{\text{in}^2}$

Maximum total dynamic pressure at  
theta = 45 degrees.

$$P_{\max}(\eta_1, 90) =$$

	0
0	0
1	0
2	0
3	0
4	0
5	0
6	0
7	0
8	0
9	0
10	0
11	0
12	0

$\frac{\text{lb}}{\text{in}^2}$

Maximum total dynamic pressure at  
theta = 90 degrees.

**RPP-RPT-28963, Rev. 1**  
**M&D-2008-005-RPT-01, Rev. 1**

Prepared by: F. G. Abatt  
M&D Professional Services  
8/17/05  
Rev. 1

Theoretical Fluid Response  
Calculations for Rigid Primary Tank  
at 460 in. Waste Level - Dytran  
Configuration

Checked by: B.G. Carpenter  
M&D Professional Services  
2/1/06

Calculate Maximum Slosh Height:

$$\text{conmax} := \begin{pmatrix} 0.837 \\ 0.073 \\ 0.028 \end{pmatrix} \quad \text{Maximum value of convective coefficients at } \eta_1=1$$

$$h_{\text{maxslosh}} := R \cdot \sqrt{\left(\text{conmax}_0 \cdot \frac{SA_{c0}}{g}\right)^2 + \left(\text{conmax}_1 \cdot \frac{SA_{c1}}{g}\right)^2 + \left(\text{conmax}_2 \cdot \frac{SA_{c2}}{g}\right)^2} \quad \text{Eqn. 4.60 BNL 1995}$$

$$h_{\text{maxslosh}} = 24.45 \text{ in} \quad \text{Maximum theoretical slosh height}$$

Calculate Maximum Total Hydrodynamic Force:

The maximum hydrodynamic force induced on the tank wall is given by Eqn. 4.31 of BNL 1995 with the instantaneous accelerations replaced by the maximum spectral accelerations. First determine the effective impulsive and convective masses.

$$m_{\text{lapprox}} := \pi \cdot R^2 \cdot H_1 \cdot \rho_1 \quad m_{\text{lapprox}} = 5 \times 10^4 \frac{\text{lb} \cdot \text{sec}^2}{\text{in}} \quad \text{Total waste mass based on circular cylinder approximation.}$$

$$m_1 := 4.95 \cdot 10^4 \frac{\text{lb} \cdot \text{sec}^2}{\text{in}} \quad \text{Actual waste mass reported by Dytran model.}$$

$$m_{c0} := \left[ \frac{2}{\lambda_0 \cdot \left[ (\lambda_0)^2 - 1 \right] \cdot \left( \frac{H_1}{R} \right)} \right] \cdot \tanh \left[ \lambda_0 \cdot \left( \frac{H_1}{R} \right) \right] \cdot m_1 \quad \text{Eqn. 4.32 BNL 1995}$$

$$m_{c0} = 2.1 \times 10^4 \frac{\text{lb} \cdot \text{sec}^2}{\text{in}} \quad \text{First mode convective mass}$$

$$m_{c1} := \left[ \frac{2}{\lambda_1 \cdot \left[ (\lambda_1)^2 - 1 \right] \cdot \left( \frac{H_1}{R} \right)} \right] \cdot \tanh \left[ \lambda_1 \cdot \left( \frac{H_1}{R} \right) \right] \cdot m_1 \quad \text{Second mode convective mass}$$

RPP-RPT-28963, Rev. 1  
M&D-2008-005-RPT-01, Rev. 1

Prepared by: F. G. Abatt  
M&D Professional Services  
8/17/05  
Rev. 1

Theoretical Fluid Response  
Calculations for Rigid Primary Tank  
at 460 in. Waste Level - Dytran  
Configuration

Checked by: B.G. Carpenter  
M&D Professional Services  
2/1/06

$$m_{c1} = 662.53 \frac{\text{lb} \cdot \text{sec}^2}{\text{in}}$$

$$m_{c2} := \left[ \frac{2}{\lambda_2 \cdot \left[ \left( \lambda_2^2 - 1 \right) \cdot \left( \frac{H_1}{R} \right) \right]} \right] \cdot \tanh \left[ \lambda_2 \cdot \left( \frac{H_1}{R} \right) \right] \cdot m_1 \quad \text{Third mode convective mass}$$

$$m_{c2} = 157.88 \frac{\text{lb} \cdot \text{sec}^2}{\text{in}}$$

$$m_i := m_1 - (m_{c0} + m_{c1} + m_{c2}) \quad \text{Impulsive mass} \quad \text{Eqn. 4.33 BNL 1995}$$

$$m_i = 2.77 \times 10^4 \frac{\text{lb} \cdot \text{sec}^2}{\text{in}}$$

$$F_{\text{max}} := m_i \cdot \text{PGA} + m_{c0} \cdot \text{SA}_{c0} + m_{c1} \cdot \text{SA}_{c1} + m_{c2} \cdot \text{SA}_{c2} \quad \text{Eqn. 4.31 BNL 1995}$$

$$F_{\text{max}} = 3.51 \times 10^6 \text{ lbf} \quad \text{Conservative estimate of maximum hydrodynamic force}$$

The above expression is a conservative estimate because it assumes that the peak impulsive and convective forces occur simultaneously. A less conservative estimate can be made via a square-root-sum-of-the-squares (SRSS) combination.

$$F_{\text{srss}} := \sqrt{(m_i \cdot \text{PGA})^2 + (m_{c0} \cdot \text{SA}_{c0})^2 + (m_{c1} \cdot \text{SA}_{c1})^2 + (m_{c2} \cdot \text{SA}_{c2})^2} \quad \text{Eqn. 4.31 BNL 1995 - SRSS}$$

$$F_{\text{srss}} = 3 \times 10^6 \text{ lbf} \quad \text{SRSS estimate of peak hydrodynamic force}$$

$$F_{\text{conmax}} := \sqrt{(m_{c0} \cdot \text{SA}_{c0})^2 + (m_{c1} \cdot \text{SA}_{c1})^2 + (m_{c2} \cdot \text{SA}_{c2})^2}$$

$$F_{\text{conmax}} = 5.21 \times 10^5 \text{ lbf} \quad \text{Peak hydrodynamic force due to convective response - shows up in free oscillations.}$$

RPP-RPT-28963, Rev. 1  
M&D-2008-005-RPT-01, Rev. 1

Prepared by: F. G. Abatt  
M&D Professional Services  
8/17/05  
Rev. 1

Theoretical Fluid Response  
Calculations for Rigid Primary Tank  
at 460 in. Waste Level - Dytran  
Configuration

Checked by: B.G. Carpenter  
M&D Professional Services  
2/1/06

Consider Vertical Excitation:

For a rigid tank, the period of the breathing mode is zero and the associated spectral acceleration is the vertical ZPA.

$ZPA_{\text{vert}} := 0.12 \cdot g$       ANSYS Haunch RS from Spectr - see also Figure 2-16 of main report.

The maximum wall pressure as a function of the dimensionless vertical distance is given by

$$P_{\text{maxv}}(\eta_1) := (0.8) \cdot \left( \cos\left(\frac{\pi}{2} \cdot \eta_1\right) \right) \cdot (\rho_1 \cdot H_1 \cdot ZPA_{\text{vert}}) \quad \text{Eqn. 4.52 BNL 1995}$$

	0
0	2.91
1	2.87
2	2.79
3	2.67
4	2.51
5	2.31
6	2.08
7	1.82
8	1.53
9	1.22
10	0.89
11	0.55
12	0.19

$P_{\text{maxv}}(\eta_1) =$        $\frac{\text{lbf}}{\text{in}^2}$

The maximum base pressure and force are given by

$$P_{\text{maxbasevert}} := \rho_1 \cdot H_1 \cdot ZPA_{\text{vert}} \quad P_{\text{maxbasevert}} = 3.65 \frac{\text{lbf}}{\text{in}^2} \quad \text{Eqn. 4.55 BNL 1995}$$

$$F_{\text{maxbasevert}} := m_1 \cdot ZPA_{\text{vert}} \quad F_{\text{maxbasevert}} = 2.3 \times 10^6 \text{ lbf} \quad \text{Eqn. 4.57 BNL 1995}$$

Reference:

BNL 1995, *Seismic Design and Evaluation Guidelines for the Department of Energy High-Level Waste Storage Tanks and Appurtenances*, BNL 52361, Rev. 10/95, Brookhaven National Laboratory, Upton, New York.

**RPP-RPT-28963, Rev. 1**  
**M&D-2008-005-RPT-01, Rev. 1**

Prepared by: F. G. Abatt  
M&D Professional Services  
8/31/05  
Rev. 2 *FA*

Theoretical Fluid Response for  
Simplified AY Flexible Wall Tank at  
422 in. Waste Level

Checked by: B.G. Carpenter  
M&D Professional Services  
*BAC* 2/1/06

$H_1 := 422\text{-in}$       Baseline waste level

$H_t := 460\text{-in}$       Height to primary tank tangent line

$\frac{H_1}{H_t} = 0.92$       Ratio of waste height to tank height

$$\frac{g}{W} := 386.4 \cdot \frac{\text{in}}{\text{sec}^2}$$

$\frac{R}{W} := 450\text{-in}$       Tank radius

$\frac{H_1}{R} = 0.94$       Ratio of waste height to tank radius

$i := 0..2$

$\lambda := \begin{pmatrix} 1.841 \\ 5.331 \\ 8.536 \end{pmatrix}$       Bessel function roots

$\theta := \begin{pmatrix} 0\text{-deg} \\ 45\text{-deg} \\ 90\text{-deg} \end{pmatrix}$       Circumferential location of waste elements for which pressures are reported

**Convective Frequencies**

$$f_{con,i} := \frac{1}{2 \cdot \pi} \cdot \left[ \sqrt{\lambda_i \cdot \frac{g}{R} \cdot \tanh \left[ \lambda_i \cdot \left( \frac{H_1}{R} \right) \right]} \right] \quad \text{Eqn. 4.14 BNL 1995}$$

$f_{con} = \begin{pmatrix} 0.19 \\ 0.34 \\ 0.43 \end{pmatrix} \text{Hz}$       First three convective frequencies

$\rho_1 := 1.59 \cdot 10^{-4} \cdot \frac{\text{lb} \cdot \text{sec}^2}{\text{in}^4}$       waste density - specific gravity = 1.7

RPP-RPT-28963, Rev. 1  
M&D-2008-005-RPT-01, Rev. 1

Prepared by: F. G. Abatt  
M&D Professional Services  
8/31/05  
Rev. 2

Theoretical Fluid Response for  
Simplified AY Flexible Wall Tank at  
422 in. Waste Level

Checked by: B.G. Carpenter  
M&D Professional Services  
2/1/06

Calculation of Impulsive Frequency:

$$\rho_t := 7.35 \cdot 10^{-4} \frac{\text{lb} \cdot \text{sec}^2}{\text{in}^4} \quad \text{Steel density}$$

$$t_{tw} := 0.65 \cdot \text{in} \quad \text{Average thickness of AY over lower 2/3.}$$

$$E_t := 29 \cdot 10^6 \frac{\text{lb} \cdot \text{sec}^2}{\text{in}^2} \quad \text{Elastic modulus for steel}$$

$$C_{iref} := 0.102 \quad \text{Table 4.4 of BNL 1995}$$

$$C_i := C_{iref} \cdot \sqrt{127 \cdot \frac{\left(\frac{t_{tw}}{R}\right)}{\left(\frac{\rho_l}{\rho_t}\right)}} \quad \text{Eqn. 4.18 BNL 1995}$$

$$C_i = 0.09 \quad \text{Impulsive coefficient for frequency calculation}$$

$$f_i := \frac{1}{2 \cdot \pi} \cdot \frac{C_i}{H_t} \cdot \sqrt{\frac{E_t}{\rho_t}} \quad f_i = 7.04 \text{ Hz} \quad \text{Eqn. 4.16 BNL 1995}$$

Determine Convective Pressures on the Tank Wall:

$$z := \begin{pmatrix} 15 \cdot \text{in} \\ 50.5 \cdot \text{in} \\ 85.8 \cdot \text{in} \\ 121.2 \cdot \text{in} \\ 156.6 \cdot \text{in} \\ 192.0 \cdot \text{in} \\ 227.4 \cdot \text{in} \\ 262.8 \cdot \text{in} \\ 298.2 \cdot \text{in} \\ 333.5 \cdot \text{in} \\ 368.9 \cdot \text{in} \\ 404.3 \cdot \text{in} \end{pmatrix}$$

Vertical location of Euler element centroids at which pressures are reported.

RPP-RPT-28963, Rev. 1  
M&D-2008-005-RPT-01, Rev. 1

Prepared by: F. G. Abatt  
M&D Professional Services  
8/31/05  
Rev. 2

Theoretical Fluid Response for  
Simplified AY Flexible Wall Tank at  
422 in. Waste Level

Checked by: B.G. Carpenter  
M&D Professional Services  
2/1/06

$$\eta_1 := \frac{z}{H_1}$$

Ratio of tank wall vertical location to waste height for waste element centroids.

	0
0	0.04
1	0.12
2	0.2
3	0.29
4	0.37
5	0.45
6	0.54
7	0.62
8	0.71
9	0.79
10	0.87
11	0.96

Determine convective coefficients as a function of dimensionless height per BNL 1995 Eqn. 4.4

$$\text{con}_0(\eta_1) := \left[ \frac{2 \cdot \cosh\left[\lambda_0 \cdot \left(\frac{H_1}{R}\right) \cdot \eta_1\right]}{(\lambda_0)^2 - 1 \cdot \cosh\left[\lambda_0 \cdot \left(\frac{H_1}{R}\right)\right]} \right]$$

$$\text{con}_1(\eta_1) := \left[ \frac{2 \cdot \cosh\left[\lambda_1 \cdot \left(\frac{H_1}{R}\right) \cdot \eta_1\right]}{(\lambda_1)^2 - 1 \cdot \cosh\left[\lambda_1 \cdot \left(\frac{H_1}{R}\right)\right]} \right]$$

$$\text{con}_2(\eta_1) := \left[ \frac{2 \cdot \cosh\left[\lambda_2 \cdot \left(\frac{H_1}{R}\right) \cdot \eta_1\right]}{(\lambda_2)^2 - 1 \cdot \cosh\left[\lambda_2 \cdot \left(\frac{H_1}{R}\right)\right]} \right]$$

RPP-RPT-28963, Rev. 1  
M&D-2008-005-RPT-01, Rev. 1

Prepared by: F. G. Abatt  
M&D Professional Services  
8/31/05  
Rev. 2

Theoretical Fluid Response for  
Simplified AY Flexible Wall Tank at  
422 in. Waste Level

Checked by: B.G. Carpenter  
M&D Professional Services  
2/1/06

$$con_0(\eta_1) =$$

	0
0	0.29
1	0.29
2	0.31
3	0.32
4	0.35
5	0.38
6	0.42
7	0.47
8	0.53
9	0.6
10	0.68
11	0.78

$$con_1(\eta_1) =$$

	0
0	$9.99 \cdot 10^{-4}$
1	$1.16 \cdot 10^{-3}$
2	$1.54 \cdot 10^{-3}$
3	$2.18 \cdot 10^{-3}$
4	$3.22 \cdot 10^{-3}$
5	$4.83 \cdot 10^{-3}$
6	$7.31 \cdot 10^{-3}$
7	0.01
8	0.02
9	0.03
10	0.04
11	0.06

$$con_2(\eta_1) =$$

	0
0	$1.93 \cdot 10^{-5}$
1	$2.78 \cdot 10^{-5}$
2	$4.91 \cdot 10^{-5}$
3	$9.35 \cdot 10^{-5}$
4	$1.82 \cdot 10^{-4}$
5	$3.55 \cdot 10^{-4}$
6	$6.94 \cdot 10^{-4}$
7	$1.36 \cdot 10^{-3}$
8	$2.66 \cdot 10^{-3}$
9	$5.19 \cdot 10^{-3}$
10	0.01
11	0.02

Impulsive pressure coefficient as a function of dimensionless wall height

$$c_i(\eta_1) := 1 - con_0(\eta_1) - con_1(\eta_1) - con_2(\eta_1)$$

Eqn. 4.7 BNL 1995

$$c_i(\eta_1) =$$

	0
0	0.71
1	0.7
2	0.69
3	0.67
4	0.65
5	0.61
6	0.57
7	0.52
8	0.45
9	0.37
10	0.27
11	0.14

**RPP-RPT-28963, Rev. 1**  
**M&D-2008-005-RPT-01, Rev. 1**

Prepared by: F. G. Abatt  
M&D Professional Services  
8/31/05  
Rev. 2

Theoretical Fluid Response for  
Simplified AY Flexible Wall Tank at  
422 in. Waste Level

Checked by: B.G. Carpenter  
M&D Professional Services  
2/1/06

Calculate maximum values of dynamic wall pressures from spectral acceleration of dome input TH.

Consider the first three convective modes

$$SA_{c0} := 0.062 \cdot g \qquad SA_{c0} = 23.96 \frac{\text{in}}{\text{sec}^2}$$

$$SA_{c1} := 0.108 \cdot g \qquad SA_{c1} = 41.73 \frac{\text{in}}{\text{sec}^2} \qquad 0.5\% \text{ Dome RS from Spectr - see Figure 2-21 of main report.}$$

$$SA_{c2} := 0.163 \cdot g \qquad SA_{c2} = 62.98 \frac{\text{in}}{\text{sec}^2}$$

Determine the spectral acceleration for the impulsive mode.

$$SA_i := 0.876 \cdot g \qquad SA_i = 338.49 \frac{\text{in}}{\text{sec}^2} \qquad 4\% \text{ Dome RS from Spectr - see Figure 2-19 of main report.}$$

$$P_{\text{maxconv}}(\eta_1, \theta) := \left[ \sqrt{(\text{con}_0(\eta_1) \cdot SA_{c0})^2 + (\text{con}_1(\eta_1) \cdot SA_{c1})^2 + (\text{con}_2(\eta_1) \cdot SA_{c2})^2} \right] \cdot (\rho_1 \cdot R \cdot \cos(\theta \cdot \text{deg}))$$

$$P_{\text{maximpulsive}}(\eta_1, \theta) := \left[ \sqrt{[c_i(\eta_1) \cdot (SA_i)]^2} \right] \cdot (\rho_1 \cdot R \cdot \cos(\theta \cdot \text{deg}))$$

$$P_{\text{max}}(\eta_1, \theta) := \left[ \sqrt{[c_i(\eta_1) \cdot (SA_i)]^2 + (\text{con}_0(\eta_1) \cdot SA_{c0})^2 + (\text{con}_1(\eta_1) \cdot SA_{c1})^2 + (\text{con}_2(\eta_1) \cdot SA_{c2})^2} \right] \cdot (\rho_1 \cdot R \cdot \cos(\theta \cdot \text{deg}))$$

Eqn. 4.24 BNL 1995

RPP-RPT-28963, Rev. 1  
M&D-2008-005-RPT-01, Rev. 1

Prepared by: F. G. Abatt  
M&D Professional Services  
8/31/05  
Rev. 2

Theoretical Fluid Response for  
Simplified AY Flexible Wall Tank at  
422 in. Waste Level

Checked by: B.G. Carpenter  
M&D Professional Services  
2/1/06

$$P_{\text{maximpulsive}}(\eta_1, 0) =$$

	0
0	17.19
1	17.05
2	16.75
3	16.29
4	15.66
5	14.83
6	13.78
7	12.48
8	10.87
9	8.9
10	6.44
11	3.36

$\frac{\text{lbf}}{\text{in}^2}$

Maximum impulsive dynamic pressures at  
theta = 0.

$$P_{\text{maxconv}}(\eta_1, 0) =$$

	0
0	0.5
1	0.51
2	0.53
3	0.56
4	0.6
5	0.66
6	0.73
7	0.81
8	0.91
9	1.03
10	1.18
11	1.36

$\frac{\text{lbf}}{\text{in}^2}$

Maximum convective dynamic pressures at  
theta = 0.

$$P_{\text{max}}(\eta_1, 0) =$$

	0
0	17.2
1	17.06
2	16.76
3	16.3
4	15.67
5	14.84
6	13.8
7	12.51
8	10.91
9	8.96
10	6.55
11	3.62

$\frac{\text{lbf}}{\text{in}^2}$

Maximum total dynamic pressure at  
theta = 0.

RPP-RPT-28963, Rev. 1  
M&D-2008-005-RPT-01, Rev. 1

Prepared by: F. G. Abatt  
M&D Professional Services  
8/31/05  
Rev. 2

Theoretical Fluid Response for  
Simplified AY Flexible Wall Tank at  
422 in. Waste Level

Checked by: B.G. Carpenter  
M&D Professional Services  
2/1/06

	0
0	12.16
1	12.06
2	11.85
3	11.53
4	11.08
5	10.5
6	9.76
7	8.84
8	7.71
9	6.33
10	4.63
11	2.56

$p_{\max}(\eta_1, 45) =$   $\frac{\text{lbf}}{\text{in}^2}$

Maximum total dynamic pressure at  
theta = 45 degrees.

	0
0	0
1	0
2	0
3	0
4	0
5	0
6	0
7	0
8	0
9	0
10	0
11	0

$p_{\max}(\eta_1, 90) =$   $\frac{\text{lbf}}{\text{in}^2}$

Maximum total dynamic pressure at  
theta = 90 degrees.

Calculate Maximum Slosh Height:

$$\text{conmax} := \begin{pmatrix} 0.837 \\ 0.073 \\ 0.028 \end{pmatrix} \quad \text{Maximum value of convective coefficients at } \eta_1=1$$

$$h_{\max\text{slosh}} := R \cdot \sqrt{\left(\text{conmax}_0 \cdot \frac{SA_{c0}}{g}\right)^2 + \left(\text{conmax}_1 \cdot \frac{SA_{c1}}{g}\right)^2 + \left(\text{conmax}_2 \cdot \frac{SA_{c2}}{g}\right)^2} \quad \text{Eqn. 4.60 BNL 1995}$$

$$h_{\max\text{slosh}} = 23.71 \text{ in}$$

RPP-RPT-28963, Rev. 1  
M&D-2008-005-RPT-01, Rev. 1

Prepared by: F. G. Abatt  
M&D Professional Services  
8/31/05  
Rev. 2

Theoretical Fluid Response for  
Simplified AY Flexible Wall Tank at  
422 in. Waste Level

Checked by: B.G. Carpenter  
M&D Professional Services  
2/1/06

Calculate Maximum Total Hydrodynamic Force:

The maximum hydrodynamic force induced on the tank wall is given by Eqn. 4.31 of BNL 1995 with the instantaneous accelerations replaced by the maximum spectral accelerations. First determine the effective impulsive and convective masses.

$$m_{l\text{approx}} := \pi R^2 H_1 \rho_1 \quad m_{l\text{approx}} = 4.27 \times 10^4 \frac{\text{lb}\cdot\text{sec}^2}{\text{in}} \quad \text{Total waste mass base on circular cylinder approximation.}$$

$$m_1 := 4.23 \times 10^4 \frac{\text{lb}\cdot\text{sec}^2}{\text{in}} \quad \text{Actual waste mass reported by Dytran model.}$$

$$m_{c0} := \left[ \frac{2}{\lambda_0 \left[ (\lambda_0)^2 - 1 \right] \left( \frac{H_1}{R} \right)} \right] \cdot \tanh \left[ \lambda_0 \left( \frac{H_1}{R} \right) \right] \cdot m_1 \quad \text{First mode convective mass - Eqn. 4.32 BNL 1995}$$

$$m_{c0} = 1.93 \times 10^4 \frac{\text{lb}\cdot\text{sec}^2}{\text{in}}$$

$$m_{c1} := \left[ \frac{2}{\lambda_1 \left[ (\lambda_1)^2 - 1 \right] \left( \frac{H_1}{R} \right)} \right] \cdot \tanh \left[ \lambda_1 \left( \frac{H_1}{R} \right) \right] \cdot m_1 \quad \text{Second mode convective mass}$$

$$m_{c1} = 617.11 \frac{\text{lb}\cdot\text{sec}^2}{\text{in}}$$

$$m_{c2} := \left[ \frac{2}{\lambda_2 \left[ (\lambda_2)^2 - 1 \right] \left( \frac{H_1}{R} \right)} \right] \cdot \tanh \left[ \lambda_2 \left( \frac{H_1}{R} \right) \right] \cdot m_1 \quad \text{Third mode convective mass}$$

$$m_{c2} = 147.06 \frac{\text{lb}\cdot\text{sec}^2}{\text{in}}$$

$$m_i := m_1 - (m_{c0} + m_{c1} + m_{c2}) \quad \text{Impulsive mass} \quad \text{Eqn. 4.33 BNL 1995}$$

$$m_i = 2.23 \times 10^4 \frac{\text{lb}\cdot\text{sec}^2}{\text{in}}$$

**RPP-RPT-28963, Rev. 1**  
**M&D-2008-005-RPT-01, Rev. 1**

Prepared by: F. G. Abatt  
M&D Professional Services  
8/31/05  
Rev. 2

Theoretical Fluid Response for  
Simplified AY Flexible Wall Tank at  
422 in. Waste Level

Checked by: B.G. Carpenter  
M&D Professional Services  
2/1/06

$$F_{\max} := m_i \cdot SA_i + m_{c0} \cdot SA_{c0} + m_{c1} \cdot SA_{c1} + m_{c2} \cdot SA_{c2} \quad \text{Eqn. 4.31 BNL 1995}$$

$$F_{\max} = 8.04 \times 10^6 \text{ lbf} \quad \text{Conservative estimate of maximum hydrodynamic force}$$

The above expression is a conservative estimate because it assumes that the peak impulsive and convective forces occur simultaneously. A less conservative estimate can be made via a square-root-sum-of-the-squares (SRSS) combination.

$$F_{\text{SRSS}} := \sqrt{(m_i \cdot SA_i)^2 + (m_{c0} \cdot SA_{c0})^2 + (m_{c1} \cdot SA_{c1})^2 + (m_{c2} \cdot SA_{c2})^2} \quad \text{Eqn. 4.31 BNL 1995 - SRSS}$$

$$F_{\text{SRSS}} = 7.56 \times 10^6 \text{ lbf} \quad \text{SRSS estimate of peak hydrodynamic force}$$

$$F_{\text{con}} := \sqrt{(m_{c0} \cdot SA_{c0})^2 + (m_{c1} \cdot SA_{c1})^2 + (m_{c2} \cdot SA_{c2})^2}$$

$$F_{\text{con}} = 4.62 \times 10^5 \text{ lbf} \quad \text{Peak hydrodynamic force due to convective effects only}$$

Consider Vertical Excitation:

Calculate the axisymmetric breathing mode frequency for the tank

$$C_{\text{vref}} := 0.088 \quad \text{Table 4.17 BNL 1995}$$

$$C_v := C_{\text{vref}} \cdot \sqrt{127 \cdot \frac{\left(\frac{t_{\text{tw}}}{R}\right)}{\left(\frac{\rho_l}{\rho_t}\right)}} \quad C_v = 0.081$$

$$f_v := \frac{1}{2 \cdot \pi} \cdot \frac{C_v}{H_1} \cdot \sqrt{\frac{E_t}{\rho_t}} \quad f_v = 6.07 \text{ Hz} \quad \text{Eqn. 4.53 BNL 1995}$$

$$S_{\text{Av}} := 0.53 \cdot g \quad S_{\text{Av}} = 204.79 \frac{\text{in}}{\text{sec}^2} \quad \text{Vert. Haunch 4 \% RS from Spectr - see Figure 2-19 of main report.}$$

The maximum dynamic wall pressure as a function of the dimensionless vertical distance is given by

$$P_{\max}(\eta_1) := (0.8) \cdot \left( \cos\left(\frac{\pi}{2} \cdot \eta_1\right) \right) \cdot (\rho_l \cdot H_1 \cdot S_{\text{Av}}) \quad \text{Eqn. 4.52 BNL 1995}$$

RPP-RPT-28963, Rev. 1  
M&D-2008-005-RPT-01, Rev. 1

Prepared by: F. G. Abatt  
M&D Professional Services  
8/31/05  
Rev. 2

Theoretical Fluid Response for  
Simplified AY Flexible Wall Tank at  
422 in. Waste Level

Checked by: B.G. Carpenter  
M&D Professional Services  
2/1/06

	0	
	0	10.98
	1	10.8
	2	10.44
	3	9.89
	4	9.18
$P_{\max v}(\eta_1) =$	5	8.3
	6	7.28
	7	6.14
	8	4.89
	9	3.56
	10	2.16
	11	0.72

$\frac{\text{lb}}{\text{in}^2}$

$$c_{\text{oprimeouter}} := 0.28 \quad c_{\text{oprimecenter}} := 0.54 \quad \text{Estimated from Figure 4.7 BNL 1995}$$

$$c_{\text{vprimeouter}} := 0.72 \quad c_{\text{vprimecenter}} := 0.46$$

$$PGA_{\text{vert}} := 0.12 \cdot g \quad \text{Figure 2-16 of main report.}$$

The maximum base pressures at the outer and center elements are given by

$$P_{\text{maxbasevertouter}} := c_{\text{oprimeouter}} \cdot \rho_1 \cdot H_1 \cdot PGA_{\text{vert}} + c_{\text{vprimeouter}} \cdot (\rho_1 \cdot H_1) \cdot S_{Av} \quad \text{Eqn. 4.55 BNL 1995}$$

$$P_{\text{maxbasevertcenter}} := c_{\text{oprimecenter}} \cdot \rho_1 \cdot H_1 \cdot PGA_{\text{vert}} + c_{\text{vprimecenter}} \cdot (\rho_1 \cdot H_1) \cdot S_{Av}$$

$$P_{\text{maxbasevertouter}} = 10.76 \frac{\text{lb}}{\text{in}^2}$$

$$P_{\text{maxbasevertcenter}} = 8 \frac{\text{lb}}{\text{in}^2}$$

Determine the maximum vertical force on the base

$$m_0 := 0.402 \cdot m_1 \quad \text{Component of waste mass participating in the motion of the tank base}$$

$$m_v := 0.598 \cdot m_1 \quad \text{Component of waste mass participating in the motion of the tank wall}$$

BNL Table 4.17

RPP-RPT-28963, Rev. 1  
M&D-2008-005-RPT-01, Rev. 1

Prepared by: F. G. Abatt  
M&D Professional Services  
8/31/05  
Rev. 2

Theoretical Fluid Response for  
Simplified AY Flexible Wall Tank at  
422 in. Waste Level

Checked by: B.G. Carpenter  
M&D Professional Services  
2/1/06

$$F_{\text{maxbasevert}} := \sqrt{(m_0 \cdot PGA_{\text{vert}})^2 + (m_v \cdot S_{Av})^2}$$

Eqn. 4.57 BNL 1995 modified for  
maximum response per p. 4-34

$$F_{\text{maxbasevert}} = 5.24 \times 10^6 \text{ lbf}$$

$$m_0 = 1.7 \times 10^4 \text{ lbf} \cdot \frac{\text{sec}^2}{\text{in}}$$

$$m_v = 2.53 \times 10^4 \text{ lbf} \cdot \frac{\text{sec}^2}{\text{in}}$$

Reference:

BNL 1995, *Seismic Design and Evaluation Guidelines for the Department of Energy High-Level Waste Storage Tanks and Appurtenances*, BNL 52361, Rev. 10/95, Brookhaven National Laboratory, Upton, New York.

Intentionally left blank.

**RPP-RPT-28963, Rev. 1**  
**M&D-2008-005-RPT-01, Rev. 1**

Prepared by: F. G. Abatt  
M&D Professional Services  
10/05/05  
Rev. 2 *FA*

Theoretical Fluid Response for  
Simplified AY Flexible Wall Tank at  
460 in. Waste Level - Dytran  
Configuration

Checked by: B.G. Carpenter  
M&D Professional Services  
2/1/06  
*BGC*

$H_1 := 460 \cdot \text{in}$       Baseline waste level

$H_t := 460 \cdot \text{in}$       Height to primary tank tangent line

$\frac{H_1}{H_t} = 1$       Ratio of waste height to tank height

$$g_w = 386.4 \cdot \frac{\text{in}}{\text{sec}^2}$$

$R := 450 \cdot \text{in}$       Tank radius

$\frac{H_1}{R} = 1.02$       Ratio of waste height to tank radius

$i := 0..2$

$\lambda := \begin{pmatrix} 1.841 \\ 5.331 \\ 8.536 \end{pmatrix}$       Bessel function roots

$\theta := \begin{pmatrix} 0 \cdot \text{deg} \\ 45 \cdot \text{deg} \\ 90 \cdot \text{deg} \end{pmatrix}$       Circumferential location of waste elements for which pressures are reported

**Convective Frequencies**

$$f_{\text{con}_i} := \frac{1}{2 \cdot \pi} \cdot \sqrt{\left[ \lambda_i \cdot \frac{g_w}{R} \cdot \tanh \left[ \lambda_i \cdot \left( \frac{H_1}{R} \right) \right] \right]} \quad \text{Eqn. 4.14 BNL 1995}$$

$f_{\text{con}} = \begin{pmatrix} 0.2 \\ 0.34 \\ 0.43 \end{pmatrix} \text{ Hz}$       First three convective frequencies

$\rho_1 := 1.71 \cdot 10^{-4} \cdot \frac{\text{lb} \cdot \text{sec}^2}{\text{in}^4}$       waste density - specific gravity = 1.83

RPP-RPT-28963, Rev. 1  
M&D-2008-005-RPT-01, Rev. 1

Prepared by: F. G. Abatt  
M&D Professional Services  
10/05/05  
Rev. 2

Theoretical Fluid Response for  
Simplified AY Flexible Wall Tank at  
460 in. Waste Level - Dytran  
Configuration

Checked by: B.G. Carpenter  
M&D Professional Services  
2/1/06

Calculation of Impulsive Frequency:

$$\rho_t := 7.35 \cdot 10^{-4} \frac{\text{lb} \cdot \text{sec}^2}{\text{in}^4} \quad \text{Steel density}$$

$$t_{tw} := 0.65 \cdot \text{in} \quad \text{Average thickness of AY over lower 2/3.}$$

$$E_t := 29 \cdot 10^6 \frac{\text{lb} \cdot \text{f}}{\text{in}^2} \quad \text{Elastic modulus for steel}$$

$$C_{iref} := 0.1062 \quad \text{Table 4.4 of BNL 1995}$$

$$C_i := C_{iref} \cdot \sqrt{127 \cdot \left( \frac{t_{tw}}{R} \right) \left( \frac{\rho_l}{\rho_t} \right)} \quad \text{Eqn. 4.18 BNL 1995}$$

$$C_i = 0.09 \quad \text{Impulsive coefficient for frequency calculation}$$

$$f_i := \frac{1}{2 \cdot \pi} \cdot \frac{C_i}{H_l} \cdot \sqrt{\frac{E_t}{\rho_t}} \quad f_i = 6.48 \text{ Hz} \quad \text{Eqn. 4.16 BNL 1995}$$

Determine Convective Pressures on the Tank Wall:

$$z := \begin{pmatrix} 15.1 \cdot \text{in} \\ 50.5 \cdot \text{in} \\ 85.8 \cdot \text{in} \\ 121.2 \cdot \text{in} \\ 156.6 \cdot \text{in} \\ 192 \cdot \text{in} \\ 227.4 \cdot \text{in} \\ 262.8 \cdot \text{in} \\ 298.2 \cdot \text{in} \\ 333.5 \cdot \text{in} \\ 368.9 \cdot \text{in} \\ 404.3 \cdot \text{in} \\ 441 \cdot \text{in} \end{pmatrix} \quad \text{Vertical location of Euler element centroids at which pressures are reported.}$$

RPP-RPT-28963, Rev. 1  
M&D-2008-005-RPT-01, Rev. 1

Prepared by: F. G. Abatt  
M&D Professional Services  
10/05/05  
Rev. 2

Theoretical Fluid Response for  
Simplified AY Flexible Wall Tank at  
460 in. Waste Level - Dytran  
Configuration

Checked by: B.G. Carpenter  
M&D Professional Services  
2/1/06

$$\eta_1 := \frac{z}{H_1}$$

Ratio of tank wall vertical location to waste height for waste element centroids.

	0
0	0.03
1	0.11
2	0.19
3	0.26
4	0.34
5	0.42
6	0.49
7	0.57
8	0.65
9	0.73
10	0.8
11	0.88
12	0.96

Determine convective coefficients as a function of dimensionless height per BNL 1995 Eqn. 4.4

$$\text{con}_0(\eta_1) := \left[ \frac{2 \cosh \left[ \lambda_0 \left( \frac{H_1}{R} \right) \eta_1 \right]}{\left( \lambda_0 \right)^2 - 1 \cosh \left[ \lambda_0 \left( \frac{H_1}{R} \right) \right]} \right]$$

$$\text{con}_1(\eta_1) := \left[ \frac{2 \cosh \left[ \lambda_1 \left( \frac{H_1}{R} \right) \eta_1 \right]}{\left( \lambda_1 \right)^2 - 1 \cosh \left[ \lambda_1 \left( \frac{H_1}{R} \right) \right]} \right]$$

$$\text{con}_2(\eta_1) := \left[ \frac{2 \cosh \left[ \lambda_2 \left( \frac{H_1}{R} \right) \eta_1 \right]}{\left( \lambda_2 \right)^2 - 1 \cosh \left[ \lambda_2 \left( \frac{H_1}{R} \right) \right]} \right]$$

RPP-RPT-28963, Rev. 1  
M&D-2008-005-RPT-01, Rev. 1

Prepared by: F. G. Abatt  
M&D Professional Services  
10/05/05  
Rev. 2

Theoretical Fluid Response for  
Simplified AY Flexible Wall Tank at  
460 in. Waste Level - Dytran  
Configuration

Checked by: B.G. Carpenter  
M&D Professional Services  
2/1/06

$$con_0(\eta_1) =$$

	0
0	0.25
1	0.25
2	0.26
3	0.28
4	0.3
5	0.33
6	0.37
7	0.41
8	0.46
9	0.52
10	0.59
11	0.68
12	0.78

$$con_1(\eta_1) =$$

	0
0	$6.37 \cdot 10^{-4}$
1	$7.43 \cdot 10^{-4}$
2	$9.8 \cdot 10^{-4}$
3	$1.39 \cdot 10^{-3}$
4	$2.05 \cdot 10^{-3}$
5	$3.08 \cdot 10^{-3}$
6	$4.66 \cdot 10^{-3}$
7	$7.07 \cdot 10^{-3}$
8	0.01
9	0.02
10	0.02
11	0.04
12	0.06

$$con_2(\eta_1) =$$

	0
0	$9.41 \cdot 10^{-6}$
1	$1.35 \cdot 10^{-5}$
2	$2.39 \cdot 10^{-5}$
3	$4.55 \cdot 10^{-5}$
4	$8.84 \cdot 10^{-5}$
5	$1.73 \cdot 10^{-4}$
6	$3.38 \cdot 10^{-4}$
7	$6.61 \cdot 10^{-4}$
8	$1.29 \cdot 10^{-3}$
9	$2.53 \cdot 10^{-3}$
10	$4.94 \cdot 10^{-3}$
11	$9.68 \cdot 10^{-3}$
12	0.02

Impulsive pressure coefficient as a function of dimensionless wall height

$$c_i(\eta_1) := 1 - con_0(\eta_1) - con_1(\eta_1) - con_2(\eta_1)$$

Eqn. 4.7 BNL 1995

$$c_i(\eta_1) =$$

	0
0	0.75
1	0.74
2	0.73
3	0.72
4	0.7
5	0.67
6	0.63
7	0.58
8	0.53
9	0.46
10	0.38
11	0.28
12	0.14

RPP-RPT-28963, Rev. 1  
M&D-2008-005-RPT-01, Rev. 1

Prepared by: F. G. Abatt  
M&D Professional Services  
10/05/05  
Rev. 2

Theoretical Fluid Response for  
Simplified AY Flexible Wall Tank at  
460 in. Waste Level - Dytran  
Configuration

Checked by: B.G. Carpenter  
M&D Professional Services  
2/1/06

Calculate maximum values of dynamic wall pressures from spectral acceleration of dome input TH.

Consider the first three convective modes

$$SA_{c0} := 0.064 \cdot g \quad SA_{c0} = 24.73 \frac{\text{in}}{\text{sec}^2}$$

$$SA_{c1} := 0.108 \cdot g \quad SA_{c1} = 41.73 \frac{\text{in}}{\text{sec}^2}$$

0.5% Dome RS from Spectr - see Figure 2-21 of main report.

$$SA_{c2} := 0.163 \cdot g \quad SA_{c2} = 62.98 \frac{\text{in}}{\text{sec}^2}$$

Determine the spectral acceleration for the impulsive mode.

$$SA_i := 0.967 \cdot g \quad SA_i = 373.65 \frac{\text{in}}{\text{sec}^2}$$

4% Dome RS from Spectr - see Figure 2-19 of main report.

$$P_{\text{maxconv}}(\eta_1, \theta) := \left[ \sqrt{(\text{con}_0(\eta_1) \cdot SA_{c0})^2 + (\text{con}_1(\eta_1) \cdot SA_{c1})^2 + (\text{con}_2(\eta_1) \cdot SA_{c2})^2} \right] \cdot (\rho_1 \cdot R \cdot \cos(\theta \cdot \text{deg}))$$

$$P_{\text{maximpulsive}}(\eta_1, \theta) := \left[ \sqrt{[c_i(\eta_1) \cdot (SA_i)]^2} \right] \cdot (\rho_1 \cdot R \cdot \cos(\theta \cdot \text{deg}))$$

$$P_{\text{max}}(\eta_1, \theta) := \left[ \sqrt{[c_i(\eta_1) \cdot (SA_i)]^2 + (\text{con}_0(\eta_1) \cdot SA_{c0})^2 + (\text{con}_1(\eta_1) \cdot SA_{c1})^2 + (\text{con}_2(\eta_1) \cdot SA_{c2})^2} \right] \cdot (\rho_1 \cdot R \cdot \cos(\theta \cdot \text{deg}))$$

Eqn. 4.24 BNL 1995

**RPP-RPT-28963, Rev. 1**  
**M&D-2008-005-RPT-01, Rev. 1**

Prepared by: F. G. Abatt  
M&D Professional Services  
10/05/05  
Rev. 2

Theoretical Fluid Response for  
Simplified AY Flexible Wall Tank at  
460 in. Waste Level - Dytran  
Configuration

Checked by: B.G. Carpenter  
M&D Professional Services  
2/1/06

$$P_{\text{maximpulsive}}(\eta_1, 0) =$$

	0
0	21.56
1	21.41
2	21.11
3	20.65
4	20
5	19.17
6	18.11
7	16.81
8	15.21
9	13.28
10	10.9
11	7.98
12	4.17

$\frac{\text{lbf}}{\text{in}^2}$

Maximum impulsive dynamic pressures at  
theta = 0.

$$P_{\text{maxconv}}(\eta_1, 0) =$$

	0
0	0.48
1	0.48
2	0.5
3	0.53
4	0.57
5	0.63
6	0.69
7	0.78
8	0.87
9	0.99
10	1.13
11	1.29
12	1.49

$\frac{\text{lbf}}{\text{in}^2}$

Maximum convective dynamic pressures at  
theta = 0.

$$P_{\text{max}}(\eta_1, 0) =$$

	0
0	21.56
1	21.42
2	21.12
3	20.65
4	20.01
5	19.18
6	18.13
7	16.83
8	15.24
9	13.31
10	10.96
11	8.08
12	4.43

$\frac{\text{lbf}}{\text{in}^2}$

Maximum total dynamic pressure at  
theta = 0.

RPP-RPT-28963, Rev. 1  
M&D-2008-005-RPT-01, Rev. 1

Prepared by: F. G. Abatt  
M&D Professional Services  
10/05/05  
Rev. 2

Theoretical Fluid Response for  
Simplified AY Flexible Wall Tank at  
460 in. Waste Level - Dytran  
Configuration

Checked by: B.G. Carpenter  
M&D Professional Services  
2/1/06

	0
0	15.25
1	15.14
2	14.93
3	14.6
4	14.15
5	13.56
6	12.82
7	11.9
8	10.78
9	9.41
10	7.75
11	5.71
12	3.13

$p_{\max}(\eta_1, 45) =$   $\frac{\text{lbf}}{\text{in}^2}$

Maximum total dynamic pressure at  
theta = 45 degrees.

	0
0	0
1	0
2	0
3	0
4	0
5	0
6	0
7	0
8	0
9	0
10	0
11	0
12	0

$p_{\max}(\eta_1, 90) =$   $\frac{\text{lbf}}{\text{in}^2}$

Maximum total dynamic pressure at  
theta = 90 degrees.

Calculate Maximum Slosh Height:

$$\text{conmax} := \begin{pmatrix} 0.837 \\ 0.073 \\ 0.028 \end{pmatrix} \quad \text{Maximum value of convective coefficients at } \eta_1=1$$

$$h_{\max\text{slosh}} := R \cdot \sqrt{\left(\text{conmax}_0 \cdot \frac{SA_{c0}}{g}\right)^2 + \left(\text{conmax}_1 \cdot \frac{SA_{c1}}{g}\right)^2 + \left(\text{conmax}_2 \cdot \frac{SA_{c2}}{g}\right)^2} \quad \text{Eqn. 4.60 BNL 1995}$$

$$h_{\max\text{slosh}} = 24.45 \text{ in}$$

RPP-RPT-28963, Rev. 1  
M&D-2008-005-RPT-01, Rev. 1

Prepared by: F. G. Abatt  
M&D Professional Services  
10/05/05  
Rev. 2

Theoretical Fluid Response for  
Simplified AY Flexible Wall Tank at  
460 in. Waste Level - Dytran  
Configuration

Checked by: B.G. Carpenter  
M&D Professional Services  
2/1/06

Calculate Maximum Total Hydrodynamic Force:

The maximum hydrodynamic force induced on the tank wall is given by Eqn. 4.31 of BNL 1995 with the instantaneous accelerations replaced by the maximum spectral accelerations. First determine the effective impulsive and convective masses.

$$m_{l\text{approx}} := \pi \cdot R^2 \cdot H_1 \cdot \rho_l \quad m_{l\text{approx}} = 5 \times 10^4 \frac{\text{lb} \cdot \text{sec}^2}{\text{in}} \quad \text{Total waste mass base on circular cylinder approximation.}$$

$$m_l := 4.95 \times 10^4 \frac{\text{lb} \cdot \text{sec}^2}{\text{in}} \quad \text{Actual waste mass reported by Dytran model.}$$

$$m_{c0} := \left[ \frac{2}{\lambda_0 \cdot \left[ (\lambda_0)^2 - 1 \right] \cdot \left( \frac{H_1}{R} \right)} \right] \cdot \tanh \left[ \lambda_0 \cdot \left( \frac{H_1}{R} \right) \right] \cdot m_l \quad \text{First mode convective mass - Eqn. 4.32 BNL 1995}$$

$$m_{c0} = 2.1 \times 10^4 \frac{\text{lb} \cdot \text{sec}^2}{\text{in}}$$

$$m_{c1} := \left[ \frac{2}{\lambda_1 \cdot \left[ (\lambda_1)^2 - 1 \right] \cdot \left( \frac{H_1}{R} \right)} \right] \cdot \tanh \left[ \lambda_1 \cdot \left( \frac{H_1}{R} \right) \right] \cdot m_l \quad \text{Second mode convective mass}$$

$$m_{c1} = 662.53 \frac{\text{lb} \cdot \text{sec}^2}{\text{in}}$$

$$m_{c2} := \left[ \frac{2}{\lambda_2 \cdot \left[ (\lambda_2)^2 - 1 \right] \cdot \left( \frac{H_1}{R} \right)} \right] \cdot \tanh \left[ \lambda_2 \cdot \left( \frac{H_1}{R} \right) \right] \cdot m_l \quad \text{Third mode convective mass}$$

$$m_{c2} = 157.88 \frac{\text{lb} \cdot \text{sec}^2}{\text{in}}$$

$$m_i := m_l - (m_{c0} + m_{c1} + m_{c2}) \quad \text{Impulsive mass - Eqn. 4.33 BNL 1995}$$

$$m_i = 2.77 \times 10^4 \frac{\text{lb} \cdot \text{sec}^2}{\text{in}}$$

**RPP-RPT-28963, Rev. 1**  
**M&D-2008-005-RPT-01, Rev. 1**

Prepared by: F. G. Abatt  
M&D Professional Services  
10/05/05  
Rev. 2

Theoretical Fluid Response for  
Simplified AY Flexible Wall Tank at  
460 in. Waste Level - Dytran  
Configuration

Checked by: B.G. Carpenter  
M&D Professional Services  
2/1/06

$$F_{\max} := m_i \cdot SA_i + m_{c0} \cdot SA_{c0} + m_{c1} \cdot SA_{c1} + m_{c2} \cdot SA_{c2} \quad \text{Eqn. 4.31 BNL 1995}$$

$$F_{\max} = 1.09 \times 10^7 \text{ lbf} \quad \text{Conservative estimate of maximum hydrodynamic force}$$

The above expression is a conservative estimate because it assumes that the peak impulsive and convective forces occur simultaneously. A less conservative estimate can be made via a square-root-sum-of-the-squares (SRSS) combination.

$$F_{\text{SRSS}} := \sqrt{(m_i \cdot SA_i)^2 + (m_{c0} \cdot SA_{c0})^2 + (m_{c1} \cdot SA_{c1})^2 + (m_{c2} \cdot SA_{c2})^2} \quad \text{Eqn. 4.31 BNL 1995 - SRSS}$$

$$F_{\text{SRSS}} = 1.03 \times 10^7 \text{ lbf} \quad \text{SRSS estimate of peak hydrodynamic force}$$

$$F_{\text{con}} := \sqrt{(m_{c0} \cdot SA_{c0})^2 + (m_{c1} \cdot SA_{c1})^2 + (m_{c2} \cdot SA_{c2})^2}$$

$$F_{\text{con}} = 5.21 \times 10^5 \text{ lbf} \quad \text{Peak hydrodynamic force due to convective effects only}$$

**Consider Vertical Excitation:**

Calculate the axisymmetric breathing mode frequency for the tank

$$C_{\text{vref}} := 0.089 \quad \text{Table 4.17 BNL 1995}$$

$$C_v := C_{\text{vref}} \sqrt{127 \cdot \frac{\left(\frac{t_{\text{tw}}}{R}\right)}{\left(\frac{\rho_l}{\rho_t}\right)}} \quad C_v = 0.079 \quad \text{Eqn. 4.16 BNL 1995}$$

$$f_v := \frac{1}{2 \cdot \pi} \cdot \frac{C_v}{H_1} \cdot \sqrt{\frac{E_t}{\rho_t}} \quad f_v = 5.43 \text{ Hz} \quad \text{Eqn. 4.53 BNL 1995}$$

$$S_{\text{Av}} := 0.38 \cdot g \quad S_{\text{Av}} = 146.83 \frac{\text{in}}{\text{sec}^2} \quad \text{Vert. Haunch 4 \% RS from Spectr - see Figure 2-19 of main report.}$$

The maximum dynamic wall pressure as a function of the dimensionless vertical distance is given by

$$P_{\text{maxv}}(\eta_1) := (0.8) \cdot \left( \cos\left(\frac{\pi}{2} \cdot \eta_1\right) \right) \cdot (\rho_l \cdot H_1 \cdot S_{\text{Av}}) \quad \text{Eqn. 4.52 BNL 1995}$$

RPP-RPT-28963, Rev. 1  
M&D-2008-005-RPT-01, Rev. 1

Prepared by: F. G. Abatt  
M&D Professional Services  
10/05/05  
Rev. 2

Theoretical Fluid Response for  
Simplified AY Flexible Wall Tank at  
460 in. Waste Level - Dytran  
Configuration

Checked by: B.G. Carpenter  
M&D Professional Services  
2/1/06

	0	
0	9.23	
1	9.1	
2	8.85	
3	8.46	
4	7.95	
5	7.32	$\frac{\text{lb}}{\text{in}^2}$
6	6.59	
7	5.76	
8	4.85	
9	3.87	
10	2.83	
11	1.75	
12	0.6	

$c_{\text{oprimeouter}} := 0.28$        $c_{\text{oprimecenter}} := 0.54$       Estimated from Figure 4.7 BNL 1995

$c_{\text{vprimeouter}} := 0.72$        $c_{\text{vprimecenter}} := 0.46$

$PGA_{\text{vert}} := 0.12 \cdot g$       Figure 2-16 of main report

The maximum base pressures at the outer and center elements are given by

$P_{\text{maxbasevertouter}} := c_{\text{oprimeouter}} \rho_1 H_1 PGA_{\text{vert}} + c_{\text{vprimeouter}} (\rho_1 H_1) S_{Av}$       Eqn. 4.55 BNL 1995

$P_{\text{maxbasevertcenter}} := c_{\text{oprimecenter}} \rho_1 H_1 PGA_{\text{vert}} + c_{\text{vprimecenter}} (\rho_1 H_1) S_{Av}$

$P_{\text{maxbasevertouter}} = 9.34 \frac{\text{lb}}{\text{in}^2}$

$P_{\text{maxbasevertcenter}} = 7.28 \frac{\text{lb}}{\text{in}^2}$

Determine the maximum vertical force on the base

$m_0 := 0.388 \cdot m_1$       Component of waste mass participating in the motion of the tank base

$m_v := 0.612 \cdot m_1$       Component of waste mass participating in the motion of the tank wall

BNL Table 4.17

RPP-RPT-28963, Rev. 1  
M&D-2008-005-RPT-01, Rev. 1

Prepared by: F. G. Abatt  
M&D Professional Services  
10/05/05  
Rev. 2

Theoretical Fluid Response for  
Simplified AY Flexible Wall Tank at  
460 in. Waste Level - Dytran  
Configuration

Checked by: B.G. Carpenter  
M&D Professional Services  
2/1/06

$$F_{\text{maxbasevert}} := \sqrt{(m_0 \cdot \text{PGA}_{\text{vert}})^2 + (m_v \cdot S_{Av})^2}$$

Eqn. 4.57 BNL 1995 modified for  
maximum response per p. 4-34

$$F_{\text{maxbasevert}} = 4.54 \times 10^6 \text{ lbf}$$

$$m_0 = 1.92 \times 10^4 \text{ lbf} \cdot \frac{\text{sec}^2}{\text{in}}$$

$$m_v = 3.03 \times 10^4 \text{ lbf} \cdot \frac{\text{sec}^2}{\text{in}}$$

Reference:

BNL 1995, *Seismic Design and Evaluation Guidelines for the Department of Energy High-Level Waste Storage Tanks and Appurtenances*, BNL 52361, Rev. 10/95, Brookhaven National Laboratory, Upton, New York.

Intentionally left blank.

## **Appendix C**

### **Reanalysis of the Rigid and Flexible Wall Tanks at the 460-Inch Initial Liquid Level with Increased Mesh Refinement**

RPP-RPT-28963, Rev. 1  
M&D-2008-005-RPT-01, Rev. 1

Intentionally left blank.

## Appendix C

### Reanalysis of the Rigid and Flexible Wall Tanks at the 460-Inch Initial Liquid Level with Increased Mesh Refinement

#### Figures

C-1	Comparison of Maximum and Minimum Pressures for Original and Refined Rigid Tank Models at $\theta=0^\circ$ .....	C.9
C-2	Comparison of Maximum and Minimum Pressures for Original and Refined Flexible Wall Tank Models at $\theta=0^\circ$ .....	C.10
C-3	Plot of Rigid Tank and Waste at 460-Inch Waste Level .....	C.13
C-4	Top View of Rigid Tank Model Showing the Angular Locations of Fluid Elements at Which Pressures Were Monitored.....	C.13
C-5	Elevation View of Rigid Tank Model Showing the Locations of “plusx_els”, “cent_press”, and “minusx_els” Fluid Elements Sets at Which Pressures Were Monitored .....	C.14
C-6	Waste Element Numbering for Element Sets “Plusx_els”, “Minusx_els”, and Cent_press” for Rigid Tank Model .....	C.14
C-7	Elevation View of Rigid Tank Model Showing the Locations of “press_45” and “plusz_els” Fluid Elements Sets at Which Pressures Were Monitored .....	C.15
C-8	Waste Element Numbering for Element Sets “press_45” and “plusz_els” for Rigid Tank Model .....	C.15
C-9	Plot of Primary Tank and Base for Flexible Tank Model .....	C.16
C-10	Plot of Flexible Tank and Waste at 460-Inch Waste Level.....	C.17
C-11	Elevation View of Model Showing the Locations of “plusx_els”, “cent_press”, and “minusx_els” Fluid Elements Sets at Which Pressures Were Monitored .....	C.17
C-12	Waste Element Numbering for Element Sets “Plusx_els”, “Minusx_els”, and Cent_press” for Flexible Tank Model .....	C.18
C-13	Elevation View of Flexible Tank Model Showing the Locations of “press_45” and “plusz_els” Fluid Elements Sets at Which Pressures Were Monitored .....	C.18
C-14	Waste Element Numbering for Element Sets “press_45” and plusz_els” for Flexible Tank Model .....	C.19
C-15	Shell Element Numbering for Tank Wall Stress Results at $\theta=0^\circ$ and $\theta=90^\circ$ for Flexible Tank Model .....	C.19
C-16	Shell Element Numbering for Tank Wall Stress Results at $\theta=45^\circ$ and $\theta=180^\circ$ for Flexible Tank .....	C.20
C-17	Comparison of Horizontal Response Spectra at 0.1% and 0.5% Damping for Low Frequencies .....	C.21

RPP-RPT-28963, Rev. 1  
M&D-2008-005-RPT-01, Rev. 1

C-18	Horizontal Spectral Comparison Showing Damping Values and Frequency Range for Impulsive Mode.....	C.21
C-19	Horizontal Coupling Surface Reaction Force for Rigid Tank at 460-Inch Waste Level Under Horizontal Seismic Excitation – Refined Mesh.....	C.25
C-20	Horizontal Coupling Surface Reaction Force for Rigid Tank at 460-Inch Waste Level Under Horizontal Seismic Excitation – Convective Response With Refined Mesh.....	C.25
C-21	Waste Pressure Time Histories for the Rigid Tank with 460 Inches of Liquid Under Horizontal Excitation at $\theta=0$ with Refined Mesh.....	C.29
C-22	Selected Liquid Pressure Time Histories for the Rigid Tank at 460 Inches of Liquid Under Horizontal Excitation at $\theta=0^\circ$ with Refined Mesh.....	C.29
C-23	Waste Pressure Time Histories for the Rigid Tank with 460 Inches of Liquid Under Horizontal Excitation at $\theta=0^\circ$ with Refined Mesh Using a 66-Hz Lowpass Filter.....	C.30
C-24	Maximum and Minimum Liquid Pressures for the Rigid Tank vs. Normalized Height from Tank Bottom for Horizontal Excitation at $\theta=0^\circ$ , Initial Liquid Height of 460 Inches, and Refined Mesh.....	C.30
C-25	Maximum and Minimum Liquid Pressures for the Rigid Tank Using a 66-Hz Lowpass Filter vs. Normalized Height from Tank Bottom for Horizontal Excitation at $\theta=0^\circ$ , Initial Liquid Height of 460 Inches, and Refined Mesh.....	C.31
C-26	Waste Pressure Time Histories for the Rigid Tank with 460 Inches of Liquid Under Horizontal Excitation at $\theta=45^\circ$ with Refined Mesh.....	C.32
C-27	Waste Pressure Time Histories for the Rigid Tank with 460 Inches of Liquid Under Horizontal Excitation at $\theta=45^\circ$ with Refined Mesh Using a 66-Hz Lowpass Filter.....	C.32
C-28	Maximum and Minimum Liquid Pressures vs. Normalized Height from Tank Bottom for Horizontal Excitation at $\theta=45^\circ$ , Initial Liquid Height of 460 Inches, and Refined Mesh.....	C.33
C-29	Maximum and Minimum Liquid Pressures Using 66-Hz Lowpass Filter vs. Normalized Height from Tank Bottom for Horizontal Excitation at $\theta=45^\circ$ , Initial Liquid Height of 460 Inches, and Refined Mesh.....	C.33
C-30	Waste Pressure Time Histories for the Rigid Tank with 460 Inches of Liquid Under Horizontal Excitation at $\theta=90^\circ$ with Refined Mesh.....	C.34
C-31	Waste Pressure Time Histories for the Rigid Tank with 460 Inches of Liquid Under Horizontal Excitation at $\theta=90^\circ$ with Refined Mesh Using a 66-Hz Lowpass Filter.....	C.35
C-32	Maximum and Minimum Liquid Pressures vs. Normalized Height from Tank Bottom for Horizontal Excitation at $\theta=90^\circ$ , Initial Liquid Height of 460 Inches, and Refined Mesh.....	C.35
C-33	Maximum and Minimum Liquid Pressures Using 66-Hz Lowpass Filter vs. Normalized Height from Tank Bottom for Horizontal Excitation at $\theta=90^\circ$ , Initial Liquid Height of 460 Inches, and Refined Mesh.....	C.36
C-34	Maximum Slosh Height Comparison for Initial Liquid Height of 460 Inches.....	C.37
C-35	Horizontal and Vertical Coupling Surface Reaction Forces for Flexible Tank at 460-Inch Waste Level Under Horizontal Seismic Excitation – Refined Mesh.....	C.39
C-36	Vertical Coupling Surface Reaction Force During Initial Gravity Loading.....	C.40
C-37	Horizontal Coupling Surface Reaction Force Immediately Following Cessation of Seismic Excitation – Impulsive Response.....	C.40

RPP-RPT-28963, Rev. 1  
M&D-2008-005-RPT-01, Rev. 1

C-38	Horizontal Reaction Force Immediately Following Cessation of Seismic Excitation – Decay of Impulsive Response .....	C.41
C-39	Horizontal Coupling Surface Reaction Force for Rigid Tank at 460-Inch Waste Level Under Horizontal Seismic Excitation – Convective Response During Unforced Oscillation .....	C.41
C-40	Liquid Pressure Time Histories for the Flexible Wall Tank with 460 Inches of Liquid Under Horizontal Excitation at $\theta=0^\circ$ with Refined Mesh .....	C.44
C-41	Selected Liquid Pressure Time Histories for the Flexible Wall Tank with 460 Inches of Liquid Under Horizontal Excitation at $\theta=0^\circ$ with Refined Mesh .....	C.45
C-42	Waste Pressure Time Histories for the Flexible Wall Tank with 460 Inches of Liquid Under Horizontal Excitation at $\theta=0^\circ$ with Refined Mesh Using a 66-Hz Lowpass Filter .....	C.45
C-43	Maximum and Minimum Liquid Pressures vs. Normalized Height from Tank Bottom for Horizontal Excitation at $\theta=0^\circ$ , Initial Liquid Height of 460 Inches, and Refined Mesh .....	C.46
C-44	Maximum and Minimum Liquid Pressures for the Flexible Wall Tank Using a 66-Hz Lowpass Filter vs. Normalized Height from Tank Bottom for Horizontal Excitation at $\theta=0^\circ$ , Initial Liquid Height of 460 Inches, and Refined Mesh .....	C.46
C-45	Liquid Pressure Time Histories for the Flexible Wall Tank with 460 Inches of Liquid Under Horizontal Excitation at $\theta=45^\circ$ with Refined Mesh .....	C.47
C-46	Waste Pressure Time Histories for the Flexible Wall Tank with 460 Inches of Liquid Under Horizontal Excitation at $\theta=45^\circ$ with Refined Mesh Using a 66-Hz Lowpass Filter .....	C.48
C-47	Maximum and Minimum Liquid Pressures vs. Normalized Height from Tank Bottom for Horizontal Excitation at $\theta=45^\circ$ , Initial Liquid Height of 460 Inches, and Refined Mesh .....	C.48
C-48	Maximum and Minimum Liquid Pressures for the Flexible Wall Tank Using a 66-Hz Lowpass Filter vs. Normalized Height from Tank Bottom for Horizontal Excitation at $\theta=45^\circ$ , Initial Liquid Height of 460 Inches, and Refined Mesh .....	C.49
C-49	Liquid Pressure Time Histories for the Flexible Wall Tank with 460 Inches of Liquid Under Horizontal Excitation at $\theta=90^\circ$ with Refined Mesh .....	C.50
C-50	Waste Pressure Time Histories for the Flexible Wall Tank with 460 Inches of Liquid Under Horizontal Excitation at $\theta=90^\circ$ with Refined Mesh Using a 66-Hz Lowpass Filter .....	C.50
C-51	Maximum and Minimum Liquid Pressures vs. Normalized Height from Tank Bottom for Horizontal Excitation at $\theta=90^\circ$ , Initial Liquid Height of 460 Inches, and Refined Mesh .....	C.51
C-52	Maximum and Minimum Liquid Pressures for the Flexible Wall Tank Using a 66-Hz Lowpass Filter vs. Normalized Height from Tank Bottom for Horizontal Excitation at $\theta=90^\circ$ , Initial Liquid Height of 460 Inches, and Refined Mesh .....	C.51
C-53	Liquid Pressure Time Histories for the Flexible Wall Tank with 460 Inches of Liquid Under Horizontal Excitation at $\theta=180^\circ$ with Refined Mesh .....	C.52
C-54	Waste Pressure Time Histories for the Flexible Wall Tank with 460 Inches of Liquid Under Horizontal Excitation at $\theta=180^\circ$ with Refined Mesh Using a 66-Hz Lowpass Filter .....	C.53

C-55	Maximum and Minimum Liquid Pressures vs. Normalized Height from Tank Bottom for Horizontal Excitation at $\theta=180^\circ$ , Initial Liquid Height of 460 Inches, and Refined Mesh.....	C.53
C-56	Maximum and Minimum Liquid Pressures for the Flexible Wall Tank Using a 66-Hz Lowpass Filter vs. Normalized Height from Tank Bottom for Horizontal Excitation at $\theta=180^\circ$ , Initial Liquid Height of 460 Inches, and Refined Mesh .....	C.54
C-57	Maximum Slosh Height Comparison for Rigid and Flexible Wall Domed Tanks at the 460-Inch Initial Liquid Level .....	C.55
C-58	Mid-Plane Hoop Stress for Flexible Wall Tank at 460-Inch Liquid Level and $\theta=0^\circ$ Extracted at 10-millisecond Intervals.....	C.56
C-59	Mid-Plane Hoop Stress for Flexible Wall Tank at 460-Inch Liquid Level and $\theta=0^\circ$ Extracted at 1-millisecond Intervals.....	C.56
C-60	Comparison of Liquid Pressure and Mid-Plane Hoop Stress in Flexible Wall Tank at 460-Inch Liquid Level at Mid-Height in the Wall and $\theta=0^\circ$ with Data Extracted Every 10 milliseconds .....	C.57
C-61	Mid-Plane Hoop Stress for Flexible Wall Tank at 460-Inch Liquid Level and $\theta=45^\circ$ Extracted at 10-millisecond Intervals.....	C.57
C-62	Mid-Plane Hoop Stress for Flexible Wall Tank at 460-Inch Liquid Level and $\theta=90^\circ$ Extracted at 10-millisecond Intervals.....	C.58
C-63	Mid-Plane Hoop Stress for Flexible Wall Tank at 460-Inch Liquid Level and $\theta=90^\circ$ Extracted at 50-millisecond Intervals.....	C.58

## Tables

C-1	Summary of Convective, Impulsive, and Breathing Mode Frequencies for Refined Models.....	C.8
C-2	Summary of Peak Horizontal Reaction Forces for Refined Models .....	C.8
C-3	Comparison of Frequencies and Slosh Heights for Original and Refined Models .....	C.9
C-4	Comparison of Peak Reaction Forces Between Original and Refined Models.....	C.9
C-5	Theoretical Hydrostatic Pressure of Liquid Elements in Rigid Tank for Initial Liquid Level of 460 Inches .....	C.22
C-6	Theoretical Hydrostatic Pressure of Liquid Elements in Flexible Tank for Initial Liquid Level of 460 Inches .....	C.23
C-7	Estimated Maximum Wall Pressures for Horizontal Excitation in Rigid Open and Equivalent Flat-Top Tanks at 460-Inch Waste Level for Elements at $\theta=0^\circ$ .....	C.27
C-8	Estimated Maximum Wall Pressures for Horizontal Excitation in Rigid Open and Equivalent Flat-Top Tanks at 460-Inch Waste Level for Elements at $\theta=45^\circ$ .....	C.28
C-9	Estimated Maximum Wall Pressures for Horizontal Excitation in Flexible Open and Equivalent Flat-Top Tanks at 460-Inch Waste Level for Elements at $\theta=0$ .....	C.42
C-10	Estimated Maximum Wall Pressures for Horizontal Excitation in Flexible Open and Equivalent Flat-Top Tanks at 460-Inch Waste Level for Elements at $\theta=45^\circ$ .....	C.43

## C.1 Introduction

This work was performed in support of a project entitled *Double-Shell Tank (DST) Integrity Project – DST Thermal and Seismic Analysis*. The analysis is directly related to work reported in Rinker and Abatt (2006) and Rinker et al. (2006) and was motivated by recommendations from a Project Review held on March 20–21, 2006 (Deibler et al. 2007, Appendix E).

Due to uncertainties in the solutions for domed tanks with an initial liquid level of 460 inches that were presented in Rinker and Abatt (2006), the reviewers recommended that the effects of liquid-roof interaction be further studied. Two of the specific recommendations made in Deibler et al. (2007, Appendix E) are shown below.

1. Solutions should be obtained for a flexible tank with a rigid, horizontal roof located at different distances above the liquid surface.
2. These solutions, along with those for the tank with the spherical dome, should be compared with the predictions of the simple, approximate procedures described in Appendix D in BNL (1995) and in Malhotra (2005).

The first recommendation is addressed in Abatt and Rinker (2008). The purpose of this study is to address the second recommendation. Revision 0 of this report documented the response of both of these configurations, but this new revision improves on that analysis with more refined models and removes the uncertainties present in the original analysis.

The uncertainty in the original models was due to unexpected behavior in the height of the liquid-free surface under gravity loading. Specifically, maximum waste-free surface heights of nearly 10 inches were recorded during the initial gravity loading of the structure before seismic excitation commenced. Investigation of the deformed shape of the waste showed that the initial change in the waste-free surface height under gravity loading was due an axisymmetric increase in the waste-free surface near the tank boundary that had the appearance of a meniscus. This effect was attributed to either a limitation of the post-processing routine used to calculate the maximum waste-free surface height, or else a limitation caused by lack of sufficient resolution in the model discretization. The uncertainty was resolved by increasing the mesh refinement in the models as described in this appendix.

The mesh refinement was increased for both the rigid and flexible wall models. Both models were subjected to horizontal seismic excitation, and the results of the Dytran<sup>®1</sup> simulations were compared with exact theoretical solutions or approximate solutions appearing in BNL (1995) and Malhotra (2005). The response parameters that are evaluated in this study are the total hydrodynamic reaction forces; the fundamental convective, impulsive, and breathing mode frequencies; liquid pressures; peak slosh heights; and to a limited extent, tank wall stresses.

One additional step taken with the simulations using the refined models is that the analyses were run a second time up through the end of the seismic excitation with results extracted at 1-millisecond increments rather than 10-millisecond increments. The liquid pressure time histories were then post-processed

---

<sup>1</sup> Dytran<sup>®</sup> is a registered trademark of MSC Software, Inc., Santa Ana, California.

using a 66-Hz lowpass filter to remove unimportant high-frequency response. Results are presented for both the unfiltered 10-millisecond data and the filtered 1-millisecond data.

Revision 1 of this report provides corrections and clarifications in response to reviewer comments arising during a project review meeting held June 7–8, 2007. The comments are reproduced in Appendix A of Deibler et al. (2008).

## C.2 Summary of Results

The following sections provide a brief summary of the results for the rigid and flexible wall tanks. Included in Section C.2.3 are four tables and two plots summarizing the key results from the analysis.

### C.2.1 Rigid Tank

The convective frequency of 0.207 Hz is approximately 3% greater than the value of 0.2 Hz reported in the original analysis. The estimated fundamental convective frequencies for a rigid open-top tank using the methodologies in BNL (1995) and Malhotra (2005) are 0.196 Hz and 0.195 Hz, respectively.

The peak total reaction force reported from the Dytran<sup>®</sup> simulation was  $3.3 \times 10^6$  lbf in the positive direction and  $3.0 \times 10^6$  lbf in the negative direction for a mean peak reaction force of  $3.15 \times 10^6$  lbf. The peak total reaction force reported for the original Dytran<sup>®</sup> model was  $3.02 \times 10^6$  lbf. The peak reaction force for an open-top tank per BNL (1995) is  $2.98 \times 10^6$  lbf. The estimated peak reaction force for an equivalent flat-top tank using the simple methodologies in BNL (1995) and Malhotra (2005) are  $3.56 \times 10^6$  lbf and  $3.42 \times 10^6$  lbf, respectively. The peak convective reaction force for the refined model was  $3.0 \times 10^5$  lbf, compared to a value of  $2.0 \times 10^5$  lbf for the original model. Apparently the increased mesh resolution improves the accuracy of the model for capturing the convective response. The differences in the estimates of the convective reaction forces are not particularly important since the convective reaction contributes roughly 10% of the total reaction force, while the impulsive component makes up the other 90%.

The additional mesh resolution of the new model combined with filtering of the pressures to remove unwanted high-frequency response led to more meaningful pressure distributions that matched closely the results for an open tank over approximately 90% of the tank wall. Deviations from the open tank solution were present only near the liquid-free surface, which is consistent with the results for flat-top tanks presented in Abatt and Rinker (2008). In fact, for the domed tank configurations, the deviations from the open-tank solution are even more localized near the liquid-free surface than for the flat-top tanks. The distributions of peak wall pressures also show that the estimates of pressures for an equivalent flat-top tank given in Appendix D in BNL (1995) are conservative, at least up the initial height of the free surface.

The peak slosh height reported from the refined Dytran<sup>®</sup> model was 27.4 inches compared to a peak height of 21.1 inches from the original model, indicating that the mesh refinement had a significant effect on the slosh height results. The Dytran<sup>®</sup> value of 27.4 inches is midway between the peak slosh height predictions 25.2 inches and 29.7 inches for an open tank using the methodologies in BNL (1995) and Malhotra (2005), respectively. This suggests that the mesh resolution in the current Dytran<sup>®</sup> model is high enough to sufficiently capture the motion of the free surface.

## C.2.2 Flexible Wall Tank

The convective response of the flexible wall tank is essentially the same as for the rigid tank as expected.

The impulsive mode frequency predicted by the Dytran<sup>®</sup> simulation was 6.25 Hz compared to a value of 6.4 Hz predicted by the original model and a theoretical impulsive frequency of 6.5 Hz for an open-top tank. The breathing mode frequency of 5.4 Hz matched the theoretical value for an open-top tank.

The peak total horizontal reaction force from the Dytran<sup>®</sup> simulation was  $9.97 \times 10^6$  lbf, which is slightly less than the value of  $1.02 \times 10^7$  lbf from the original model and also slightly less than the peak reaction force expected for a flexible wall open-top tank. The peak total horizontal reaction force for an equivalent flat-top tank is approximately  $1.3 \times 10^7$  lbf, but depends slightly on the assumptions and the methodology.

The peak convective reaction force of  $3.0 \times 10^5$  lbf is slightly greater than the value of  $2.85 \times 10^5$  lbf from the original model, but the differences in the estimates of the convective reactions are of little significance since the convective reaction force constitutes less than 5% of the total reaction force for the flexible wall tank.

Just as in the case of the rigid tank, additional mesh resolution of the new flexible wall tank model combined with filtering of the pressures to remove unwanted high-frequency response led to more meaningful pressure distributions that matched closely the results for an open tank over approximately 90% of the tank wall. Again, deviations from the open-tank solution were present only near the liquid-free surface and are more localized near the liquid-free surface than for the flat-top tanks. The distributions of peak wall pressures show that the estimates of pressures for an equivalent flat-top tank given in Appendix D in BNL (1995) are more conservative for the flexible wall tank than for the rigid tank.

The peak slosh height reported from the refined Dytran<sup>®</sup> model was 26.9 inches compared to a peak height of 20.1 inches from the original model, indicating that the mesh refinement had a significant effect on the slosh height results. The peak slosh height for an open tank per BNL (1995) is 25.2 inches.

Mid-plane hoop stress time histories are presented for the flexible wall tank along the plane of seismic excitation ( $\theta=0^\circ$ ) and at  $45^\circ$  and  $90^\circ$  from the plane of excitation. At  $\theta=0^\circ$ , unfiltered results are shown for stresses extracted at both 10-millisecond and 1-millisecond intervals. The time histories appear essentially the same in both cases indicating that no important information is gained by extracting the stresses at increments smaller than 10 milliseconds.

Also presented is a comparison of a hoop stress time history to a pressure time history near the mid-height of the tank wall, where the hoop stress is taken adjacent to the pressure element. It is evident in that plot that the stress time history is smoother than the pressure time history. This also shows that the primary tank wall naturally filters out high-frequency response in the pressures.

## C.2.3 Summary of Key Parameters

The following tables and plots provide a summary of the important parameters from this study. Included are convective, impulsive, and breathing mode frequencies; horizontal reaction forces; maximum slosh heights; and wall pressure distributions.

**RPP-RPT-28963, Rev. 1**  
**M&D-2008-005-RPT-01, Rev. 1**

**Table C-1. Summary of Convective, Impulsive, and Breathing Mode Frequencies for Refined Models (Hz)**

<b>Configuration/Solution</b>	<b>First Convective Mode Frequency (Hz)</b>	<b>Impulsive Mode Frequency (Hz)</b>	<b>Breathing Mode Frequency (Hz)</b>
Rigid 460 Open Top (BNL)	0.196	Rigid	Rigid
Rigid 460 Open Top (Malhotra)	0.195	Rigid	Rigid
Rigid 460 Domed -Dytran®	0.207	Rigid	Rigid
Rigid Equivalent Flat Top (BNL Estimate)	0.196 <sup>(a)</sup>	Rigid	Rigid
Rigid Equivalent Flat Top (Malhotra Estimate)	0.195 <sup>(a)</sup>	Rigid	Rigid
Flexible 460 Domed - Dytran®	0.207	6.25	5.41
Flexible 460 Open Top (BNL Estimate)	0.196	6.48	5.43
Flexible 460 Open Top (Malhotra)	0.195	5.36	Not applicable
Flexible Wall Equivalent Flat Top (BNL Estimate)	0.196 <sup>(a)</sup>	6.48 <sup>(a)</sup>	Not applicable
Flexible Wall Equivalent Flat Top (Malhotra Estimate)	0.195 <sup>(a)</sup>	5.36 <sup>(a)</sup>	Not applicable

(a) Assumed to be the same as for the open tank.

**Table C-2. Summary of Peak Horizontal Reaction Forces for Refined Models (lbf)**

<b>Configuration/Solution</b>	<b>Peak Reaction Force (lbf)</b>	<b>Reference</b>
Rigid Open Top (BNL Estimate)	2.98 x 10 <sup>6</sup>	p. D-10
Rigid Equivalent Flat Top (BNL Estimate)	3.56 x 10 <sup>6</sup>	p. D-20
Rigid Equivalent Flat Top (Malhotra Estimate)	3.42 x 10 <sup>6</sup>	p. D-21
Rigid Domed (Dytran Simulation)	3.15 x 10 <sup>6</sup>	pp. C-28 and C-29
Flexible Open Top (BNL Estimate at 6.5 Hz and 3.5% Damping)	1.07 x 10 <sup>7</sup>	p. D-32
Flexible Open Top (BNL Estimate at 6.25 Hz and 5.5% Damping)	1.01 x 10 <sup>7</sup>	p. D-45
Flexible Open Top (Malhotra Estimate at 5.4 Hz and 3.5% Damping)	1.14 x 10 <sup>7</sup>	p. D-33
Flexible Open Top (Malhotra Estimate at 5.4 Hz and 5.5% Damping)	9.81 x 10 <sup>6</sup>	p. D-46
Flexible Equivalent Flat Top (BNL Estimate at 6.5 Hz and 3.5% Damping)	1.28 x 10 <sup>7</sup>	p. D-58
Flexible Equivalent Flat Top (Malhotra Estimate at 5.4 Hz and 3.5% Damping)	1.32x 10 <sup>7</sup>	p. D-59
Flexible Equivalent Flat Top (BNL Estimate at 6.25 Hz and 5.5% Damping)	1.2 x 10 <sup>7</sup>	p. D-70
Flexible Equivalent Flat Top (Malhotra Estimate at 5.4 Hz and 5.5% Damping)	1.13 x 10 <sup>7</sup>	p. D-71
Flexible Domed (Dytran Simulation)	9.97 x 10 <sup>6</sup>	pp. C-42 and C-44

Table C-3. Comparison of Frequencies and Slosh Heights for Original and Refined Models

Configuration	Fundamental Convective Frequency (Hz)		Impulsive Mode Frequency (Hz)		Breathing Mode Frequency (Hz)		Maximum Slosh Height (in)	
	Theory	Dytran®	Theory	Dytran®	Theory	Dytran®	Theory	Dytran®
Original Rigid	0.196	0.2	Rigid	Rigid	Rigid	Rigid	24.5	21.1
Refined Rigid	0.196	0.207	Rigid	Rigid	Rigid	Rigid	25.2	27.4
Original Flexible Wall	0.196	0.2	6.5	6.4	5.5	5.5	24.5	20.1
Refined Flexible Wall	0.196	0.207	6.5	6.25	5.43	5.41	25.2	26.9

Table C-4. Comparison of Peak Reaction Forces Between Original and Refined Models

Configuration	Peak Reaction Force (lbf)	
	Theory	Dytran®
Original Rigid	$3.0 \times 10^6$	$3.02 \times 10^6$
Refined Rigid	$2.98 \times 10^6$	$3.15 \times 10^6$
Original Flexible Wall	$1.03 \times 10^7$	$1.02 \times 10^7$
Refined Flexible Wall <sup>(a)</sup>	$1.07 \times 10^7$	$9.97 \times 10^6$

(a) Based on an open-top tank with a 6.5-Hz impulsive frequency and 3.5% damping.

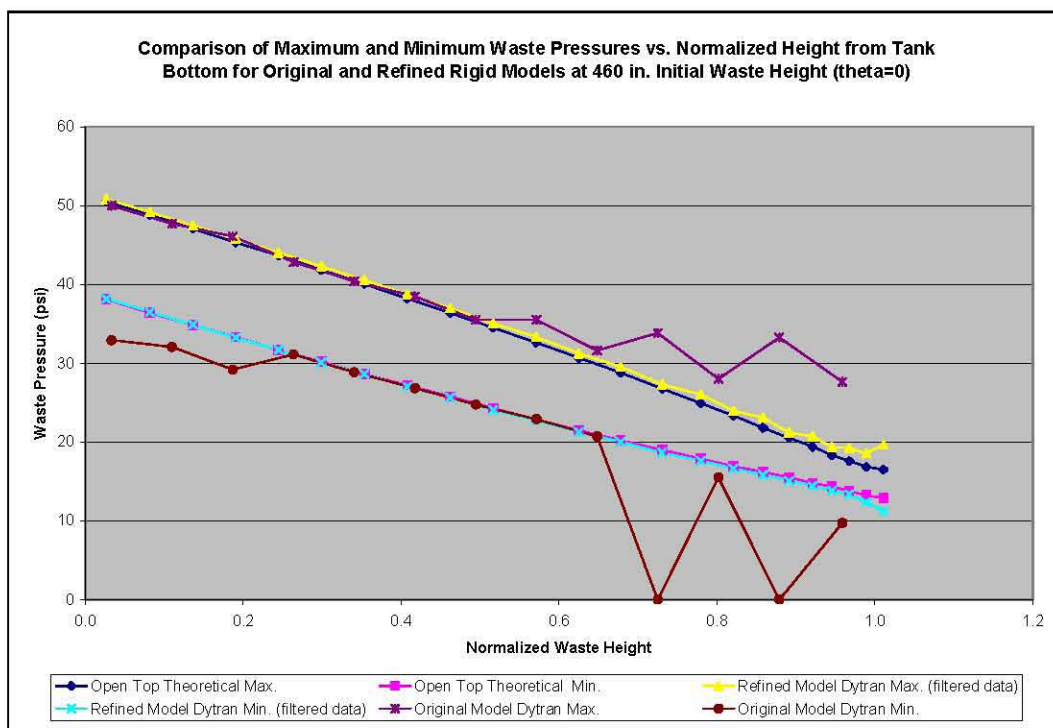


Figure C-1. Comparison of Maximum and Minimum Pressures for Original and Refined Rigid Tank Models at  $\theta=0^\circ$

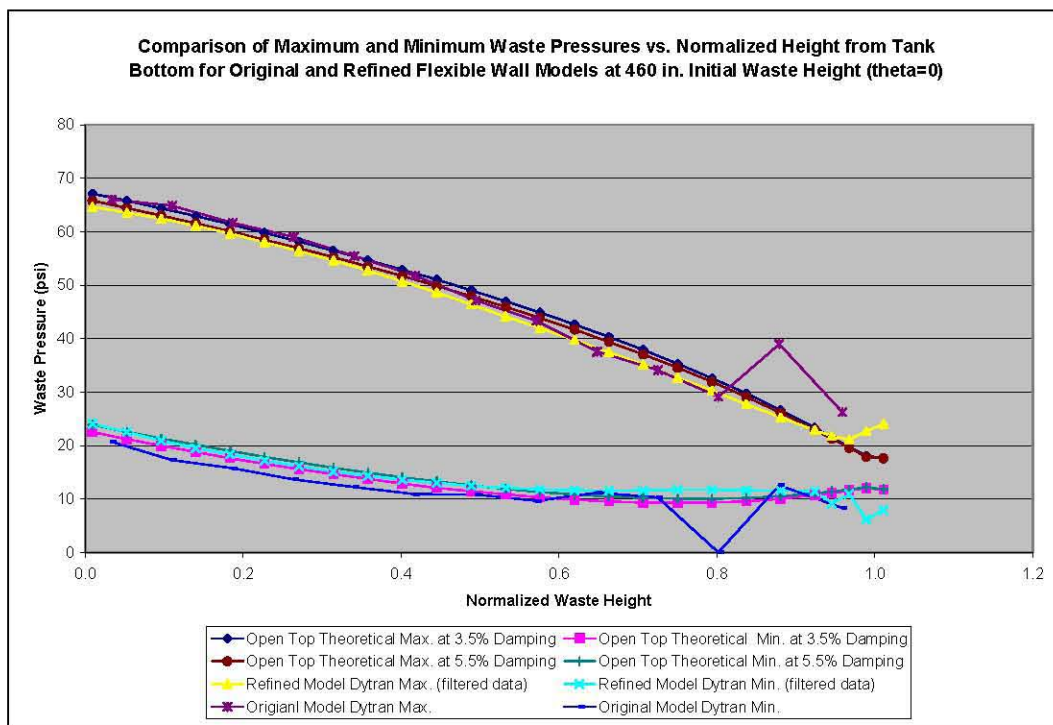


Figure C-2. Comparison of Maximum and Minimum Pressures for Original and Refined Flexible Wall Tank Models at  $\theta=0^\circ$

### C.3 Discussion

Refined models of the rigid and flexible wall tank configurations were created to address uncertainties in the solutions associated with the original less refined models. In both the rigid model and flexible wall model, the mesh resolution was increased in both the fluid mesh and the structural mesh. However, the fluid mesh is different between the rigid tank model and the flexible wall model. In the case of the rigid tank model, a biased fluid mesh was employed as shown in Figure C-3. This scheme allowed for increased mesh density near the waste-free surface while minimizing the total number of fluid elements. However, in order to maintain solution stability in the flexible wall tank model, increased mesh resolution was required throughout the Euler domain as shown in Figure C-10. The difference in fluid mesh resolution led to a 1% difference in the waste mass calculated by Dytran<sup>®</sup> for the two models and thus led to some very minor differences in the theoretical or estimated solutions for the two models based on waste mass. The differences had no significant effect on the results.

The damping or dynamic relaxation in the model was selected to give approximately 4% damping in the impulsive response. The damping was initially calibrated based on the decay of the vertical reaction force during the initial gravity loading. This reaction actually reflects the breathing mode response of the system rather than the impulsive response, but it was expected that calibrating the damping to the breathing mode response would be essentially equivalent to calibrating to the impulsive response and it saves computer time since the decay of the breathing mode response occurs at the beginning of the simulation. The damping calculated in this manner was approximately 3.5% of critical and was used to select the spectral acceleration associated with the impulsive response that was used in the benchmark

solutions from BNL (1995) and Malhotra (2005). The impulsive frequency used to select the spectral acceleration was the theoretically calculated value of 6.5 Hz from the open-tank solution.

A better estimate of impulsive response can be isolated by viewing the decay of the horizontal reaction force immediately following the cessation of the seismic signal (or equivalently, looking at the difference of the horizontal reaction force between the rigid and flexible wall tank models). The impulsive response as shown by the decay of the horizontal reaction force immediately after the termination of the seismic excitation showed that the impulsive frequency from the Dytran<sup>®</sup> solution was 6.25 Hz rather than the value of 6.5 Hz for the open tank. The response also indicated slightly higher damping of approximately 4.3% to 5.2% of critical. In order to provide a second estimate of the impulsive response, the benchmark solutions were also calculated using an impulsive spectral acceleration based on the 6.25-Hz impulsive frequency from the Dytran<sup>®</sup> simulation and a damping of 5.5%. Results using both estimates are presented.

Because spectral accelerations decrease between 6.25 Hz and 6.5 Hz as shown in Figure C-18, the higher damping value of 5.5% occurs with the higher spectral acceleration at 6.25 Hz, and the lower damping value of 3.5% occurs with the lower spectral acceleration at 6.5 Hz. Thus, the differences using the two estimates are relatively minor.

The total horizontal reaction force for the flexible wall tank as predicted by the Dytran<sup>®</sup> simulation was slightly less than that calculated for an open-top tank. Although the difference is small, this is not the expected result since the interaction of the liquid with the dome should increase the impulsive response. The effect may be due to the fact that some of the interaction between the liquid and the dome occurs in the rigid region of the dome and thus will not be amplified by the tank flexibility. This will reduce the overall reaction force relative to a completely flexible tank as is assumed in the open-top solution. The total horizontal reaction force for the rigid domed tank is greater than for the rigid open-top tank, as expected.

Investigation of hoop stress time histories for the flexible wall tank show that the primary tank wall does not respond to high-frequency content in the pressure time histories. That is, the primary tank structure acts as a natural mechanical lowpass filter.

## C.4 Conclusions

The fundamental conclusion from this study is that Dytran<sup>®</sup> is a useful tool for the simulation of seismically induced fluid-structure interaction effects in domed tanks. A list of technical conclusions and observations is presented below.

1. Increased mesh resolution in the tank models removed the anomalous behavior of the liquid-free surface under gravity loading that was present in the original models.
2. The frequencies and reaction forces predicted by the refined tank models agree fairly well with the frequencies and reaction forces predicted by the original tank models.
3. The original models did not have enough resolution to accurately predict slosh heights, but this deficiency appears to be corrected with increased mesh resolution.

4. In the case of the rigid tank, the convective reaction force is approximately 10% of the total reaction force, while in the case of the flexible wall tank, the convective reaction force is less than 5% of the total reaction force. Since the total reaction force is dominated by impulsive effects, the differences in estimates of the peak convective reaction forces are relatively unimportant.
5. The increased mesh resolution plus data filtering show that the solution for the domed tank is very similar to the solution for an open tank up to at least 90% of the normalized tank height based on the initial liquid level. This behavior is consistent with results document in Abatt and Rinker (2008) for flat-top tanks, but the agreement between the solutions for the domed tanks and for open-top tanks extends further up the tank wall than for flat-top tanks.
6. The estimates of peak wall pressures using the methodology of Appendix D in BNL (1995) are conservative, especially for the flexible wall tank.
7. The primary tank wall does not respond to high-frequency content in the pressure time histories. That is, the primary tank structure acts as a natural mechanical lowpass filter.

## C.5 Description of Refined Models

The refined rigid and flexible wall models are described in the following two sections. In both cases, the applied loads include gravity loading and seismic loading, with seismic loading applied in a single horizontal direction.

### C.5.1 Rigid Model

The mesh density for the refined model was increased in both the structural and fluid elements. The tank mesh was increased from 8 to 14 elements vertically in the tank wall and the transition from the vertical wall to the rigid dome now has two facets instead of only one. The number of structural elements in the tank in the circumferential direction has been increased from 28 to 36. The number of structural elements in the tank was increased from 488 to 898.

The new fluid mesh is biased with increasing vertical mesh density near the top of the tank. The new fluid elements measure 25.75 inches laterally each way and decreased from 25 inches tall near the bottom of the tank to 10 inches tall near the top of the tank. The old fluid elements measured approximately 35 inches in all three directions. The total number of fluid elements was increased from 15,137 to 62,400.

An overall plot of the refined model of the rigid tank and contained liquid at the 460-inch level is shown in Figure C-3. The location and numbering of fluid element sets “plusx\_els”, “cent\_press”, “minusx\_els”, “press\_45”, and “plusz\_els” are shown in Figure C-4 through Figure C-8.

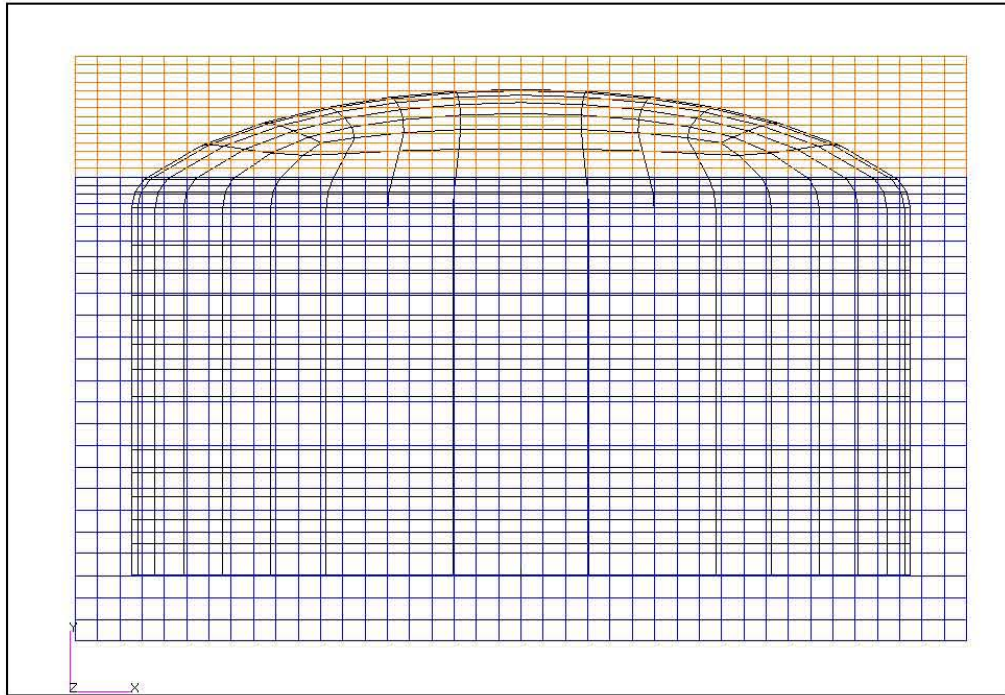


Figure C-3. Plot of Rigid Tank and Waste at 460-Inch Waste Level

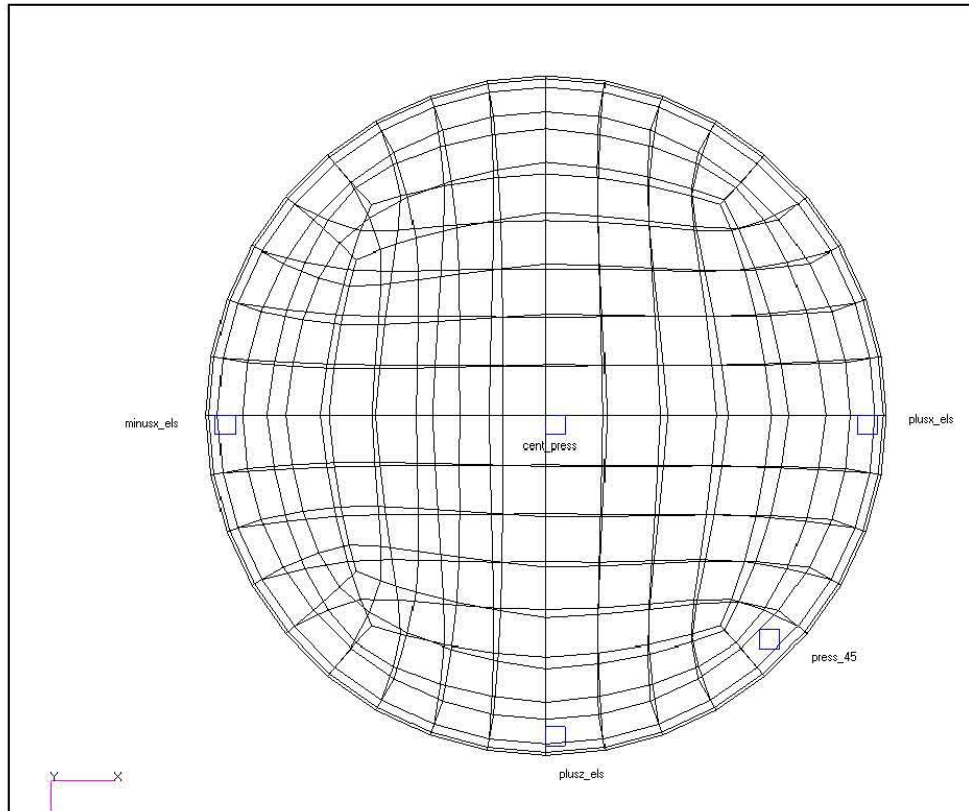
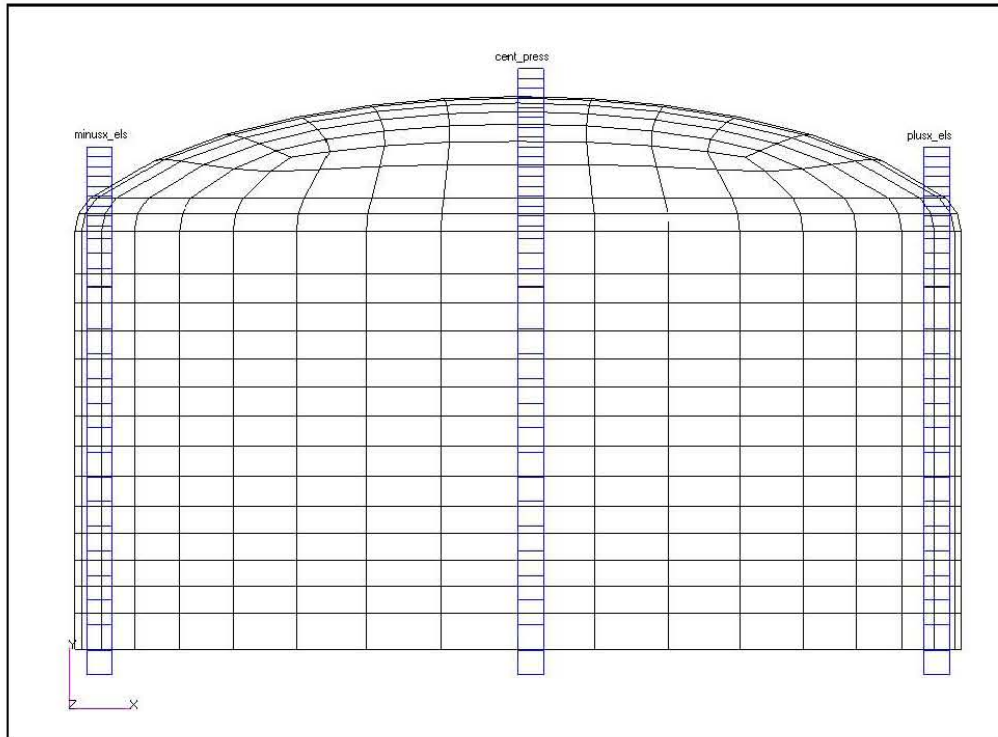
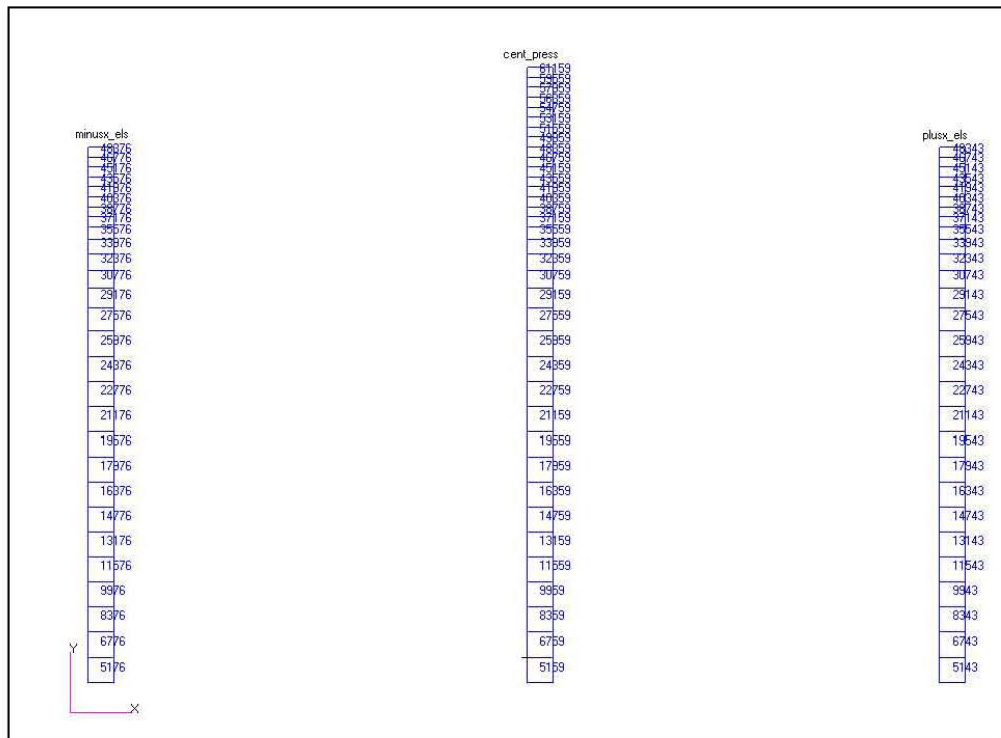


Figure C-4. Top View of Rigid Tank Model Showing the Angular Locations of Fluid Elements at Which Pressures Were Monitored

RPP-RPT-28963, Rev. 1  
M&D-2008-005-RPT-01, Rev. 1



**Figure C-5.** Elevation View of Rigid Tank Model Showing the Locations of “plusx\_els,” “cent\_press,” and “minusx\_els” Fluid Elements Sets at Which Pressures Were Monitored



RPP-RPT-28963, Rev. 1  
M&D-2008-005-RPT-01, Rev. 1

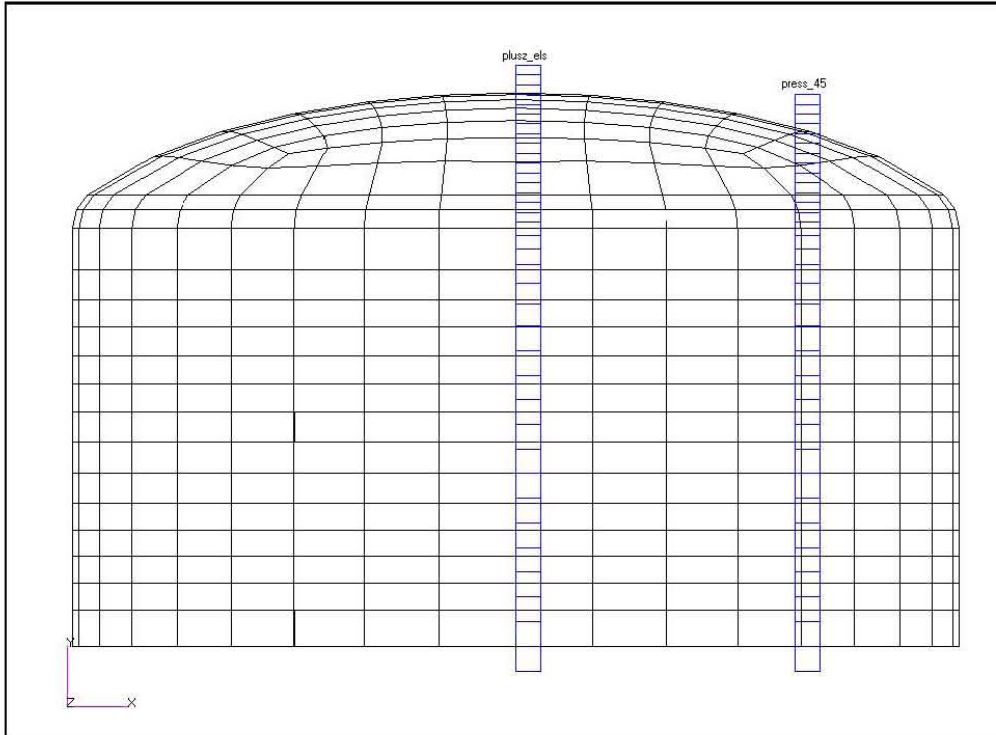


**Figure C-7.** Elevation View of Rigid Tank Model Showing the Locations of “press\_45” and “plusz\_els” Fluid Elements Sets at Which Pressures Were Monitored

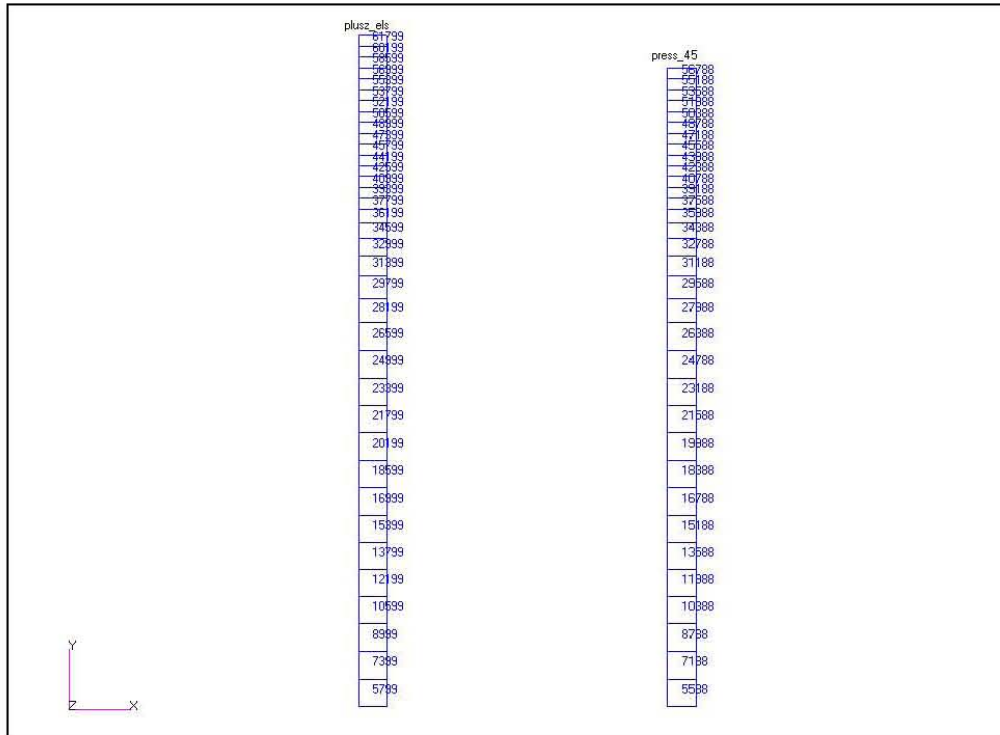


**Figure C-8.** Waste Element Numbering for Element Sets “press\_45” and “plusz\_els” for Rigid Tank Model

### C.5.1.1 Flexible Wall Model

The structural mesh for the flexible wall model is the same as in the rigid model described in the previous section, but the mesh density of the fluid elements was increased. In the flexible wall tank model, all fluid elements measure 25.75 x 25.75 inches laterally and are 10 inches tall. That is, the fluid elements are no longer biased in the vertical direction. In this model, the total number of fluid elements is increased to 107,200.

Overall plots of the flexible tank model are shown in Figure C-9 and Figure C-10. The location and numbering for fluid element sets “plusx\_els”, “cent\_press”, “minusx\_els”, “press\_45”, and “plusz\_els” is shown in Figure C-11 through Figure C-14. The shell element numbering for the tank structural element sets “plusx\_outstrip”, “plusz\_outstrip”, “press45\_outstrip”, and “minusx\_outstrip” are shown in Figure C-15 and Figure C-16.

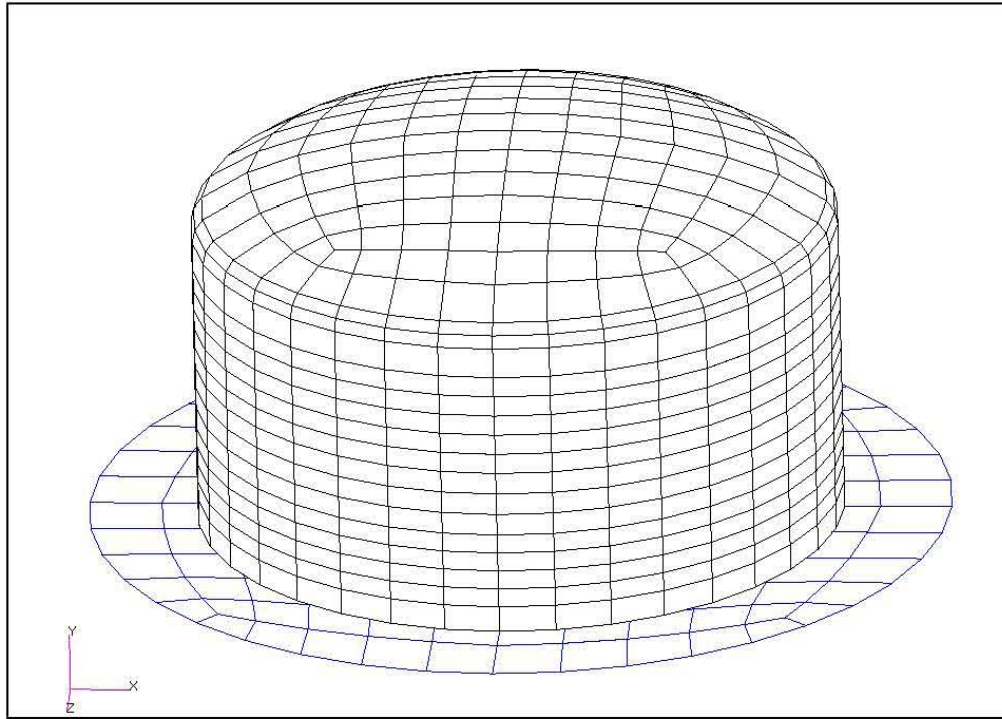


**Figure C-9.** Plot of Primary Tank and Base for Flexible Tank Model

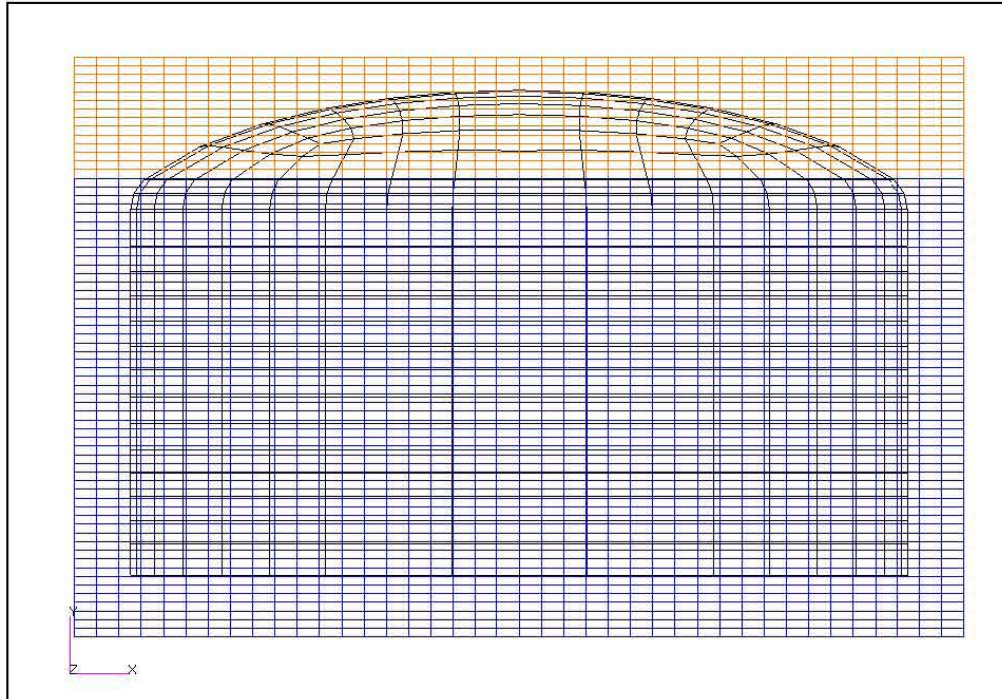


**Figure C-10.** Plot of Flexible Tank and Waste at 460-Inch Waste Level

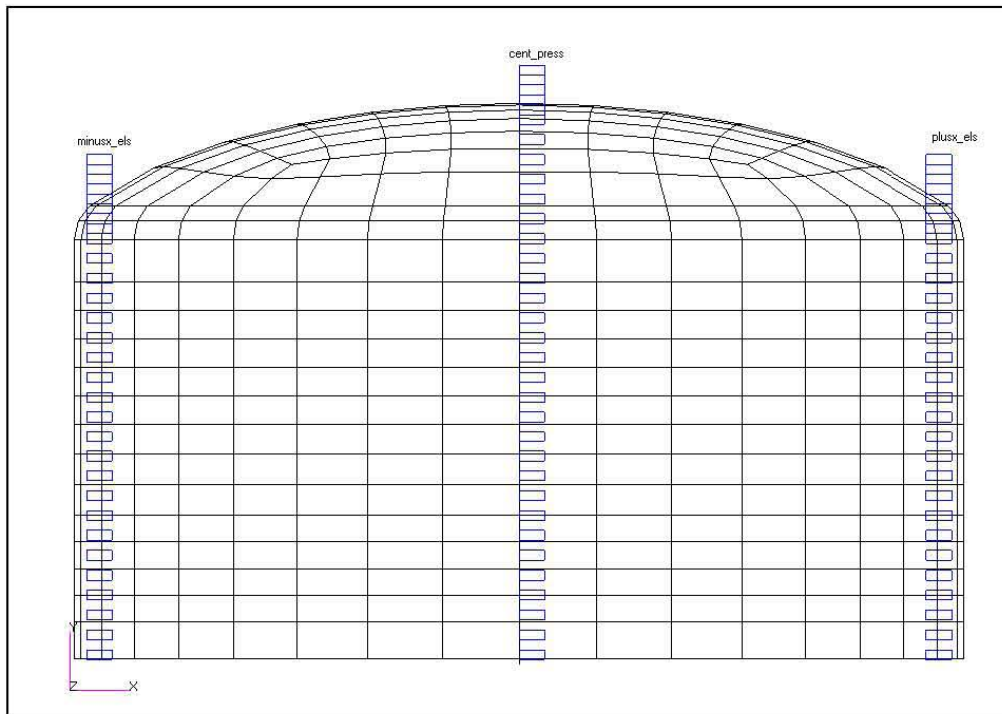


**Figure C-11.** Elevation View of Model Showing the Locations of “plusx\_els”, “cent\_press”, and “minusx\_els” Fluid Elements Sets at Which Pressures Were Monitored



RPP-RPT-28963, Rev. 1  
M&D-2008-005-RPT-01, Rev. 1

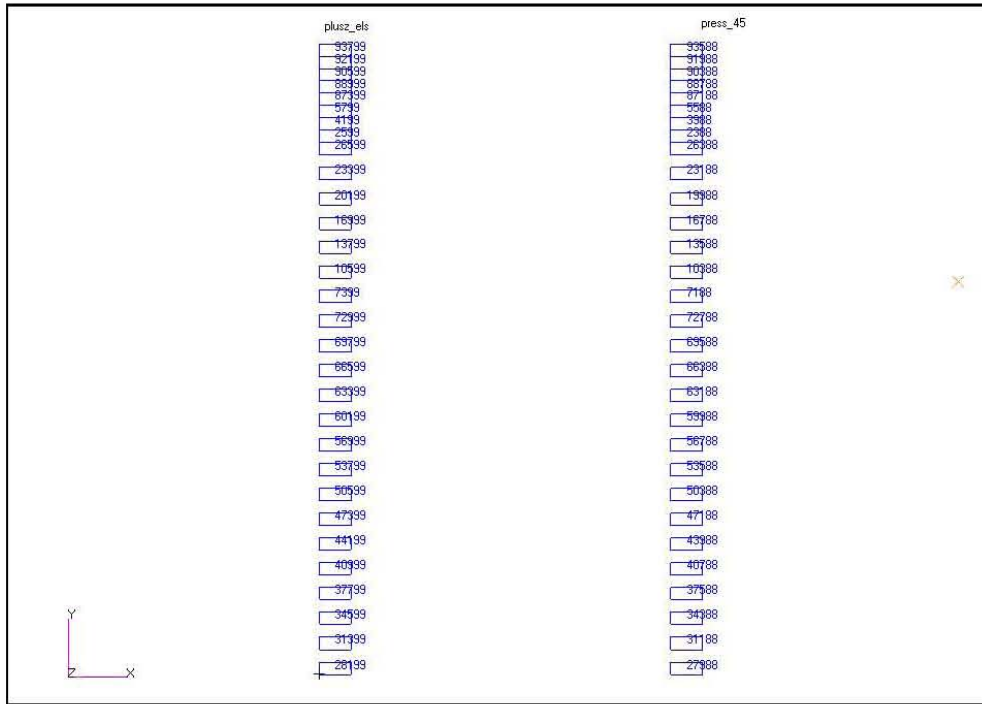


Figure C-14. Waste Element Numbering for Element Sets “press\_45” and plusz\_els” for Flexible Tank Model

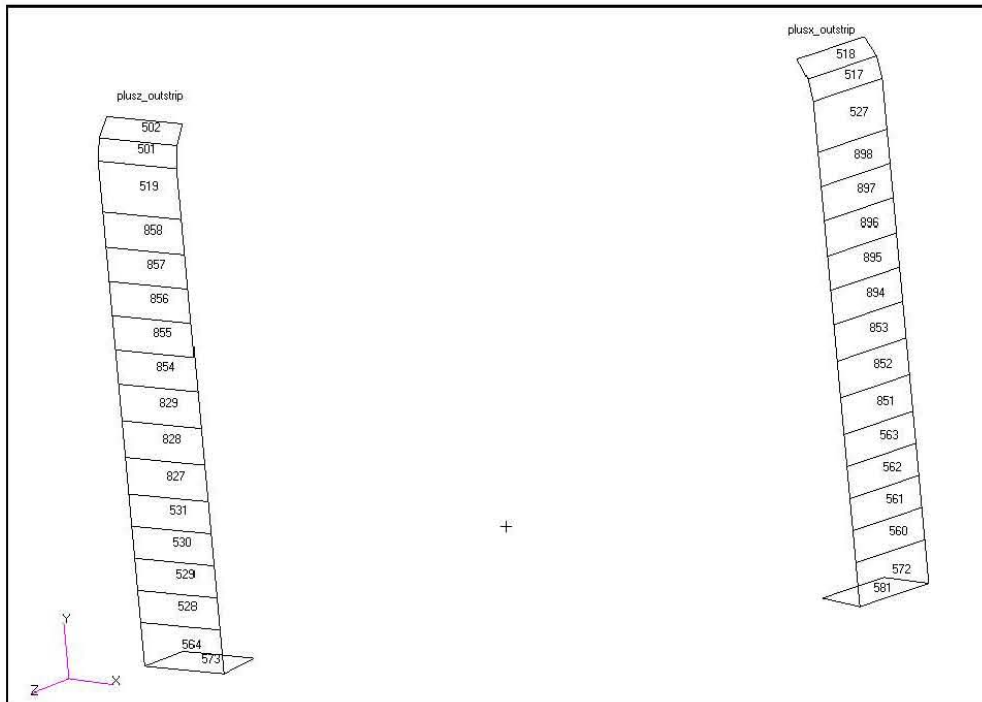
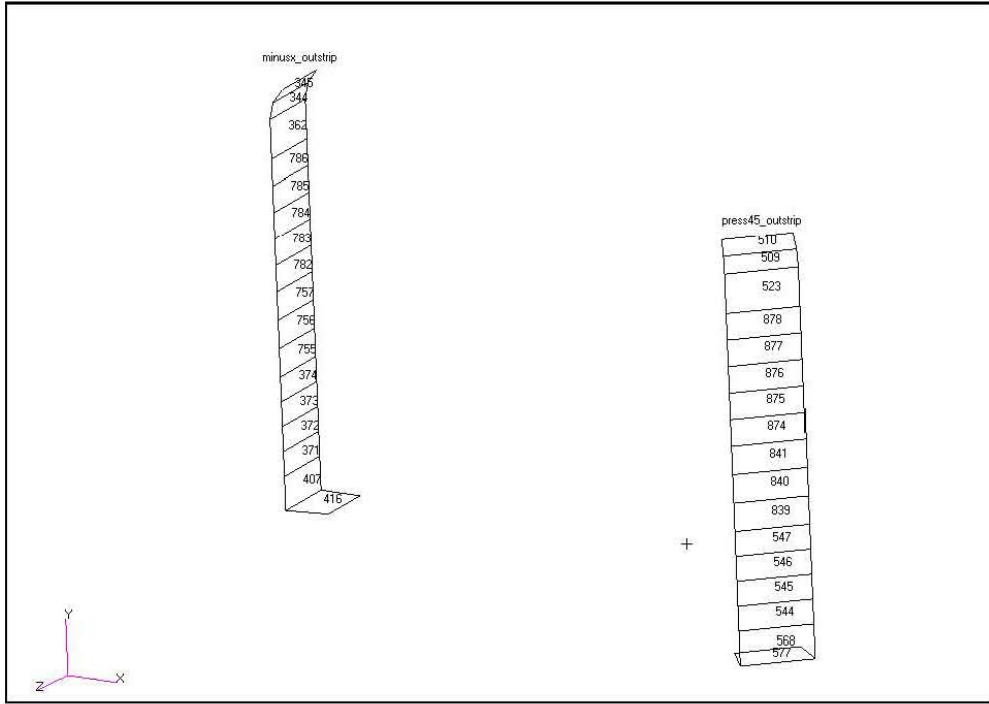


Figure C-15. Shell Element Numbering for Tank Wall Stress Results at  $\theta=0^\circ$  and  $\theta=90^\circ$  for Flexible Tank Model



**Figure C-16.** Shell Element Numbering for Tank Wall Stress Results at  $\theta=45^\circ$  and  $\theta=180^\circ$  for Flexible Tank

### C.5.1.2 Seismic Input Response Spectra

Figure C-17 shows that the spectral accelerations in the range of 0.1 to 0.5 Hz (typical convective frequencies) are nearly the same for 0.1% and 0.5% damping. That is, in this range of frequencies and damping values, the convective response is not sensitive to damping. The spectral accelerations for frequencies and damping values appropriate for the impulsive response of the system are shown in Figure C-18. The plots will be referred to subsequently when discussing the selection of spectral accelerations for the calculation of benchmark solutions.

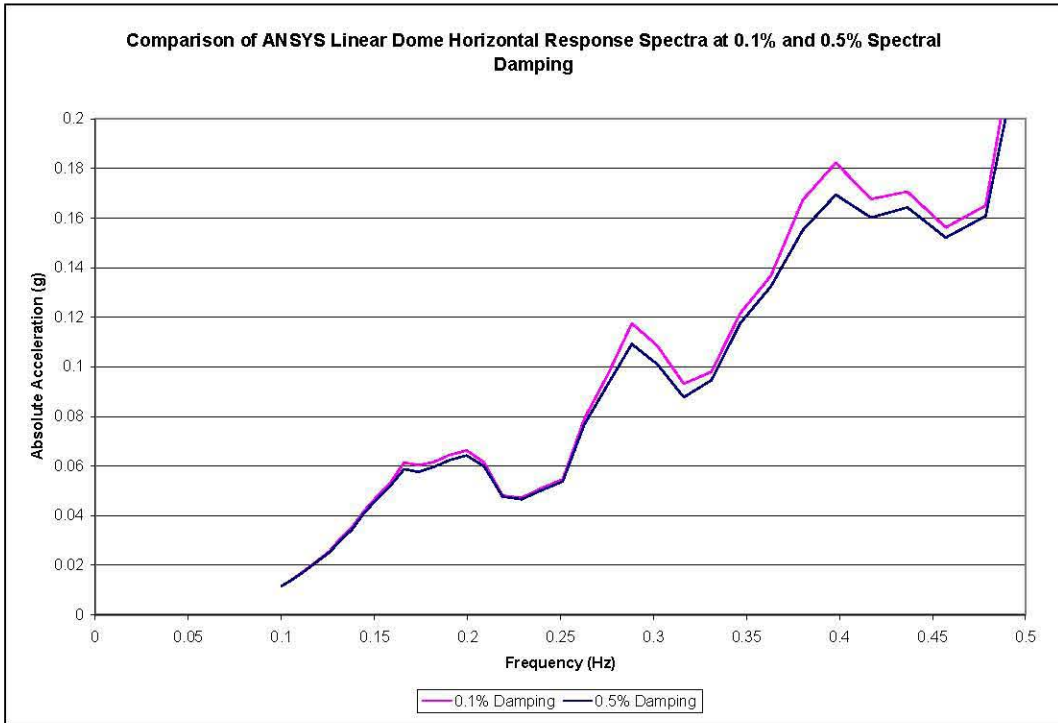


Figure C-17. Comparison of Horizontal Response Spectra at 0.1% and 0.5% Damping for Low Frequencies

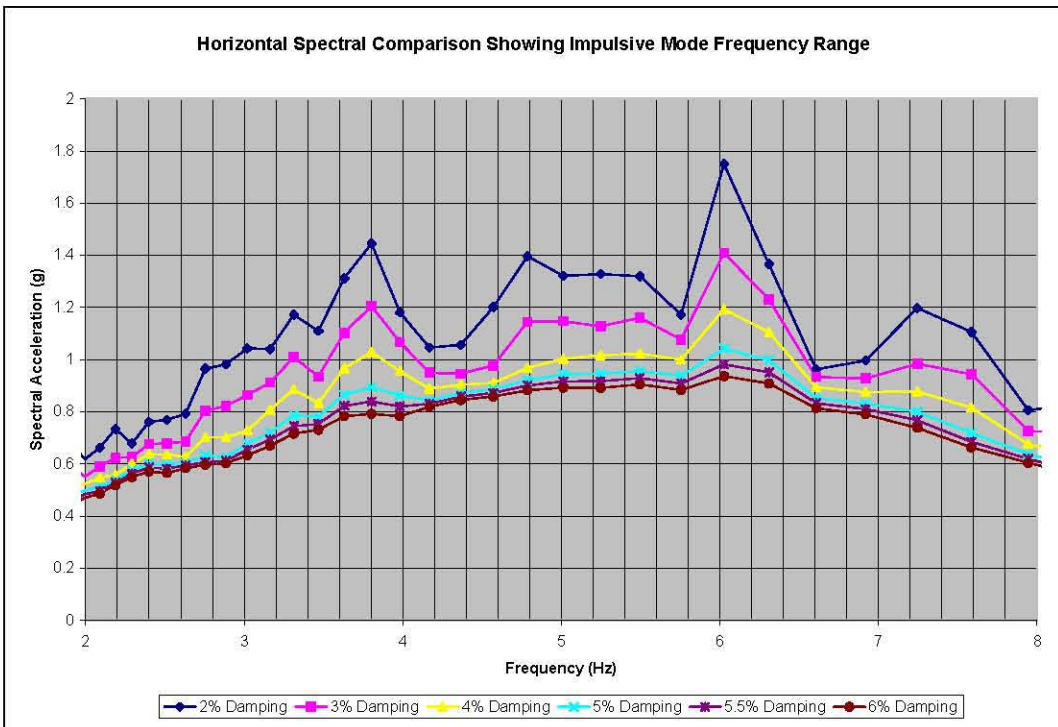


Figure C-18. Horizontal Spectral Comparison Showing Damping Values and Frequency Range for Impulsive Mode

### C.5.2 Theoretical Hydrostatic Pressures

The theoretical hydrostatic pressures for selected element sets in the fluid meshes of the rigid and flexible wall tank models are shown in Table C-5 and Table C-6, respectively.

**Table C-5.** Theoretical Hydrostatic Pressure of Liquid Elements in Rigid Tank for Initial Liquid Level of 460 Inches

<b>“Plusx_els”</b>	<b>“Press_45”</b>	<b>“Plusz_els”</b>	<b>“Cent_press”</b>	<b>“Minusx_els”</b>	<b>Theoretical Hydrostatic Pressure (psi absolute)</b>
<b>Element</b>	<b>Element</b>	<b>Element</b>	<b>Element</b>	<b>Element</b>	
43543	43988	44199	43559	43576	14.7
41943	42388	42599	41959	41976	14.7
40343	40788	40999	40359	40376	15.0
38743	39188	39399	38759	38776	15.7
37143	37588	37799	37159	37176	16.4
35543	35988	36199	35559	35576	17.1
33943	34388	34599	33959	33976	18.0
32343	32788	32999	32359	32376	19.0
30743	31188	31399	30759	30776	20.1
29143	29588	29799	29159	29176	21.4
27543	27988	28199	27559	27576	22.9
25943	26388	26599	25959	25976	24.5
24343	24788	24999	24359	24376	26.1
22743	23188	23399	22759	22776	27.7
21143	21588	21799	21159	21176	29.4
19543	19988	20199	19559	19576	31.1
17943	18388	18599	17959	17976	32.7
16343	16788	16999	16359	16376	34.4
14743	15188	15399	14759	14776	36.0
13143	13588	13799	13159	13176	37.7
11543	11988	12199	11559	11576	39.3
9943	10388	10599	9959	9976	41.0
8343	8788	8999	8359	8376	42.6
6743	7188	7399	6759	6776	44.3

RPP-RPT-28963, Rev. 1  
M&D-2008-005-RPT-01, Rev. 1

Table C-6. Theoretical Hydrostatic Pressure of Liquid Elements in Flexible Tank for Initial Liquid Level of 460 Inches

“Plusx_els”	“Press_45”	“Plusz_els”	“Cent_press”	“Minusx_els”	Theoretical Hydrostatic Pressure (psi absolute)
Element	Element	Element	Element	Element	
5143	5588	5799	89959	86776	15.0
3543	3988	4199	86759	5176	15.7
1943	2388	2599	3559	3576	16.4
25943	26388	26599	25959	1976	17.0
22743	23188	23399	22759	22776	18.3
19543	19988	20199	19559	19576	19.7
16343	16788	16999	16359	16376	21.0
13143	13588	13799	13159	13176	22.3
9943	10388	10599	9959	9976	23.6
6743	7188	7399	6759	6776	24.9
72343	72788	72399	72359	72376	26.3
69143	69588	69799	69159	69176	27.6
65943	66388	66599	65959	65876	28.9
62743	63188	63399	62759	62776	30.2
59543	59988	60199	59559	59576	31.6
56343	56788	56999	56359	56376	32.9
53143	53588	53799	53159	53176	34.2
49943	50388	50599	49959	49876	35.5
46743	47188	47399	46759	46776	36.9
43543	43988	44199	43559	43576	38.2
40343	40788	40999	40359	40376	39.5
37143	37588	37799	37159	37176	40.9
33943	34388	34599	33959	33876	42.2
30743	31188	31399	30759	30776	43.5
27543	27988	28199	27559	27576	44.8

## C.6 Rigid Tank Results

In the case of the rigid tank, the gravity load was run for 2 seconds before beginning the seismic input. The 20.48-second seismic input was followed by 20 seconds of unforced motion giving a total simulation time of 42.5 seconds. In the initial simulation, the reaction forces and liquid pressures were extracted every 10 millisecond. In order to further investigate high-frequency response in the pressures, the problem was rerun up to a time of 25 seconds with pressures extracted every 1 millisecond. Results from both simulations are presented.

### C.6.1 Hydrodynamic Forces

When the logarithmic decrement discussed in Section 5.1 of the main body of this report is used to quantify the damping present in the convective response during the free-oscillation period shown in Figure C-20, the resulting critical damping ratio is on the order of a few tenths of a percent. Consequently, the convective accelerations from the 0.1% damped spectrum are used for the calculation of the reaction forces for the benchmark solutions. As shown in Figure C-17, the spectral accelerations are insensitive to the damping values in the range of damping values and frequencies associated with the convective response.

In the case of an open-top tank, the peak hydrodynamic force induced against the tank wall due to horizontal excitation can be calculated via Equation 4.31 in BNL (1995) with the instantaneous accelerations replaced by the appropriate spectral accelerations. If the contributions of the impulsive mode and first three convective modes are combined in a square-root-sum-of-squares (SRSS) fashion, the theoretical maximum horizontal hydrodynamic force is  $2.98 \times 10^6$  lbf, based on a zero-period acceleration for the impulsive response, and convective accelerations from the 0.1% damped spectrum. The supporting calculations using the methodology in BNL (1995) are included in Appendix D of this report.

The horizontal coupling surface reaction force time history reported by Dytran<sup>®</sup> is shown in Figure C-19. The peak positive reaction force is  $3.3 \times 10^6$  lbf, while the peak negative reaction force is  $3.0 \times 10^6$  lbf. The peak positive reaction force is approximately 11% greater than the open-top SRSS value, while the mean of the peak positive and peak negative reaction forces is 6% greater than the SRSS open-top estimate. The slight positive bias in the reaction force record may be due to an inherent slight positive bias in the seismic acceleration record. The mean of the peak positive and negative reaction forces will negate any inherent bias in the seismic record.

Either way, the peak reaction force reported by Dytran<sup>®</sup> is slightly higher than the SRSS open-top estimate. This is expected since the interaction with the dome curvature should have the effect of slightly increasing the impulsive response and slightly decreasing the convective response. Since the total reaction force is dominated by the impulsive response, any interaction with the dome is expected to lead to a net increase in the total reaction force relative to the open-tank solution.

According to the approximate estimate using the methodology of Appendix D in BNL (1995), the maximum total reaction force for an equivalent flat-top tank with the roof at 484 inches above the bottom of the tank per Kennedy (2003) is  $3.56 \times 10^6$  lbf. The estimate given by Malhotra (2005) for the equivalent flat-top tank is  $3.42 \times 10^6$  lbf.

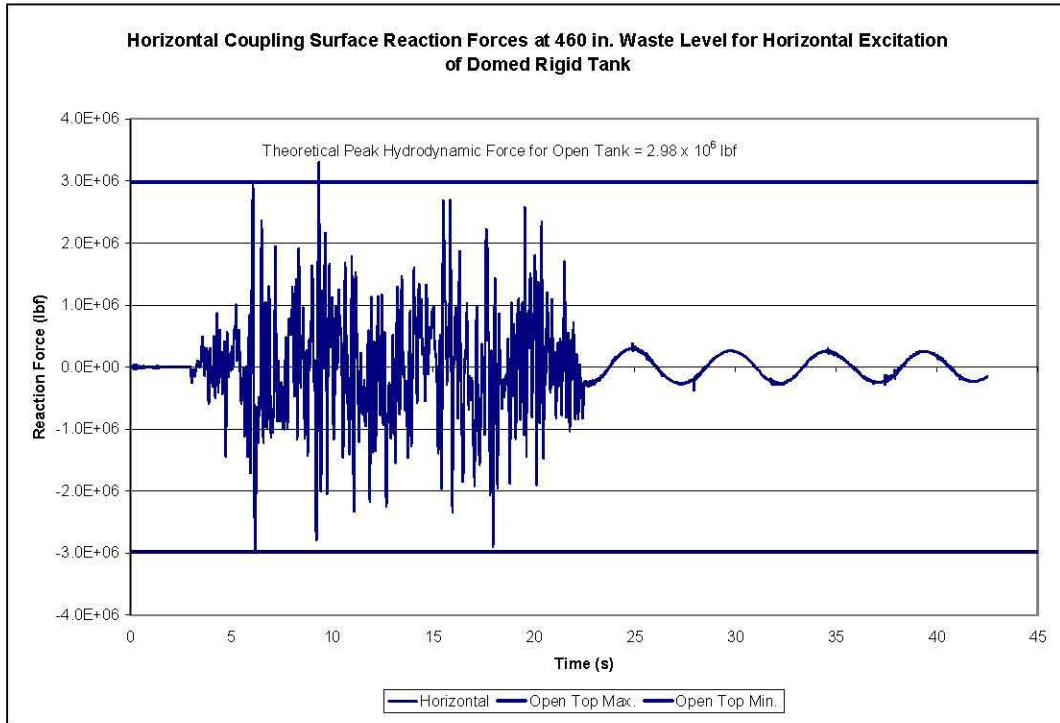


Figure C-19. Horizontal Coupling Surface Reaction Force for Rigid Tank at 460-Inch Waste Level Under Horizontal Seismic Excitation – Refined Mesh

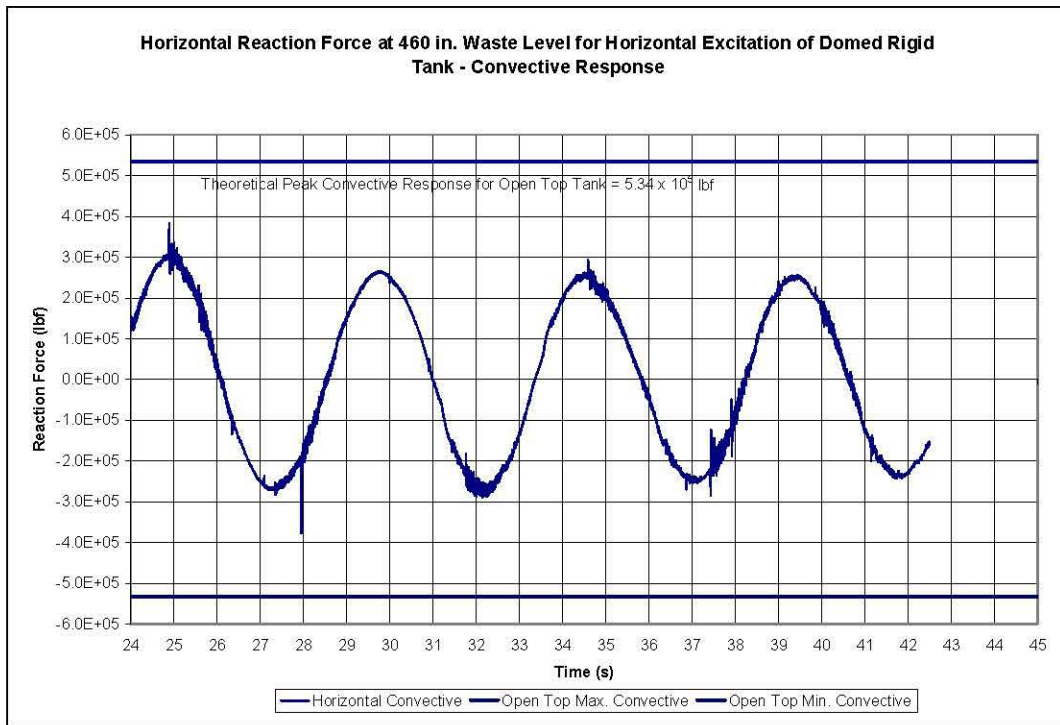


Figure C-20. Horizontal Coupling Surface Reaction Force for Rigid Tank at 460-Inch Waste Level Under Horizontal Seismic Excitation – Convective Response With Refined Mesh

The peak reaction force for the fundamental convective mode predicted from the Dytran<sup>®</sup> simulation was approximately  $3.0 \times 10^5$  lbf as shown in Figure C-20. The estimate of the peak convective reaction force for an open-top tank is  $5.34 \times 10^5$  lbf. As expected, the peak convective reaction force for the domed tank is lower than for an open-top tank.

The convective frequency displayed in Figure C-20 is 0.207 Hz, which represents a slight increase relative to the convective frequency of 0.196 Hz for an open tank. The slight increase in the apparent convective frequency is consistent with the interaction between the liquid and the dome. Similar behavior is documented in Abatt and Rinker (2008).

## C.6.2 Liquid Pressures

Estimates of peak wall pressures for fluid elements along the plane of excitation and  $45^\circ$  from the plane of excitation are summarized in Table C-7 and Table C-8, respectively. Each table shows the wall pressures predicted for an open tank and for an equivalent flat-top tank according to BNL (1995). As before, the roof of the equivalent flat-top tank is 484 inches above the bottom of the tank per Kennedy (2003). The  $45^\circ$  location lies outside the central angle of  $17.8^\circ$  per Appendix D in BNL (1995) so that the open-tank solution and equivalent flat-top tank solution are the same in this region. This is reflected in Table C-8.

Pressure time histories for selected fluid elements near the wall of the tank at  $\theta=0^\circ$  are shown in Figure C-21 and Figure C-22. In each of these plots, some isolated peaks occur that are characteristic of a high-frequency response that may be due to spurious numerics, and that in any case are unimportant to any structural analysis. To investigate the nature of the isolated peaks and to remove the unnecessary high-frequency response, the simulation was rerun up to 25 seconds simulation time with pressures extracted every 1 millisecond instead of every 10 millisecond. The resulting pressure time histories were then post-processed using a 66 Hz-lowpass 6-pole Butterworth filter with re-filtering for phase correction. The cutoff frequency of 66 Hz was selected since it is twice the 33 Hz frequency that is commonly accepted as the cutoff frequency above which no dynamic amplification will occur.

The filtered pressure time histories at  $\theta=0^\circ$  are shown in Figure C-23. Plots of the maximum and minimum liquid pressures as a function of normalized wall height are shown in Figure C-24 and Figure C-25. The data in Figure C-24 are based on the original simulation with pressure output taken every 10 millisecond. The plot in Figure C-25 is based on pressure data extracted every 1 millisecond and then passed through the 66 Hz-lowpass filter. In this case, the filter has had the effect of slightly increasing the minimum pressures in fluid elements near the free surface. In particular, the minimum pressure in element 41943 near the waste-free surface was increased from  $7 \text{ lbf/in}^2$  to  $11 \text{ lbf/in}^2$ .

RPP-RPT-28963, Rev. 1  
M&D-2008-005-RPT-01, Rev. 1

Table C-7. Estimated Maximum Wall Pressures for Horizontal Excitation in Rigid Open and Equivalent Flat-Top Tanks at 460-Inch Waste Level for Elements at  $\theta=0^\circ$

“plusx_els”					
Element No.	Hydrostatic Pressure (psi absolute)	Peak Hydrodynamic Pressure for Open Tank (psi absolute)	Peak Hydrodynamic Pressure for Equivalent Flat-Top Tank (psi absolute)	Peak Total Pressure for Open Tank (psi absolute)	Peak Total Pressure for Equivalent Flat-Top Tank (psi absolute)
43543	14.7	1.8	8.2	16.5	22.9
41943	14.7	1.8	8.2	16.5	22.9
40343	15.0	1.8	8.2	16.8	23.2
38743	15.7	1.9	8.2	17.6	23.9
37143	16.4	2.0	8.2	18.4	24.6
35543	17.1	2.3	8.2	19.4	25.3
33943	18.0	2.5	8.2	20.5	26.2
32343	19.0	2.8	8.2	21.8	27.2
30743	20.1	3.2	8.2	23.3	28.3
29143	21.4	3.5	8.2	24.9	29.6
27543	22.9	3.9	8.2	26.8	31.1
25943	24.5	4.3	8.2	28.8	32.7
24343	26.1	4.6	8.2	30.7	34.3
22743	27.7	4.9	8.2	32.6	36.0
21143	29.4	5.1	8.2	34.5	37.6
19543	31.1	5.3	8.2	36.4	39.3
17943	32.7	5.5	8.2	38.2	40.9
16343	34.4	5.7	8.2	40.1	42.6
14743	36.0	5.8	8.2	41.8	44.2
13143	37.7	6.0	8.2	43.7	45.9
11543	39.3	6.0	8.2	45.3	47.5
9943	41.0	6.1	8.2	47.1	49.2
8343	42.6	6.2	8.2	48.8	50.8
6743	44.3	6.2	8.2	50.5	52.5

RPP-RPT-28963, Rev. 1  
M&D-2008-005-RPT-01, Rev. 1

**Table C-8.** Estimated Maximum Wall Pressures for Horizontal Excitation in Rigid Open and Equivalent Flat-Top Tanks at 460-Inch Waste Level for Elements at  $\theta=45^\circ$

“press_45” Element No.	Hydrostatic Pressure (psi absolute)	Peak Hydrodynamic Pressure for Open or Equivalent Flat-Top Tank (psi absolute)	Peak Total Pressure for Open or Equivalent Flat-Top Tank (psi absolute)
43988	14.7	0	14.7
42388	14.7	0	14.7
40788	15.0	1.2	16.2
39188	15.7	1.2	16.9
37588	16.4	1.3	17.7
35988	17.1	1.4	18.5
34388	18.0	1.5	19.5
32788	19.0	1.7	20.7
31188	20.1	1.8	21.9
29588	21.4	2.0	23.4
27988	22.9	2.1	25.0
26388	24.5	2.3	26.8
24788	26.1	2.5	28.6
23188	27.7	2.6	30.3
21588	29.4	2.7	32.1
19988	31.1	2.8	33.9
18388	32.7	2.9	35.6
16788	34.4	3.0	37.4
15188	36.0	3.1	39.1
13588	37.7	3.1	40.8
11988	39.3	3.2	42.5
10388	41.0	3.2	44.2
8788	42.6	3.2	45.8
7188	44.3	3.3	47.6

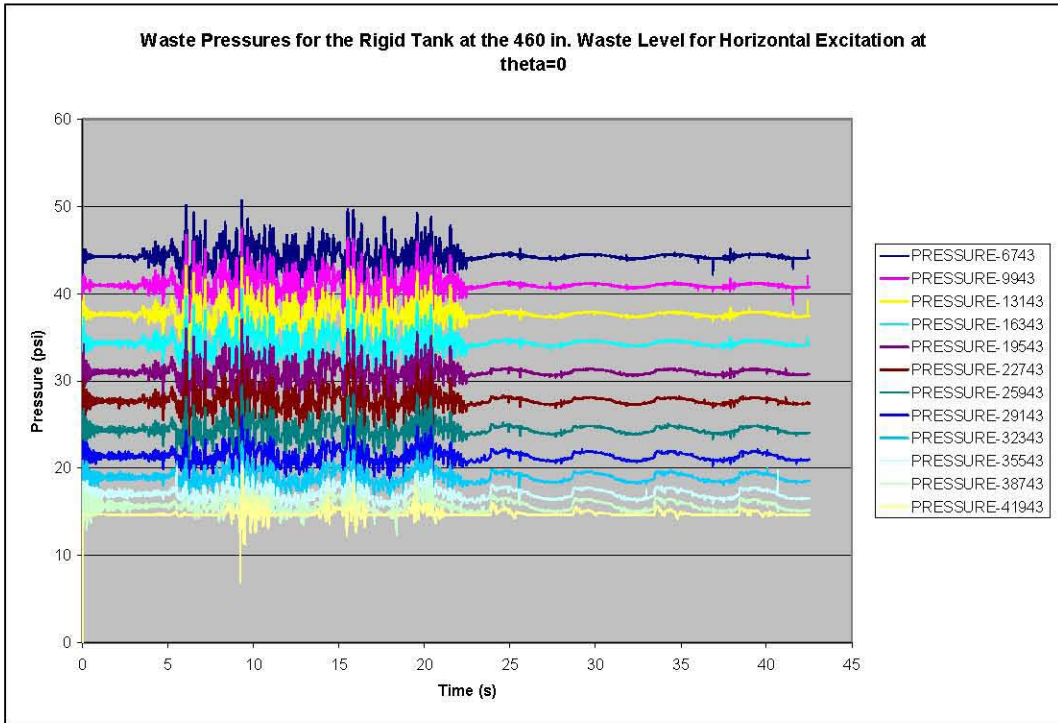


Figure C-21. Waste Pressure Time Histories for the Rigid Tank with 460 Inches of Liquid Under Horizontal Excitation at  $\theta=0$  with Refined Mesh

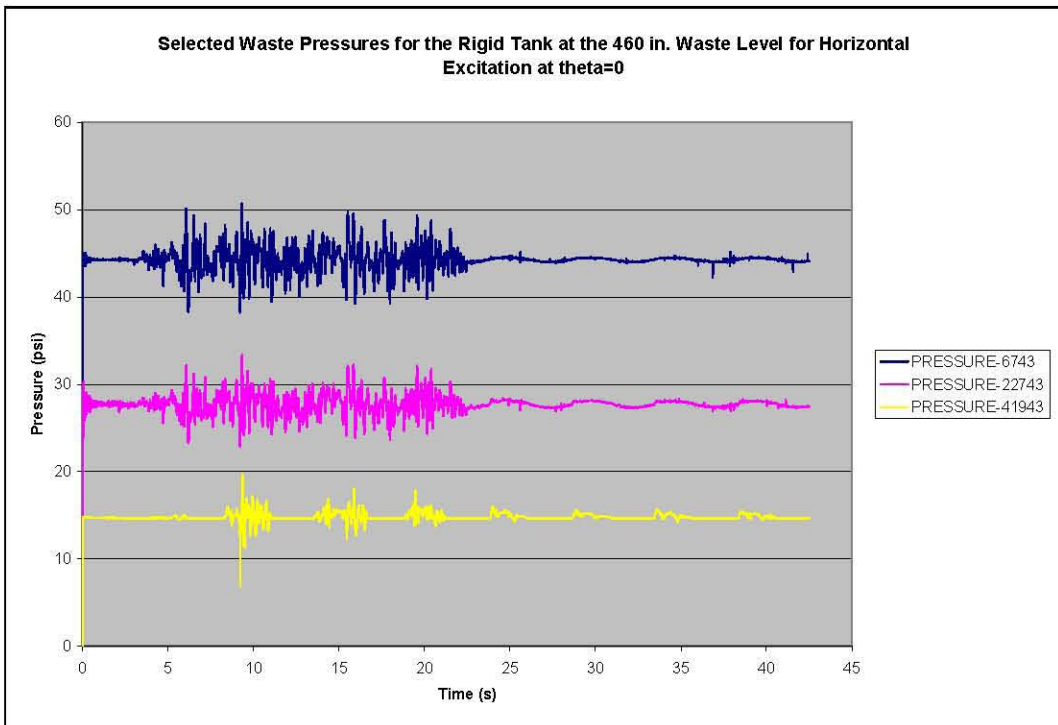


Figure C-22. Selected Liquid Pressure Time Histories for the Rigid Tank at 460 Inches of Liquid Under Horizontal Excitation at  $\theta=0^\circ$  with Refined Mesh

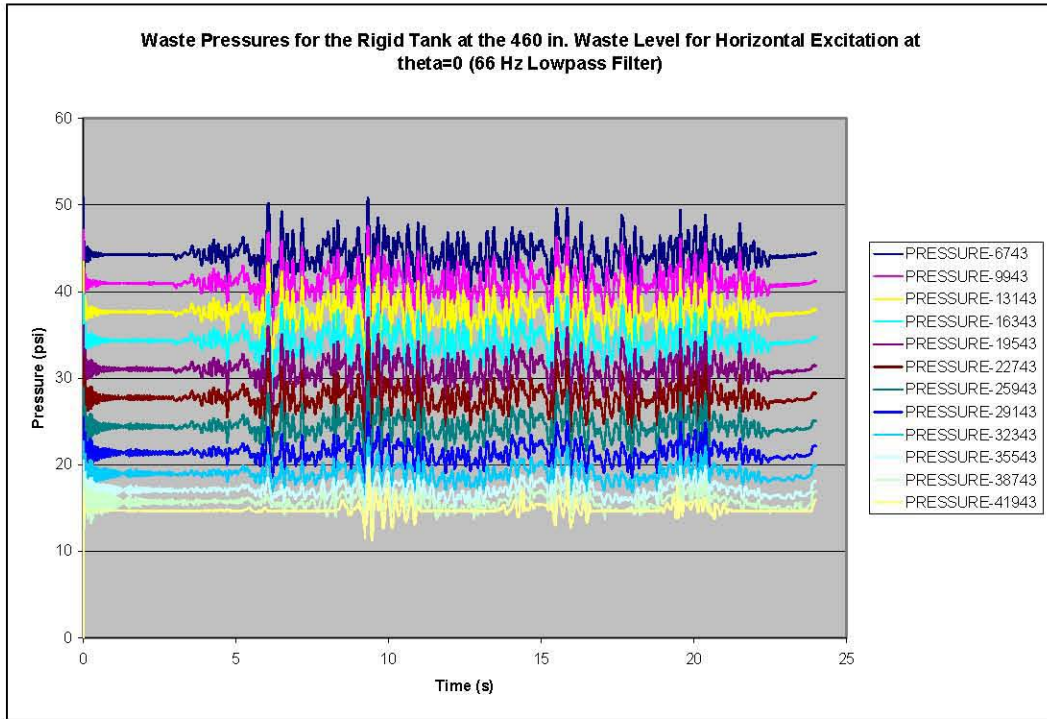


Figure C-23. Waste Pressure Time Histories for the Rigid Tank with 460 Inches of Liquid Under Horizontal Excitation at  $\theta=0^\circ$  with Refined Mesh Using a 66-Hz Lowpass Filter

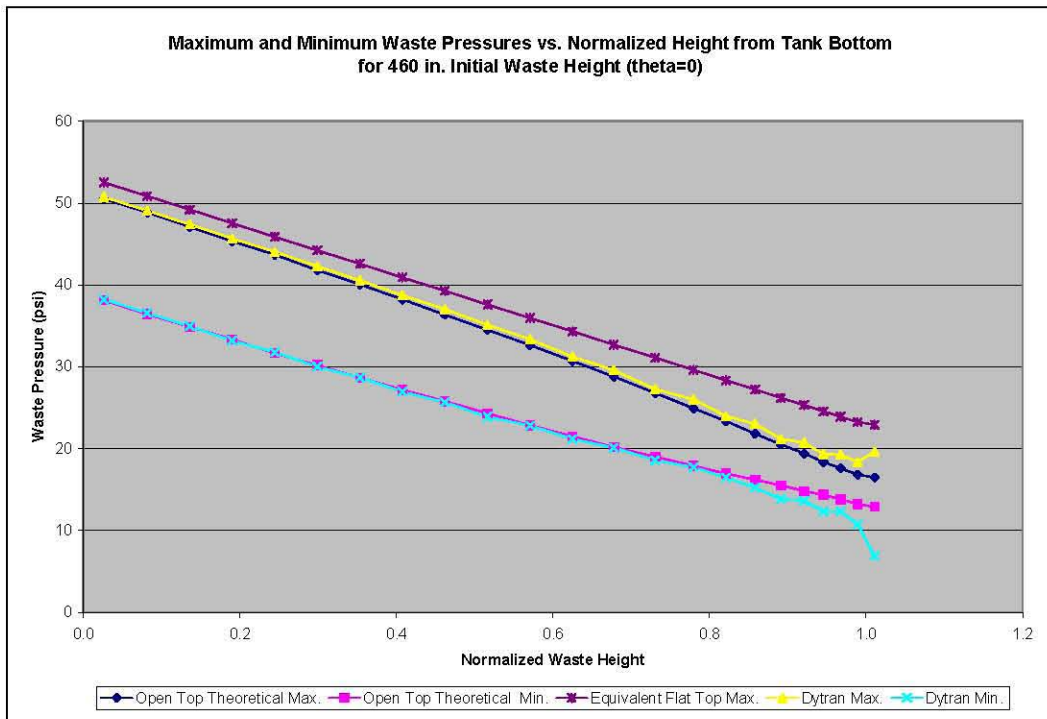


Figure C-24. Maximum and Minimum Liquid Pressures for the Rigid Tank vs. Normalized Height from Tank Bottom for Horizontal Excitation at  $\theta=0^\circ$ , Initial Liquid Height of 460 Inches, and Refined Mesh

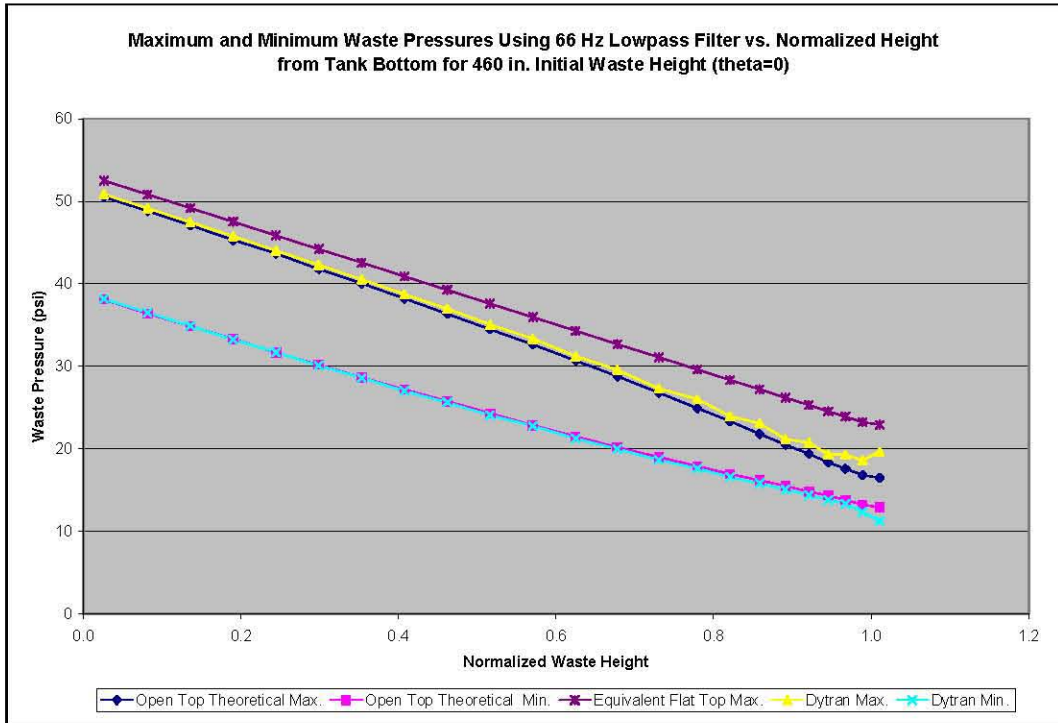


Figure C-25. Maximum and Minimum Liquid Pressures for the Rigid Tank Using a 66-Hz Lowpass Filter vs. Normalized Height from Tank Bottom for Horizontal Excitation at  $\theta=0^\circ$ , Initial Liquid Height of 460 Inches, and Refined Mesh

Plots of pressure time histories for fluid elements located  $45^\circ$  from the plane of excitation are shown in Figure C-26 and Figure C-27. The first plot shows the original data extracted at 10-millisecond intervals, and the second plot shows the histories that were extracted at 1-millisecond intervals and then passed through the 66-Hz lowpass filter. The effect of the filtering is seen most clearly when comparing Figure C-28 and Figure C-29. The filtering somewhat improves the match to the open-tank solution lower in the tank, but primarily it reduces isolated spikes in minimum pressures in fluid elements closer to the free surface.

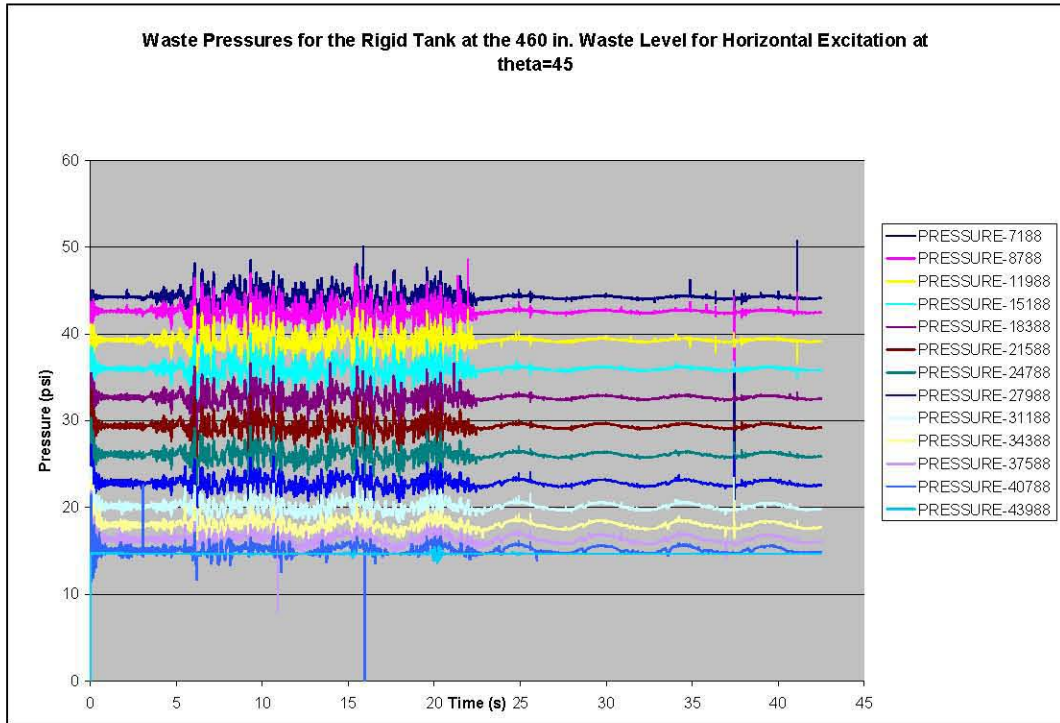


Figure C-26. Waste Pressure Time Histories for the Rigid Tank with 460 Inches of Liquid Under Horizontal Excitation at  $\theta=45^\circ$  with Refined Mesh

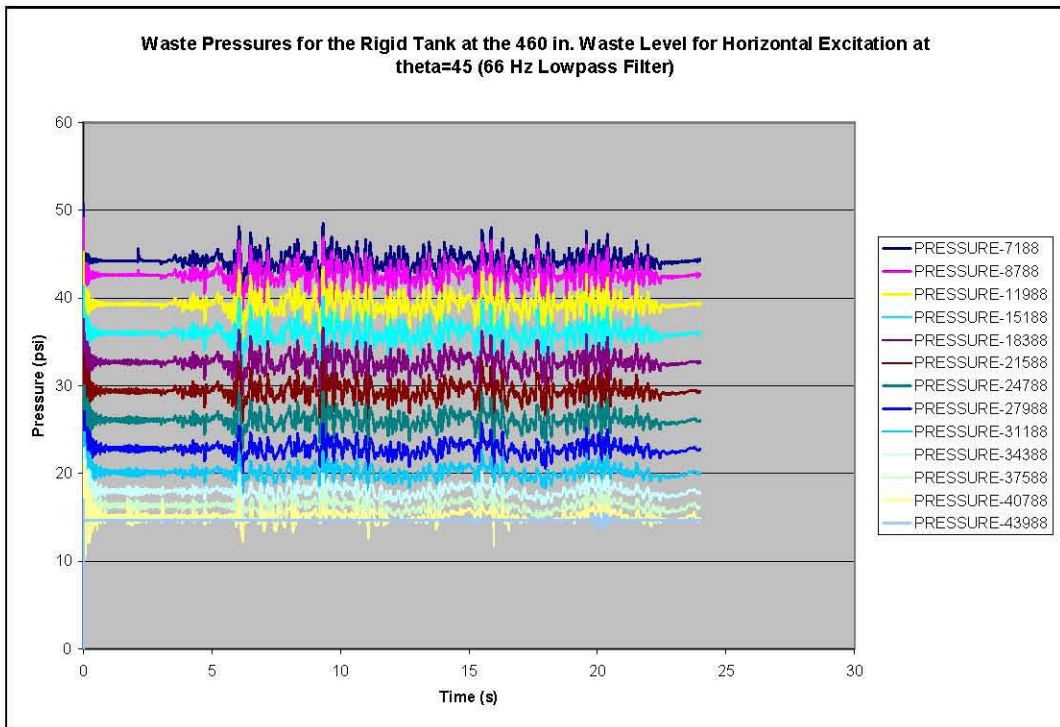


Figure C-27. Waste Pressure Time Histories for the Rigid Tank with 460 Inches of Liquid Under Horizontal Excitation at  $\theta=45^\circ$  with Refined Mesh Using a 66-Hz Lowpass Filter

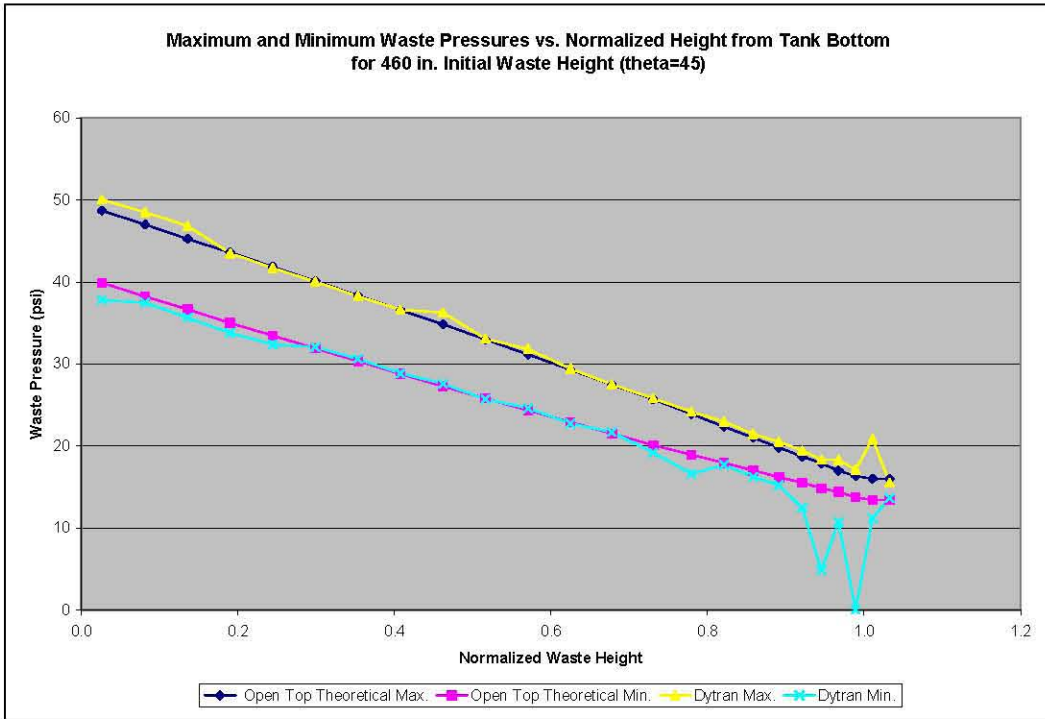


Figure C-28. Maximum and Minimum Liquid Pressures vs. Normalized Height from Tank Bottom for Horizontal Excitation at  $\theta=45^\circ$ , Initial Liquid Height of 460 Inches, and Refined Mesh

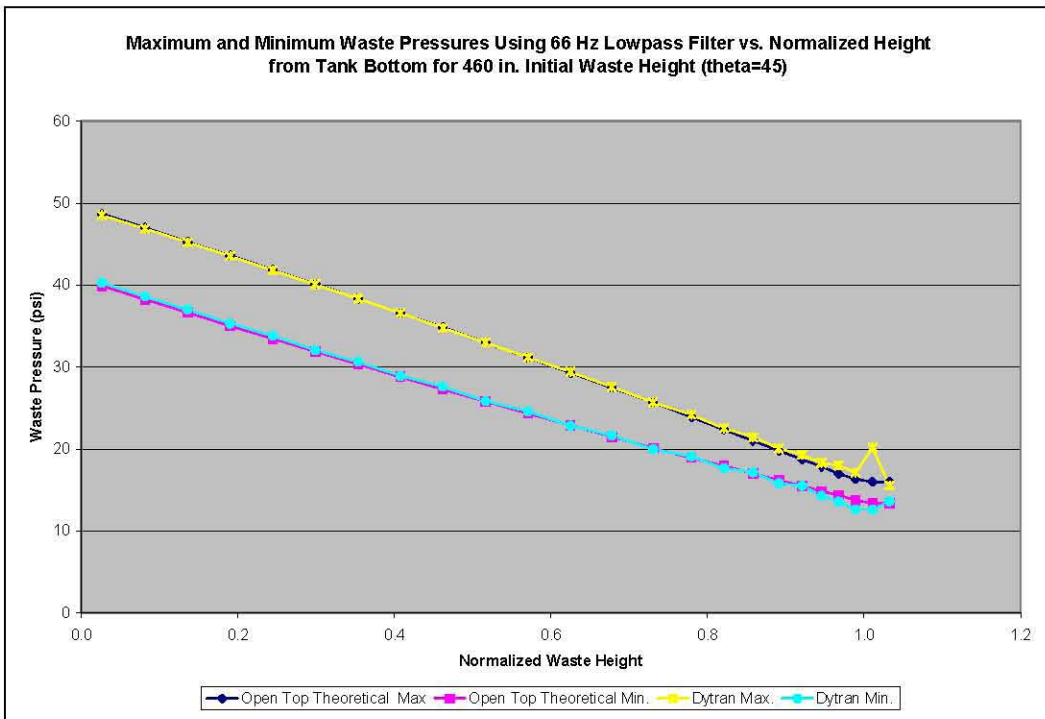


Figure C-29. Maximum and Minimum Liquid Pressures Using 66-Hz Lowpass Filter vs. Normalized Height from Tank Bottom for Horizontal Excitation at  $\theta=45^\circ$ , Initial Liquid Height of 460 Inches, and Refined Mesh

Plots of pressure time histories  $90^\circ$  from the plane of excitation are shown in Figure C-30 and Figure C-31. The first plot shows the original data at 10-millisecond intervals, and the second plot shows the filtered data at 1-millisecond intervals. Maximum and minimum plots for the original and filtered data are shown in Figure C-32 and Figure C-33. All plots show low dynamic pressures at this location as expected.

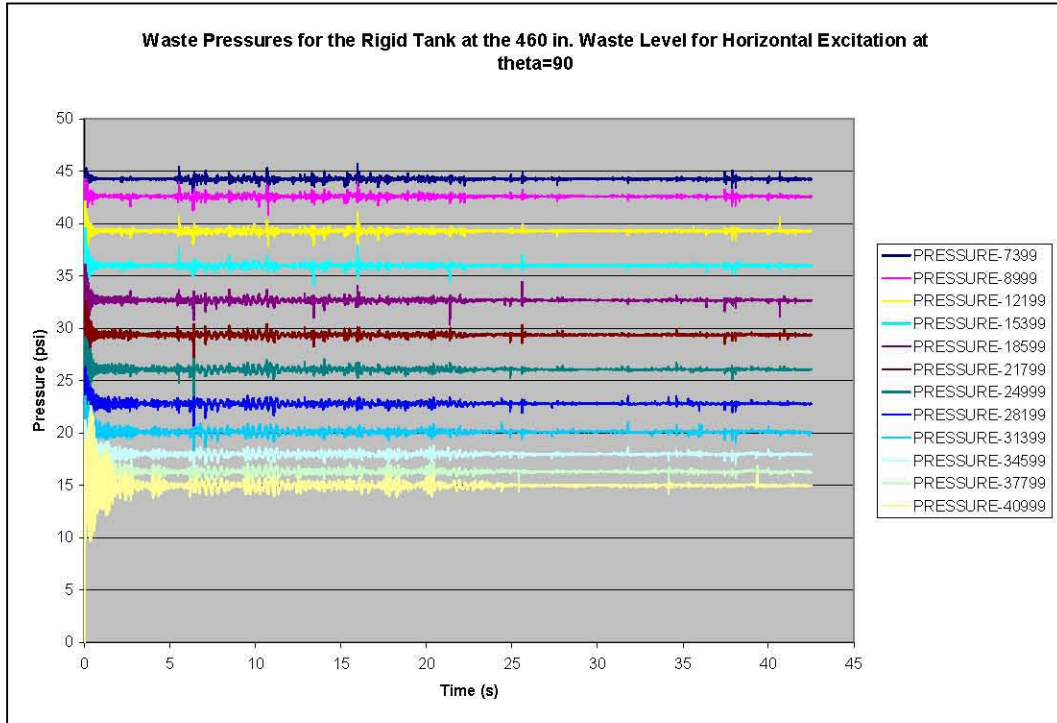


Figure C-30. Waste Pressure Time Histories for the Rigid Tank with 460 Inches of Liquid Under Horizontal Excitation at  $\theta=90^\circ$  with Refined Mesh

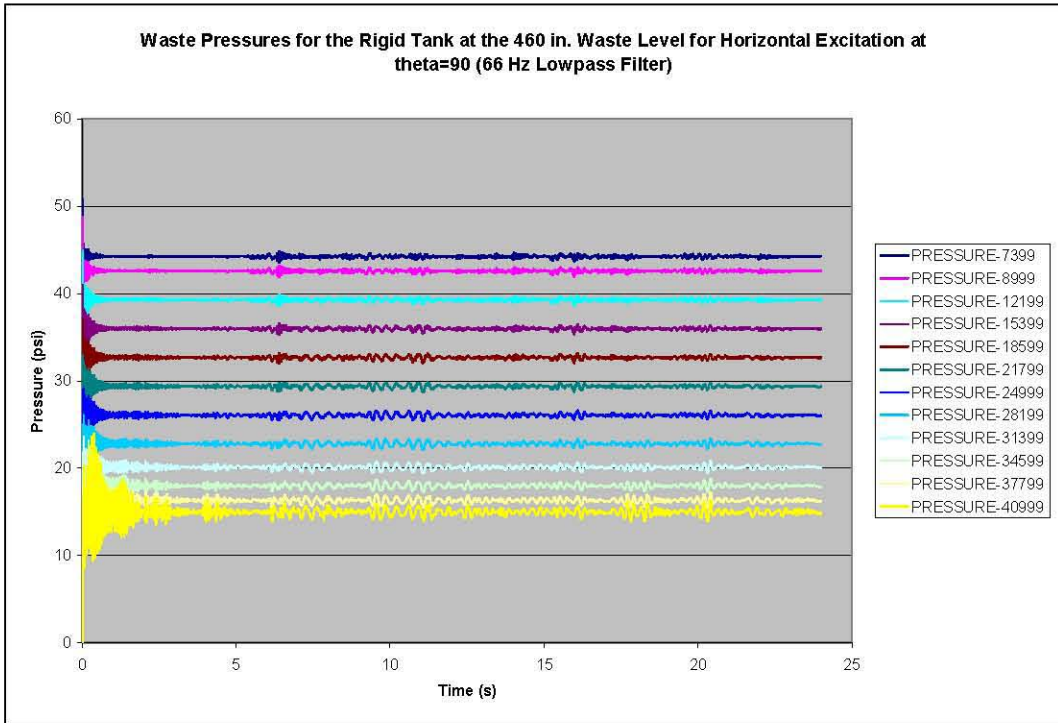


Figure C-31. Waste Pressure Time Histories for the Rigid Tank with 460 Inches of Liquid Under Horizontal Excitation at  $\theta=90^\circ$  with Refined Mesh Using a 66-Hz Lowpass Filter

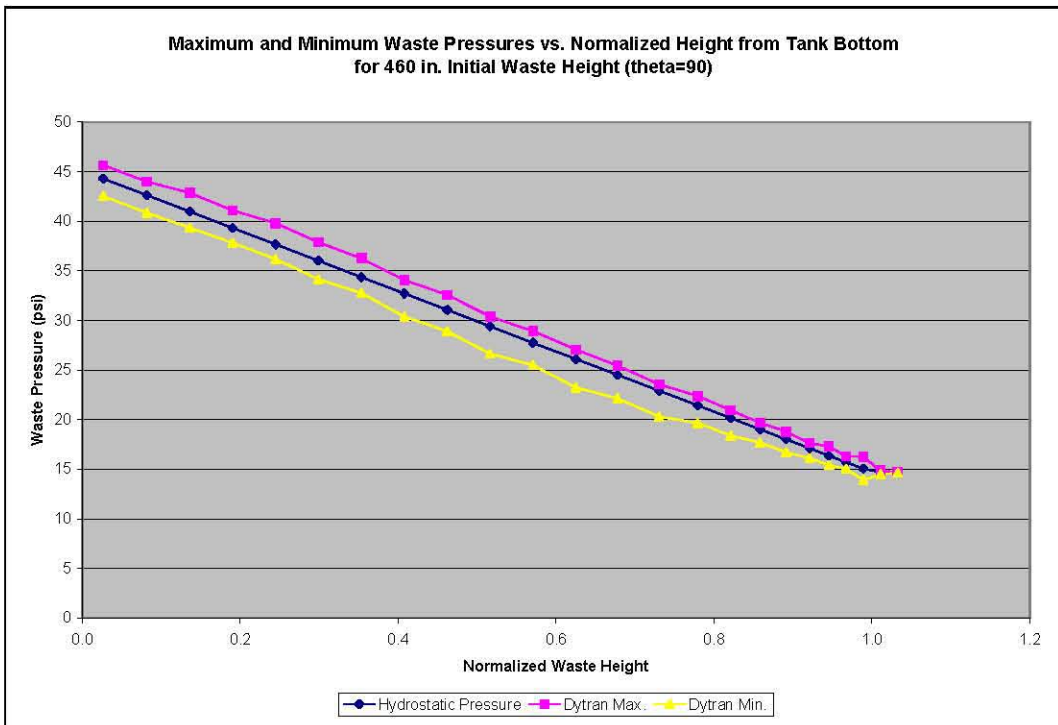


Figure C-32. Maximum and Minimum Liquid Pressures vs. Normalized Height from Tank Bottom for Horizontal Excitation at  $\theta=90^\circ$ , Initial Liquid Height of 460 Inches, and Refined Mesh

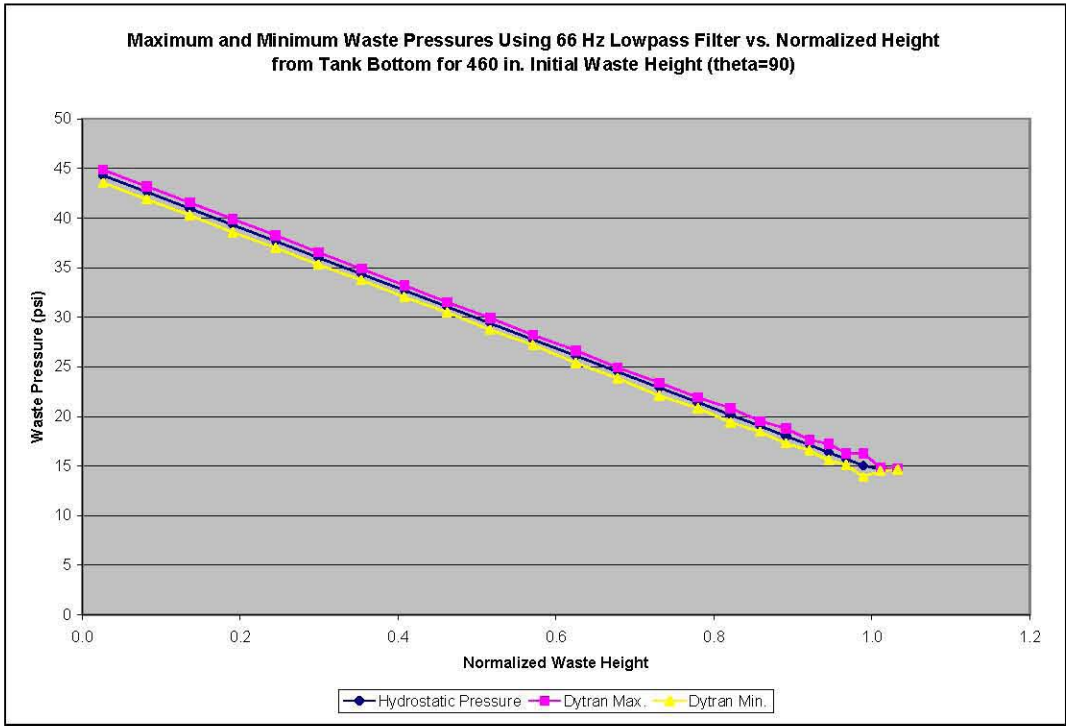


Figure C-33. Maximum and Minimum Liquid Pressures Using 66-Hz Lowpass Filter vs. Normalized Height from Tank Bottom for Horizontal Excitation at  $\theta=90^\circ$ , Initial Liquid Height of 460 Inches, and Refined Mesh

### C.6.3 Maximum Slosh Height

Slosh height traces for the domed rigid tank and for an open rigid tank (vertical walls with no dome) at the 460-in. initial liquid height are shown in Figure C-34. The peak slosh height predicted for the domed tank is 27.4 inches, while the peak slosh height for the open tank is 26.9 inches. The maximum theoretical value for an open tank is 25.2 inches per the methodology in BNL (1995) and 29.7 inches using the procedure in Malhotra (2005).

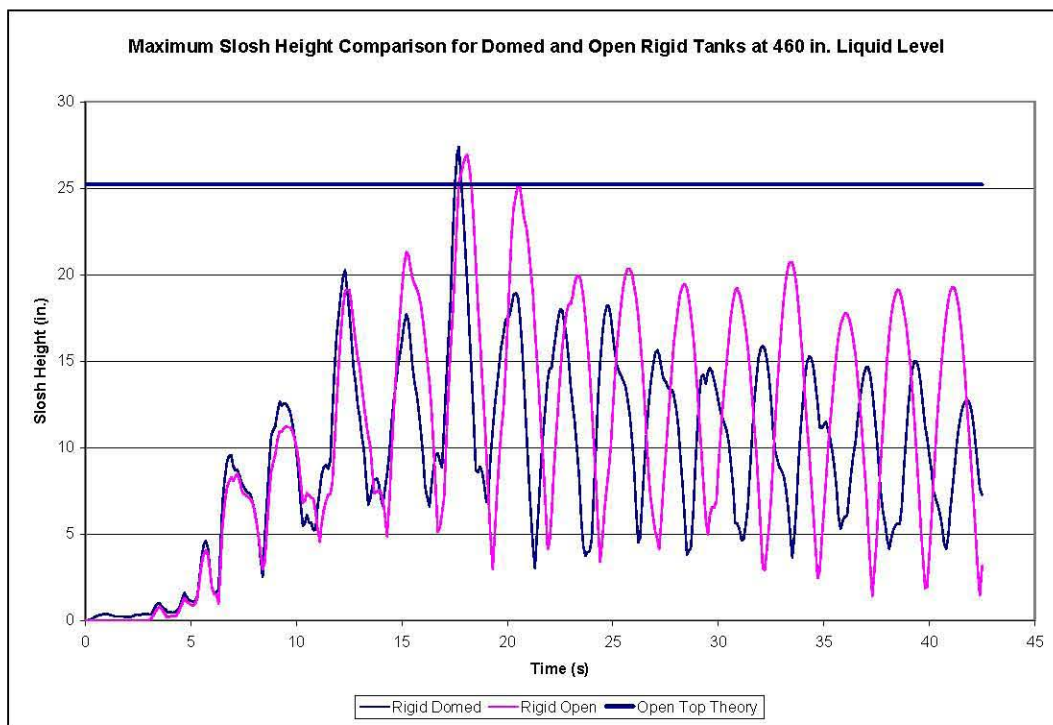


Figure C-34. Maximum Slosh Height Comparison for Initial Liquid Height of 460 Inches

## C.7 Flexible Tank Results

In the case of the flexible wall tank, the gravity load was run for 5 seconds before beginning the seismic input. The 20.48-second seismic input was followed by 20 seconds of unforced motion giving a total simulation time of 45.5 seconds. In the initial simulation, the reaction forces, liquid pressures, and tank stresses were extracted every 10 milliseconds. In order to further investigate high-frequency response in the pressures, the problem was rerun up to a time of 27.5 seconds (which completely captures the seismic event) with forces, pressures, and stresses extracted every 1 millisecond. Results from both simulations are presented.

### C.7.1 Characterization of Damping

The value of the dynamic relaxation factor was set to 0.02 based on the initial decay of the vertical coupling surface reaction force during gravity loading. As discussed in Section 5.1 of the main body of this report, the intent was to achieve an effective damping of 2-4% for the impulsive response of the tank and liquid system. The initial decay of the vertical reaction force actually represents the effective damping of the breathing mode response of the system, but this was expected to be a good indicator of the impulsive response of the system. Based on the decay of the breathing mode response, the effective impulsive damping is approximately 3.5% of critical.

A more direct way of determining the effective damping for the impulsive response may be to quantify the decay of the horizontal reaction force immediately following the cessation of the seismic excitation. Based on this approach, the effective damping for the impulsive response is in the range of 4.3% to 5.2% of critical damping.

Reference to benchmark solutions calculated at both 3.5% and 5.5% damping will be made in the following sections.

## C.7.2 Hydrodynamic Forces

The theoretical impulsive and convective frequencies for an open flexible wall tank at the 460-inch liquid level are 6.5 Hz and 0.196 Hz, respectively. The impulsive and convective frequencies for the domed flexible wall tank from the Dytran<sup>®</sup> simulation are 6.25 Hz and 0.207 Hz, respectively. The slight shift in the impulsive frequency as well as the slight uncertainty in the effective impulsive damping both affect the spectral acceleration used in the benchmark solution. References are made to two benchmark solutions – one at the theoretical impulsive frequency of 6.5 Hz using 3.5% damping, and the other at the Dytran<sup>®</sup> frequency of 6.25 Hz using 5.5% damping.

Because spectral accelerations decrease between 6.25 Hz and 6.5 Hz, both are intermediate solutions. That is, the upper bound solution would occur at 6.25 Hz using the lower damping value of 3.5%, and the lower bound solution would occur using the lower spectral accelerations at 6.5 Hz and the higher damping of 5.5%.

The horizontal and vertical coupling surface reaction forces are shown in Figure C-35. The maximum horizontal reaction force reported by Dytran<sup>®</sup> is  $9.97 \times 10^6$  lbf. This result is 7% lower than the value of  $1.07 \times 10^7$  lbf predicted for a flexible wall open-top tank with the theoretical frequency of 6.5 Hz at 3.5% damping and 1% lower than the value of  $1.01 \times 10^7$  lbf for an open wall tank at 6.25 Hz using 5.5% damping. The conservative estimates provided by Appendix D in BNL (1995) and Malhotra (2005) for an equivalent flat-top tank with a roof height of 484 inches per Kennedy (2003) are  $1.28 \times 10^7$  lbf and  $1.32 \times 10^7$  lbf, respectively, based on a 6.5 Hz impulsive frequency and 3.5% damping for the BNL estimate, and 5.4 Hz and 3.5% damping for the Malhotra estimate.

Normally one would expect that the reaction force for the domed tank would be greater than that for the corresponding open tank. However, the comparison here is not a direct one since some of the interaction between the tank and contained liquid in this problem occurs in the rigid dome area. The interaction between the liquid and rigid portion of the tank is not amplified by the impulsive frequency, and this may lead to a slightly lower overall reaction force.

The effective damping present in the flexible wall configuration was evaluated by quantifying the decay in the vertical reaction force during the initial period in which the gravity load is equilibrating in the absence of seismic excitation. The initial decay of the vertical reaction force during gravity loading is shown in Figure C-35 and in more detail in Figure C-36. The response of the tank to the initial gravity load is the breathing mode response with a theoretically calculated frequency of 5.43 Hz. The breathing mode frequency of the Dytran<sup>®</sup> response that is shown in Figure C-36 is 5.41 Hz, and the decay of the response corresponds to an effective critical damping ratio of approximately 3.5%.

The horizontal reaction force immediately following the cessation of the seismic excitation is shown as Figure C-37. This brief transient is expected to be a good indicator of the impulsive response of the system. The frequency of this response is 6.25 Hz compared to a theoretical impulsive frequency of 6.48 Hz for an open tank. The decay of the horizontal reaction force is shown in more detail in Figure C-38. A nearly complete decay of the impulsive response occurs in 14 to 17 cycles indicating an effective damping for the impulsive mode of 4.3% to 5.2% of critical damping using this approach.

The convective response following the seismic excitation is shown as Figure C-39. The convective frequency from the dome tank simulation is 0.207 Hz compared to a theoretical convective frequency of 0.196 Hz for an open tank. This is the same result reported for the rigid tank configuration. The slight upward shift of the convective frequency is consistent with interaction between the liquid and the dome. Similar results were reported in Abatt and Rinker (2008) for flat-top tanks.

The peak convective reaction force from the Dytran<sup>®</sup> simulation was approximately  $3.0 \times 10^5$  lbf. This is the same value as for the rigid tank, and as before it is less than the value of  $5.39 \times 10^5$  predicted for an open tank.

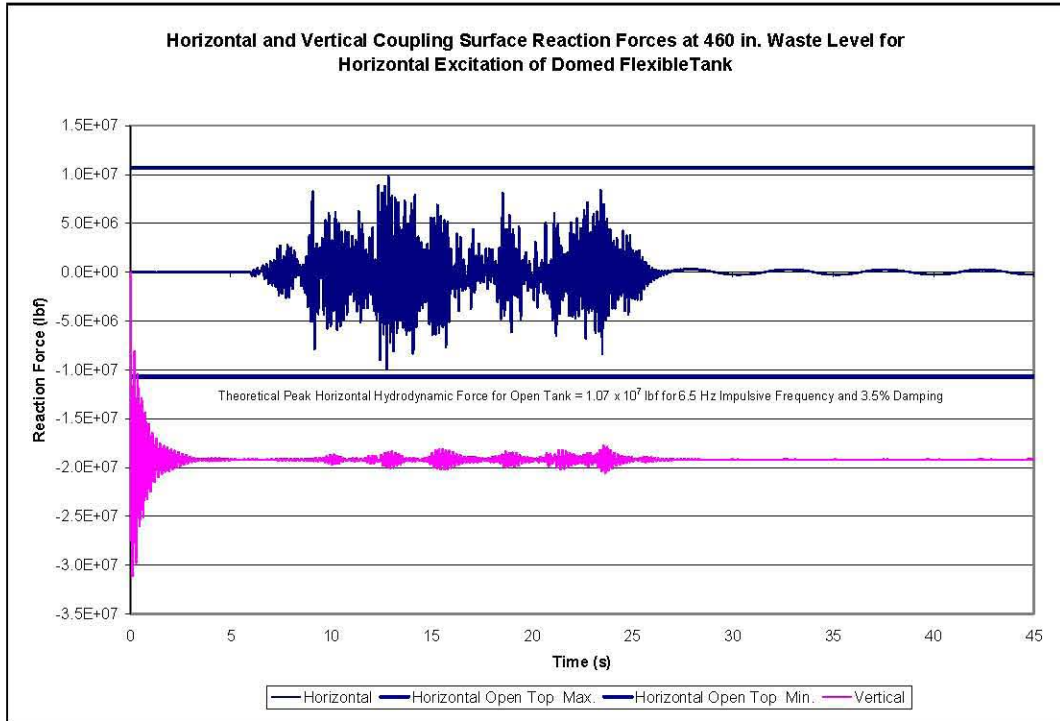


Figure C-35. Horizontal and Vertical Coupling Surface Reaction Forces for Flexible Tank at 460-Inch Waste Level Under Horizontal Seismic Excitation – Refined Mesh

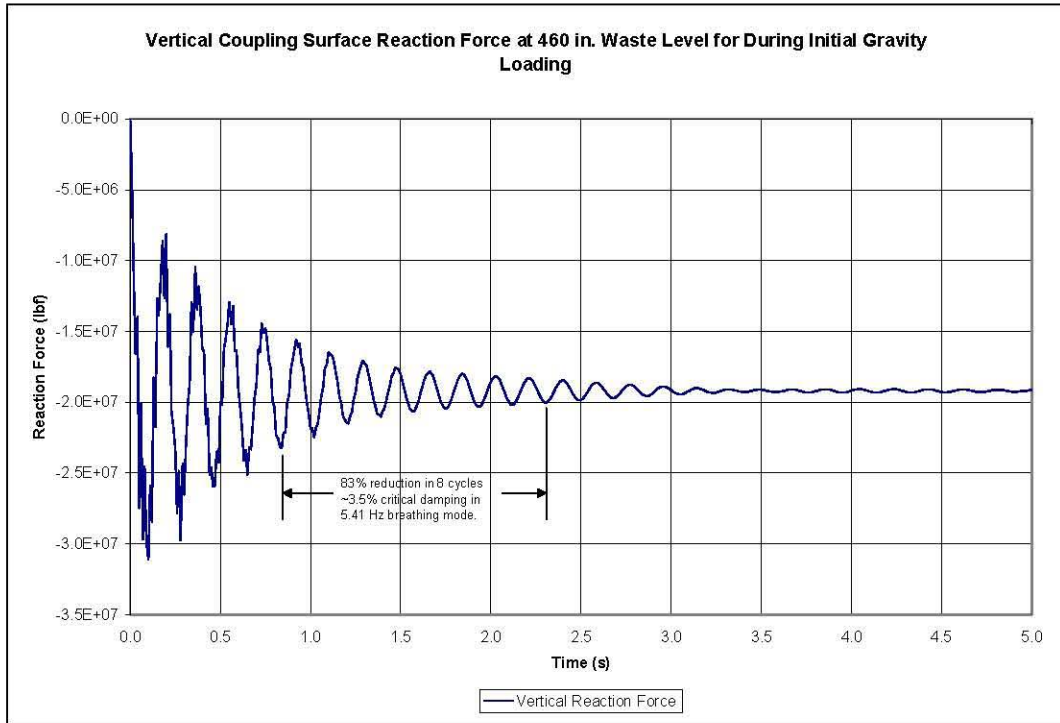


Figure C-36. Vertical Coupling Surface Reaction Force During Initial Gravity Loading

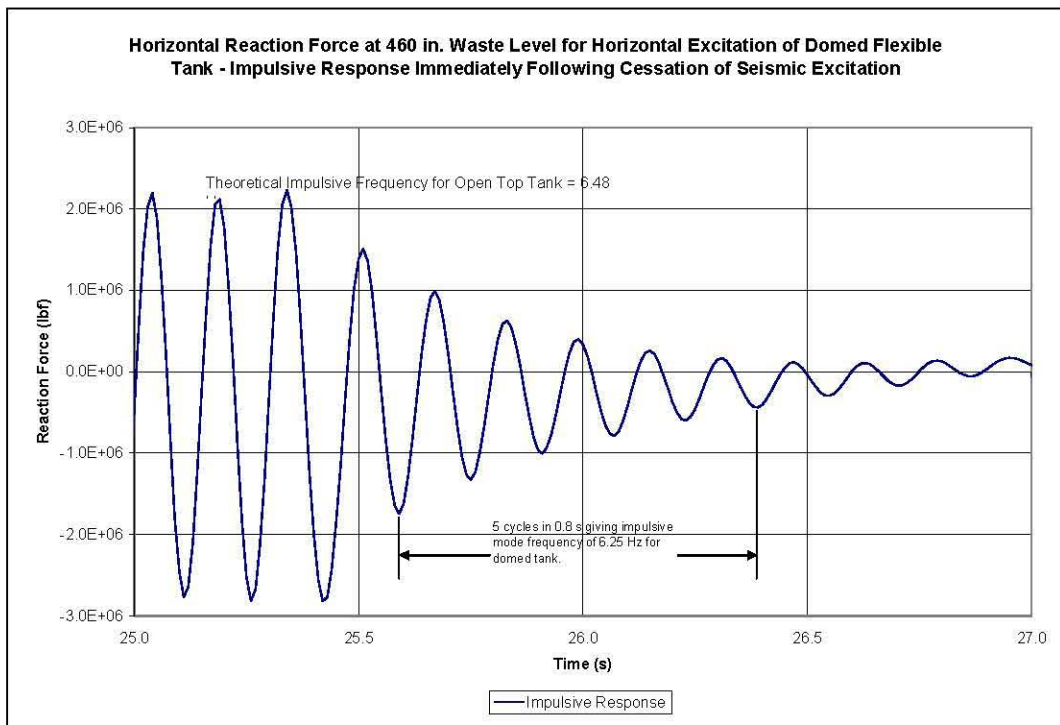


Figure C-37. Horizontal Coupling Surface Reaction Force Immediately Following Cessation of Seismic Excitation – Impulsive Response

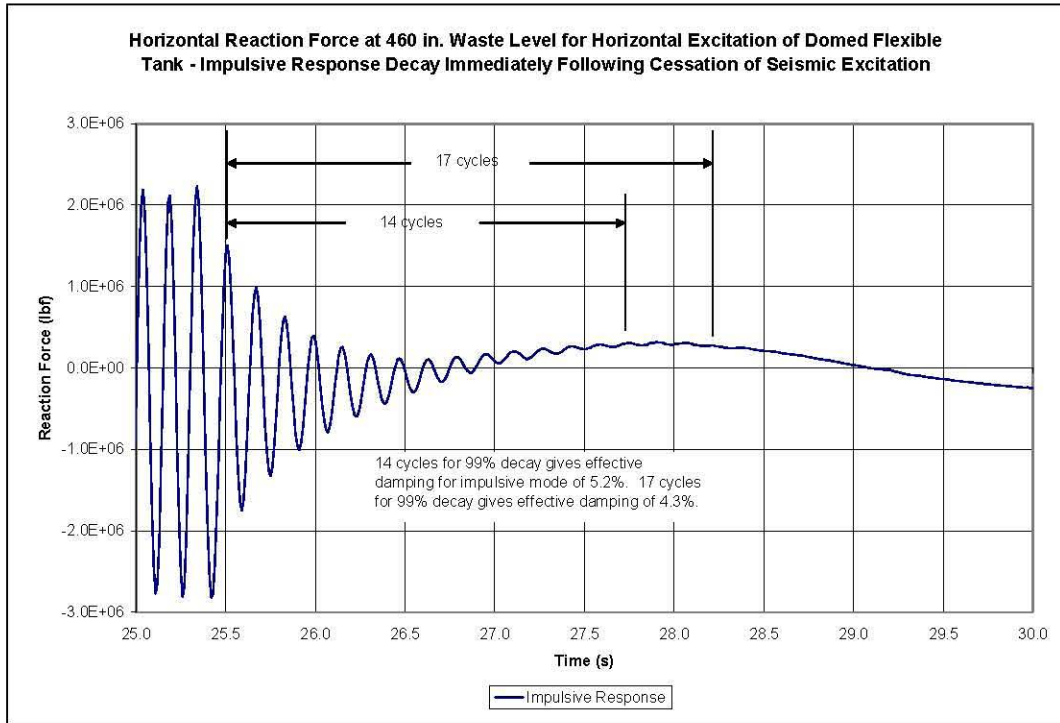


Figure C-38. Horizontal Reaction Force Immediately Following Cessation of Seismic Excitation – Decay of Impulsive Response

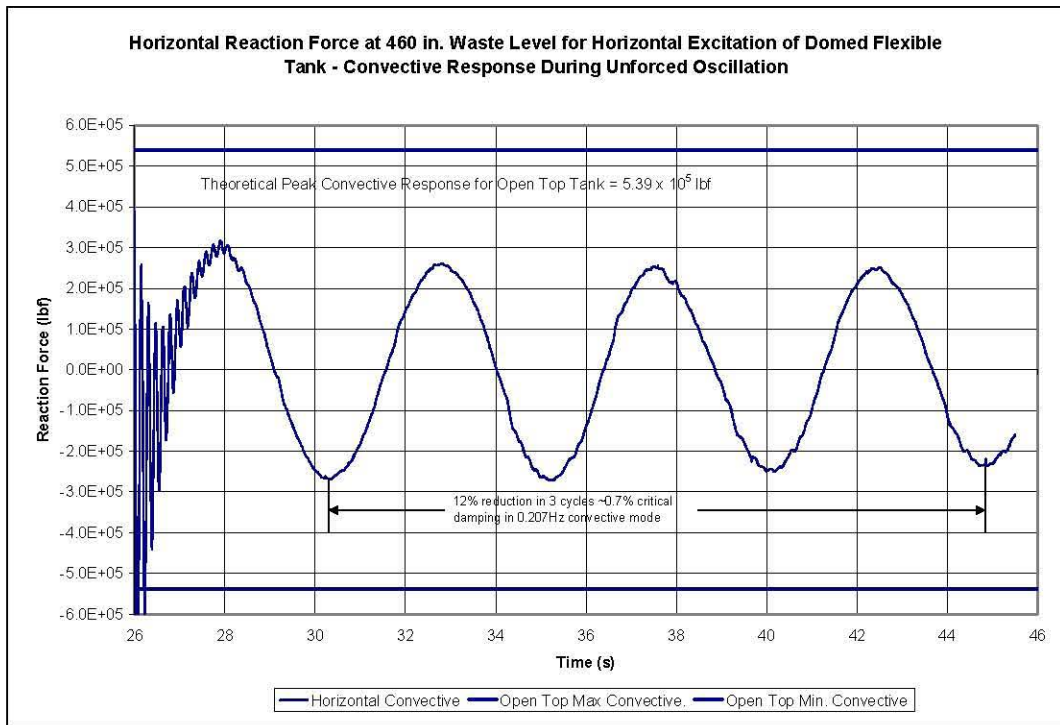


Figure C-39. Horizontal Coupling Surface Reaction Force for Rigid Tank at 460-Inch Waste Level Under Horizontal Seismic Excitation – Convective Response During Unforced Oscillation

### C.7.3 Liquid Pressures

Estimates of peak wall pressures for fluid elements along the plane of excitation and 45° from the plane of excitation are summarized in Table C-9 and Table C-10, respectively. Each table shows the wall pressures predicted for an open tank and for an equivalent flat-top tank according to BNL (1995). As before, the roof of the equivalent flat-top tank is 484 inches above the bottom of the tank per Kennedy (2003). The dynamic pressures in these two tables are based on an impulsive frequency of 6.5 Hz, and 3.5% damping. The 45° location lies outside the central angle of 17.8° per Appendix D in BNL (1995) so that the open-tank solution and equivalent flat-top tank solution are the same in this region. This is reflected in Table C-10.

**Table C-9.** Estimated Maximum Wall Pressures for Horizontal Excitation in Flexible Open and Equivalent Flat-Top Tanks at 460-Inch Waste Level for Elements at  $\theta=0$

<b>“plusx_els”</b>					
<b>Element No.</b>	<b>Hydrostatic Pressure (psi absolute)</b>	<b>Peak Hydrodynamic Pressure for Open Tank (psi absolute)</b>	<b>Peak Hydrodynamic Pressure for Equivalent Flat-Top Tank (psi absolute)</b>	<b>Peak Total Pressure for Open Tank (psi absolute)</b>	<b>Peak Total Pressure for Equivalent Flat-Top Tank (psi absolute)</b>
5143	15.0	3.0	29.7	18.0	44.8
3543	15.7	4.1	29.7	19.8	45.4
1943	16.4	5.2	29.7	21.6	46.1
25943	17.0	6.3	29.7	23.3	46.7
22743	18.3	8.3	29.7	26.6	48.1
19543	19.7	10.1	29.7	29.8	49.4
16343	21.0	11.6	29.7	32.6	50.7
13143	22.3	13.0	29.7	35.3	52.0
9943	23.6	14.3	29.7	37.9	53.4
6743	24.9	15.4	29.7	40.3	54.7
72343	26.3	16.4	29.7	42.7	56.0
69143	27.6	17.3	29.7	44.9	57.3
65943	28.9	18.1	29.7	47.0	58.6
62743	30.2	18.8	29.7	49.0	60.0
59543	31.6	19.5	29.7	51.1	61.3
56343	32.9	20.0	29.7	52.9	62.6
53143	34.2	20.5	29.7	54.7	64.0
49943	35.5	20.9	29.7	56.4	65.3
46743	36.9	21.3	29.7	58.2	66.6
43543	38.2	21.6	29.7	59.8	67.9
40343	39.5	21.9	29.7	61.4	69.3
37143	40.9	22.1	29.7	63.0	70.6
33943	42.2	22.2	29.7	64.4	71.9
30743	43.5	22.3	29.7	65.8	73.2
27543	44.8	22.3	29.7	67.1	74.6

Table C-10. Estimated Maximum Wall Pressures for Horizontal Excitation in Flexible Open and Equivalent Flat-Top Tanks at 460-Inch Waste Level for Elements at  $\theta=45^\circ$

<b>“press_45”</b>			
<b>Element No.</b>	<b>Hydrostatic Pressure (psi absolute)</b>	<b>Peak Hydrodynamic Pressure for Open or Equivalent Flat-Top Tank (psi absolute)</b>	<b>Peak Total Pressure for Open or Equivalent Flat-Top Tank (psi absolute)</b>
5588	15.0	2.1	17.1
3988	15.7	2.9	18.6
2388	16.4	3.7	20.1
26388	17.0	4.5	21.5
23188	18.3	5.9	24.5
19988	19.7	7.1	26.8
16788	21.0	8.2	29.2
13588	22.3	9.2	31.5
10388	23.6	10.1	33.7
7188	24.9	10.9	35.8
72788	26.3	11.6	37.9
69588	27.6	12.2	39.8
66388	28.9	12.8	41.7
63188	30.2	13.3	43.5
59988	31.6	13.8	45.4
56788	32.9	14.2	47.1
53588	34.2	14.5	48.7
50388	35.5	14.8	50.3
47188	36.9	15.1	52.0
43988	38.2	15.3	53.5
40788	39.5	15.5	55.0
37588	40.9	15.6	56.5
34388	42.2	15.7	57.9
31188	43.5	15.7	59.2
27988	44.8	15.8	60.6

Pressures were monitored along the plane of excitation at the 0 and 180° positions, and at 45° and 90° from the plane of excitation. Pressure time histories for individual fluid elements and maximum and minimum pressures as a function of normalized wall height are shown in the following plots.

Pressure time histories for selected fluid elements near the wall of the tank at  $\theta=0^\circ$  are shown in Figure C-40 and Figure C-41. As in the case of the rigid tank, some of the time history plots show isolated peaks that are characteristic of a high-frequency response that may be due to spurious numerics, and that in any case are unimportant to any structural analysis.

In order to remove the unnecessary high-frequency response, the simulation was rerun up to 27.5 seconds simulation time with pressures extracted every 1 millisecond instead of every 10 millisecond. The resulting pressure time histories were then post-processed using a 66-Hz lowpass 6-pole Butterworth filter

with re-filtering for phase correction. The cutoff frequency of 66 Hz was selected since it is twice the 33-Hz frequency that is commonly accepted as the cutoff frequency above which no dynamic amplification will occur.

The filtered pressure time histories at  $\theta=0^\circ$  are shown as Figure C-42. The pressures appear essentially the same as the unfiltered time histories shown in Figure C-40, showing that little high-frequency content was present in the original time histories.

The original unfiltered maximum and minimum pressures at  $\theta=0^\circ$  are shown in Figure C-43 and the filtered maximum and minimum pressures are shown in Figure C-44. In both plots, the results of the Dytran<sup>®</sup> simulation are compared with the theoretical open-top tank pressure distributions at 6.5-Hz impulsive frequency and 3.5% damping and at 6.25-Hz impulsive frequency and 5.5% damping. The maximum pressures for the equivalent flat-top tank at 6.5-Hz impulsive frequency and 3.5% damping are also shown. The wall pressures from the Dytran<sup>®</sup> solution are close to the open-tank solutions and only deviate somewhat near the liquid-free surface. The equivalent flat-top tank estimate of the wall pressures is quite conservative relative to the Dytran<sup>®</sup> solution.

The maximum and minimum pressures are plotted up to the normalized wall height of 1.01, or 465 inches. Above this level, the pressure traces contained spurious data, and thus were not included in the plots.

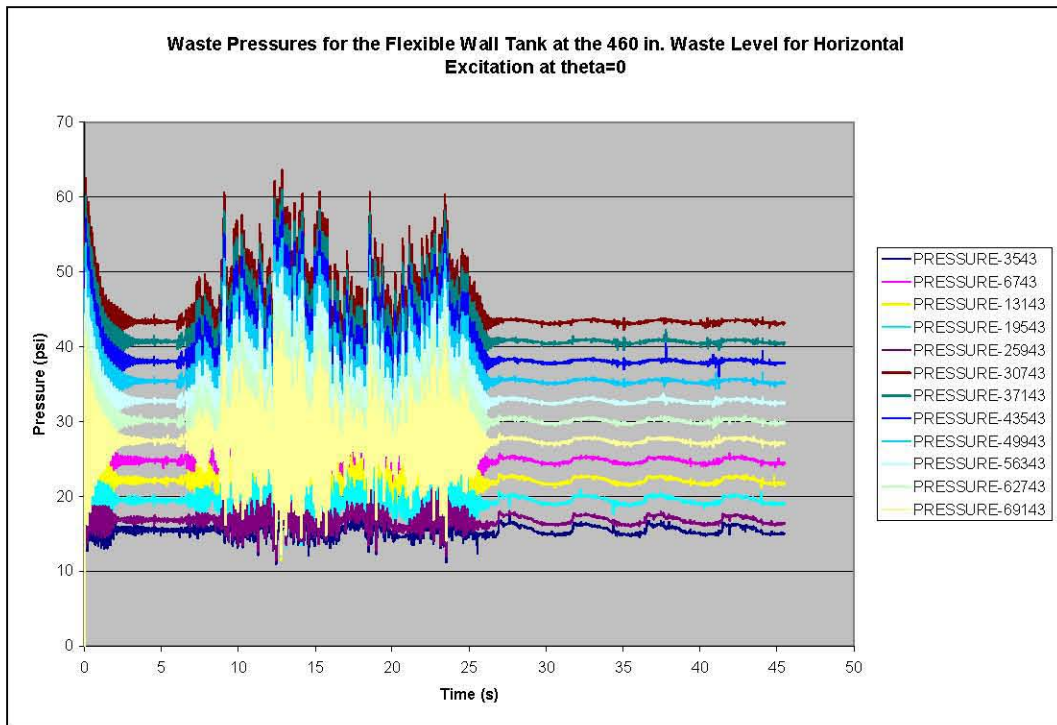


Figure C-40. Liquid Pressure Time Histories for the Flexible Wall Tank with 460 Inches of Liquid Under Horizontal Excitation at  $\theta=0^\circ$  with Refined Mesh

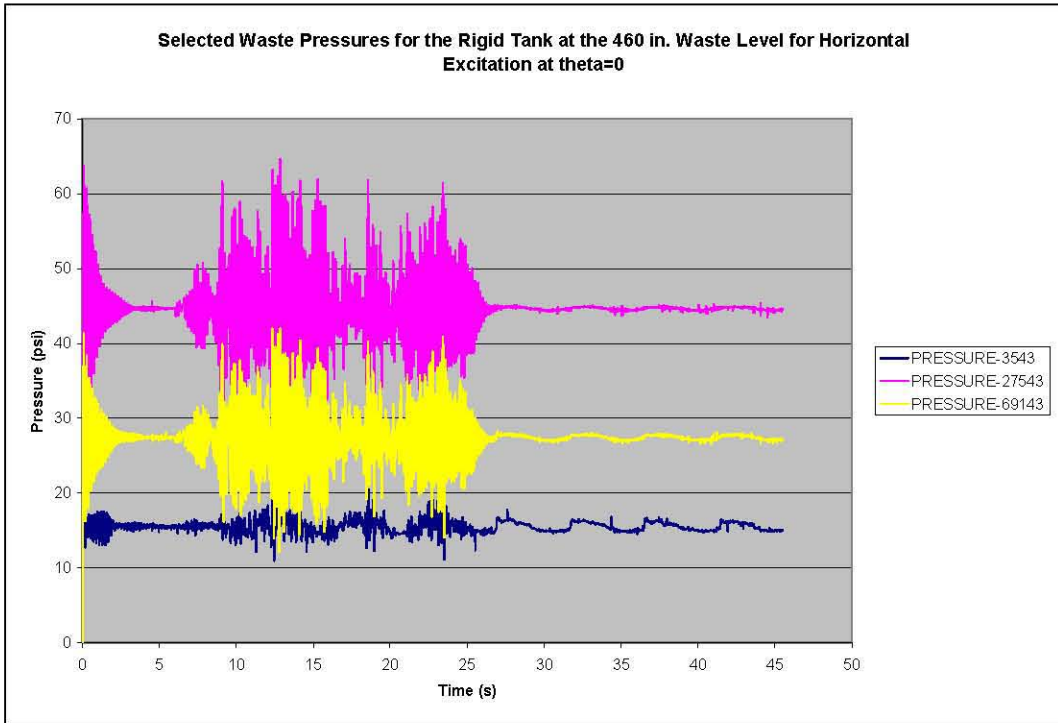


Figure C-41. Selected Liquid Pressure Time Histories for the Flexible Wall Tank with 460 Inches of Liquid Under Horizontal Excitation at  $\theta=0^\circ$  with Refined Mesh

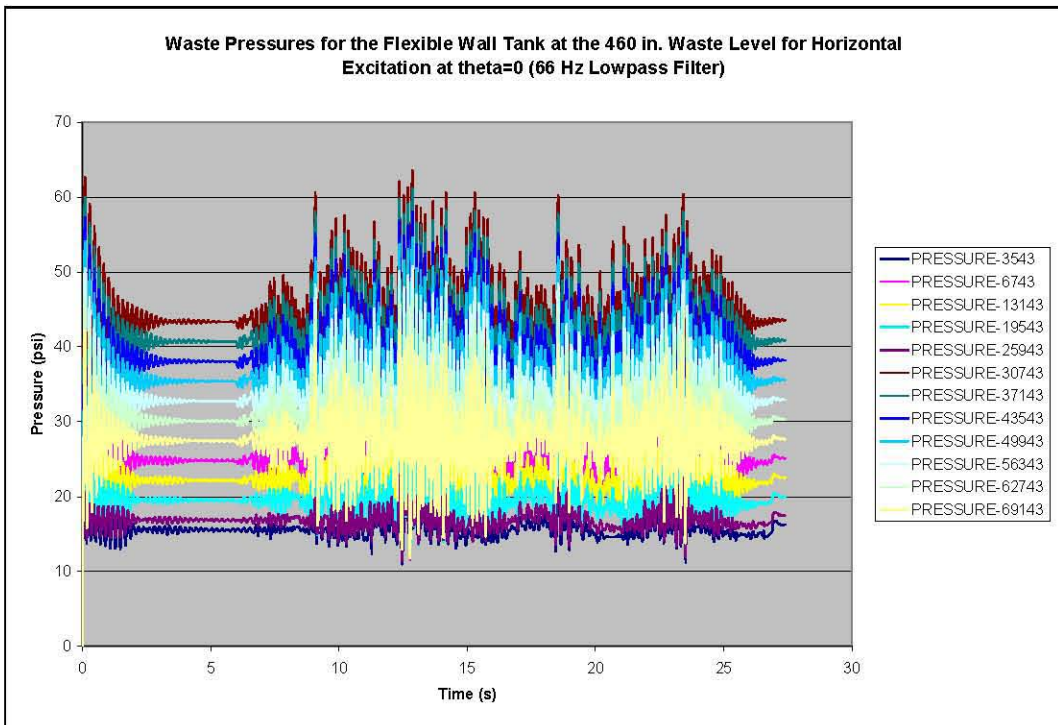


Figure C-42. Waste Pressure Time Histories for the Flexible Wall Tank with 460 Inches of Liquid Under Horizontal Excitation at  $\theta=0^\circ$  with Refined Mesh Using a 66-Hz Lowpass Filter

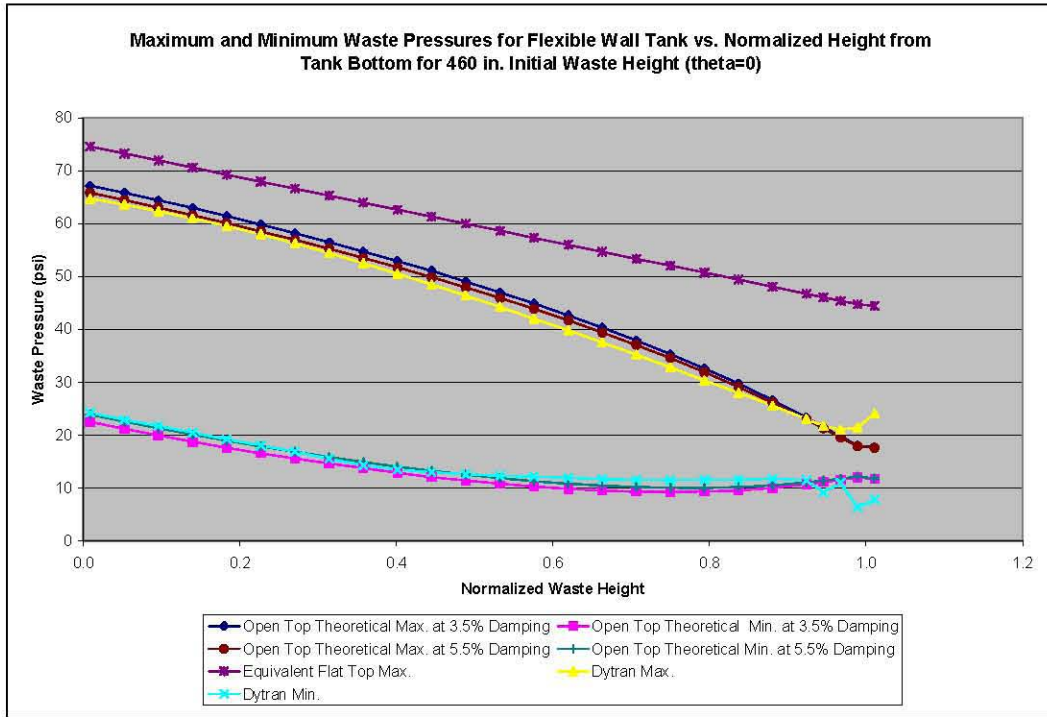


Figure C-43. Maximum and Minimum Liquid Pressures vs. Normalized Height from Tank Bottom for Horizontal Excitation at  $\theta=0^\circ$ , Initial Liquid Height of 460 Inches, and Refined Mesh

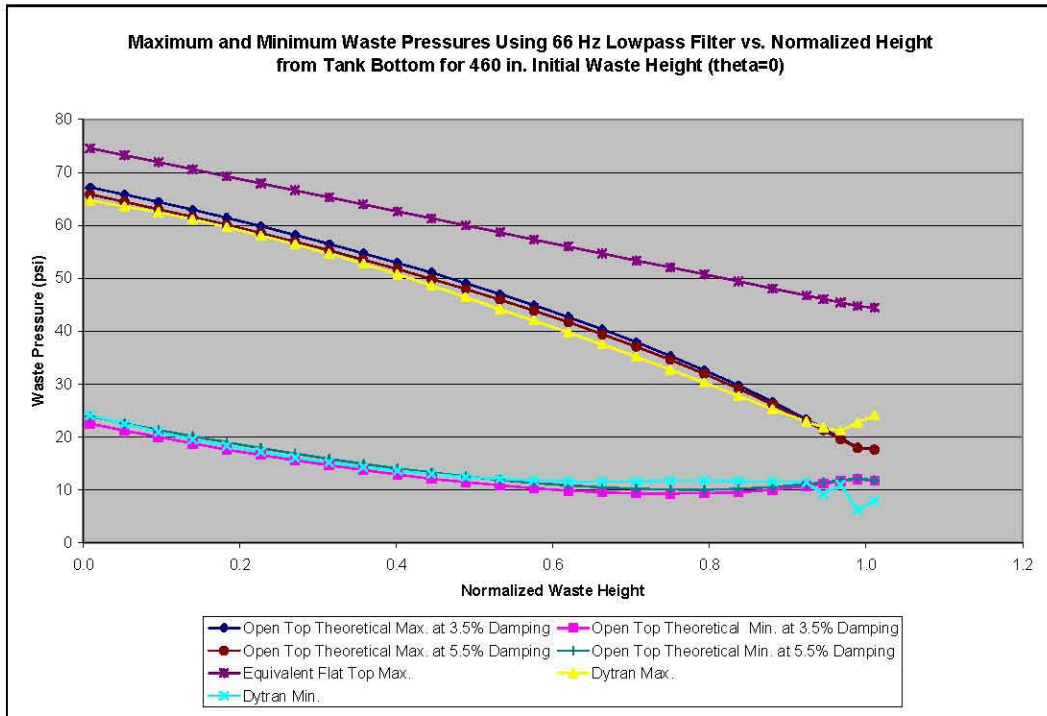


Figure C-44. Maximum and Minimum Liquid Pressures for the Flexible Wall Tank Using a 66-Hz Lowpass Filter vs. Normalized Height from Tank Bottom for Horizontal Excitation at  $\theta=0^\circ$ , Initial Liquid Height of 460 Inches, and Refined Mesh

Unfiltered pressure time histories for selected fluid elements near the wall of the tank at  $\theta=45^\circ$  are shown in Figure C-45. In this plot, isolated peaks are evident in the traces, particularly during the unforced motion following the seismic excitation. The filtered time histories are shown in Figure C-46. The filtered data show that high-frequency low peaks in elements 2388 and 3988 near the free surface were that occurred approximately 15 seconds into the simulation were removed during filtering.

The unfiltered and filtered maximum and minimum pressure plots at  $\theta=45^\circ$  are shown as Figure C-47 and Figure C-48, respectively. The maximum and minimum pressures from the Dytran<sup>®</sup> solutions are reasonably close to the open-tank solutions, but the dynamic pressures from the simulation were somewhat less than the theoretical values at this location. The pressures agree fairly well with the theoretical open-top tank solution except near the liquid-free surface where the dynamic pressures increase. The  $45^\circ$  location lies outside the central angle of  $17.8^\circ$  per Appendix D in BNL (1995) so that the open-tank solution and equivalent flat-top tank solution are the same in this region.

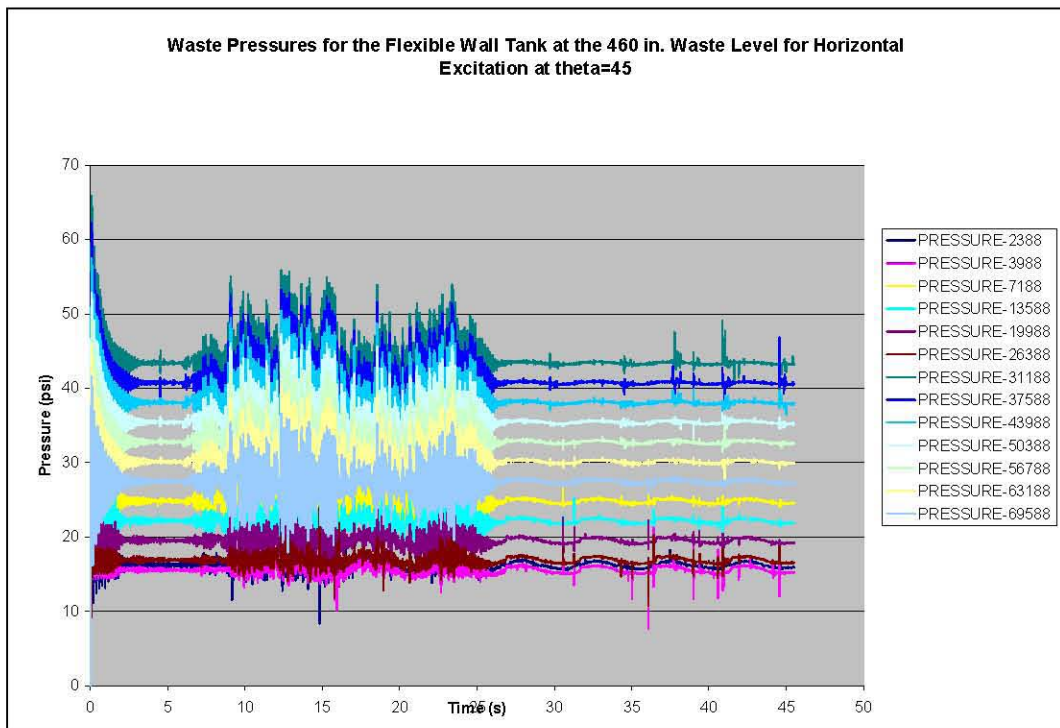


Figure C-45. Liquid Pressure Time Histories for the Flexible Wall Tank with 460 Inches of Liquid Under Horizontal Excitation at  $\theta=45^\circ$  with Refined Mesh

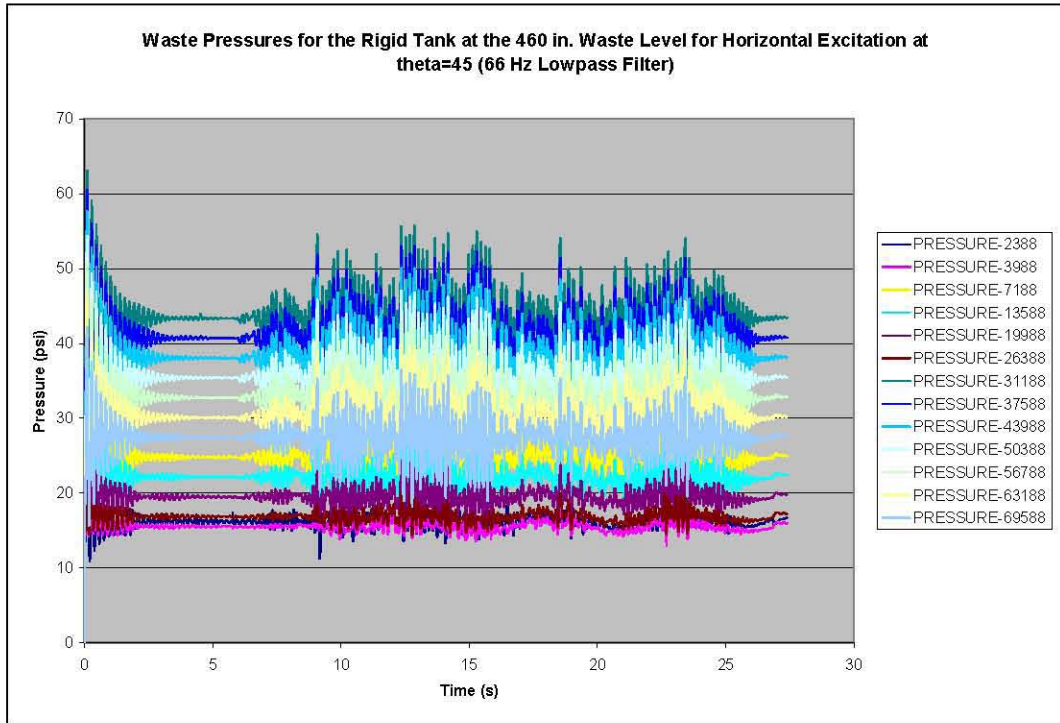


Figure C-46. Waste Pressure Time Histories for the Flexible Wall Tank with 460 Inches of Liquid Under Horizontal Excitation at  $\theta=45^\circ$  with Refined Mesh Using a 66-Hz Lowpass Filter

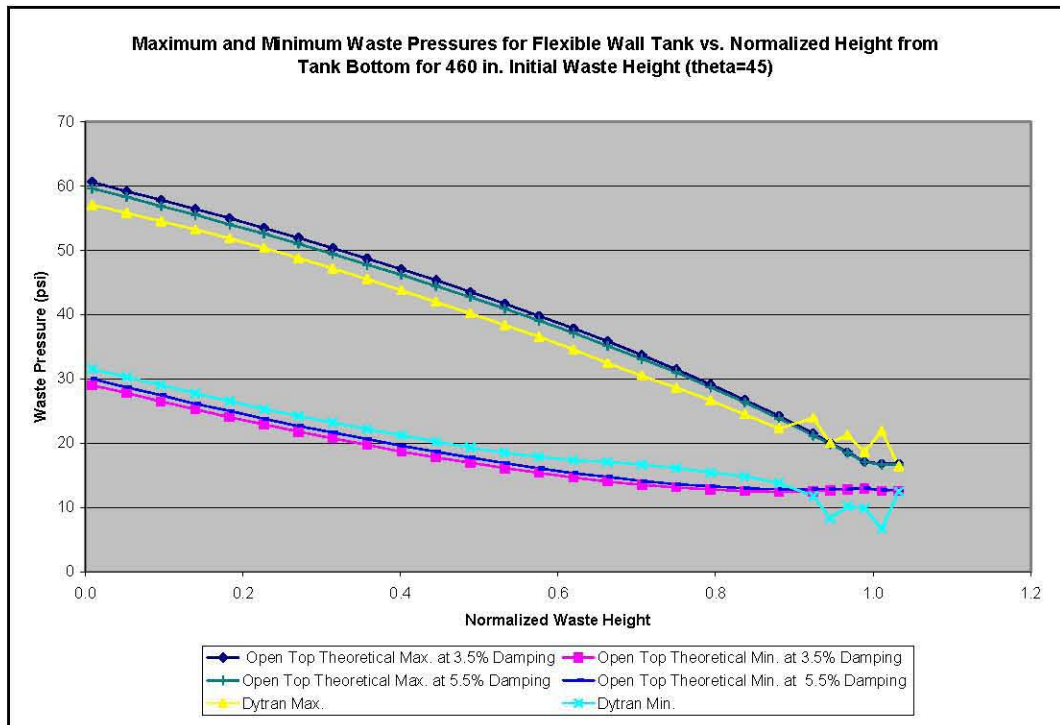
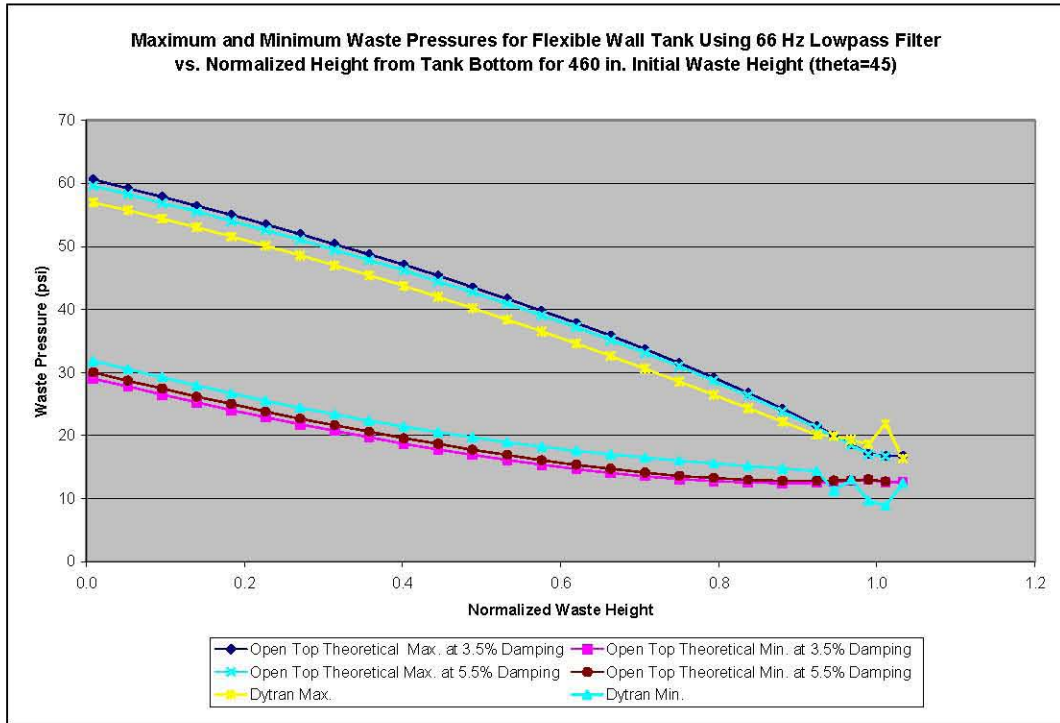


Figure C-47. Maximum and Minimum Liquid Pressures vs. Normalized Height from Tank Bottom for Horizontal Excitation at  $\theta=45^\circ$ , Initial Liquid Height of 460 Inches, and Refined Mesh



**Figure C-48.** Maximum and Minimum Liquid Pressures for the Flexible Wall Tank Using a 66-Hz Lowpass Filter vs. Normalized Height from Tank Bottom for Horizontal Excitation at  $\theta=45^\circ$ , Initial Liquid Height of 460 Inches, and Refined Mesh

Unfiltered and filtered pressure time histories near the wall at  $\theta=90^\circ$  are shown in Figure C-49 and Figure C-50, respectively, and the dynamic pressures are low as expected. The unfiltered and filtered maximum and minimum pressures are shown as Figure C-51 and Figure C-52, respectively. As expected, the maximum and minimum pressures follow the hydrostatic line fairly closely with maximum deviation of approximately 2 lbf/in<sup>2</sup>, except near the liquid-free surface where the deviations are greater.

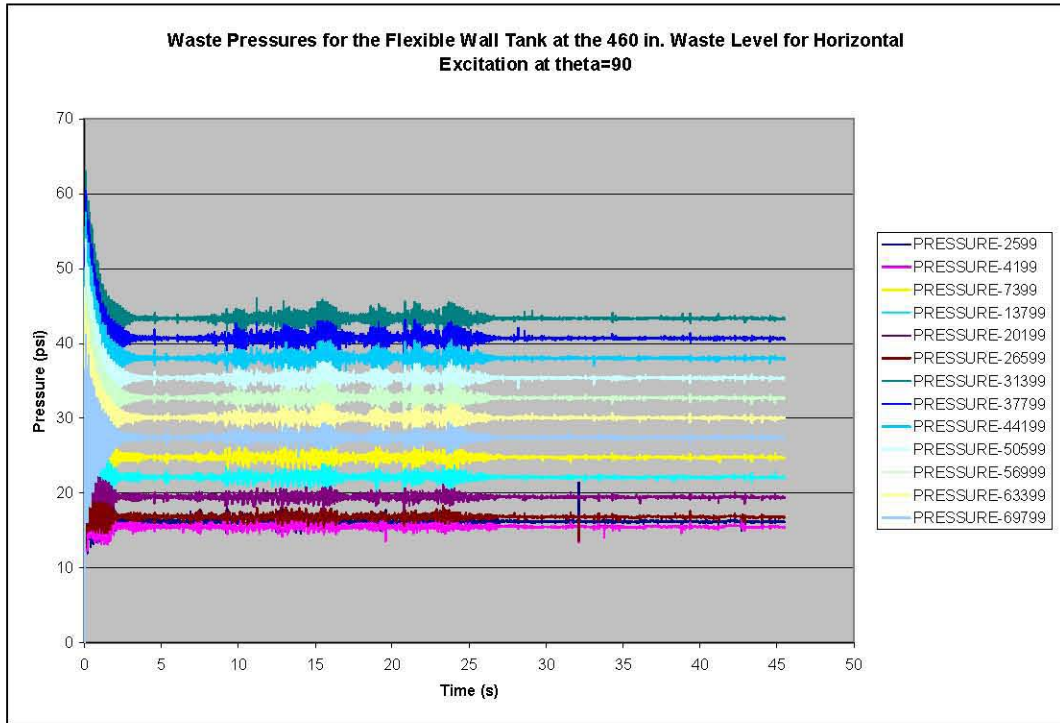


Figure C-49. Liquid Pressure Time Histories for the Flexible Wall Tank with 460 Inches of Liquid Under Horizontal Excitation at  $\theta=90^\circ$  with Refined Mesh

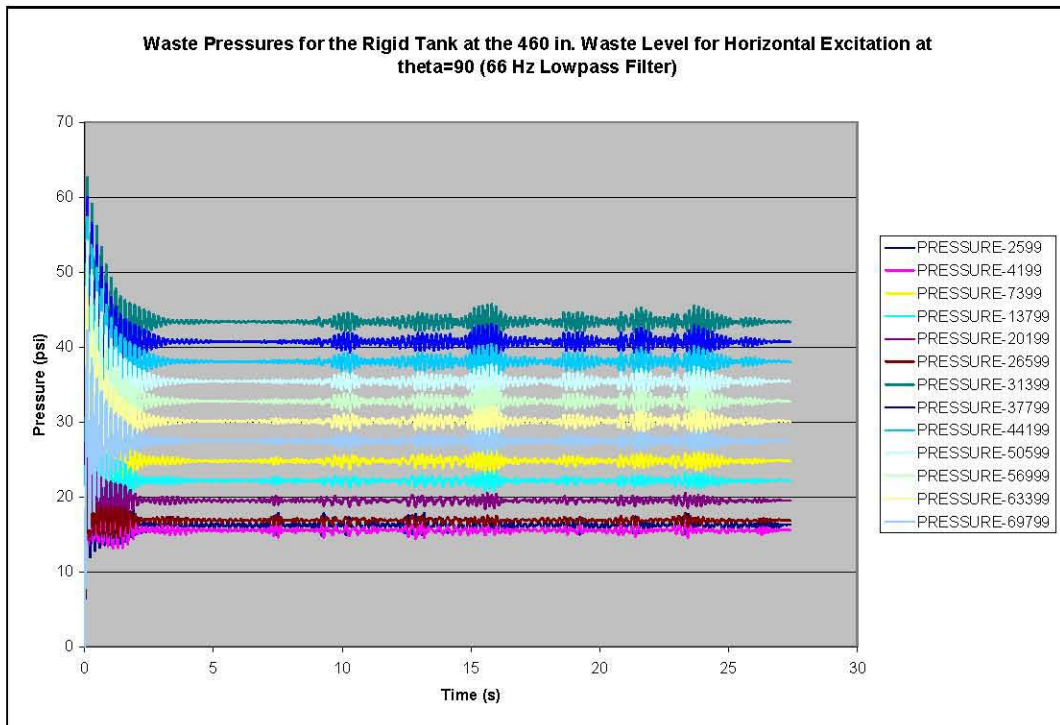


Figure C-50. Waste Pressure Time Histories for the Flexible Wall Tank with 460 Inches of Liquid Under Horizontal Excitation at  $\theta=90^\circ$  with Refined Mesh Using a 66-Hz Lowpass Filter

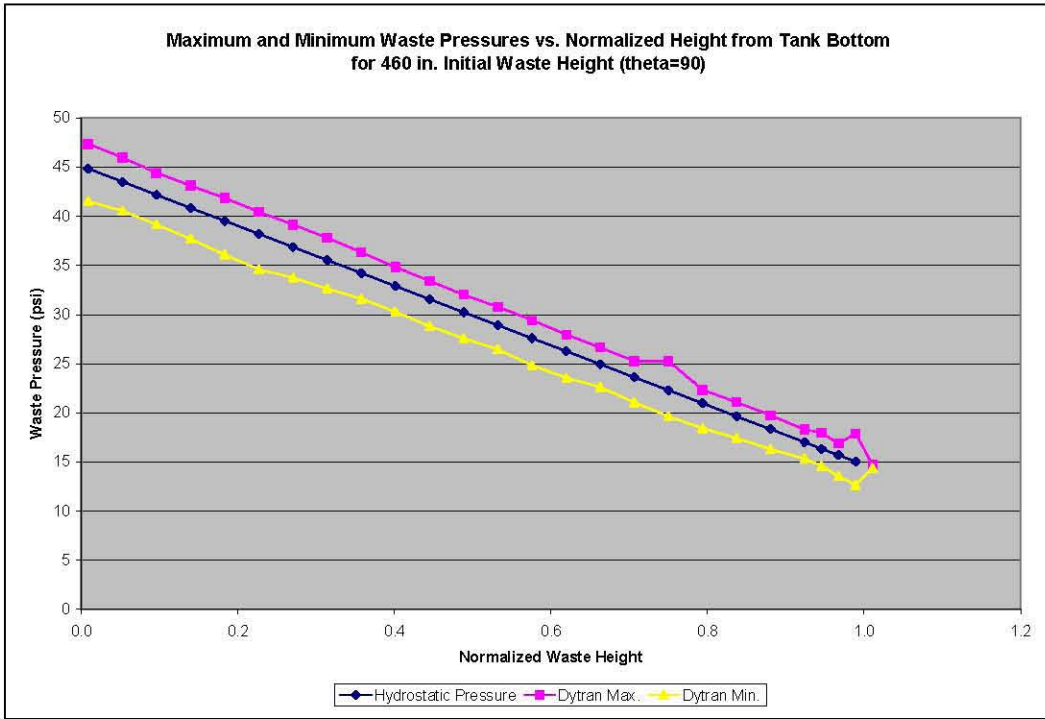


Figure C-51. Maximum and Minimum Liquid Pressures vs. Normalized Height from Tank Bottom for Horizontal Excitation at  $\theta=90^\circ$ , Initial Liquid Height of 460 Inches, and Refined Mesh

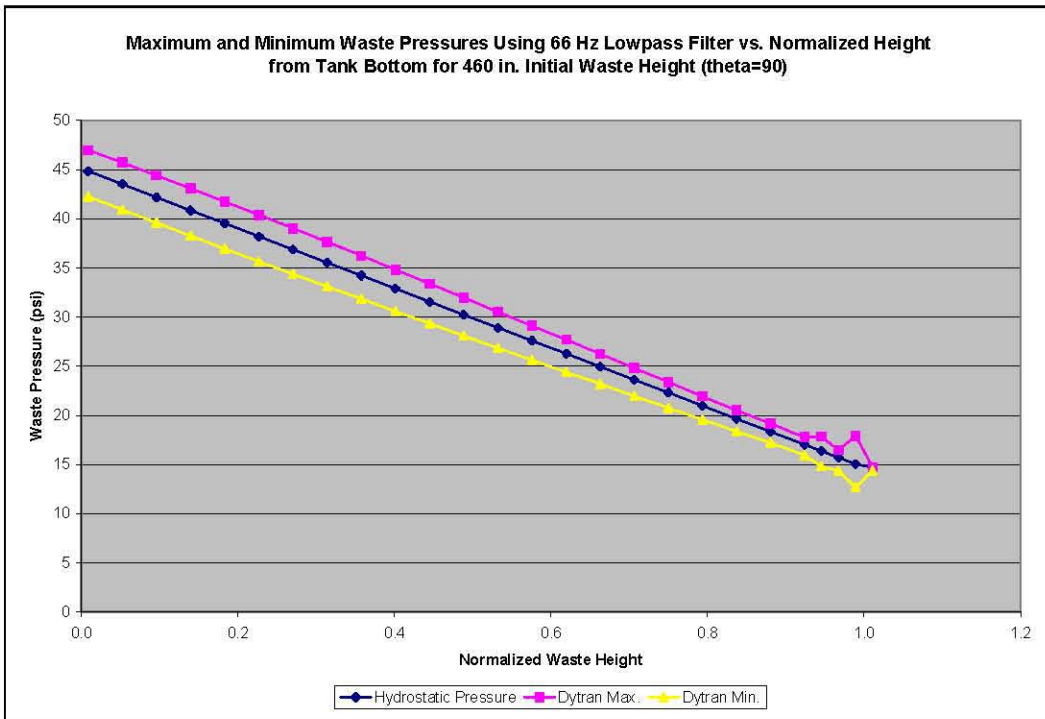


Figure C-52. Maximum and Minimum Liquid Pressures for the Flexible Wall Tank Using a 66-Hz Lowpass Filter vs. Normalized Height from Tank Bottom for Horizontal Excitation at  $\theta=90^\circ$ , Initial Liquid Height of 460 Inches, and Refined Mesh

The final set of wall pressure traces are along the plane of excitation at  $\theta=180^\circ$ . Unfiltered and filtered pressure traces are shown in Figure C-53 and Figure C-54, respectively. Unfiltered and filtered maximum and minimum pressure plots are shown in Figure C-55 and Figure C-56, respectively.

In theory, the peak pressures should be the same at  $\theta=0^\circ$  and  $\theta=180^\circ$ . However, comparison of Figure C-55 to Figure C-43 or Figure C-55 to Figure C-44 shows that peak wall pressures along the majority of the tank height are greater at  $\theta=180^\circ$  than they are at  $\theta=0^\circ$ . However, the peak dynamic pressures near the liquid-free surface are higher at  $\theta=0^\circ$ .

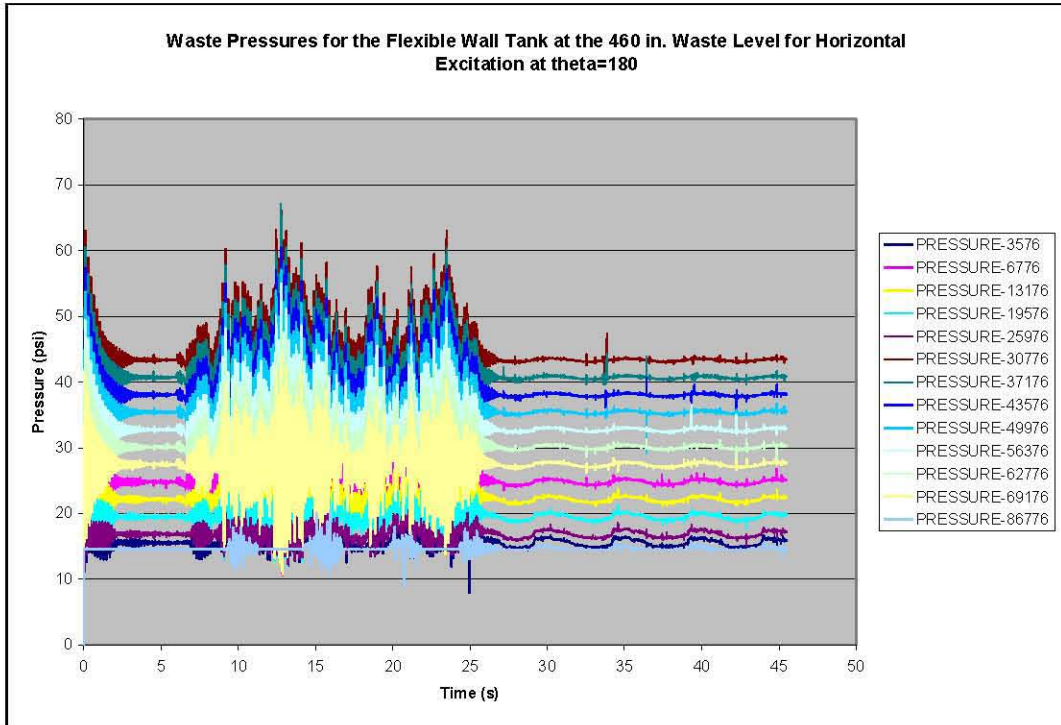


Figure C-53. Liquid Pressure Time Histories for the Flexible Wall Tank with 460 Inches of Liquid Under Horizontal Excitation at  $\theta=180^\circ$  with Refined Mesh

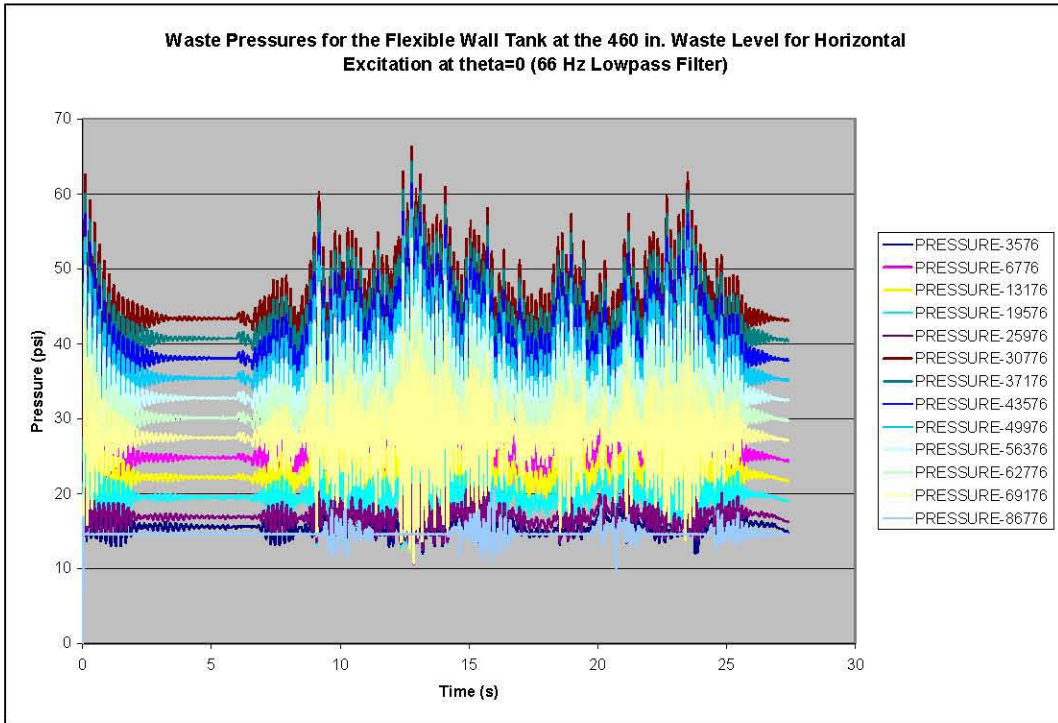


Figure C-54. Waste Pressure Time Histories for the Flexible Wall Tank with 460 Inches of Liquid Under Horizontal Excitation at  $\theta=180^\circ$  with Refined Mesh Using a 66-Hz Lowpass Filter

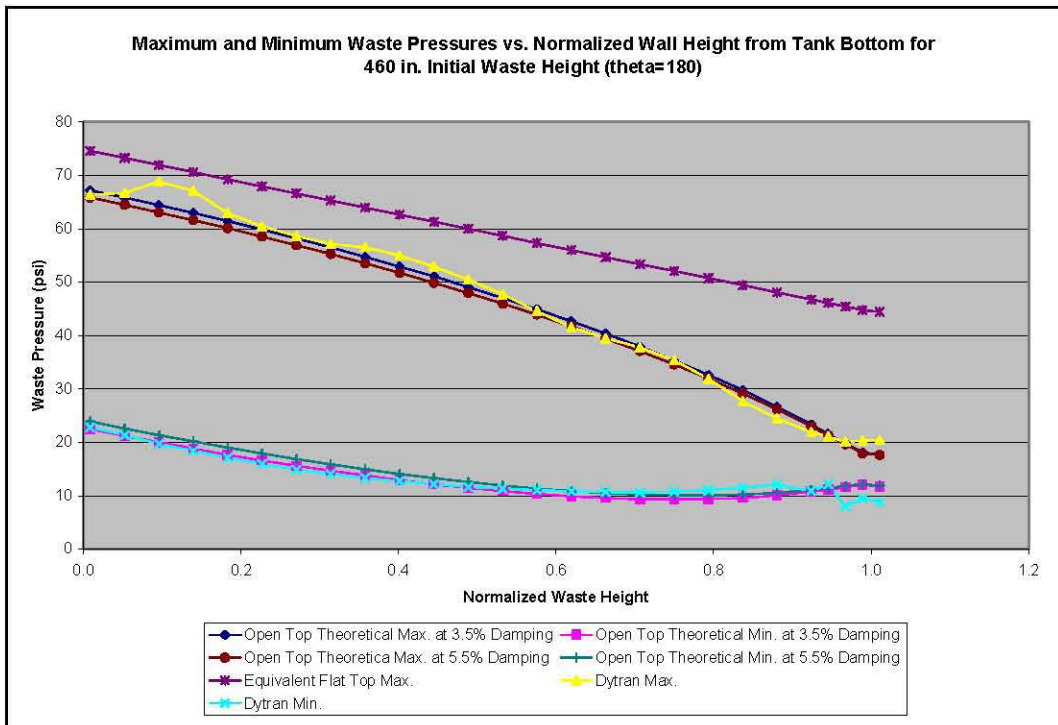


Figure C-55. Maximum and Minimum Liquid Pressures vs. Normalized Height from Tank Bottom for Horizontal Excitation at  $\theta=180^\circ$ , Initial Liquid Height of 460 Inches, and Refined Mesh

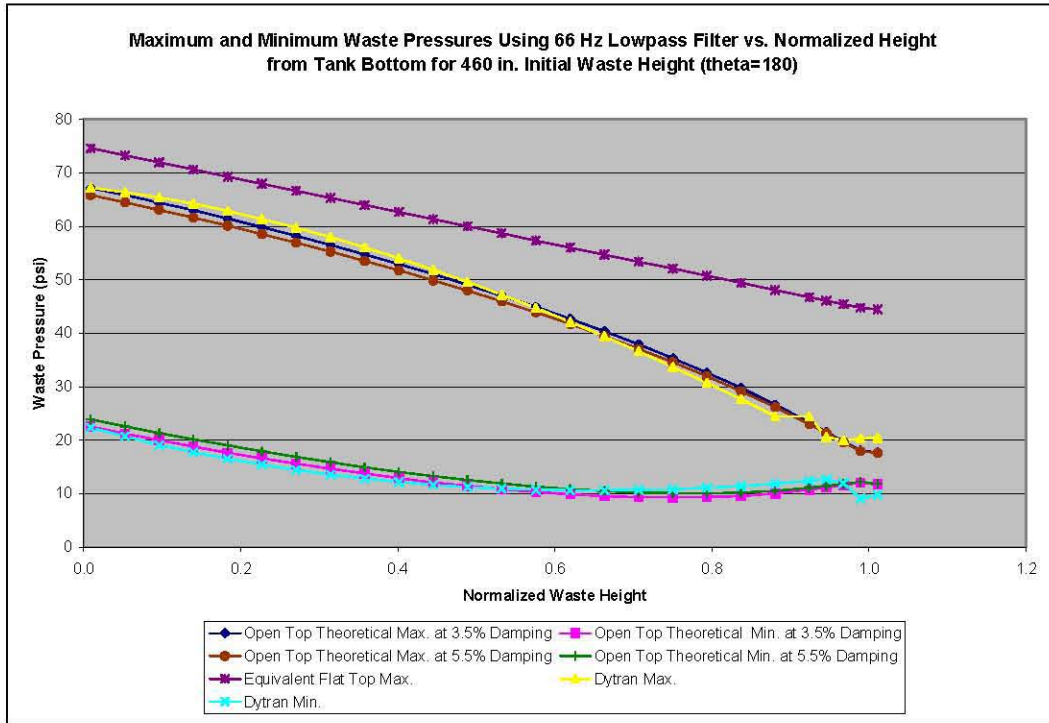


Figure C-56. Maximum and Minimum Liquid Pressures for the Flexible Wall Tank Using a 66-Hz Lowpass Filter vs. Normalized Height from Tank Bottom for Horizontal Excitation at  $\theta=180^\circ$ , Initial Liquid Height of 460 Inches, and Refined Mesh

### C.7.4 Maximum Slosh Height

The maximum slosh height trace for the flexible wall tank is shown in Figure C-57 along with the maximum slosh height trace for a rigid open tank at the same liquid level. The details of the two traces are slightly different, but each shows a maximum slosh height of 26.9 inches. The maximum theoretical value for an open tank is 25.2 inches per the methodology in BNL (1995) and 29.7 inches using the procedure in Malhotra (2005).

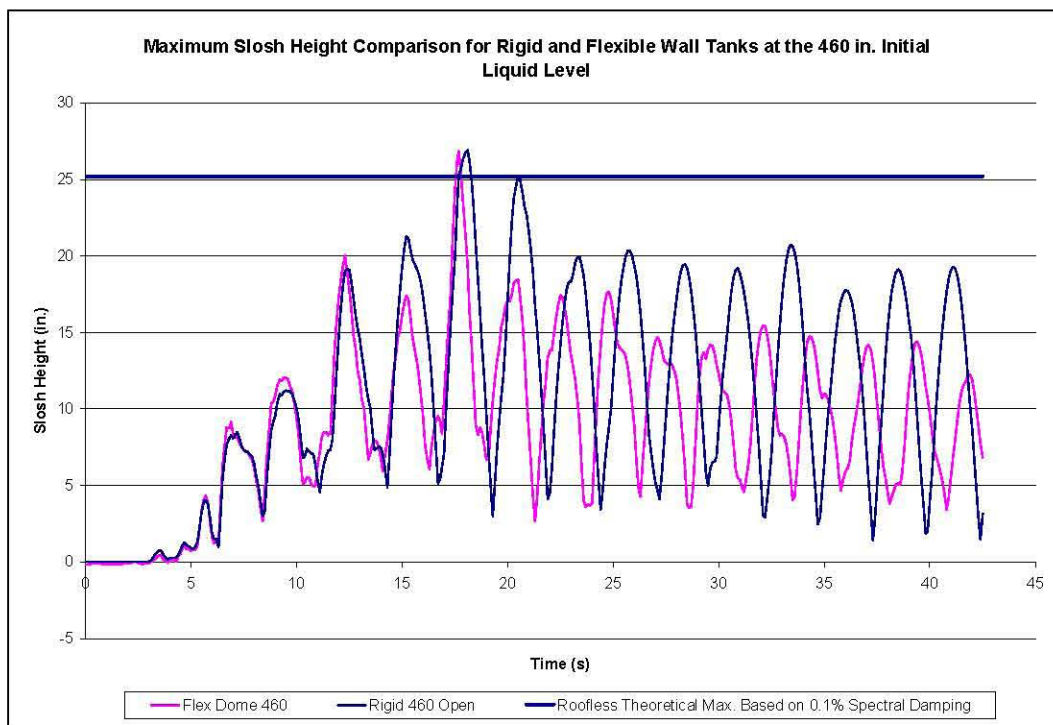


Figure C-57. Maximum Slosh Height Comparison for Rigid and Flexible Wall Domed Tanks at the 460-Inch Initial Liquid Level

### C.7.5 Element Stresses

Time histories of mid-plane hoop stresses for primary tank elements at  $\theta=0^\circ$ ,  $45^\circ$ ,  $90^\circ$ , and  $180^\circ$  from the plane of seismic excitation are presented in this section (see Figure C-15 and Figure C-16 for numbering of tank shell elements). Hoop stress time histories for tank elements at  $\theta=0^\circ$  with the data extracted at 10-millisecond intervals are shown in Figure C-58. The same data are presented in Figure C-59, except that in that figure, the data were extracted at 1-millisecond intervals. There is little apparent difference in the two sets of data indicating that little, if any, additional information is gained by sampling the stresses more frequently. This is expected since the flexible tank wall should act to mechanically filter high-frequency content in the liquid pressures. This behavior is also evident in Figure C-60, which shows a comparison of liquid pressure trace and a mid-plane hoop stress trace at mid-height in the tank wall and at  $\theta=0^\circ$ . The natural filtering provided by the primary tank is most evident in the lack of high-frequency content in the stress trace relative to the pressure trace during the 20 seconds of free oscillation following the termination of the seismic excitation.

Hoop stress traces for tank elements at  $\theta=45^\circ$ ,  $\theta=90^\circ$ , and  $\theta=180^\circ$  are shown in Figure C-61, Figure C-62, and Figure C-63. The data at  $\theta=45^\circ$  and  $\theta=90^\circ$  were extracted at 10-millisecond intervals. The data at  $\theta=180^\circ$  were extracted at 50-millisecond intervals. The stresses in Figure C-63 at  $\theta=180^\circ$  are very similar to the stresses shown in Figure C-58 at  $\theta=0^\circ$ , suggesting that the essence of the stress signal is captured even when sampled at 50-millisecond intervals.

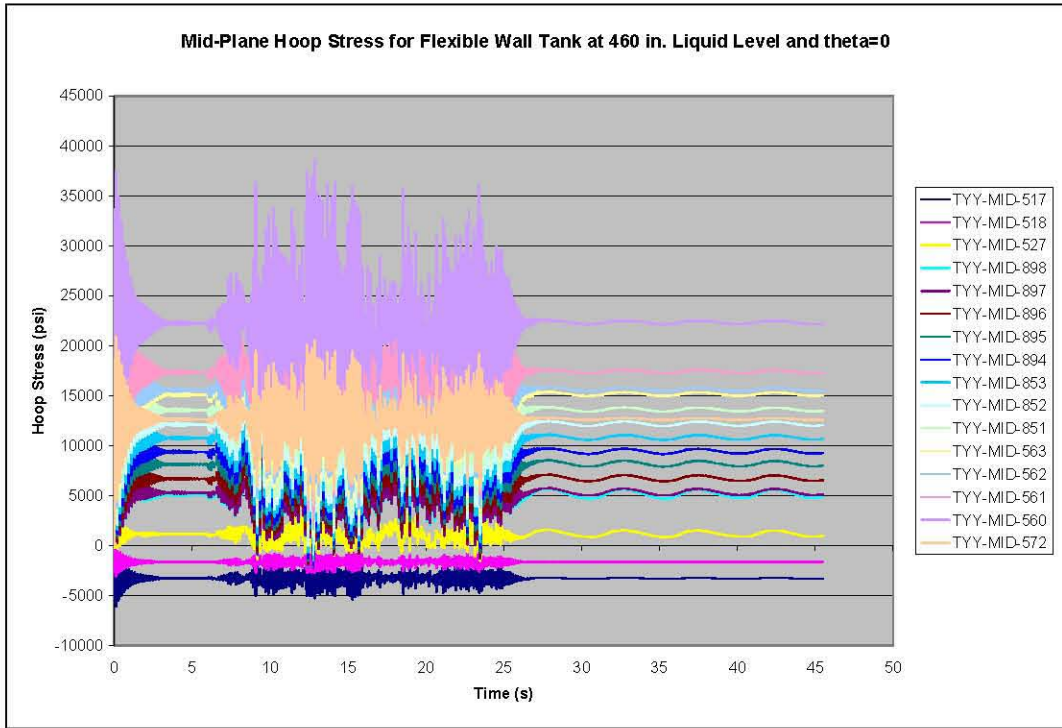


Figure C-58. Mid-Plane Hoop Stress for Flexible Wall Tank at 460-Inch Liquid Level and  $\theta=0^\circ$  Extracted at 10-millisecond Intervals

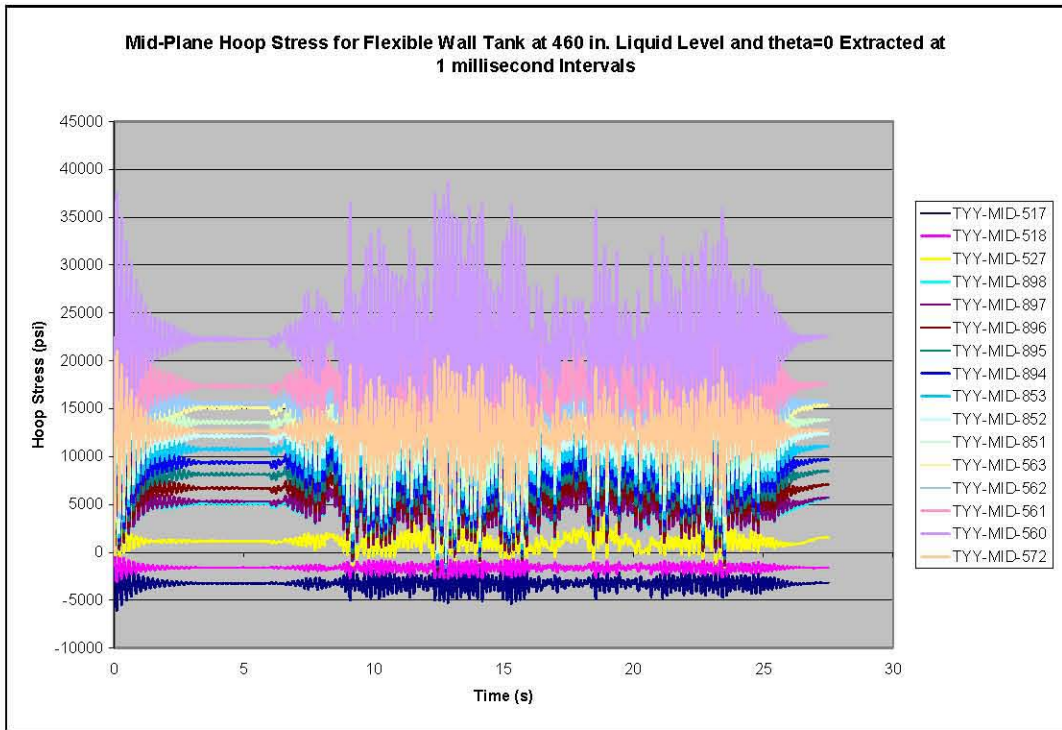


Figure C-59. Mid-Plane Hoop Stress for Flexible Wall Tank at 460-Inch Liquid Level and  $\theta=0^\circ$  Extracted at 1-millisecond Intervals

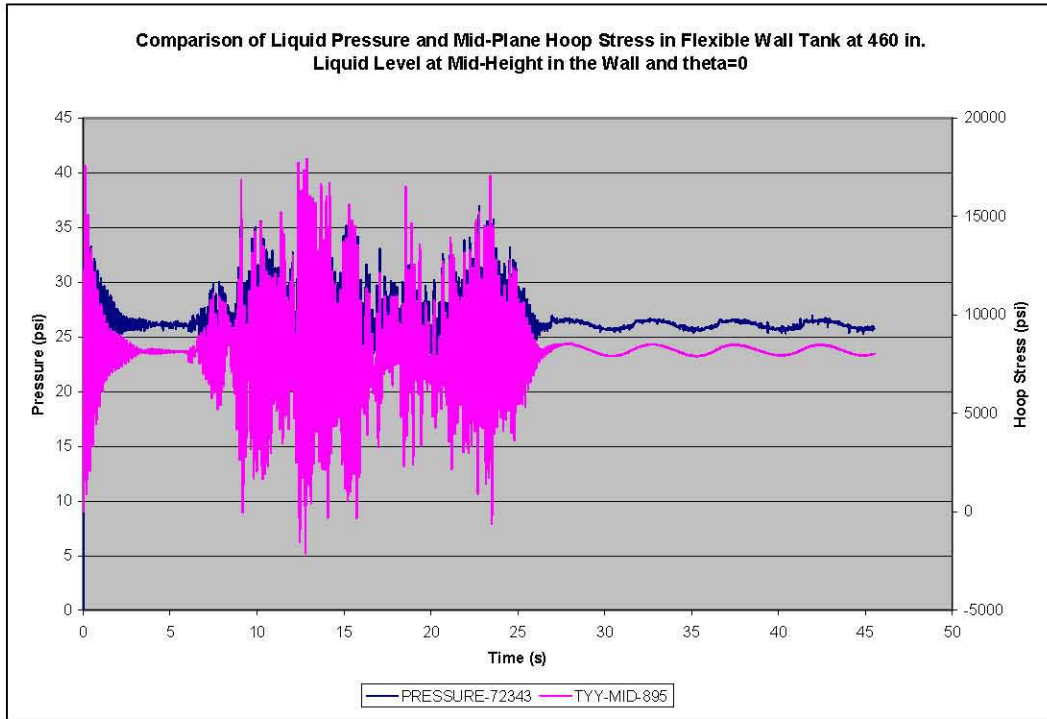


Figure C-60. Comparison of Liquid Pressure and Mid-Plane Hoop Stress in Flexible Wall Tank at 460-Inch Liquid Level at Mid-Height in the Wall and  $\theta=0^\circ$  with Data Extracted Every 10 milliseconds

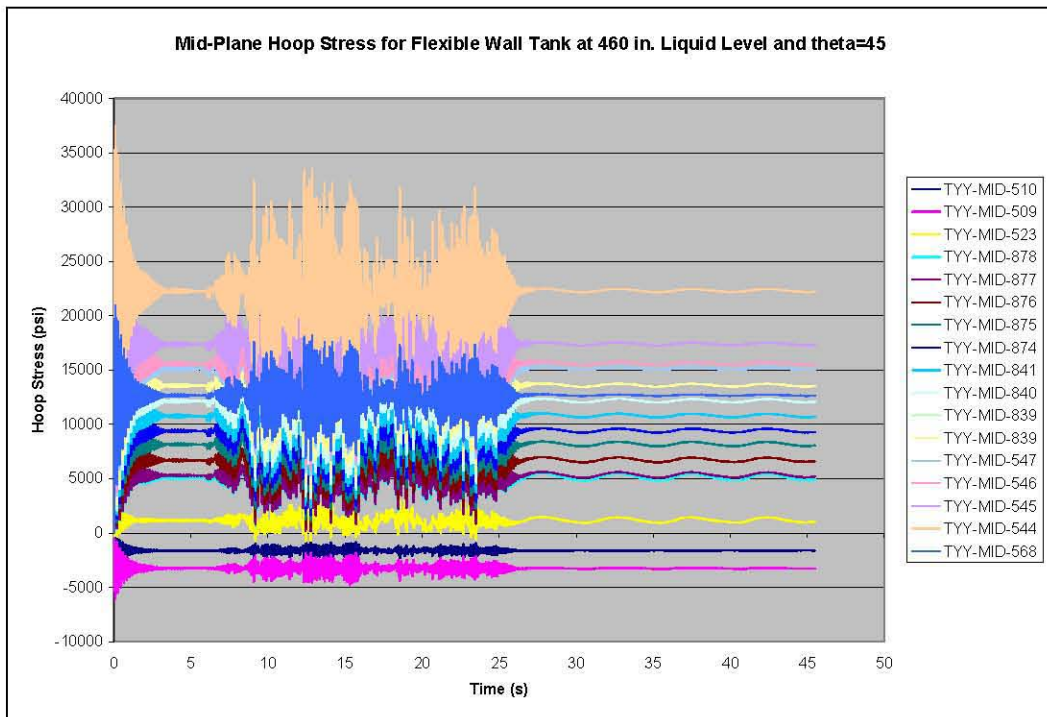


Figure C-61. Mid-Plane Hoop Stress for Flexible Wall Tank at 460-Inch Liquid Level and  $\theta=45^\circ$  Extracted at 10-millisecond Intervals

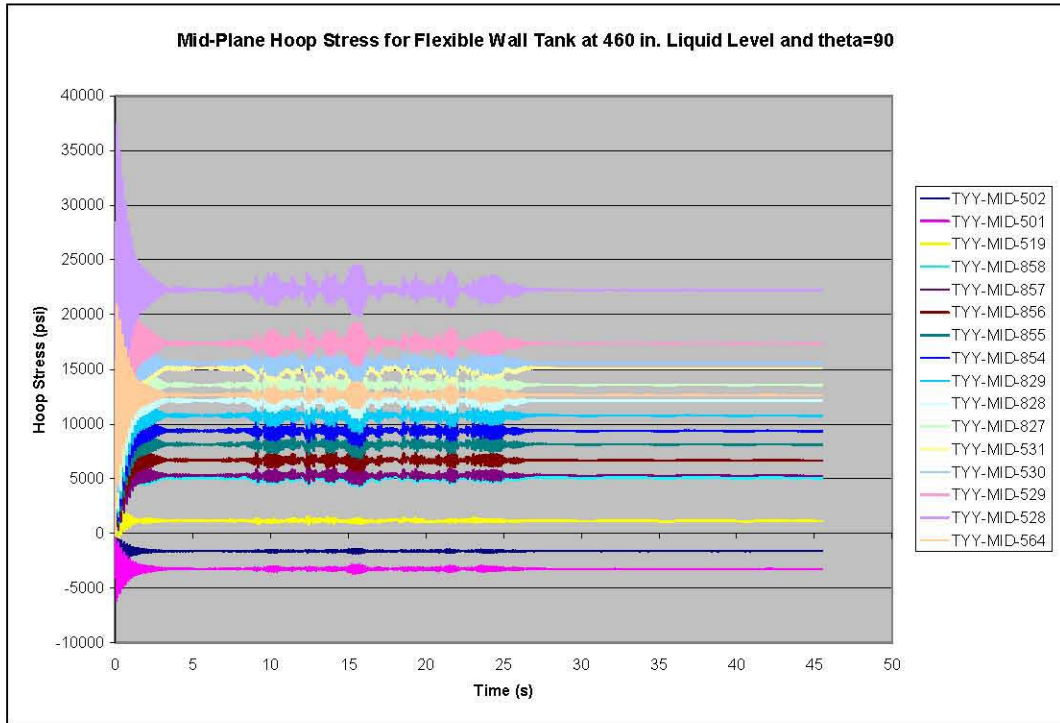


Figure C-62. Mid-Plane Hoop Stress for Flexible Wall Tank at 460-Inch Liquid Level and  $\theta=90^\circ$   
Extracted at 10-millisecond Intervals

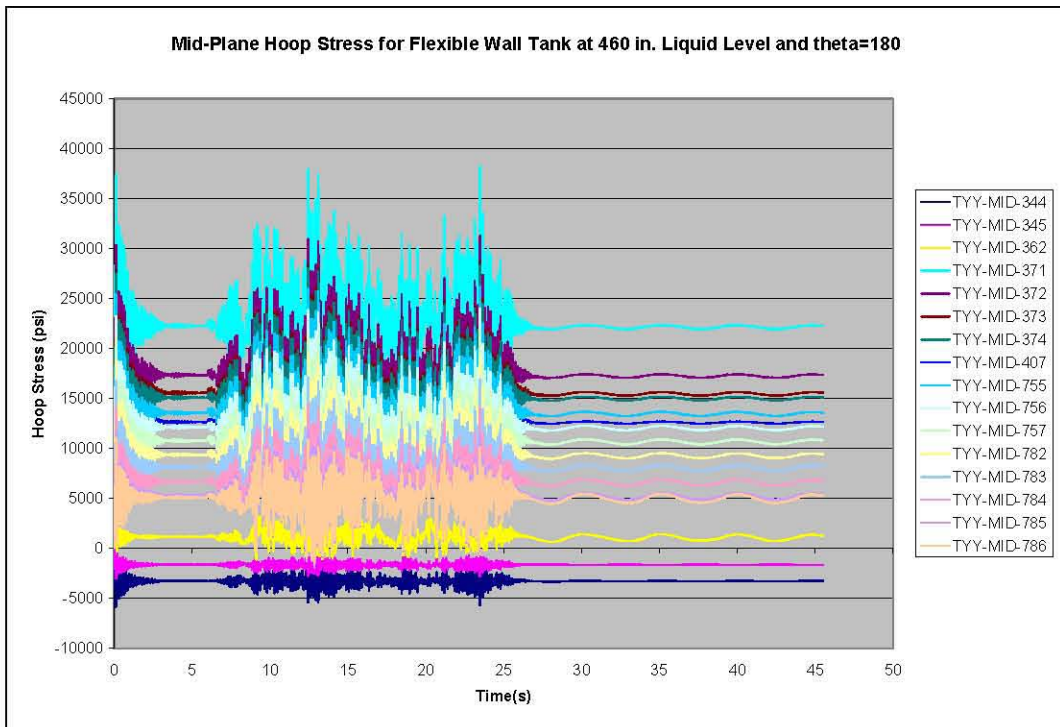


Figure C-63. Mid-Plane Hoop Stress for Flexible Wall Tank at 460-Inch Liquid Level and  $\theta=90^\circ$   
Extracted at 50-millisecond Intervals

## C.8 References

Abatt FG and MW Rinker. 2008. *Dytran Analysis of Seismically Induced Fluid-Structure Interaction in Flat-Top Tanks*. RPP-RPT-30807, Rev. 1, prepared by M&D Professional Services, Inc. for Pacific Northwest National Laboratory, Richland, Washington.

BNL. 1995. *Seismic Design and Evaluation Guidelines for the Department of Energy High-Level Liquid Storage Tanks and Appurtenances*. Report No. 52361, October 1995, Engineering Research and Applications Division, Department of Advanced Technology, Brookhaven National Laboratory, Associated Universities, Inc., Upton, New York.

Deibler JE, KI Johnson, SP Pilli, MW Rinker, FG Abatt, and NK Karri. 2008. *Hanford Double-Shell Tank Thermal and Seismic Project – Increased Liquid Level Analysis for 241-AP Tank Farm*. RPP-RPT-32237, Rev. 1, Pacific Northwest National Laboratory, Richland, Washington.

Deibler JE, KI Johnson, NK Karri, SP Pilli, MW Rinker, FG Abatt, BF Carpenter, and C Hendrix. 2007. *Hanford Double-Shell Tank Thermal and Seismic Project - Summary of Combined Thermal and Operating Loads with Seismic Analysis*. RPP-RPT-28969, Rev. 0A, Pacific Northwest National Laboratory, Richland, Washington.

Kennedy RP. 2003. *Review Comments Concerning Evaluation of Proposed Increase to Double-Shell Tank Liquid Level*. RPK Structural Mechanics Consulting, Escondido, California.

Malhotra PK. 2005. “Sloshing Loads in Liquid-Storage Tanks with Insufficient Freeboard.” *Earthquake Spectra* 21(4):1185-1192.

Rinker MW and FG Abatt. 2006. *Dytran Benchmark Analysis of Seismically Induced Fluid-Structure Interaction in a Hanford Double Shell Primary Tank*. RPP-RPT-28963, Rev. 0 and Rev. 0A, prepared by M&D Professional Services, Inc. for Pacific Northwest National Laboratory, Richland, Washington.

Rinker MW, BG Carpenter, and FG Abatt. 2006. *ANSYS Benchmark Analysis of Seismically Induced Fluid-Structure Interaction in a Hanford Double Shell Primary Tank*. RPP-RPT-28965, Rev. 0, prepared by M&D Professional Services, Inc. for Pacific Northwest National Laboratory, Richland, Washington.

Intentionally left blank.

## **Appendix D**

### **Benchmark Solutions in Support of Reanalysis Contained in Appendix C**

RPP-RPT-28963, Rev. 1  
M&D-2008-005-RPT-01, Rev. 1

Intentionally left blank.

RPP-RPT-28963, Rev. 1  
M&D-2008-005-RPT-01, Rev. 1

Prepared by: F. G. Abatt  
M&D Professional Services  
1/14/08  
Rev. 1

Theoretical Fluid Response  
Calculations for Rigid Open Tank at  
460 in. Waste Level - Biased Mesh

Checked by: Milon Meyer

This worksheet contains calculations for a rigid open top tank with an initial liquid level of 460 in. The calculations are performed using the methodology in Chapter 4 of BNL (1995). The location of the fluid elements corresponds to the Dytran model of the rigid domed tank.

$H_1 := 460.0 \cdot \text{in}$     Baseline liquid level

$$g := 386.4 \cdot \frac{\text{in}}{\text{sec}^2}$$

$R := 450 \cdot \text{in}$     Tank radius

$\frac{H_1}{R} = 1.02$     Ratio of waste height to tank radius

$i := 0..2$

$\lambda := \begin{pmatrix} 1.841 \\ 5.331 \\ 8.536 \end{pmatrix}$     Bessel function roots - Eqn. 4.5 BNL (1995)

$\theta := \begin{pmatrix} 0 \cdot \text{deg} \\ 45 \cdot \text{deg} \\ 90 \cdot \text{deg} \end{pmatrix}$     Circumferential location of waste elements for which pressures are reported

**Convective Frequencies**

$$f_{con_i} := \frac{1}{2 \cdot \pi} \cdot \left[ \sqrt{\lambda_i \cdot \frac{g}{R} \cdot \tanh \left[ \lambda_i \cdot \left( \frac{H_1}{R} \right) \right]} \right] \quad \text{Eqn. 4.14 BNL (1995)}$$

$f_{con} = \begin{pmatrix} 0.196 \\ 0.341 \\ 0.431 \end{pmatrix} \frac{1}{s}$     First three convective frequencies

$\rho_1 := 1.71 \cdot 10^{-4} \cdot \frac{\text{lb} \cdot \text{sec}^2}{\text{in}^4}$     waste density - specific gravity = 1.83

**RPP-RPT-28963, Rev. 1**  
**M&D-2008-005-RPT-01, Rev. 1**

Prepared by: F. G. Abatt  
M&D Professional Services  
1/14/08  
Rev. 1

Theoretical Fluid Response  
Calculations for Rigid Open Tank at  
460 in. Waste Level - Biased Mesh

Checked by: Milon Meyer

Determine Convective Pressures on the Tank Wall:

- z :=
- ( 12.in )
  - 37.5.in
  - 62.5.in
  - 87.5.in
  - 112.5.in
  - 137.5.in
  - 162.5.in
  - 187.5.in
  - 212.5.in
  - 237.5.in
  - 262.5.in
  - 287.5.in
  - 311.8.in
  - 336.0.in
  - 358.5.in
  - 377.7.in
  - 394.8.in
  - 410.0.in
  - 423.6.in
  - 435.0.in
  - 445.0.in
  - ( 455.0.in )

Vertical location of Euler element centroids at which pressures are reported.

$$\eta_1 := \frac{z}{H_1}$$

Ratio of tank wall vertical location to waste height for waste element centroids.

	0
0	0.026
1	0.082
2	0.136
3	0.19
4	0.245
5	0.299
6	0.353
7	0.408
8	0.462
9	0.516
10	0.571
11	0.625
12	0.678
13	0.73
14	0.779
15	0.821
16	0.858
17	0.891
18	0.921
19	0.946
20	0.967
21	0.989

**RPP-RPT-28963, Rev. 1**  
**M&D-2008-005-RPT-01, Rev. 1**

Prepared by: F. G. Abatt  
M&D Professional Services  
1/14/08  
Rev. 1

Theoretical Fluid Response  
Calculations for Rigid Open Tank at  
460 in. Waste Level - Biased Mesh

Checked by: Milon Meyer

Determine convective coefficients as a function of dimensionless height per Eqn. 4.4 BNL (1995).

$$\text{con}_0(\eta_1) := \frac{2 \cdot \cosh\left[\lambda_0 \cdot \left(\frac{H_1}{R}\right) \cdot \eta_1\right]}{(\lambda_0)^2 - 1 \cdot \cosh\left[\lambda_0 \cdot \left(\frac{H_1}{R}\right)\right]}$$

$$\text{con}_1(\eta_1) := \frac{2 \cdot \cosh\left[\lambda_1 \cdot \left(\frac{H_1}{R}\right) \cdot \eta_1\right]}{(\lambda_1)^2 - 1 \cdot \cosh\left[\lambda_1 \cdot \left(\frac{H_1}{R}\right)\right]}$$

$$\text{con}_2(\eta_1) := \frac{2 \cdot \cosh\left[\lambda_2 \cdot \left(\frac{H_1}{R}\right) \cdot \eta_1\right]}{(\lambda_2)^2 - 1 \cdot \cosh\left[\lambda_2 \cdot \left(\frac{H_1}{R}\right)\right]}$$

	0
0	0.25
1	0.25
2	0.26
3	0.27
4	0.28
5	0.29
6	0.31
7	0.33
8	0.35
9	0.38
10	0.41
11	0.44
12	0.48
13	0.52
14	0.57
15	0.61
16	0.65
17	0.69
18	0.73
19	0.76
20	0.79
21	0.82

	0
0	6.33·10 <sup>-4</sup>
1	6.9·10 <sup>-4</sup>
2	8.07·10 <sup>-4</sup>
3	9.95·10 <sup>-4</sup>
4	1.27·10 <sup>-3</sup>
5	1.66·10 <sup>-3</sup>
6	2.2·10 <sup>-3</sup>
7	2.92·10 <sup>-3</sup>
8	3.91·10 <sup>-3</sup>
9	5.25·10 <sup>-3</sup>
10	7.04·10 <sup>-3</sup>
11	9.46·10 <sup>-3</sup>
12	1.26·10 <sup>-2</sup>
13	1.68·10 <sup>-2</sup>
14	2.19·10 <sup>-2</sup>
15	2.75·10 <sup>-2</sup>
16	3.37·10 <sup>-2</sup>
17	4.03·10 <sup>-2</sup>
18	4.74·10 <sup>-2</sup>
19	5.42·10 <sup>-2</sup>
20	6.11·10 <sup>-2</sup>
21	6.87·10 <sup>-2</sup>

	0
0	9.27·10 <sup>-6</sup>
1	1.14·10 <sup>-5</sup>
2	1.62·10 <sup>-5</sup>
3	2.46·10 <sup>-5</sup>
4	3.87·10 <sup>-5</sup>
5	6.17·10 <sup>-5</sup>
6	9.88·10 <sup>-5</sup>
7	1.58·10 <sup>-4</sup>
8	2.55·10 <sup>-4</sup>
9	4.09·10 <sup>-4</sup>
10	6.57·10 <sup>-4</sup>
11	1.06·10 <sup>-3</sup>
12	1.67·10 <sup>-3</sup>
13	2.65·10 <sup>-3</sup>
14	4.06·10 <sup>-3</sup>
15	5.84·10 <sup>-3</sup>
16	8.08·10 <sup>-3</sup>
17	1.08·10 <sup>-2</sup>
18	1.4·10 <sup>-2</sup>
19	1.73·10 <sup>-2</sup>
20	2.09·10 <sup>-2</sup>
21	2.53·10 <sup>-2</sup>

RPP-RPT-28963, Rev. 1  
M&D-2008-005-RPT-01, Rev. 1

Prepared by: F. G. Abatt  
M&D Professional Services  
1/14/08  
Rev. 1

Theoretical Fluid Response  
Calculations for Rigid Open Tank at  
460 in. Waste Level - Biased Mesh

Checked by: Milon Meyer

Impulsive pressure coefficient as a function of dimensionless wall height

$$c_i(\eta_i) := 1 - \cos_0(\eta_i) - \cos_1(\eta_i) - \cos_2(\eta_i) \quad \text{Eqn. 4.7 BNL (1995)}$$

	0
0	0.75
1	0.75
2	0.74
3	0.73
4	0.72
5	0.71
6	0.69
7	0.67
8	0.65
9	0.62
10	0.59
11	0.55
12	0.5
13	0.46
14	0.41
15	0.36
16	0.31
17	0.26
18	0.21
19	0.17
20	0.13
21	0.09

Calculate maximum values of dynamic wall pressures from spectral acceleration of dome input TH.

Consider the first three convective mode spectral accelerations for the 0.1% damped spectrum

$$SA_{c0} := 0.066 \cdot g$$

$$SA_{c0} = 25.5 \frac{\text{in}}{\text{sec}^2}$$

$$SA_{c1} := 0.11 \cdot g$$

$$SA_{c1} = 42.5 \frac{\text{in}}{\text{sec}^2}$$

ANSYS dome RS from Spectr

$$SA_{c2} := 0.17 \cdot g$$

$$SA_{c2} = 65.69 \frac{\text{in}}{\text{sec}^2}$$

RPP-RPT-28963, Rev. 1  
M&D-2008-005-RPT-01, Rev. 1

Prepared by: F. G. Abatt  
M&D Professional Services  
1/14/08  
Rev. 1

Theoretical Fluid Response  
Calculations for Rigid Open Tank at  
460 in. Waste Level - Biased Mesh

Checked by: Milon Meyer

Associate the impulsive mode with the peak ground acceleration (PGA), since the tank is rigid.

PGA := 0.276·g      PGA = 106.65  $\frac{\text{in}}{\text{sec}^2}$       ANSYS dome RS from Spectr

$$P_{\text{maxconv}}(\eta_1, \theta) := \left[ \sqrt{(\text{con}_0(\eta_1) \cdot SA_{c0})^2 + (\text{con}_1(\eta_1) \cdot SA_{c1})^2 + (\text{con}_2(\eta_1) \cdot SA_{c2})^2} \right] \cdot (\rho_1 \cdot R \cdot \cos(\theta \cdot \text{deg}))$$

$$P_{\text{maximpulsive}}(\eta_1, \theta) := \left[ \sqrt{[c_i(\eta_1) \cdot (PGA)]^2} \right] \cdot (\rho_1 \cdot R \cdot \cos(\theta \cdot \text{deg}))$$

$$P_{\text{max}}(\eta_1, \theta) := \left[ \sqrt{[c_i(\eta_1) \cdot (PGA)]^2 + (\text{con}_0(\eta_1) \cdot SA_{c0})^2 + (\text{con}_1(\eta_1) \cdot SA_{c1})^2 + (\text{con}_2(\eta_1) \cdot SA_{c2})^2} \right] \cdot (\rho_1 \cdot R \cdot \cos(\theta \cdot \text{deg}))$$

Previous expression is Eqn. 4.24 of BNL (1995).

	0	
	0	6.15
	1	6.13
	2	6.09
	3	6.02
	4	5.93
	5	5.82
	6	5.67
	7	5.5
	8	5.3
	9	5.07
$P_{\text{maximpulsive}}(\eta_1, 0) =$	10	4.8
	11	4.49
	12	4.14
	13	3.75
	14	3.33
	15	2.92
	16	2.52
	17	2.12
	18	1.74
	19	1.39
	20	1.05
	21	0.7

$\frac{\text{lb}}{\text{in}^2}$

Maximum impulsive dynamic pressures at  
theta = 0.

RPP-RPT-28963, Rev. 1  
M&D-2008-005-RPT-01, Rev. 1

Prepared by: F. G. Abatt  
M&D Professional Services  
1/14/08  
Rev. 1

Theoretical Fluid Response  
Calculations for Rigid Open Tank at  
460 in. Waste Level - Biased Mesh

Checked by: Milon Meyer

$P_{\max\text{conv}}(\eta_1, 0) =$

	0
0	0.49
1	0.49
2	0.51
3	0.52
4	0.54
5	0.57
6	0.6
7	0.64
8	0.69
9	0.74
10	0.8
11	0.87
12	0.94
13	1.03
14	1.12
15	1.2
16	1.28
17	1.36
18	1.44
19	1.5
20	1.57
21	1.63

$\frac{\text{lbf}}{\text{in}^2}$

Maximum convective dynamic pressures at theta = 0.

$P_{\max}(\eta_1, 0) =$

	0
0	6.17
1	6.15
2	6.11
3	6.04
4	5.95
5	5.84
6	5.71
7	5.54
8	5.35
9	5.12
10	4.87
11	4.57
12	4.25
13	3.88
14	3.51
15	3.16
16	2.83
17	2.52
18	2.25
19	2.04
20	1.89
21	1.77

$\frac{\text{lbf}}{\text{in}^2}$

Maximum total dynamic pressure at theta = 0.

RPP-RPT-28963, Rev. 1  
M&D-2008-005-RPT-01, Rev. 1

Prepared by: F. G. Abatt  
M&D Professional Services  
1/14/08  
Rev. 1

Theoretical Fluid Response  
Calculations for Rigid Open Tank at  
460 in. Waste Level - Biased Mesh

Checked by: Milon Meyer

	0	
0	4.37	
1	4.35	
2	4.32	
3	4.27	
4	4.21	
5	4.13	
6	4.03	
7	3.92	
8	3.78	
9	3.62	
$P_{\max}(\eta_1, 45) =$	10	3.44
	11	3.23
	12	3
	13	2.75
	14	2.48
	15	2.23
	16	2
	17	1.78
	18	1.59
	19	1.45
	20	1.33
	21	1.25

$\frac{\text{lb}}{\text{in}^2}$

Maximum total dynamic pressure at theta = 45 degrees.

Maximum total dynamic pressure at theta = 90 degrees is zero by inspection of Eqn. 4.24 of BNL (1995)

Calculate Maximum Slosh Height:

$$\text{conmax} := \begin{pmatrix} 0.837 \\ 0.073 \\ 0.028 \end{pmatrix} \quad \text{Maximum value of convective coefficients at } \eta_1=1$$

$$h_{\text{maxslosh}} := R \cdot \sqrt{\left(\text{conmax}_0 \cdot \frac{SA_{c0}}{g}\right)^2 + \left(\text{conmax}_1 \cdot \frac{SA_{c1}}{g}\right)^2 + \left(\text{conmax}_2 \cdot \frac{SA_{c2}}{g}\right)^2} \quad \text{Eqn. 4.60 BNL (1995)}$$

$$h_{\text{maxslosh}} = 25.21 \text{ in} \quad \text{Maximum theoretical slosh height}$$

RPP-RPT-28963, Rev. 1  
M&D-2008-005-RPT-01, Rev. 1

Prepared by: F. G. Abatt  
M&D Professional Services  
1/14/08  
Rev. 1

Theoretical Fluid Response  
Calculations for Rigid Open Tank at  
460 in. Waste Level - Biased Mesh

Checked by: Milon Meyer

Calculate Maximum Total Hydrodynamic Force:

The maximum hydrodynamic force induced on the tank wall is given by Eqn. 4.31 of BNL 1995 with the instantaneous accelerations replaced by the maximum spectral accelerations. First determine the effective impulsive and convective masses.

$$m_{lapprox} := \pi \cdot R^2 \cdot H_1 \cdot \rho_l \quad m_{lapprox} = 5 \times 10^4 \frac{\text{lb} \cdot \text{sec}^2}{\text{in}} \quad \text{Total waste mass based on circular cylinder approximation.}$$

$$m_l := 4.92 \cdot 10^4 \frac{\text{lb} \cdot \text{sec}^2}{\text{in}} \quad \text{Actual waste mass reported by Dytran model.}$$

$$m_{c0} := \left[ \frac{2}{\lambda_0 \cdot \left[ (\lambda_0)^2 - 1 \right] \cdot \left( \frac{H_1}{R} \right)} \right] \cdot \tanh \left[ \lambda_0 \cdot \left( \frac{H_1}{R} \right) \right] \cdot m_l \quad \text{Eqn. 4.32 BNL (1995)}$$

$$m_{c0} = 20891.92 \frac{\text{lb} \cdot \text{sec}^2}{\text{in}} \quad \text{First mode convective mass}$$

$$m_{c1} := \left[ \frac{2}{\lambda_1 \cdot \left[ (\lambda_1)^2 - 1 \right] \cdot \left( \frac{H_1}{R} \right)} \right] \cdot \tanh \left[ \lambda_1 \cdot \left( \frac{H_1}{R} \right) \right] \cdot m_l \quad \text{Eqn. 4.32 BNL (1995)}$$

$$m_{c1} = 658.51 \frac{\text{lb} \cdot \text{sec}^2}{\text{in}} \quad \text{Second mode convective mass}$$

$$m_{c2} := \left[ \frac{2}{\lambda_2 \cdot \left[ (\lambda_2)^2 - 1 \right] \cdot \left( \frac{H_1}{R} \right)} \right] \cdot \tanh \left[ \lambda_2 \cdot \left( \frac{H_1}{R} \right) \right] \cdot m_l \quad \text{Eqn. 4.32 BNL (1995)}$$

$$m_{c2} = 1.57 \times 10^2 \frac{\text{lb} \cdot \text{sec}^2}{\text{in}} \quad \text{Third mode convective mass}$$

$$m_i := m_l - (m_{c0} + m_{c1} + m_{c2}) \quad \text{Impulsive mass - Eqn. 4.33 BNL (1995)}$$

$$m_i = 2.75 \times 10^4 \frac{\text{lb} \cdot \text{sec}^2}{\text{in}}$$

RPP-RPT-28963, Rev. 1  
M&D-2008-005-RPT-01, Rev. 1

Prepared by: F. G. Abatt  
M&D Professional Services  
1/14/08  
Rev. 1

Theoretical Fluid Response  
Calculations for Rigid Open Tank at  
460 in. Waste Level - Biased Mesh

Checked by: Milon Meyer

$$F_{\max} := m_i \cdot PGA + m_{c0} \cdot SA_{c0} + m_{c1} \cdot SA_{c1} + m_{c2} \cdot SA_{c2}$$

$$F_{\max} = 3.5 \times 10^6 \text{ lbf} \quad \text{Conservative estimate of maximum hydrodynamic force}$$

The above expression is a conservative estimate because it assumes that the peak impulsive and convective forces occur simultaneously. A less conservative estimate can be made via a square-root-sum-of-the-squares (SRSS) combination.

$$F_{\text{srss}} := \sqrt{(m_i \cdot PGA)^2 + (m_{c0} \cdot SA_{c0})^2 + (m_{c1} \cdot SA_{c1})^2 + (m_{c2} \cdot SA_{c2})^2}$$

$$F_{\text{srss}} = 2.98 \times 10^6 \text{ lbf} \quad \text{SRSS estimate of peak hydrodynamic force}$$

$$F_{\text{conmax}} := \sqrt{(m_{c0} \cdot SA_{c0})^2 + (m_{c1} \cdot SA_{c1})^2 + (m_{c2} \cdot SA_{c2})^2}$$

$$F_{\text{conmax}} = 5.34 \times 10^5 \text{ lbf} \quad \text{Peak hydrodynamic force due to convective response - shows up in free oscillations.}$$

Reference:

BNL 1995, *Seismic Design and Evaluation Guidelines for the Department of Energy High-Level Waste Storage Tanks and Appurtenances*, BNL 52361, Rev. 10/95, Brookhaven National Laboratory, Upton, New York.

Intentionally left blank.

**RPP-RPT-28963, Rev. 1**  
**M&D-2008-005-RPT-01, Rev. 1**

Prepared by: F. G. Abatt  
M&D Professional Services  
1/11/08  
Rev. 1

Theoretical Fluid Response  
Calculations for Equivalent Rigid  
Flat Top Tank at 460 in. Waste  
Level

Checked by: Milon Meyer

This worksheet contains calculations for a rigid equivalent flat-top tank with an initial liquid level of 460 in. The calculations are performed using the methodology in Chapter 4 and Appendix D of BNL (1995) and in Malthotra (2005). The freeboard distance is such that minor interaction occurs between the liquid and the flat roof. The location of the fluid elements corresponds to the Dytran model of the domed rigid tank in Appendix C. Revision 1 incorporates corrections and clarifications regarding the interpretation of solutions in BNL (1995) per reviewer comments from a June 7-8, 2007 review meeting. The complete set of review comments from that meeting appear as Appendix A of Deibler et al. (2008).

$H_1 := 460.0 \text{ in}$     Baseline liquid level

$H_t := 484.0 \text{ in}$     Height of equivalent flat top tank per Kennedy (2003)

$h_0 := H_t - H_1$      $h_0 = 24 \text{ in}$     Freeboard distance

$\frac{H_1}{H_t} = 0.95$     Ratio of waste height to tank height

$\frac{g}{W} := 386.4 \frac{\text{in}}{\text{sec}^2}$

$R := 450 \text{ in}$     Tank radius

$\frac{H_1}{R} = 1.02$     Ratio of waste height to tank radius

$i := 0..2$

$\lambda := \begin{pmatrix} 1.841 \\ 5.331 \\ 8.536 \end{pmatrix}$     Bessel function roots - Eqn. 4.5 BNL (1995)

$\theta := \begin{pmatrix} 0 \text{ deg} \\ 45 \text{ deg} \\ 90 \text{ deg} \end{pmatrix}$     Circumferential location of waste elements for which pressures are reported.

$\rho_1 := 1.71 \cdot 10^{-4} \frac{\text{lb} \cdot \text{sec}^2}{\text{in}^4}$     Liquid mass density - specific gravity of 1.83

**Convective Frequencies**

$f_{con_i} := \frac{1}{2 \cdot \pi} \cdot \sqrt{\lambda_i \cdot \left[ \frac{g}{R} \cdot \tanh \left[ \lambda_i \cdot \left( \frac{H_1}{R} \right) \right] \right]}$     Eqn. 4.14 BNL (1995)

**RPP-RPT-28963, Rev. 1**  
**M&D-2008-005-RPT-01, Rev. 1**

Prepared by: F. G. Abatt  
M&D Professional Services  
1/11/08  
Rev. 1

Theoretical Fluid Response  
Calculations for Equivalent Rigid  
Flat Top Tank at 460 in. Waste  
Level

Checked by: Milon Meyer

$$f_{con} = \begin{pmatrix} 0.2 \\ 0.34 \\ 0.43 \end{pmatrix} \frac{1}{s} \quad \text{First three convective frequencies}$$

Recalculate the Fundamental Convective Frequency Using the Methodology of Malhotra (2005)

$$j := 0..1$$

$$HR := \begin{pmatrix} 1.0 \\ 1.5 \end{pmatrix} \quad C_{cref} := \begin{pmatrix} 1.52 \\ 1.48 \end{pmatrix} \quad \text{Table 1 of Malhotra (2005)}$$

$$linterp\left(HR, C_{cref}, \frac{H_1}{R}\right) = 1.52$$

$$C_c := linterp\left(HR, C_{cref}, \frac{H_1}{R}\right) \frac{sec}{\sqrt{m}}$$

$$T_{conMalhotra} := C_c \cdot \sqrt{R} \quad T_{conMalhotra} = 5.13 \text{ s}$$

$$f_{conMalhotra} := \frac{1}{T_{conMalhotra}} \quad f_{conMalhotra} = 0.19 \frac{1}{s} \quad \text{Fundamental convective frequency per Eqn. (2) of Malhotra (2005).}$$

The fundamental convective frequencies calculated using the methodologies of BNL (1995) and Malhotra (2005) are nearly the same. Consequently, the spectral accelerations associated with the fundamental convective modes are essentially the same using either methodology.

Consider the first three convective mode spectral accelerations for the 0.1% damped spectrum

$$SA_{c0} := 0.066 \cdot g \quad SA_{c0} = 25.5 \frac{in}{sec^2}$$

$$SA_{c1} := 0.11 \cdot g \quad SA_{c1} = 42.5 \frac{in}{sec^2} \quad \text{ANSYS dome RS from Spectr}$$

$$SA_{c2} := 0.17 \cdot g \quad SA_{c2} = 65.69 \frac{in}{sec^2}$$

Associate the impulsive mode with the peak ground acceleration, since the tank is rigid.

$$PGA := 0.276 \cdot g \quad PGA = 106.65 \frac{in}{sec^2} \quad \text{ANSYS dome RS from Spectr}$$

**RPP-RPT-28963, Rev. 1**  
**M&D-2008-005-RPT-01, Rev. 1**

Prepared by: F. G. Abatt  
M&D Professional Services  
1/11/08  
Rev. 1

Theoretical Fluid Response  
Calculations for Equivalent Rigid  
Flat Top Tank at 460 in. Waste  
Level

Checked by: Milon Meyer

Calculate Maximum Slosh Height per BNL (1995):

$$\text{conmax} := \begin{pmatrix} 0.837 \\ 0.073 \\ 0.028 \end{pmatrix} \quad \text{Maximum value of convective coefficients at } \eta_1=1$$

$$h_s := R \cdot \sqrt{\left(\text{conmax}_0 \cdot \frac{SA_{c0}}{g}\right)^2 + \left(\text{conmax}_1 \cdot \frac{SA_{c1}}{g}\right)^2 + \left(\text{conmax}_2 \cdot \frac{SA_{c2}}{g}\right)^2} \quad \text{Eqn. 4.60 BNL (1995)}$$

$h_s = 25.2 \text{ in}$       Maximum theoretical slosh height for roofless tank

Recalculate the Maximum Slosh Height per Malhotra (2005):

$$h_{s\text{Malhotra}} := R \cdot \frac{SA_{c0}}{g} \quad \text{Eqn. (9) of Malhotra (2005)}$$

$h_{s\text{Malhotra}} = 29.7 \text{ in}$       Maximum slosh height for roofless tank per Malhotra (2005)

Calculate the Central Half-Angle for Wetted Portion of Tank Roof:

$$\theta_0 := \arccos\left(\frac{h_0}{h_s}\right) \quad \text{Central half-angle of maximum impacted roof area per Eqn. D.2 BNL (1995)}$$

$\theta_0 = 17.8 \text{ deg}$       Central half-angle per Appendix D BNL (1995)

$$\frac{h_0}{h_{s\text{Malhotra}}} = 0.81 \quad \text{Used to calculate } x_f \text{ from Figure 3 of Malhotra (2005)}$$

$x_f = 0.2 R$        $x_f = 90 \text{ in}$       Wetted width of tank roof per Figures 2 and 3 of Malhotra (2005)

$$\psi_0 := \arccos\left(\frac{x_f}{R} - 1\right) \quad \psi_0 = 2.5$$

$\theta_{0\text{Malhotra}} := \pi - \psi_0$        $\theta_{0\text{Malhotra}} = 36.9 \text{ deg}$       Central half-angle per Malhotra (2005)

Maximum Roof Pressure:

$r := 424.875 \text{ in}$       Typical centroidal radius of Dytran elements for which results are monitored

$p_r(r, \theta) := p_1 \cdot r \cdot \text{PGA} \cdot \cos(\theta)$       for  $|\theta| < |\theta_0|$       Peak roof pressure per Eqn. D.4 BNL (1995)

**RPP-RPT-28963, Rev. 1**  
**M&D-2008-005-RPT-01, Rev. 1**

Prepared by: F. G. Abatt  
M&D Professional Services  
1/11/08  
Rev. 1

Theoretical Fluid Response  
Calculations for Equivalent Rigid  
Flat Top Tank at 460 in. Waste  
Level

Checked by: Milon Meyer

$$p_r(R, 0) = 8.21 \frac{\text{lb}_f}{\text{in}^2}$$

$$p_r(r, 0) = 7.75 \frac{\text{lb}_f}{\text{in}^2}$$

Predicted peak roof pressure for Dytran element per BNL (1995)

$$P_{\text{maxroofMalhotra}} := \rho_1 \cdot x_f \cdot SA_{c0}$$

Peak roof pressure per Eqn. (10) and (12) of Malhotra (2005)

$$P_{\text{maxroofMalhotra}} = 0.39 \frac{\text{lb}_f}{\text{in}^2}$$

Calculate the Maximum Wall Pressure per Appendix D BNL (1995) :

$$p_{ic}(\theta) := \rho_1 \cdot R \cdot PGA \cdot \cos(\theta)$$

Impulsive component of pressure due to the constrained portion of the liquid per Eqn. D.5 of BNL (1995). This term represents the total hydrodynamic pressure within the central half-angle  $\theta_0$ .

$$p_{ic}(\theta) = \begin{pmatrix} 8.21 \\ 5.8 \\ 0 \end{pmatrix} \frac{\text{lb}_f}{\text{in}^2}$$

z :=  $\begin{pmatrix} 12\text{-in} \\ 37.5\text{-in} \\ 62.5\text{-in} \\ 87.5\text{-in} \\ 112.5\text{-in} \\ 137.5\text{-in} \\ 162.5\text{-in} \\ 187.5\text{-in} \\ 212.5\text{-in} \\ 237.5\text{-in} \\ 262.5\text{-in} \\ 287.5\text{-in} \\ 311.8\text{-in} \\ 336.0\text{-in} \\ 358.5\text{-in} \\ 377.7\text{-in} \\ 394.8\text{-in} \\ 410.0\text{-in} \\ 423.6\text{-in} \\ 435.0\text{-in} \\ 445.0\text{-in} \\ 455.0\text{-in} \end{pmatrix}$

Vertical location of Euler element centroids at which pressures are reported.

**RPP-RPT-28963, Rev. 1**  
**M&D-2008-005-RPT-01, Rev. 1**

Prepared by: F. G. Abatt  
M&D Professional Services  
1/11/08  
Rev. 1

Theoretical Fluid Response  
Calculations for Equivalent Rigid  
Flat Top Tank at 460 in. Waste  
Level

Checked by: Milon Meyer

$$\eta_1 := \frac{z}{H_1}$$

Ratio of tank wall vertical location to waste height for waste element centroids.

	0
0	0.03
1	0.08
2	0.14
3	0.19
4	0.24
5	0.3
6	0.35
7	0.41
8	0.46
9	0.52
$\eta_1 =$ 10	0.57
11	0.63
12	0.68
13	0.73
14	0.78
15	0.82
16	0.86
17	0.89
18	0.92
19	0.95
20	0.97
21	0.99

Determine convective coefficients as a function of dimensionless height per Eqn. 4.4 BNL (1995).

$$\text{con}_0(\eta_1) := \frac{2}{\left(\lambda_0\right)^2 - 1} \cdot \frac{\cosh\left[\lambda_0 \cdot \left(\frac{H_1}{R}\right) \cdot \eta_1\right]}{\cosh\left[\lambda_0 \cdot \left(\frac{H_1}{R}\right)\right]}$$

$$\text{con}_1(\eta_1) := \frac{2}{\left(\lambda_1\right)^2 - 1} \cdot \frac{\cosh\left[\lambda_1 \cdot \left(\frac{H_1}{R}\right) \cdot \eta_1\right]}{\cosh\left[\lambda_1 \cdot \left(\frac{H_1}{R}\right)\right]}$$

$$\text{con}_2(\eta_1) := \frac{2}{\left(\lambda_2\right)^2 - 1} \cdot \frac{\cosh\left[\lambda_2 \cdot \left(\frac{H_1}{R}\right) \cdot \eta_1\right]}{\cosh\left[\lambda_2 \cdot \left(\frac{H_1}{R}\right)\right]}$$

**RPP-RPT-28963, Rev. 1**  
**M&D-2008-005-RPT-01, Rev. 1**

Prepared by: F. G. Abatt  
M&D Professional Services  
1/11/08  
Rev. 1

Theoretical Fluid Response  
Calculations for Equivalent Rigid  
Flat Top Tank at 460 in. Waste  
Level

Checked by: Milon Meyer

Impulsive pressure coefficient as a function of normalized wall height

$$c_i(\eta_1) := 1 - \cos_0(\eta_1) \quad \text{Eqn. 4.7 BNL (1995) - 1st term}$$

$$P_{iu}(\eta_1, \theta) := c_i(\eta_1) \cdot \rho_1 \cdot R \cdot PGA \cdot \cos(\theta)$$

Impulsive component of maximum wall pressure induced by unconstrained portion of liquid beneath the non-impacted portion of the roof - same as for roofless tank ( Eqn. D.6 BNL [1995]). This is the impulsive component of the hydrodynamic pressure outside the central half-angle  $\theta_0$ .

$$P_{cu}(\eta_1, \theta) := \cos_0(\eta_1) \cdot \rho_1 \cdot R \cdot SA_{c0} \cdot \cos(\theta)$$

Convective component of maximum wall pressure induced by unconstrained portion of liquid beneath the non-impacted portion of the roof outside the central half-angle  $\theta_0$  - same as for roofless tank ( Eqn. D.7 BNL [1995]).

$$P_{totaloutside}(\eta_1, \theta) := \sqrt{P_{iu}(\eta_1, \theta)^2 + P_{cu}(\eta_1, \theta)^2} \quad \text{Total dynamic wall pressure outside central half-angle } \theta_0 \text{ - same as open tank solution.}$$

$$P_{totalinside}(\eta_1, \theta) := P_{ic}(\theta) \quad \text{Total dynamic wall pressure inside central half-angle } \theta_0 \text{ - same as completely full tank solution.}$$

$$P_{totalinside}(\eta_1, 0) = 8.21 \frac{\text{lb}}{\text{in}^2}$$

	0	
0	3.25	
1	3.23	
2	3.21	
3	3.18	
4	3.13	
5	3.08	
6	3.01	
7	2.92	
8	2.83	
9	2.72	
$P_{totaloutside}(\eta_1, 45) =$	10	2.59
	11	2.45
	12	2.29
	13	2.12
	14	1.95
	15	1.79
	16	1.65
	17	1.51
	18	1.4
	19	1.3
	20	1.22
	21	1.15

psi

**RPP-RPT-28963, Rev. 1**  
**M&D-2008-005-RPT-01, Rev. 1**

Prepared by: F. G. Abatt  
M&D Professional Services  
1/11/08  
Rev. 1

Theoretical Fluid Response  
Calculations for Equivalent Rigid  
Flat Top Tank at 460 in. Waste  
Level

Checked by: Milon Meyer

	0
0	0.25
1	0.25
2	0.26
3	0.27
4	0.28
5	0.29
6	0.31
7	0.33
8	0.35
9	0.38
10	0.41
11	0.44
12	0.48
13	0.52
14	0.57
15	0.61
16	0.65
17	0.69
18	0.73
19	0.76
20	0.79
21	0.82

	0
0	0.75
1	0.75
2	0.74
3	0.73
4	0.72
5	0.71
6	0.69
7	0.67
8	0.65
9	0.62
10	0.59
11	0.56
12	0.52
13	0.48
14	0.43
15	0.39
16	0.35
17	0.31
18	0.27
19	0.24
20	0.21
21	0.18

**RPP-RPT-28963, Rev. 1**  
**M&D-2008-005-RPT-01, Rev. 1**

Prepared by: F. G. Abatt  
M&D Professional Services  
1/11/08  
Rev. 1

Theoretical Fluid Response  
Calculations for Equivalent Rigid  
Flat Top Tank at 460 in. Waste  
Level

Checked by: Milon Meyer

$$P_{iu}(\eta_1, 45) = \begin{array}{|c|c|} \hline & 0 \\ \hline 0 & 3.24 \\ \hline 1 & 3.22 \\ \hline 2 & 3.2 \\ \hline 3 & 3.17 \\ \hline 4 & 3.12 \\ \hline 5 & 3.06 \\ \hline 6 & 2.99 \\ \hline 7 & 2.9 \\ \hline 8 & 2.8 \\ \hline 9 & 2.69 \\ \hline 10 & 2.56 \\ \hline 11 & 2.4 \\ \hline 12 & 2.24 \\ \hline 13 & 2.05 \\ \hline 14 & 1.86 \\ \hline 15 & 1.68 \\ \hline 16 & 1.5 \\ \hline 17 & 1.34 \\ \hline 18 & 1.18 \\ \hline 19 & 1.04 \\ \hline 20 & 0.91 \\ \hline 21 & 0.77 \\ \hline \end{array} \frac{\text{lb}}{\text{in}^2}$$

$$P_{cu}(\eta_1, 45) = \begin{array}{|c|c|} \hline & 0 \\ \hline 0 & 0.26 \\ \hline 1 & 0.26 \\ \hline 2 & 0.27 \\ \hline 3 & 0.27 \\ \hline 4 & 0.28 \\ \hline 5 & 0.3 \\ \hline 6 & 0.32 \\ \hline 7 & 0.34 \\ \hline 8 & 0.36 \\ \hline 9 & 0.39 \\ \hline 10 & 0.42 \\ \hline 11 & 0.46 \\ \hline 12 & 0.5 \\ \hline 13 & 0.54 \\ \hline 14 & 0.59 \\ \hline 15 & 0.63 \\ \hline 16 & 0.67 \\ \hline 17 & 0.71 \\ \hline 18 & 0.75 \\ \hline 19 & 0.78 \\ \hline 20 & 0.81 \\ \hline 21 & 0.85 \\ \hline \end{array} \frac{\text{lb}}{\text{in}^2}$$

Total dynamic wall pressure at  $\theta=45$  degrees (outside the central half-angle  $\theta_0$ ).

$$P_{\text{totaloutside}}(\eta_1, 45) = \begin{array}{|c|c|} \hline & 0 \\ \hline 0 & 3.25 \\ \hline 1 & 3.23 \\ \hline 2 & 3.21 \\ \hline 3 & 3.18 \\ \hline 4 & 3.13 \\ \hline 5 & 3.08 \\ \hline 6 & 3.01 \\ \hline 7 & 2.92 \\ \hline 8 & 2.83 \\ \hline 9 & 2.72 \\ \hline 10 & 2.59 \\ \hline 11 & 2.45 \\ \hline 12 & 2.29 \\ \hline 13 & 2.12 \\ \hline 14 & 1.95 \\ \hline 15 & 1.79 \\ \hline 16 & 1.65 \\ \hline 17 & 1.51 \\ \hline 18 & 1.4 \\ \hline 19 & 1.3 \\ \hline 20 & 1.22 \\ \hline 21 & 1.15 \\ \hline \end{array} \frac{\text{lb}}{\text{in}^2}$$

RPP-RPT-28963, Rev. 1  
M&D-2008-005-RPT-01, Rev. 1

Prepared by: F. G. Abatt  
M&D Professional Services  
1/11/08  
Rev. 1

Theoretical Fluid Response  
Calculations for Equivalent Rigid  
Flat Top Tank at 460 in. Waste  
Level

Checked by: Milon Meyer

Calculate Maximum Total Hydrodynamic Force:

The maximum hydrodynamic force induced on the tank wall is given by the sum of the terms in Equations D.12, D.13, and D.14 of BNL 1995.

$$m_1 := 4.97 \cdot 10^4 \frac{\text{lb} \cdot \text{sec}^2}{\text{in}} \quad \text{Actual waste mass reported by Dytran model.}$$

$$m_{c0} := \left[ \frac{2}{\lambda_0 \left[ (\lambda_0)^2 - 1 \right]} \cdot \left( \frac{H_1}{R} \right) \right] \cdot \tanh \left[ \lambda_0 \cdot \left( \frac{H_1}{R} \right) \right] \cdot m_1 \quad \text{Eqn. 4.32 BNL (1995)}$$

$$m_{c0} = 2.11 \times 10^4 \frac{\text{lb} \cdot \text{sec}^2}{\text{in}} \quad \text{First mode convective mass for roofless tank}$$

$$m_i := m_1 - m_{c0} \quad m_i = 2.86 \times 10^4 \frac{\text{lb} \cdot \text{sec}^2}{\text{in}} \quad \text{Impulsive mass for roofless tank - Eqn. 4.33 BNL (1995)}$$

$$\frac{m_{c0}}{m_1} = 0.42 \quad \frac{m_i}{m_1} = 0.58$$

$$\text{epsilon} := \frac{2 \cdot \theta_0 + \sin(2 \cdot \theta_0)}{2 \cdot \pi} \quad \text{Dimensionless factor for wall force calculation Eqn. D.9 of BNL (1995).}$$

$$F_{ic} := \text{epsilon} \cdot \frac{H_t}{H_1} \cdot m_i \cdot \text{PGA} \quad \text{Impulsive component of force due to constrained portion of liquid Eqn. D.12 of BNL (1995) with force notation changed to "F".}$$

$$F_{ic} = 1.07 \times 10^6 \text{ lbf}$$

$$F_{iu} := (1 - \text{epsilon}) \cdot m_i \cdot \text{PGA} \quad \text{Impulsive component of force due to unconstrained portion of liquid Eqn. D.13 of BNL (1995) with force notation changed to "F".}$$

$$F_{iu} = 2.46 \times 10^6 \text{ lbf}$$

$$F_{cu} := (1 - \text{epsilon}) \cdot m_{c0} \cdot S A_{c0} \quad \text{Convective component of force due to unconstrained portion of liquid Eqn. D.14 of BNL (1995) with force notation changed to "F".}$$

$$F_{cu} = 4.35 \times 10^5 \text{ lbf}$$

RPP-RPT-28963, Rev. 1  
M&D-2008-005-RPT-01, Rev. 1

Prepared by: F. G. Abatt  
M&D Professional Services  
1/11/08  
Rev. 1

Theoretical Fluid Response  
Calculations for Equivalent Rigid  
Flat Top Tank at 460 in. Waste  
Level

Checked by: Milon Meyer

$$F_{\text{total}} := \sqrt{(F_{\text{ic}} + F_{\text{iu}})^2 + F_{\text{cu}}^2} \quad \text{Total peak hydrodynamic force per BNL (1995)}$$

$$F_{\text{total}} = 3.56 \times 10^6 \text{ lbf}$$

Recalculate Maximum Hydrodynamic Force Using Methodology of Malhotra (2005):

The hydrodynamic force can be calculated by excluding the structural masses from Eqn. (3) of Malhotra (2005). First calculate the impulsive and convective masses.

$$\beta := 0..1$$

$$\frac{HR}{H_1} := \begin{pmatrix} 1.0 \\ 1.5 \end{pmatrix} \quad \text{ImpMassRatio} := \begin{pmatrix} 0.548 \\ 0.686 \end{pmatrix} \quad \text{Table 1 of Malhotra (2005)}$$

$$\text{linterp}\left(HR, \text{ImpMassRatio}, \frac{H_1}{R}\right) = 0.55$$

$$m_{\text{iMalhotra}} := \text{linterp}\left(HR, \text{ImpMassRatio}, \frac{H_1}{R}\right) m_1 \quad m_{\text{iMalhotra}} = 2.75 \times 10^4 \frac{\text{lbf}\cdot\text{sec}^2}{\text{in}}$$

$$m_{\text{cMalhotra}} := m_1 - m_{\text{iMalhotra}} \quad m_{\text{cMalhotra}} = 2.22 \times 10^4 \frac{\text{lbf}\cdot\text{sec}^2}{\text{in}}$$

$$R_i := m_{\text{iMalhotra}} \cdot \text{PGA} \quad \text{Eqn. (3) Malhotra (2005)}$$

$$R_c := m_{\text{cMalhotra}} \cdot \text{SA}_{c0} \quad \text{Eqn. (4) Malhotra (2005)}$$

Modify the impulsive and convective masses to account for interaction with the tank roof per Eqns. (15) and (16) of Malhotra (2005).

$$m_{\text{ibar}} := m_{\text{iMalhotra}} + m_{\text{cMalhotra}} \left(1 - \frac{h_0}{h_{\text{sMalhotra}}}\right) \quad m_{\text{ibar}} = 3.18 \times 10^4 \frac{\text{lbf}\cdot\text{sec}^2}{\text{in}}$$

$$m_{\text{cbar}} := m_{\text{cMalhotra}} \left(\frac{h_0}{h_{\text{sMalhotra}}}\right) \quad m_{\text{cbar}} = 1.79 \times 10^4 \frac{\text{lbf}\cdot\text{sec}^2}{\text{in}}$$

$$R_{\text{ibar}} := m_{\text{ibar}} \cdot \text{PGA} \quad R_{\text{ibar}} = 3.39 \times 10^6 \text{ lbf} \quad \text{Impulsive component of peak reaction force}$$

$$R_{\text{cbar}} := m_{\text{cbar}} \cdot \text{SA}_{c0} \quad R_{\text{cbar}} = 4.57 \times 10^5 \text{ lbf} \quad \text{Convective component of peak reaction force}$$

RPP-RPT-28963, Rev. 1  
M&D-2008-005-RPT-01, Rev. 1

Prepared by: F. G. Abatt  
M&D Professional Services  
1/11/08  
Rev. 1

Theoretical Fluid Response  
Calculations for Equivalent Rigid  
Flat Top Tank at 460 in. Waste  
Level

Checked by: Milon Meyer

$$R_{\text{bar}} := \sqrt{R_{\text{ibar}}^2 + R_{\text{cbar}}^2}$$

Total peak reaction force per Malhotra (2005)

$$R_{\text{bar}} = 3.42 \times 10^6 \text{ lbf}$$

References:

BNL 1995, *Seismic Design and Evaluation Guidelines for the Department of Energy High-Level Waste Storage Tanks and Appurtenances*, BNL 52361, Rev. 10/95, Brookhaven National Laboratory, Upton, New York.

Deibler, J.E., K.I. Johnson, S.P. Pilli, M.W. Rinker, F.G. Abatt, and N.K. Karri, 2008, *Hanford Double-Shell Tank Thermal and Seismic Project Increased Liquid Level Analysis for 241AP Tank Farm*, RPP-RPT-32237, Rev. 1, Pacific Northwest National Laboratory, Richland, Washington.

Malhotra, Praveen K, 2005, *Sloshing Loads in Liquid Storage Tanks With Insufficient Freeboard*, Earthquake Spectra, Volume 21, No. 4, pp. 1185-1192, November 2005.

Kennedy, R.P., 2003, *Review Comments Concerning Evaluation of Proposed Increase to Double-Shell Tank Liquid Level*, May 2003, RPK Structural Mechanics Consulting, Escondido, California.

Intentionally left blank.

**RPP-RPT-28963, Rev. 1**  
**M&D-2008-005-RPT-01, Rev. 1**

Prepared by: F. G. Abatt  
M&D Professional Services  
1/11/08  
Rev. 1

Theoretical Fluid Response for  
Flexible Wall Open Top Tank at 460  
in. Waste Level

Checked by: Milon Meyer

This worksheet contains calculations for a flexible wall open top tank with an initial liquid level of 460 in. The calculations are performed using the methodology in Chapter 4 of BNL (1995) and in Malhotra (2005). The benchmark solutions are based on an impulsive frequency of 6.5 Hz and impulsive damping of 3.5% critical. The location of the fluid elements corresponds to the flexible wall Dytran model with the refined mesh as described in Appendix C. Revision 1 modifies the total reaction force using the method of Malhotra to be the SRSS combination of the impulsive and convective components rather than the direct sum.

$H_1 := 460 \cdot \text{in}$       Baseline waste level

$$\frac{g}{\omega} := 386.4 \frac{\text{in}}{\text{sec}^2}$$

$R := 450 \cdot \text{in}$       Tank radius

$\frac{H_1}{R} = 1.02$       Ratio of waste height to tank radius

$H_t := 460 \cdot \text{in}$       Assumed tank height used for calculation

$\frac{H_1}{H_t} = 1$       Ratio of liquid height to tank height - only used for calculation of  $C_{\text{ref}}$  from Table 4.4 of BNL (1995)

$i := 0..2$

$\lambda := \begin{pmatrix} 1.841 \\ 5.331 \\ 8.536 \end{pmatrix}$       Bessel function roots - Eqn. 4.5 BNL (1995)

$\theta := \begin{pmatrix} 0 \cdot \text{deg} \\ 45 \cdot \text{deg} \\ 90 \cdot \text{deg} \end{pmatrix}$       Circumferential location of waste elements for which pressures are reported

Convective Frequencies per BNL (1995)

$$f_{\text{con}_i} := \frac{1}{2 \cdot \pi} \left[ \sqrt{\lambda_i \left[ \frac{g}{R} \cdot \tanh \left[ \lambda_i \left( \frac{H_1}{R} \right) \right] \right]} \right] \quad \text{Eqn. 4.14 BNL (1995)}$$

$f_{\text{con}} = \begin{pmatrix} 0.196 \\ 0.341 \\ 0.431 \end{pmatrix} \frac{1}{\text{s}}$       First three convective frequencies

**RPP-RPT-28963, Rev. 1**  
**M&D-2008-005-RPT-01, Rev. 1**

Prepared by: F. G. Abatt  
M&D Professional Services  
1/11/08  
Rev. 1

Theoretical Fluid Response for  
Flexible Wall Open Top Tank at 460  
in. Waste Level

Checked by: Milon Meyer

$$\rho_l := 1.71 \cdot 10^{-4} \frac{\text{lb} \cdot \text{sec}^2}{\text{in}^4} \quad \text{waste density - specific gravity} = 1.83$$

Recalculate Maximum Slosh Height per Malhotra (2005):

$$j := 0..1$$

$$H_r := \begin{pmatrix} 1.0 \\ 1.5 \end{pmatrix}$$

$$C_{\text{cref}} := \begin{pmatrix} 1.52 \\ 1.48 \end{pmatrix}$$

Table 1 of Malhotra (2005)

$$C_c := \text{linterp}\left(H_r, C_{\text{cref}}, \frac{H_1}{R}\right) \frac{\text{sec}}{\sqrt{\text{m}}} \quad C_c = 1.52 \frac{\text{sec}}{\text{m}^{0.5}}$$

$$T_{\text{con}} := C_c \cdot \sqrt{R} \quad T_{\text{con}} = 5.13 \text{ s}$$

$$f_{\text{cMalhotra}} := \frac{1}{T_{\text{con}}} \quad f_{\text{cMalhotra}} = 0.195 \frac{1}{\text{s}} \quad \text{Fundamental convective frequency per Malhotra (2005)}$$

Calculation of Impulsive Frequency per BNL (1995):

$$\rho_t := 7.35 \cdot 10^{-4} \frac{\text{lb} \cdot \text{sec}^2}{\text{in}^4} \quad \text{Steel density}$$

$$t_{\text{tw}} := 0.65 \cdot \text{in} \quad \text{Tank wall thickness used in Dytran model.}$$

$$E_t := 29 \cdot 10^6 \frac{\text{lb} \cdot \text{f}}{\text{in}^2} \quad \text{Elastic modulus for steel}$$

$$C_{\text{iref}} := 0.1062 \quad \text{Table 4.4 of BNL (1995) - } H_1=R=H_t, \text{ hinged top boundary condition.}$$

$$C_i := C_{\text{iref}} \cdot \sqrt{127 \cdot \frac{t_{\text{tw}}}{R} \cdot \frac{\rho_l}{\rho_t}} \quad \text{Eqn. 4.18 BNL (1995)}$$

$$C_i = 0.09 \quad \text{Impulsive coefficient for frequency calculation}$$

$$f_i := \frac{1}{2 \cdot \pi} \cdot \frac{C_i}{H_1} \cdot \sqrt{\frac{E_t}{\rho_t}} \quad f_i = 6.48 \frac{1}{\text{s}} \quad \text{Eqn. 4.16 BNL (1995)}$$

**RPP-RPT-28963, Rev. 1**  
**M&D-2008-005-RPT-01, Rev. 1**

Prepared by: F. G. Abatt  
M&D Professional Services  
1/11/08  
Rev. 1

Theoretical Fluid Response for  
Flexible Wall Open Top Tank at 460  
in. Waste Level

Checked by: Milon Meyer

Recalculate the Fundamental Impulsive Frequency Using the Methodology of Malhotra (2005):

$$\omega = 0..1$$

$$HR := \begin{pmatrix} 1.0 \\ 1.5 \end{pmatrix} \quad C_{irefMalhotra} := \begin{pmatrix} 6.36 \\ 6.06 \end{pmatrix}$$

$$linterp\left(HR, C_{irefMalhotra}, \frac{H_1}{R}\right) = 6.35$$

$$C_{iMalhotra} := linterp\left(HR, C_{irefMalhotra}, \frac{H_1}{R}\right)$$

$$T_{impMalhotra} := C_{iMalhotra} \cdot \frac{\sqrt{\rho_1} \cdot H_1}{\sqrt{\frac{t_{tw}}{R} \cdot \sqrt{E_t}}} \quad T_{impMalhotra} = 0.19 \text{ s}$$

$$f_{impMalhotra} := \frac{1}{T_{impMalhotra}} \quad f_{impMalhotra} = 5.36 \frac{1}{s} \quad \text{Fundamental impulsive frequency per Malhotra (2005)}$$

**RPP-RPT-28963, Rev. 1**  
**M&D-2008-005-RPT-01, Rev. 1**

Prepared by: F. G. Abatt  
M&D Professional Services  
1/11/08  
Rev. 1

Theoretical Fluid Response for  
Flexible Wall Open Top Tank at 460  
in. Waste Level

Checked by: Milon Meyer

Determine Convective Pressures on the Tank Wall per BNL (1995):

- z :=
- 4.0-in
  - 24.1-in
  - 44.2-in
  - 64.2-in
  - 84.3-in
  - 104.4-in
  - 124.4-in
  - 144.5-in
  - 164.6-in
  - 184.6-in
  - 204.7-in
  - 224.8-in
  - 244.8-in
  - 264.9-in
  - 285-in
  - 305-in
  - 325-in
  - 345-in
  - 365-in
  - 385-in
  - 405-in
  - 425-in
  - 435-in
  - 445-in
  - 455-in

Vertical location of Euler element centroids at which pressures are reported.

$$\eta_1 := \frac{z}{H_1}$$

	0
0	$8.7 \cdot 10^{-3}$
1	0.05
2	0.1
3	0.14
4	0.18
5	0.23
6	0.27
7	0.31
8	0.36
9	0.4
10	0.45
11	0.49
12	0.53
13	0.58
14	0.62
15	0.66
16	0.71
17	0.75
18	0.79
19	0.84
20	0.88
21	0.92
22	0.95
23	0.97
24	0.99

Ratio of tank wall vertical location to waste height for waste element centroids.

**RPP-RPT-28963, Rev. 1**  
**M&D-2008-005-RPT-01, Rev. 1**

Prepared by: F. G. Abatt  
M&D Professional Services  
1/11/08  
Rev. 1

Theoretical Fluid Response for  
Flexible Wall Open Top Tank at 460  
in. Waste Level

Checked by: Milon Meyer

Determine convective coefficients as a function of dimensionless height per Eqn. 4.4 BNL (1995).

$$\text{con}_0(\eta_1) := \frac{2 \cdot \cosh\left[\lambda_0 \cdot \left(\frac{H_1}{R}\right) \eta_1\right]}{\left(\lambda_0\right)^2 - 1 \cdot \cosh\left[\lambda_0 \cdot \left(\frac{H_1}{R}\right)\right]}$$

$$\text{con}_1(\eta_1) := \frac{2 \cdot \cosh\left[\lambda_1 \cdot \left(\frac{H_1}{R}\right) \eta_1\right]}{\left(\lambda_1\right)^2 - 1 \cdot \cosh\left[\lambda_1 \cdot \left(\frac{H_1}{R}\right)\right]}$$

$$\text{con}_2(\eta_1) := \frac{2 \cdot \cosh\left[\lambda_2 \cdot \left(\frac{H_1}{R}\right) \eta_1\right]}{\left(\lambda_2\right)^2 - 1 \cdot \cosh\left[\lambda_2 \cdot \left(\frac{H_1}{R}\right)\right]}$$

$\text{con}_0(\eta_1) =$

	0
0	0.25
1	0.25
2	0.25
3	0.26
4	0.26
5	0.27
6	0.28
7	0.29
8	0.31
9	0.32
10	0.34
11	0.36
12	0.38
13	0.41
14	0.44
15	0.47
16	0.5
17	0.54
18	0.58
19	0.63
20	0.68
21	0.73
22	0.76
23	0.79
24	0.82

$\text{con}_1(\eta_1) =$

	0
0	6.28·10 <sup>-4</sup>
1	6.53·10 <sup>-4</sup>
2	7.15·10 <sup>-4</sup>
3	8.17·10 <sup>-4</sup>
4	9.67·10 <sup>-4</sup>
5	1.17·10 <sup>-3</sup>
6	1.44·10 <sup>-3</sup>
7	1.79·10 <sup>-3</sup>
8	2.25·10 <sup>-3</sup>
9	2.83·10 <sup>-3</sup>
10	3.57·10 <sup>-3</sup>
11	4.52·10 <sup>-3</sup>
12	5.72·10 <sup>-3</sup>
13	7.24·10 <sup>-3</sup>
14	9.19·10 <sup>-3</sup>
15	0.01
16	0.01
17	0.02
18	0.02
19	0.03
20	0.04
21	0.05
22	0.05
23	0.06
24	0.07

$\text{con}_2(\eta_1) =$

	0
0	9.06·10 <sup>-6</sup>
1	10·10 <sup>-6</sup>
2	1.24·10 <sup>-5</sup>
3	1.66·10 <sup>-5</sup>
4	2.33·10 <sup>-5</sup>
5	3.34·10 <sup>-5</sup>
6	4.83·10 <sup>-5</sup>
7	7.03·10 <sup>-5</sup>
8	1.03·10 <sup>-4</sup>
9	1.5·10 <sup>-4</sup>
10	2.2·10 <sup>-4</sup>
11	3.21·10 <sup>-4</sup>
12	4.7·10 <sup>-4</sup>
13	6.88·10 <sup>-4</sup>
14	1.01·10 <sup>-3</sup>
15	1.47·10 <sup>-3</sup>
16	2.15·10 <sup>-3</sup>
17	3.14·10 <sup>-3</sup>
18	4.59·10 <sup>-3</sup>
19	6.71·10 <sup>-3</sup>
20	9.8·10 <sup>-3</sup>
21	0.01
22	0.02
23	0.02
24	0.03

RPP-RPT-28963, Rev. 1  
M&D-2008-005-RPT-01, Rev. 1

Prepared by: F. G. Abatt  
M&D Professional Services  
1/11/08  
Rev. 1

Theoretical Fluid Response for  
Flexible Wall Open Top Tank at 460  
in. Waste Level

Checked by: Milon Meyer

Impulsive pressure coefficient as a function of dimensionless wall height

$$c_i(\eta_1) := 1 - c_{n0}(\eta_1) - c_{n1}(\eta_1) - c_{n2}(\eta_1) \quad \text{Eqn. 4.7 BNL (1995)}$$

	0
0	0.75
1	0.75
2	0.75
3	0.74
4	0.73
5	0.73
6	0.72
7	0.7
8	0.69
9	0.67
10	0.65
11	0.63
12	0.61
13	0.58
14	0.55
15	0.52
16	0.48
17	0.44
18	0.39
19	0.34
20	0.28
21	0.21
22	0.17
23	0.13
24	0.09

Calculate maximum values of dynamic wall pressures from spectral acceleration of dome input TH.

Consider the first three convective modes with accelerations from the 0.1% damped spectrum

$$SA_{c0} := 0.066 \cdot g$$

$$SA_{c0} = 25.5 \frac{\text{in}}{\text{sec}^2}$$

$$SA_{c1} := 0.11 \cdot g$$

$$SA_{c1} = 42.5 \frac{\text{in}}{\text{sec}^2}$$

ANSYS Dome RS from Spectr

$$SA_{c2} := 0.17 \cdot g$$

$$SA_{c2} = 65.69 \frac{\text{in}}{\text{sec}^2}$$

RPP-RPT-28963, Rev. 1  
M&D-2008-005-RPT-01, Rev. 1

Prepared by: F. G. Abatt  
M&D Professional Services  
1/11/08  
Rev. 1

Theoretical Fluid Response for  
Flexible Wall Open Top Tank at 460  
in. Waste Level

Checked by: Milon Meyer

Determine the spectral acceleration for the impulsive mode.

$$SA_i := 1.0g \quad SA_i = 386.4 \frac{\text{in}}{\text{sec}^2} \quad 3.5\% \text{ Dome RS from Spectr based on damping during initial gravity loading in Dytran model taken at 6.5 Hz.}$$

$$P_{\max\text{conv}}(\eta_1, \theta) := \left[ \sqrt{(\cos_0(\eta_1) \cdot SA_{c0})^2 + (\cos_1(\eta_1) \cdot SA_{c1})^2 + (\cos_2(\eta_1) \cdot SA_{c2})^2} \right] \cdot (\rho_1 \cdot R \cdot \cos(\theta \cdot \text{deg}))$$

$$P_{\max\text{impulsive}}(\eta_1, \theta) := \left[ \sqrt{[c_i(\eta_1) \cdot (SA_i)]^2} \right] \cdot (\rho_1 \cdot R \cdot \cos(\theta \cdot \text{deg}))$$

$$P_{\max}(\eta_1, \theta) := \left[ \sqrt{[c_i(\eta_1) \cdot (SA_i)]^2 + (\cos_0(\eta_1) \cdot SA_{c0})^2 + (\cos_1(\eta_1) \cdot SA_{c1})^2 + (\cos_2(\eta_1) \cdot SA_{c2})^2} \right] \cdot (\rho_1 \cdot R \cdot \cos(\theta \cdot \text{deg}))$$

Eqn. 4.24 BNL (1995)

Determine the spectral acceleration for the impulsive frequency calculated per Malhotra (2005).

$$SA_{i\text{Malhotra}} := 1.07g \quad SA_{i\text{Malhotra}} = 413.45 \frac{\text{in}}{\text{sec}^2} \quad 3.5\% \text{ Dome RS from Spectr based on damping during initial gravity loading in Dytran model taken at 5.4 Hz.}$$

RPP-RPT-28963, Rev. 1  
M&D-2008-005-RPT-01, Rev. 1

Prepared by: F. G. Abatt  
M&D Professional Services  
1/11/08  
Rev. 1

Theoretical Fluid Response for  
Flexible Wall Open Top Tank at 460  
in. Waste Level

Checked by: Milon Meyer

	0
0	22.3
1	22.27
2	22.18
3	22.04
4	21.85
5	21.6
6	21.3
7	20.94
8	20.51
9	20.02
10	19.46
11	18.82
12	18.1
13	17.29
14	16.39
15	15.38
16	14.25
17	12.99
18	11.57
19	9.98
20	8.18
21	6.14
22	5.02
23	3.82
24	2.53

$$P_{\text{maximpulsive}}(\eta_1, 0) =$$

$$\frac{\text{lbf}}{\text{in}^2}$$

Maximum impulsive dynamic pressures at  
theta = 0.

	0
0	0.49
1	0.49
2	0.5
3	0.51
4	0.52
5	0.53
6	0.55
7	0.58
8	0.6
9	0.64
10	0.67
11	0.71
12	0.76
13	0.81
14	0.86
15	0.92
16	0.99
17	1.06
18	1.15
19	1.24
20	1.34
21	1.44
22	1.5
23	1.57
24	1.63

$$P_{\text{maxconv}}(\eta_1, 0) =$$

$$\frac{\text{lbf}}{\text{in}^2}$$

Maximum convective  
dynamic pressures at  
theta = 0.

RPP-RPT-28963, Rev. 1  
M&D-2008-005-RPT-01, Rev. 1

Prepared by: F. G. Abatt  
M&D Professional Services  
1/11/08  
Rev. 1

Theoretical Fluid Response for  
Flexible Wall Open Top Tank at 460  
in. Waste Level

Checked by: Milon Meyer

	0
0	22.31
1	22.27
2	22.19
3	22.05
4	21.86
5	21.61
6	21.31
7	20.94
8	20.52
9	20.03
10	19.47
11	18.83
12	18.12
13	17.31
14	16.41
15	15.41
16	14.28
17	13.03
18	11.63
19	10.05
20	8.29
21	6.31
22	5.24
23	4.13
24	3.01

Maximum total dynamic pressure at  
theta = 0.

$\frac{\text{lbf}}{\text{in}^2}$

	0
0	15.8
1	15.7
2	15.7
3	15.6
4	15.5
5	15.3
6	15.1
7	14.8
8	14.5
9	14.2
10	13.8
11	13.3
12	12.8
13	12.2
14	11.6
15	10.9
16	10.1
17	9.2
18	8.2
19	7.1
20	5.9
21	4.5
22	3.7
23	2.9
24	2.1

$\frac{\text{lbf}}{\text{in}^2}$

Maximum total dynamic pressure at  
theta = 45 degrees.

RPP-RPT-28963, Rev. 1  
M&D-2008-005-RPT-01, Rev. 1

Prepared by: F. G. Abatt  
M&D Professional Services  
1/11/08  
Rev. 1

Theoretical Fluid Response for  
Flexible Wall Open Top Tank at 460  
in. Waste Level

Checked by: Milon Meyer

Calculate Maximum Slosh Height per BNL (1995):

$$\text{conmax} := \begin{pmatrix} 0.837 \\ 0.073 \\ 0.028 \end{pmatrix} \quad \text{Maximum value of convective coefficients at } \eta_i=1$$

$$h_{\text{maxslosh}} := R \cdot \sqrt{\left(\text{conmax}_0 \cdot \frac{SA_{c0}}{g}\right)^2 + \left(\text{conmax}_1 \cdot \frac{SA_{c1}}{g}\right)^2 + \left(\text{conmax}_2 \cdot \frac{SA_{c2}}{g}\right)^2} \quad \text{Eqn. 4.60 BNL (1995)}$$

$$h_{\text{maxslosh}} = 25.21 \text{ in}$$

Recalculate the Maximum Slosh Height per Malhotra (2005):

Since the fundamental convective frequency calculated per Malhotra agrees with the frequency calculated via BNL (1995), the convective acceleration is the same in both cases.

$$h_{\text{sMalhotra}} := R \cdot \frac{SA_{c0}}{g} \quad \text{Eqn. (9) of Malhotra (2005)}$$

$$h_{\text{sMalhotra}} = 29.7 \text{ in} \quad \text{Maximum slosh height for roofless tank per Malhotra (2005)}$$

Calculate Maximum Total Hydrodynamic Force per BNL (1995):

The maximum hydrodynamic force induced on the tank wall is given by Eqn. 4.31 of BNL (1995) with the instantaneous accelerations replaced by the maximum spectral accelerations. First determine the effective impulsive and convective masses.

$$m_{\text{lapprox}} := \pi \cdot R^2 \cdot H_1 \cdot \rho_1 \quad m_{\text{lapprox}} = 5 \times 10^4 \frac{\text{lb} \cdot \text{sec}^2}{\text{in}} \quad \text{Total waste mass based on circular cylinder approximation.}$$

$$m_1 := 4.97 \times 10^4 \frac{\text{lb} \cdot \text{sec}^2}{\text{in}} \quad \text{Actual waste mass reported by Dytran model.}$$

**RPP-RPT-28963, Rev. 1**  
**M&D-2008-005-RPT-01, Rev. 1**

Prepared by: F. G. Abatt  
M&D Professional Services  
1/11/08  
Rev. 1

Theoretical Fluid Response for  
Flexible Wall Open Top Tank at 460  
in. Waste Level

Checked by: Milon Meyer

$$m_{c0} := \left[ \frac{2}{\lambda_0 \cdot \left[ (\lambda_0)^2 - 1 \right] \cdot \left( \frac{H_1}{R} \right)} \right] \cdot \tanh \left[ \lambda_0 \cdot \left( \frac{H_1}{R} \right) \right] \cdot m_i \quad \text{First mode convective mass - Eqn. 4.32 BNL (1995)}$$

$$m_{c0} = 2.11 \times 10^4 \frac{\text{lb} \cdot \text{sec}^2}{\text{in}}$$

$$m_{c1} := \left[ \frac{2}{\lambda_1 \cdot \left[ (\lambda_1)^2 - 1 \right] \cdot \left( \frac{H_1}{R} \right)} \right] \cdot \tanh \left[ \lambda_1 \cdot \left( \frac{H_1}{R} \right) \right] \cdot m_i \quad \text{Second mode convective mass}$$

$$m_{c1} = 665.21 \frac{\text{lb} \cdot \text{sec}^2}{\text{in}}$$

$$m_{c2} := \left[ \frac{2}{\lambda_2 \cdot \left[ (\lambda_2)^2 - 1 \right] \cdot \left( \frac{H_1}{R} \right)} \right] \cdot \tanh \left[ \lambda_2 \cdot \left( \frac{H_1}{R} \right) \right] \cdot m_i \quad \text{Third mode convective mass}$$

$$m_{c2} = 158.52 \frac{\text{lb} \cdot \text{sec}^2}{\text{in}}$$

$$m_i := m_1 - (m_{c0} + m_{c1} + m_{c2}) \quad \text{Impulsive mass - Eqn. 4.33 BNL (1995)}$$

$$m_i = 2.78 \times 10^4 \frac{\text{lb} \cdot \text{sec}^2}{\text{in}}$$

$$F_{\max} := m_i \cdot SA_i + m_{c0} \cdot SA_{c0} + m_{c1} \cdot SA_{c1} + m_{c2} \cdot SA_{c2} \quad \text{Eqn. 4.31 BNL (1995)}$$

$$F_{\max} = 1.13 \times 10^7 \text{ lbf} \quad \text{Conservative estimate of maximum hydrodynamic force}$$

The above expression is a conservative estimate because it assumes that the peak impulsive and convective forces occur simultaneously. A less conservative estimate can be made via a square-root-sum-of-the-squares (SRSS) combination.

$$F_{\text{SRSS}} := \sqrt{(m_i \cdot SA_i)^2 + (m_{c0} \cdot SA_{c0})^2 + (m_{c1} \cdot SA_{c1})^2 + (m_{c2} \cdot SA_{c2})^2} \quad \text{Eqn. 4.31 BNL (1995) - SRSS}$$

$$F_{\text{SRSS}} = 1.07 \times 10^7 \text{ lbf} \quad \text{SRSS estimate of peak hydrodynamic force}$$

**RPP-RPT-28963, Rev. 1**  
**M&D-2008-005-RPT-01, Rev. 1**

Prepared by: F. G. Abatt  
M&D Professional Services  
1/11/08  
Rev. 1

Theoretical Fluid Response for  
Flexible Wall Open Top Tank at 460  
in. Waste Level

Checked by: Milon Meyer

$$F_{con} := \sqrt{(m_{c0} \cdot SA_{c0})^2 + (m_{c1} \cdot SA_{c1})^2 + (m_{c2} \cdot SA_{c2})^2}$$

$$F_{con} = 5.39 \times 10^5 \text{ lbf} \quad \text{Peak hydrodynamic force due to convective effects only}$$

Recalculate Maximum Hydrodynamic Force Using Methodology of Malhotra (2005):

The hydrodynamic force can be calculated by excluding the structural masses from Eqn. (3) of Malhotra (2005). First calculate the impulsive and convective masses.

$$j := 0..1$$

$$\frac{HR}{R} := \begin{pmatrix} 1.0 \\ 1.5 \end{pmatrix} \quad \text{ImpMassRatio} := \begin{pmatrix} 0.548 \\ 0.686 \end{pmatrix} \quad \text{Table 1 of Malhotra (2005)}$$

$$\text{linterp}\left(HR, \text{ImpMassRatio}, \frac{H_1}{R}\right) = 0.55$$

$$m_{i\text{Malhotra}} := \text{linterp}\left(HR, \text{ImpMassRatio}, \frac{H_1}{R}\right) \cdot m_1 \quad m_{i\text{Malhotra}} = 2.75 \times 10^4 \frac{\text{lbf} \cdot \text{sec}^2}{\text{in}}$$

$$m_{c\text{Malhotra}} := m_1 - m_{i\text{Malhotra}} \quad m_{c\text{Malhotra}} = 2.22 \times 10^4 \frac{\text{lbf} \cdot \text{sec}^2}{\text{in}}$$

$$R_i := m_{i\text{Malhotra}} \cdot SA_{i\text{Malhotra}} \quad R_i = 1.14 \times 10^7 \text{ lbf} \quad \text{Impulsive reaction - Eqn. (3) Malhotra (2005)}$$

$$R_c := m_{c\text{Malhotra}} \cdot SA_{c0} \quad R_c = 5.65 \times 10^5 \text{ lbf} \quad \text{Convective reaction - Eqn. (4) Malhotra (2005)}$$

$$R_{\text{total}} := \sqrt{R_i^2 + R_c^2} \quad R_{\text{total}} = 1.14 \times 10^7 \text{ lbf} \quad \text{Total reaction force per Malhotra (2005)}$$

Consider Vertical Excitation:

Calculate the axisymmetric breathing mode frequency for the tank as a benchmark for the Dytran simulation.

$$C_{v\text{ref}} := 0.089 \quad \text{Table 4.17 BNL (1995)}$$

$$C_v := C_{v\text{ref}} \cdot \sqrt{127 \cdot \frac{t_{tw}}{R} \cdot \frac{\rho_1}{\rho_t}} \quad C_v = 0.079 \quad \text{Eqn. 4.16 BNL (1995)}$$

$$f_v := \frac{1}{2 \cdot \pi} \cdot \frac{C_v}{H_1} \cdot \sqrt{\frac{E_t}{\rho_t}} \quad f_v = 5.43 \frac{1}{s} \quad \text{Eqn. 4.53 BNL (1995)}$$

References:

BNL (1995), *Seismic Design and Evaluation Guidelines for the Department of Energy High-Level Waste Storage Tanks and Appurtenances*, BNL 52361, Rev. 10/95, Brookhaven National Laboratory, Upton, New York.

Deibler, J.E., K.I. Johnson, S.P. Pilli, M.W. Rinker, F.G. Abatt, and N.K. Karri, 2008, *Hanford Double-Shell Tank Thermal and Seismic Project Increased Liquid Level Analysis for 241AP Tank Farm*, RPP-RPT-32237, Rev. 1, Pacific Northwest National Laboratory, Richland, Washington.

Malhotra, Praveen K, 2005, *Sloshing Loads in Liquid Storage Tanks With Insufficient Freeboard*, *Earthquake Spectra*, Volume 21, No. 4, pp. 1185-1192, November 2005.

Intentionally left blank.

**RPP-RPT-28963, Rev. 1**  
**M&D-2008-005-RPT-01, Rev. 1**

Prepared by: F. G. Abatt  
M&D Professional Services  
1/11/08  
Rev. 1

Theoretical Fluid Response for  
Flexible Wall Open Top Tank at 460  
in. Waste Level

Checked by: Milon Meyer

This worksheet contains calculations for a flexible wall open top tank with an initial liquid level of 460 in. The calculations are performed using the methodology in Chapter 4 of BNL (1995) and in Malhotra (2005). The impulsive response per BNL (1995) is calculated using the Dytran calculated impulsive frequency of 6.25 Hz and damping of 5.5%. Total reaction forces using the methodology of Malhotra (2005) are calculated at the Malhotra impulsive frequency of 5.4 Hz at damping values of 3.5% and 5.5%. The location of the fluid elements corresponds to the flexible wall Dytran model with the refined mesh as described in Appendix C. Revision 1 modifies the total reaction force using the method of Malhotra to be the SRSS combination of the impulsive and convective components rather than the direct sum.

$H_1 := 460 \cdot \text{in}$       Baseline waste level

$$g_w := 386.4 \frac{\text{in}}{\text{sec}^2}$$

$R_{\text{tank}} := 450 \cdot \text{in}$       Tank radius

$\frac{H_1}{R} = 1.02$       Ratio of waste height to tank radius

$H_t := 460 \cdot \text{in}$       Assumed tank height used for calculation

$\frac{H_1}{H_t} = 1$       Ratio of liquid height to tank height - only used for calculation of  $C_{\text{iref}}$  from Table 4.4 of BNL (1995)

$i := 0..2$

$\lambda := \begin{pmatrix} 1.841 \\ 5.331 \\ 8.536 \end{pmatrix}$       Bessel function roots - Eqn. 4.5 BNL (1995)

$\theta := \begin{pmatrix} 0 \cdot \text{deg} \\ 45 \cdot \text{deg} \\ 90 \cdot \text{deg} \end{pmatrix}$       Circumferential location of waste elements for which pressures are reported

Convective Frequencies per BNL (1995)

$$f_{\text{con}_i} := \frac{1}{2 \cdot \pi} \sqrt{\lambda_i \left[ \frac{g_w}{R} \cdot \tanh \left[ \lambda_i \cdot \left( \frac{H_1}{R} \right) \right] \right]} \quad \text{Eqn. 4.14 BNL (1995)}$$

$f_{\text{con}} = \begin{pmatrix} 0.196 \\ 0.341 \\ 0.431 \end{pmatrix} \frac{1}{\text{s}}$       First three convective frequencies

**RPP-RPT-28963, Rev. 1**  
**M&D-2008-005-RPT-01, Rev. 1**

Prepared by: F. G. Abatt  
M&D Professional Services  
1/11/08  
Rev. 1

Theoretical Fluid Response for  
Flexible Wall Open Top Tank at 460  
in. Waste Level

Checked by: Milon Meyer

$$\rho_l := 1.71 \cdot 10^{-4} \frac{\text{lb} \cdot \text{sec}^2}{\text{in}^4} \quad \text{waste density - specific gravity} = 1.83$$

Recalculate Convective Frequency per Malhotra (2005):

$$j := 0..1$$

$$H_r := \begin{pmatrix} 1.0 \\ 1.5 \end{pmatrix} \quad C_{\text{cref}} := \begin{pmatrix} 1.52 \\ 1.48 \end{pmatrix} \quad \text{Table 1 of Malhotra (2005)}$$

$$C_c := \text{linterp}\left(H_r, C_{\text{cref}}, \frac{H_1}{R}\right) \frac{\text{sec}}{\sqrt{\text{m}}} \quad C_c = 1.52 \frac{\text{sec}}{0.5 \text{ m}}$$

$$T_{\text{con}} := C_c \sqrt{R} \quad T_{\text{con}} = 5.13 \text{ s}$$

$$f_{\text{cMalhotra}} := \frac{1}{T_{\text{con}}} \quad f_{\text{cMalhotra}} = 0.195 \frac{1}{\text{s}} \quad \text{Fundamental convective frequency per Malhotra (2005)}$$

Calculation of Impulsive Frequency per BNL (1995):

$$\rho_t := 7.35 \cdot 10^{-4} \frac{\text{lb} \cdot \text{sec}^2}{\text{in}^4} \quad \text{Steel density}$$

$$t_{\text{tw}} := 0.65 \text{ in} \quad \text{Tank wall thickness used in Dytran model.}$$

$$E_t := 29 \cdot 10^6 \frac{\text{lb} \cdot \text{f}}{\text{in}^2} \quad \text{Elastic modulus for steel}$$

$$C_{\text{iref}} := 0.1062 \quad \text{Table 4.4 of BNL (1995) - } H_1=R=H_t, \text{ hinged top boundary condition.}$$

$$C_i := C_{\text{iref}} \sqrt{127 \cdot \frac{t_{\text{tw}}}{R} \cdot \frac{\rho_l}{\rho_t}} \quad \text{Eqn. 4.18 BNL (1995)}$$

$$C_i = 0.09 \quad \text{Impulsive coefficient for frequency calculation}$$

$$f_i := \frac{1}{2 \cdot \pi} \cdot \frac{C_i}{H_1} \sqrt{\frac{E_t}{\rho_t}} \quad f_i = 6.48 \frac{1}{\text{s}} \quad \text{Eqn. 4.16 BNL (1995)}$$

**RPP-RPT-28963, Rev. 1**  
**M&D-2008-005-RPT-01, Rev. 1**

Prepared by: F. G. Abatt  
M&D Professional Services  
1/11/08  
Rev. 1

Theoretical Fluid Response for  
Flexible Wall Open Top Tank at 460  
in. Waste Level

Checked by: Milon Meyer

Recalculate the Fundamental Impulsive Frequency Using the Methodology of Malhotra (2005):

$$j_w = 0..1$$

$$HR := \begin{pmatrix} 1.0 \\ 1.5 \end{pmatrix} \quad C_{irefMalhotra} := \begin{pmatrix} 6.36 \\ 6.06 \end{pmatrix}$$

$$linterp\left(HR, C_{irefMalhotra}, \frac{H_1}{R}\right) = 6.35$$

$$C_{iMalhotra} := linterp\left(HR, C_{irefMalhotra}, \frac{H_1}{R}\right)$$

$$T_{impMalhotra} := C_{iMalhotra} \cdot \frac{\sqrt{\rho_1} \cdot H_1}{\sqrt{\frac{t_{tw}}{R}} \cdot \sqrt{E_t}} \quad T_{impMalhotra} = 0.19 \text{ s}$$

$$f_{impMalhotra} := \frac{1}{T_{impMalhotra}} \quad f_{impMalhotra} = 5.36 \frac{1}{s} \quad \text{Fundamental impulsive frequency per Malhotra (2005)}$$

**RPP-RPT-28963, Rev. 1**  
**M&D-2008-005-RPT-01, Rev. 1**

Prepared by: F. G. Abatt  
M&D Professional Services  
1/11/08  
Rev. 1

Theoretical Fluid Response for  
Flexible Wall Open Top Tank at 460  
in. Waste Level

Checked by: Milon Meyer

Determine Convective Pressures on the Tank Wall per BNL (1995):

z :=

4.0-in
24.1-in
44.2-in
64.2-in
84.3-in
104.4-in
124.4-in
144.5-in
164.6-in
184.6-in
204.7-in
224.8-in
244.8-in
264.9-in
285-in
305-in
325-in
345-in
365-in
385-in
405-in
425-in
435-in
445-in
455-in

Vertical location of Euler element centroids at which pressures are reported.

$$\eta_1 := \frac{z}{H_1}$$

0	0
1	$8.7 \cdot 10^{-3}$
2	0.05
3	0.1
4	0.14
5	0.18
6	0.23
7	0.27
8	0.31
9	0.36
10	0.4
11	0.45
12	0.49
13	0.53
14	0.58
15	0.62
16	0.66
17	0.71
18	0.75
19	0.79
20	0.84
21	0.88
22	0.92
23	0.95
24	0.97
25	0.99

Ratio of tank wall vertical location to waste height for waste element centroids.

**RPP-RPT-28963, Rev. 1**  
**M&D-2008-005-RPT-01, Rev. 1**

Prepared by: F. G. Abatt  
M&D Professional Services  
1/11/08  
Rev. 1

Theoretical Fluid Response for  
Flexible Wall Open Top Tank at 460  
in. Waste Level

Checked by: Milon Meyer

Determine convective coefficients as a function of dimensionless height per Eqn. 4.4 BNL (1995).

$$\text{con}_0(\eta_1) := \frac{2 \cdot \cosh\left[\lambda_0 \cdot \left(\frac{H_1}{R}\right) \cdot \eta_1\right]}{\left(\lambda_0\right)^2 - 1 \cdot \cosh\left[\lambda_0 \cdot \left(\frac{H_1}{R}\right)\right]}$$

$$\text{con}_1(\eta_1) := \frac{2 \cdot \cosh\left[\lambda_1 \cdot \left(\frac{H_1}{R}\right) \cdot \eta_1\right]}{\left(\lambda_1\right)^2 - 1 \cdot \cosh\left[\lambda_1 \cdot \left(\frac{H_1}{R}\right)\right]}$$

$$\text{con}_2(\eta_1) := \frac{2 \cdot \cosh\left[\lambda_2 \cdot \left(\frac{H_1}{R}\right) \cdot \eta_1\right]}{\left(\lambda_2\right)^2 - 1 \cdot \cosh\left[\lambda_2 \cdot \left(\frac{H_1}{R}\right)\right]}$$

$\text{con}_0(\eta_1) =$

	0
0	0.25
1	0.25
2	0.25
3	0.26
4	0.26
5	0.27
6	0.28
7	0.29
8	0.31
9	0.32
10	0.34
11	0.36
12	0.38
13	0.41
14	0.44
15	0.47
16	0.5
17	0.54
18	0.58
19	0.63
20	0.68
21	0.73
22	0.76
23	0.79
24	0.82

$\text{con}_1(\eta_1) =$

	0
0	6.28·10 <sup>-4</sup>
1	6.53·10 <sup>-4</sup>
2	7.15·10 <sup>-4</sup>
3	8.17·10 <sup>-4</sup>
4	9.67·10 <sup>-4</sup>
5	1.17·10 <sup>-3</sup>
6	1.44·10 <sup>-3</sup>
7	1.79·10 <sup>-3</sup>
8	2.25·10 <sup>-3</sup>
9	2.83·10 <sup>-3</sup>
10	3.57·10 <sup>-3</sup>
11	4.52·10 <sup>-3</sup>
12	5.72·10 <sup>-3</sup>
13	7.24·10 <sup>-3</sup>
14	9.19·10 <sup>-3</sup>
15	0.01
16	0.01
17	0.02
18	0.02
19	0.03
20	0.04
21	0.05
22	0.05
23	0.06
24	0.07

$\text{con}_2(\eta_1) =$

	0
0	9.06·10 <sup>-6</sup>
1	10·10 <sup>-6</sup>
2	1.24·10 <sup>-5</sup>
3	1.66·10 <sup>-5</sup>
4	2.33·10 <sup>-5</sup>
5	3.34·10 <sup>-5</sup>
6	4.83·10 <sup>-5</sup>
7	7.03·10 <sup>-5</sup>
8	1.03·10 <sup>-4</sup>
9	1.5·10 <sup>-4</sup>
10	2.2·10 <sup>-4</sup>
11	3.21·10 <sup>-4</sup>
12	4.7·10 <sup>-4</sup>
13	6.88·10 <sup>-4</sup>
14	1.01·10 <sup>-3</sup>
15	1.47·10 <sup>-3</sup>
16	2.15·10 <sup>-3</sup>
17	3.14·10 <sup>-3</sup>
18	4.59·10 <sup>-3</sup>
19	6.71·10 <sup>-3</sup>
20	9.8·10 <sup>-3</sup>
21	0.01
22	0.02
23	0.02
24	0.03

RPP-RPT-28963, Rev. 1  
M&D-2008-005-RPT-01, Rev. 1

Prepared by: F. G. Abatt  
M&D Professional Services  
1/11/08  
Rev. 1

Theoretical Fluid Response for  
Flexible Wall Open Top Tank at 460  
in. Waste Level

Checked by: Milon Meyer

Impulsive pressure coefficient as a function of dimensionless wall height

$$c_i(\eta_1) := 1 - \text{con}_0(\eta_1) - \text{con}_1(\eta_1) - \text{con}_2(\eta_1) \quad \text{Eqn. 4.7 BNL (1995)}$$

	0
0	0.75
1	0.75
2	0.75
3	0.74
4	0.73
5	0.73
6	0.72
7	0.7
8	0.69
9	0.67
10	0.65
11	0.63
12	0.61
13	0.58
14	0.55
15	0.52
16	0.48
17	0.44
18	0.39
19	0.34
20	0.28
21	0.21
22	0.17
23	0.13
24	0.09

$c_i(\eta_1) =$

Calculate maximum values of dynamic wall pressures from spectral acceleration of dome input TH.

Consider the first three convective modes with accelerations from the 0.1% damped spectrum

$$SA_{c0} := 0.066 \cdot g$$

$$SA_{c0} = 25.5 \frac{\text{in}}{\text{sec}^2}$$

$$SA_{c1} := 0.11 \cdot g$$

$$SA_{c1} = 42.5 \frac{\text{in}}{\text{sec}^2}$$

ANSYS Dome RS from Spectr

$$SA_{c2} := 0.17 \cdot g$$

$$SA_{c2} = 65.69 \frac{\text{in}}{\text{sec}^2}$$

RPP-RPT-28963, Rev. 1  
M&D-2008-005-RPT-01, Rev. 1

Prepared by: F. G. Abatt  
M&D Professional Services  
1/11/08  
Rev. 1

Theoretical Fluid Response for  
Flexible Wall Open Top Tank at 460  
in. Waste Level

Checked by: Milon Meyer

Determine the spectral acceleration for the impulsive mode.

$$SA_i := 0.94 \cdot g \quad SA_i = 363.22 \frac{\text{in}}{\text{sec}^2} \quad \text{5.5\% Dome RS from Spectr based on damping during initial gravity loading in Dytran model taken at 6.25 Hz.}$$

$$P_{\text{maxconv}}(\eta_1, \theta) := \left[ \sqrt{(\cos_0(\eta_1) \cdot SA_{c0})^2 + (\cos_1(\eta_1) \cdot SA_{c1})^2 + (\cos_2(\eta_1) \cdot SA_{c2})^2} \right] \cdot (\rho_1 \cdot R \cdot \cos(\theta \cdot \text{deg}))$$

$$P_{\text{maximpulsive}}(\eta_1, \theta) := \left[ \sqrt{[c_1(\eta_1) \cdot (SA_i)]^2} \right] \cdot (\rho_1 \cdot R \cdot \cos(\theta \cdot \text{deg}))$$

$$P_{\text{max}}(\eta_1, \theta) := \left[ \sqrt{[c_1(\eta_1) \cdot (SA_i)]^2 + (\cos_0(\eta_1) \cdot SA_{c0})^2 + (\cos_1(\eta_1) \cdot SA_{c1})^2 + (\cos_2(\eta_1) \cdot SA_{c2})^2} \right] \cdot (\rho_1 \cdot R \cdot \cos(\theta \cdot \text{deg}))$$

Eqn. 4.24 BNL (1995)

Determine the spectral acceleration for the impulsive frequency calculated per Malhotra (2005).

$$SA_{i\text{Malhotra}_{35}} := 1.07 \cdot g \quad SA_{i\text{Malhotra}_{35}} = 413.45 \frac{\text{in}}{\text{sec}^2} \quad \text{3.5\% Dome RS from Spectr based on damping during initial gravity loading in Dytran model taken at 5.4 Hz.}$$

$$SA_{i\text{Malhotra}_{55}} := 0.92 \cdot g \quad SA_{i\text{Malhotra}_{55}} = 355.49 \frac{\text{in}}{\text{sec}^2} \quad \text{5.5\% Dome RS from Spectr based on damping during initial gravity loading in Dytran model taken at 5.4 Hz.}$$

RPP-RPT-28963, Rev. 1  
M&D-2008-005-RPT-01, Rev. 1

Prepared by: F. G. Abatt  
M&D Professional Services  
1/11/08  
Rev. 1

Theoretical Fluid Response for  
Flexible Wall Open Top Tank at 460  
in. Waste Level

Checked by: Milon Meyer

	0	
0	20.97	
1	20.93	
2	20.85	
3	20.72	
4	20.54	
5	20.31	
6	20.02	
7	19.68	
8	19.28	
9	18.82	
10	18.29	
11	17.69	$P_{\text{maximpulsive}}(\eta_1, 0) = \frac{\text{lb}}{\text{in}^2}$
12	17.02	
13	16.26	
14	15.4	
15	14.46	
16	13.39	
17	12.21	
18	10.88	
19	9.38	
20	7.69	
21	5.78	
22	4.72	
23	3.59	
24	2.38	

Maximum impulsive dynamic pressures at  
theta = 0.

	0	
0	0.49	
1	0.49	
2	0.5	
3	0.51	
4	0.52	
5	0.53	
6	0.55	
7	0.58	
8	0.6	
9	0.64	
10	0.67	
11	0.71	$P_{\text{maxconv}}(\eta_1, 0) = \frac{\text{lb}}{\text{in}^2}$
12	0.76	
13	0.81	
14	0.86	
15	0.92	
16	0.99	
17	1.06	
18	1.15	
19	1.24	
20	1.34	
21	1.44	
22	1.5	
23	1.57	
24	1.63	

Maximum convective  
dynamic pressures at  
theta = 0.

RPP-RPT-28963, Rev. 1  
M&D-2008-005-RPT-01, Rev. 1

Prepared by: F. G. Abatt  
M&D Professional Services  
1/11/08  
Rev. 1

Theoretical Fluid Response for  
Flexible Wall Open Top Tank at 460  
in. Waste Level

Checked by: Milon Meyer

$p_{\max}(\eta_1, 0) =$

	0
0	20.97
1	20.94
2	20.86
3	20.73
4	20.55
5	20.31
6	20.03
7	19.69
8	19.29
9	18.83
10	18.3
11	17.7
12	17.03
13	16.28
14	15.43
15	14.48
16	13.43
17	12.25
18	10.94
19	9.46
20	7.81
21	5.95
22	4.95
23	3.92
24	2.88

$\frac{\text{lbf}}{\text{in}^2}$

Maximum total dynamic pressure at  
theta = 0.

$p_{\max}(\eta_1, 45) =$

	0
0	14.8
1	14.8
2	14.7
3	14.7
4	14.5
5	14.4
6	14.2
7	13.9
8	13.6
9	13.3
10	12.9
11	12.5
12	12
13	11.5
14	10.9
15	10.2
16	9.5
17	8.7
18	7.7
19	6.7
20	5.5
21	4.2
22	3.5
23	2.8
24	2

$\frac{\text{lbf}}{\text{in}^2}$

Maximum total dynamic pressure at  
theta = 45 degrees.

RPP-RPT-28963, Rev. 1  
M&D-2008-005-RPT-01, Rev. 1

Prepared by: F. G. Abatt  
M&D Professional Services  
1/11/08  
Rev. 1

Theoretical Fluid Response for  
Flexible Wall Open Top Tank at 460  
in. Waste Level

Checked by: Milon Meyer

Calculate Maximum Slosh Height per BNL (1995):

$$\text{conmax} := \begin{pmatrix} 0.837 \\ 0.073 \\ 0.028 \end{pmatrix} \quad \text{Maximum value of convective coefficients at } \eta_1=1$$

$$h_{\text{maxslosh}} := R \cdot \sqrt{\left(\text{conmax}_0 \cdot \frac{SA_{c0}}{g}\right)^2 + \left(\text{conmax}_1 \cdot \frac{SA_{c1}}{g}\right)^2 + \left(\text{conmax}_2 \cdot \frac{SA_{c2}}{g}\right)^2} \quad \text{Eqn. 4.60 BNL (1995)}$$

$$h_{\text{maxslosh}} = 25.21 \text{ in}$$

Recalculate the Maximum Slosh Height per Malhotra (2005):

Since the fundamental convective frequency calculated per Malhotra agrees with the frequency calculated via BNL (1995), the convective acceleration is the same in both cases.

$$h_{s\text{Malhotra}} := R \cdot \frac{SA_{c0}}{g} \quad \text{Eqn. (9) of Malhotra (2005)}$$

$$h_{s\text{Malhotra}} = 29.7 \text{ in} \quad \text{Maximum slosh height for roofless tank per Malhotra (2005)}$$

Calculate Maximum Total Hydrodynamic Force per BNL (1995):

The maximum hydrodynamic force induced on the tank wall is given by Eqn. 4.31 of BNL (1995) with the instantaneous accelerations replaced by the maximum spectral accelerations. First determine the effective impulsive and convective masses.

$$m_{l\text{approx}} := \pi \cdot R^2 \cdot H_1 \cdot \rho_1 \quad m_{l\text{approx}} = 5 \times 10^4 \frac{\text{lb} \cdot \text{sec}^2}{\text{in}} \quad \text{Total waste mass based on circular cylinder approximation.}$$

$$m_1 := 4.97 \times 10^4 \frac{\text{lb} \cdot \text{sec}^2}{\text{in}} \quad \text{Actual waste mass reported by Dytran model.}$$

RPP-RPT-28963, Rev. 1  
M&D-2008-005-RPT-01, Rev. 1

Prepared by: F. G. Abatt  
M&D Professional Services  
1/11/08  
Rev. 1

Theoretical Fluid Response for  
Flexible Wall Open Top Tank at 460  
in. Waste Level

Checked by: Milon Meyer

$$m_{c0} := \left[ \frac{2}{\lambda_0 \left[ (\lambda_0)^2 - 1 \right] \left( \frac{H_1}{R} \right)} \right] \cdot \tanh \left[ \lambda_0 \left( \frac{H_1}{R} \right) \right] \cdot m_1 \quad \text{First mode convective mass - Eqn. 4.32 BNL (1995)}$$

$$m_{c0} = 2.11 \times 10^4 \frac{\text{lbf} \cdot \text{sec}^2}{\text{in}}$$

$$m_{c1} := \left[ \frac{2}{\lambda_1 \left[ (\lambda_1)^2 - 1 \right] \left( \frac{H_1}{R} \right)} \right] \cdot \tanh \left[ \lambda_1 \left( \frac{H_1}{R} \right) \right] \cdot m_1 \quad \text{Second mode convective mass}$$

$$m_{c1} = 665.21 \frac{\text{lbf} \cdot \text{sec}^2}{\text{in}}$$

$$m_{c2} := \left[ \frac{2}{\lambda_2 \left[ (\lambda_2)^2 - 1 \right] \left( \frac{H_1}{R} \right)} \right] \cdot \tanh \left[ \lambda_2 \left( \frac{H_1}{R} \right) \right] \cdot m_1 \quad \text{Third mode convective mass}$$

$$m_{c2} = 158.52 \frac{\text{lbf} \cdot \text{sec}^2}{\text{in}}$$

$$m_i := m_1 - (m_{c0} + m_{c1} + m_{c2}) \quad \text{Impulsive mass - Eqn. 4.33 BNL (1995)}$$

$$m_i = 2.78 \times 10^4 \frac{\text{lbf} \cdot \text{sec}^2}{\text{in}}$$

$$F_{\max} := m_i \cdot SA_i + m_{c0} \cdot SA_{c0} + m_{c1} \cdot SA_{c1} + m_{c2} \cdot SA_{c2} \quad \text{Eqn. 4.31 BNL (1995)}$$

$$F_{\max} = 1.07 \times 10^7 \text{ lbf} \quad \text{Conservative estimate of maximum hydrodynamic force}$$

The above expression is a conservative estimate because it assumes that the peak impulsive and convective forces occur simultaneously. A less conservative estimate can be made via a square-root-sum-of-the-squares (SRSS) combination.

$$F_{\text{SRSS}} := \sqrt{(m_i \cdot SA_i)^2 + (m_{c0} \cdot SA_{c0})^2 + (m_{c1} \cdot SA_{c1})^2 + (m_{c2} \cdot SA_{c2})^2} \quad \text{Eqn. 4.31 BNL (1995) - SRSS}$$

$$F_{\text{SRSS}} = 1.01 \times 10^7 \text{ lbf} \quad \text{SRSS estimate of peak hydrodynamic force}$$

RPP-RPT-28963, Rev. 1  
M&D-2008-005-RPT-01, Rev. 1

Prepared by: F. G. Abatt  
M&D Professional Services  
1/11/08  
Rev. 1

Theoretical Fluid Response for  
Flexible Wall Open Top Tank at 460  
in. Waste Level

Checked by: Milon Meyer

$$F_{con} := \sqrt{(m_{c0} \cdot SA_{c0})^2 + (m_{c1} \cdot SA_{c1})^2 + (m_{c2} \cdot SA_{c2})^2}$$

$$F_{con} = 5.39 \times 10^5 \text{ lbf} \quad \text{Peak hydrodynamic force due to convective effects only}$$

Recalculate Maximum Hydrodynamic Force Using Methodology of Malhotra (2005):

The hydrodynamic force can be calculated by excluding the structural masses from Eqn. (3) of Malhotra (2005). First calculate the impulsive and convective masses.

$$j := 0..1$$

$$\frac{HR}{\omega} = \begin{pmatrix} 1.0 \\ 1.5 \end{pmatrix} \quad \text{ImpMassRatio} := \begin{pmatrix} 0.548 \\ 0.686 \end{pmatrix} \quad \text{Table 1 of Malhotra (2005)}$$

$$\text{linterp}\left(HR, \text{ImpMassRatio}, \frac{H_1}{R}\right) = 0.55$$

$$m_{i\text{Malhotra}} := \text{linterp}\left(HR, \text{ImpMassRatio}, \frac{H_1}{R}\right) \cdot m_1 \quad m_{i\text{Malhotra}} = 2.75 \times 10^4 \frac{\text{lbf} \cdot \text{sec}^2}{\text{in}}$$

$$m_{c\text{Malhotra}} := m_1 - m_{i\text{Malhotra}} \quad m_{c\text{Malhotra}} = 2.22 \times 10^4 \frac{\text{lbf} \cdot \text{sec}^2}{\text{in}}$$

**Total reaction force at 5.4 Hz and 3.5% damping per Malhotra (2005)**

$$R_{i\_35} := m_{i\text{Malhotra}} \cdot SA_{i\text{Malhotra\_35}} \quad R_{i\_35} = 1.14 \times 10^7 \text{ lbf} \quad \text{Impulsive reaction - Eqn. (3) Malhotra (2005)}$$

$$R_c := m_{c\text{Malhotra}} \cdot SA_{c0} \quad R_c = 5.65 \times 10^5 \text{ lbf} \quad \text{Convective reaction - Eqn. (4) Malhotra (2005)}$$

$$R_{\text{total\_35}} := \sqrt{R_{i\_35}^2 + R_c^2} \quad R_{\text{total\_35}} = 1.14 \times 10^7 \text{ lbf} \quad \text{Total reaction force per Malhotra (2005)}$$

**Total reaction force at 5.4 Hz and 5.5% damping per Malhotra (2005)**

$$R_{i\_55} := m_{i\text{Malhotra}} \cdot SA_{i\text{Malhotra\_55}} \quad R_{i\_55} = 9.79 \times 10^6 \text{ lbf} \quad \text{Impulsive reaction - Eqn. (3) Malhotra (2005)}$$

$$R_{\text{total\_55}} := \sqrt{R_{i\_55}^2 + R_c^2} \quad R_{\text{total\_55}} = 9.81 \times 10^6 \text{ lbf} \quad \text{Total reaction force per Malhotra (2005)}$$

RPP-RPT-28963, Rev. 1  
M&D-2008-005-RPT-01, Rev. 1

Prepared by: F. G. Abatt  
M&D Professional Services  
1/11/08  
Rev. 1

Theoretical Fluid Response for  
Flexible Wall Open Top Tank at 460  
in. Waste Level

Checked by: Milon Meyer

Consider Vertical Excitation:

Calculate the axisymmetric breathing mode frequency for the tank as a benchmark for the Dytran simulation.

$C_{vref} := 0.089$  Table 4.17 BNL (1995)

$$C_v := C_{vref} \sqrt{127 \cdot \frac{t_{tw}}{R} \cdot \frac{\rho_l}{\rho_t}} \quad C_v = 0.079 \quad \text{Eqn. 4.16 BNL (1995)}$$

$$f_v := \frac{1}{2 \cdot \pi} \cdot \frac{C_v}{H_l} \cdot \sqrt{\frac{E_t}{\rho_t}} \quad f_v = 5.43 \frac{1}{s} \quad \text{Eqn. 4.53 BNL (1995)}$$

References:

BNL (1995), *Seismic Design and Evaluation Guidelines for the Department of Energy High-Level Waste Storage Tanks and Appurtenances*, BNL 52361, Rev. 10/95, Brookhaven National Laboratory, Upton, New York.

Malhotra, Praveen K, 2005, *Sloshing Loads in Liquid Storage Tanks With Insufficient Freeboard*, *Earthquake Spectra*, Volume 21, No. 4, pp. 1185-1192, November 2005.

Intentionally left blank.

**RPP-RPT-28963, Rev. 1**  
**M&D-2008-005-RPT-01, Rev. 1**

Prepared by: F. G. Abatt  
M&D Professional Services  
1/14/08  
Rev. 2

Theoretical Fluid Response  
Calculations for Equivalent Flexible  
Wall Flat-Top Tank at 460 in. Waste  
Level

Checked by: Milon Meyer

This worksheet contains calculations for a flexible wall equivalent flat-top tank with an initial liquid level of 460 in. The calculations are performed using the methodology in Chapter 4 and Appendix D of BNL (1995) and in Malhotra (2005). The impulsive response per BNL (1995) is calculated using is based on an impulsive frequency of 6.5 Hz and damping of 3.5%. Total reaction forces using the methodology of Malhotra (2005) are calculated at the Malhotra impulsive frequency of 5.4 Hz at a damping value of 3.5%. The freeboard distance is such that minor interaction occurs between the liquid and the flat roof. The location of the fluid elements corresponds to the Dytran model of the domed flexible wall tank in Appendix C. Revision 2 of this file incorporates corrections and clarifications regarding the interpretation of solutions in BNL (1995) per reviewer comments from a June 7-8, 2007 review meeting. The complete set of review comments from that meeting appear as Appendix A of Deibler et al. (2008).

- $H_1 := 460.0 \text{ in}$                       Baseline liquid level
  
- $H_t := 484.0 \text{ in}$                       Height of equivalent flat top tank per Kennedy (2003)
  
- $h_0 := H_t - H_1$        $h_0 = 24 \text{ in}$                       Freeboard distance
  
- $\frac{H_1}{H_t} = 0.95$                               Ratio of waste height to tank height
  
- $g := 386.4 \frac{\text{in}}{\text{sec}^2}$
  
- $R := 450 \text{ in}$                               Tank radius
  
- $\frac{H_1}{R} = 1.02$                               Ratio of waste height to tank radius
  
- $i := 0..2$
  
- $\lambda := \begin{pmatrix} 1.841 \\ 5.331 \\ 8.536 \end{pmatrix}$                               Bessel function roots - Eqn. 4.5 BNL (1995)
  
- $\theta := \begin{pmatrix} 0 \text{ deg} \\ 45 \text{ deg} \\ 90 \text{ deg} \end{pmatrix}$                               Circumferential location of waste elements for which pressures are reported.
  
- $\rho_1 := 1.71 \cdot 10^{-4} \frac{\text{lb} \cdot \text{sec}^2}{\text{in}^4}$                               Liquid mass density - specific gravity of 1.83

**RPP-RPT-28963, Rev. 1**  
**M&D-2008-005-RPT-01, Rev. 1**

Prepared by: F. G. Abatt  
M&D Professional Services  
1/14/08  
Rev. 2

Theoretical Fluid Response  
Calculations for Equivalent Flexible  
Wall Flat-Top Tank at 460 in. Waste  
Level

Checked by: Milon Meyer

**Convective Frequencies**

$$f_{con,i} := \frac{1}{2 \cdot \pi} \left[ \sqrt{\lambda_i \left[ \frac{g}{R} \cdot \tanh \left[ \lambda_i \left( \frac{H_1}{R} \right) \right] \right]} \right] \quad \text{Eqn. 4.14 BNL (1995)}$$

$$f_{con} = \begin{pmatrix} 0.196 \\ 0.341 \\ 0.431 \end{pmatrix} \frac{1}{s} \quad \text{First three convective frequencies}$$

Recalculate the Fundamental Convective Frequency Using the Methodology of Malhotra (2005)

$$j := 0..1$$

$$HR := \begin{pmatrix} 1.0 \\ 1.5 \end{pmatrix} \quad C_{cref} := \begin{pmatrix} 1.52 \\ 1.48 \end{pmatrix} \quad \text{Table 1 of Malhotra (2005)}$$

$$linterp \left( HR, C_{cref}, \frac{H_1}{R} \right) = 1.52$$

$$C_c := linterp \left( HR, C_{cref}, \frac{H_1}{R} \right) \frac{sec}{\sqrt{m}}$$

$$T_{conMalhotra} := C_c \sqrt{R} \quad T_{conMalhotra} = 5.13 \text{ s}$$

$$f_{conMalhotra} := \frac{1}{T_{conMalhotra}} \quad f_{conMalhotra} = 0.19 \frac{1}{s} \quad \text{Fundamental convective frequency per Eqn. (2) of Malhotra (2005)}$$

The fundamental convective frequencies calculated using the methodologies of BNL (1995) and Malhotra (2005) are nearly the same. Consequently, the spectral accelerations associated with the fundamental convective modes are essentially the same using either methodology.

Consider the first three convective mode spectral accelerations for the 0.1% damped spectrum

$$SA_{c0} := 0.066 \cdot g \quad SA_{c0} = 25.5 \frac{in}{sec^2}$$

$$SA_{c1} := 0.11 \cdot g \quad SA_{c1} = 42.5 \frac{in}{sec^2} \quad \text{ANSYS dome RS from Spectr}$$

$$SA_{c2} := 0.17 \cdot g \quad SA_{c2} = 65.69 \frac{in}{sec^2}$$

**RPP-RPT-28963, Rev. 1**  
**M&D-2008-005-RPT-01, Rev. 1**

Prepared by: F. G. Abatt  
M&D Professional Services  
1/14/08  
Rev. 2

Theoretical Fluid Response  
Calculations for Equivalent Flexible  
Wall Flat-Top Tank at 460 in. Waste  
Level

Checked by: Milon Meyer

Calculation of Impulsive Frequency per BNL (1995):

$$\rho_t := 7.35 \cdot 10^{-4} \cdot \frac{\text{lbf} \cdot \text{sec}^2}{\text{in}^4} \quad \text{Steel density}$$

$$t_{tw} := 0.65 \cdot \text{in} \quad \text{Tank wall thickness used in Dytran model.}$$

$$E_t := 29 \cdot 10^6 \cdot \frac{\text{lbf}}{\text{in}^2} \quad \text{Elastic modulus for steel}$$

$$C_{iref} := 0.1062 \quad \text{Table 4.4 of BNL (1995)}$$

$$C_i := C_{iref} \sqrt{127 \cdot \frac{\frac{t_{tw}}{R}}{\frac{\rho_l}{\rho_t}}} \quad \text{Eqn. 4.18 BNL (1995)}$$

$$C_i = 9.43 \times 10^{-2} \quad \text{Impulsive coefficient for frequency calculation}$$

$$f_i := \frac{1}{2 \cdot \pi} \cdot \frac{C_i}{H_1} \sqrt{\frac{E_t}{\rho_t}} \quad f_i = 6.48 \frac{1}{s} \quad \text{Eqn. 4.16 BNL (1995)}$$

Recalculate the Fundamental Impulsive Frequency Using the Methodology of Malhotra (2005):

$$j = 0..1$$

$$\overline{HR} := \begin{pmatrix} 1.0 \\ 1.5 \end{pmatrix} \quad C_{irefMalhotra} := \begin{pmatrix} 6.36 \\ 6.06 \end{pmatrix}$$

$$linterp\left(HR, C_{irefMalhotra}, \frac{H_1}{R}\right) = 6.35$$

$$C_{iMalhotra} := linterp\left(HR, C_{irefMalhotra}, \frac{H_1}{R}\right)$$

RPP-RPT-28963, Rev. 1  
M&D-2008-005-RPT-01, Rev. 1

Prepared by: F. G. Abatt  
M&D Professional Services  
1/14/08  
Rev. 2

Theoretical Fluid Response  
Calculations for Equivalent Flexible  
Wall Flat-Top Tank at 460 in. Waste  
Level

Checked by: Milon Meyer

$$T_{\text{impMalhotra}} := C_{i\text{Malhotra}} \frac{\sqrt{\rho_l \cdot H_l}}{\sqrt{\frac{t_w}{R} \cdot \sqrt{E_t}}} \quad T_{\text{impMalhotra}} = 0.19 \text{ s}$$

$$f_{\text{impMalhotra}} := \frac{1}{T_{\text{impMalhotra}}} \quad f_{\text{impMalhotra}} = 5.36 \frac{1}{\text{s}} \quad \text{Fundamental impulsive frequency per Eqn. (1) of Malhotra (2005)}$$

Spectral acceleration for the impulsive mode at 3.5% damping using impulsive frequency 6.5 Hz from BNL methodology.

$$SA_i := 1.0 \cdot g \quad SA_i = 3.86 \times 10^2 \frac{\text{in}}{\text{sec}^2} \quad \text{ANSYS dome RS from Spectr at 3.5% damping and impulsive frequency of 6.5 Hz.}$$

Calculate Maximum Slosh Height per BNL (1995):

$$\text{conmax} := \begin{pmatrix} 0.837 \\ 0.073 \\ 0.028 \end{pmatrix} \quad \text{Maximum value of convective coefficients at } \eta_l=1$$

$$h_s := R \cdot \sqrt{\left( \text{conmax}_0 \cdot \frac{SA_{c0}}{g} \right)^2 + \left( \text{conmax}_1 \cdot \frac{SA_{c1}}{g} \right)^2 + \left( \text{conmax}_2 \cdot \frac{SA_{c2}}{g} \right)^2} \quad \text{Eqn. 4.60 BNL (1995)}$$

$$h_s = 25.2 \text{ in} \quad \text{Maximum theoretical slosh height for roofless tank per BNL (1995)}$$

Recalculate the Maximum Slosh Height per Malhotra (2005):

$$h_{s\text{Malhotra}} := R \cdot \frac{SA_{c0}}{g} \quad \text{Eqn. (9) of Malhotra (2005)}$$

$$h_{s\text{Malhotra}} = 29.7 \text{ in} \quad \text{Maximum slosh height for roofless tank per Malhotra (2005)}$$

Calculate the Central Half-Angle for Wetted Portion of Tank Roof:

$$\theta_0 := \arccos\left(\frac{h_0}{h_s}\right) \quad \text{Central half-angle of maximum impacted roof area per Eqn. D.2 BNL (1995)}$$

$$\theta_0 = 17.8 \text{ deg} \quad \text{Central half-angle per Appendix D BNL (1995)}$$

**RPP-RPT-28963, Rev. 1**  
**M&D-2008-005-RPT-01, Rev. 1**

Prepared by: F. G. Abatt  
M&D Professional Services  
1/14/08  
Rev. 2

Theoretical Fluid Response  
Calculations for Equivalent Flexible  
Wall Flat-Top Tank at 460 in. Waste  
Level

Checked by: Milon Meyer

$$\frac{h_0}{h_{s\text{Malhotra}}} = 0.81 \quad \text{Used to calculate } x_f \text{ from Figure 3 of Malhotra (2005)}$$

$$x_f := 0.2 \cdot R \quad x_f = 90 \text{ in} \quad \text{Wetted width of tank roof per Figures 2 and 3 of Malhotra (2005)}$$

$$\psi_0 := \arccos\left(\frac{x_f}{R} - 1\right) \quad \psi_0 = 2.5$$

$$\theta_{0\text{Malhotra}} := \pi - \psi_0 \quad \theta_{0\text{Malhotra}} = 36.9 \text{ deg} \quad \text{Central half-angle per Malhotra (2005)}$$

**Maximum Roof Pressure:**

$r := 424.875 \text{ in}$  Typical centroidal radius of Dytran elements for which results are monitored

$$p_f(r, \theta) := \rho_1 \cdot r \cdot SA_f \cdot \cos(\theta) \quad \text{for } |\theta| < |\theta_0| \quad \text{Peak roof pressure per Eqn. D.4 BNL (1995)}$$

$$p_f(R, 0) = 29.73 \frac{\text{lb}_f}{\text{in}^2} \quad \text{Peak roof pressure per BNL (1995)}$$

$$p_f(r, 0) = 28.07 \frac{\text{lb}_f}{\text{in}^2} \quad \text{Predicted peak roof pressure for Dytran element per BNL (1995)}$$

$$P_{\text{maxroofMalhotra}} := \rho_1 \cdot x_f \cdot SA_{c0} \quad \text{Peak roof pressure per Eqns. (10) and (12) of Malhotra (2005)}$$

$$P_{\text{maxroofMalhotra}} = 0.39 \frac{\text{lb}_f}{\text{in}^2}$$

**Calculate the Maximum Wall Pressure per Appendix D BNL (1995) :**

$p_{ic}(\theta) := \rho_1 \cdot R \cdot SA_f \cdot \cos(\theta)$  Impulsive component of pressure due to constrained portion of the liquid per Eqn. D.5 BNL (1995). This term represents the total hydrodynamic wall pressure inside the central half-angle  $\theta_0$ .

$$p_{ic}(\theta) = \begin{pmatrix} 29.73 \\ 21.02 \\ 0 \end{pmatrix} \frac{\text{lb}_f}{\text{in}^2}$$

**RPP-RPT-28963, Rev. 1**  
**M&D-2008-005-RPT-01, Rev. 1**

Prepared by: F. G. Abatt  
M&D Professional Services  
1/14/08  
Rev. 2

Theoretical Fluid Response  
Calculations for Equivalent Flexible  
Wall Flat-Top Tank at 460 in. Waste  
Level

Checked by: Milon Meyer

z :=

4.0-in
24.1-in
44.2-in
64.2-in
84.3-in
104.4-in
124.4-in
144.5-in
164.6-in
184.6-in
204.7-in
224.8-in
244.8-in
264.9-in
285-in
305-in
325-in
345-in
365-in
385-in
405-in
425-in
435-in
445-in
455-in

Vertical location of Euler element centroids at which pressures are reported.

$$\eta_1 := \frac{z}{H_1}$$

0	0
1	0.01
2	0.05
3	0.1
4	0.14
5	0.18
6	0.23
7	0.27
8	0.31
9	0.36
10	0.4
11	0.45
12	0.49
13	0.53
14	0.58
15	0.62
16	0.66
17	0.71
18	0.75
19	0.79
20	0.84
21	0.88
22	0.92
23	0.95
24	0.97
25	0.99

Ratio of tank wall vertical location to waste height for waste element centroids.

**RPP-RPT-28963, Rev. 1**  
**M&D-2008-005-RPT-01, Rev. 1**

Prepared by: F. G. Abatt  
M&D Professional Services  
1/14/08  
Rev. 2

Theoretical Fluid Response  
Calculations for Equivalent Flexible  
Wall Flat-Top Tank at 460 in. Waste  
Level

Checked by: Milon Meyer

Determine convective coefficients as a function of dimensionless height per Eqn. 4.4 BNL (1995).

$$\text{con}_0(\eta_1) := \frac{2 \cdot \cosh\left[\lambda_0 \cdot \left(\frac{H_1}{R}\right) \cdot \eta_1\right]}{\left(\lambda_0\right)^2 - 1 \cdot \cosh\left[\lambda_0 \cdot \left(\frac{H_1}{R}\right)\right]}$$

$$\text{con}_1(\eta_1) := \frac{2 \cdot \cosh\left[\lambda_1 \cdot \left(\frac{H_1}{R}\right) \cdot \eta_1\right]}{\left(\lambda_1\right)^2 - 1 \cdot \cosh\left[\lambda_1 \cdot \left(\frac{H_1}{R}\right)\right]}$$

$$\text{con}_2(\eta_1) := \frac{2 \cdot \cosh\left[\lambda_2 \cdot \left(\frac{H_1}{R}\right) \cdot \eta_1\right]}{\left(\lambda_2\right)^2 - 1 \cdot \cosh\left[\lambda_2 \cdot \left(\frac{H_1}{R}\right)\right]}$$

Impulsive pressure coefficient as a function of normalized wall height

$$c_i(\eta_1) := 1 - \text{con}_0(\eta_1)$$

BNL (1995) Eqn. 4.7 - 1st term

$$P_{iu}(\eta_1, \theta) := c_i(\eta_1) \cdot \rho_1 \cdot R \cdot SA_i \cdot \cos(\theta)$$

Impulsive component of maximum wall pressure induced by unconstrained portion of liquid beneath the non-impacted portion of the roof - same as for roofless tank (Eqn. D.6 BNL [1995]). This is the impulsive component of the hydrodynamic pressure outside the central half-angle  $\theta_0$ .

$$P_{cu}(\eta_1, \theta) := \text{con}_0(\eta_1) \cdot \rho_1 \cdot R \cdot SA_{c0} \cdot \cos(\theta)$$

Convective component of maximum wall pressure induced by unconstrained portion of liquid beneath the non-impacted portion of the roof outside the central half-angle  $\theta_0$  - same as for roofless tank (Eqn. D.7 BNL [1995]).

$$P_{\text{totaloutside}}(\eta_1, \theta) := \sqrt{P_{iu}(\eta_1, \theta)^2 + P_{cu}(\eta_1, \theta)^2}$$

Total dynamic wall pressure outside central half-angle  $\theta_0$  - same as open tank solution.

$$P_{\text{totalinside}}(\eta_1, \theta) := P_{ic}(\theta)$$

Total dynamic wall pressure inside central half-angle  $\theta_0$  - same as completely full tank solution.

$$P_{\text{totalinside}}(\eta_1, 0) = 29.73 \frac{\text{lbf}}{\text{in}^2}$$

Dynamic wall pressure at  $\theta=0$ .

RPP-RPT-28963, Rev. 1  
M&D-2008-005-RPT-01, Rev. 1

Prepared by: F. G. Abatt  
M&D Professional Services  
1/14/08  
Rev. 2

Theoretical Fluid Response  
Calculations for Equivalent Flexible  
Wall Flat-Top Tank at 460 in. Waste  
Level

Checked by: Milon Meyer

	0
0	0.25
1	0.25
2	0.25
3	0.26
4	0.26
5	0.27
6	0.28
7	0.29
8	0.31
9	0.32
10	0.34
11	0.36
12	0.38
13	0.41
14	0.44
15	0.47
16	0.5
17	0.54
18	0.58
19	0.63
20	0.68
21	0.73
22	0.76
23	0.79
24	0.82

$c_{n_0}(\eta_1) =$

	0
0	0.75
1	0.75
2	0.75
3	0.74
4	0.74
5	0.73
6	0.72
7	0.71
8	0.69
9	0.68
10	0.66
11	0.64
12	0.62
13	0.59
14	0.56
15	0.53
16	0.5
17	0.46
18	0.42
19	0.37
20	0.32
21	0.27
22	0.24
23	0.21
24	0.18

$c_i(\eta_1) =$

**RPP-RPT-28963, Rev. 1**  
**M&D-2008-005-RPT-01, Rev. 1**

Prepared by: F. G. Abatt  
M&D Professional Services  
1/14/08  
Rev. 2

Theoretical Fluid Response  
Calculations for Equivalent Flexible  
Wall Flat-Top Tank at 460 in. Waste  
Level

Checked by: Milon Meyer

	0
0	11.73
1	11.71
2	11.66
3	11.59
4	11.49
5	11.37
6	11.21
7	11.03
8	10.81
9	10.56
10	10.28
11	9.96
12	9.61
13	9.21
14	8.77
15	8.28
16	7.75
17	7.16
18	6.52
19	5.81
20	5.04
21	4.2
22	3.76
23	3.29
24	2.8

$$P_{iu}(\eta_1, 45) =$$

$$\frac{\text{lb}}{\text{in}^2}$$

$$P_{cu}(\eta_1, 45) =$$

	0
0	0.26
1	0.26
2	0.26
3	0.27
4	0.27
5	0.28
6	0.29
7	0.3
8	0.32
9	0.33
10	0.35
11	0.37
12	0.4
13	0.42
14	0.45
15	0.48
16	0.52
17	0.56
18	0.6
19	0.65
20	0.7
21	0.75
22	0.78
23	0.81
24	0.85

$$\frac{\text{lb}}{\text{in}^2}$$

Total dynamic wall pressure at  $\theta=45$  degrees (outside the central half-angle  $\theta_0$ ).

$$P_{\text{totaloutside}}(\eta_1, 45) =$$

	0
0	11.73
1	11.71
2	11.67
3	11.6
4	11.5
5	11.37
6	11.22
7	11.03
8	10.82
9	10.57
10	10.29
11	9.97
12	9.61
13	9.22
14	8.78
15	8.3
16	7.77
17	7.18
18	6.55
19	5.85
20	5.09
21	4.27
22	3.84
23	3.39
24	2.92

$$\frac{\text{lb}}{\text{in}^2}$$

RPP-RPT-28963, Rev. 1  
M&D-2008-005-RPT-01, Rev. 1

Prepared by: F. G. Abatt  
M&D Professional Services  
1/14/08  
Rev. 2

Theoretical Fluid Response  
Calculations for Equivalent Flexible  
Wall Flat-Top Tank at 460 in. Waste  
Level

Checked by: Milon Meyer

Calculate Maximum Total Hydrodynamic Force:

The maximum hydrodynamic force induced on the tank wall is given by the sum of the terms in Equations D.12, D.13, and D.14 of BNL (1995).

$$m_1 := 4.97 \cdot 10^4 \frac{\text{lb} \cdot \text{sec}^2}{\text{in}} \quad \text{Actual waste mass reported by Dytran model.}$$

$$m_{c0} := \left[ \frac{2}{\lambda_0 \cdot [(\lambda_0)^2 - 1] \cdot \left(\frac{H_1}{R}\right)} \right] \cdot \tanh \left[ \lambda_0 \cdot \left(\frac{H_1}{R}\right) \right] \cdot m_1 \quad \text{Eqn. 4.32 BNL (1995)}$$

$$m_{c0} = 2.11 \times 10^4 \frac{\text{lb} \cdot \text{sec}^2}{\text{in}} \quad \text{First mode convective mass for roofless tank}$$

$$m_i := m_1 - m_{c0} \quad m_i = 2.86 \times 10^4 \frac{\text{lb} \cdot \text{sec}^2}{\text{in}} \quad \text{Impulsive mass for roofless tank - Eqn. 4.33 BNL (1995).}$$

$$\frac{m_{c0}}{m_1} = 0.42 \quad \frac{m_i}{m_1} = 0.58$$

$$\text{epsilon} := \frac{2 \cdot \theta_0 + \sin(2 \cdot \theta_0)}{2 \cdot \pi} \quad \text{Dimensionless factor for wall force calculation Eqn. D.9 of BNL (1995).}$$

$$F_{ic} := \text{epsilon} \cdot \frac{H_1}{H_1} \cdot m_i \cdot SA_i \quad \text{Impulsive component of force due to constrained portion of liquid Eqn. D.12 of BNL (1995).}$$

$$F_{ic} = 3.88 \times 10^6 \text{ lbf}$$

$$F_{iu} := (1 - \text{epsilon}) \cdot m_i \cdot SA_i \quad \text{Impulsive component of force due to unconstrained portion of liquid Eqn. D.13 of BNL (1995).}$$

$$F_{iu} = 8.93 \times 10^6 \text{ lbf}$$

$$F_{cu} := (1 - \text{epsilon}) \cdot m_{c0} \cdot SA_{c0} \quad \text{Convective component of force due to unconstrained portion of liquid Eqn. D.14 of BNL (1995).}$$

$$F_{cu} = 4.35 \times 10^5 \text{ lbf}$$

RPP-RPT-28963, Rev. 1  
M&D-2008-005-RPT-01, Rev. 1

Prepared by: F. G. Abatt  
M&D Professional Services  
1/14/08  
Rev. 2

Theoretical Fluid Response  
Calculations for Equivalent Flexible  
Wall Flat-Top Tank at 460 in. Waste  
Level

Checked by: Milon Meyer

$$F_{\text{total}} := \sqrt{(F_{\text{ic}} + F_{\text{iu}})^2 + F_{\text{cu}}^2} \quad \text{Total peak hydrodynamic force per BNL (1995)}$$

$$F_{\text{total}} = 1.28 \times 10^7 \text{ lbf}$$

Recalculate Maximum Hydrodynamic Force Using Methodology of Malhotra (2005):

The hydrodynamic force can be calculated by excluding the structural masses from Eqn. (3) of Malhotra (2005). First calculate the impulsive and convective masses.

$$j := 0..1$$

$$\overline{HR}_j := \begin{pmatrix} 1.0 \\ 1.5 \end{pmatrix} \quad \text{ImpMassRatio} := \begin{pmatrix} 0.548 \\ 0.686 \end{pmatrix} \quad \text{Table 1 of Malhotra (2005)}$$

$$\text{linterp}\left(\overline{HR}_j, \text{ImpMassRatio}, \frac{H_1}{R}\right) = 0.55$$

$$m_{i\text{Malhotra}} := \text{linterp}\left(\overline{HR}_j, \text{ImpMassRatio}, \frac{H_1}{R}\right) m_1 \quad m_{i\text{Malhotra}} = 2.75 \times 10^4 \frac{\text{lbf}\cdot\text{sec}^2}{\text{in}}$$

$$m_{c\text{Malhotra}} := m_1 - m_{i\text{Malhotra}} \quad m_{c\text{Malhotra}} = 2.22 \times 10^4 \frac{\text{lbf}\cdot\text{sec}^2}{\text{in}}$$

$$SA_{i\text{Malhotra}} := 1.07 \cdot g \quad SA_{i\text{Malhotra}} = 4.13 \times 10^2 \frac{\text{in}}{\text{sec}^2} \quad \text{ANSYS dome RS from Spectr at 3.5\% damping using impulsive frequency of 5.4 Hz.}$$

$$R_i := m_{i\text{Malhotra}} \cdot SA_{i\text{Malhotra}} \quad \text{Eqn. (3) Malhotra (2005)}$$

$$R_c := m_{c\text{Malhotra}} \cdot SA_{c0} \quad \text{Eqn. (4) Malhotra (2005)}$$

Modify the impulsive and convective masses to account for interaction with the tank roof per Eqns. (15) and (16) of Malhotra (2005).

$$m_{\text{ibar}} := m_{i\text{Malhotra}} + m_{c\text{Malhotra}} \left(1 - \frac{h_0}{h_{s\text{Malhotra}}}\right) \quad m_{\text{ibar}} = 3.18 \times 10^4 \frac{\text{lbf}\cdot\text{sec}^2}{\text{in}}$$

$$m_{\text{cbar}} := m_{c\text{Malhotra}} \left(\frac{h_0}{h_{s\text{Malhotra}}}\right) \quad m_{\text{cbar}} = 1.79 \times 10^4 \frac{\text{lbf}\cdot\text{sec}^2}{\text{in}}$$

**RPP-RPT-28963, Rev. 1**  
**M&D-2008-005-RPT-01, Rev. 1**

Prepared by: F. G. Abatt  
M&D Professional Services  
1/14/08  
Rev. 2

Theoretical Fluid Response  
Calculations for Equivalent Flexible  
Wall Flat-Top Tank at 460 in. Waste  
Level

Checked by: Milon Meyer

$$R_{i\text{bar}} := m_{i\text{bar}} \cdot S_{A_i} \text{Malhotra} \quad R_{i\text{bar}} = 1.31 \times 10^7 \text{ lbf} \quad \text{Impulsive component of peak reaction force}$$

$$R_{c\text{bar}} := m_{c\text{bar}} \cdot S_{A_c0} \quad R_{c\text{bar}} = 4.57 \times 10^5 \text{ lbf} \quad \text{Convective component of peak reaction force}$$

$$R_{\text{bar}} := \sqrt{R_{i\text{bar}}^2 + R_{c\text{bar}}^2} \quad \text{Total peak reaction force per Malhotra (2005)}$$

$$R_{\text{bar}} = 1.32 \times 10^7 \text{ lbf}$$

**References:**

BNL (1995), *Seismic Design and Evaluation Guidelines for the Department of Energy High-Level Waste Storage Tanks and Appurtenances*, BNL 52361, Rev. 10/95, Brookhaven National Laboratory, Upton, New York.

Deibler, J.E., K.I. Johnson, S.P. Pilli, M.W. Rinker, F.G. Abatt, and N.K. Karri, 2008, *Hanford Double-Shell Tank Thermal and Seismic Project Increased Liquid Level Analysis for 241AP Tank Farm*, RPP-RPT-32237, Rev. 1, Pacific Northwest National Laboratory, Richland, Washington.

Malhotra, Praveen K, 2005, *Sloshing Loads in Liquid Storage Tanks With Insufficient Freeboard*, *Earthquake Spectra*, Volume 21, No. 4, pp. 1185-1192, November 2005.

Kennedy, R.P., 2003, *Review Comments Concerning Evaluation of Proposed Increase to Double-Shell Tank Liquid Level*, May 2003, RPK Structural Mechanics Consulting, Escondido, California.

**RPP-RPT-28963, Rev. 1**  
**M&D-2008-005-RPT-01, Rev. 1**

Prepared by: F. G. Abatt  
M&D Professional Services  
1/14/08  
Rev. 2

Theoretical Fluid Response  
Calculations for Equivalent Flexible  
Wall Flat-Top Tank at 460 in. Waste  
Level

Checked by : Milon Meyer

This worksheet contains calculations for a flexible wall equivalent flat-top tank with an initial liquid level of 460 in. The calculations are performed using the methodology in Chapter 4 and Appendix D of BNL (1995) and in Malhotra (2005). The impulsive response per BNL (1995) is calculated using is based on the Dytran calculated impulsive frequency of 6.25 Hz and damping of 5.5%. Total reaction forces using the methodology of Malhotra (2005) are calculated at the Malhotra impulsive frequency of 5.4 Hz at a damping value of 5.5%. The freeboard distance is such that minor interaction occurs between the liquid and the flat roof. The location of the fluid elements corresponds to the Dytran model of the domed flexible wall tank in Appendix C. Revision 2 of this file incorporates corrections and clarifications regarding the interpretation of solutions in BNL (1995) per reviewer comments from a June 7-8, 2007 review meeting. The complete set of review comments from that meeting appear as Appendix A of Deibler et al. (2008).

$$H_l := 460.0 \text{ in} \quad \text{Baseline liquid level}$$

$$H_t := 484.0 \text{ in} \quad \text{Height of equivalent flat top tank per Kennedy (2003)}$$

$$h_0 := H_t - H_l \quad h_0 = 24 \text{ in} \quad \text{Freeboard distance}$$

$$\frac{H_l}{H_t} = 0.95 \quad \text{Ratio of waste height to tank height}$$

$$\omega := 386.4 \frac{\text{in}}{\text{sec}^2}$$

$$R := 450 \text{ in} \quad \text{Tank radius}$$

$$\frac{H_l}{R} = 1.02 \quad \text{Ratio of waste height to tank radius}$$

$$i := 0..2$$

$$\lambda := \begin{pmatrix} 1.841 \\ 5.331 \\ 8.536 \end{pmatrix} \quad \text{Bessel function roots - Eqn. 4.5 BNL (1995)}$$

$$\theta := \begin{pmatrix} 0 \text{ deg} \\ 45 \text{ deg} \\ 90 \text{ deg} \end{pmatrix} \quad \text{Circumferential location of waste elements for which pressures are reported}$$

$$\rho_l := 1.71 \cdot 10^{-4} \frac{\text{lb} \cdot \text{sec}^2}{\text{in}^4} \quad \text{Liquid mass density - specific gravity of 1.83}$$

**RPP-RPT-28963, Rev. 1**  
**M&D-2008-005-RPT-01, Rev. 1**

Prepared by: F. G. Abatt  
M&D Professional Services  
1/14/08  
Rev. 2

Theoretical Fluid Response  
Calculations for Equivalent Flexible  
Wall Flat-Top Tank at 460 in. Waste  
Level

Checked by : Milon Meyer

**Convective Frequencies**

$$f_{con_i} := \frac{1}{2 \cdot \pi} \cdot \left[ \sqrt{\lambda_i \cdot \left[ \frac{g}{R} \cdot \tanh \left[ \lambda_i \cdot \left( \frac{H_1}{R} \right) \right] \right]} \right] \quad \text{Eqn. 4.14 BNL (1995)}$$

$$f_{con} = \begin{pmatrix} 0.196 \\ 0.341 \\ 0.431 \end{pmatrix} \frac{1}{s} \quad \text{First three convective frequencies}$$

Recalculate the Fundamental Convective Frequency Using the Methodology of Malhotra (2005)

$$j := 0..1$$

$$HR := \begin{pmatrix} 1.0 \\ 1.5 \end{pmatrix} \quad C_{cref} := \begin{pmatrix} 1.52 \\ 1.48 \end{pmatrix} \quad \text{Table 1 of Malhotra (2005)}$$

$$linterp \left( HR, C_{cref}, \frac{H_1}{R} \right) = 1.52$$

$$C_c := linterp \left( HR, C_{cref}, \frac{H_1}{R} \right) \frac{\text{sec}}{\sqrt{m}}$$

$$T_{conMalhotra} := C_c \cdot \sqrt{R} \quad T_{conMalhotra} = 5.13 \text{ s}$$

$$f_{conMalhotra} := \frac{1}{T_{conMalhotra}} \quad f_{conMalhotra} = 0.19 \frac{1}{s} \quad \text{Fundamental convective frequency per Eqn. (2) of Malhotra (2005)}$$

The fundamental convective frequencies calculated using the methodologies of BNL (1995) and Malhotra (2005) are nearly the same. Consequently, the spectral accelerations associated with the fundamental convective modes are essentially the same using either methodology.

Consider the first three convective mode spectral accelerations for the 0.1% damped spectrum

$$SA_{c0} := 0.066 \cdot g \quad SA_{c0} = 25.5 \frac{\text{in}}{\text{sec}^2}$$

$$SA_{c1} := 0.11 \cdot g \quad SA_{c1} = 42.5 \frac{\text{in}}{\text{sec}^2} \quad \text{ANSYS dome RS from Spectr}$$

$$SA_{c2} := 0.17 \cdot g \quad SA_{c2} = 65.69 \frac{\text{in}}{\text{sec}^2}$$

**RPP-RPT-28963, Rev. 1**  
**M&D-2008-005-RPT-01, Rev. 1**

Prepared by: F. G. Abatt  
M&D Professional Services  
1/14/08  
Rev. 2

Theoretical Fluid Response  
Calculations for Equivalent Flexible  
Wall Flat-Top Tank at 460 in. Waste  
Level

Checked by : Milon Meyer

Calculation of Impulsive Frequency per BNL (1995):

$$\rho_t := 7.35 \cdot 10^{-4} \frac{\text{lb} \cdot \text{sec}^2}{\text{in}^4} \quad \text{Steel density}$$

$$t_{tw} := 0.65 \text{ in} \quad \text{Tank wall thickness used in Dytran model.}$$

$$E_t := 29 \cdot 10^6 \frac{\text{lb} \cdot \text{f}}{\text{in}^2} \quad \text{Elastic modulus for steel}$$

$$C_{iref} := 0.1062 \quad \text{Table 4.4 of BNL (1995)}$$

$$C_i := C_{iref} \sqrt{127 \cdot \frac{t_{tw}}{R} \cdot \frac{\rho_l}{\rho_t}} \quad \text{Eqn. 4.18 BNL (1995)}$$

$$C_i = 9.43 \times 10^{-2} \quad \text{Impulsive coefficient for frequency calculation}$$

$$f_i := \frac{1}{2 \cdot \pi} \cdot \frac{C_i}{H_1} \cdot \sqrt{\frac{E_t}{\rho_t}} \quad f_i = 6.48 \frac{1}{s} \quad \text{Eqn. 4.16 BNL (1995)}$$

Recalculate the Fundamental Impulsive Frequency Using the Methodology of Malhotra (2005):

$$j_w := 0..1$$

$$HR := \begin{pmatrix} 1.0 \\ 1.5 \end{pmatrix} \quad C_{irefMalhotra} := \begin{pmatrix} 6.36 \\ 6.06 \end{pmatrix}$$

$$l_{interp} \left( HR, C_{irefMalhotra}, \frac{H_1}{R} \right) = 6.35$$

$$C_{iMalhotra} := l_{interp} \left( HR, C_{irefMalhotra}, \frac{H_1}{R} \right)$$

**RPP-RPT-28963, Rev. 1**  
**M&D-2008-005-RPT-01, Rev. 1**

Prepared by: F. G. Abatt  
M&D Professional Services  
1/14/08  
Rev. 2

Theoretical Fluid Response  
Calculations for Equivalent Flexible  
Wall Flat-Top Tank at 460 in. Waste  
Level

Checked by : Milon Meyer

$$T_{\text{impMalhotra}} := C_{\text{iMalhotra}} \cdot \frac{\sqrt{\rho_l \cdot H_l}}{\sqrt{\frac{t_{\text{tw}}}{R}} \cdot \sqrt{E_t}} \quad T_{\text{impMalhotra}} = 0.19 \text{ s}$$

$$f_{\text{impMalhotra}} := \frac{1}{T_{\text{impMalhotra}}} \quad f_{\text{impMalhotra}} = 5.36 \frac{1}{\text{s}} \quad \text{Fundamental impulsive frequency per Eqn. (1) of Malhotra (2005)}$$

Spectral acceleration for the impulsive mode at 5.5% damping using impulsive frequency 6.25 Hz from Dytran simulation.

$$SA_i := 0.94 \cdot g \quad SA_i = 3.63 \times 10^2 \frac{\text{in}}{\text{sec}^2} \quad \text{ANSYS dome RS from Spectr at 5.5% damping and impulsive frequency of 6.25 Hz.}$$

Calculate Maximum Slosh Height per BNL (1995):

$$\text{conmax} := \begin{pmatrix} 0.837 \\ 0.073 \\ 0.028 \end{pmatrix} \quad \text{Maximum value of convective coefficients at } \eta_l=1$$

$$h_s := R \cdot \sqrt{\left( \text{conmax}_0 \cdot \frac{SA_{c0}}{g} \right)^2 + \left( \text{conmax}_1 \cdot \frac{SA_{c1}}{g} \right)^2 + \left( \text{conmax}_2 \cdot \frac{SA_{c2}}{g} \right)^2} \quad \text{Eqn. 4.60 BNL (1995)}$$

$$h_s = 25.2 \text{ in} \quad \text{Maximum theoretical slosh height for roofless tank per BNL (1995)}$$

Recalculate the Maximum Slosh Height per Malhotra (2005):

$$h_{s\text{Malhotra}} := R \cdot \frac{SA_{c0}}{g} \quad \text{Eqn. (9) of Malhotra (2005)}$$

$$h_{s\text{Malhotra}} = 29.7 \text{ in} \quad \text{Maximum slosh height for roofless tank per Malhotra (2005)}$$

Calculate the Central Half-Angle for Wetted Portion of Tank Roof:

$$\theta_0 := \arccos\left(\frac{h_0}{h_s}\right) \quad \text{Central half-angle of maximum impacted roof area per Eqn. D.2 BNL (1995)}$$

$$\theta_0 = 17.8 \text{ deg} \quad \text{Central half-angle per Appendix D BNL (1995)}$$

**RPP-RPT-28963, Rev. 1**  
**M&D-2008-005-RPT-01, Rev. 1**

Prepared by: F. G. Abatt  
M&D Professional Services  
1/14/08  
Rev. 2

Theoretical Fluid Response  
Calculations for Equivalent Flexible  
Wall Flat-Top Tank at 460 in. Waste  
Level

Checked by : Milon Meyer

$$\frac{h_0}{h_{s\text{Malhotra}}} = 0.81 \quad \text{Used to calculate } x_f \text{ from Figure 3 of Malhotra (2005)}$$

$$x_f := 0.2 \cdot R \quad x_f = 90 \text{ in} \quad \text{Wetted width of tank roof per Figures 2 and 3 of Malhotra (2005)}$$

$$\psi_0 := \arccos\left(\frac{x_f}{R} - 1\right) \quad \psi_0 = 2.5$$

$$\theta_{0\text{Malhotra}} := \pi - \psi_0 \quad \theta_{0\text{Malhotra}} = 36.9 \text{ deg} \quad \text{Central half-angle per Malhotra (2005)}$$

**Maximum Roof Pressure:**

$r := 424.875 \text{ in}$  Typical centroidal radius of Dytran elements for which results are monitored

$$p_r(r, \theta) := \rho_1 \cdot r \cdot SA_i \cdot \cos(\theta) \quad \text{for } |\theta| < |\theta_0| \quad \text{Peak roof pressure per Eqn. D.4 BNL (1995)}$$

$$p_r(R, 0) = 27.95 \frac{\text{lb}}{\text{in}^2} \quad \text{Peak roof pressure per BNL (1995)}$$

$$p_r(r, 0) = 26.39 \frac{\text{lb}}{\text{in}^2} \quad \text{Predicted peak roof pressure for Dytran element per BNL (1995)}$$

$$P_{\text{maxroofMalhotra}} := \rho_1 \cdot x_f \cdot SA_{c0} \quad \text{Peak roof pressure per Eqns. (10) and (12) of Malhotra (2005)}$$

$$P_{\text{maxroofMalhotra}} = 0.39 \frac{\text{lb}}{\text{in}^2}$$

**Calculate the Maximum Wall Pressure per Appendix D BNL (1995) :**

$$p_{ic}(\theta) := \rho_1 \cdot R \cdot SA_i \cdot \cos(\theta) \quad \text{Impulsive component of pressure due to constrained portion of the liquid per Eqn. D.5 BNL (1995). This term represents the total hydrodynamic pressure within the central half-angle } \theta_0.$$

$$p_{ic}(\theta) = \begin{pmatrix} 27.95 \\ 19.76 \\ 0 \end{pmatrix} \frac{\text{lb}}{\text{in}^2}$$

**RPP-RPT-28963, Rev. 1**  
**M&D-2008-005-RPT-01, Rev. 1**

Prepared by: F. G. Abatt  
M&D Professional Services  
1/14/08  
Rev. 2

Theoretical Fluid Response  
Calculations for Equivalent Flexible  
Wall Flat-Top Tank at 460 in. Waste  
Level

Checked by : Milon Meyer

z :=

4.0-in
24.1-in
44.2-in
64.2-in
84.3-in
104.4-in
124.4-in
144.5-in
164.6-in
184.6-in
204.7-in
224.8-in
244.8-in
264.9-in
285-in
305-in
325-in
345-in
365-in
385-in
405-in
425-in
435-in
445-in
455-in

Vertical location of Euler element centroids at which pressures are reported.

$$\eta_1 := \frac{z}{H_1}$$

0	0.01
1	0.05
2	0.1
3	0.14
4	0.18
5	0.23
6	0.27
7	0.31
8	0.36
9	0.4
10	0.45
11	0.49
12	0.53
13	0.58
14	0.62
15	0.66
16	0.71
17	0.75
18	0.79
19	0.84
20	0.88
21	0.92
22	0.95
23	0.97
24	0.99

$$\eta_1 =$$

Ratio of tank wall vertical location to waste height for waste element centroids.

**RPP-RPT-28963, Rev. 1**  
**M&D-2008-005-RPT-01, Rev. 1**

Prepared by: F. G. Abatt  
M&D Professional Services  
1/14/08  
Rev. 2

Theoretical Fluid Response  
Calculations for Equivalent Flexible  
Wall Flat-Top Tank at 460 in. Waste  
Level

Checked by : Milon Meyer

Determine convective coefficients as a function of dimensionless height per Eqn. 4.4 BNL (1995).

$$\text{con}_0(\eta_1) := \frac{2 \cdot \cosh\left[\lambda_0 \cdot \left(\frac{H_1}{R}\right) \cdot \eta_1\right]}{\left(\lambda_0\right)^2 - 1 \cdot \cosh\left[\lambda_0 \cdot \left(\frac{H_1}{R}\right)\right]}$$

$$\text{con}_1(\eta_1) := \frac{2 \cdot \cosh\left[\lambda_1 \cdot \left(\frac{H_1}{R}\right) \cdot \eta_1\right]}{\left(\lambda_1\right)^2 - 1 \cdot \cosh\left[\lambda_1 \cdot \left(\frac{H_1}{R}\right)\right]}$$

$$\text{con}_2(\eta_1) := \frac{2 \cdot \cosh\left[\lambda_2 \cdot \left(\frac{H_1}{R}\right) \cdot \eta_1\right]}{\left(\lambda_2\right)^2 - 1 \cdot \cosh\left[\lambda_2 \cdot \left(\frac{H_1}{R}\right)\right]}$$

Impulsive pressure coefficient as a function of normalized wall height

$$c_i(\eta_1) := 1 - \text{con}_0(\eta_1)$$

BNL (1995) Eqn. 4.7 - 1st term

$$P_{iu}(\eta_1, \theta) := c_i(\eta_1) \cdot \rho_1 \cdot R \cdot S A_i \cdot \cos(\theta)$$

Impulsive component of maximum wall pressure induced by unconstrained portion of liquid beneath the non-impacted portion of the roof - same as for roofless tank (Eqn. D.6 BNL [1995]). This is the impulsive component of the hydrodynamic pressure outside the central half-angle  $\theta_0$ .

$$P_{cu}(\eta_1, \theta) := \text{con}_0(\eta_1) \cdot \rho_1 \cdot R \cdot S A_{c0} \cdot \cos(\theta)$$

Convective component of maximum wall pressure induced by unconstrained portion of liquid beneath the non-impacted portion of the roof outside the central half-angle  $\theta_0$  - same as for roofless tank (Eqn. D.7 BNL [1995]).

$$P_{\text{totaloutside}}(\eta_1, \theta) := \sqrt{P_{iu}(\eta_1, \theta)^2 + P_{cu}(\eta_1, \theta)^2}$$

Total dynamic pressure outside central half-angle  $\theta_0$  - same as open tank solution.

$$P_{\text{totalinside}}(\eta_1, \theta) := P_{ic}(\theta)$$

Total dynamic wall pressure inside central half-angle  $\theta_0$  - same as completely full tank solution.

$$P_{\text{totalinside}}(\eta_1, 0) = 27.95 \frac{\text{lbf}}{\text{in}^2}$$

RPP-RPT-28963, Rev. 1  
M&D-2008-005-RPT-01, Rev. 1

Prepared by: F. G. Abatt  
M&D Professional Services  
1/14/08  
Rev. 2

Theoretical Fluid Response  
Calculations for Equivalent Flexible  
Wall Flat-Top Tank at 460 in. Waste  
Level

Checked by : Milon Meyer

$$c_{n0}(\eta_1) =$$

	0
0	0.25
1	0.25
2	0.25
3	0.26
4	0.26
5	0.27
6	0.28
7	0.29
8	0.31
9	0.32
10	0.34
11	0.36
12	0.38
13	0.41
14	0.44
15	0.47
16	0.5
17	0.54
18	0.58
19	0.63
20	0.68
21	0.73
22	0.76
23	0.79
24	0.82

$$c_i(\eta_1) =$$

	0
0	0.75
1	0.75
2	0.75
3	0.74
4	0.74
5	0.73
6	0.72
7	0.71
8	0.69
9	0.68
10	0.66
11	0.64
12	0.62
13	0.59
14	0.56
15	0.53
16	0.5
17	0.46
18	0.42
19	0.37
20	0.32
21	0.27
22	0.24
23	0.21
24	0.18

**RPP-RPT-28963, Rev. 1**  
**M&D-2008-005-RPT-01, Rev. 1**

Prepared by: F. G. Abatt  
M&D Professional Services  
1/14/08  
Rev. 2

Theoretical Fluid Response  
Calculations for Equivalent Flexible  
Wall Flat-Top Tank at 460 in. Waste  
Level

Checked by : Milon Meyer

$$P_{iu}(\eta_1, 45) = \frac{\text{lb}}{\text{in}^2}$$

	0
0	11.02
1	11.01
2	10.96
3	10.9
4	10.8
5	10.68
6	10.54
7	10.37
8	10.16
9	9.93
10	9.66
11	9.36
12	9.03
13	8.66
14	8.24
15	7.79
16	7.28
17	6.73
18	6.13
19	5.47
20	4.74
21	3.95
22	3.53
23	3.09
24	2.63

$$P_{cu}(\eta_1, 45) = \frac{\text{lb}}{\text{in}^2}$$

	0
0	0.3
1	0.3
2	0.3
3	0.3
4	0.3
5	0.3
6	0.3
7	0.3
8	0.3
9	0.3
10	0.4
11	0.4
12	0.4
13	0.4
14	0.5
15	0.5
16	0.5
17	0.6
18	0.6
19	0.6
20	0.7
21	0.8
22	0.8
23	0.8
24	0.8

$$P_{\text{totaloutside}}(\eta_1, 45) = \frac{\text{lb}}{\text{in}^2}$$

	0
0	11.03
1	11.01
2	10.97
3	10.9
4	10.81
5	10.69
6	10.54
7	10.37
8	10.17
9	9.94
10	9.67
11	9.37
12	9.04
13	8.67
14	8.25
15	7.8
16	7.3
17	6.76
18	6.16
19	5.5
20	4.79
21	4.02
22	3.62
23	3.19
24	2.76

Total dynamic wall pressure at  $\theta=45$  degrees (outside the central half-angle  $\theta_0$ ).

**RPP-RPT-28963, Rev. 1**  
**M&D-2008-005-RPT-01, Rev. 1**

Prepared by: F. G. Abatt  
M&D Professional Services  
1/14/08  
Rev. 2

Theoretical Fluid Response  
Calculations for Equivalent Flexible  
Wall Flat-Top Tank at 460 in. Waste  
Level

Checked by : Milon Meyer

Calculate Maximum Total Hydrodynamic Force:

The maximum hydrodynamic force induced on the tank wall is given by the sum of the terms in Equations D.12, D.13, and D.14 of BNL (1995).

$$m_1 := 4.97 \cdot 10^4 \frac{\text{lb} \cdot \text{sec}^2}{\text{in}} \quad \text{Actual waste mass reported by Dytran model.}$$

$$m_{c0} := \left[ \frac{2}{\lambda_0 \left[ \left( \lambda_0 \right)^2 - 1 \right] \left( \frac{H_1}{R} \right)} \right] \cdot \tanh \left[ \lambda_0 \left( \frac{H_1}{R} \right) \right] \cdot m_1 \quad \text{Eqn. 4.32 BNL (1995)}$$

$$m_{c0} = 2.11 \times 10^4 \frac{\text{lb} \cdot \text{sec}^2}{\text{in}} \quad \text{First mode convective mass for roofless tank}$$

$$m_i := m_1 - m_{c0} \quad m_i = 2.86 \times 10^4 \frac{\text{lb} \cdot \text{sec}^2}{\text{in}} \quad \text{Impulsive mass for roofless tank - Eqn. 4.33 BNL (1995).}$$

$$\frac{m_{c0}}{m_1} = 0.42 \quad \frac{m_i}{m_1} = 0.58$$

$$\text{epsilon} := \frac{2 \cdot \theta_0 + \sin(2 \cdot \theta_0)}{2 \cdot \pi} \quad \text{Dimensionless factor for wall force calculation Eqn. D.9 of BNL (1995).}$$

$$F_{ic} := \text{epsilon} \cdot \frac{H_t}{H_1} \cdot m_i \cdot SA_i \quad \text{Impulsive component of force due to constrained portion of liquid Eqn. D.12 of BNL (1995).}$$

$$F_{ic} = 3.64 \times 10^6 \text{ lbf}$$

$$F_{iu} := (1 - \text{epsilon}) \cdot m_i \cdot SA_i \quad \text{Impulsive component of force due to unconstrained portion of liquid Eqn. D.13 of BNL (1995).}$$

$$F_{iu} = 8.39 \times 10^6 \text{ lbf}$$

$$F_{cu} := (1 - \text{epsilon}) \cdot m_{c0} \cdot SA_{c0} \quad \text{Convective component of force due to unconstrained portion of liquid Eqn. D.14 of BNL (1995).}$$

$$F_{cu} = 4.35 \times 10^5 \text{ lbf}$$

**RPP-RPT-28963, Rev. 1**  
**M&D-2008-005-RPT-01, Rev. 1**

Prepared by: F. G. Abatt  
M&D Professional Services  
1/14/08  
Rev. 2

Theoretical Fluid Response  
Calculations for Equivalent Flexible  
Wall Flat-Top Tank at 460 in. Waste  
Level

Checked by : Milon Meyer

$$F_{\text{total}} := \sqrt{(F_{\text{ic}} + F_{\text{iu}})^2 + F_{\text{cu}}^2} \quad \text{Total peak hydrodynamic force per BNL (1995)}$$

$$F_{\text{total}} = 1.2 \times 10^7 \text{ lbf}$$

Recalculate Maximum Hydrodynamic Force Using Methodology of Malhotra (2005):

The hydrodynamic force can be calculated by excluding the structural masses from Eqn. (3) of Malhotra (2005). First calculate the impulsive and convective masses.

$$\alpha_j := 0..1$$

$$\text{HR} := \begin{pmatrix} 1.0 \\ 1.5 \end{pmatrix} \quad \text{ImpMassRatio} := \begin{pmatrix} 0.548 \\ 0.686 \end{pmatrix} \quad \text{Table 1 of Malhotra (2005)}$$

$$\text{linterp}\left(\text{HR}, \text{ImpMassRatio}, \frac{H_1}{R}\right) = 0.55$$

$$m_{i\text{Malhotra}} := \text{linterp}\left(\text{HR}, \text{ImpMassRatio}, \frac{H_1}{R}\right) m_1 \quad m_{i\text{Malhotra}} = 2.75 \times 10^4 \frac{\text{lbf}\cdot\text{sec}^2}{\text{in}}$$

$$m_{c\text{Malhotra}} := m_1 - m_{i\text{Malhotra}} \quad m_{c\text{Malhotra}} = 2.22 \times 10^4 \frac{\text{lbf}\cdot\text{sec}^2}{\text{in}}$$

$$SA_{i\text{Malhotra}} := 0.92\text{-g} \quad SA_{i\text{Malhotra}} = 3.55 \times 10^2 \frac{\text{in}}{\text{sec}^2} \quad \text{ANSYS dome RS from Spectr at 5.5\% damping using impulsive frequency of 5.4 Hz.}$$

$$R_i := m_{i\text{Malhotra}} \cdot SA_{i\text{Malhotra}} \quad \text{Eqn. (3) Malhotra (2005)}$$

$$R_c := m_{c\text{Malhotra}} \cdot SA_{c0} \quad \text{Eqn. (4) Malhotra (2005)}$$

Modify the impulsive and convective masses to account for interaction with the tank roof per Eqns. (15) and (16) of Malhotra (2005).

$$m_{i\text{bar}} := m_{i\text{Malhotra}} + m_{c\text{Malhotra}} \left(1 - \frac{h_0}{h_{s\text{Malhotra}}}\right) \quad m_{i\text{bar}} = 3.18 \times 10^4 \frac{\text{lbf}\cdot\text{sec}^2}{\text{in}}$$

$$m_{c\text{bar}} := m_{c\text{Malhotra}} \left(\frac{h_0}{h_{s\text{Malhotra}}}\right) \quad m_{c\text{bar}} = 1.79 \times 10^4 \frac{\text{lbf}\cdot\text{sec}^2}{\text{in}}$$

**RPP-RPT-28963, Rev. 1**  
**M&D-2008-005-RPT-01, Rev. 1**

Prepared by: F. G. Abatt  
M&D Professional Services  
1/14/08  
Rev. 2

Theoretical Fluid Response  
Calculations for Equivalent Flexible  
Wall Flat-Top Tank at 460 in. Waste  
Level

Checked by : Milon Meyer

$$R_{i\bar{b}ar} := m_{i\bar{b}ar} \cdot SA_{i\bar{b}ar} \quad R_{i\bar{b}ar} = 1.13 \times 10^7 \text{ lbf} \quad \text{Impulsive component of peak reaction force}$$

$$R_{c\bar{b}ar} := m_{c\bar{b}ar} \cdot SA_{c\bar{b}ar} \quad R_{c\bar{b}ar} = 4.57 \times 10^5 \text{ lbf} \quad \text{Convective component of peak reaction force}$$

$$R_{\bar{b}ar} := \sqrt{R_{i\bar{b}ar}^2 + R_{c\bar{b}ar}^2} \quad \text{Total peak reaction force per Malhotra (2005)}$$

$$R_{\bar{b}ar} = 1.13 \times 10^7 \text{ lbf}$$

References:

BNL (1995), *Seismic Design and Evaluation Guidelines for the Department of Energy High-Level Waste Storage Tanks and Appurtenances*, BNL 52361, Rev. 10/95, Brookhaven National Laboratory, Upton, New York.

Deibler, J.E., K.I. Johnson, S.P. Pilli, M.W. Rinker, F.G. Abatt, and N.K. Karri, 2008, *Hanford Double-Shell Tank Thermal and Seismic Project Increased Liquid Level Analysis for 241AP Tank Farm*, RPP-RPT-32237, Rev. 1, Pacific Northwest National Laboratory, Richland, Washington.

Malhotra, Praveen K, 2005, *Sloshing Loads in Liquid Storage Tanks With Insufficient Freeboard*, *Earthquake Spectra*, Volume 21, No. 4, pp. 1185-1192, November 2005.

Kennedy, R.P., 2003, *Review Comments Concerning Evaluation of Proposed Increase to Double-Shell Tank Liquid Level*, May 2003, RPK Structural Mechanics Consulting, Escondido, California.